Justus-Liebig-Universität Gießen

Fachbereich Medizin

Klinische Forschungseinheit

Leiter: Prof. Dr. Thomas Linn

Medizinische Klinik und Poliklinik III

Endokrinologie, Diabetologie, Stoffwechsel und Ernährungsmedizin

Direktor: Prof. Dr. Andreas Schäffler

Die Bedeutung der Glutaredoxine und Thioredoxine für die pankreatische β-Zelle bei Diabetes mellitus

Kumulative Habilitationsschrift

zur Erlangung der Lehrbefähigung für das Fach Innere Medizin

im Fachbereich Medizin der Justus-Liebig-Universität Gießen

vorgelegt von

Dr. med. Sebastian Friedrich Petry

Gießen 2023

Inhaltsverzeichnis

1. Einführung

1.1 Diabetes mellitus

1.1.1 Definition und Diagnostik

Der Diabetes mellitus umfasst eine ätiologisch heterogene Gruppe von chronischen, nichtübertragbaren Stoffwechselerkrankungen, deren gemeinsames Merkmal die chronische Hyperglykämie ist. Die häufigsten und klinisch am relevantesten Diabetesformen sind der Typ 1 und Typ 2 Diabetes mellitus (T1 bzw. T2DM). Sonstige Formen werden als Typ 3 zusammengefasst, und eine in der Schwangerschaft erstmals diagnostizierte Glukosestoffwechselstörung wird als Schwangerschaftsdiabetes (GDM) bezeichnet.

Zur Diagnose der Erkrankung wird die Plasmaglukose nüchtern (NPG), die Gelegenheitsplasmaglukose (GPG) und/oder die Plasmaglukose zwei Stunden nach Ingestion einer Lösung mit 75 g Glukoseäquivalent im oralen Glukosetoleranztest (OGTT) herangezogen, zudem der HbA1c-Wert. Die Diagnose eines Diabetes mellitus wird gestellt, wenn die NPG $\geq$ 126 mg/dl, die GPG $\geq$ 200 mg/dl oder der HbA1c-Wert $\geq$ 6,5% beträgt. Ein Graubereich, auch definiert als Prädiabetes, liegt bei einem HbA1c-Wert von 5,7 - 6,4% oder einer NPG von 100 bis 125 mg/dl vor, wobei letzterer Zustand als gestörte Nüchternglukose (impaired fasting glucose / IFG) bezeichnet wird. In dieser Situation, oder bei diskrepanten Werten für die NPG und den HbA1c-Wert, wird ein OGTT durchgeführt. Eine Plasmaglukose von $\geq$ 200 mg/dl zum Zeitpunkt 2 h nach Ingestion der Glukoselösung gilt als pathologisch, bei 140 - 199 mg/dl liegt eine gestörte Glukosetoleranz (impaired glucose tolerance / IGT) vor. In der Praxis empfiehlt sich bei grenzwertigen oder diskrepanten Werten eine Zweitbestimmung von NPG, GPG und HbA1c-Wert. Für die Diagnose des GDM gelten strengere Grenzwerte [1].

1.1.2 Epidemiologie

Weltweit sind gemäß Erhebungen der International Diabetes Federation (IDF) rund 540 Millionen Menschen zwischen 20 und 79 Jahren an Diabetes mellitus erkrankt, was einem von zehn Erwachsenen entspricht. Die IDF schätzt die Prävalenz des Diabetes mellitus auf rund 640

Millionen im Jahr 2030 und rund 780 Millionen im Jahr 2045 [2]. Gemäß dem Gesundheitsbericht Diabetes 2023 gehen Erhebungen für Deutschland von knapp 400.000 Menschen mit T1DM und knapp 9 Millionen mit T2DM aus, wobei für letztere Gruppe eine Dunkelziffer von mindestens 2 Millionen Menschen angenommen wird. Rund 90 - 95% der Betroffenen leiden folglich an einem T2DM, in etwa 7% an einem T1DM. Der Anteil der als Typ 3 klassifizierten Formen liegt in einstelligen Prozentbereich [3–5]. Die Prävalenz des GDM wird für Deutschland mit rund 7% aller Schwangeren angegeben [6]. Die epidemiologischen Daten deuten auf einen weiteren Anstieg der Prävalenz des Diabetes mellitus, insbesondere des T2DM und vor allem in der Gruppe der über 65-Jährigen, hin [7].

Die Systemerkrankung Diabetes mellitus geht mit einer massiven Erhöhung von Mortalität und Morbidität einher. Das Risiko für kardiovaskuläre Erkrankungen ist bei Menschen mit Diabetes mellitus zwei- bis achtfach erhöht, sodass die Betroffenen trotz moderner Therapiemöglichkeiten bis zu acht Lebensjahre verlieren [8]. Die diabetesassoziierte Krankheitslast wird zudem wesentlich durch typische Folgeerkrankungen mitbedingt. In etwa jeder fünfte Mensch mit Diabetes erleidet eine potentiell zur Blindheit führende diabetische Retinopathie, jeder dritte Dialysepatient benötigt die Nierenersatztherapie wegen einer diabetischen Nephropathie, und pro Jahr erfolgen bei Menschen mit diabetischem Fußsyndrom aufgrund einer diabetischen Polyneuropathie 40.000 - 50.000 Amputationen, was 2/3 aller durchgeführten Amputationen entspricht [3]. Aufgrund der zunehmenden Prävalenz und Inzidenz der Erkrankung stellt die „Diabetes-Pandemie“ eine globale medizinische und sozioökonomische Herausforderung dar. Im Jahr 2021 lagen die diabetesassoziierten Kosten für das deutsche Gesundheitssystem bei rund 39 Milliarden Euro [3].

1.1.3 Ätiologie und Pathogenese

1.1.3.1 Typ 1 Diabetes mellitus

Beim T1DM kommt es unter den Einfluss genetischer und Umweltfaktoren zu einer autoimmun bedingten Zerstörung des endokrinen Pankreas mit einem absoluten Insulinmangel. Die genetische Prädisposition eines Individums wird wesentlich durch Gene der human leukocyte antigen (HLA) Klasse II bestimmt, allerdings spielen rund 50 weitere nicht-HLA-Gene, welche zumeist für die Immunität verantwortlich sind, eine Rolle [9]. Diese genetische Suszeptibilität

für T1DM ist Voraussetzung für die Erkrankung, jedoch nicht ausreichend. Man geht davon aus, dass Umweltfaktoren wie Infektionen, Vakzinierungen, das Mikrobiom des Darms, die Ernährung und Hygiene die Entstehung der Autoimmunität auf der Grundlage der permissiven Genetik auslösen. Die exakte Ursache für die Entstehung der gegen die β-Zellen gerichteten Immunreaktion ist bisher aber nicht bekannt [10]. Bei dem Immunprozess gegen die β-Zellen spielen sowohl die humorale als auch die zelluläre Immunantwort eine Rolle. Inflammatorische Zytokine wie Interleukine (IL), u.a. IL-2 [11], -4 [12], -6 [13] und -9 [14], Tumornekrosefaktor (TNF)-α und Interferon (IFN)-γ sowie autoreaktive T-Zellen [15, 16] unterhalten die lokale Inflammation der Langerhans'schen Inseln („Insulitis"). Eine wesentliche Bedeutung für die β-Zellautoimmunität haben zudem spezifische Antikörper. Es wurden über ein dutzend Inselautoantigene, welche mit T1DM assoziiert sind, entdeckt [17]. Wesentlich für die klinische Diagnostik sind jene gegen Insulin (IAA), Oberflächenantigene der β-Zelle (ICA), die Glutamatcarboxylase (GAD65), die Tyrosinphosphatase (IA2) und den pankreas-spezifischen Zinktransporter (ZnT8).

Die Erkrankung verläuft in drei Stadien [18–20]: Im Stadium I ist eine β-Zellautoimmunität, definiert als das Vorliegen von zwei oder mehr typischen, β-zellspezifischen Autoantikörpern, ohne Beeinträchtigung der Glukosehomöstase, detektierbar. Je mehr Antikörper vorliegen, desto höher ist das Risiko zur Entwicklung einer Glukosestoffwechselstörung, wobei das Lebenszeitrisiko ab dem Vorliegen von zwei Antikörpern nahezu 100% beträgt [21, 22]. Das zweite Stadium kennzeichnet eine präsymptomatische Phase mit IFG und/oder IGT als Zeichen der Dysglykämie, das dritte schließlich die symptomatische, dysglykämische Phase, welche einem klinisch manifesten Diabetes mellitus entspricht. Die zeitliche Latenz zwischen den einzelnen Stadien ist interindividuell unterschiedlich und kann Monate bis Jahrzehnte betragen [23].

1.1.3.2 Typ 2 Diabetes mellitus

Der T2DM stellt eine komplexe und multifaktoriell bedingte Stoffwechselerkrankung dar. Wesentliche Merkmale sind eine dysfunktionale Insulinsekretion und eine gestörte Insulinwirkung durch eine ausgeprägte Insulinresistenz der insulinabhängigen Gewebe, vor allem der Leber, des Fettgewebes, der Skelettmuskulatur, der Nieren, des Gehirns und des Darms. Auch bei dem T2DM wird der genetischen Prädisposition eine entscheidende Bedeutung zuteil. Es han-

delt sich um eine polygenetische Erkrankung [24], wobei die meisten Genloci die Insulinsekretion betreffen, eine weitaus geringere Zahl die Insulinwirkung [25, 26]. Treffen auf diese nicht-modifizierbaren, genetischen Risikofaktoren nun diabetogene, modifizierbare Faktoren, häufig zusammengefasst als „westlicher Lebensstil“, kann ein T2DM entstehen. Die wesentlichen Treiber des T2DM sind Adipositas [27], körperliche Inaktivität [28, 29] und Über- bzw. Fehlernährung. Die sogenannte „westliche Diät“ beinhaltet hochverarbeitete Nahrungsmittel mit hoher Energiedichte, ein Übermaß an rotem Fleisch und tierischen Fetten, raffiniertes Getreide und einen Überfluss an Kohlenhydraten [30]. Zusammengefasst stellen diese Faktoren somit ein Ungleichgewicht aus zu geringem Energieverbrauch und zu hoher Energiezufuhr dar. Korrelat des Substratüberschusses sind die Hyperglykämie, erhöhte freie Fettsäuren (FFS), eine Zunahme an viszeralem Fettgewebe, ektope Fetteinlagerungen und eine chronische Inflammation („Metaflammation“) [31]. Diese Faktoren bedingen zum einen Insulinresistenz, zum anderen eine Beeinträchtigung der β-Zellfunktion. Weitere Risikofaktoren sind u.a. eine Dysbalance des Darmmikrobioms [32, 33], Schadstoffe und endokrine Disruptoren [34], gestörter Schlaf [35] und das Lebensalter [36]. Typischerweise entwickelt sich über Jahre hinweg zunächst eine IGT bzw. IFG und somit ein Prädiabetes. Schließlich, mit der zunehmend nachlassenden β-Zellreserve, manifestiert sich eine Hyperglykämie [37, 38]. Häufig findet sich eine Assoziation mit weiteren metabolischen Erkrankungen, insbesondere des metabolischen Syndroms, wie arterielle Hypertonie, Adipositas, Dyslipidämie, Steatosis hepatis und dem Schlafapnoesyndrom [1]. Modernere Klassifikationsmodelle tragen der Tatsache Rechnung, dass das klinische Erscheinungsbild je nach Ausprägung der Insulinresistenz und des sekretorischen Defizits der β-Zellen zwischen einem vornehmlich insulinresistenten hyperinsulinämen Phänotyp und einem solchen mit ausgeprägtem sekretorischen Defizit variiert. Es lassen sich gemäß einer datenbasierten Erhebung fünf „Cluster“ des Diabetes mellitus definieren: severe autoimmune diabetes (SAID), welcher dem klassischen T1DM entspricht, severe insulin-deficient diabetes (SIDD), severe insulin-resistent diabetes (SIRD), moderate obesity diabetes (MOD) und moderate age-related diabetes (MARD), welche dem T2DM zuzuordnen sind [39]. Diese moderne Einteilung erlaubt die Identifizierung von Risikokonstellationen, da je nach Cluster eine unterschiedlich hohe Suszeptibilität gegenüber bestimmten Folgeerkrankungen beschrieben wurde.

Zudem ermöglicht sie die individuellere Therapie der Betroffenen.

1.1.4 Therapie

Die Therapie des Diabetes mellitus richtet sich nach den individuellen Bedürfnissen der Menschen mit Diabetes. Grundlage jeder Therapie ist die adäquate und eingehende Schulung der Betroffenen für das Leben mit der Erkrankung im Rahmen von strukturierten und evaluierten Schulungsprogrammen. Zumeist ist eine Pharmakotherapie jedoch unumgänglich. Der T1DM setzt per defitionem die Therapie mit exogenem Insulin im Rahmen einer intensivierten Insulintherapie voraus, wobei dieses mittels Insulinpens oder einer Insulinpumpe verabreicht werden kann. In der Praxis kommen zumeist schnellwirksame Insulinanaloga und (ultra)langwirksame Basalinsulinanaloga zur Anwendung, prinzipiell sind aber auch die älteren, schnell- und langwirksamen Humaninsuline verfügbar. Der T2DM ist primär die Domäne von nicht insulinbasierten Therapien. Hierzu gehören Substanzen wie Sulfonylharnstoffe, Glitazone, die Acarbose, das Biguanid Metformin, sodium glucose transporter 2 (SGLT2)-Hemmer und glucagon-like Peptide 1 (GLP1)- und/oder glukoseabhängiges insulinotropes Peptid (GIP)-Agonisten.
Die moderne Diabetestherapie adressiert zunehmend Komorbiditäten und das kardiovaskuläre Risiko der Menschen mit Diabetes, was vor allem durch die modernen Substanzen wie SGLT2-Hemmer und GLP1/GIP-basierte Therapien ermöglicht wird. Wesentlich sind je nach individuellen Komorbiditäten und Risikoprofil darüber hinaus lipidsenkende, antihypertensive und Adipositastherapien. Die reine Glukosekontrolle („Glukozentrik“) ist zwar weiterhin entscheidend, wird aber insbesondere beim T2DM als primäres Therapieziel zunehmend abgelöst. Der Typ 3 Diabetes stellt zumeist einen Insulinmangeldiabetes dar und wird daher vornehmlich mit Insulin behandelt, der GDM aufgrund begrenzter bzw. nicht vorhandener Erfahrungen mit anderen Substanzen ebenso. Als Surrogatparameter für die Glukosekontrolle dient der HbA1c-Wert, zunehmend aber auch durch Systeme zur kontinuierlichen Glukosemessung etablierte Parameter wie die Zeit im, unter und über dem Zielbereich [40, 41]. Insbesondere die Therapie des T1DM ist mehr und mehr Domäne von technologischen Hilfsmitteln, u.a. automatisierten Systemen zur Insulinabgabe (automated insulin delivery / AID), welche das Diabetesmanagement zunehmend autark vom Zutun der betroffenen Menschen mit Diabetes übernehmen [42]. In Einzelfällen kommt eine Insel- oder Pankreastransplantation infrage.

1.1.5 Pathophysiologie

Auf der molekularen Ebene sorgen die Hyperglykämie, eine chronische Fettstoffwechselstörung mit erhöhten FFS sowie ektopen Fetteinlagerungen, ein anhaltendes Inflammationsgeschehen sowie oxidativer Disstress für die Schädigung der insulinproduzierenden pankreatischen β-Zellen.

1.1.5.1 Hyperglykämie

Die sogenannte „Glukotoxizität“ wird klassischerweise als eine Schädigung der β-Zellen durch die chronische Exposition gegenüber supraphysiologischen Konzentrationen von Glukose definiert [43]. Allerdings gibt es in experimentellen Untersuchungen keine eindeutige Schwelle, welche Konzentration als „toxisch“ anzusehen ist. Vielmehr scheint insbesondere die Dauer der Hyperglykämie wesentlich für das Eintreten abträglicher Effekte zu sein [44–46]. Kongruent dazu fanden Colagiuri et al. in einer Datenanalyse von rund 45.000 Menschen mit Diabetes als Schwellenwerte für die Entwicklung einer diabetischen Retinopathie eine FBG von rund 6,5 mmol/l (117 mg/dl), einen Zweistundenwert im OGTT von rund 10 - 13 mmol/l (180 - 234 mmol/l) und einen HbA1c-Wert von rund 6,5% (entsprechend einer durchschnittlichen Glukosekonzentration von ca. 140 mg/dl [47]) [48]. Diese Werte entsprechen in etwa jenen Grenzwerten, die sich als diagnostische Kriterien des Diabetes mellitus etabliert haben. Dieser Ansatz definiert die Glukotoxizität folglich über die Glukosewerte, welche dauerhaft zur Entwicklung einer diabetischen Retinopathie führen, und ist daher für klinische Zwecke praktikabel.

Auf der molekluaren Ebene ist ein wesentlicher Treiber der Glukotoxizität die Entstehung von reaktiven Sauerstoffspezies (ROS) über verschiedene Stoffwechselwege. Es handelt sich unter anderem um Superoxid (O_2^-), das Hydroxylradikal (HO^-) und Peroxide (O_2^{2-}) inkl. Wasserstoffperoxid (H_2O_2). Diese können in der Summe zu oxidativem Disstress („oxidative distress“) führen. Die Glukoselast führt zum einen zu einer gesteigerten Glykierung von Proteinen. In diesem im Rahmen werden über die Schiff’sche Base und die Amadori-Umlagerung neben ROS auch glykierte Reaktionsprodukte (advanced glycation endproducts [AGEs]), welche insbesondere für die Entwicklung von diabetischen Folgeschäden wesentlich sind, gebildet [49]. Zum anderen kommt es auch über den Hexosaminsignalweg durch das vermehrte Anfallen von Glu-

cosamin insbesondere zur Bildung von H_2O_2 [50]. Der hyperglykämiebedingte erhöhte Substratumsatz in den Mitochondrien begünstigt ebenso die Entstehung von ROS [51]. In der Summe führt die Glukotoxizität unter anderem zu einer Verringerung der Transkription des Insulingens, aber auch von regulatorischen Genen, u.a. von pancreatic and duodenal homeobox 1 (PDX1), welches wesentlich für die Funktion und die Viabilität der β-Zellen ist [52]. Die Aktivität des Insulinpromotors und der Glukokinase wird reduziert [53], die Insulinbiosynthese und schließlich die Insulinsekretion nehmen ab [54]. Überlastet die Insulinbiosynthese unter Bedingungen ausgeprägter Hyperglykämie die Proteinfaltungskapazität des endoplasmatischen Retikulums (ER), führt dies des Weiteren zu ER-Stress und somit zur Dysfunktion und zum Untergang der β-Zelle [55]. Darüber hinaus ist davon auszugehen, dass Hyperglykämie die Produktion inflammatorischer Zytokine in den Inseln auslöst [56].

1.1.5.2 Diabetesassoziierte Fettstoffwechselstörung und mitochondriale Dysfunktion

Der Begriff der sogenannten „Lipotoxizität“ wurde 1994 von Lee et al. geprägt und beschreibt die negativen Effekte freier Fettsäuren auf die β-Zellfunktion und die Insulinsensitivität im T2DM [57]. Die komplexen, schädlichen Auswirkungen von Fetten auf den Metabolismus werden u.a. über oxidativen Disstress [58], ER-Stress [59], die Induktion von Insulinresistenz [60] und eines Inflammationsgeschehens [61] sowie β-Zellapoptose [62] vermittelt. Sowohl FFS als auch intrazelluläre Ablagerungen von Neutralfetten, sogenannte „lipid droplets“ bzw. Lipidtropfen, in anderen Zellen als den Adipozyten, sind hierfür relevant. Metabolische Effekte werden durch ektope Ablagerungen im Pankreas, aber auch in Leber, Niere, Herz und Skelettmuskel hervorgerufen (für einen Überblick siehe [63, 64]). Aus dieser Definition und den involvierten Mechanismen geht hervor, dass der Begriff der Lipotoxizität sehr undifferenziert und stark vereinfachend ist. Er umfasst hochkomplexe pathophysiologische Abläufe, die einer detailliertern Betrachtung bedürfen. Als besonders kritisch ist unserer Ansicht nach zu sehen, dass die Effekte von Fettsäuren stark von ihren biologischen Parametern und den experimentellen Bedingungen abhängig sind. Darüber hinaus gibt es keine eindeutig definierte, feste „Schwelle“ für das Eintreten lipotoxischer Effekte, und diese sind in der Literatur nur selten quantifiziert worden - im Gegensatz beispielsweise zum eindeutig nachgewiesenen Zusammenhang zwischen der Höhe des low density lipoprotein (LDL)-Cholesterins und der Entstehung von Atherosklerose. Wir

halten den Begriff der Lipotoxizität daher für stark vereinfacht und schlagen eine differenziertere Betrachtung der darunter subsumierten Vorgänge, wie im Rahmen der vorliegenden Arbeit thematisiert, vor.

In Kürze dargestellt, ist die zelluläre Verstoffwechslung der FFS, von der Aufnahme in die β-Zelle bis hin zur Speicherung, in Phasen der Lipotoxizität beeinträchtigt. Okamura et al. konnten zeigen, dass langkettige FFS über den FFS-Transporter cluster of differentiation (CD) 36 ein Inflammationsgeschehen und zudem oxidativen Disstress auslösen [61]. Eine gestörte Verstoffwechselung der FFS über die β-Oxidation führt zur Akkumulation von Zwischenprodukten, u.a. Diacylglycerol (DAG) und Ceramiden. Diese fördern über u.a. Proteinkinasen im Skelettmuskel Insulinresistenz [65, 66] und in der β-Zelle PDX1-abhängig die Insulinexpression [67,68]. Ceramide induzieren zudem über die induzierbare Stickstoffmonoxid-Synthase [69] und die Nicotinamidadenindinukleotidphosphat (NADPH)-Oxidase 2 [70] die Entstehung von Stick- und Superoxiden, hochreaktiven Sauerstoffspezies, welche zu oxidativem Disstress beitragen. Zwei weitere wesentliche Aspekte sind diesbezüglich insbesondere die Entstehung von ROS über die Atmungskette durch den Substratüberschuss [71] und der Abbau von langkettigen FFS in den Peroxisomen, was zur Entstehung von H_2O_2 führt [58]. DAG wiederum kumuliert nach einer FFS-Belastung im ER, wie Akoumi et al. feststellten, und könnte somit ein wesentlicher Treiber des lipotoxisch bedingten ER-Stresses sein [72]. Das vermehrte Anfallen von FFS in der Zelle beeinträchtigt zudem die Wiederauffüllung der Kalziumspeicher und verhindert damit die glukosedinduzierte Insulinsekretion (glucose-stimulated insulin secretion bzw. GSIS) [73]. Der gesamte Energiestoffwechsel der Zelle leidet unter einer eingeschränkten Anaplerose durch die gestörte Funktion von Enzymen des Zitratzyklus [68] sowie einer beeinträchtigen Funktionalität der Pyruvatdecarboxylase und damit der Glukoseutilisation [74].

Eine weitere Konsequenz der diabetesassoziierten Fettstöffwechselstörung ist die mitochondriale Dysfunktion. Ihr wird eine wesentliche Rolle für den Verlust endokrin aktiver β-Zellmasse durch Apoptose und Dedifferenzierung zugeschrieben. Insbesondere mitochondriale ROS spielen eine kritische Rolle, indem sie die Adenosintriphosphat (ATP)-Produktion und die GSIS stören und schließlich die Viabilität und Funktionalität der β-Zelle beeinträchtigen [75]. Im Diabetes vermindert sich die Anzahl der Mitochondrien und sowohl ihre Morphologie als auch

ihre Bioenergetik verändert sich [76] als Korrelat der mitochondrialen Funktionseinschränkung. Die Auswirkungen der Lipotoxizität auf die Zelle sind folglich komplex und basieren auf zahlreichen verschiedenen Signal- und Stoffwechselwegen. Somit ist die Lipotoxizität unserer Ansicht nach nicht als toxischer Effekt von freien Fettsäuren oder Lipidakkumulationen im Gewebe anzusehen, sondern als eine komplexe Stoffwechselstörung des gesamten Energiemetabolismus mit vielen unterschiedlichen Facetten, die für sich genommen betrachtet werden müssen. In diesem Kontext ist darauf hinzuweisen, dass zahlreiche Publikationen auch förderliche Effekte von FFS auf die Funktion von Leber- und β-Zellen zeigen konnten, und diese über die gleichen Signalwege wie die abträglichen vermittelt werden (für eine Übersicht siehe [77]). Auch rund 30 Jahre nach der Prägung des Begriffs der Lipotoxizität durch Lee et al. sind die zugrundeliegenden Mechanismen folglich noch nicht vollständig verstanden.

1.1.5.3 Oxidativer Disstress

Der Begriff „oxidativer Stress“ wurde 1985 vom deutschen Mediziner und Biochemiker Helmut Sies geprägt [78]. Die ursprüngliche Vorstellung war, dass es ein physiologisches Gleichgewicht zwischen pro- und antioxidativ wirksamen Substanzen gibt. Folglich ging man davon aus, dass aus einer Imbalance durch einen Überfluss an Oxidanzien, in der Regel ROS bzw. freien Radikalen, oxidativer Stress resultiert. Weniger verbreitet ist die Bezeichnung „reduktiver Stress“ durch den Überfluss an reduzierenden Substanzen. In beiden Fällen kommt es zu irreversiblen Schädigungen zellulärer Strukturen und einer Dysfunktion der jeweiligen Gewebe. Bereits früh wurde daher die Bedeutung von Veränderungen im Redoxgleichgewicht für Erkrankungen erkannt und intensiv erforscht [79]. Durchbrüche in der klinischen Anwendung von Antioxidanzien waren jedoch nicht zu verzeichnen [80]. Im Verlauf entdeckte man, dass Redoxmodifikationen tief in grundlegende Signalwege der Zellen eingebettet sind, und die Vorstellung einer „Redoxbalance“ die komplexe Realität nicht angemessen beschreibt. Diese sogenannten „redox-regulierten Signalwege“ („redox signaling“) sind nach heutigem Kenntnisstand kompartimentalisiert ablaufende, ultraschnelle, hochspezifische und reversible translationale Modifikationen an Cysteinresten. Diese Veränderungen an sogenannten „Thiolschaltern“ („thiol switches“) werden durch ROS, in diesem Kontext als redoxaktive sekundäre Botenstoffe („second messengers“) bezeichnet, vermittelt [81]. Somit entsteht ein deutlich komplexeres

Bild der physiologischen aber auch pathophysiologischen Rolle der ROS. Diese Redoxsignalwege sind letztlich für jegweden Krankheitszustand relevant, so auch den Diabetes mellitus. Die β-Zelle unterliegt von ihrer physiologischen Reifung bis zum pathologischen Untergang Redoxregulationen [82]. Sie ist metabolisch hochaktiv und damit in hohem Maße auf die reibungslose oxidative Phosphorylierung angewiesen. Zugleich weist sie im Vergleich zu anderen Zelltypen eine geringere antioxidative Kapazität auf. So werden z.B. diverse Schlüsselenzyme, darunter die Superoxiddismutase, Katalase und Glutathionperoxidase (Gpx), in den Langerhans'schen Inseln von Mäusen deutlich geringer als in anderen Geweben oder überhaupt nicht exprimiert [83], was zu einer hohen Anfälligkeit der sensiblen Insulinsekretionskaskade gegenüber Veränderungen im Redoxstoffwechsel führt. Durch diese Verknüpfung der Atmungskette mit dem Anfallen von H_2O_2 als redoxaktiver sekundärer Botenstoff entsteht ein wesentlicher Einfluss auf den Insulinsignalweg und damit die endokrine Funktion der β-Zelle [84–86]. Tatsächlich wurde in Inselzellen von Menschen mit T2DM eine veränderte Expression von für redox-regulierte Signalwege wesentlichen Genen gefunden [87]. Auch Veränderungen in anderen Geweben haben Relevanz für die Entwicklung eines Diabetes. So führt die Überexpression der Gpx1 in Mäusen zur Entwicklung einer Insulinresistenz und Adipositas [88]. In Nierenzellen von Ratten, in welchen mittels dem inselspezifischen Alkylanz Streptozotocin (STZ) ein T1DM induziert wurde, fand sich eine verminderte Menge des gesamten Glutathions (GSH) sowie ein vermindertes GSH/GSSG- und NADPH/NADP-Verhältnis als Zeichen eines deutlich veränderten Redoxzustands [89].

Diese komplexen Vorgänge sind nach wie vor Gegenstand intensiver Forschung. Aufgrund der skizzierten Erkenntnisse der letzten 35 Jahre wird von Sies und anderen Autoren eine moderne Sicht auf oxidativen Stress vorgeschlagen [90]. Wie in einem aktuellen Review von Loreto Palacio et al. dargestellt, wurde für den physiologischen Redoxzustand der Begriff „Redoxeustress" eingeführt. Durch einen Überschuss oder einen Verbrauch an ROS kann es dann zu oxidativem oder reduktivem Disstress kommen. In beiden pathologischen Zuständen ist die Redoxregulation gestört, und zelluläre Strukturen werden irreversibel geschädigt anstatt reversibel modifiziert zu werden [91].

Aus Sicht der translationalen Forschung wäre eine Möglichkeit der Quantifizierung von Re-

doxdisstress wünschenswert. Eine anerkannte Definition existiert jedoch bisher nicht. Sies diskutiert die Problematik in mehreren Reviews und beschreibt den oxidativen Eustress als eine physiologische Spanne, welche sowohl kurz- als auch langfristig einer kontinuierlichen Kontrolle durch räumlich und zeitlich eng abgestimmte Prozesse unterliegt, und darüber hinaus auch durch externe Einflüsse wie der Ernährung und Lebensstilfaktoren beeinflusst wird [92]. Er weist darauf hin, das für verschiedene Organsysteme und Erkrankungen möglicherweise unterschiedliche Biomarker für eine Quantifizierung infrage kommen [93]. Solche sind bisher klinisch nicht etabliert und unterliegen intra- und interindividuellen Schwankungen. Möglichkeiten der Quantifizierung werden zudem von Lushchak in einem eingehenden Übersichtsartikel diskutiert [94]. Denkbar sind z.B. die Quantifizierung anhand oxidativ modifizierter Zellbestandteile, der Aktivität von antioxidativ wirkenden Enzymen oder ROS-sensitiver Parameter sowie solchen der biologischen Zellfunktion. Letztere wären für die klinische Forschung besonders wertvoll.

1.2 Proteine der Thioredoxinfamilie

Die Proteinfamilie der Thioredoxine (Trx) stellt eine hochkonservierte und im Säuger ubiquitär vorkommende Proteinfamilie dar. Diese Proteine spielen eine wesentliche Rolle für den zellulären Redoxstoffwechsel und sind darüber in zahlreiche Stoffwechselwege involviert. Ihre Bedeutung für insbesondere chronische und/oder inflammatorische Erkrankungen ist in den letzten Jahren zunehmend in den Fokus von Forschungsbemühungen gerückt. Hanschmann et al. geben in einem ausführlichen Review einen Überblick über die Proteinfamilie, zu welcher die Thioredoxine, die Glutaredoxine (Glrx) und die Peroxiredoxine (Prx) gehören, und betonen ihr translationales Potential [95].

1.2.1 Thioredoxine

Trx wurde 1964 als essentieller Elektronendonor für die Ribonukleotidreduktase und, gemeinsam mit seiner Reduktase (TrxR), als elementarer Faktor für jedes Lebewesen [96] entdeckt. Das Säugetiergenom kodiert zwei Thioredoxin-Systeme: Das zytosolische (Trx1, TrxR1) sowie das mitochondriale (Trx2, TrxR2). Trx1 wird zudem sezerniert [97, 98]. Durch ihre breite Substratspezifität haben die Thioredoxine eine Vielzahl an Funktionen in der Regulation der

DNA-Synthese [96], Genexpression [99], Proliferation sowie Apoptose [100] und Immunmodulation [98, 101]. Antidiabetogene Effekte sind in der Literatur gut dokumentiert. Prinzipiell sind verminderte Gehalte von Trx1 mit einer erhöhten Diabetessuszeptibilität assoziiert. Es ist bekannt, dass Trx1 Einfluss auf die Insulinsekretion nimmt [102] und eine Überexpression in Modellen des T1DM und T2DM das Überleben der β-Zelle verbessert [103, 104]. Bestimmte Polymorphismen des *TRX1*-Gens hingegen korrelierten mit der Entwicklung eines Diabetes [105]. Der endogene Inhibitor von Trx1, Txnip, ist in Tiermodellen und humanen Patienten deutlich hochreguliert [106, 107]. Eine besondere Rolle scheint auch die Sekretion von Trx1 zu spielen. In Probanden mit einer gestörten Glukosetoleranz bzw. einem manifesten Diabetes waren deutlich erhöhte Plasmakonzentration des Proteins zu messen [108]. Diese korrelierten im manifesten T2DM interessanterweise mit dem Plasmaspiegel freier Fettsäuren [109]. Bemerkenswerterweise verhinderte die intravenöse Gabe von Trx1 im Mausmodell die Entwicklung eines Typ 1 Diabetes über eine Immunmodulation [110]. Diesbezüglich ist beschrieben, dass Trx1 die Proliferation von Immunzellen anregt [111], die Sekretion von sowohl pro- als auch anti-inflammatorischen Zytokinen vermittelt und die Chemotaxis von peripheren mononukleären Blutzellen (PBMC) beeinflusst [98, 112].

1.2.2 Glutaredoxine

Das Glutaredoxinsystem wurde in den 1970er Jahren als Wasserstofftransportsystem, bestehend aus NAPDH, GSH, der Glutathionreduktase (GR) und Glrx, beschrieben. Man erkannte, dass es in E. coli Ribonukleotide reduzierte und somit die DNA-Synthese sicherstellte [113, 114]. NAPDH dient als Elektronendonor für Glutathion, von welchem Elektronen über die GR und Glrx zum entsprechenden Ziel transferiert werden [115]. In den Genomen von Säugetieren sind vier Glutaredoxine kodiert, welche gemäß der Anzahl der redoxaktiven Cysteinreste in ihrem aktiven Zentrum als Dithiole (Glrx1 und 2) und Monothiole (Glrx3 und 5) klassifiziert werden können.

Glrx1 und 2 sind Hauptakteure der zytosolischen und mitochondrialen Redoxregulation und spielen somit eine zentrale Rolle bei der Aufrechterhaltung der Redoxbalance. Glrx3 und 5 hingegen sind insbesondere für die Biosynthese der mitochondrialen Eisen-Schwefel (FeS)-Kofaktoren und damit für die Reifung von FeS-Proteinen von Bedeutung [116, 117]. Einen

Überblick über die Historie, Eigenschaften und Funktionen der Glrx als komplex in zelluläre Prozesse eingebundene Faktoren gibt ein aktueller Übersichtsartikel von Ogata et al. [118].
Es existieren nur wenige Untersuchungen über die Glrx in der β-Zelle. Vor allem translationale Daten sind rar (71 Ergebnisse auf PubMed für „(glutaredoxin* OR grx OR glrx) AND (diabetes OR „beta-cell“)“, Stand 08/2023). Es ist bekannt, dass die Glrx sowohl in β-Zellmodellen als auch in primären Inseln deutlich exprimiert werden, insbesondere Glrx1, 2 und 5 [119]. Die aktuell verfügbare Literatur über die Glrx und den Diabetes mellitus bezieht sich größtenteils auf Glrx1 und 2. Im Rahmen dieser Arbeit wurden vornehmlich Glrx1 und 5 untersucht.

1.2.2.1 Glutaredoxin 1

Das Dithiol Glrx1 wurde im Zytoplasma, Zellkern, extrazellulär [120] und den Mitochondrien [121] nachgewiesen. Durch seine Rolle im Thiol-Disulfid-Austausch [122] steuert es über verschiedene Signalwege und Transkriptionsfaktoren, u.a. Nuclear factor kappa B (NFκB) [123, 124], Akt [125], Forkhead-Box-Protein O (FOXO) [126] und cAMP response element-binding protein (CREB) [123], die Zelldifferenzierung [127] und Apoptose [125, 128]. Glrx1-knockout-Mäuse sind lebensfähig, aber embryonale Fibroblasten waren anfälliger gegenüber den schädlichen Effekten von Diquat und Paraquat, aber nicht H_2O_2 [129]. Glrx1 wirkt, u.a. über den zellulären Kupferstoffwechsel [130], neuroprotektiv [131]. Darüber hinaus wurden protektive Effekte gegen H_2O_2-induzierte Apoptose in Endothelzellen [132, 133], gegen ischämie- bzw. reperfusionsinduzierten Schaden im Myokard [126] sowie gegen eine glukoseinduzierte Kardiotoxizität [134] beschrieben.
In murinen β-Zellen (mouse insulinoma 6 [MIN6]) führte die exogene Zugabe oder die endogene Überexpression von Glrx1 zur Verstärkung der NADPH-vermittelten Insulinsekretion, wohingegen diese durch die Geninaktivierung von Glrx1 in Ratteninseln und Ratten-β-Zellen (INS-1) inhibiert wurde [102, 135]. Shao et al. zeigten, dass Glrx1$^{-/-}$-Mäuse eine Glukoseintoleranz und Insulinresistenz ausbilden [136]. Es finden sich Hinweise darauf, dass Glrx1 in der β-Zelle über die Deglutathionylierung grundlegende Proteine beeinflusst, u.a. Fas, Caspase-3, Proteinkinase C (PKC)-α, inhibitor of nuclear factor kappa-B kinase subunit beta (IKKβ), NF-κB, Adenosine monophosphate-activated protein kinase (AMPK), Protein-tyrosine phosphatase-1B (PTP1B) und Aldosereduktase. Die Aktivierung des PKC-Signalwegs kann bei-

spielsweise die Apoptose der β-Zelle inhibieren [137], und es wurde gezeigt, dass Glrx1 die durch Glutathionylierung deaktivierte PKC zu reaktivieren vermag [138]. Dong et al. beschreiben die Phosphorylierung der AMPK durch Glrx1 und 2, wohingegen die Geninaktivierung beider Glrx wieder zur Dephosphorylierung führte [139].

1.2.2.2 Glutaredoxin 5

Das mitochondriale Protein Glrx5 fungiert als zentraler Faktor bei der Umverteilung von FeS-Cluster-Vorstufen in verschiedene FeS-Proteinbiogenesewegen, u.a. über eine Interaktion mit den eisenbindenden Proteinen IscA 1/2 [140]. Damit übt es eine grundlegende Funktion für die mitochondriale Atmungskette, deren reibungslose Funktion insbesondere wegen des hohen Energiebedarfs der metabolisch hochaktiven β-Zelle essentiell ist, aus [141]. Glrx5 nimmt damit unter den Proteinen der Thioredoxinfamilie eine Sonderstellung ein, und eine Glrx5-Defizienz führt zu einer gestörten zellulären Eisenverwertung [141]. Besonders eindrücklich lassen sich die Konsequenzen an einem Patienten mit homozygotem *GLRX5* RNA-Splicing-defekt beobachten. Dieser präsentierte auf dem Boden der Fe-Verwertungsstörung u.a. eine mikrozytäre Anämie, eine Hepatosplenomegalie mit Leberzirrhose sowie einen Typ 2 bzw. 3c Diabetes mellitus [142]. Dieser Fall zeigt eindrücklich die Relevanz einer Glrx5-Defizienz und unterstreicht die Bedeutung des Proteins für die Aufrechterhaltung der Glukosehomöostase. Laborchemische und histologische Untersuchungen deckten eine ausgeprägte Eisenüberladung bei gleichzeitig vorliegender Eisenverwertungsstörung als ursächliche Pathologie auf. Unter Eisenchelatortherapie zeigte sich klinisch wie laborchemisch eine deutliche Verbesserung der entsprechenden Parameter [142]. In einem zweiten Fall zeigten sich die gleichen Pathologien [143]. Ähnliche Ergebnisse erbrachte die Behandlung diabetischer Nager mit einem Eisenchelator bzw. diätetischer Eisenrestriktion. Beide Ansätze wirken sich positiv auf die Glukosehomöostase aus [144]. Diese Befunde stehen auch im Einklang mit Untersuchungen zur experimentellen Depletion des Divalent metal transporter 1 (Dmt1) Eisentransporters in Mäusen, in welchen der konsekutiv geringere intrazelluläre Eisengehalt eine höhere β-Zellviabilität zur Folge hatte [145].

Darüber hinaus nimmt Glrx5 eine protektive Rolle gegen oxidativen Stress ein. In Glrx5-defizienten Hefezellen konnte im Vergleich zu Wildtypen eine höhere Empfindlichkeit gegenüber

intrinsischem und extrinsisch provoziertem oxidativem Stress beobachtet werden, was in einer Wachstumshemmung resultierte. Zudem fielen eine erhöhte Carbonylierung und Oxidierung des Proteoms auf [146]. Bemerkenswerterweise hatten Mutationen der einzelnen anderen Glutaredoxine (1-4) keine derartigen Konsequenzen, was die Sonderstellung von Glrx5 betont. Des Weiteren konnte auch in Säugetierzellen (Osteoblasten) eine protektive Funktion gegen oxidativen Stress und eine Verhinderung von Apoptose nachgewiesen werden [147]. Eine Überexpression von Glrx5 führte hier zu einer verminderten DNA-Fragmentierung, weniger Annexin V-positiven Zellen und einer geringen Caspase-Aktivität, wohingegen ein Verlust an Glrx5 die gegenteiligen Effekte zur Folge hatte. Interessant ist an dieser Arbeit auch, dass ein Mangel an Glrx5 eine vermehrte ROS-Produktion nach sich zog, wohingegen die Überexpression die Menge an zellulären ROS verminderte. Wingert et al. konnten zeigen, dass homozygot Glrx5-defiziente Zebrafische aufgrund einer schweren Anämie nicht lebensfähig sind [148]. Das Pankreas des Stammes ist nicht untersucht worden.

1.2.3 Peroxiredoxine

Die Prx werden je nach Isoform (1-6) in nahezu allen Kompartimenten der Zelle reichlich exprimiert und auch sezerniert [149]. Klassischerweise fungieren sie als Peroxidasen und machen rund 1% des löslichen Proteins aus [150]. Sie haben Relevanz für die Viabilität der Zelle [151], und ein Mangel führt in der Regel zu einem Überschuss an ROS [152–155]. Da die Prx in dieser Arbeit nicht untersucht wurden, sei für weitere Informationen auf entsprechende Übersichtsarbeiten verwiesen [95, 156, 157].

1.3 Neue Therapien für den Diabetes mellitus

Ein wesentliches Problem aller Diabetesformen im klinischen Alltag ist der Verlust der funktionalen β-Zellmasse, welcher durch bisherige Therapieformen nicht aufgehalten werden kann. Die Erhaltung, Substitution und Regeneration insulinproduzierender Zellen ist daher Objekt intensiver Forschung. Verschiedene Strategien der Stimulation einer endogenen Regeneration oder exogenen Supplementation wurden geprüft, haben aber bisher keinen Weg in die breite Patientenversorgung gefunden.

1.3.1 Mitochondrien als therapeutisches Ziel

Das Forschungsfeld der mitochondrialen Dysfunktion im Diabetes mellitus ist hochaktuell. Momentane Forschungsansätze zielen auf die Identifizierung von antidiabetischen Substanzen, welche direkt am mitochondrialen Stoffwechsel ansetzen, ab. Potenzielle Kandidaten sind beispielsweise Modulatoren der oxidativen Phosphorylierung (OXPHOS), AMPK-Aktivatoren und Komplex I-Inhibitoren. So konnte Imeglimin, ein OXPHOS-Modulator, über eine Verlagerung des Substratflusses von Komplex I zu Komplex II der Atmungskette in menschlichen Probanden die Nüchternblutglukose und den HbA1c absenken [158, 159]. Die Mitochondrien sind auch im Hinblick auf mögliche regenerative Faktoren in den Fokus aktueller Forschungsbemühungen gerückt, beispielsweise über die Manipulation der FOXO3-vermittelten Stressantwort [160].

1.3.2 Pankreas- und Inselzelltransplantation

Die Gesamtpankreastransplantation und die Inseltransplantation sind seit über 100 Jahren Gegenstand intensiver Forschung. Die Transplantation eines gesamten Pankreas wird stark durch die Anzahl der zur Verfügung stehenden Spenderorgane limitiert und kommt vornehmlich als Pankreas/Niere-Kotransplantation zum Einsatz. Fridell et al. und Aref et al. geben in ihren Übersichtsarbeiten einen Überblick über den aktuellen Kenntnisstand [161, 162]. Für eine Inseltransplantation werden Inseln aus Pankreata isoliert, aufgereinigt und kultiviert. Die Transplantation wird überlicherweise durch die Injektion in die Pfortader durchgeführt. Diese perkutane Methode ist deutlich schonender als die Transplantation des Gesamtpankreas [163]. Die Anzahl der Transplantatempfänger, welche nach fünf Jahren kein exogenes Insulin benötigen, lag zuletzt teilweise bei über 50% und ist damit vergleichbar mit der Pankreastransplantation [164]. Ein besonders interessantes Konzept ist die Inselautotransplantation, beispielsweise vor einer geplanten Pankreatektomie, da im Anschluss keine Immunsuppression erfolgen muss. Eine Übersicht über die Thematik geben Shapiro et al. [165]. Trotz der Fortschritte und bemerkenswerten Ergebnisse der Inseltransplantation besteht auch hier das Problem der geringen Verfügbarkeit von Spenderorganen. Aktuelle Forschungsbemühungen untersuchen daher insbesondere die Möglichkeit der Transplantation von aus Stammzellen gewonnenen β-Zellen

[166–168]. Darüber hinaus stellen die sogenannte instant blood-mediated inflammatory response (IBMIR), eine durch das angeborene Immunsystem vermittelte sofortige Immunreaktion, welche durch eine Aktivierung der Gerinnung und des Komplementsystems, eine Leukozyteninfiltration und Thrombozytenaggregation gekennzeichnet ist, und die Transplantathypoxie aufgrund fehlender Vaskularisierung eine wesentliche Hürde dar und sind entscheidende Ursachen für ein frühes Transplantatversagen innerhalb der ersten 24 h. Folglich werden immunprotektive und die Perfusion fördernde Ansätze zur Optimierung der Transplantationsergebnisse verfolgt [166, 169–171].

1.3.3 β-Zell(re)generation

Eine weitere therapeutische Option besteht in der Regeneration vorhandener β-Zellen bzw. der Erzeugung von β-Zellen aus endogenen Vorläuferzellen oder exogenen Stammzellen. Dieses spannende Themenfeld wird eingehend in diversen Übersichtsarbeiten diskutiert [172–174]. Trotz enormer Fortschritte auf diesem Feld gibt es nach wie vor ungelöste Probleme, wie z.B. das Potential zur malignen Entartung und Immunreaktionen des Wirts. In mehreren Versuchen wurde von uns die Möglichkeit der Induktion einer Differenzierung von mesenchymalen Stammzellen und duktalen Pankreaszellen durch small molecules untersucht [175–177]. Zwar gelang es, (Trans)Differenzierungsprozesse einzuleiten, jedoch sind die zugrundeliegenden, hochkomplexen regulatorischen Prozesse noch weitesgehend unverstanden und noch nicht für eine Anwendung am Menschen geeignet. Ein entscheidender Faktor für die bisher gescheiterte Translation dürfte die deutlich geringere Plastizität humaner Inseln im Vergleich zu jenen von Nagern sein [178, 179].

1.3.4 Proteine der Thioredoxinfamilie als potenzielle therapeutische Ziele im Diabetes mellitus

Die vorhandene wissenschaftliche Literatur gibt Hinweise darauf, dass die Proteine der Thioredoxinfamilie endogen für die Erhaltung der Viabilität und endokrinen Funktion sowie die Regeneration der β-Zellen von Bedeutung sind. Darüber hinaus besteht Potential zur exogenen Nutzung als Therapeutikum. Diese Annahme fußt auf der Funktion der Proteine für die redoxregulierten Signalwege [82], die Förderung der β-Zellproliferation über verschiedene Media-

toren, u.a. PI3K/AKT [180], den mitochondrialen- und den Eisenstoffwechsel [142] sowie die Immunmodulation [98, 101]. Insbesondere die β-zellspezifischen Effekte und deren zugrundeliegenden Mechanismen sind jedoch bei Weitem noch nicht vollständig bekannt und verstanden. Im Rahmen der vorliegenden Arbeit wurden die Glutaredoxine und die Thioredoxine im Kontext diabetischer Stoffwechselpathologien im Hinblick auf ihre Bedeutung für die β-Zelle anhand von murinen, porcinen und humanen Modellen untersucht. Insbesondere stand Glrx5 als mitochondriales Glutaredoxin im Kontext der mitochondrialen Dysfunktion sowie die Bedeutung der Lipotoxizität für seine Regulation und Trx1 im Kontext der Hypoxie und Reoxygenierung im Rahmen der Inseltransplantation im Fokus.

2. Ergebnisse

2.1 Das Glutaredoxinsystem als potenzielles therapeutisches Ziel im Kontext der Lipotoxizität

Römer A, Linn T, **Petry SF**. Lipotoxic Impairment of Mitochondrial Function in β-Cells: A Review. Antioxidants (Basel)., 10(2):293, Feb 2021. doi:10.3390/antiox10020293.

Römer A, Rawat D, Linn T, **Petry SF**. Preparation of fatty acid solutions exerts significant impact on experimental outcomes in cell culture models of lipotoxicity. Biol MethodsProtoc., 7(1):bpab023, 2022. doi:10.1093/biomethods/bpab023.

2.1.1 Bedeutung der experimentellen Bedingungen für Untersuchungen zum Einfluss freier Fettsäuren

Die wissenschaftliche Literatur zur Lipotoxizität selbst sowie zu den zugrundeliegenden experimentellen Bedingungen ist äußerst heterogen. Die verfügbaren Daten zu den Effekten freier Fettsäuren sowie die methodischen Hintergründe und die Relevanz der Mitochondrien wurde von uns ausführlich in einer Übersichtsarbeit zusammengetragen [77]. Diese inkludiert 130 Arbeiten zur Thematik (Abbildung 2.1).

Demnach wird die Konzentration freier Fettsäuren im Blut von Menschen mit Diabetes mit 3,5 bis 15 mM angegeben, wovon die Palmitin- und die Ölsäure den größten Anteil ausmachen [181]. Nager weisen Serumkonzentrationen von 0,8 bis 1,5 mM auf [182]. Im Diabetes mellitus kommt es zu einem teils deutlichen, bis zu dreifachen Anstieg der FFS im Vergleich zu gesunden Kontrollen [183]. Die meisten in die Übersichtsarbeit eingeflossenen Studien hatten in diesem Kontext als relativ niedrig erscheinende Konzentrationen von 0,5 mM angewendet (Tabelle 2.1). Die Mehrzahl der Protokolle führte zu einer Verminderung des ATP-Gehalts der β-Zellen und der Insulinsekretion in verschiedenen, größtenteils Nager-β-Zelllinien (INS-1

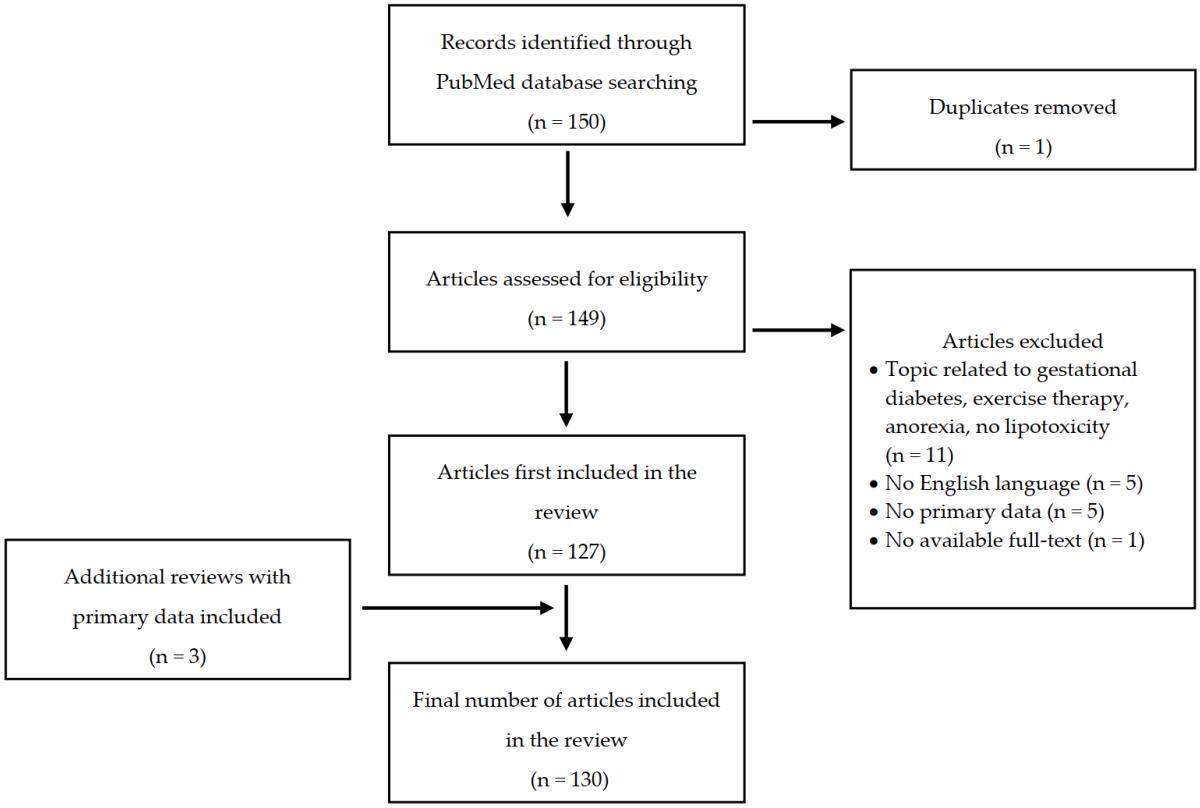

Abbildung 2.1: **Graphische Zusammenfassung der Literaturrecherche der Übersichtsarbeit.**

oder MIN6), nur selten humanen Zellreihen (n = 12 Publikationen), wobei die Resultate aufgrund großer methodischer Unterschiede in der Zubereitung der Fettsäurelösungen nur sehr eingeschränkt vergleichbar sind. Hauptsächlich war Palmitinsäure alleinig oder in Kombination mit Ölsäure verwendet worden (Tabelle 2.1). Als Lösungsmittel kam vor allem Ethanol, seltener Natriumhydroxid (NaOH) / Kochsalzlösung (NaCl) oder Dimethylsulfoxid (DMSO) zur Anwendung. Bemerkenswert ist, dass in den meisten Publikationen nicht angegeben wird, welches Lösungsmittel zur Anwendung kam (Tabelle 2.1). In vivo wurden vor allem C57BL/6-Mäuse, Wistar und Sprague Dawley Ratten unter Fütterung mit einer fettreichen Kost (high fat diet / HFD) untersucht.

Interessanterweise werden sowohl die als positiv als auch die als negativ aufgefassten Auswirkungen der FFS auf die β-Zelle über die gleichen Signalwege vermittelt. Diese umfassen u.a. die Aufnahme der FFS in die Zelle [184], ihre mitochondriale aber auch peroxisomale Verstoffwechslung inklusive dem vermehrten Anfallen von Intermediaten wie Acyl-CoA [185], Ceramiden [62] sowie DAG [72] und dadurch beeinträchtigten zellulären Funktionen [186],

Konzentration der FFS	**Anzahl der Studien**
501 - 2000 μM	18
500 μM	49
100 - 499 μM	53
10 - 99 μM	12
FFS	
Palmitinsäure	52
+ Ölsäure	20
+ sonstige	6
+ Ölsäure + sonstige	8
Ölsäure	6
sonstige	4
Lösungsmittel	
Ethanol	25
NaOH / NaCl	12
DMSO	4
Methanol	3
nicht angegeben	54

Tabelle 2.1: **Übersicht über die Häufigkeit der in der Literatur verwendeten FFS, ihrer Konzentration und der Lösungsmittel.**

eine gestörte Anaplerose [68] und Kalziumhomöstase [187], eine Beeinträchtigung der FeS-Clusterbiosynthese [141], die Induktion von Ferroptose [188], den Beitrag zu oxidativem Disstress [61] durch mitochondriale und peroxisomale ROS, ein verändertes mitochondriales Membranpotential [189] und die gesteigerte Autophagie [190], Apoptose [62] und Aktivität des Peroxisome proliferator-activated receptor (PPAR)γ [191]. Die Vielzahl der involvierten Mechanismen verdeutlicht die Komplexität der Veränderungen des Fettstoffwechsels im Diabetes mellitus. Die als schädlich bewerteten Effekte, wie z.B. eine reduzierte Insulinsekretion, werden gemäß unserer eingehenden Literaturrecherche tendenziell durch höhere Konzentrationen und langkettigere FFS sowie eine längere Behandlungsdauer verursacht. Als Beispiel für positive Effekte von FFS sei die in Anlehnung an die GSIS als „fatty acid stimulated insulin secretion“ (FASIS) bezeichnete Stimulation der Insulinsekretion durch die kurzzeitige Behandlung mit niedrigen FFS-Konzentrationen (i.d.R. $<$ 500 μM über wenige Stunden) genannt. Im Rahmen dieser Reaktion auf FFS kommt es vermittelt durch den free fatty acid receptor 1 (FFA1), auch bezeichnet als GPR40, zu einer Kalziumfreisetzung und konsekutiv zur Insulinausschüttung [192]. Auch den im Rahmen dieser Verstoffwechslung physiologischerweise in

geringem Maße anfallenden mitochondrialen ROS wird ein der Insulinsekretion förderlicher Effekt zugeschrieben. Dieser wird in Konkordanz als „redox stimulated insulin secretion“ (RSIS) bezeichnet [193].

Ein enormes Problem der Beurteilung der vorhandenen Publikationen ist neben der Heterogenität der untersuchten Modelle insbesondere jene der angewandten Methodik. Obgleich Einflüsse der verwendeten Lösungsmittel und Zellkulturzusätzen, dem molaren Verhältnis von Albumin zur Fettsäure und der Kultivierungs- bzw. Expositionszeiten auf experimentell gewonnene Ergebnisse sowie Interferenzen mit spezifischen Assays prinzipiell bekannt sind, gibt es nur sehr wenige systematische methodische Untersuchungen zur Behandlung mit FFS, insbesondere nicht anhand der β-Zelle. Daher untersuchten wir die Einflüsse von verschiedenen Parametern der Zubereitung und Anwendung von Fettsäurelösungen und ihre Effekte auf die murine MIN6-Zelle erstmals in einer Originalarbeit [194]. Zum Einsatz kamen der 3-(4,5-Dimethylthiazol-2-yl)-2,5-diphenyltetrazoliumbromid (MTT)-Assay, der Insulin-ELISA und die Luciferase-basierte Lumineszenzanalyse des ATP-Gehalts.

2.1.1.1 Einfluss der BSA-Konzentration auf den MTT-Assay

BSA ist ein essentieller Zusatz für Fettsäurelösungen. Der MTT-Assay wird häufig als Test für die Effekte experimenteller Bedingungen auf den Zellstoffwechsel verwendet. Aus diesem Grund untersuchten wir die Effekte verschiedener BSA-Konzentrationen auf die Ergebnisse des MTT-Assays in unseren MIN6-Zellen. Die 24-stündige Kultivierung von MIN6-Zellen mit Medium von unterschiedlichem BSA-Gehalt führte bis zu 6% BSA zu einer stetigen Zunahme der Umwandlung von MTT zu Formazan, gemessen anhand der optischen Dichte (OD). Diese war im Vergleich zum Medium ohne BSA ab 2% BSA signifikant erhöht und erreichte bei 6% das Maximum von +60% ($0,16 \pm 0,02$ OD bei 6% vs. $0,09 \pm 0,004$ OD bei 0%, **** $p < 0,001$). Bei 12,5% BSA zeigte sich hingegen eine verminderte Umwandlung, welche jedoch rund 25% höher war als die Kontrolle (Abbildung 2.2A). Die Kultivierung über 120 h zeigte gegensätzliche Ergebnisse, nämlich eine signifikant verminderte Assayaktivität von bis zu -50% ab 6% BSA ($1,098 \pm 0,05$ OD bei 6% vs. $1,49 \pm 0,07$ OD bei 0%, ** $p < 0,005$), wohingegen geringe Konzentrationen (1 bzw. 3% BSA) keinen relevanten Effekt hatten. Die maximale Verminderung von rund -60% wurde bei 10% BSA erreicht ($0,77 \pm 0,11$ OD bei

10% vs. $1,49 \pm 0,07$ OD bei 0%, **** $p < 0,0001$, Abbildung 2.2B).

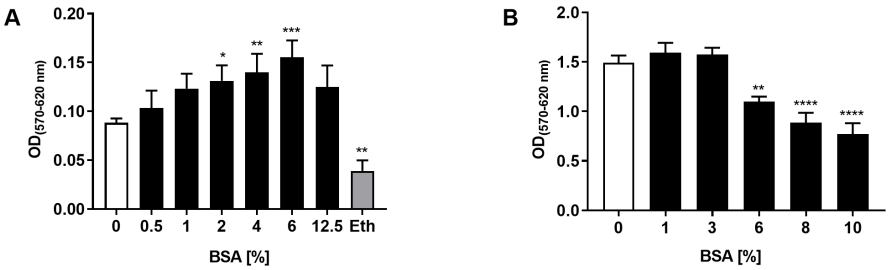

Abbildung 2.2: **Die optische Dichte des MTT-Assays unter dem Einfluss verschieder Kultivierungszeiten und BSA-Konzentrationen.** Dargestellt sind die optischen Dichtewerte des MTT-Assays nach (A) 24 h und (B) 120 h Kultivierung von MIN6-Zellen mit verschiedenen BSA-Konzentrationen sowie unbehandelten Kontrollen und einer Positivkontrolle (5% Ethanol). Mittelwerte $\pm$ SD, n = 3-4, weiß: Negativkontrolle, schwarz: Behandlung, grau: Positivkontrolle (5% Ethanol), **** $p < 0,0001$, *** $p < 0,001$, ** $p < 0,005$ und * $p < 0,05$ im Vergleich mit 0% BSA (einfaktorielle Anova).

Der direkte Einfluss des BSA auf den MTT-Assay wurde anhand der Quantifizierung der Umwandlung von MTT zu Formazan nach 24-stündiger Kultivierung von MIN6-Zellen und Medium ohne Zellen untersucht. Es wurde mit BSA-Konzentrationen von 1, 2, 4, 8 und 10% gearbeitet. Eine Steigerung der Umwandlung von MTT zu Formazan war nicht nur unter Zellkulturbedingungen (Abbildung 2.3A), sondern auch unter dem Einfluss von reinem Medium (Abbildung 2.3B) messbar. Der relative Effekt des BSA auf den MTT-Assay war signifikant, wobei die absolute Zunahme der gemessenen OD gering war ($0,03 \pm 0,016$ OD bei 10% vs. $0,007 \pm 0,002$ OD bei 1%, * $p < 0,05$).

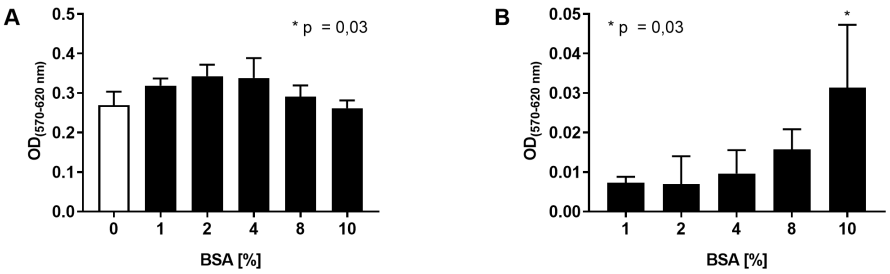

Abbildung 2.3: **Die optische Dichte des MTT-Assays mit und ohne MIN6-Zellen.** Dargestellt sind die optischen Dichtewerte des MTT-Assays nach 24 h (A) Kultivierung von MIN6-Zellen und (B) Mediums mit jeweils verschiedenen BSA-Konzentrationen sowie einer unbehandelten Kontrolle. Mittelwerte $\pm$ SD, n = 3, weiß: Negativkontrolle, schwarz: Behandlung, n = 3, * $p < 0,05$ im Vergleich mit 1% und 2% BSA. Einfaktorielle Anova, * p = 0,03.

Um den rein durch BSA- und unabhängig von den MIN6-Zellen auftretenden Effekt auf den MTT-Assay zu berücksichtigen, wurden die OD-Werte des Mediums von jenen der MIN6-Zellen subtrahiert. Somit resultierte eine rund 25%ige Verminderung der OD bei 10% BSA ($0,23 \pm 0,04$ OD bei 10% vs. $0,31 \pm 0,02$ OD bei 1%, * $p < 0,05$, Abbildung 2.4) im Gegensatz zur rund 17% ohne Normalisierung (Abbildung 2.3A).

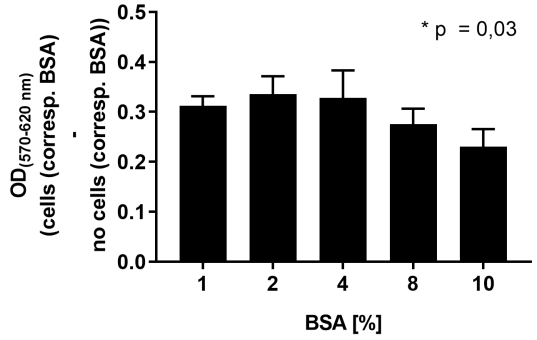

Abbildung 2.4: **Die normalisierte optische Dichte des MTT-Assays nach Behandlung mit BSA.** Dargestellt sind die optischen Dichtewerte des MTT-Assays nach 24 h Kultivierung von MIN6-Zellen nach Subtraktion jener Werte des Mediums. Mittelwerte ± SD, n = 3, einfaktorielle Anova, * p = 0,03.

2.1.1.2 Einfluss der Kultivierungsdauer und des Lösungsmittels auf den MTT-Assay

Sowohl die Kultivierungsdauer als auch das verwendete Lösungsmittel wurde im Hinblick auf die optische Dichte im MTT-Assay in unseren MIN6-Zellen untersucht. Die 24-stündige Behandlung mit 0,5, 0,75, 1,5 und 3 mM Ölsäure führte dosisabhängig zu niedrigeren OD-Werten im MTT-Assay. Nach 120 h Kultur war die OD mit und ohne Behandlung rund 50 bis 75% höher und die Verminderung durch die Ölsäurebehandlung stärker ausgeprägt.

Der Vergleich der Lösungsmittel DMSO und Ethanol erbrachte nach 24 h Kultivierung von MIN6-Zellen eine deutlich geringere OD im Sinne einer geringeren Viabilität und somit messbaren Toxizität für höhere Konzentrationen beider Substanzen, wobei ein signifikanter Einfluss durch DMSO erst bei 4% auftrat ($0,16 \pm 0,019$ OD bei 4% vs. $0,23 \pm 0,03$ OD in der Kontrolle, *** $p < 0,001$), durch Ethanol hingegen schon bei 1% ($0,195 \pm 0,015$ OD bei 1% vs. $0,23 \pm 0,03$ OD in der Kontrolle, * $p < 0,05$, Abbildung 2.5). DMSO hatte demnach bis 3%, Ethanol bis 1% keinen signifikanten Einfluss auf die Messwerte des MTT-Assays, wobei sich für die niedrigen DMSO-Konzentrationen initial ein nicht signifikanter Anstieg der OD zeigte, während sie bei Ethanol stetig abfiel.

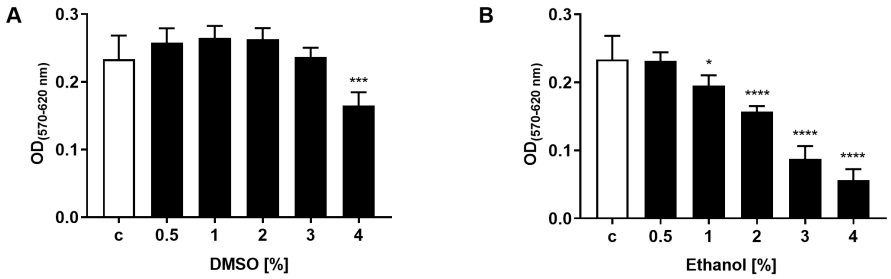

Abbildung 2.5: **Die optische Dichte des MTT-Assays nach 24-stündiger Behandlung mit dem Lösungsmittel DSMO oder Ethanol.** Dargestellt sind die optischen Dichtewerte des MTT-Assays nach 24-stündiger Behandlung mit entweder (A) DMSO oder (B) Ethanol als Lösungsmittel und einer DMEM-Kontrolle. Mittelwerte ± SD, n = 5, weiß: Negativkontrolle, schwarz: Behandlung, **** $p < 0,0001$, *** $p < 0,001$, * $p < 0,05$ im Vergleich mit der Kontrolle sowie 0,5 mM (einfaktorielle Anova).

2.1.1.3 Einfluss des Lösungsmittels auf biologische Variablen

Neben dem Einfluss auf die gemessene metabolische Aktivität via MTT-Assay ließ sich auch ein Einfluss des gewählten Lösungsmittels und dessen Konzentration auf den ATP-Gehalt und den Insulingehalt der MIN6-Zellen feststellen. Die Behandlung mit Ethanol für 24 h führte zu einer signifikanten, rund 50%igen Reduktion des zellulären ATP-Gehalts ($2,08 \pm 0,78$ µM bei 0.9% vs. $3,99 \pm 0,95$ µM in der Kontrolle, *** $p < 0,001$, Abbildung 2.6).

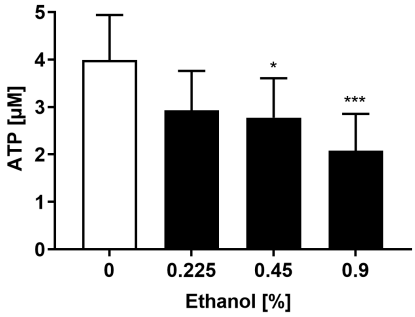

Abbildung 2.6: **Der ATP-Gehalt von MIN6-Zellen nach 24-stündiger Behandlung mit Ethanol.** Dargestellt ist der ATP-Gehalt von MIN6-Zellen nach 24 h Kultivierung mit verschiedenen Konzentrationen Ethanol. Mittelwerte ± SD, n = 8, weiß: Negativkontrolle, schwarz: Behandlung, *** $p < 0,001$, * $p < 0,05$ (einfaktorielle Anova).

Der Effekt des jeweiligen Lösungsmittels wurde nach Lösen von 1,5 mM Ölsäure untersucht. Es zeigte sich sowohl für DMSO (finale Konzentration 0,96%) als auch für Ethanol (finale Konzentration 0,45%) eine signifikante Verminderung des zellulären Insulingehalts. Diese war für Ethanol deutlich stärker ausgeprägt ($7,39 \pm 4,71$% für Ethanol vs. $60,8 \pm 4,27$% für DMSO vs.

$100 \pm 16,48\%$ in der Kontrolle, **** $p < 0,0001$ für Ethanol, ** $p < 0,005$ für DMSO, Abbildung 2.7A). Beide Lösungsmittel hatten einen ähnlich starken Effekt auf den Insulingehalt im Medium als Korrelat einer verminderten Insulinsekretion und reduzierten diesen deutlich ($12,2 \pm 1,699\%$ für Ethanol vs. $20,88 \pm 5,4\%$ für DMSO vs. $100 \pm 14,26\%$ in der Kontrolle, **** $p < 0,0001$, Abbildung 2.7B). Der Effekt war für Ethanol trotz der geringeren Konzentration deutlicher ausgeprägt als für DMSO.

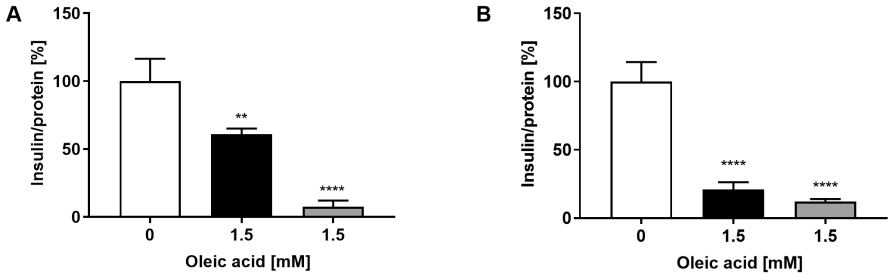

Abbildung 2.7: **Der Insulingehalt von Zelllysat und Kulturmedium nach 24-stündiger Behandlung von MIN6-Zellen Behandlung mit 1.5 mM Ölsäure, gelöst in DMSO oder Ethanol.** Dargestellt ist der Insulingehalt von (A) MIN6-Zelllysat und (B) -Zellkulturmedium nach 24 h Kultivierung mit 1.5 mM Ölsäure gelöst in DMSO 0,9% oder Ethanol 0,45%. Mittelwerte $\pm$ SD, n = 4, weiß: Negativkontrolle, schwarz: DMSO, grau: Ethanol, **** $p < 0,0001$, ** $p < 0,01$ im Vergleich mit der Kontrolle (einfaktorielle Anova).

2.1.1.4 Haupterkenntnisse

- **Die Auswirkungen freier Fettsäuren auf die β-Zelle sind in hohem Maße von den experimentellen Bedingungen abhängig. Eine Quantifizierung der Lipotoxizität sowie die Abgrenzung zwischen als physiologisch und als pathologisch anzusehenden Effekten ist eine Herausforderung und muss im Kontext des verwendeten Modells erfolgen.**

- **Die Zusammensetzung von Fettsäurelösungen kann je nach Lösungsmittel und Zellkulturzusätzen einen signifikanten Einfluss auf experimentelle Resultate haben. Sie muss daher sorgfältig kontrolliert und dokumentiert werden, um die Vergleichbarkeit und Reproduzierbarkeit zu gewährleisten.**

Petry SF, Sharifpanah F, Sauer H, et al. Differential expression of islet glutaredoxin 1and 5 with high reactive oxygen species production in a mouse model of diabesity. PLoSOne., 12(5):e0176267, May 2017. doi:10.1371/journal.pone.0176267

Petry SF, Sun LM, Knapp A, et al. Distinct Shift in Beta-Cell Glutaredoxin 5 ExpressionIs Mediated by Hypoxia and Lipotoxicity Both In Vivo and In Vitro. Front Endocrinol(Lausanne)., 9:84, May 2018. doi:10.3389/fendo.2018.00084.

2.1.2 Untersuchung von Glutaredoxin 1 und 5 in der db-Maus als transgenes murines Modell der Lipotoxizität

In zwei Studien untersuchten wir erstmals das Glutaredoxinsystem der Langerhans'schen Inseln anhand der db/db-Maus in vivo. Es handelte sich um reine Beobachtungsstudien ohne Intervention. Aufgrund der dominanten Expressionsmuster von Glrx1 und 5 im Pankreas [119] lag der Fokus auf diesen beiden Glutaredoxinen.

2.1.3 Die db-Maus als Modell des latenten Diabetes mellitus

In dieser ersten Studie wurden homozygote db/db- mit heterozygoten db/+-Tieren (BKS(D)-Leprdb/JOrlRj) verglichen. Sie wurden im Alter von 5 Wochen von Charles River in unsere Tierhalteeinrichtung überführt. Im Alter von 6, 12 und 18 Wochen wurden Daten erhoben. Die insuläre Expression von Glrx1 und 5 wurde mit Gewicht, Nüchternplasmaglukose, histologischen Untersuchungen der Langerhans'schen Inseln, u.a. der Inselfläche, der Anzahl der proliferierenden und der apoptotischen Zellen, sowie der Bildung von insulären ROS korreliert. Die Methodik umfasst die Immunhistologie, qPCR und die Fluoreszenzanalyse der 2',7'-Dichlorfluorescein-Diacetat (DCFH-DA)-Färbung mit dem konfokalen Mikroskop [195].

2.1.3.1 Phänotyp und Inselpathologien der db/db-Maus

Die homozygoten Tiere entwickelten eine ausgeprägt Adipositas mit einem signifikant höheren Gewicht (6 Wochen: 27,4 $\pm$ 0,3 vs. 18,9 $\pm$ 0,2 g; 12 Wochen: 48,1 $\pm$ 1 vs. 23,9 $\pm$ 0,3 g; 18 Wochen: 56,92 $\pm$ 1 vs. 26,29 $\pm$ 0,5 g, *** $p < 0,001$, Abbildung 2.8A) und Nüchternblutzucker (6 Wochen: 129 $\pm$ 5,5 vs. 76,7 $\pm$ 3,2 mg/dl; 12 Wochen: 180,3 $\pm$ 12,9 vs. 99,4 $\pm$ 7,1

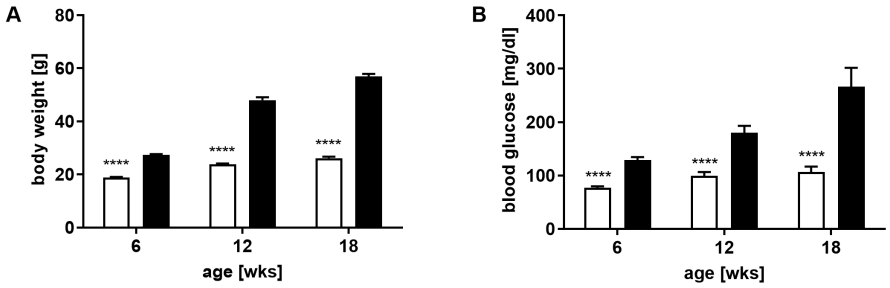

Abbildung 2.8: **Körpergewicht und Nüchternblutzucker der db/db- und db/+-Tiere.** Dargestellt sind (A) Körpergewicht und (B) Nüchternplasmaglukose der Tiere im Alter von 6, 12 und 18 Wochen. Mittelwerte ± SEM, n = 11-40 Tiere, weiß: db/+-Tiere, schwarz: db/db-Tiere, **** $p < 0,0001$ (zweifaktorielle Anova).

mg/dl; 18 Wochen: 266,5 ± 35,3 vs. 106,7 ± 0,1 mg/dl, **** $p < 0,0001$, Abbildung 2.8B) als die heterozygoten Kontrolltiere.

Die Studie war stark auf histologische Untersuchungen der Langerhans'schen Inseln fokussiert, sodass eine ausführliche Charakterisierung der Inselmorphologie und Fläche sowie der immunhistologisch angefärbten Antigene (Insulin, Ki-67, aktivierte Caspase-3, Glutaredoxine) erfolgte. Die Inseln präsentierten bei den homozygoten Tieren eine bis zum Alter von 12 Wochen eklatant zunehmende Größe. Die Inselfläche war zu diesem Zeitpunkt gemäß der Quantifizierung nach etablierter Methodik mittels der Software ImageJ [196] signifikant größer als bei den Kontrollen (0,02 ± 0,004 vs. 0,004 ± 0,0003 mm^2, *** $p < 0,001$). Die Inseln wiesen eine signifikant höhere Anzahl an Ki-67-positiven, jedoch auch Caspase-3 positiven Zellen auf [195].

2.1.3.2 Korrelation des Verlusts der Insulin- und Glutaredoxinexpression

Die Inseln der homozygoten db-Mäuse wiesen ein qualitativ deutlich weniger intensives Fluoreszenzsignal für die immunhistologische Färbung gegen Insulin auf. Das Signal als Korrelat für die Insulinexpression wurde in Anlehnung an etablierte Methoden [197, 198] quantifiziert. Die Analyse der Fluoreszenzintensität erbrachte eine signifikant geringere Intensität in den Inseln der diabetischen Tiere. Im Rahmen der Inselisolationen wurde mRNA aus diesen gewonnen und für die qPCR verwendet. Auch auf der mRNA-Ebene fand sich eine verminderte Expression der *Ins1* mRNA (db/+ vs. db/db 6 Wochen: 2,1-fach, ** $p < 0,005$; 12 Wochen: 2-fach, *** $p < 0,001$; 18 Wochen: 44,5-fach, *** $p < 0,001$, Abbildung 2.9A).

Die vier in Säugern vorkommenden Glutaredoxine 1, 2, 3 und 5 wurden als Screening in Inseln

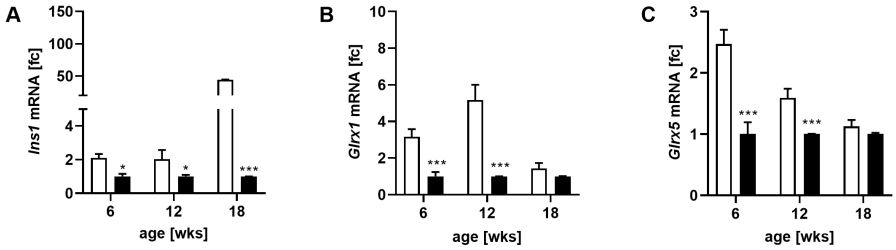

Abbildung 2.9: **PCR aus isolierten Inseln auf *Ins1*, *Glrx1* und *Glrx5*.** Dargestellt sind die qPCR-Daten für die mRNA von (A) *Ins1*, (B) *Glrx1* und (C) *Glrx5* in den isolierten Inseln der homozygoten und heterozygten db-Mäuse, für jeden Zeitpunkt dargestellt als x-fache Veränderung von db/+ gegenüber db/db. Mittelwerte $\pm$ SEM, n = 3, weiß: db/+-Tiere, schwarz: db/db-Tiere, *** $p < 0,001$, ** $p < 0,005$ (zweifaktorielle Anova).

homo- und heterozygoter Tiere im Alter von 12 Wochen untersucht und gegenübergestellt. Diese immunhistologischen Studien zeigten bereits optisch ein unterschiedliches Färbemuster. In den Inseln der diabetischen Tiere fand sich eine auffällig spärlichere Färbung als in den Kontrollen. Der Befund war am stärksten für Glrx1 und 5 ausgeprägt (Abbildung 2.10). Die Quantifizierung der jeweiligen Fluorezenzintensität erbrachte für beide Redoxine signifikant geringere Messwerte in den diabetischen Inseln. Auch die Quantifizierung anhand des Verhältnisses von Glutaredoxin- zu Insulinfärbefläche, einer weiteren in der Literatur beschriebenen Möglichkeit der Quantifizierung einer immunhistologischen Färbung, wies auf einen Verlust von Glrx1 und 5 in den diabetischen Inseln hin (Abbildung 2.11). Somit korrelierte die verminderte *Ins1* mRNA-Expression und das reduzierte Färbesignal mit der deutlich geringeren *Glrx1* und *5* mRNA-Expression (Abbildung 2.9B, C) sowie dem Verlust des Immunfluoreszenzsignals.

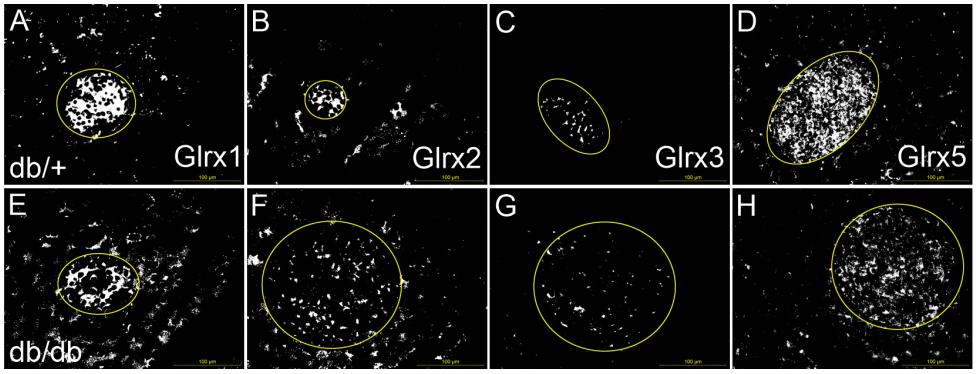

Abbildung 2.10: **Qualitativer immunhistologischer Vergleich des Glutaredoxinsystems in db/db- und db/+-Inseln.** Dargestellt sind repräsentative, Schwarzweißaufnahmen von immunhistologischen Färbungen gegen Glrx1, 2, 3 und 5 in pankreatischen Inseln. weiß: Glutaredoxin, gelbe Ellipse: Inselkontur, der gelbe Balken entspricht 100 μm.

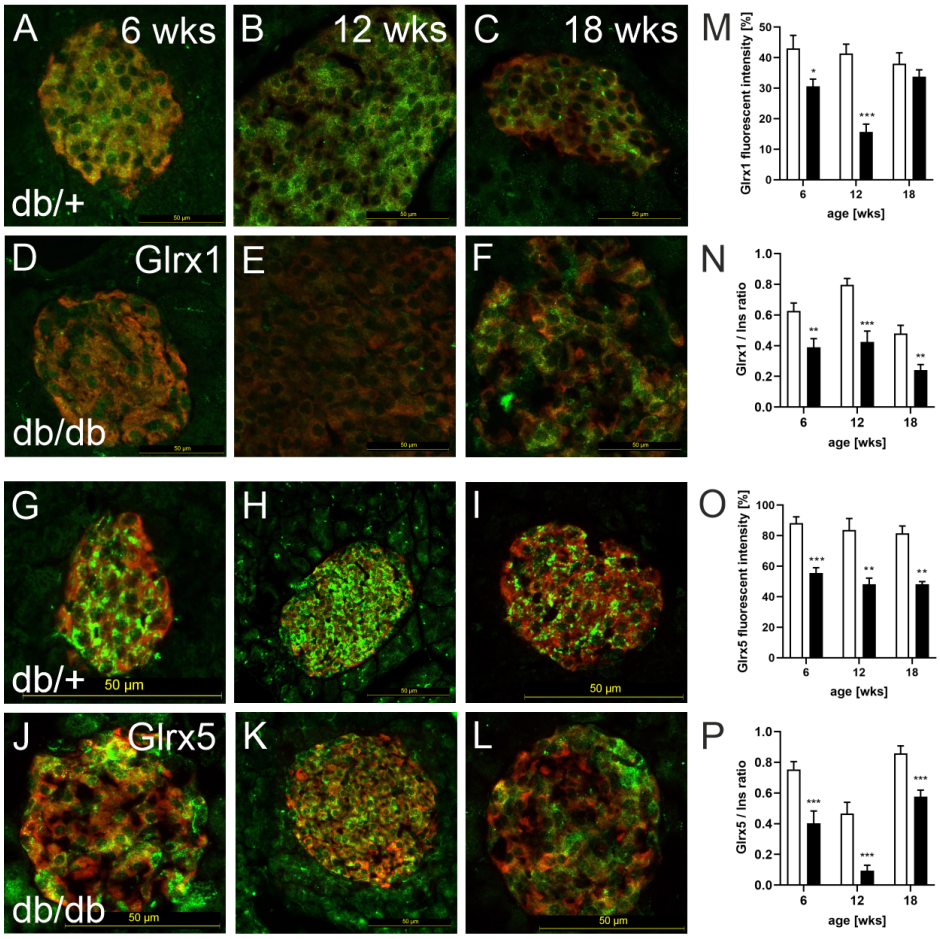

Abbildung 2.11: **Immunhistologische Färbungen von Glrx1 und 5, Quantifizierung der jeweiligen Fluoreszenz und Färbefläche.** Dargestellt sind repräsentative Aufnahmen von immunhistologischen Färbungen gegen (A-F) Glrx1 bzw. (G-L) 5 in pankreatischen Inseln der db/db bzw. db/+-Tiere. rot: Insulin, grün: Glutaredoxin mit der jeweiligen Quantifizierung der (M, O) Fluoreszenz und der (N, P) Gluataredoxin-Färbefläche, normalisiert anhand der Insulinfärbefläche. Mittelwerte ± SEM, n = 3, *** $p < 0,0001$, ** $p < 0,005$, * $p < 0,05$ (zweifaktorielle Anova).

2.1.3.3 Elevierte ROS-Produktion in den Inseln der db-Maus

Isolierte Inseln von Tieren beider Gruppen wurden ex vivo mit DCFH-DA, einem redoxaktiven Färbemittel, welches ROS, vor allem H_2O_2, nachweist, behandelt. Die Enstehung wurde mittels konfokalem Mikroskop quantifiziert, und zwar in Inseln ohne Behandlung, nach Kultivierung mit 20 mM Glukose über 2 h oder nach 15 min 1 μM TNF-α. Bereits im Ausgangszustand wiesen die db/db-Inseln eine stärkere Fluoreszenz als Korrelat von vermehrten ROS auf. Die Stimulation mit Glukose sowie TNF-α führte zu einer Steigerung der ROS-Produktion in beiden Arten von Inseln, war jedoch in den db/db-Inseln stärker ausgeprägt als in den Kontrollen (db/+ vs. db/db: Kontrolle: 75.3 ± 2,4 vs. 119,7 ± 6,4%; Glukose: 106,9 ± 3,4 vs. 186,2 ± 3,7%;

TNF-α: 117,2 $\pm$ 3,8 vs. 173,1 $\pm$ 3,6%) [195].

2.1.4 Die akut diabetische db-Maus sowie die murine β-Zelllinie MIN6

Für diese zweite Studie wurden homozygote db/db-Mäuse und Wildtypen (C57BL/6-Tiere) als Kontrollen im Alter von 10 Wochen bei Charles River erworben. Ursprünglich war das Ziel gewesen, korrelierend mit der zuvor beschriebenen Studie an den beiden Zeitpunkten 12 und 18 Wochen weitere Daten zu erheben. Unerwarteterweise wiesen die db/db-Tiere jedoch im Alter von 12 bis 14 Wochen einen entgleisten diabetischen Phänotyp mit Polyurie und -dipsie auf, sodass der Versuch frühzeitig abgebrochen wurde. Die Datenerhebung beschränkte sich somit auf diese Altersspanne. In dieser Studie stand die Inselmorphologie und Komposition im Fokus, und es wurden zum ersten Mal Untersuchungen von Glrx5 in murinen β-Zellen durchgeführt. Die Immunhistologie, qPCR, der Insulin- sowie Glrx5-ELISA und die DCFH-DA-Färbung kamen zur Anwendung [199]. Glrx5 wurde vor allem im Kontext der Inselmorphologie und Komposition untersucht, und es wurden zum ersten Mal Untersuchungen von Glrx5 in murinen β-Zellen durchgeführt [199].

Die Spontanglukosewerte der db/db-Mäuse waren im Vergleich zu den gleichaltrigen Wildtypen signifikant erhöht (471,1 $\pm$ 232,4 vs. 178,4 $\pm$ 11,9 mg/dl, *** $p < 0,0001$, Abbildung 2.12A). Ebenso waren die Tiere signifikant schwerer (51,9 $\pm$ 0,98 vs. 28,6 $\pm$ 0,9 g, *** $p < 0,0001$, Abbildung 2.12B).

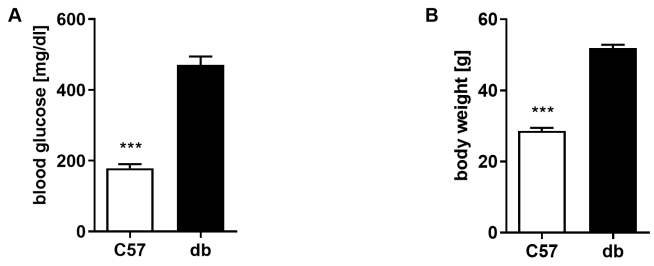

Abbildung 2.12: **Blutglukose und Körpergewicht der Tiere.** Dargestellt sind die (A) Spontanglukosewerte und das (B) Körpergewicht der C57- und db/db-Mäuse. Mittelwerte $\pm$ SEM, n = 12 - 15 Mäuse, weiß: C57BL/6, schwarz: db/db, *** $p < 0,0001$ (ungepaarter t-Test).

2.1.4.1 Gestörte Inselarchitektur und veränderte Glrx5-Expression

Die Inselfläche der akut diabetischen Tiere war in etwa so groß wie jene der zuvor untersuchten db/db-Mäuse und signifikant größer als jene der Wildtypen (0,022 $\pm$ 0,007 vs. 0,005 $\pm$

0,0001 mm^2, * $p < 0,05$). Die histologischen Analysen zeigten eine sehr hohe, nicht weiter quantifizierte Anzahl kleiner, destruiert wirkender Inseln ohne eindeutige Abgrenzung zum exokrinen Gewebe.

Die histologischen Pankreaspräparate wurden immunhistochemisch gegen Insulin, Glukagon und Glrx5 gefärbt. In den Inseln der db-Tiere war nahezu kein Fluoreszenzsignal der Insulinfärbung zu detektieren (Abbildung 2.13 und 2.14). Die Quantifizierung der Insulinfärbefläche (15,2 $\pm$ 3,4 vs. 45,1 $\pm$ 2,3% der jeweiligen Inselfläche, ** $p < 0,005$, Abbildung 2.13G) und -intensität (13,2 $\pm$ 3,5 vs. 59,7 $\pm$ 12,9%, ** $p < 0,005$, Abbildung 2.13H) erbrachte signifikant niedrigere Werte im Vergleich zu den Kontrollen. Bemerkenswerterweise zeigte sich für Glukagon ein gegensetzlicher Befund. Die db-Inseln hatten eine signifikant größere Glukagonfärbefläche als die Kontrollinseln (0,002 $\pm$ 0,0004 vs. 0,0009 $\pm$ 0,00002 mm^2, * $p < 0,05$, Abbildung 2.13I, K) mit jedoch verminderter Fluoreszenzintensität (14,52 $\pm$ 13,08 vs. 36,28 $\pm$ 10,39%, * $p < 0,05$, Abbildung 2.13J).

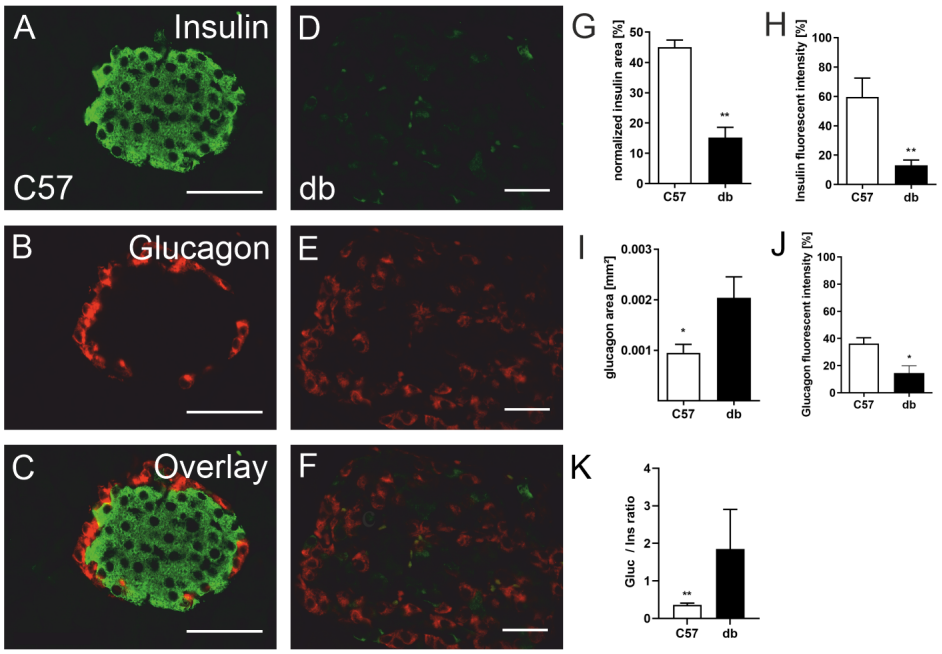

Abbildung 2.13: **Die Inselmorphologie und die Färbung gegen Insulin und Glukagon samt Quantifizierung.** (A-F) Dargestellt sind repräsentative immunhistologische Färbungen von db/db- und C57BL/6-Inseln gegen Insulin (grün) und Glukagon (rot), der weiße Balken entspricht 50 μm. (G, H, I, J) Quantifizierung der Färbefläche und der Fluoreszenzintensität des Signals der Färbung gegen (G, H) Insulin und (I, J) Glukagon. (K) Quantifizierung der Glukagonfärbefläche als Verhältnis von Glukagon zu Insulin. Mittelwerte $\pm$ SEM, n = 6 Mäuse, weiß: C57BL/6, schwarz: db/db, ** $p < 0,005$, * $p < 0,05$ (ungepaarter t-Test).

Die Muster der immunhistochemischen Färbung gegen Glrx5 zeigten deutliche Unterschiede

zwischen den akut diabetischen db-Tieren und den Wildtypen. In beiden Inseltypen zeigte sich ubiquitär ein Signal gegen Glrx5. Es erschien der Eindruck eines betont nukleären Färbemusters (Abbildung 2.14A-F und G, H). Die Glrx5-Färbung war in den db-Inseln deutlich schwächer ausgeprägt, was anhand des Verhältnisses der Färbefläche von Glrx5 zu Insulin (0,52 $\pm$ 0,05 vs. 0,19 $\pm$ 0,04, *** $p < 0,0001$) und der Fluoreszenzintensität (16,6 $\pm$ 3,4 vs. 6,7 $\pm$ 1,7%, * $p < 0,05$) quantifiziert wurde (Abbildung 2.14J, K). Der Eindruck einer nukleären Färbung herrschte in den Wildtypinseln deutlich vor, wohingegen in den db-Inseln ein eher diffus in der Insel verteiltes Färbemuster vorherrschte. Die Anzahl der Glrx5-positiven Kerne wurde quantifiziert und war in den db-Inseln signifikant geringer (49,7 $\pm$ 4,8 vs. 25,2 $\pm$ 3,1 Kerne / Insel, ** $p < 0,005$, Abbildung 2.14L). Somit konnten wir zeigen, dass die pathologische Inselmorphologie mit einer veränderten Glrx5-Expression einhergeht.

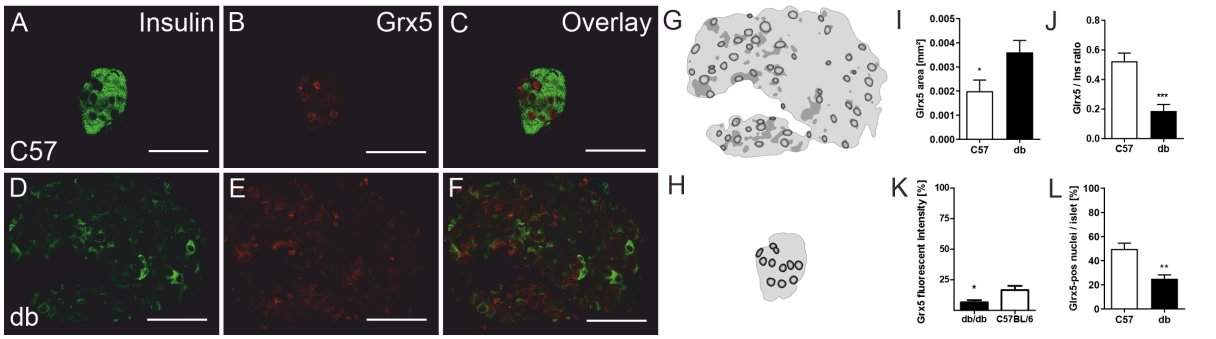

Abbildung 2.14: **Das Glrx5-Expressionsmuster und seine Quantifizierung.** (A–C, D–F) Dargestellt sind repräsentative immunhistologische Färbungen von db/db- und C57BL/6-Inseln gegen Insulin (grün) und Glrx5 (rot), der weiße Balken entspricht 50 μm. (G, H) Schematische Darstellung des Glrx5-Färbemusters von schwarz: hohe Signalintensität zu weiß: kein Signal detektiert. (I) Die Quantifizierung der Glrx5-Färbefläche, normalisiert gegen die Inselfläche, (J) der Glrx5-Färbefläche als Glrx5/Insulin-Verhältnis, (K) der Glrx5-Fluoreszenzintensität und (L) der Glrx5-positiven Nuclei. Mittelwerte $\pm$ SEM, n = 6 Mäuse, weiß: C57BL/6, schwarz: db/db, *** $p < 0,0001$, ** $p < 0,005$, * $p < 0,05$ (ungepaarter t-Test).

2.1.4.2 Einfluss von Leptin, Ölsäure und Hypoxie auf die Glrx5-Expression in MIN6-Zellen

Der Einfluss des Leptins auf die murine β-Zelle wurde anhand von MIN6-Zellen untersucht. Die Zellen wurden für 2 h oder 48 h mit rekombinantem Leptin (0, 0,075, 0,2, 0,45 oder 2 ng/ml) behandelt. Es zeigte sich in diesem Zellmodell weder ein Einfluss auf den Insulingehalt bzw. die -sekretion, noch den Gehalt an Glrx5 oder seiner mRNA-Expression [199]. In einem

zweiten Versuchsaufbau wurde der Einfluss von Ölsäure und Hypoxie auf die MIN6-Zelle, ihre Insulinsekretion und ihren Glrx5-Gehalt untersucht. MIN6-Zellen wurden für 24 h gegenüber 0, 0,5 bzw. 0,75 mM Ölsäure in normaler oder hypoxischer (2% O_2) Atmosphäre exponiert. Es zeigte sich sowohl als Reaktion auf die Ölsäure als auch die Hypoxie eine signifikante Verminderung der per ELISA gemessenen Glrx5-Proteinmenge [199].

2.1.4.3 Haupterkenntnisse

- **Im murinen Diabetes mellitus mit Adipositas zeigen die Langerhans'schen Inseln im Vergleich zu gesunden Kontrollen stark abweichende Expressionsmuster der Glutaredoxine. Die mRNA-Expression und der Proteingehalt von Glrx1 und 5 sind signifikant vermindert. Diese Befunde sind umso deutlicher, je stärker der diabetische Phänotyp ausgeprägt ist.**

- **Der Verlust der Glutaredoxine korreliert mit einer pathologisch veränderten Morphologie, zellulären Zusammensetzung und Funktion der Inseln sowie einer deutlich gesteigerten ROS-Bildung.**

- **In der murinen MIN6-β-Zelle wird Glrx5 durch Hypoxie oder Ölsäure herabreguliert. Leptin hat keinen Effekt auf Glrx5. Es ist folglich davon auszugehen ist, dass der Glutaredoxinmangel kein für die db-Maus spezifischer Befund ist.**

2.1.5 Untersuchung der Expression von Glutaredoxin 5 in einem murinen Modell der diätetisch induzierten Lipotoxizität sowie mechanistische Untersuchungen in der murinen β-Zelllinie MIN6

Petry SF, Römer A, Rawat D, Brunner L, Lerch N, Zhou M, Grewal R, Sharifpanah F, Sauer H, Eckert GP, Linn T. Loss and Recovery of Glutaredoxin 5 Is Inducible by Diet in a Murine Model of Diabesity and Mediated by Free Fatty Acids In Vitro. Antioxidants (Basel). 2022 Apr15;11(4):788. doi: 10.3390/antiox11040788.

Nachdem die beiden vorherigen Studien mit der db-Maus als monogenetisches Modell für den Diabetes mellitus gearbeitet hatten, zielte diese Studie darauf ab, den Befund eines Verlusts des insulären Glrx5 im Diabetes anhand eines Modells, welches besser mit dem humanen metabolischen Syndrom vergleichbar ist, zu untersuchen. Hierfür wurde in C57BL/6J-Mäusen diätetisch mittels einer HFD eine Adipositas und ein Überfluss an freien Fettsäuren induziert. Des Weiteren wurden in der Studie diabetische Bedingungen in der Zellkultur (MIN6) simuliert. Der Einfluss der typischen diabetischen Stressoren Hyperglykämie, freie Fettsäuren und inflammatorische Zytokine auf Glrx5 wurde untersucht. Zur Anwendung kamen die Immunhistologie und -zytologie, die DCFH-DA-Färbung, die qPCR, der MTT-Assay, die Luciferase-basierte Lumineszenzanalyse des ATP-Gehalts, die Respirometrie zur Analyse der mitochondrialen Atmung und der Insulin- sowie Glrx5-ELISA.

Männliche C57BL/6J-Mäuse wurden im Alter von fünf Wochen von Charles River gekauft und hatten zwei Wochen lang Gelegenheit, sich an die Tierhalteeinrichtung zu gewöhnen. In diesen Zeitraum wurde ihnen eine kohlenhydratreiche Kost, ähnlich der Standardnagerkost (Pellets) gefüttert (CD, 3514 kcal/kg, 10% der Energie aus Fett, 66% aus Kohlenhydraten, 24% aus Protein, Diät C 1090-10, Altromin). Anschließen wurden die Tiere in eine Experimental- (Exp) und eine Kontrollgruppe (Ctrl) aufgeteilt. Die Kontrollgruppe wurde durch den gesamten Versuch mit der CD gefüttert. Die Experimentaltiere erhielten für 13 Wochen eine Hochfettdiät (HFD, 5389 kcal/kg, 70% der Energie aus Fett, 14% aus Kohlenhydraten, 16% aus Protein, Diät C 1090-70, Altromin). Anschließend wurde die Diät für drei Wochen auf die CD umge-

stellt, schließlich für vier Wochen erneut die HFD gefüttert (Abbildung 2.15). Im Alter von 7, 20, 23 und 27 Wochen wurden Gewicht und Nüchternplasmaglukose gemessen und Blut sowie das Pankreas entnommen.

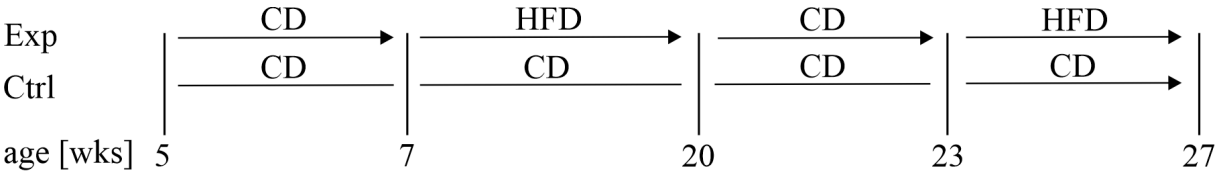

Abbildung 2.15: **Der Ablauf des Tierversuchs.** Exp = Experimentalgruppe, Ctrl = Kontrollgruppe, CD = kohlenhydratreiche Kontrolldiät, HFD = fettreiche Diät.

2.1.5.1 Ein diätinduzierter adipöser und prädiabetischer Phänotyp der Lipotoxizität

Die HFD-gefütterten Tiere hatten ab 20 Wochen ein signifikant höheres Körpergewicht als die Kontrolltiere, wobei die dreiwöchige CD-Fütterung zu einem deutlichen Gewichtsverlust führte (Exp vs. Ctrl: $37,3 \pm 1,1$ g vs. $27,9 \pm 0,3$ g, *** $p < 0,001$ mit 20 Wochen; $31,8 \pm 0,7$ g vs. $29 \pm 0,5$ g, * $p < 0,05$ mit 23 Wochen; $43 \pm 1,3$ vs. $28,8 \pm 1,4$ g, *** $p < 0,001$ 27 Wochen, Abbildung 2.16A). Die Nüchternblutglukose war lediglich im Alter von 27 Wochen signifikant unterschiedlich mit höheren Werten in der Experimentalgruppe (Exp vs. Ctrl: $102,6 \pm 5,76$ vs. $78,6 \pm 5,1$ mg/dl, ** $p < 0,005$, Abbildung 2.16B). Die freien Fettsäuren im Blut der Nager, gemessen mittels ELISA, waren nach den HFD-Fütterungen signifikant erhöht und fielen nach der CD-Fütterung deutlich ab (Exp vs. Ctrl: $2,32 \pm 0,03$ mM vs. $1,24 \pm 0,2$ mM, * $p < 0,05$ mit 20 Wochen; $1,5 \pm 0,04$ mM vs. $1 \pm 0,2$ mM, n.s. mit 23 Wochen; $2,77 \pm 0,1$ vs. $1,43 \pm 0,6$ mM, ** $p < 0,005$ mit 27 Wochen, 2.16C). Das Pankreasgewicht der Tiere war nicht signifikant unterschiedlich (2.16D). Um den dynamischen Glukosestoffwechsel zu prüfen, wurden intraperitoneale Glukosetoleranztests (IPGTT, Injektion von 1 mg Glukose / g Körpergewicht, Messung der kapillären Plasmaglukose nach 30, 60, 90 und 120 min) durchgeführt. Diese zeigten nach den HFD-Phasen jeweils eine signifikant höhere Fläche unter der Kurve bei den Experimentaltieren als bei den Kontrolltieren (Exp vs. Ctrl: 29403 ± 1512 vs. 22667 ± 1610 mg/dl x min, * $p < 0,05$ mit 20 Wochen; 32393 ± 2211 vs. 25377 ± 1732 mg/dl x min, * $p < 0,05$, Abbildung 2.16E-H).

Die Tiere bildeten somit einen adipösen Phänotyp mit nachweisbarer Einschränkung der GSIS sowie einer erhöhten Nüchternglukose i.S. eines Prädiabetes bzw. latenten Typ 2 Diabetes mel-

litus aus. Die phänotypischen Auffälligkeiten und die Stoffwechselpathologien waren jedoch deutlich weniger ausgeprägt als in den zuvor verwendeten db-Tieren.

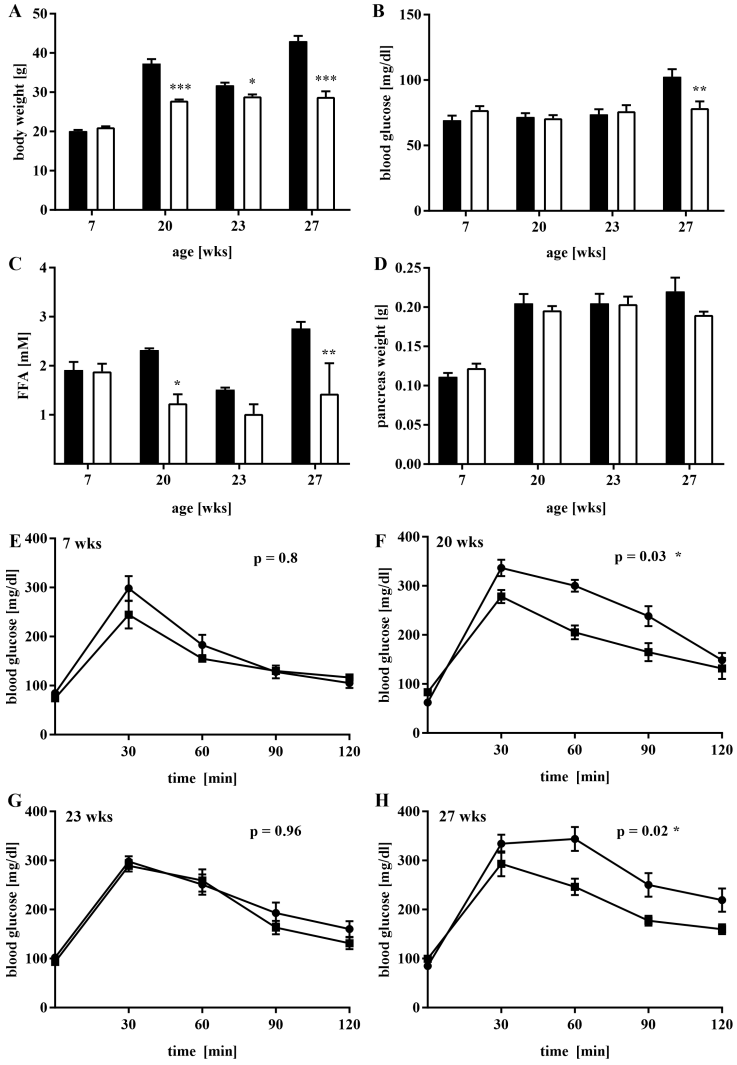

Abbildung 2.16: **Glukosewerte, Körpergewicht, freie Fettsäuren und Pankreasgewicht der Tiere.** (A) Körpergewicht und (B) Nüchternplasmaglukose, n = 5-33 Mäuse. (C) freie Fettsäuren, n = 3 Mäuse und (D) Pankreasgewicht, n = 6 Mäuse. (E-H): Glukosewerte der intraperitonealen Glukosetoleranztests, n = 5 Mäuse. Mittelwerte $\pm$ SEM, schwarz bzw Kreise: Exp-Tiere, weiß bzw. Quadrate: Ctrl-Tiere, *** $p < 0,001$, ** $p < 0,005$, * $p < 0,05$ (zweifaktorielle Anova bzw. ungepaarter t-Test).

2.1.5.2 Diätabhängige Expression des insulären Glrx5

In dem beschriebenen Phänotyp wurden nun Glrx5 und Insulin untersucht. Beide Antigene wurden in den Inseln immunhistologisch angefärbt. Die Quantifizierung fand wie in einer vorherigen Studie über das Verhältnis der Glrx5- zur Insulinfärbefläche statt und wurde mittels ImageJ quantifiziert [98]. Zudem wurde die mRNA-Expression von *Glrx5* und *Ins1* in isolierten Inseln gemessen. Bemerkenswerterweise zeigte sich eine Korrelation von sowohl dem Glrx5/Insulin-

Verhältnis und seiner mRNA-Expression als auch von Insulin mit den freien Fettsäuren im Blut und der schlechteren Glukosetoleranz gemäß IPGTT bzw. der erhöhten Nüchternglukose der Tiere. Die Quantifizierung des Verhältnisses der Glrx5- zur Insulinfläche war für die Experimentalgruppe ab dem Alter von 20 Wochen signifikant niedriger ($0,102 \pm 0,076$ vs. $0,107 \pm 0,103$, n.s. mit 7 Wochen, $0,02 \pm 0,019$ vs. $0,135 \pm 0,212$, **** $p < 0,0001$ mit 20 Wochen, $0,056 \pm 0,081$ vs. $0,147 \pm 0,104$, ** $p < 0,005$ mit 23 Wochen, $0,008 \pm 0,007$ vs. $0,048 \pm 0,058$, **** $p < 0,0001$ mi 27 Wochen, Abbildung 2.17). Die *Glrx5* mRNA-Expression war nach den HFD-Phasen mit 20 und 27 Wochen signifikant geringer (dCT $0,003246 \pm 0,03456$ vs. $0,002977 \pm 0,002821$, n.s. mit 7 Wochen, $0,00192 \pm 0,0008917$ vs. $0,005226 \pm 0,001592$, * $p < 0,05$ mit 20 Wochen, $0,004078 \pm 0,004273$ vs. $0,004983 \pm 0,0047$, n.s. mit 23 Wochen, $0,00121 \pm 0,0009342$ vs. $0,003442 \pm 0,0009659$, * $p < 0,05$ mit 27 Wochen, Abbildung 2.17). Ein ähnliches Muster war für die mRNA-Expression von *Ins1* zu erkennen, wobei diese nur zum Zeitpunkt 20 Wochen signifikant geringer war (dCT $0,0009357 \pm 0,001047$ vs. $0,001009 \pm 0,0001171$, n.s. mit 7 Wochen, $0,0004324 \pm 0,0001747$ vs. $0,001239 \pm 0,0002954$, * $p < 0,05$ mit 20 Wochen, $0,0008023 \pm 0,0003196$ vs. $0,0004618 \pm 0,0003729$, n.s. mit 23 Wochen, $0,0004204 \pm 0,0002157$ vs. $0,0005973 \pm 0,0002814$, mit 27 Wochen, Abbildung 2.17).

Isolierte Mausinseln wurden zudem auf ihre ROS-Menge sowie ihre GSIS untersucht. Die Inseln der Experimentalgruppe wiesen signifikant mehr ROS, gemessen per Fluoreszenzanalyse mit dem konfokalen Mikroskop, auf ($148,5 \pm 29,5\%$ vs. $99,8 \pm 24,5\%$, **** $p < 0,0001$ mit 20 Wochen, $131,7 \pm 24,2\%$ vs. $88 \pm 15\%$, **** $p < 0,0001$ mit 23 Wochen). Die Inseln der 27 Wochen alten Tiere wurden einer Glukosestimulation ex vivo unterzogen und wiesen im Gegensatz zu den nichtdiabetischen Kontrolltieren keine GSIS mehr auf [200].

Somit ging der diätetisch induzierbare Verlust in vivo mit dem (prä)diabetischen Phänotyp der HFD-gefütterten Tiere und den gemessenen Störungen des Glukosestoffwechsels sowie mit signifikant erhöhten Leveln von FFS und ex vivo mit einer vermehrten Produktion von ROS sowie einer gestörten GSIS einher. Die Regeneration des insulären Glrx5 korrelierte mit den gegenteiligen Effekten.

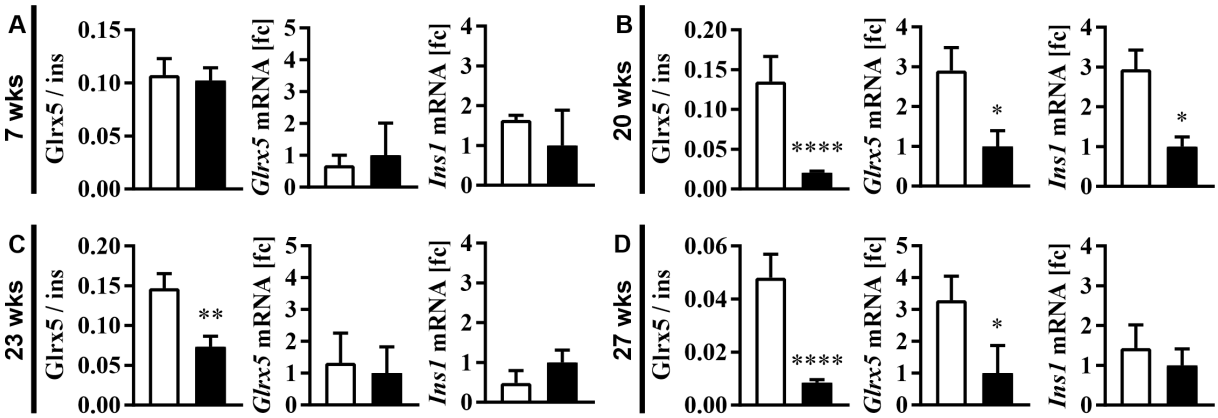

Abbildung 2.17: **Quantifizierung der Glrx5-Färbefläche, *Glrx5* und *Ins1* mRNA-Expression in den Inseln.** Dargestellt ist jeweils das Verhältnis der Glrx5- zur Insulinfärbefläche sowie die *Glrx5* und *Ins1* mRNA-Expression im Alter von (A) 7, (B) 20, (C) 23 und (D) 27 Wochen. n = 3-4 Mäuse (Histologie) bzw. 6 Mäuse (qPCR). Mittelwerte ± SEM, schwarz: Exp-Tiere, weiß: Ctrl-Tiere, **** $p < 0,0001$, ** $p < 0,005$, * $p < 0,05$ (zweifaktorielle Anova).

2.1.5.3 Regulation von Glrx5 durch FFS in vitro

Auf den ersten Zellversuchen der vorhergehenden Studie aufbauend, wurde nun der Einfluss diabetischer Stressoren auf die MIN6-Zelle untersucht, um die im Tiermodell nicht zu separierenden Effekte von Hyperglykämie, FFS und Inflammation voneinander zu trennen und in ihrer Wirkung auf die β-Zelle zu untersuchen.

Der Glrx5-Gehalt der Zellen sowie die Insulinmenge im Medium als Korrelat der Insulinsekretion wurden jeweils per ELISA untersucht. Die Präinkubation mit 400 µM Palmitinsäure, gefolgt von einer Stunde Glukosedeprivation und der konsekutiven Behandlung mit 3 bzw. 16 mM Glukose für 24 h führte zu einer signifikanten Verminderung von Glrx5, wohingehen die Zellen ohne Palmitinsäure keine relevanten Veränderungen aufwiesen ($46,3 \pm 11,8$ vs. $82,8 \pm 9,5$ pg / mg, * $p < 0,05$ bei 3 mM Glukose, Abbildung 2.18A). Erwartungsgemäß kam es bei ansteigenden Glukosekonzentrationen zu einer gesteigerten Insulinsekretion, welche allerdings nach der Präinkubation mit Palmitinsäure signifikant schwächer ausfiel ($0,14 \pm 0,03$ vs. $0,56 \pm 0,14$ µg / mg, * $p < 0,05$ bei 16 mM Glukose, Abbildung 2.18B). Die Behandlung mit jeweils Öl- und Palmitinsäure für 24 h führte zu einer dosisabhängigen Verminderung sowohl des zellulären Glrx5-Gehalts ($91,32 \pm 13,11$ vs. $43,03 \pm 10,91$ vs. $20,82 \pm 7,56$ vs. $8,76 \pm 0,85$ pg / mg, **** $p < 0,0001$, Abbildung 2.18C, Daten für Palmitinsäure nicht ge-

zeigt) als auch der Insulinmenge im Medium ($0,38 \pm 0,2$ vs. $0,08 \pm 0,01$ vs. $0,03 \pm 0,01$ vs. $0,02 \pm 0,002$ µg / mg, ** $p < 0,005$ bei 0,75 mM, *** $p < 0,001$ bei 1,5 und 3 mM, Abbildung 2.18D).

Die Behandlung mit 5, 10, 20 und 30 mM Glukose für 24 h nach zwei Stunden Glukosedeprivation hingegen zog keine signifikante Veränderung der zellulären Glrx5-Menge nach sich ($41,17 \pm 13,93$ vs. $58,63 \pm 14,24$ vs. $48,44 \pm 2,43$ vs. $58,05 \pm 19,05$ vs. $40,11 \pm 3,85$ pg / mg, n.s., Abbildung 2.18E). Die Insulinsekretion hingegen stieg plausiblerweise an ($0,074 \pm 0,002$ vs. $0,089 \pm 0,001$ vs. $0,094 \pm 0,004$ vs. $0,091 \pm 0,003$ vs. $0,093 \pm 0,005$ µg / mg, * $p < 0,05$ bei 5 mM Glukose, *** $p < 0,001$ bei 10 mM Glukose, ** $p < 0,005$ bei 20 und 30 mM Glucose, Abbildung 2.18F). Zudem wurden MIN6-Zellen gegenüber einem Zytokinmix, bestehend aus 10 ng/ml TNF-α, 5 ng/ml IL-1β und 100 ng/ml IFN-γ [98], für jeweils 24 und 48 h exponiert. Zu keine Zeitpunkt war ein signifikanter Einfluss auf Glrx5 zu finden ($385,1 \pm 190,6$ vs. $352 \pm 154,9$ pg / mg nach 24 h, $275,1 \pm 57,64$ vs. 268.4 ± 84.34 pg / mg nach 48 h, n.s., Abbildung 2.18G) Das Insulin im Kulturmedium wies einen abfallenden Trend auf ($0,16 \pm 0,07$ vs. $0,08 \pm 0,02$ µg / mg nach 24 h, $0,14 \pm 0,1$ vs. $0,11 \pm 0,05$ µg / mg nach 48 h, n.s., Abbildung 2.18H).

In einer ergänzenden immunzytologischen Untersuchung wurden Glrx5 und Insulin in MIN6-Zellen gefärbt. Mittels der Software ImageJ wurde die normalisierte integrierte Dichte als Korrelat der Färbeintensität und damit zur Quantifizierung des jeweiligen Antigens ermittelt. Sowohl unter der Behandlung mit 1,5 mM Ölsäure als auch in der Kontrolle korrelierte der Glrx5- mit dem Insulingehalt (r = 0,78; **** $p < 0,0001$ für 0 mM Ölsäure; r = 0,83; **** $p < 0,0001$ für 1,5 mM Ölsäure). Dies gilt als Hinweis darauf, dass auf Einzelzellebene eine hohe Insulinexpression mit einem hohen Gehalt an Glrx5 korreliert und umgekehrt [200].

2.1.5.4 Einfluss der Ölsäure auf die Atmungskette

Um eine Verbindung zwischen dem Mangel an Glrx5 und der gestörten Insulinsekretion herzustellen, wurde die mitochondriale Funktion mit Ölsäure behandelter MIN6-Zellen untersucht. Es zeigte sich sowohl durch die Präinkubation mit Palmitinsäure als auch dosisabhängig unter Ölsäure eine verminderte Menge an ATP ($3,99 \pm 0,87$ vs. $2,12 \pm 0,63$ vs. $1,6 \pm 0,45$ vs. $0,89 \pm 0,25$ µM, **** $p < 0,0001$, Abbildung 2.19A and $3,6 \pm 0,43$ vs. $2,69 \pm 0,46$ µM bei

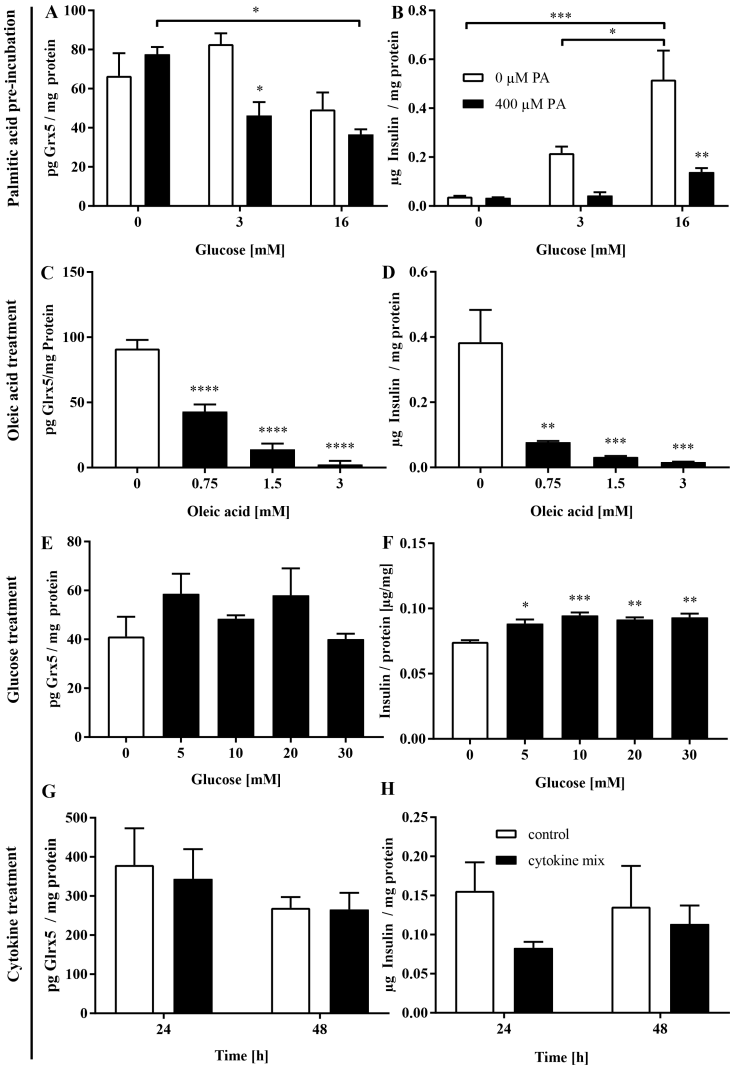

Abbildung 2.18: **MIN6 Glrx5 und Insulinsekretion.** Gezeigt sind die Proteinmenge von Glrx5 im Lysat und von Insulin im Medium von MIN6-Zellen, welche mit (A, B) Glukose für 24 h nach und ohne Präinkubation mit 400 µM Palmitinsäure sowie einer Stunde Glukosedeprivation, (C, D) Ölsäure für 24 h, (E, F) Glukose für 24 h nach 2 h Glukosedeprivation und (G, H) einem Zytokinmix aus 10 ng/ml TNF-α, 5 ng/ml IL-1β und 100 ng/ml IFN-γ für 24 bzw. 48 h behandelt wurden. Mittelwert $\pm$ SEM. n = 3-5. Schwarz: (vor)behandelte Zellen, weiß: Kontrollen. **** $p < 0,0001$, *** $p < 0,001$, ** $p < 0,005$, * $p < 0,05$ (Ein- bzw. zweifaktorielle Anova).

3 mM Glukose, ** $p < 0,005$, Abbildung 2.19B). Der Sauerstoffffluss durch die Atmungskette wurde mithilfe einer Sauerstoffelektrode untersucht. Die basale, endogene Atmung war in den behandelten Zellen signifikant erhöht, was als gesteigerter, aber durch vermehrte Entkopplung ineffizienterer Substratumsatz gewertet wurde ($363,5 \pm 54,5$ vs. $330,3 \pm 25,98$ pmol/(s*U), * $p < 0,05$, Abbildung 2.19C). Die bei maximaler ADP-, Phosphat-, O_2- und Substratsättigung gemessene maximale Leistung der oxidativen Phosphorylierung von Komplex I und II war gemäß den erhobenen Daten in den behandelten Zellen signifikant geringer als in den Kontrollen

(1170 ± 199,7 vs. 1467 ± 268,6 pmol/(s*U), *** $p < 0,001$, Abbildung 2.19D). Das galt auch für die maximale Kapazität der oxidativen Phosphorylierung der Atmungskette (492,3 ± 78,34 vs. 665,9 ± 115 pmol/(s*U), *** $p < 0,001$, Abbildung 2.19F, 1029 ± 185 vs. 1269 ± 197,3 pmol/(s*U), *** $p < 0,001$, Abbildung 2.19G). Komplex IV war nicht betroffen (1218 ± 187,5 vs. 1258 ± 208,4 pmol/(s*U), n.s., Abbildung 2.19H).

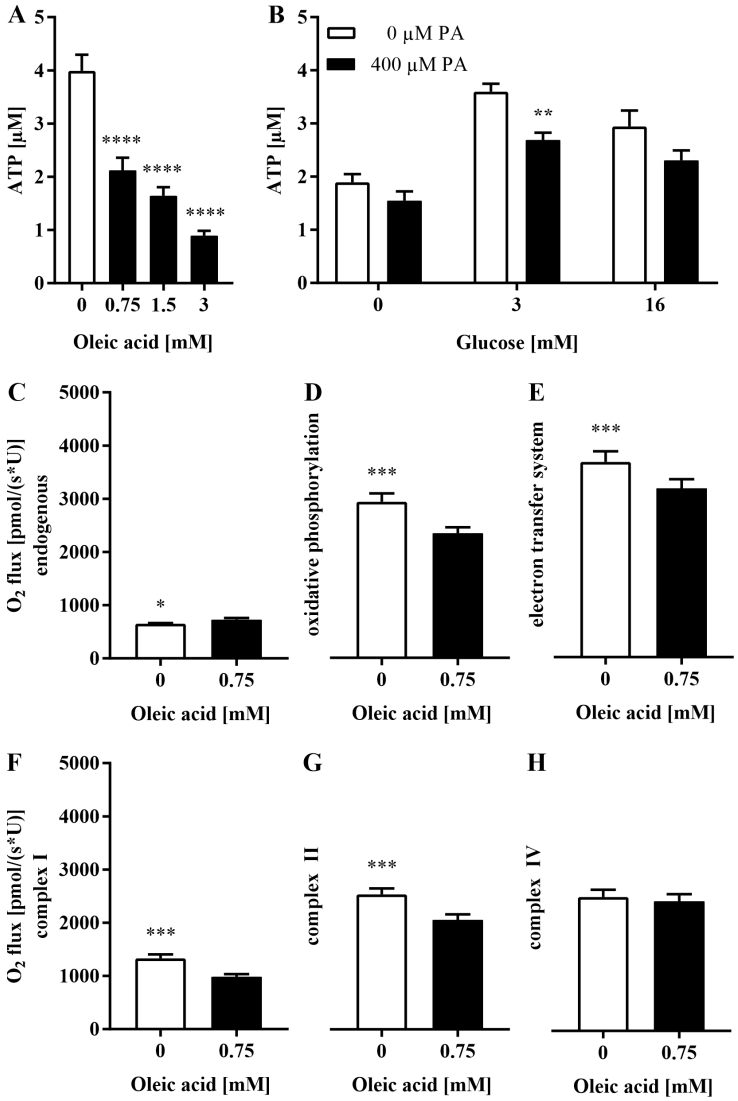

Abbildung 2.19: **ATP-Produktion und Sauerstoffffluss durch die Atmungskette nach Behandlung mit Ölsäure.** (A) ATP nach Behandlung mit Ölsäure für 24 h und (B) Präinkubation mit 400 µM Palmitinsäure, 1 h Glukosedeprivation und Glukosebehandlung. (C-H) O_2-Fluss in der Atmungskette nach Behandlung mit 0,75 mM Ölsäure für 24 h. Mittelwerte ± SEM. n = 12. Schwarz: (Vor)behandelte Zellen, weiß: Kontrollen. **** $p < 0,0001$, *** $p < 0,001$, ** $p < 0,005$, * $p < 0,05$ (einfaktorielle Anova bzw. ungepaarter t-Test).

2.1.5.5 Haupterkenntnisse

- **Der murine Diabetes mellitus mit Adipositas ist durch einen Verlust der insulären Glutaredoxine, insbesondere Glrx1 und 5, gekennzeichnet. Glrx-defiziente Inseln weisen eine gestörte Insulinsekretion und vermehrte ROS-Bildung auf. Eine diätetisch induzierte Rekonvaleszenz geht mit der Rekonstitution von Glrx5 einher.**

- **In der murinen MIN6-β-Zelle wird Glrx5 durch Hypoxie oder freie Fettsäuren herabreguliert. Glukose oder ein Zytokinmix (TNF-α, IL-1β und IFN-γ) hat keinen Einfluss.**

2.2 Thioredoxin als therapeutische Option zur Erhaltung der β-Zellviabilität und -funktion

Hanschmann EM*, **Petry SF***, Eitner S, Maresch CC, Lingwal N, Lillig CH, Linn T. Paracrine regulation and improvement of β-cell function by thioredoxin. Redox Biol., 34:101570, Jul 2020. doi:10.1016/j.redox.2020.101570. *Gleichberechtige Erstautorenschaft.

In unserer Studie wurde das Thioredoxinsystem in einem Schwein-zu-Maus-Inseltransplantationsmodell, MIN6-Zellen, porcinen Inseln und humanen Blutproben aus dem Gießener Inseltransplantationsprogramm untersucht. Ziel war es, die Regulation im Kontext der Hypoxie und Reoxygenierung sowie die Bedeutung des sezernierten Trx1 zu untersuchen. Die Methodik umfasste den Western Blot, den ELISA, die Immunhistologie, die Durchflusszytometrie, die qPCR, den MTT- und den Makrophagenmigrationsassay sowie einige kommerzielle Kits (Trx1-, Laktat-Dehydrogenase (LDH)-, und Caspase3/7-Aktivität) [98].

2.2.1 Gegensätzliche Regulation der Thioredoxinsysteme durch Hypoxie und Reoxygenierung und Sekretion von Trx1

Zunächst wurden MIN6-Zellen unter hypoxischen Bedingungen bei 1% bzw. 2% Sauerstoffgehalt für 12 h mit und ohne anschließende Reoxygenierung bei 20% Sauerstoffgehalt für 12 bzw. 24h kultiviert. Bemerkenswerterweise zeigten sich unterschiedliche Reaktionen des zytosolischen und mitochondrialen Thioredoxinsystems. Das zytosolische Trx1 und seine Reduktase zeigten im Vergleich zur Normoxie signifikant verminderte Proteinmengen nach der hypoxischen Behandlung. Dieser Befund änderte sich nicht wesentlich nach der Reoxygenierung (Abbildung 2.20A, C). Die Proteinmenge des mitochondrialen Trx2 und seiner Reduktase hingegen verhielten sich gegensätzlich. Es kam zu einem signifikanten Ansteigen sowohl nach Hypoxie als auch nach Reoxygenierung im Vergleich mit den normoxischen Kontrollen (Abbildung 2.20B, D). Txnip war interessanterweise nur nach der Hypoxiebehandlung zu detektieren. Die Menge stieg nach der Redoxygenierung weiter an (Abbildung 2.20F). Die Hypoxie löste in den MIN6-Zellen eine Sekretion des Trx1 aus, welche unter Reoxygenierung sistierte (Abbil-

dung 2.20E). Um sicherzustellen, dass diese Freisetzung nicht durch einen Zellschaden bedingt ist, wurden zudem das extrazelluläre Aktin und Tubulin gemessen, welche per Western Blot nicht detektiert wurden [98]. Darüber hinaus wurde die Aktivität der LDH gemessen. Diese war lediglich bei 1% O_2 und nach der 24-stündigen normoxischen Kultur vergleichen mit der 12-stündigen signifikant erhöht. Eine passive Freisetzung des Trx1 war somit nicht plausibel.

Nachdem die Zellkultur deutliche Unterschiede und eine gegensätzliche Reaktion der Trx als Reaktion auf die Hypoxie bzw. Reoxygenierung gezeigt hatte, zielten wir darauf ab, diesen Befund in vivo zu bestätigen. Hierfür wurden Transplantate aus einem Schwein-zu-Maus-Inseltransplantationsversuch untersucht. In diesem Versuch wurde in 12 Wochen alten Nacktmäusen (NRMI nu/nu) ein Diabetes durch die Injektion von STZ induziert. Tiere mit einem nachgewiesenen Diabetes (GPG $>$ 300 mg/dl) wurden als Empfänger ausgewählt. Ihnen wurden nach dem etablierten Protokoll aus der Arbeitsgruppe per Injektion 2.000 Schweineinseläquivalente über die Pfortader transplantiert [201]. Nach 30 min wurden die Lebern und Portalvenenblut entnommen. Die immunhistologische Untersuchung der Trx bestätigte das in den MIN6-Zellen dokumentierte Muster: Trx1 und TrxR1 ließen sich deutlich in den Kontrollpankreata, aber so gut wie nicht in den Transplantaten anfärben (-70% für Trx1, ** $p < 0,005$ und -95% für TrxR1, * $p < 0,05$ im Vergleich Transplantat gegen Nativpankreas, Abbildung 2.21A-H). Für Trx2 und TrxR2 sowie Txnip verhielt es sich umgekehrt (+80% für Trx2, **** $p < 0,0001$ und +95% für TrxR2, **** $p < 0,0001$ sowie +45% für Txnip, ** $p < 0,005$ im Vergleich Transplantat gegen Nativpankreas, Abbildung 2.21I-T).

2.2.2 Sekretion von Trx1 in vivo

Als nächstes untersuchten wir, ob die im MIN6-Modell festgestellte Sekretion von Trx1 auch in vivo stattfindet. Hierfür wurde das gemeinsam mit den Transplantaten 30 min nach Transplantation asservierte Pfortaderblut der Empfängermäuse auf Trx1 untersucht. Tatsächlich fand sich im Gegensatz zu den Kontrolltieren, in deren Blut kein Trx1 messbar war, eine deutliche Sekretion des Proteins. Eine Subgruppe der Transplantatempfängertiere war mit dem TrxR-Inhibitor Auranofin behandelt worden. Bemerkenswerterweise fanden wir im Pfortaderblut dieser Tiere nur eine minimale, im Vergleich zu den unbehandelten Tieren signifikant, um rund 85%, verminderte Menge Trx1 (1,78 $\pm$ 0,66 vs. 0,22 $\pm$ 0,18 vs. 0,008 $\pm$ 0,004 OD, **** $p < 0,0001$,

Abbildung 2.22A). Die Transplantate der mit Auranofin behandelten Tiere wiesen zudem eine drastisch verkürzte und signifikant verminderte Überlebenszeit auf (50% der Transplantate versagten nach 2,5 vs. 14 Tagen, **** $p < 0,0001$, Abbildung 2.22B). Korrelierend mit dieser

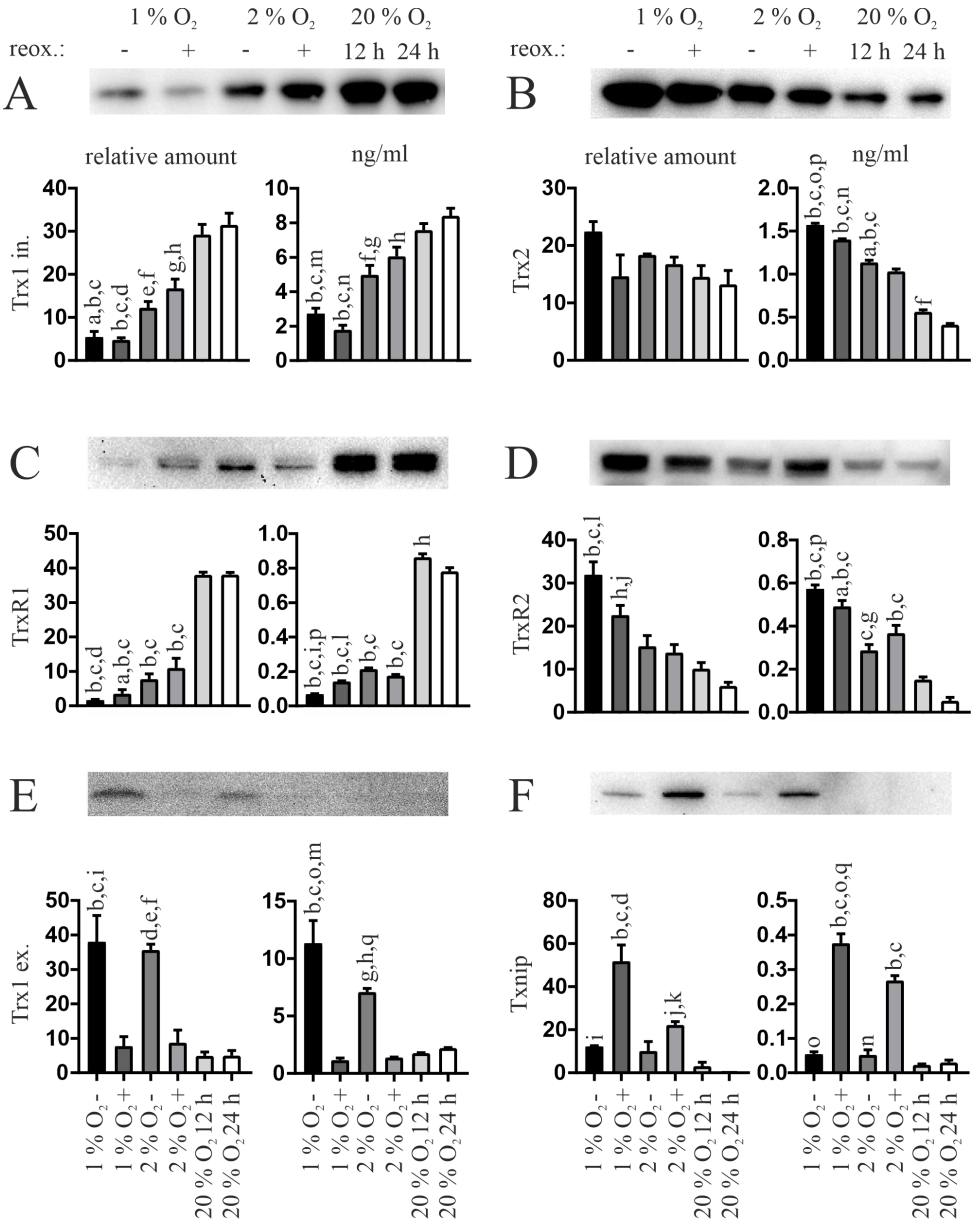

Abbildung 2.20: **Die Effekte von Hypoxie und Reoxygenierung auf die Thioredoxine in MIN6-Zellen.** Abgebildet sind jeweils ein repräsentativer Western Blot sowie die jeweilige Densitometrie und die ELISA-Analyse. (A) Intrazelluläres Trx1, (B) Trx2, (C) TrxR1, (D) TrxR2, (E) extrazelluläres Trx1, (F) Txnip. (+) mit Reoxygenierung, (-) ohne. Mittelwerte ± SD. n = 3-5. [a]$p < 0,05$ vs. 2% O_2 +; [b]$p < 0,0001$ vs. 20% O_2 12 h; [c]$p < 0,0001$ vs. 20% O_2 24 h; [d]$p < 0,01$ vs. 2% O_2 +; [e]$p < 0,001$ vs. 20% O_2 12 h; [f]$p < 0,001$ vs. 20% O_2 24 h; [g]$p < 0,01$ vs. 20% O_2 12 h; [h]$p < 0,01$ vs. 20% O_2 24 h; [i]$p < 0,001$ vs. 1% O_2 +; [j]$p < 0,05$ vs. 20% O_2 12 h, [k]$p < 0,05$ vs. 20% O_2 24 h; [l]$p < 0,01$ vs. 2% O_2 -; [m]$p < 0,05$ vs. 2% O_2 -; [n]$p < 0,0001$ vs. 2% O_2 +; [o]$p < 0,0001$ vs. 1% O_2 +; [p]$p < 0,0001$ vs. 2% O_2 –; [q]$p < 0,001$ vs. 2% O_2 + (einfaktorielle Anova).

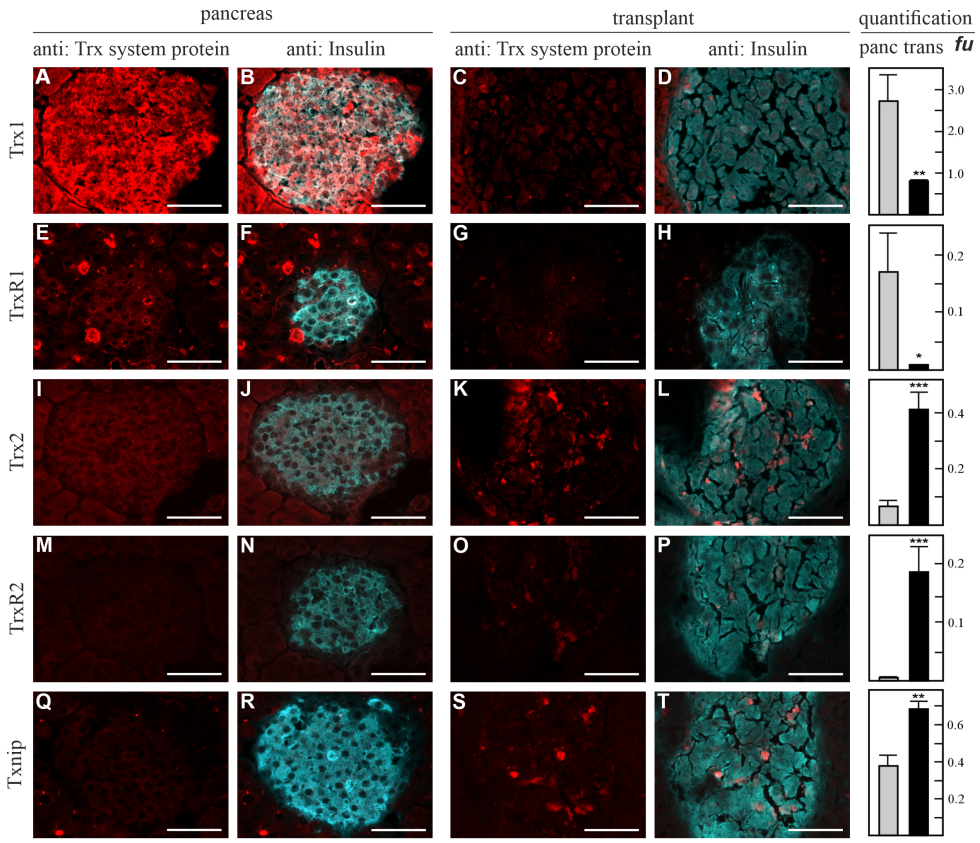

Abbildung 2.21: **Immunhistochemische Analyse der Thoredoxine, ihrer Reduktasen und Txnip in pankreatischen Inseln und Transplantaten.** Färbung gegen (A, E, I, M, Q) das jeweilige Thioredoxinprotein bzw. (B, F, J, N, R) Insulin im nativen Mauspankreas, Färbung gegen (C, G, K, O, S) das jeweilige Thioredoxinprotein bzw. (D, H, L, P, T) Insulin im Transplantat. Rechts im Panel befindet sich die Quantifizierung der Thioredoxinfärbefläche gegen die Insulinfärbefläche, Mittelwerte ± SD. n = 6-12 Objektträger. *** $p < 0,0001$, ** $p < 0,005$, * $p < 0,05$ (ungepaarter t-Test).

Messung wiesen die mit Auranofin behandelten Tiere eine signifikant höhere Blutglukose auf (18,7 ± 3,2 vs. 11,3 ± 3,5 mM, **** $p < 0,0001$, 2.22C).

Konsekutiv wurde Trx1 nach intravenöser Glukosebelastung mit 0,3 g/kg Körpergewicht im Blut von Personen aus dem Gießener Inseltransplantationsprogramm gemessen. Die Versuche wurden jeweils vor und ein Jahr nach der Inseltransplantation durchgeführt. Als Kontrollen wurden gesunde Menschen mit abgeglichenem Alter, Geschlecht und Körpergewicht rekrutiert. Der bereits in vitro und in Tiermodell in vivo erhobene Befund der Trx1-Sekretion konnte auch im Humanmodell bestätigt werden. Die Betroffenen zeigten vor Transplantation keine Trx1-Sekretion, wohingegen eine solche nach Transplantation deutlich und signifikant messbar war. Die höchste Sekretion war in den Proben Gesunder zu messen (3,98 ± 0,57 vs. 2,28 ± 0,27 vs. 0,03 ± 0,08 ng/ml, * $p < 0,05$, Abbildung 2.22D, E).

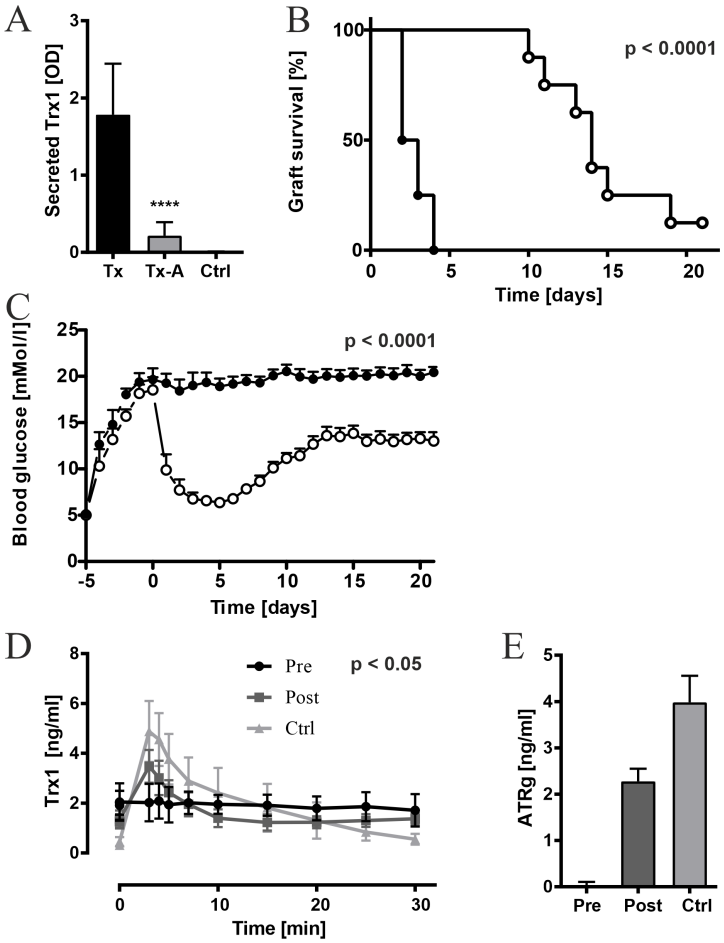

Abbildung 2.22: **Trx-Sekretion in Schweine- und humanen Inseltransplantaten nach Transplantation.** (A) Trx1 im Pfortaderblut von transplantierten Mäusen. Tx: Transplantierte Tiere, Tx-A: Transplantierte Tiere mit Auranofinbehandlung, Ctrl: Kontrollen, n = 8. Einfaktorielle Anova. (B) Das Transplantatüberleben mit und ohne Auranofinbehandlung der Mäuse und ihre (C) Blutglukose. Ausgefüllte Kreise: Auranofingruppe, offene Kreise Kontrollgruppe, n = 8, Chi-Square bzw. zweifaktorielle Anova. (D) Die glukosestimulierte Trx1-Antwort der humanen Probanden (pre: vor Transplantation, post: nach Transplantation, Ctrl: gesunde Kontrolle) und (E) die entsprechende Quantifizierung. n = 8. Zweifaktorielle Anova. Mittelwerte $\pm$ SD. **** $p < 0,0001$.

2.2.3 Parakrine Regulation der β-Zelle durch sezerniertes Trx1

Da Trx1 unter Hypoxie bemerkenswerterweise in allen bisherigen Modellen sezerniert wurde, untersuchten wir als nächstes den Einfluss von extrazellulärem rekombinanten humanen hTrx1 auf die Viabilität und Funktion der β-Zelle bzw. Insel. Per Durchflusszytometrie wurde die Viabilität von Schweineinseln, gemessen am Verhältnis von Annexin V als Marker der Apoptose und Propidiumiodid als Marker der Nekrose bzw. späten Apoptose, unter dem Einfluss von 30 oder 60 μg/ml hTrx1 beurteilt. Die Analyse zeigte eine Verminderung der doppelt positiven Zellen unter Hypoxie (2% O_2, 9,8 $\pm$ 1,3 auf 5.7 $\pm$ 0,5% für 30 μg/ml hTrx1 und auf 2,0 $\pm$

1,6% für 60 μg/ml hTrx1, **** $p < 0,0001$). Unter Normoxie vermochte 60 μg/ml Trx1 eine signifikante Reduktion (20% O_2, 4,3 ± 0.3% auf 2,5 ± 1,3%, ** $p < 0,001$) zu erreichen. Um sicherzustellen, dass die Effekte durch Trx1 und seine Redoxaktivität vermittelt werden, wurden die redox-inaktive Cys32Ser-Mutante des humanen rekombinanten Thioredoxin 1 (C32S) und das denaturierte humane Trx1 (dhTrx1) als Kontrollen angewendet. Diese übten keinen Einfluss auf die Ergebnisse der Durchflusszytometrie aus. Die Daten sind in Abbildung 2.23 dargestellt.

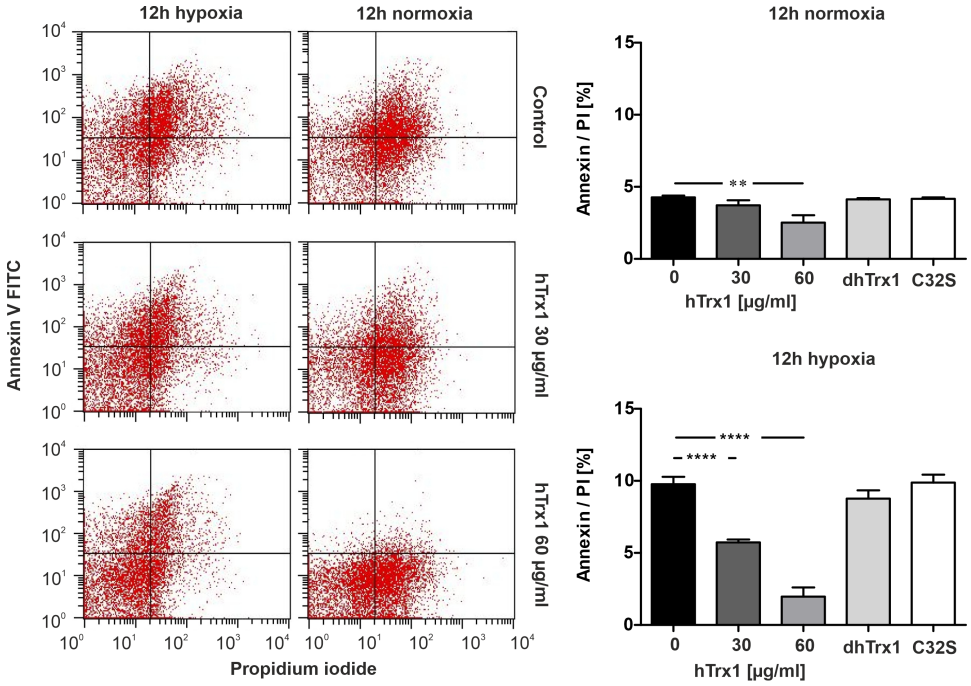

Abbildung 2.23: **Der Einfluss von hTrx1 auf die Viabilität porciner Inseln.** Links: Die Ergebnisse der Durchflusszytometrie porciner Inseln unter dem Einfluss von rekombinantem hTrx unter Hypoxie und Normoxie. Rechts: Die Quantifizierung der Doppelfärbung für Annexin V und Propidiumiodid. n = 6. Einfaktorielle Anova. Mittelwerte ± SD. **** $p < 0,0001$, ** $p < 0,001$.

In den Schweineinseln wurde darüber hinaus die mRNA-Expression der proapoptotischen Gene Bax/Bcl-2, des antiapoptotischen Gens c-FLIP sowie von HIF-1α und Vascular Endothelial Growth Factor-A (VEGF-A) per qPCR gemessen. Die Zugabe des hTrx1 verminderte die Transkription von Bax/Bcl-2 unter Hypoxie sowie unter hypoxischer Zytokinbehandlung. Ein Einfluss auf c-FLIP wurde nicht detektiert, jedoch auf VEGF-A und HIF-1α. Es zeigte sich unter Hypoxie sowie unter der Zugabe der Zytokine zur normoxischen und hypoxischen Kultur eine vermehrte Transkription beider Gene. Weder Cys32Ser noch dhTrx1 hatten einen Einfluss auf die Transkription [98].

Die Effekte des exogenen Trx1 wurden zudem in MIN6-Zellen untersucht. Hier zeigte sich

unter Normoxie kein Effekt auf die Zellviabilität, gemessen per MTT-Assay. Unter Hypoxie jedoch steigerte Trx1 dosisabhängig die Viabilität der Zellen (Hypoxie: 39,12 $\pm$ 2,21% ohne Trx1, 68,97 $\pm$ 3,96% mit 60 μg/ml Trx1, **** $p < 0,0001$). Die zusätzliche Behandlung mit einem Zytokinmix bestehend aus 100 ng/ml IFN-γ, 5 ng/ml IL-1β und 10 ng/ml TNF-α führte sowohl unter Normoxie als auch unter Hypoxie zu einer Verminderung der Viabilität. In beiden Zuständen wurde diese durch Zugabe von Trx1 signifikant gesteigert (Normoxie + Zytokine: 63,08 $\pm$ 0,78% ohne Trx1, 89,73 $\pm$ 1,65% mit 60 μg/ml Trx1 und Hypoxie + Zytokine: 28,09 $\pm$ 3,68% ohne Trx1, 77,51 $\pm$ 1,47% mit 60 μg/ml Trx1, **** $p < 0,0001$). Auch in diesem Versuch wurden keine Effekte durch C32S oder dhTrx1 vermittelt (Abbildung 2.24). Im gleichen Versuchsaufbau konnte mit dem exogenen Trx1 eine dosisabhängige Verminderung der Caspase3/7 und NF-κB p65 als früher und später Marker der Apoptose erreicht werden [98].

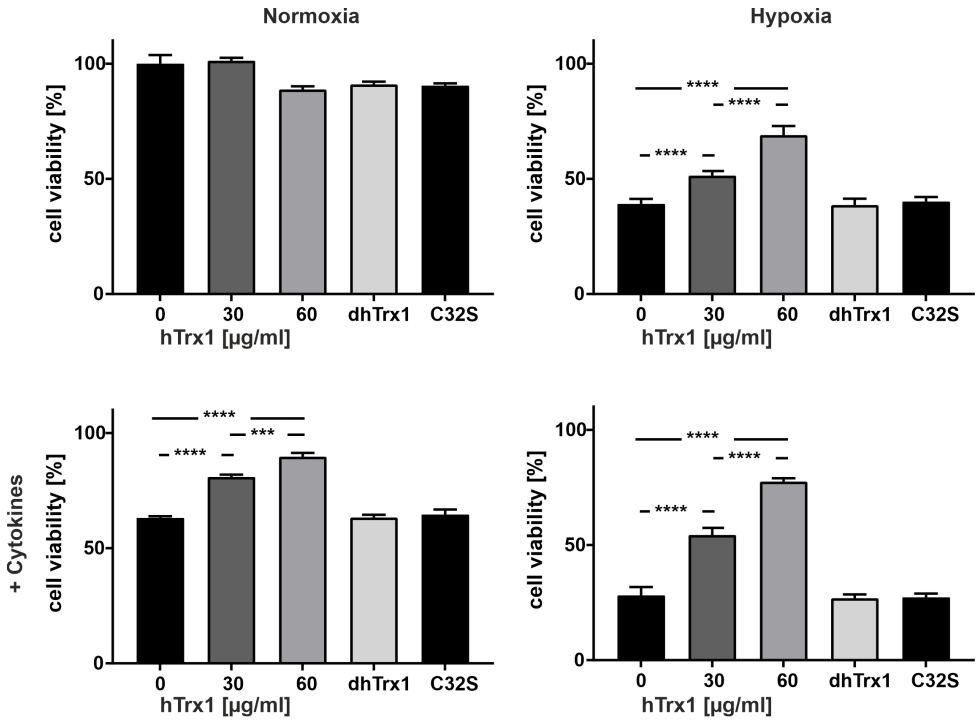

Abbildung 2.24: **Der Einfluss von hTrx1 auf die Viabilität der MIN6-Zelle.** Gezeigt sind die Werte des MTT-Assays von normoxisch und hypoxisch kultivierten MIN6-Zellen unter dem Einfluss von exogenem hTrx1 sowie dem redox-inaktiven C32S-Trx1 und dem denaturierten dhTrx1. n = 5. Einfaktorielle Anova. Mittelwerte $\pm$ SEM. **** $p < 0,0001$, *** $p < 0,005$.

Nachdem wir einen deutlichen antiapoptotischen Effekt des sezernierten Trx1 auf die Inseln bzw. β-Zellen nachweisen konnten, untersuchten wir einen möglichen Einfluss auf die endokrine Funktion. Hierfür wurden zunächst MIN6-Zellen für 12 h unter Hypoxie (2% O_2) kultiviert und das Insulin im Lysat und im Kulturmedium untersucht. Das Insulin im Medium als

Korrelat des sezernierten Insulins stieg dosisabhängig signifikant an (2,5 ± 1,06 ng/ml ohne hTrx1 vs. 10,28 ± 2,22 ng/ml mit 60 μg/ml hTrx1, **** $p < 0,0001$). Kongruent dazu nahm der zelluläre Gehalt an Insulin, gemessen im Zelllysat, ab (8,1 ± 0,9 ng/ml ohne hTrx1 vs. 4,4 ± 0,44 ng/ml mit 60 μg/ml hTrx1, **** $p < 0,0001$, Abbildung 2.25A). Der Effekt ließ sich auch in porcinen Inseln unter dem Einfluss von Hypoxie und Zytokinen zeigen. Es wurde der Stimulationsindex als das Verhältnis des stimulierten und basalen Insulins im Medium, gemessen bei 22 und 2,8 mM (396 und 50 mg/dl) Glukose, berechnet. Unter Hypoxie und Zytokinen stieg der Index signifikant an (1,03 ± 0,1 ohne hTrx1 vs. 1,95 ± 0,31 mit 60 μg/ml hTrx1, ** $p < 0,01$), wohingegen unter Normoxie und Hypoxie ohne Zytokine kein Effekt zu messen war (Abbildung 2.25B).

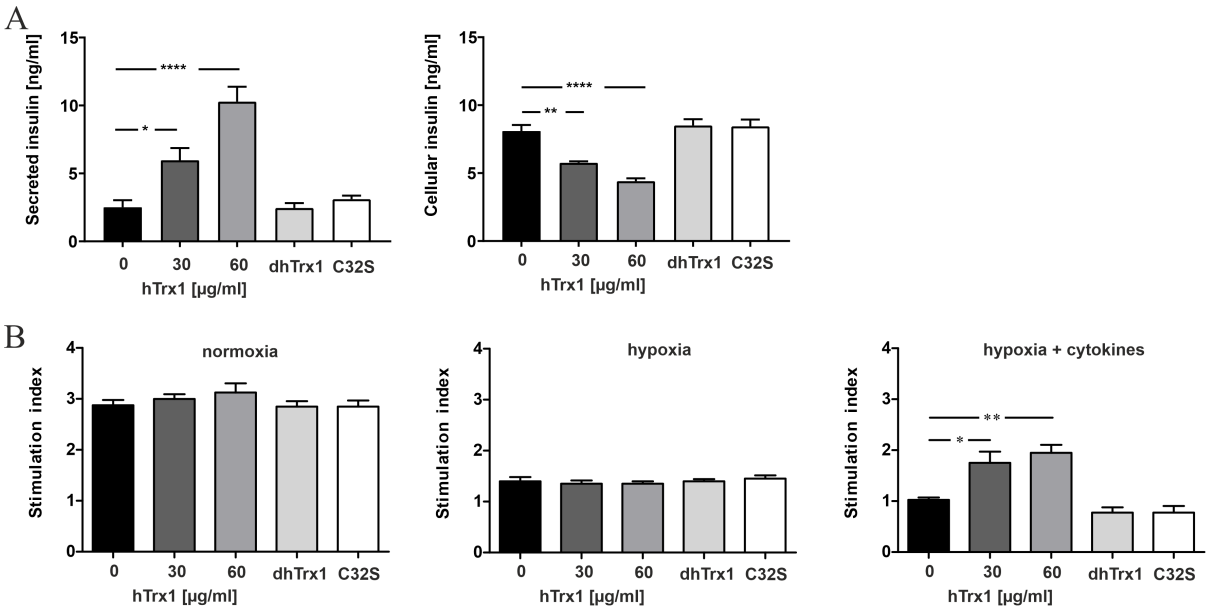

Abbildung 2.25: **Der Einfluss von hTrx1 auf die Insulinsekretion porciner Inseln und MIN6-Zellen.** (A) Der Insulingehalt im Zellkulturmedium bzw. im Zelllysat nach Behandlung mit hTrx1. n = 4. Einfaktorielle Anova. Mittelwerte ± SD. **** $p < 0,0001$, ** $p < 0,01$, * $p < 0,05$. (B) Der Insulinstimulationsindex von porcinen Inseln unter Normoxie, Hypoxie und Hypoxie mit Zytokinen. n = 4. Einfaktorielle Anova. Mittelwerte ± SD. ** $p < 0,01$, * $p < 0,05$.

2.2.4 Exogenes Trx1 hemmt die Makrophagenmigration

Da für Trx1 immunmodulatorische Effekte beschrieben sind, untersuchten wir zuletzt einen möglichen Einfluss des hTrx1 auf die Migration muriner Makrophagen zu Kulturmedium der porcinen Inseln in einem entsprechenden Makrophagenmigrationsassay. Wir konnten nachwei-

sen, dass das Kulturmedium eine Migration der Makrophagen auslöst, und, dass hTrx1 diese dosisabhängig signifikant vermindert (50,65 $\pm$ 3,87 bei Kulturmedium ohne hTrx1 vs. 33,5 $\pm$ 2,59 fiktive Einheit des Calceins $* 10^3$ mit 90 μg/ml hTrx1, **** $p < 0,0001$). Auch in diesem Experiment hatten C32S und dhTrx1 keinen Einfluss auf die Messwerte. Der hemmende Effekt durch das hTrx1 persistierte unter Zugabe des Endotoxininhibitors Polymyxin B. Eine Vermittlung durch residuelle bakterielle Endotoxine oder eine Kontamination des rekombinanten hTrx1 mit selbigen als Stimulus für die Makrophagenmigration konnte also ausgeschlossen werden (Abbildung 2.26).

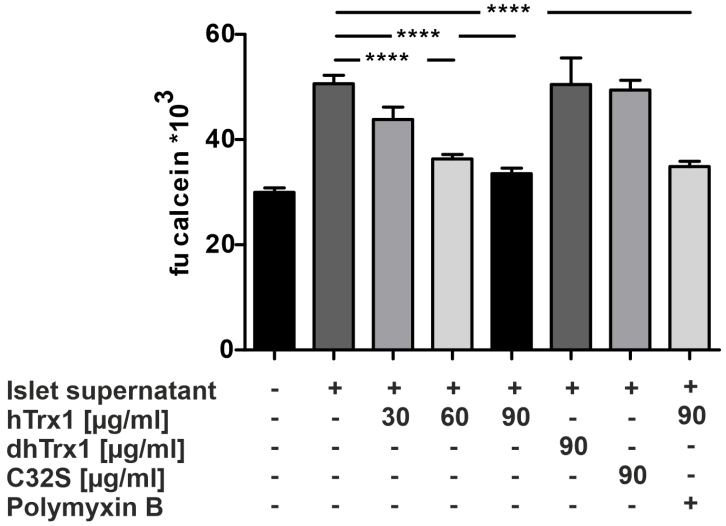

Abbildung 2.26: **Der Einfluss von Trx1 auf die Migration muriner Makrophagen.** Gezeigt ist die Menge der Makrophagen, quantifiziert über ihre Calceinmarkierung, unter Zugabe von exogenem hTrx1 sowie den entsprechenden Kontrollen. n = 6. Einfaktorielle Anova. Mittelwerte $\pm$ SD. **** $p < 0,0001$.

2.2.5 Haupterkenntnisse

- **Hypoxie und Reoxygenierung induzieren kompartimentalisierte Redoxreaktionen der mitochondrialen, zytosolischen und extrazellulären Thioredoxine zur Aufrechterhaltung der β-Zellviabilität und Insulinsekretion.**
- **Sowohl Hypoxie als auch Glukose induzieren die Sekretion von Trx1. Das Protein fungiert folglich als Surrogatparameter für β-Zellen.**
- **Das sezernierte Trx1 fördert mittels seiner Redoxaktivität parakrin Viabilität und Insulinsekretion der β-Zelle. Zudem inhibiert es die Chemotaxis von Mausmakrophagen.**

3. Diskussion

3.1 Experimentelle Modelle der Lipotoxizität

Trotz der zahlreichen Publikationen zu der komplexen und dynamischen Fettstoffwechselstörung im Diabetes mellitus, zumeist vereinfacht zusammengefasst unter dem Begriff der Liptoxizität, gibt es keine einheitliche Definition des Begriffs. Das Überschreiten einer bestimmten Konzentration einzelner oder mehrerer Fettsäuren wird der Komplexität der durch FFS vermittelten Effekte nicht gerecht. Diese werden über verschiedene Signalwege vermittelt und betreffen multiple Station des FFS-Stoffwechsels von ihrer Aufnahme in die β-Zelle bis hin zu ihrem Abbau [62, 72, 184, 184, 185, 202]. Eine klare Abgrenzung zwischen als physiologisch und als pathologisch anzusehenden Auswirkungen von FFS ist nicht trivial, zumal zumeist negativ konnotierte Vorgänge wie die Apoptose [62] oder Autophagozytose [190] physiologische und notwendige Prozesse darstellen. Konsekutiv weist die wissenschaftliche Literatur zu den Effekten von Fettsäuren auf die pankreatische β-Zelle eine große Heterogenität hinsichtlich der experimentellen Bedingungen und deren Resultaten auf. Die biologischen Effekte sind in hohen Maße abhängig von der jeweiligen Fettsäure und der Kettenlänge des Kohlenstoffgerüsts, ihrer Sättigung, ihrer Konzentration und der Behandlungsdauer [77, 194].

Mit unserer Übersichtsarbeit konnten wir herausarbeiten, dass insbesondere die Mitochondrien der β-Zelle auf mannigfaltige Art in die komplexen Veränderungen des Fettstoffwechsels im Diabetes mellitus eingebunden sind und in Konsequenz Funktionsstörungen auftreten [77]. Dies fügt sich in die vorhandene Literatur und die daraus abzuleitende potenzielle Nutzbarkeit der Mitochondrien und mitochondrialer Proteine für Therapiezwecke ein [158, 159]. Ein in diesem Kontext selten berücksichtigter Aspekt ist das Zusammenspiel zwischen ER und Mitochondrium. Obgleich man die molekularen Vorgänge der ER-Stressantwort und der mitochondrialen Dysfunktion voneinander separieren kann, bilden beide Organellen eine funktionelle Einheit mit reziproker Beziehung. Eine wesentliche Bedeutung kommt beispielsweise dem Austausch von Kalzium und Lipiden zwischen beiden Organellen über direkte Kontakte zu [203–205]. Für

gewöhnlich wird in der Literatur jedoch nicht zwischen durch das ER und durch die Mitochondrien vermittelte Effekte unterschieden.

Die zugrundeliegenden Signalwege und Mechanismen der Lipotoxizität sind also vielschichtig und komplex, und die experimentellen Bedingungen müssen bei der Arbeit mit FFS-Lösungen genau kontrolliert werden. Wesentliche dieser Faktoren wurden im Laufe der Jahre für unsere MIN6-Zellen untersucht und schließlich als Publikation zusammengefasst [194]. Die MIN6-Zellreihe gehört zu den am weitesten verbreiteten β-Zellmodellen. Die murine, immortalisierte Zelllinie war ursprünglich aus dem Insulinom von transgenen C57BL/6-Mäusen, welche aus der Mikroinjektion des an das Simian-Virus 40 gekoppelten humanen Insulinpromotor entstanden waren, isoliert worden [206]. Die MIN6-Zelle weist typische β-Zelleigenschaften auf und exprimiert unter anderem die Glukokinase, den Glukosetransporter Typ 2 (GLUT2) und Insulin und verfügt über eine funktionierende GSIS [207]. Die Studie befasste sich insbesondere mit dem MTT-Assay. Mit diesem lässt sich anhand der Reduktion von MTT zu Formazan kolorimetrisch die Zellviabilität messen. Während man initial annahm, dass die Reaktion vor allem durch die Succinat-Dehydrogenase (SDH) vermittelt wird, und somit ein Indikator für die Zellatmung und respektive die mitochondriale Funktion ist [208], deuten spätere Erkenntnisse darauf hin, dass die Reaktion vornehmlich von NADH/NADPH und damit dem ER abhängig ist [209]. Damit ist die Umwandlung von MTT zu Formazan ein Marker der zellulären Glykolyse. Der MTT-Assay wird daher häufig als Standardtest für die Auswirkungen experimenteller Bedingungen auf den Zellstoffwechsel verwendet. Es gibt viele Variablen, welche die Resultate des Assays maßgeblich beeinflussen können, unter anderem die Anzahl der verwendeten Zellen, die Inkubationszeit, die Konzentration des MTTs und Zusätze zum Zellkulturmedium [210]. Bovines Serumalbumin (BSA) ist ein essentieller Zusatz in der Zellkultur. Im experimentellen Setting von Lipotoxizitätsuntersuchungen wird es benötigt, um die FFS in wässriger Lösung zu binden [211], ähnlich der physiologischen Rolle des Albumins als Transporter vieler komplexgebundener Moleküle.

Wir konnten zeigen, dass BSA signifikanten Einfluss auf die Ergebnisse des MTT-Assays nimmt. Der Einfluss von BSA auf Zellkulturexperimente ist wenig erforscht. Bekannt ist, dass es die Bioverfügbarkeit von FFS erhöht [212]. Insbesondere die ungebundenen FFS vermitteln die

biologischen Effekte [69], sodass diese experimentelle Bedingung kontrolliert werden muss. Empfohlen wird ein Verhältnis von 5:1 für FFS zu BSA. In der Literatur werden Verhältnisse von 1:3 bis 74:1 angegeben, und die BSA-Konzentrationen reichen beispielsweise für eine FFS-Lösung von 0,5 mM von 0,045% bis 16,6%, was die enorme Heterogenität der Protokolle verdeutlicht. Es ist unklar, ob die festgestellten Einflüsse auf die Umwandlung von Formazan aufgrund einer Interferenz oder einer veränderten zellulären Funktion eintreten. Mögliche Mechanismen sind generelle proteotoxische Effekte [213], die Aktivierung mitochondrialer Enzyme, z.B. der SDH [214], sowie Interaktionen mit Wachstumsfaktoren und sonstigen Zusätzen zum Zellkulturmedium und die Bindung toxischer Substanzen [215, 216]. Unsere Studie beschrieb veränderte MTT-Messwerte in Abhängigkeit der Kultivierungsdauer der verwendeten Zellen sowie von dem verwendeten Lösungsmittel. Letzteres hatte zudem auch biologische Effekte. Auswirkungen der Kultivierungsdauer auf die Messwerte des MTT-Assays sind beschrieben [210], die Einflüsse des Lösungsmittels von Fettsäurelösungen hingegen nicht. Häufig verwendete Lösungsmittel sind Ethanol und DMSO. Letzteres bietet den Vorteil einer geringeren Toxizität bei gleicher Konzentration [217, 218], jedoch ermöglicht Ethanol eine effizientere Lösung, sodass höhere FFS-Konzentrationen erreicht werden können [219]. Letztlich muss das Lösungsmittel nach der gewünschten Konzentration der FFS-Lösungen und möglichen bekannten Effekten auf die zu untersuchenden Parameter gewählt werden, wobei die Auswahl limitiert ist, und die verfügbaren Substanzen allesamt Vor- und Nachteile aufweisen. Für hohe FFS-Konzentrationen bietet sich Ethanol aufgrund der guten Lösbarkeit an, zumal ist er günstig und gut verfügbar. Die Verseifung wird in der Literatur gelegentlich verwendet, ist aber aufwendiger. Eine gute, aber eher selten zur Anwendung kommende Alternative scheint Methanol zu sein. Während die Lösbarkeit von FFS ähnlich jener des Ethanols ist, werden weniger toxische Nebeneffekte berichtet [220]. Als absolut wesentlich erscheint uns unabhängig vom gewählten Lösungsmittel die Verwendung von entsprechenden Kontrollen, um die FFS-induzierten Effekte von jenen des Lösungsmittel separieren zu können.

Aus dieser Veröffentlichung entstand ein Standardprotokoll zur Herstellung von Fettsäurelösungen (Supplement von [194]), welches potenzielle Fallstricke berücksichtigt und die Zubereitung von Lösungen unterschiedlicher Molarität mit definiertem FFS:BSA-Verhältnis, ver-

gleichbarer Konzentrationen von BSA und dem verwendeten Lösungsmittel sowie die Erstellung adäquater Kontrollen sicherstellt. Somit kann ein Experiment mit FFS standardisiert dokumentiert, durchgeführt und die Vergleichbarkeit gewährleistet werden. Dieses Protokoll wurde von anderen Autoren bereits als Referenz verwendet [221–223] (sowie über die persönliche Kommunikation via E-Mail).

Eine besondere Herausforderung ist die Quantifizierung von Lipotoxizität in vivo. Turpin et al. untersuchten den Einfluss einer Lipidinfusion, einer HFD sowie einer genetisch determinierten Leptindefizienz (ob/ob-Mäuse) auf verschiedene Parameter der Skelettmuskulatur, u.a. der Apoptose, Proteolyse und Autophagozytose. Bemerkenswerterweise führten diese Methoden zur Induktion einer Lipotoxizität nicht zu kongruenten Veränderungen der genannten Messparameter. So wiesen die ob/ob-Mäuse beispielsweise die höchsten Werte für die freien Fettsäuren im Plasma, aber keine vermehrte Apoptose des Skelettmuskels auf [224]. Wir schließen uns den Schlussfolderungen der Autoren, wonach ex vivo bzw. in vitro gewonnene Erkenntnisse aufgrund der Komplexität der Thematik nur eingeschränkt auf in vitro-Modelle übertragen werden können und folglich entsprechend kritisch geprüft werden müssen, an.

3.2 Die Glutaredoxine im Kontext des Diabetes mellitus

Die ersten in vivo-Untersuchungen der Glutaredoxinexpression der Langerhans'schen Inseln wurden im Rahmen dieser Arbeit anhand der db/db-Maus durchgeführt. Diese wurde erstmals 1966 beschrieben [225]. Der Stamm weist eine Punktmutation, welche eine Splicingmutation verursacht, im Downstreamintron des transmembranösen Leptinrezeptors Ob-Rb auf [226]. Dadurch sind die Mäuse unempfindlich gegenüber der Wirkung des Leptins. Dieses von Adipozyten ausgeschüttete und daher zur Gruppe der Adipokine gehörende Hormon ist wesentlich für die Energiehomöstase und das Ernährungsverhalten [227]. Insbesondere sorgt es über seine hypothalamische Wirkung für das Eintreten eines Sättigungsgefühls bzw. Inappetenz. Homozygote Tiere weisen somit eine Hyperphagie mit einer massiv gesteigerten Nahrungsaufnahme auf und entwickeln eine ausgeprägte Adipositas sowie eine diabetische Stoffwechsellage [228, 229]. Typischerweise prägen sich auch ausgeprägte Störungen des Lipidstoffwechsels mit einem Überfluss an FFS [230–232] sowie ektopen Fetteinlagerungen [233] aus, sodass sich das Modell zur Untersuchung von Lipotoxizität in vivo eignet.

In diesem Modell wurde die Expression der Glutaredoxine untersucht. Als Grundlage der Untersuchung dienten die Vorarbeiten der Arbeitsgruppe von Prof. Lillig, welche 2011 erstmals systematisch die Expression der Proteine der Thioredoxinfamilie in verschiedenen Geweben der Labormaus untersucht hatten [119]. Die mittels größtenteils eigens hergestellten Antikörpern entstandenen histologischen Präparate zeigen sowohl unterschiedliche Expressionsmuster in den verschiedenen Geweben als auch Unterschiede der Redoxine im jeweiligen Gewebe [119]. Die Autoren weisen ausdrücklich auf die Limitationen der Immunhistologie hin und diskutieren die Interpretation der Färbung als geeignete Methode zum Nachweis des Zielproteins – somit der Sensitivität und Spezifität der Analysen – und zur Zuordnung zu zellulären Strukturen [234, 235]. Dennoch stellte diese strukturierte Untersuchung der Redoxine ein Novum dar und lieferte erste Hinweise für eine differenzierte Funktion im Pankreas der Maus. Die Autoren konnten zeigen, dass Glrx1 und 5 relativ starke Fluoreszenzsignale erzeugen, und Glrx3 und 5 ein nukleäres Muster aufweisen. Dies wurde durch die eigene, vorliegende Arbeit bestätigt.

Unsere beiden Studien [195, 199] beschrieben erstmals den Verlust der Glutaredoxine 1 und 5 in den Inseln diabetischer Nager. Sie wiesen eine Korrelation mit dem diabetischen Phänotyp, dem Verlust des Insulingehalts und der Insulinexpression der Inseln sowie einer gesteigerten Anfälligkeit gegenüber der durch Glukose und TNF-α-vermittelten ROS-Produktion nach. Der Verlust von Glutaredoxin in MIN6-Zellen durch die Behandlung mit Ölsäure bzw. Hypoxie erbrachte erste Hinweise auf die zugrundeliegenden Mechanismen.

Die Ergebnisse fügen sich in die vorhandene Literatur, welche der Insulinsekretion und der β-Zellviabilität förderliche Effekte des Glutaredoxinsystems, v.a. durch Glrx1, beschreibt, ein [102,135,136,138,139]. Daten zur konkreten Bedeutung der Glutaredoxine für die β-Zelle bzw. die pankreatische Insel waren damals [95] wie heute sehr begrenzt [236]. Insbesondere Untersuchungen zur Relevanz für die Inseln im diabetischen Tiermodell wurden nicht durchgeführt, was die Bedeutung unserer Studien betont.

Es gibt zahlreiche Mausmodelle für den Typ 2 Diabetes, die sich in ihrer Diabetessuszeptibilität stark voneinander unterscheiden. Je nach dem genetischen Hintergrund gibt es diesbezüglich auch enorme Divergenzen innerhalb der jeweiligen Stämme [237], so auch bei der db-Maus. Auf dem BKS-Hintergrund weisen diese Tiere beispielsweise einen raschen Verlust

an β-Zellmasse und konsekutiv des messbaren Plasmainsulins sowie eine starke Hyperglykämie auf [238], wohingegen der B6-Hintergrund über eine vergrößerte Inselzellmasse und daraus resultierender Hyperinsulinämie zu einer Kompensation in der Lage ist und eher mäßig erhöhte Glukosewerte zeigt [239]. Die im Rahmen der Studie verwendeten BKS(D)-Leprdb/JOrlRj-Mäuse (Charles River) entwickelten im Einklang mit der Literatur einen stark adipösen und diabetischen Phänotyp. Dieser war in der ersten Studie kompensiert, die Tiere präsentierten keine ausgeprägte Polyurie oder -dipsie [195]. In der zweiten Studie [199] hingegen kam es zu einer Dekompensation des Stoffwechsels mit ausgeprägter Symptomatik. Warum die db-Tiere des gleichen Stamms diesen deutlich stärker ausgeprägteren diabetischen Phänotyp aufwiesen, ist nicht eindeutig geklärt. Der einzige Unterschied zu den zuvor verwendeten Mäusen war das Alter, mit welchen die Tiere in unsere Tierhaltung übernommen wurden (4 bzw. 10 Wochen), sodass die Haltungslokalisation und -bedingungen inkl. Käfigart und Gruppengröße pro Käfig die Unterschiede bedingt haben können. Es gibt in der wissenschaftlichen Literatur zahlreiche Belege für einen signifikanten Einfluss dieser Größen auf die Entwicklung und den Phänotyp von Labormäusen bis hin zu histopathologischen Veränderungen der Langerhans'schen Inseln in Diabetesmodellen [240–242], sodass diese Erklärung plausibel erscheint.

Die deutlich größere Inselfläche der diabetischen db/db-Tiere wurde als Kompensationsmechanismus der Insulinresistenz und Hyperglykämie interpretiert. Passend dazu wiesen die Inseln eine signifikant höhere Anzahl an Ki-67-positiven, jedoch auch Caspase-3 positiven Zellen auf. Eine solche Inselplastizität ist für Nagerinseln beschrieben worden, ist jedoch für Primaten untypisch [178, 179]. Diese Inselplastizität und ausgeprägte Veränderungen der Inselkomposition wurde in der Literatur vielfach beschrieben [243–246]. Es ist davon auszugehen, dass dies durch verschiedene Mechanismen verursacht wird. Neben der β-Zellapoptose [247–249] ist die De- bzw. Redifferenzierung von β-Zellen dokumentiert [250–252]. Es gibt Hinweise darauf, dass FoxO1 eine Rolle für diese Entdifferenzierungprozesse bis hin zur Redifferenzierung in α-Zellen spielt [250]. Dies wurde von uns in einem Modell der mesenchymalen Stammzelle gezeigt [170], in der db-Maus allerdings nicht weiter verfolgt.

Über einige Befunde kann auch retrospektiv nur spekuliert werden. Hervorzuheben ist beispielsweise die Tatsache, dass die *Glrx1* mRNA-Expression in den db/db-Tieren negativ mit

der mittleren Inselgröße und den Ki-67-positiven Inselzellen, aber positiv mit der Inselanzahl korrelierte. Der Befund steht möglicherweise mit der antiapoptotischen und proproliferativen Funktion von Glrx1 in Zusammenhang. Ob hier aber ein vermehrter Verbrauch, eine Sekretion von Glrx1 oder ein ganz anderer Effekt vorliegt, ist unklar. Im Alter von 18 Wochen fand sich keine signifikant unterschiedliche mRNA-Expression beider Glrx zwischen den diabetischen und den nichtdiabetischen Tieren, obwohl sich ihr Phänotype maximal unterschied – die Größe der Inseln und ihre KI67-positive Zellen jedoch nicht. Es könnte sein, dass das Alter der Tiere eine Rolle spielt. Ob die murine insuläre Glrx-Expression sich im Laufe des Alters verändert, ist bisher nicht untersucht worden. Es ist allerdings auch denkbar, dass die heterozygote db-Mutation der im Rahmen der ersten Studie verwendeten Kontrolltiere für diese Befunde relevant ist.

Kritisch anzumerken ist, dass sich beiden Untersuchungen vornehmlich auf immunhistochemische Analysen stützen. Es wurden allerdings die von Godoy et al. validierten Antikörper verwendet, und die Expressionsmuster entsprachen den von der Arbeitsgruppe vorbeschriebenen [119]. Zusätzlich korrelierten diese mit der mRNA-Expressionen der Glrx.

Die db-Maus weist aufgrund ihres Leptinrezeptordefekts überdies hohe Leptinspiegel auf [253]. Kieffer und Habener hatten im Jahr 2000 den Begriff der sogenannten „adipo-insulären-Feedbackschleife“ bzw. -achse geprägt [254]. Der Theorie nach beeinflussen sich die Inselzellen des Pankreas und das Fettgewebe gegenseitig. Gemäß einiger Daten inhibiert Leptin die Transkription [255] und Sekretion von Insulin [256], welches wiederum die Leptintranskription [257] und -sekretion stimuliert [258]. Allerdings gibt es auch widersprüchliche bzw. konträre Befunde [259–261]. In den 2000er Jahren gab es daraufhin zahlreiche Publikationen zu der Thematik [262]. Insbesondere wurde der Frage nach einer therapeutischen Nutzbarkeit des Leptins nachgegangen. Coppari und Bjørbæk geben in ihrem Review aus 2012 einen Überblick über mehrere klinische Studien, welche die Wirksamkeit von rekombinantem Leptin im Diabetes mellitus im Kontext des Leptinspiegels untersucht haben [263]. Es lässt sich daraus ableiten, dass Leptin insbesondere bei Menschen mit einem niedrigen basalen Leptinspiegel eine positive Wirkung auf die Insulinwirkung und das Körpergewicht erzielt, wohingegen die meisten adipösen Patienten eine endogene Leptinresistenz aufweisen und somit nicht auf die exogene

Zufuhr ansprechen. Ein aktuelles Review von Obradovic et al. zeigt keine wesentlichen neuen Befunde. Die Ergebnisse der Leptintherapie im Menschen variieren stark und sind nicht kongruent. Positive Effekte waren insbesondere mit der Koapplikation von Amylin, einem von den β-Zellen sezernierten Peptidhormon, zu verzeichnen [264].

Der Einfluss des Leptins auf die murine β-Zelle wurde anhand von MIN6-Zellen untersucht. Unsere Untersuchung konnte keinen Effekt des Leptins auf den Insulingehalt oder die -sekretion sowie den Glrx5-Gehalt der MIN6-Zelle zeigen. Damit war davon auszugehen, dass der Effekt nicht spezifisch für die db-Maus ist. Es sei erwähnt, dass die Literaturrecherche nach „leptin AND (glutaredoxin* OR glrx OR grx)“ neben unserer Studie nur eine einzige weitere, welche sich nicht auf die β-Zelle bezieht, findet (PubMed, Stand: 08/2023).

In einem zweiten Versuchsaufbau wurde der Einfluss von Ölsäure und Hypoxie auf die MIN6-Zelle, ihre Insulinsekretion und ihren Glrx5-Gehalt untersucht. Das mitochondriale Glrx5 ist aufgrund seiner Lokalisation im Mitochondrium im Kontext der Lipotoxizität besonders interessant, zudem konnten wir einen ausgeprägten Anstieg der ROS in den Inseln der diabetischen db/db-Tiere zeigen. Da die DCFH-DA-Methode vor allem H_2O_2 nachweist, und die Mitochondrien hierfür die Hauptquelle darstellen [265], ist davon auszugehen, dass es sich vornehmlich um mitochondriale ROS handelt. MIN6-Zellen wurden für 24 h gegenüber 0, 0,5 bzw. 0,75 mM Ölsäure in normaler oder hypoxischer (2% O_2) Atmosphäre exponiert. Es zeigte sich sowohl als Reaktion auf die Ölsäure als auch die Hypoxie eine signifikante Verminderung der per ELISA gemessenen Glrx5-Proteinmenge als Hinweis auf einen Zusammenhang mit der Lipotoxizität. Hypoxie ist ein unspezifischer Stressor, jedoch gibt es Hinweise darauf, dass in der β-Zelle in Phasen von hoher metabolischer Belastung hypoxieähnliche Zustände, welche die Insulinsekretion von Ratten- und Hundeinseln kompromittieren [266], herrschen [267]. Als Folge wurde Apoptose, eine Hochregulation von NF-κB und oxidativer Disstress [268] beschrieben. In den Inseln diabetischer db-Mäuse wurde eine Hochregulation von in die Hypoxiestressantwort involvierten Genen entdeckt [269]. Watanabe et. al konnten nachweisen, dass ein Mangel an Glrx1 in einem Modell der murinen Extremitätenischämie den hypoxieinduzierten Faktor (HIF) 1α stabilisiert und somit die Revaskularisierung fördert [270]. Der Zusammenhang zwischen Glutaredoxinen und der β-Zell- oder Inselhypoxie ist außer durch uns bisher nicht untersucht

worden. Die beiden Studien konnten noch keinen direkten Bezug zwischen dem Protein und der mitochondrialen Funktion herstellen. Insbesondere die Regulation der Redoxine im Diabetes mellitus blieb ungeklärt. Diesen offenen Fragen wurde in der nächsten Studie nachgegangen.

In einer dritten Studie konnten wir anhand eines weiteren Mausmodells den Verlust von Glutaredoxin 5 im Zustand der Adipositas mit Glukoseintoleranz bzw. Diabetes mellitus zeigen. Hierfür wurde in C57BL/6J-Mäusen diätetisch mittels einer HFD eine Adipositas und ein Überfluss an freien Fettsäuren induziert. Der Stamm ist bekannt für seine Empfänglichkeit gegenüber der Entwicklung eines diätetisch induzierten Typ 2 Diabetes mellitus [271, 272]. Verschiedene Autoren konnten zeigen, dass die Makronährstoffzusammensetzung der Nahrung relevanten Einfluss auf die Inselfunktion haben kann [273, 274]. Aus diesem Grund wurde im Rahmen der diätetischen Intervention zudem überprüft, ob ein Diätwechsel Einfluss auf die insuläre Glrx5-Expression hat.

Das HFD-Mausmodell konnte darlegen, dass dieser Glrx5-Verlust auch in einem weniger stark ausgeprägten Phänotyp als jenem der db-Maus auftritt und per Diät induzierbar ist. Zwei Befunde der Studie sind besonders bemerkenswert: Zum einen, dass der insuläre Glrx5-Gehalt durch den Diätwechsel von HFD auf die kohlenhydratreiche Diät und umgekehrt verändert wurde, und zum anderen, dass zwar Ölsäure (und Palmitinsäure) den Glrx5-Gehalt in MIN6-Zellen beeinflusst, nicht aber die Behandlung mit Glukose oder Zytokinen.

HFD werden in der Literatur häufig verwendet, um eine Adipositas und/oder einen (Prä)Diabetes in Mäusen zu induzieren [275]. Eine Alternative stellt die saccharosereiche Ernährung dar. Diätwechsel hingegen werden weitaus seltener durchgeführt. Interessanterweise konnten Sumiyoshi et al. feststellen, dass beide Diäten eine unterschiedliche Art der Glukoseintoleranz verursachen. Mäuse, die eine HFD erhielten, entwickelten ein deutlich höheres Körpergewicht und eine stärker ausgeprägte Insulinresistenz [276]. Zudem führt der Wechsel von einer HFD zu einer Standarddiät zu einem rascheren Gewichtsverlust. Die HFD erschien uns folglich als besser geeignetes Mittel zur Erzeugung eines murinen T2DM, vor allem im Hinblick auf den Diätwechsel mit dem Ziel der Normalisierung des Phänotyps.

Kluth et al. beschreiben einen ähnlichen Diätwechsel in einem Versuch mit New Zealand

Obese (NZO)-Mäusen. Diese Mäuse entwickeln eine schwere viszerale und subkutane Adipositas und eine gestörte Glukosetoleranz [277]. Im Versuch erhielten die Tiere nach dem Absetzen von den Muttertieren für 15 Wochen eine kohlenhydratfreie (fettreiche) Diät, unter welcher die Mäuse eine Adipositas und Insulinresistenz, aber keine Hyperglykämie entwickelten. Anschließend wurde einem Teil der Tiere für 16 Tage eine kohlenhydratreiche (fettarme) Diät gefüttert, die restlichen Tiere erhielten weiter die ursprüngliche Kost. Die Umstellung auf die kohlenhydratreiche Diät führte in diesem Modell zu einer deutlichen Hyperglykämie und nach einem initialen Anstieg des Plasmainsulingehalts zum β-Zellversagen mit schwindendem Plasmainsulingehalt [278]. In den Inseln der kohlenhydratreich gefütterten Mäuse kam es zu einem deutlichen Verlust von PDX1 und Insulin, gemessen per Histologie. Somit konnte auch in dieser Studie ein deutlicher Effekt der Diät auf Parameter der Inseln und ihre Proteinexpression gezeigt werden. Interessanterweise reagierten die Mäuse jedoch im Vergleich zu unserem Versuch nahezu gegenteilig auf die Einführung von Kohlenhydraten. Anzumerken ist hier, dass Kluth et al. eine ketogene Diät ohne jeglichen Kohlenhydratgehalt verwendeten, und die NZO-Maus ein völlig anderes Mausmodell, welches auch ohne Diätintervention die beschriebenen Stoffwechselpathologien ausbildet, darstellt. Da keine Rückumstellung von der kohlenhydratreichen auf die ketogene Diät erfolgt war, ist unklar, ob eine Regeneration der Inselfunktion wie in unserem Versuch erfolgt wäre. Eine solche ist in der Literatur dokumentiert [279, 280], wobei je nach Mausmodell und Diät auch gegenteilige Effekte, nämlich eine Beeinträchtigung bzw. ein Ausbleiben der Inselerholung, beschrieben sind [281]. Während zahlreiche Humanstudien den Einfluss eines Gewichtsverlusts auf Funktionsparameter der Inseln dokumentieren [282, 283], gibt es aus Gründen der Verfügbarkeit keine gute Datenbasis für humanes Pankreasgewebe. Eine Übersicht über den Einfluss von Ernährung und Bewegung auf die β-Zellen geben Lv et al. in einem aktuellen Review [284].

Anhand unserer erhobenen Daten kann die Frage, ob Glrx5 eine kausale Rolle für die Inselfunktion und -viabilität aufweist, oder ob der Verlust schlichtweg Zeichen einer generellen Funktionsstörung und eines Schadens der Inseln darstellt, nicht beantwortet werden. Unsere Zellkulturdaten konnten die Effekte der Lipo-, Glukotoxizität und der Inflammation separieren. Zusammengefasst veränderten nur die Fettsäureprotokolle den Glrx5-Gehalt der MIN6-Zelle,

nicht jedoch die Glukose oder die inflammatorischen Zytokine. Somit lieferten diese Daten Hinweise darauf, dass der Verlust von Glrx5 durch Lipotoxizität, nicht aber durch Hyperglykämie oder Inflammation vermittelt wird. Es lässt sich mutmaßen, dass die Lipotoxizität der wesentliche Treiber des Verlusts von Glrx5 darstellt. Ob hier ein spezifischer Effekt vorliegt, oder ein Korrelat des β-Zellschadens gemessen wird, verbleibt unklar. Ebenso stellt sich die Frage, ob der Glrx5-Verlust als spezifischer Effekt einer durch die FFS induzierten mitochondrialen Dysfunktion zu werten ist. MIN6-Zellen sind überdies Tumorzellen, sodass eine andersartige Regulation im Vergleich zu reinen β-Zellen möglich ist. Präliminäre, noch nicht publizierte Daten der Arbeitsgruppe zeigen jedoch dieselben Effekte einer Exposition gegenüber Ölsäure auf den Glrx5- und Insulingehalt sowie die Insulinsekretion in humanen β-Zellen (EndoC-βH3), sodass wir nicht von einem zell- oder speziesspezifischen Effekt ausgehen.
Betrachtet man die Literatur zur Lipotoxizität, fällt auf, dass sowohl die Öl- als auch die Palmitinsäure zu einer Verringerung der Glrx5-Menge und mRNA-Expression führten. Der Ölsäure wird eigentlich eine protektive Rolle zugeschrieben [285, 286]. So konnten Liu et al. zeigen, dass sie in Ratten-β-Zellen (INS-1E) protektiv gegen die palmitinsäureinduzierten Lipotoxizität wirkt und so die Zellviabilität erhält und ER-Stress mindert [287]. In Ratteninseln steigerte Ölsäure auch die Insulinsekretion [288], und eine ölsäurehaltige Diät verbesserte in Zucker fatty rats die Plasmaglukose sowie das Lipidprofil und verringerte das Körperfett, die Fettgewebsinflammation und erhielt die Inselkapazität aufrecht [289]. In diesen Studien wurden jedoch weitaus geringere Ölsäurekonzentrationen angewendet bzw. im Tiermodell gemessen (i.d.R. ca. 0,5 mM oder weniger) als von uns angewendet (bis rund 3 mM in der Zellkultur und in den mit HFD gefütterten C57BL/6-Tieren), was erneut die Relevanz der experimentellen Bedingungen verdeutlicht.

In unseren Studien wurde nach unserer Kenntnis zudem zum ersten Mal in vivo und in vitro eine Regulation des *Glrx5*-Gens in der β-Zelle bzw. den Langerhans'schen Inseln im Kontext des Diabetes mellitus beschrieben. Die Regulation der Glrx war lange ungeklärt bzw. strittig. Das *GLRX*-Gen im Säuger wurde erst 1997, rund 20 Jahre nach der Erstbeschreibung der Glrx, durch Park und Levine beschrieben [290]. Die Autoren detektierten damals auch Bindungs-

stellen für redoxaktive Substanzen im Glrx-Promotor, was als Bestätigung der Rolle der Glrx in der zellulären Redoxhomöostase gewertet wurde. Die genaue Regulation von Glrx5 in der β-Zelle im Diabetes mellitus und die von der *Glrx5*-Expression abhängigen Gene sind nicht abschließend geklärt. Cai et al. untersuchten die Expression von *Glrx5* in bovinen Adipozyten und fanden u.a. eine Abhängigkeit der PPARγ-Expression von jener des Glrx5 [291]. Aufgrund der Bedeutung des Faktors für den Glukosestoffwechsel lässt es sich darüber spekulieren, ob die durch uns beschriebenen Stoffwechselpathologien im Rahmen der verminderten Glrx5-Expression möglicherweise über PPARγ vermittelt werden. Die Regulation des *Glrx5*-Gens in der β-Zelle im Diabetes mellitus ist Neuland, Schlussfolgerungen sind folglich sehr spekulativ, und es gibt reichlich Raum für zukünftige Experimente.

Zusammenfassend konnten die Studien eine bis dato nicht beschriebene, ausgeprägte Veränderung der insulären Verteilungsmuster von Glrx1 und 5 und ihres insulären Gehalts zeigen. Die Befunde korrelieren mit einer für Mausmodelle des T2DM typischen funktionellen und morphologischen Inselplastizität und der Ausprägung des diabetischen Phänotyps. Es konnte dargelegt werden, dass Glrx5 durch Lipotoxizität reguliert wird und eng mit dem mitochondrialen Status zusammenhängt. Zukünftige Studien werden zeigen müssen, ob sich Glrx5 als therapeutisches oder diagnostisches Zielprotein eignet. Präliminäre, noch nicht publizierte Daten der Arbeitsgruppe zeigen eine Abhängigkeit der *GLRX5* mRNA-Expression im Blut von Menschen mit Diabetes von ihrer residuellen Insulineigensekretion – jene mit höherem C-Peptid hatten auch eine höhere *GLRX5*-Expression. Zudem ergeben sich erste Hinweise auf eine Resistenz einer Glrx5-überexprimierenden MIN6-Zelle gegenüber schädlichen Effekten der Ölsäure auf die Aktivität der Aconitase 1, und erste PCR-Daten aus Glrx5-unterexprimierenden Zellen deuten auf eine verminderte *Ins1* und *Ins2* mRNA-Expression hin. Die Glutaredoxine, vor allem Glrx5, erscheinen daher im Hinblick auf β-zellprotektive Therapie und als potenzielle messbare Parameter für die insuläre Funktion als vielversprechende Forschungsobjekte.

3.3 Die Thioredoxine im Kontext des Diabetes mellitus

Godoy et al. beschreiben in der bereits erwähnten, eingehenden histologischen Analyse des Mauspankreas ein stark ausgeprägtes Signal für Trx1 und TrxR1 im endokrinen, aber auch exokrinen Pankreasgewebe, wohingegen für Trx2 und TrxR2 nur ein sehr schwaches Signal zu messen war. Wie auch Glrx5 zeigte Trx1 Zeichen einer nukleären Lokalisation [119]. Die Relevanz der beiden Thioredoxinsysteme für die β-Zelle ist weitesgehend ungeklärt. Interessanterweise gibt es eine etwas breitere Datenbasis zu Txnip. Dieser nach zu urteilen wirkt eine Txnip-Defizienz durch die Verbesserung der β-Zellviabilität protektiv. In Inseln diabetischer Nager ist das Protein jedoch von mehreren Autoren als hochreguliert beschrieben worden [292] (eine Übersicht geben [293, 294]).

Die wesentlichen Befunde der vorliegenden Arbeit sind zum einen die gegensätzliche Regulation des zytosolischen und mitochondrialen Thioredoxinsystems unter Hypoxie, zum anderen die hypoxieinduzierte Sekretion von Trx1, welche im Transplantationsmodell aber nur mit funktionierenden TrxR erfolgte. Das sezernierte Trx1 hatte nicht nur eine apoptosehemmende und immunsuppressive, sondern bemerkenswerterweise auch eine parakrine, die Insulinsekretion fördernde Wirkung auf die β-Zelle.

Diese Erkenntnisse fügen sich in die vorhandene Literatur ein, bieten aber auch Raum für Spekulationen. Chou et al. haben bereits 2009 beschrieben, dass die insuläre Überexpression von Trx1 im Maus-zu-Maus-Inseltransplantationsmodell (Non-Obese Diabetic [NOD]-Mäuse) das Überleben der transplantierten Inseln steigert, wodurch die Plasmaglukose der Transplantatempfänger länger kontrolliert wird. Der Trx-Proteingehalt wurde allerdings nur vor der Transplantation untersucht, die Trx1-Sekretion gar nicht [295]. Anhand unserer erhobenen Daten erscheint es als plausibel, dass die festgestellten positiven Effekte durch sezerniertes Trx1 vermittelt werden, welches im Rahmen der Überexpression in größerer Menge zur Verfügung steht. Diese Hypothese der parakrinen Wirkung wird durch die Tatsache, dass die endogene Überexpression weder unter hypoglykämen (50 mg/dl), noch unter hyperglykämen Bedingungen (301 mg/dl) eine gesteigerte Insulinsekretion zur Folge hatte, gestützt. Interessanterweise konnten Cohen-Kutner et al. bereits 2013 zeigen, dass die exogene Anwendung von Trx-ähnlichen Peptiden die auranofininduzierte Apoptose und Störung der Insulinsekretion in INS

832/13-Zellen milderte bzw. wiederherstellte [296]. Darüber hinaus hatten Ivarsson et al. schon 2005 gezeigt, dass das intrazelluläre Trx1 im Gegensatz zu Glrx1 die NADPH-vermittelte Exozytose in Ratteninseln und INS-1-Zellen hemmt statt fördert [102]. Protektive Effekte durch die insuläre Überexpression von Trx1 wurden von Hotta et al. beschrieben. Die Autoren entdeckten, dass die insuläre Überexpression von Trx1 protektiv gegen sowohl die spontane als auch die STZ-induzierte Entwicklung eines Diabetes in NOD-Mäusen wirkt [103]. Auch in dieser Studie wurde der Trx1-Gehalt vor Beginn der Experimente gemessen und eine mögliche Sekretion nicht untersucht. Der zugrundeliegende Mechanismus könnte unter anderem durch die von uns gezeigte Hemmung der Makrophagenmigration mitbedingt sein, da die Infiltration mononukleärer Zellen in die Inseln ein wesentlicher Befund in diabetischen NOD-Mäusen ist [297]. Obgleich bisher kein entsprechender Rezeptor identifiziert werden konnte, gibt es in der Literatur zahlreiche Hinweise auf eine Bedeutung von sezerniertem Trx1 für das Immunsystem [298–300]. Wir konnten zeigen, dass die Chemotaxis von Mausmakrophagen durch die Redoxaktivität des Proteins vermittelt wird, sodass es denkbar ist, dass es sich nicht um einen rezeptorvermittelten Effekt handelt.

Ein weiterer Aspekt der protektiven Wirkung der Thioredoxine für die β-Zelle könnte der Schutz vor H_2O_2 sein. Trx1 sorgt gemeinsam mit Prx wesentlich für dessen Entgiftung [301]. Dementsprechend wurde gezeigt, dass die Trx1-Überexpression den schädlichen Einfluss von H_2O_2 auf die Inselviabilität vermindert [295]. In Trx1 überexprimierenden Ratteninseln und INS-1E-Zellen konnte ein Schutz vor durch Mycophenolsäure induzierter Apoptose und ROS-Entstehung gezeigt werden, wohin die Herabregulation von Trx1 die gegenteiligen Effekte zeigte [302]. Inwieweit diese eher klassische Funktion des Thioredoxinsystems in unserer Studie im Kontext der Trx1-Sekretion unter Hypoxie und Inflammation eine Rolle spielt, und ob das Trx2-System diesbezüglich möglicherweise eine kompensatorische Funktion einnimmt, ist unklar, denn über das Trx2-System und beide TrxR sind weitaus weniger Daten verfügbar. Unserer Interpretation nach ist die gegensätzlichen Regulation und die schädliche Folge des auranofin-induzierten Verlustes von Trx2/TrxR2 ein Zeichen der kompartimentalisierten aber dennoch miteinander verwobenen Redoxreaktionen.

Liu et al. haben den Einfluss der Inhibierung von Trx2 durch Methylglyoxal auf INS-1-Zellen

untersucht. Diese wiesen eine gesteigerte Menge an mitochodrialen ROS (vornehmlich H_2O_2 und O_2^-) und Zeichen der mitochondrialen Dysfunktion, nämlich eine morphologische Degeneration, eine verminderte Expression der Cytochrom-c-Oxidase (COX) Untereinheit 1 und 4 und eine geringere Menge ATP, auf. Die Überexpression von Trx2 wirkte dem entgegen [303]. Der homozygote Knockout von Trx2 ist nicht mit dem Leben vereinbar, wie anhand eines Mausmodells gezeigt werden konnte. Die Embryonen verstarben innerhalb der ersten 14 Tage und zeigten eine ausgeprägte Apoptose [304]. Unabhängig von der Sekretion des Trx1 ist der Verlust des mitochondrialen Trx2-Systems für die Zelle folglich nicht zu kompensieren.

Es gibt wenige Daten zur Relevanz der TrxR für die β-Zelle. Eine β-zellspezifische TrxR1-Knockout-Maus wurde von Stancill et al. charakterisiert. Die Inseln der Tiere zeigten eine gestörte GSIS, wobei ihre Glukosetoleranz bemerkenswerterweise unverändert war. Auch die Empfindlichkeit gegenüber H_2O_2-induzierten Zellschäden war nicht größer als bei den Kontrollen. Die TrxR1-defizienten β-Zellen wiesen jedoch einen Verlust der Expression von Genen, welche für die β-Zellidentität relevant sind, u.a. PDX1, auf. Die Autoren schlussfolgern, dass es über die vermehrte Expression von nuclear factor erythroid 2-related factor 2 (Nrf2)-regulierten Genen zu einer adaptiven und kompensatorischen Antwort kommt, da für diese eine gesteigerte Expression zu verzeichnen war [305]. Der TrxR1-Knockout führte nicht zu einer kompensatorischen Mehrexpression von Trx1 oder Prx1/2. Brüning et al. haben den Effekt einer chemischen Inhibition von TrxR1 in MIN6-Zellen und NMRI-Inseln untersucht [306]. Sie konnten in diesen Modellen eine geringere Viabilität nachweisen. Die Inseln zeigten unter Behandlung eine unveränderte basale, aber unter Stimulation mit 541 mg/dl Glukose leicht gesteigerte Insulinsekretion. Der Verlust der TrxR1 scheint also zumindest kurzfristig keine drastischen Effekte auf die β-Zelle zu haben, wobei die Datenbasis äußerst gering ist. Hinsichtlich einer Überexpression oder eines Knockouts der TrxR2 sind im Kontext der β-Zelle keine Daten verfügbar. In C57BL/6-Mäusen wurde der nach großflächigen Verbrennungsverletzungen gestörte Glukosestoffwechsel, welcher auf Hypoxie, oxidativen Disstress und Inflammation zurückgeführt wird, untersucht. Hier zeigte sich eine mitochondriale Dysfunktion mit einer gesteigerten ROS-Bildung, und die Aktivität und Proteinmenge der TrxR2 war signifikant vermindert. Das gleiche galt für die Proteinmenge des Trx2, nicht jedoch für Trx1 und TrxR1 [307].

Das lokale pankreatische / Inselmilieu wurde nicht untersucht, sodass unklar ist, welchen Bedingungen die Langerhans'schen Inseln ausgesetzt waren. Es ist jedoch davon auszugehen, dass unser Modell lokal einen ausgeprägteren hypoxischen und inflammatorischen Reiz auf die Inseln auslöst, sodass sich die diskrepanten Resultate hierdurch erklären lassen.

Die Gruppe um Stancill et al. führte ähnlich zu unserer Studie eine Auranofinbehandlung durch und zeigte eine signifikante Sensibilisierung von Ratteninseln und der Ratteninsulinomzellreihe INS 832/13 gegenüber dem Einfluss von H_2O_2 [308]. Das Ausschalten beider TrxR erzeugt demnach offenbar stärkere Effekte als die Hemmung nur einer der beiden Reduktasen. ROS sind in unserer Studie nicht gemessen worden, ihr vermehrtes Anfallen sind jedoch ein typisches Merkmal der hypoxischen Stressantwort der β-Zelle. Sie werden darüber hinaus durch Gluko- und Lipotoxizität induziert [107, 309]. Somit erklärt sich das rasche Transplantatversagen in den auranofinbehandelten Tieren offenbar zumindest teilweise durch eine drastisch herabgesetzte Viabilität ob der fehlenden Abwehrkapazität gegen ROS.

Eine graphische Zusammenfassung der gewonnenen Erkenntnisse über das Thioredoxinsystem im Kontext des Diabetes mellitus gibt Abbildung 3.1. Die wenigen vorhandenen Daten bestätigen unsere Hypothese, dass beide Trx-Systeme gemeinsam für die Viabilität und endokrine Funktion der β-Zelle entscheidend und der Verlust des einen nicht einfach durch das andere kompensiert werden kann. Interessant wäre die Prüfung einer systemischen Gabe von Thioredoxin aus therapeutischer Intention.

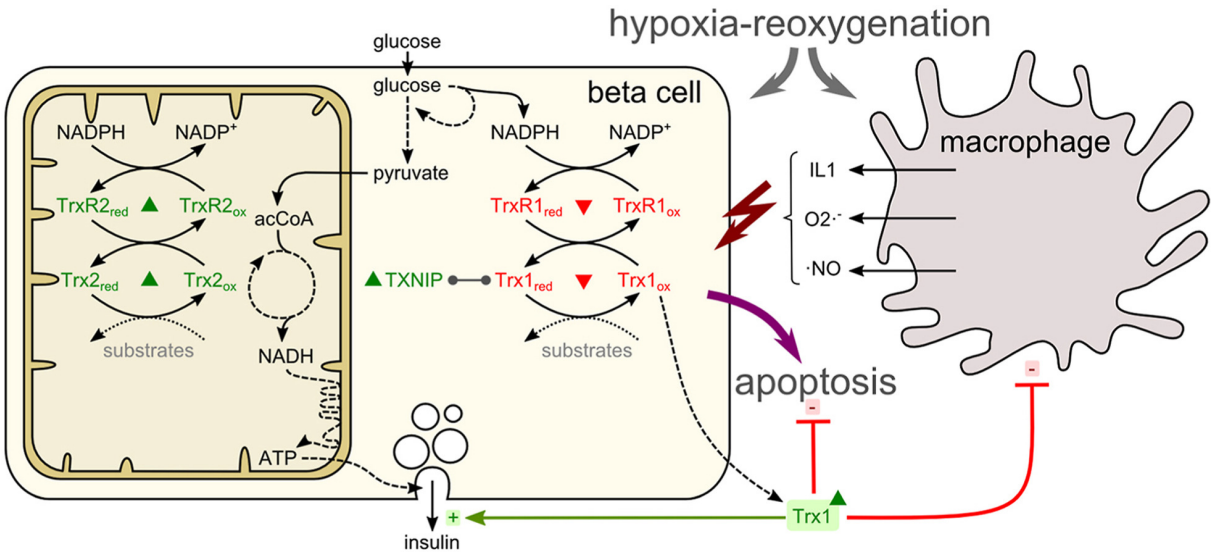

Abbildung 3.1: **Graphische Zusammenfassung der Erkenntnisse über das Thioredoxinsystem im Kontext des Diabetes mellitus.** Unter hypoxischem und immunvermitteltem Stress wird das zytosolische Trx-System (Trx1, TrxR1) herab- und das mitochondriale (Trx2, TrxR2) hochreguliert. Trx1 wird aus der β-Zelle sezerniert. Es wirkt antiinflammatorisch, protektiv und fördert die Insulinsekretion. Das Ausschalten beider Trx-Systeme führt zum Untergang der β-Zelle [98].

4. Zusammenfassung

Die Diabetologie erlebt eine rasante technologische und pharmakologische Entwicklung mit zahlreichen neuen Behandlungsmöglichkeiten. Die Insuffizienz und der Verlust der pankreatischen, einzig insulinproduzierenden β-Zellen ist bisher im klinischen Alltag jedoch nach wie vor nicht gezielt therapierbar. In der vorliegenden Arbeit wurden die Gluta- und Thioredoxine als potentielle Zielproteine für neuartige Therapien in verschiedenen Modellen des Diabetes mellitus untersucht. Diese ubiquitär exprimierten Proteine beeinflussen grundlegende zelluläre Funktionen. Glutaredoxin (Glrx) 1 und 2 sind wesentlich für die zelluläre Redoxregulation. Glrx3 und 5 werden für die Biosynthese der mitochondrialen Eisen-Schwefel (FeS)-Kofaktoren und die Reifung von FeS-Proteinen benötigt. Die Thioredoxine (Trx1 und 2) sind in die Regulation der DNA-Synthese, Genexpression, den Zellzyklus und die Immunmodulation eingebunden.

Das Glutaredoxinsystem wurde im Kontext der Lipotoxizität untersucht. Die verfügbaren Erkenntnisse zur Auswirkung letzterer auf die β-Zellen wurden in einer ausführlichen Übersichtsarbeit zusammengestellt und diskutiert. Es konnte herausgearbeitet werden, dass die Beurteilung der vorhandenen Literatur wesentlich durch die heterogenen methodischen Ansätze erschwert wird. Parameter wie die Zusammensetzung der Fettsäurelösungen, die Kultivierungszeit, die Kettenlänge der Fettsäuren, ihre Sättigung und vor allem ihre Konzentration führen zu mitunter stark divergierenden Ergebnissen. Solche Einflüsse wurde im murinen β-Zellmodell anhand der MIN6-Zelle untersucht. Es zeigte sich, dass z.B. die optische Dichte des MTT-Assays und die Insulinsekretion in hohem Maße von der Zusammensetzung der Fettsäurelösung, des verwendeten Lösungsmittels und der Behandlungsdauer abhängig sind. Aus der Untersuchung erwuchs ein Standardprotokoll zur Herstellung von Fettsäurelösungen zwecks Sicherstellung der Vergleichbarkeit und Reproduzierbarkeit, welches bereits von anderen Autoren angewendet wurde.

Anhand von homozygoten, leptinresistenten db-Mäusen, welche spontan eine Adipositas mit Diabetes mellitus entwickeln, konnte erstmals den Verlust der insulären Glutaredoxine, ins-

besondere 1 und 5, nachgewiesen werden. Dieser Befund korrelierte mit dem diabetischen Phänotyp der Tiere und tiefgreifenden, pathologischen Veränderungen der Proliferation, Apoptose, Morphologie, zellulären Zusammensetzung und Funktion ihrer Langerhans'schen Inseln sowie einer gesteigerten insulären ROS-Produktion im Vergleich zu den gesunden Kontrollen, heterozygoten db-Tieren bzw. C57BL/6-Wildtypen. In einer weiteren Studie wurde der Verlust des insulären mitochondrialen Glrx5 auch in einem Mausmodell des per stark fetthaltiger Diät induzierten Diabetes mellitus mit Adipositas nachgewiesen. Bemerkenswerterweise führte die Umstellung der Ernährung auf eine Standardkost neben der Regredienz des Phänotyps und der Wiederherstellung der Glukosetoleranz in C57BL/6-Tieren auch zu einer Rekonstitution der insulären Glrx5-Expression. Anhand von MIN6-Zellen wurden die Effekte der Lipo-, Glukotoxizität und Inflammation separiert. Die Lipotoxizität stellte sich als Mediator des Glrx5-Verlusts heraus, wohingegen die Hyperglykämie und inflammatorische Zytokine keinen Einfluss auf die Expression des Redoxins nahmen. Die β-Zellen mit Glrx5-Verlust wiesen eine ausgeprägte mitochondriale Dysfunktion, charakterisiert durch den Mangel an ATP, dem Überfluss von ROS und der gestörten mitochondrialen Bioenergetik auf. In Folge dessen war die endokrine Funktion, gemessen an der Insulinsekretion, signifikant beeinträchtigt. Als Schlussfolgerung wird Glrx5 als potenzielles Bindeglied zwischen der Lipotoxizität, der mitochondrialen Dysfunktion und der gestörten Insulinsekretion der β-Zelle im Diabetes mellitus angesehen.

Das Thioredoxinsystem wurde im Kontext der Inflammation sowie der Hypoxie und Reoxygenierung untersucht. Erstmals wurde im Modell der Schwein-zu-Maus-Inseltransplantation, der MIN6-Zelle sowie humanen Blutproben aus der klinischen Inseltransplantation eine kompartimentalisierte Regulation der zytosolischen, mitochondrialen und extrazellulären Thioredoxine nachgewiesen. Zudem konnte die Sekretion von Trx1 aus der β-Zelle, welche jedoch eine funktionierende Trx-Reduktase voraussetzt, gezeigt werden. Das sezernierte Trx1 übte eine redoxvermittelte parakrine Wirkung auf die Langerhans'schen Inseln und MIN6-Zellen aus und förderte deren Viabilität und Insulinsekretion.

Folglich wird für die Gluta- und Thioredoxine Potential für weitere translationale Forschungsbemühungen im Hinblick auf β-zellerhaltende und -regenerative Therapien gesehen.

5. Summary

Diabetology is experiencing rapid technological and pharmacological progress. However, the insufficiency and loss of the insulin-producing pancreatic β-cells cannot yet be specifically treated in daily clinical practice. In the present work, the significance of glutaredoxins and thioredoxins as potential novel therapeutic targets in different models of diabetes mellitus has been studied. These ubiquitously expressed proteins control basic cellular functions. Glutaredoxin (Glrx) 1 and 2 are major actors in cellular redox regulation. Glrx3 and 5 are involved in the biosynthesis of mitochondrial iron-sulfur (FeS) cofactors and required for the maturation of FeS proteins. Thioredoxins (Trx1 and 2) regulate DNA synthesis, gene expression, and cell cycle and exert immunomodulatory effects.

Glutaredoxins were studied in the context of lipotoxicity. The current knowledge of its impact on the β-cell was summarized and discussed in a thorough review. It was concluded that the methodological approaches to model lipotoxicity differ significantly, which makes the interpretation of the available data complex. This comprises the composition of the fatty acid solutions, the chain length, saturation, and concentration of the employed fatty acids, and the time of exposure and cultivation. The impact of such parameters on the murine β-cell was investigated with the MIN6-cell. The data showed a significant impact on e.g., the optical density of the MTT-assay and the insulin secretion dependent on the composition of the fatty acid solution, the employed solvent, and the duration of the treatment. This study led to a standard protocol for the preparation of fatty acid solutions to ensure comparability and reproducibility. It has since been employed by other authors.

By employing homozygous, leptin-resistant db-mice, which spontaneously develop obesity and diabetes mellitus, a loss of the insular glutaredoxins, specially 1 and 5, was detected for the first time. This depreviation of glutaredoxins correlated with the diabetic phenotype of the animals and profound, pathological changes in proliferation, apoptosis, morphology, cellular composition, and function of their islets of Langerhans, as well as increased insular ROS production when compared with healthy controls, heterozygous db animals and C57BL/6 wild-type animals, re-

spectively. Furthermore, the loss of the mitochondrial Glrx5 in islets of C57BL/6 mice in which obesity and diabetes were induced by a high fat diet was found. Remarkably, the shift to a standard diet led to the reconstitution of the insular expression of Glrx5 concomittant with a relief from the diabetic phenotype and the amelioration of the glucose homeostasis. In MIN6-cells, the effects of lipotoxicity, glucotoxicity, and inflammation were separated by respective culture conditions. Interestingly, only lipotoxicity as modelled by free fatty acids mediated the loss of glutaredoxin 5, whereas it was not affected by hyperglycemia and inflammatory cytokines. β-cells which were depraved of Glrx5 exhibited a marked level of mitochondrial dysfunction as characterized by the lack of ATP, the excess of ROS, and impaired mitochondrial bioenergetics. Their endocrine function, as measured by insulin secretion, was significantly impaired. In conclusion, Glrx5 is considered a potential link between lipotoxicity, mitochondrial dysfunction, and the impaired insulin secretion of the β-cell in diabetes mellitus.

The thioredoxin system was studied in the context of inflammation and hypoxia and reoxygenation. In a pig-to-mouse model of islet transplantation, MIN6-cells, and human blood samples derived from clinical islet transplantation, a compartmentalized regulation of the cytosolic, mitochondrial, and extracellular thioredoxins was shown for the first time. A secretion of Trx1 by the β-cell, which required a functional Trx reductase, was detected. Secreted Trx1 increased the viability of islets and MIN6-cells and improved their insulin secretion via its redox activity.

In conclusion, glutaredoxins and thioredoxis are considered potential targets for further translational research efforts with regard to β-cell-maintaining and -regenerative therapies.

6. Abkürzungsverzeichnis

Abkürzung	Bedeutung
AGE	advanced glycation endproduct
AID	automated insulin delivery
AMPK	Adenosine monophosphate-activated protein kinase
ATP	Adenosintriphosphat
BSA	bovines Serumalbumin
C32S	redox-inaktive Cys32Ser Mutante von humanem rekombinantem Thioredoxin 1
CD	cluster of differentiation
COX	Cytochrom-c-Oxidase
CREB	cAMP response element-binding protein
DAG	Diacylglycerol
DCFH-DA	2',7'-Dichlorfluorescein-Diacetat
dhTrx1	denaturiertes humanes rekombinantes Thioredoxin 1
DMSO	Dimethylsulfoxid
Dmt1	Divalent metal transporter 1
ER	endoplasmatisches Retikulums
FASIS	fatty acid stimulated insulin secretion
Fe	Eisen
FeS	Eisen-Schwefel
FFA1	free fatty acid receptor 1
FFS	freie Fettsäure
FOXO	Forkhead-Box-Protein O
GAD65	Glutamatcarboxylase
GDM	Gestationsdiabetes mellitus
Glrx	Glutaredoxin

GLUT2	Glukosetransporter Typ 2
Gpx	Glutathionperoxidase
GIP	glukoseabhängiges insulinotropes Peptid
GLP1	glucagon-like Peptide 1
GPG	Gelegenheitsplasmaglukose
GR	Glutathionreduktase
GSH	Glutathion (reduzierte Form)
GSIS	glukosestimulierte Insulinsekretion / glucose-stimulated insulin secretion
GSSG	Glutathion (oxidierte Form)
HFD	fettreiche Diät / high fat diet
HIF	hdypoxieinduzierter Faktor
HLA	human leukocyte antigen
hTrx1	humanes rekombinantes Thioredoxin 1
IA2	Tyrosinphosphatase
IAA	Insulin-Autoantikörper
IBMIR	instant blood-mediated inflammatory response
ICA	Inselzellantikörper
IFG	gestörte Nüchternglukose / impaired fasting glucose
IGF	gestörte Glukosetoleranz / impaired glucose tolerance
IKKβ	inhibitor of nuclear factor kappa-B kinase subunit beta
IL	Interleukin
IPGTT	intraperitonealer Glukosetoleranztest
LDH	Laktat-Dehydrogenase
LDL	low density lipoprotein
MARD	moderate age-related diabetes
MIN6	mouse insulinoma 6
MOD	moderate obesity diabetes
MTT	3-(4,5-Dimethylthiazol-2-yl)-2,5-diphenyltetrazoliumbromid
NaCl	Natriumchlorid

NADP	Nicotinamidadenindinukleotidphosphat (oxidierte Form)
NADPH	Nicotinamidadenindinukleotidphosphat (reduzierte Form)
NaOH	Natriumhydroxid
NF-κB	Nuclear factor kappa B
NOD	Non-Obese Diabetic
NPG	Nüchternplasmaglukose
NZO	New Zealand Obese
OGTT	oraler Glukosetoleranztest
OXPHOS	oxidative Phosphorylierung
PBMC	periphere mononukleäre Blutzellen
PDX1	pancreatic and duodenal homeobox 1
PPAR	peroxisome proliferator-activated receptor
PKC	Proteinkinase C
Prx	Peroxiredoxin
PTP1B	protein-tyrosine phosphatase-1B
ROS	reaktive Sauerstoffspezies
RSIS	redox stimulated insulin secretion
SAID	severe autoimmune diabetes
SDH	Succinat-Dehydrogenase
SGLT2	sodium glucose transporter 2
SIDD	severe insulin-deficient diabetes
SIRD	severe insulin-resistent diabetes
STZ	Streptozotocin
IDF	International Diabetes Federation
IFN	Interferon
T1DM	Typ 1 Diabetes mellitus
T2DM	Typ 2 Diabetes mellitus
TNF	Tumornekrosefaktor
Trx	Thioredoxin

TrxR	Thioredoxinreduktase
VEGF-A	Vascular Endothelial Growth Factor-A
ZnT8	pankreas-spezifischer Zinktransporter

7. Literaturverzeichnis

[1] Landgraf R, Heinemann L, Schleicher E, et al. Definition, Klassifikation, Diagnostik und Differenzialdiagnostik des Diabetes mellitus: Update 2022. Diabetol und Stoffwechsel., 17 (S 02):S98–S110, 2022. doi:10.1055/a-1789-5615.

[2] International Diabetes Federation. IDF Diabetes Atlas, 10th edn. Brussels, Belgium. https://www.diabetesatlas.org, 2021.

[3] Deutsche Diabetes Gesellschaft (DDG) und diabetesDE - Deutsche Diabetes-Hilfe. Deutscher Gesundheitsbericht Diabetes 2023, November 2022. ISSN 1614-824X.

[4] Tönnies T, Röckl S, Hoyer A, et al. Projected number of people with diagnosed Type 2 diabetes in Germany in 2040. Diabet Med., 36(10):1217–1225, Oct 2019. doi:10.1111/dme.13902.

[5] Rosenbauer J, Neu A, Rothe U, et al. Types of diabetes are not limited to age groups: type 1 diabetes in adults and type 2 diabetes in children and adolescents. J Health Monit., 4(2):29–49, Jun 2019. doi:10.25646/5987.

[6] Reitzle L, Schmidt C, Heidemann C, et al. Gestationsdiabetes in Deutschland: Zeitliche Entwicklung von Screeningquote und Prävalenz. J Health Monit., 6(2), June 2021. doi:10.25646/8324.

[7] Heidemann C and Scheidt-Nave C. Prevalence, incidence and mortality of diabetes mellitus in adults in Germany – A review in the framework of the Diabetes Surveillance. J Health Monit., 2(3), 2017. doi:10.17886/RKI-GBE-2017-062.

[8] Heald AH, Stedman M, Davies M, et al. Estimating life years lost to diabetes: outcomes from analysis of National Diabetes Audit and Office of National Statistics data. Cardiovasc Endocrinol Metab., 9(4):183–185, Dec 2020. doi:10.1097/XCE.0000000000000210.

[9] Pociot F, Akolkar B, Concannon P, et al. Genetics of type 1 diabetes: what's next? Diabetes., 59(7):1561–71, Jul 2010. doi:10.2337/db10-0076.

[10] Quinn LM, Wong FS, and Narendran P. Environmental Determinants of Type 1 Diabetes: From Association to Proving Causality. Front Immunol., 12:737964, 2021. doi:10.3389/fimmu.2021.737964.

[11] Tang Q, Adams JY, Penaranda C, et al. Central role of defective interleukin-2 production in the triggering of islet autoimmune destruction. Immunity., 28(5):687–97, May 2008. doi:10.1016/j.immuni.2008.03.016.

[12] Kent SC, Chen Y, Clemmings SM, et al. Loss of IL-4 secretion from human type 1a diabetic pancreatic draining lymph node NKT cells. J Immunol., 175(7):4458–64, Oct 2005. doi:10.4049/jimmunol.175.7.4458.

[13] Chen YL, Qiao YC, Pan YH, et al. Correlation between serum interleukin-6 level and type 1 diabetes mellitus: A systematic review and meta-analysis. Cytokine., 94:14–20, Jun 2017. doi:10.1016/j.cyto.2017.01.002.

[14] Shruthi S, Mohan V, Amutha A, et al. Increased serum levels of novel T cell cytokines IL-33, IL-9 and IL-17 in subjects with type-1 diabetes. Cytokine., 86:6–9, Oct 2016. doi:10.1016/j.cyto.2016.07.007.

[15] Bottazzo GF, Dean BM, McNally JM, et al. In situ characterization of autoimmune phenomena and expression of HLA molecules in the pancreas in diabetic insulitis. N Engl J Med., 313(6):353–60, Aug 1985. doi:10.1056/nejm198508083130604.

[16] Roep BO. T-cell responses to autoantigens in IDDM. The search for the Holy Grail. Diabetes., 45(9):1147–56, Sep 1996. doi:10.2337/diab.45.9.1147.

[17] Pietropaolo M, Towns R, and Eisenbarth GS. Humoral autoimmunity in type 1 diabetes: prediction, significance, and detection of distinct disease subtypes. Cold Spring Harb Perspect Med., 2(10):a012831, Oct 2012. doi:10.1101/cshperspect.a012831.

[18] Eisenbarth GS. Type I diabetes mellitus. A chronic autoimmune disease. N Engl J Med., 314(21):1360–8, May 1986. doi:10.1056/NEJM198605223142106.

[19] Atkinson MA and Eisenbarth GS. Type 1 diabetes: new perspectives on disease pathogenesis and treatment. Lancet., 358(9277):221–9, Jul 2001. doi:10.1016/s0140-6736(01)05415-0.

[20] Atkinson MA, Eisenbarth GS, and Michels AW. Type 1 diabetes. Lancet., 383(9911):69–82, Jan 2014. doi:10.1016/s0140-6736(13)60591-7.

[21] Lieberman SM and DiLorenzo TP. A comprehensive guide to antibody and T-cell responses in type 1 diabetes. Tissue antigens., 62(5):359–77, Nov 2003. doi:10.1034/j.1399-0039.2003.00152.x.

[22] Roep BO and Peakman M. Antigen targets of type 1 diabetes autoimmunity. Cold Spring Harb Perspect Med., 2(4):a007781, Apr 2012. doi:10.1101/cshperspect.a007781.

[23] Insel RA, Dunne JL, Atkinson MA, et al. Staging presymptomatic type 1 diabetes: a scientific statement of JDRF, the Endocrine Society, and the American Diabetes Association. Diabetes Care., 38(10):1964–74, Oct 2015. doi:10.2337/dc15-1419.

[24] Fuchsberger C, Flannick J, Teslovich TM, et al. The genetic architecture of type 2 diabetes. Nature., 536(7614):41–47, Aug 2016. doi:10.1038/nature18642.

[25] Dimas AS, Lagou V, Barker A, et al. Impact of type 2 diabetes susceptibility variants on quantitative glycemic traits reveals mechanistic heterogeneity. Diabetes., 63(6):2158–71, Jun 2014. doi:10.2337/db13-0949.

[26] Hara K, Shojima N, Hosoe J, et al. Genetic architecture of type 2 diabetes. Biochem Biophys Res Commun., 452(2):213–20, Sep 2014. doi:10.1016/j.bbrc.2014.08.012.

[27] Carey VJ, Walters EE, Colditz GA, et al. Body fat distribution and risk of non-insulin-dependent diabetes mellitus in women. The Nurses' Health Study. Am J Epidemiol., 145(7):614–9, Apr 1997. doi:10.1093/oxfordjournals.aje.a009158.

[28] Weinstein AR, Sesso HD, Lee IM, et al. Relationship of physical activity vs body mass index with type 2 diabetes in women. JAMA., 292(10):1188–94, Sep 2004. doi:10.1016/j.accreview.2004.11.012.

[29] Lynch J, Helmrich SP, Lakka TA, et al. Moderately intense physical activities and high levels of cardiorespiratory fitness reduce the risk of non-insulin-dependent diabetes mellitus in middle-aged men. Arch Intern Med., 156(12):1307–14, Jun 1996. doi:10.1001/archinte.1996.00440110073010.

[30] van Dam RM, Rimm EB, Willett WC, et al. Dietary patterns and risk for type 2 diabetes mellitus in U.S. men. Ann Intern Med., 136(3):201–9, Feb 2002. doi:10.7326/0003-4819-136-3-200202050-00008.

[31] DeFronzo RA. Pathogenesis of type 2 diabetes mellitus. Med Clin North Am., 88(4):787–835, Jul 2004. doi:10.1002/9781118387658.ch25.

[32] Tremaroli V and Bäckhed F. Functional interactions between the gut microbiota and host metabolism. Nature., 489(7415):242–9, Sep 2012. doi:10.1038/nature11552.

[33] Qin J, Li Y, Cai Z, et al. A metagenome-wide association study of gut microbiota in type 2 diabetes. Nature, 490(7418):55–60, Oct 2012. doi:10.1038/nature11450.

[34] Hectors TLM, Vanparys C, van der Ven K, et al. Environmental pollutants and type 2 diabetes: a review of mechanisms that can disrupt beta cell function. Diabetologia., 54(6):1273–90, Jun 2011. doi:10.1007/s00125-011-2109-5.

[35] Schmid SM, Hallschmid M, and Schultes B. The metabolic burden of sleep loss. Lancet Diabetes Endocrinol., 3(1):52–62, Jan 2015. doi:10.1016/s2213-8587(14)70012-9.

[36] Fazeli PK, Lee H, and Steinhauser ML. Aging Is a Powerful Risk Factor for Type 2 Diabetes Mellitus Independent of Body Mass Index. Gerontology., 66(2):209–210, 2020. doi:10.1159/000501745.

[37] Levy J, Atkinson AB, Bell PM, et al. Beta-cell deterioration determines the onset and rate of progression of secondary dietary failure in type 2 diabetes mellitus: the 10-year

follow-up of the Belfast Diet Study. Diabet Med., 15(4):290–6, Apr 1998. doi:10.1002/(sici)1096-9136(199804)15:4⟨290::aid-dia570⟩3.0.co;2-m.

[38] Calles-Escandon J and Robbins DC. Loss of early phase of insulin release in humans impairs glucose tolerance and blunts thermic effect of glucose. Diabetes., 36(10):1167–72, Oct 1987. doi:10.2337/diab.36.10.1167.

[39] Ahlqvist E, Storm P, Käräjämäki A, et al. Novel subgroups of adult-onset diabetes and their association with outcomes: a data-driven cluster analysis of six variables. Lancet Diabetes Endocrinol., 6(5):361–369, May 2018. doi:10.1016/S2213-8587(18)30051-2.

[40] Haak T, Gölz S, Fritsche A, et al. Therapie des Typ-1-Diabetes. Diabetol und Stoffwechsel., 16 (Suppl 2):S142–S153, 2021. doi:10.1055/a-1515-8682.

[41] Landgraf R, Aberle J, Birkenfeld AL, et al. Therapie des Typ-2-Diabetes. Diabetol und Stoffwechsel., 16 (Suppl 2):S168–206, 2021. doi:10.1055/a-1394-2313.

[42] Phillip M, Nimri R, Bergenstal RM, et al. Consensus Recommendations for the Use of Automated Insulin Delivery Technologies in Clinical Practice. Endocr Rev., 44(2):254–280, Mar 2023. doi:10.1210/endrev/bnac022.

[43] Robertson RP, Harmon J, Tran PO, et al. Glucose toxicity in beta-cells: type 2 diabetes, good radicals gone bad, and the glutathione connection. Diabetes., 52(3):581–7, Mar 2003. doi:10.2337/diabetes.52.3.581.

[44] Gleason CE, Gonzalez M, Harmon JS, et al. Determinants of glucose toxicity and its reversibility in the pancreatic islet beta-cell line, HIT-T15. Am J Physiol Endocrinol Metab., 279(5):E997–1002, Nov 2000. doi:10.1152/ajpendo.2000.279.5.E997.

[45] Flax H, Matthews DR, Levy JC, et al. No glucotoxicity after 53 hours of 6.0 mmol/l hyperglycaemia in normal man. Diabetologia., 34:570–5, Aug 1991. doi:10.1007/bf00400275.

[46] Merovci A, Tripathy D, Chen X, et al. Effect of Mild Physiologic Hyperglycemia on Insulin Secretion, Insulin Clearance, and Insulin Sensitivity in Healthy Glucose-Tolerant Subjects. Diabetes., 70(1):204–213, Jan 2021. doi:10.2337/db20-0039.

[47] Nathan DM, Kuenen J, Borg R, et al. Translating the A1C assay into estimated average glucose values. Diabetes Care., 31(8):1473–8, Aug 2008. doi:10.2337/dc08-0545.

[48] Colagiuri S, Lee CMY, Wong TY, et al. Glycemic thresholds for diabetes-specific retinopathy: implications for diagnostic criteria for diabetes. Diabetes Care., 34(1):145–50, Jan 2011. doi:10.2337/dc10-1206.

[49] Kaneto H, Fujii J, Myint T, et al. Reducing sugars trigger oxidative modification and apoptosis in pancreatic beta-cells by provoking oxidative stress through the glycation reaction. Biochem J., 320 (Pt 3):855–63, Dec 1996. doi:10.1042/bj3200855.

[50] Kaneto H, Xu G, Song KH, et al. Activation of the hexosamine pathway leads to deterioration of pancreatic beta-cell function through the induction of oxidative stress. J Biol Chem., 276(33):31099–104, Aug 2001. doi:10.1074/jbc.M104115200.

[51] Nishikawa T, Edelstein D, Du XL, et al. Normalizing mitochondrial superoxide production blocks three pathways of hyperglycaemic damage. Nature., 404(6779):787–790, Apr 2000. doi:10.1038/35008121.

[52] Olson LK, Redmon JB, Towle HC, et al. Chronic exposure of HIT cells to high glucose concentrations paradoxically decreases insulin gene transcription and alters binding of insulin gene regulatory protein. J Clin Invest., 92(1):514–9, July 1993. doi:10.1172/JCI116596.

[53] Kajimoto Y, Matsuoka T, Kaneto H, et al. Induction of glycation suppresses glucokinase gene expression in HIT-T15 cells. Diabetologia., 42(12):1417–24, Dec 1999. doi:10.1007/s001250051313.

[54] Kawamori D, Kaneto H, Nakatani Y, et al. The forkhead transcription factor Foxo1 bridges the JNK pathway and the transcription factor PDX-1 through its intracellular translocation. J Biol Chem., 281:1091–8, Jan 2006. doi:10.1074/jbc.m508510200.

[55] Elouil H, Bensellam M, Guiot Y, et al. Acute nutrient regulation of the unfolded protein response and integrated stress response in cultured rat pancreatic islets. Diabetologia., 50(7):1442–52, May 2007. doi:10.1007/s00125-007-0674-4.

[56] Maedler K, Sergeev P, Ris F, et al. Glucose-induced beta cell production of IL-1beta contributes to glucotoxicity in human pancreatic islets. J Clin Invest., 110(6):851–860, Sep 2002. doi:10.1172/JCI15318.

[57] Lee Y, Hirose H, Ohneda M, et al. Beta-cell lipotoxicity in the pathogenesis of non-insulin-dependent diabetes mellitus of obese rats: impairment in adipocyte-beta-cell relationships. Proc Natl Acad Sci U S A., 91(23):10878–82, Nov 1994. doi:10.1073/pnas.91.23.10878.

[58] Elsner M, Gehrmann W, and Lenzen S. Peroxisome-generated hydrogen peroxide as important mediator of lipotoxicity in insulin-producing cells. Diabetes., 60(1):200–8, Jan 2011. doi:10.2337/db09-1401.

[59] Cunha DA, Hekerman P, Ladrière L, et al. Initiation and execution of lipotoxic ER stress in pancreatic beta-cells. J Cell Sci., 121(14):2308–2318, Jul 2008. doi:10.1242/jcs.026062.

[60] Solinas G, Naugler W, Galimi F, et al. Saturated fatty acids inhibit induction of insulin gene transcription by JNK-mediated phosphorylation of insulin-receptor substrates. Proc Natl Acad Sci U S A., 103(44):16454–16459, Oct 2006. doi:10.1073/pnas.0607626103.

[61] Okamura DM, Pennathur S, Pasichnyk K, et al. CD36 regulates oxidative stress and inflammation in hypercholesterolemic CKD. J Am Soc Nephrol., 20(3):495–505, Mar 2009. doi:10.1681/asn.2008010009.

[62] Maedler K, Spinas GA, Dyntar D, et al. Distinct effects of saturated and monounsaturated fatty acids on beta-cell turnover and function. Diabetes., 50(1):69–76, Jan 2001. doi:10.2337/diabetes.50.1.69.

[63] Lipke K, Kubis-Kubiak A, and Piwowar A. Molecular Mechanism of Lipotoxicity as an Interesting Aspect in the Development of Pathological States-Current View of Knowledge. Cells., 11(5):844, Mar 2022. doi:10.3390/cells11050844.

[64] Snel M, Jonker JT, Schoones J, et al. Ectopic fat and insulin resistance: pathophysiology and effect of diet and lifestyle interventions. Int J Endocrinol., 2012:983814, 2012. doi:10.1155/2012/983814.

[65] Koves TR, Ussher JR, Noland RC, et al. Mitochondrial overload and incomplete fatty acid oxidation contribute to skeletal muscle insulin resistance. Cell Metab., 7(1):45–56, Jan 2008. doi:10.1016/j.cmet.2007.10.013.

[66] Itani SI, Ruderman NB, Schmieder F, et al. Lipid-induced insulin resistance in human muscle is associated with changes in diacylglycerol, protein kinase C, and IkappaB-alpha. Diabetes., 51(7):2005–11, Jul 2002. doi:10.2337/diabetes.51.7.2005.

[67] Tordjman K, Standley KN, Bernal-Mizrachi C, et al. PPARalpha suppresses insulin secretion and induces UCP2 in insulinoma cells. J Lipid Res., 43(6):936–43, Jun 2002. doi:10.1016/S0022-2275(20)30468-5.

[68] Maris M, Robert S, Waelkens E, et al. Role of the saturated nonesterified fatty acid palmitate in beta cell dysfunction. J Proteome Res., 12(1):347–62, Jan 2013. doi:10.1021/pr300596g.

[69] Cnop M, Hannaert JC, Hoorens A, et al. Inverse relationship between cytotoxicity of free fatty acids in pancreatic islet cells and cellular triglyceride accumulation. Diabetes., 50(8):1771–7, Aug 2001. doi:10.2337/diabetes.50.8.1771.

[70] Syed I, Szulc ZM, Ogretmen B, et al. L- threo -C6-pyridinium-ceramide bromide, a novel cationic ceramide, induces NADPH oxidase activation, mitochondrial dysfunction and loss in cell viability in INS 832/13 β-cells. Cell Physiol Biochem., 30(4):1051–8, 2012. doi:10.1159/000341481.

[71] Koshkin V, Wang X, Scherer PE, et al. Mitochondrial functional state in clonal pancreatic beta-cells exposed to free fatty acids. J Biol Chem., 278(22):19709–15, May 2003. doi:10.1074/jbc.M209709200.

[72] Akoumi A, Haffar T, Mousterji M, et al. Palmitate mediated diacylglycerol accumulation causes endoplasmic reticulum stress, Plin2 degradation, and cell death in H9C2 cardiomyoblasts. Exp Cell Res., 354(2):85–94, May 2017. doi:10.1016/j.yexcr.2017.03.032.

[73] Ly LD, Ly DD, Nguyen NT, et al. Mitochondrial Ca(2+) Uptake Relieves Palmitate-Induced Cytosolic Ca(2+) Overload in MIN6 Cells. Mol Cells., 43(1):66–75, Jan 2020. doi:10.14348/molcells.2019.0223.

[74] Zhou YP, Berggren PO, and Grill V. A fatty acid-induced decrease in pyruvate dehydrogenase activity is an important determinant of beta-cell dysfunction in the obese diabetic db/db mouse. Diabetes., 45(5):580–6, May 1996. doi:10.2337/diab.45.5.580.

[75] Anello M, Lupi R, Spampinato D, et al. Functional and morphological alterations of mitochondria in pancreatic beta cells from type 2 diabetic patients. Diabetologia., 48(2):282–9, Feb 2005. doi:10.1007/s00125-004-1627-9.

[76] Ma Z, Wirström T, Borg LA, et al. Diabetes reduces beta-cell mitochondria and induces distinct morphological abnormalities, which are reproducible by high glucose in vitro with attendant dysfunction. Islets., 4(3):233–42, 2012. doi:10.4161/isl.20516.

[77] Römer A, Linn T, and Petry SF. Lipotoxic Impairment of Mitochondrial Function in β-Cells: A Review. Antioxidants (Basel)., 10(2):293, Feb 2021. doi:10.3390/antiox10020293.

[78] Cadenas E and Sies H. Oxidative stress: excited oxygen species and enzyme activity. Adv Enzyme Regul., 23:217–37, 1985. doi:10.1016/0065-2571(85)90049-4.

[79] Sies H. Oxidative stress: from basic research to clinical application. Am J Med., 91(3C):31S–38S, Sep 1991. doi:10.1016/0002-9343(91)90281-2.

[80] Davies AM and Holt AG. Why antioxidant therapies have failed in clinical trials. J Theor Biol., 457:1–5, Nov 2018. doi:10.1016/j.jtbi.2018.08.014.

[81] Forman HJ, Ursini F, and Maiorino M. An overview of mechanisms of redox signaling. J Mol Cell Cardiol., 73:2–9, Aug 2014. doi:10.1016/j.yjmcc.2014.01.018.

[82] Benáková S, Holendová B, and Plecitá-Hlavatá L. Redox Homeostasis in Pancreatic β-Cells: From Development to Failure. Antioxidants (Basel)., 10(4):526, Mar 2021. doi:10.3390/antiox10040526.

[83] Lenzen S, Drinkgern J, and Tiedge M. Low antioxidant enzyme gene expression in pancreatic islets compared with various other mouse tissues. Free Radic Biol Med., 20(3):463–6, 1996. doi:10.1016/0891-5849(96)02051-5.

[84] Plecitá-Hlavatá L, Engstová H, Holendová B, et al. Mitochondrial Superoxide Production Decreases on Glucose-Stimulated Insulin Secretion in Pancreatic β Cells Due to Decreasing Mitochondrial Matrix NADH/NAD(+) Ratio. Antioxid Redox Signal., 33(12):789–815, Oct 2020. doi:10.1089/ars.2019.7800.

[85] Janjic D, Maechler P, Sekine N, et al. Free radical modulation of insulin release in INS-1 cells exposed to alloxan. Biochem Pharmacol., 57(6):639–48, Mar 1999. doi:10.1016/s0006-2952(98)00346-3.

[86] Maechler P, Jornot L, and Wollheim CB. Hydrogen peroxide alters mitochondrial activation and insulin secretion in pancreatic beta cells. J Biol Chem., 274(39):27905–13, Sep 1999. doi:10.1074/jbc.274.39.27905.

[87] Marques ES, Formato E, Liang W, et al. Relationships between type 2 diabetes, cell dysfunction, and redox signaling: A meta-analysis of single-cell gene expression of human pancreatic α- and β-cells. J Diabetes., 14(1):34–51, Jan 2022. doi:10.1111/1753-0407.13236.

[88] Lei XG and Cheng WH. Selenium, chapter New roles of glutathione peroxidase-1 in oxidative stress and diabetes, pages 173–182. Springer US, Boston, MA, 2006. ISBN 978-0-387-33827-9. doi:10.1007/0-387-33827-6_16.

[89] Grunewald RW, Weber II, Kinne-Saffran E, et al. Control of sorbitol metabolism in renal inner medulla of diabetic rats: regulation by substrate, cosubstrate and products of the aldose reductase reaction. Biochim Biophys Acta., 1225(1):39–47, Nov 1993. doi:10.1016/0925-4439(93)90119-l.

[90] Sies H, Berndt C, and Jones DP. Oxidative Stress. Annu Rev Biochem., 86(1):715–748, 2017. doi:10.1146/annurev-biochem-061516-045037.

[91] Loreto Palacio P, Godoy JR, Aktas O, et al. Changing Perspectives from Oxidative Stress to Redox Signaling-Extracellular Redox Control in Translational Medicine. Antioxidants (Basel)., 11, Jun 2022. doi:10.3390/antiox11061181.

[92] Sies H. Oxidative eustress: On constant alert for redox homeostasis. Redox Biol., 41:101867, May 2021. doi:10.1016/j.redox.2021.101867.

[93] Sies H. Oxidative Stress: Concept and Some Practical Aspects. Antioxidants (Basel)., 9(9):852, Sep 2020. doi:10.3390/antiox9090852.

[94] Lushchak VI. Free radicals, reactive oxygen species, oxidative stress and its classification. Chem Biol Interact., 224:164–75, Dec 2014. doi:10.1016/j.cbi.2014.10.016.

[95] Hanschmann EM, Godoy JR, Berndt C, et al. Thioredoxins, glutaredoxins, and peroxiredoxins–molecular mechanisms and health significance: from cofactors to antioxidants to redox signaling. Antioxid Redox Signal., 19(13):1539–605, Nov 2013. doi:10.1089/ars.2012.4599.

[96] Laurent TC, Moore EC, and Reichard P. Enzymatic synthesis of deoxyribonucleotides. IV. ISOLATION AND CHARACTERIZATION OF THIOREDOXIN, THE HYDROGEN DONOR FROM ESCHERICHIA COLI B. J Biol Chem., 239:3436–44, Oct 1964. doi:10.1016/S0021-9258(18)97742-2.

[97] Rubartelli A, Bajetto A, Allavena G, et al. Secretion of thioredoxin by normal and neoplastic cells through a leaderless secretory pathway. J Biol Chem., 267(34):24161–4, Dec 1992. doi:10.1016/s0021-9258(18)35742-9.

[98] Hanschmann EM, Petry SF, Eitner S, et al. Paracrine regulation and improvement of β-cell function by thioredoxin. Redox Biol., 34:101570, Jul 2020. doi:10.1016/j.redox.2020.101570.

[99] Abate C, Patel L, Rauscher FJ, et al. Redox regulation of fos and jun DNA-binding activity in vitro. Science., 4973(249):1157–61, Sep 1990. doi:10.1126/science.2118682.

[100] Saitoh M, Nishitoh H, Fujii M, et al. Mammalian thioredoxin is a direct inhibitor of apoptosis signal-regulating kinase (ASK) 1. EMBO J., 17(9):2596–606, May 1998. doi:10.1093/emboj/17.9.2596.

[101] Steinbrenner H, Speckmann B, and Klotz LO. Selenoproteins: Antioxidant selenoenzymes and beyond. Arch Biochem Biophys., 595:113–9, Apr 2016. doi:10.1016/j.abb.2015.06.024.

[102] Ivarsson R, Quintens R, Dejonghe S, et al. Redox control of exocytosis: regulatory role of NADPH, thioredoxin, and glutaredoxin. Diabetes., 54(7):2132–42, Jul 2005. doi:10.2337/diabetes.54.7.2132.

[103] Hotta M, Tashiro F, Ikegami H, et al. Pancreatic beta cell-specific expression of thioredoxin, an antioxidative and antiapoptotic protein, prevents autoimmune and streptozotocin-induced diabetes. J Exp Med., 188(8):1445–51, Oct 1998. doi:10.1084/jem.188.8.1445.

[104] Yamamoto M, Yamato E, Toyoda S, et al. Transgenic expression of antioxidant protein thioredoxin in pancreatic beta cells prevents progression of type 2 diabetes mellitus. Antioxid Redox Signal., 10(1):43–9, Jan 2008. doi:10.1089/ars.2007.1586.

[105] Ikegami H, Ono M, Fujisawa T, et al. Molecular scanning of the gene for thioredoxin, an antioxidative and antiapoptotic protein, and genetic susceptibility to type 1 diabetes. Ann N Y Acad Sci., 1150:103–5, Dec 2008. doi:10.1196/annals.1447.060.

[106] Parikh H, Carlsson E, Chutkow WA, et al. TXNIP Regulates Peripheral Glucose Metabolism in Humans. PLoS Med., 4(5):e158, May 2007. doi:10.1371/journal.pmed.0040158.

[107] Schulze PC, Yoshioka J, Takahashi T, et al. Hyperglycemia promotes oxidative stress through inhibition of thioredoxin function by thioredoxin-interacting protein. J Biol Chem., 279(29):30369–74, Jul 2004. doi:10.1074/jbc.m400549200.

[108] Miyamoto S, Kawano H, Hokamaki J, et al. Increased plasma levels of thioredoxin in patients with glucose intolerance. Intern Med., 44(11):1127–32, Nov 2005. doi:10.2169/internalmedicine.44.1127.

[109] Kakisaka Y, Nakashima T, Sumida Y, et al. Elevation of serum thioredoxin levels in patients with type 2 diabetes. Horm Metab Res., 34(3):160–4, Mar 2002. doi:10.1055/s-2002-23201.

[110] Chernatynskaya AV, Looney B, Hu H, et al. Administration of recombinant human thioredoxin-1 significantly delays and prevents autoimmune diabetes in nonobese diabetic mice through modulation of autoimmunity. Diabetes Metab Res Rev., 27(8):809–12, Nov 2011. doi:10.1002/dmrr.1232.

[111] Pekkari K, Gurunath R, Arner ES, et al. Truncated thioredoxin is a mitogenic cytokine for resting human peripheral blood mononuclear cells and is present in human plasma. J Biol Chem., 275(48):37474–80, Dec 2000. doi:10.1074/jbc.m001012200.

[112] Bizzarri C, Holmgren A, Pekkari K, et al. Requirements for the different cysteines in the chemotactic and desensitizing activity of human thioredoxin. Antioxid Redox Signal., 7(9-10):1189–94, Sep-Oct 2005. doi:10.1089/ars.2005.7.1189.

[113] Holmgren A. Hydrogen donor system for Escherichia coli ribonucleoside-diphosphate reductase dependent upon glutathione. Proc Natl Acad Sci U S A., 73(7):2275–9, Jul 1976. doi:10.1073/pnas.73.7.2275.

[114] Holmgren A. Glutathione-dependent synthesis of deoxyribonucleotides. Purification and characterization of glutaredoxin from Escherichia coli. J Biol Chem., 254(9):3664–71, May 1979. doi:10.1016/s0021-9258(18)50813-9.

[115] Lillig CH, Berndt C, and Holmgren A. Glutaredoxin systems. Biochim Biophys Acta., 1780(11):1304–17, Nov 2008. doi:10.1016/j.bbagen.2008.06.003.

[116] Lill R, Dutkiewicz R, Freibert SA, et al. The role of mitochondria and the CIA machinery in the maturation of cytosolic and nuclear iron-sulfur proteins. Eur J Cell Biol., 94(7-9):280–91, Jul-Sep 2015. doi:10.1016/j.ejcb.2015.05.002.

[117] Stehling O, Wilbrecht C, and Lill R. Mitochondrial iron-sulfur protein biogenesis and human disease. Biochimie., 100:61–77, May 2014. doi:10.1016/j.biochi.2014.01.010.

[118] Ogata FT, Branco V, Vale FF, et al. Glutaredoxin: Discovery, redox defense and much more. Redox Biol., 43:101975, Jul 2021. doi:10.1016/j.redox.2021.101975.

[119] Godoy JR, Funke M, Ackermann W, et al. Redox atlas of the mouse. Immunohistochemical detection of glutaredoxin-, peroxiredoxin-, and thioredoxin-family proteins in various tissues of the laboratory mouse. Biochim Biophys Acta., 1810(1):2–92, Jan 2011. doi:10.1016/j.bbagen.2010.05.006.

[120] Lundberg M, Fernandes AP, Kumar S, et al. Cellular and plasma levels of human glutaredoxin 1 and 2 detected by sensitive ELISA systems. Biochem Biophys Res Commun., 319(3):801–9, Jul 2004. doi:10.1016/j.bbrc.2004.04.199.

[121] Pai HV, Starke DW, Lesnefsky EJ, et al. What is the functional significance of the unique location of glutaredoxin 1 (GRx1) in the intermembrane space of mitochondria? Antioxid Redox Signal., 9(11):2027–33, Nov 2007. doi:10.1089/ars.2007.1642.

[122] Holmgren A. Thioredoxin and glutaredoxin systems. J Biol Chem., 264(24):13963–6, Aug 1989. doi:10.1016/s0021-9258(18)71625-6.

[123] Hirota K, Matsui M, Murata M, et al. Nucleoredoxin, glutaredoxin, and thioredoxin differentially regulate NF-kappaB, AP-1, and CREB activation in HEK293 cells. Biochem Biophys Res Commun., 274(1):177–82, Jul 2000. doi:10.1006/bbrc.2000.3106.

[124] Daily D, Vlamis-Gardikas A, Offen D, et al. Glutaredoxin protects cerebellar granule neurons from dopamine-induced apoptosis by activating NF-kappa B via Ref-1. J Biol Chem., 276(2):1335–44, Jan 2001. doi:10.1074/jbc.M008121200.

[125] Murata H, Ihara Y, Nakamura H, et al. Glutaredoxin exerts an antiapoptotic effect by regulating the redox state of Akt. J Biol Chem., 278(50):50226–33, Dec 2003. doi:10.1074/jbc.m310171200.

[126] Lekli I, Mukherjee S, Ray D, et al. Functional recovery of diabetic mouse hearts by glutaredoxin-1 gene therapy: role of Akt-FoxO-signaling network. Gene Ther., 17(4):478–85, Apr 2010. doi:10.1038/gt.2010.9.

[127] Takashima Y, Hirota K, Nakamura H, et al. Differential expression of glutaredoxin and thioredoxin during monocytic differentiation. Immunol Lett., 68(2-3):397–401, Jun 1999. doi:10.1016/s0165-2478(99)00087-5.

[128] Chrestensen CA, Starke DW, and Mieyal JJ. Acute cadmium exposure inactivates thioltransferase (Glutaredoxin), inhibits intracellular reduction of protein-glutathionyl-mixed disulfides, and initiates apoptosis. J Biol Chem., 275(34):26556–65, Aug 2000. doi:10.1074/jbc.m004097200.

[129] Ho YS, Xiong Y, Ho DS, et al. Targeted disruption of the glutaredoxin 1 gene does not sensitize adult mice to tissue injury induced by ischemia/reperfusion and hyperoxia. Free Radic Biol Med., 43(9):1299–312, Nov 2007. doi:10.1016/j.freeradbiomed.2007.07.025.

[130] Cater MA, Materia S, Xiao Z, et al. Glutaredoxin1 protects neuronal cells from copper-induced toxicity. Biometals., 27(4):661–72, Aug 2014. doi:10.1007/s10534-014-9748-1.

[131] Miller OG, Behring JB, Siedlak SL, et al. Upregulation of Glutaredoxin-1 Activates Microglia and Promotes Neurodegeneration: Implications for Parkinson's Disease. Antioxid Redox Signal., 25(18):967–982, Dec 2016. doi:10.1089/ars.2015.6598.

[132] Ho FM, Liu SH, Liau CS, et al. High glucose-induced apoptosis in human endothelial cells is mediated by sequential activations of c-Jun NH(2)-terminal kinase and caspase-3. Circulation., 101(22):2618–24, Jun 2000. doi:10.1161/01.cir.101.22.2618.

[133] Li S, Sun Y, Qi X, et al. Protective effect and mechanism of glutaredoxin 1 on coronary arteries endothelial cells damage induced by high glucose. Biomed Mater Eng., 24(6):3897–903, 2014. doi:10.3233/bme-141221.

[134] Qi X, Xu A, Gao Y, et al. Cardiac damage and dysfunction in diabetic cardiomyopathy are ameliorated by Grx1. Genet Mol Res., 15(3), Sep 2016. doi:10.4238/gmr.15039000.

[135] Reinbothe TM, Ivarsson R, Li DQ, et al. Glutaredoxin-1 mediates NADPH-dependent stimulation of calcium-dependent insulin secretion. J Mol Endocrinol., 23(6):893–900, Jun 2009. doi:10.1210/me.2008-0306.

[136] Shao D, Han J, Hou X, et al. Glutaredoxin-1 Deficiency Causes Fatty Liver and Dyslipidemia by Inhibiting Sirtuin-1. Antioxid Redox Signal., 27(6):313–327, Aug 2017. doi:10.1089/ars.2016.6716.

[137] Zhang L, Wang Y, Wang J, et al. Protein kinase C pathway mediates the protective effects of glucagon-like peptide-1 on the apoptosis of islet β-cells. Mol Med Rep., 12(5):7589–94, Nov 2015. doi:10.3892/mmr.2015.4355.

[138] Ward NE, Stewart JR, Ioannides CG, et al. Oxidant-induced S-glutathiolation inactivates protein kinase C-alpha (PKC-alpha): a potential mechanism of PKC isozyme regulation. Biochemistry., 39(33):10319–29, Aug 2000. doi:10.1021/bi000781g.

[139] Dong K, Wu M, Liu X, et al. Glutaredoxins concomitant with optimal ROS activate AMPK through S-glutathionylation to improve glucose metabolism in type 2 diabetes. Free Radic Biol Med., 101:334–47, Dec 2016. doi:10.1016/j.freeradbiomed.2016.10.007.

[140] Beilschmidt LK, Ollagnier de Choudens S, Fournier M, et al. ISCA1 is essential for mitochondrial Fe4S4 biogenesis in vivo. Nat Commun., 8:15124, 05 2017. doi:10.1038/ncomms15124.

[141] Rodríguez-Manzaneque MT, Tamarit J, Bellí G, et al. Grx5 is a mitochondrial glutaredoxin required for the activity of iron/sulfur enzymes. Mol Biol Cell., 13(4):1109–21, Apr 2002. doi:10.1091/mbc.01-10-0517.

[142] Camaschella C, Campanella A, De Falco L, et al. The human counterpart of zebrafish shiraz shows sideroblastic-like microcytic anemia and iron overload. Blood., 110(4):1353–8, Aug 2007. doi:10.1182/blood-2007-02-072520.

[143] Liu G, Guo S, Anderson GJ, et al. Heterozygous missense mutations in the GLRX5 gene cause sideroblastic anemia in a Chinese patient. Blood., 124(17):2750–1, Oct 2014. doi:10.1182/blood-2014-08-598508.

[144] Cooksey RC, Jones D, Gabrielsen S, et al. Dietary iron restriction or iron chelation protects from diabetes and loss of beta-cell function in the obese (ob/ob lep-/-) mouse. Am J Physiol Endocrinol Metab., 298(6):E1236–43, Jun 2010. doi:10.1152/ajpendo.00022.2010.

[145] Hansen JB, Tonnesen MF, Madsen AN, et al. Divalent metal transporter 1 regulates iron-mediated ROS and pancreatic β cell fate in response to cytokines. Cell Metab., 16(4):449–61, Oct 2012. doi:10.1016/j.cmet.2012.09.001.

[146] Rodríguez-Manzaneque MT, Ros J, Cabiscol E, et al. Grx5 glutaredoxin plays a central role in protection against protein oxidative damage in Saccharomyces cerevisiae. Mol Cell Biol., 19(12):8180–90, Dec 1999. doi:10.1128/MCB.19.12.8180.

[147] Linares GR, Xing W, Govoni KE, et al. Glutaredoxin 5 regulates osteoblast apoptosis by protecting against oxidative stress. Bone., 44(5):795–804, May 2009. doi:10.1016/j.bone.2009.01.003.

[148] Wingert RA, Galloway JL, Barut B, et al. Deficiency of glutaredoxin 5 reveals Fe-S clusters are required for vertebrate haem synthesis. Nature., 436(7053):1035–9, Aug 2005. doi:10.1038/nature03887.

[149] Wood ZA, Schröder E, Harris JR, et al. Structure, mechanism and regulation of peroxiredoxins. Trends Biochem Sci., 28(1):32–40, Jan 2003. doi:10.1016/s0968-0004(02)00003-8.

[150] Seo MS, Kang SW, Kim K, et al. Identification of a new type of mammalian peroxiredoxin that forms an intramolecular disulfide as a reaction intermediate. J Biol Chem., 275(27):20346–54, Jul 2000. doi:10.1074/jbc.m001943200.

[151] Fujii J and Ikeda Y. Advances in our understanding of peroxiredoxin, a multifunctional, mammalian redox protein. Redox Rep., 7(40):123–30, Feb 2002. doi:10.1179/135100002125000352.

[152] Neumann CA, Krause DS, Carman CV, et al. Essential role for the peroxiredoxin Prdx1 in erythrocyte antioxidant defence and tumour suppression. Nature., 424(6948):561–5, Jul 2003. doi:10.1038/nature01819.

[153] Lee TH, Kim SU, Yu SL, et al. Peroxiredoxin II is essential for sustaining life span of erythrocytes in mice. Blood., 101(12):5033–8, Jun 2003. doi:10.1182/blood-2002-08-2548.

[154] Li L, Shoji W, Takano H, et al. Increased susceptibility of MER5 (peroxiredoxin III) knockout mice to LPS-induced oxidative stress. Biochem Biophys Res Commun., 355(3):715–22, Apr 2007. doi:10.1016/j.bbrc.2007.02.022.

[155] Wang X, Phelan SA, Forsman-Semb K, et al. Mice with targeted mutation of peroxiredoxin 6 develop normally but are susceptible to oxidative stress. J Biol Chem., 278(27):25179–90, Jul 2003. doi:10.1074/jbc.m302706200.

[156] Heo S, Kim S, and Kang D. The Role of Hydrogen Peroxide and Peroxiredoxins throughout the Cell Cycle. Antioxidants (Basel)., 9(4):280, Mar 2020. doi:10.3390/antiox9040280.

[157] Lee YJ. Knockout Mouse Models for Peroxiredoxins. Antioxidants (Basel)., 9(2):182, Feb 2020. doi:10.3390/antiox9020182.

[158] Pirags V, Lebovitz H, and Fouqueray P. Imeglimin, a novel glimin oral antidiabetic, exhibits a good efficacy and safety profile in type 2 diabetic patients. Diabetes Obes Metab., 14(9):852–8, Sep 2012. doi:10.1111/j.1463-1326.2012.01611.x.

[159] Krako Jakovljevic N, Pavlovic K, Jotic A, et al. Targeting Mitochondria in Diabetes. Int J Mol Sci., 22(12), Jun 2021. doi:10.3390/ijms22126642.

[160] Accili D, Talchai SC, Kim-Muller JY, et al. When β-cells fail: lessons from dedifferentiation. Diabetes Obes Metab., 18 Suppl 1:117–22, Sep 2016. doi:10.1111/dom.12723.

[161] Aref A, Zayan T, Pararajasingam R, et al. Pancreatic transplantation: Brief review of the current evidence. World J Transplant., 9(4):81–93, Aug 2019. doi:10.5500/wjt.v9.i4.81.

[162] Fridell JA, Stratta RJ, and Gruessner AC. Pancreas Transplantation: Current Challenges, Considerations, and Controversies. J Clin Endocrinol Metab., 108(3):614–623, Feb 2023. doi:10.1210/clinem/dgac644.

[163] Weimar B, Rauber K, Brendel MD, et al. Percutaneous transhepatic catheterization of the portal vein: A combined CT- and fluoroscopy-guided technique. Cardiovasc Intervent Radiol., 22(4):342–4, Jul-Aug 1999. doi:10.1007/s002709900403.

[164] Gruessner AC. 2011 update on pancreas transplantation: comprehensive trend analysis of 25,000 cases followed up over the course of twenty-four years at the International Pancreas Transplant Registry (IPTR). Rev Diabet Stud., 8(1):6–16, Spring 2011. doi:10.1900/RDS.2011.8.6.

[165] Shapiro AMJ, Pokrywczynska M, and Ricordi C. Clinical pancreatic islet transplantation. Nat Rev Endocrinol., 13(5):268–277, May 2017. doi:10.1038/nrendo.2016.178.

[166] Takaichi S, Tomimaru Y, Akagi T, et al. Three-dimensional Vascularized β-cell Spheroid Tissue Derived From Human Induced Pluripotent Stem Cells for Subcutaneous Islet Transplantation in a Mouse Model of Type 1 Diabetes. Transplantation., 106(1):48–59, Jan 2022. doi:10.1097/TP.0000000000003745.

[167] Velazco-Cruz L, Song J, Maxwell KG, et al. Acquisition of Dynamic Function in Human Stem Cell-Derived β Cells. Stem Cell Reports., 12(2):351–365, Feb 2019. doi:10.1016/j.stemcr.2018.12.012.

[168] Wang X, Gao M, Wang Y, et al. The progress of pluripotent stem cell-derived pancreatic β-cells regeneration for diabetic therapy. Front Endocrinol (Lausanne)., 13:927324, 2022. doi:10.3389/fendo.2022.927324.

[169] Kanak MA, Takita M, Itoh T, et al. Alleviation of instant blood-mediated inflammatory reaction in autologous conditions through treatment of human islets with NF-κB inhibitors. Transplantation., 98(5):578–84, Sep 2014. doi:10.1097/tp.0000000000000107.

[170] Khatri R, Mazurek S, Petry SF, et al. Mesenchymal stem cells promote pancreatic β-cell regeneration through downregulation of FoxO1 pathway. Stem Cell Res Ther., 11(1):497, Nov 2020. doi:10.1186/s13287-020-02007-9.

[171] Khatri R, Petry SF, and Linn T. Intrapancreatic MSC transplantation facilitates pancreatic islet regeneration. Stem Cell Res Ther., 12(1):121, Feb 2021. doi:10.1186/s13287-021-02173-4.

[172] Zhong F and Jiang Y. Endogenous Pancreatic β Cell Regeneration: A Potential Strategy for the Recovery of β Cell Deficiency in Diabetes. Front Endocrinol (Lausanne)., 10:101, 2019. doi:10.3389/fendo.2019.00101.

[173] Wang P, Karakose E, Choleva L, et al. Human Beta Cell Regenerative Drug Therapy for Diabetes: Past Achievements and Future Challenges. Front Endocrinol (Lausanne)., 12:671946, 2021. doi:10.3389/fendo.2021.671946.

[174] Basile G, Qadir MMF, Mauvais-Jarvis F, et al. Emerging diabetes therapies: Bringing back the β-cells. Mol Metab., 60:101477, Jun 2022. doi:10.1016/j.molmet.2022.101477.

[175] Doering L, Khatri R, Petry SF, et al. Regulation of somatostatin expression by vitamin D3 and valproic acid in human adipose-derived mesenchymal stem cells. Stem Cell Res Ther., 10(1):240, Aug 2019. doi:10.1186/s13287-019-1330-x.

[176] Schröder C, Khatri R, Petry SF, et al. Class I and II Histone Deacetylase Inhibitor LBH589 Promotes Endocrine Differentiation in Bone Marrow Derived Human

Mesenchymal Stem Cells and Suppresses Uncontrolled Proliferation. Exp Clin Endocrinol Diabetes., 129(5):357–364, May 2021. doi:10.1055/a-1103-1900.

[177] Petry SF, Kandula ND, Günther S, et al. Valproic Acid Initiates Transdifferentiation of the Human Ductal Adenocarcinoma Cell-line Panc-1 Into α-Like Cells. Exp Clin Endocrinol Diabetes., Apr 2022. doi:10.1055/a-1750-9190.

[178] Puff R, Dames P, Weise M, et al. Reduced proliferation and a high apoptotic frequency of pancreatic beta cells contribute to genetically-determined diabetes susceptibility of db/db BKS mice. Horm Metab Res., 43(5):306–11, May 2011. doi:10.1055/s-0031-1271817.

[179] Kim A, Miller K, Jo J, et al. Islet architecture: A comparative study. Islets., 1(2):129–36, Sep-Oct 2009. doi:10.4161/isl.1.2.9480.

[180] Lei Z, Chen Y, Wang J, et al. Txnip deficiency promotes β-cell proliferation in the HFD-induced obesity mouse model. Endocr Connect., 11(4):e210641, Apr 2022. doi:10.1530/ec-21-0641.

[181] Sergeant S, Ruczinski I, Ivester P, et al. Impact of methods used to express levels of circulating fatty acids on the degree and direction of associations with blood lipids in humans. Br J Nutr., 115(2):251–61, Jan 2016. doi:10.1017/S0007114515004341.

[182] Christeff N, Homo-Delarche F, Thobie N, et al. Free fatty acid profiles in the non-obese diabetic (NOD) mouse: basal serum levels and effects of endocrine manipulation. Prostaglandins Leukot Essent Fatty Acids., 51(2):125–31, Aug 1994. doi:10.1016/0952-3278(94)90088-4.

[183] Spiller S, Blüher M, and Hoffmann R. Plasma levels of free fatty acids correlate with type 2 diabetes mellitus. Diabetes Obes Metab., 20(11):2661–2669, Nov 2018. doi:10.1111/dom.13449.

[184] Wu P, Yang L, and Shen X. The relationship between GPR40 and lipotoxicity of the pancreatic β-cells as well as the effect of pioglitazone. Biochem Biophys Res Commun., 403(1):36–9, Dec 2010. doi:10.1016/j.bbrc.2010.10.105.

[185] Frigerio F, Chaffard G, Berwaer M, et al. The antiepileptic drug topiramate preserves metabolism-secretion coupling in insulin secreting cells chronically exposed to the fatty acid oleate. Biochem Pharmacol., 72(8):965–73, Oct 2006. doi:10.1016/j.bcp.2006.07.013.

[186] Boucher A, Lu D, Burgess SC, et al. Biochemical mechanism of lipid-induced impairment of glucose-stimulated insulin secretion and reversal with a malate analogue. J Biol Chem., 279(26):27263–71, Jun 2004. doi:10.1074/jbc.m401167200.

[187] Chen Y, Ren Q, Zhou Z, et al. HWL-088, a new potent free fatty acid receptor 1 (FFAR1) agonist, improves glucolipid metabolism and acts additively with metformin in ob/ob diabetic mice. Br J Pharmacol., 177(10):2286–2302, May 2020. doi:10.1111/bph.14980.

[188] Koulajian K, Ivovic A, Ye K, et al. Overexpression of glutathione peroxidase 4 prevents β-cell dysfunction induced by prolonged elevation of lipids in vivo. Am J Physiol Endocrinol Metab., 305(2):E254–62, Jul 2013. doi:10.1152/ajpendo.00481.2012.

[189] Köhnke D, Ludwig B, and Kadenbach B. A threshold membrane potential accounts for controversial effects of fatty acids on mitochondrial oxidative phosphorylation. FEBS Lett., 336(1):90–4, Dec 1993. doi:10.1016/0014-5793(93)81616-8.

[190] Assali EA, Shlomo D, Zeng J, et al. Nanoparticle-mediated lysosomal reacidification restores mitochondrial turnover and function in β cells under lipotoxicity. FASEB J., 33(3):4154–4165, Mar 2019. doi:10.1096/fj.201801292R.

[191] Jiang L, Wan J, Ke Lq, et al. Activation of PPARγ promotes mitochondrial energy metabolism and decreases basal insulin secretion in palmitate-treated β-cells. Mol Cell Biochem., 343(1-2):249–56, Oct 2010. doi:10.1007/s11010-010-0520-8.

[192] Remizov O, Jakubov R, Düfer M, et al. Palmitate-induced Ca2+-signaling in pancreatic beta-cells. Mol Cell Endocrinol., 212(1-2):1–9, Dec 2003. doi:10.1016/j.mce.2003.09.026.

[193] Ježek J, Dlasková A, Zelenka J, et al. H_2O_2-Activated Mitochondrial Phospholipase iPLA$_2\gamma$ Prevents Lipotoxic Oxidative Stress in Synergy with UCP2, Amplifies Signaling via G-Protein-Coupled Receptor GPR40, and Regulates Insulin Secretion in Pancreatic β-Cells. Antioxid Redox Signal., 23(12):958–72, Oct 2015. doi:10.1089/ars.2014.6195.

[194] Römer A, Rawat D, Linn T, et al. Preparation of fatty acid solutions exerts significant impact on experimental outcomes in cell culture models of lipotoxicity. Biol Methods Protoc., 7(1):bpab023, 2022. doi:10.1093/biomethods/bpab023.

[195] Petry SF, Sharifpanah F, Sauer H, et al. Differential expression of islet glutaredoxin 1 and 5 with high reactive oxygen species production in a mouse model of diabesity. PLoS One., 12(5):e0176267, May 2017. doi:10.1371/journal.pone.0176267.

[196] Kilimnik G, Kim A, Jo J, et al. Quantification of pancreatic islet distribution in situ in mice. Am J Physiol Endocrinol Metab., 297(6):E1331–E8, Dec 2009. doi:10.1152/ajpendo.00479.2009.

[197] Schlederer M, Mueller KM, Haybaeck J, et al. Reliable quantification of protein expression and cellular localization in histological sections. PLoS One., 9(7):e100822, 2014. doi:10.1371/journal.pone.0100822.

[198] Tenbaum SP, Pálmer HG, Arqués O, et al. Standardized Relative Quantification of Immunofluorescence Tissue Staining. Nat Protoc., 2012. doi:10.1038/protex.2012.008.

[199] Petry SF, Sun LM, Knapp A, et al. Distinct Shift in Beta-Cell Glutaredoxin 5 Expression Is Mediated by Hypoxia and Lipotoxicity Both In Vivo and In Vitro. Front Endocrinol (Lausanne)., 9:84, May 2018. doi:10.3389/fendo.2018.00084.

[200] Petry SF, Römer A, Rawat D, et al. Loss and Recovery of Glutaredoxin 5 Is Inducible by Diet in a Murine Model of Diabesity and Mediated by Free Fatty Acids In Vitro. Antioxidants (Basel)., 11, Apr 2022.

[201] Chen C, Kuehn C, Bretzel RG, et al. Anti-inflammatory thalidomide improves islet grafts survival and functions in a xenogenic environment. PLoS One., 4(7):e6312, Jul 2009. doi:10.1371/journal.pone.0006312.

[202] Plötz T, von Hanstein AS, Krümmel B, et al. Structure-toxicity relationships of saturated and unsaturated free fatty acids for elucidating the lipotoxic effects in human EndoC-βH1 beta-cells. Biochim Biophys Acta Mol Basis Dis., 1865(11):165525, Nov 2019. doi:10.1016/j.bbadis.2019.08.001.

[203] Malhotra JD and Kaufman RJ. ER stress and its functional link to mitochondria: role in cell survival and death. Cold Spring Harb Perspect Biol., 3(9):a004424, Sep 2011. doi:10.1101/cshperspect.a004424.

[204] Bravo R, Gutierrez T, Paredes F, et al. Endoplasmic reticulum: ER stress regulates mitochondrial bioenergetics. Int J Biochem Cell Biol., 44(1):16–20, Jan 2012. doi:10.1016/j.biocel.2011.10.012.

[205] Vannuvel K, Renard P, Raes M, et al. Functional and morphological impact of ER stress on mitochondria. J Cell Physiol., 228(9):1802–18, Sep 2013. doi:10.1002/jcp.24360.

[206] Miyazaki J, Araki K, Yamato E, et al. Establishment of a pancreatic beta cell line that retains glucose-inducible insulin secretion: special reference to expression of glucose transporter isoforms. Endocrinology., 127(1):126–32, 1990. doi:10.1210/endo-127-1-126.

[207] Ishihara H, Asano T, Tsukuda K, et al. Pancreatic beta cell line MIN6 exhibits characteristics of glucose metabolism and glucose-stimulated insulin secretion similar to those of normal islets. Diabetologia., 36(11):1139–45, Nov 1993. doi:10.1007/bf00401058.

[208] Mosmann T. Rapid colorimetric assay for cellular growth and survival: application to proliferation and cytotoxicity assays. J Immunol Methods., 65(1-2):55–63, Dec 1983. doi:10.1016/0022-1759(83)90303-4.

[209] Berridge MV and Tan AS. Characterization of the cellular reduction of 3-(4,5-dimethylthiazol-2-yl)-2,5-diphenyltetrazolium bromide (MTT): subcellular localization, substrate dependence, and involvement of mitochondrial electron transport in MTT reduction. Arch Biochem Biophys., 303(2):474–82, Jun 1993. doi:10.1006/abbi.1993.1311.

[210] Ghasemi M, Turnbull T, Sebastian S, et al. The MTT Assay: Utility, Limitations, Pitfalls, and Interpretation in Bulk and Single-Cell Analysis. Int J Mol Sci., 22(23):12827, Nov 2021. doi:10.3390/ijms222312827.

[211] van der Vusse GJ. Albumin as fatty acid transporter. Drug Metab Pharmacokinet., 24(4):300–7, 2009. doi:10.2133/dmpk.24.300.

[212] Saifer A and Goldman L. The free fatty acids bound to human serum albumin. J Lipid Res., 2(3):268–270, July 1961. doi:10.1016/s0022-2275(20)39014-3.

[213] Boyer F, Diotel N, Girard D, et al. Enhanced oxidative stress in adipose tissue from diabetic mice, possible contribution of glycated albumin. Biochem Biophys Res Commun., 473(1):154–160, Apr 2016. doi:10.1016/j.bbrc.2016.03.068.

[214] Panov AV, Vavilin VA, Lyakhovich VV, et al. Effect of bovine serum albumin on mitochondrial respiration in the brain and liver of mice and rats. Bull Exp Biol Med., 149(2):187–90, Aug 2010. doi:10.1007/s10517-010-0904-5.

[215] Lane BP and Miller SL. Preparation of large numbers of uniform tracheal organ cultures for long term studies. I. Effects of serum on establishment in culture. In Vitro., 12(2):147–54, Feb 1976. doi:10.1007/bf02796363.

[216] Keenan J, Doherty G, and Clynes M. Separation of growth-stimulating activity of BSA fraction V from the bulk of albumin using Heparin Sepharose Chromatography. Cytotechnology., 19(1):63–72, Jan 1995. doi:10.1007/bf00749756.

[217] Tapani E, Taavitsainen M, Lindros K, et al. Toxicity of ethanol in low concentrations. Experimental evaluation in cell culture. Acta radiol., 37(6):923–6, Nov 1996. doi:10.3109/02841859609175470.

[218] Hallare A, Nagel K, Köhler HR, et al. Comparative embryotoxicity and proteotoxicity of three carrier solvents to zebrafish (Danio rerio) embryos. Ecotoxicol Environ Saf., 63(3):378–88, Mar 2006. doi:10.1016/j.ecoenv.2005.07.006.

[219] Wehinger S, Ortiz R, Díaz MI, et al. Phosphorylation of caveolin-1 on tyrosine-14 induced by ROS enhances palmitate-induced death of beta-pancreatic cells. Biochim Biophys Acta., 1852(5):693–708, May 2015. doi:10.1016/j.bbadis.2014.12.021.

[220] Jover R, Ponsoda X, Castell JV, et al. Evaluation of the cytotoxicity of ten chemicals on human cultured hepatocytes: Predictability of human toxicity and comparison with rodent cell culture systems. Toxicol In Vitro., 6(1):47–52, Jan 1992. doi:10.1016/0887-2333(92)90084-5.

[221] Shiragannavar VD, Sannappa Gowda NG, Puttahanumantharayappa LD, et al. The ameliorating effect of withaferin A on high-fat diet-induced non-alcoholic fatty liver disease by acting as an LXR/FXR dual receptor activator. Front Pharmacol., 14:1135952, 2023. doi:10.3389/fphar.2023.1135952.

[222] Li X, Chen R, Kemper S, et al. Production, Exacerbating Effect, and EV-Mediated Transcription of Hepatic CCN2 in NASH: Implications for Diagnosis and Therapy of NASH Fibrosis. Int J Mol Sci., 24(16):12823, 2023. ISSN 1422-0067. doi:10.3390/ijms241612823.

[223] Nelson BN. Insights Into Mechanisms of Antifungal Activity by Innate Immune Cells. Ph.D. thesis, Oklahoma State University, United States – Oklahoma, https://www.proquest.com/dissertations-theses/insights-into-mechanisms-antifungal-activity/docview/2847236505/se-2, 2023.

[224] Turpin SM, Ryall JG, Southgate R, et al. Examination of 'lipotoxicity' in skeletal muscle of high-fat fed and ob/ob mice. J Physiol., 587(Pt 7):1593–605, Apr 2009. doi:10.1113/jphysiol.2008.166033.

[225] Hummel KP, Dickie MM, and Coleman DL. Diabetes, a new mutation in the mouse. Science., 153(3740):1127–8, Sep 1966. doi:10.1126/science.153.3740.1127.

[226] Chen H, Charlat O, Tartaglia LA, et al. Evidence that the diabetes gene encodes the leptin receptor: identification of a mutation in the leptin receptor gene in db/db mice. Cell., 84(3):491–5, Feb 1996. doi:10.1016/s0092-8674(00)81294-5.

[227] Friedman JM and Halaas JL. Leptin and the regulation of body weight in mammals. Nature., 395(6704):763–70, Oct 1998. doi:10.1038/27376.

[228] Coleman DL. Obese and diabetes: two mutant genes causing diabetes-obesity syndromes in mice. Diabetologia., 14(3):141–8, Mar 1978. doi:10.1007/bf00429772.

[229] Tuman RW and Doisy RJ. The influence of age on the development of hypertriglyceridaemia and hypercholesterolaemia in genetically diabetic mice. Diabetologia., 13(1):7–11, Jan 1977. doi:10.1007/bf00996320.

[230] Nishina PM, Lowe S, Wang J, et al. Characterization of plasma lipids in genetically obese mice: the mutants obese, diabetes, fat, tubby, and lethal yellow. Metabolism., 43(4):549–53, May 1994. doi:10.1016/0026-0495(94)90194-5.

[231] Kim KE, Jung Y, Min S, et al. Caloric restriction of db/db mice reverts hepatic steatosis and body weight with divergent hepatic metabolism. Sci Rep., 6:30111, Jul 2016. doi:10.1038/srep30111.

[232] Kobayashi K, Forte TM, Taniguchi S, et al. The db/db mouse, a model for diabetic dyslipidemia: molecular characterization and effects of Western diet feeding. Metabolism., 49(1):22–31, Jan 2000. doi:10.1016/s0026-0495(00)90588-2.

[233] Wang MY, Grayburn P, Chen S, et al. Adipogenic capacity and the susceptibility to type 2 diabetes and metabolic syndrome. Proc Natl Acad Sci U S A., 105(16):6139–44, Apr 2008. doi:10.1097/01.ogx.0000325912.87929.06.

[234] Yaziji H and Barry T. Diagnostic Immunohistochemistry: what can go wrong? Arch Pathol Lab Med., 13(5):238–46, Sep 2006. doi:10.1097/01.pap.0000213041.39070.2f.

[235] Bussolati G and Leonardo E. Technical pitfalls potentially affecting diagnoses in immunohistochemistry. J Clin Pathol., 61(11):1184–92, Nov 2008. doi:10.1136/jcp.2007.047720.

[236] Burns M, Rizvi SHM, Tsukahara Y, et al. Role of Glutaredoxin-1 and Glutathionylation in Cardiovascular Diseases. Int J Mol Sci., 21(18):6803, Sep 2020. doi:10.3390/ijms21186803.

[237] Clee SM and Attie AD. The genetic landscape of type 2 diabetes in mice. Endocr Rev., 28(1):48–83, Feb 2007. doi:10.1210/er.2006-0035.

[238] Hummel KP, Coleman DL, and Lane PW. The influence of genetic background on expression of mutations at the diabetes locus in the mouse. I. C57BL-KsJ and C57BL-6J strains. Biochem Genet., 7(1):1–13, Aug 1972. doi:10.1007/bf00487005.

[239] Coleman DL and Hummel KP. Symposium IV: Diabetic syndrome in animals. Influence of genetic background on the expression of mutations at the diabetes locus in the mouse. II. Studies on background modifiers. Isr J Med Sci., 11:708–13, Jul 1975.

[240] Sbierski-Kind J, Kath J, Brachs S, et al. Distinct Housing Conditions Reveal a Major Impact of Adaptive Immunity on the Course of Obesity-Induced Type 2 Diabetes. Front Immunol., 9:1069, 2018. doi:10.3389/fimmu.2018.01069.

[241] Morgan JL, Svenson KL, Lake JP, et al. Effects of housing density in five inbred strains of mice. PLoS One., 9(3):e90012, 2014. doi:10.1371/journal.pone.0090012.

[242] McKie GL, Medak KD, Knuth CM, et al. Housing temperature affects the acute and chronic metabolic adaptations to exercise in mice. J Physiol., 597(17):4581–4600, Sep 2019. doi:10.1113/jp278221.

[243] McEvoy RC and Hegre OD. Morphometric quantitation of the pancreatic insulin-, glucagon-, and somatostatin-positive cell populations in normal and alloxan-diabetic rats. Diabetes., 26(12):1140–6, Dec 1977. doi:10.2337/diab.26.12.1140.

[244] Pipeleers D, in't Veld PI, Maes E, et al. Glucose-induced insulin release depends on functional cooperation between islet cells. Proc Natl Acad Sci U S A., 79(23):7322–5, Dec 1982. doi:10.1073/pnas.79.23.7322.

[245] Cerf ME, Chapman CS, and Louw J. High-fat programming of hyperglycemia, hyperinsulinemia, insulin resistance, hyperleptinemia, and altered islet architecture in 3-month-old wistar rats. ISRN Endocrinol., 2012:627270, 2012. doi:10.5402/2012/627270.

[246] Brereton MF, Iberl M, Shimomura K, et al. Reversible changes in pancreatic islet structure and function produced by elevated blood glucose. Nat Commun., 22(5):4639, Aug 2014. doi:10.1038/ncomms5639.

[247] Butler AE, Janson J, Bonner-Weir S, et al. Beta-cell deficit and increased beta-cell apoptosis in humans with type 2 diabetes. Diabetes., 52(1):102–10, Jan 2003. doi:10.2337/diabetes.52.1.102.

[248] Maedler K and Donath MY. Beta-cells in type 2 diabetes: a loss of function and mass. Horm Res., 62(Suppl 3):67–73, 2004. doi:10.1159/000080503.

[249] Marchetti P, Del Guerra S, Marselli L, et al. Pancreatic islets from type 2 diabetic patients have functional defects and increased apoptosis that are ameliorated by metformin. J Clin Endocrinol Metab., 89(11):5535–41., Nov 2004. doi:10.1210/jc.2004-0150.

[250] Talchai C, Xuan S, Lin HV, et al. Pancreatic beta cell dedifferentiation as a mechanism of diabetic beta cell failure. Cell., 150(6):1223–34, Sep 2012. doi:10.1016/j.cell.2012.07.029.

[251] White MG, Marshall HL, Rigby R, et al. Expression of mesenchymal and alpha-cell phenotypic markers in islet beta-cells in recently diagnosed diabetes. Diabetes Care., 36(11):3818–20, Nov 2013. doi:10.2337/dc13-0705.

[252] Gao T, McKenna B, Li C, et al. Pdx1 maintains beta cell identity and function by repressing an alpha cell program. Cell Metab., 19(2):259–71, Feb 2014. doi:10.1016/j.cmet.2013.12.002.

[253] Maffei M, Fei H, Lee GH, et al. Increased expression in adipocytes of ob RNA in mice with lesions of the hypothalamus and with mutations at the db locus. Proc Natl Acad Sci U S A., 92(15):6957–60, Jul 1995. doi:10.1073/pnas.92.15.6957.

[254] Kieffer TJ and Habener JF. The adipoinsular axis: effects of leptin on pancreatic beta-cells. Am J Physiol Endocrinol Metab., 278(1):E1–E14, Jan 2000. doi:10.1152/ajpendo.2000.278.1.E1.

[255] Seufert J, Kieffer TJ, and Habener JF. Leptin inhibits insulin gene transcription and reverses hyperinsulinemia in leptin-deficient ob/ob mice. Proc Natl Acad Sci U S A., 96(2):674–9, Jan 1999. doi:10.1073/pnas.96.2.674.

[256] Kulkarni RN, Wang ZL, Wang RM, et al. Leptin rapidly suppresses insulin release from insulinoma cells, rat and human islets and, in vivo, in mice. J Clin Invest., 100(11):2729–36, Dec 1997. doi:10.1172/jci119818.

[257] Moreno-Aliaga MJ, Stanhope KL, and Havel PJ. Transcriptional regulation of the leptin promoter by insulin-stimulated glucose metabolism in 3t3-l1 adipocytes. Biochem Biophys Res Commun., 283(3):544–8, May 2001. doi:10.1006/bbrc.2001.4822.

[258] Laferrère B, Caixas A, Fried SK, et al. A pulse of insulin and dexamethasone stimulates serum leptin in fasting human subjects. Eur J Endocrinol., 146(6):839–45, Jun 2002. doi:10.1530/eje.0.1460839.

[259] Leclercq-Meyer V and Malaisse WJ. Failure of human and mouse leptin to affect insulin, glucagon and somatostatin secretion by the perfused rat pancreas at physiological glucose concentration. Mol Cell Endocrinol., 141(1-2):111–8., Jun 1998. doi:10.1016/s0303-7207(98)00087-2.

[260] Leclercq-Meyer V, Considine RV, Sener A, et al. Do leptin receptors play a functional role in the endocrine pancreas? Biochem Biophys Res Commun., 229(3):794–8, Dec 1996. doi:10.1006/bbrc.1996.1882.

[261] Lupi R, Marchetti P, Maffei M, et al. Effects of acute or prolonged exposure to human leptin on isolated human islet function. Biochem Biophys Res Commun., 256(3):637–41, Mar 1999. doi:10.1006/bbrc.1999.0384.

[262] Vickers MH, Reddy S, Ikenasio BA, et al. Dysregulation of the adipoinsular axis – a mechanism for the pathogenesis of hyperleptinemia and adipogenic diabetes induced by fetal programming. J Endocrinol., 170(2):323–32, Aug 2001. doi:10.1677/joe.0.1700323.

[263] Coppari R and Bjørbæk C. Leptin revisited: its mechanism of action and potential for treating diabetes. Nat Rev Drug Discov., 11(9):692–708, Sep 2012. doi:10.1038/nrd3757.

[264] Obradovic M, Sudar-Milovanovic E, Soskic S, et al. Leptin and Obesity: Role and Clinical Implication. Front Endocrinol (Lausanne)., 12:585887, 2021. doi:10.3389/fendo.2021.585887.

[265] Chance B, Sies H, and Boveris A. Hydroperoxide metabolism in mammalian organs. Physiol Rev., 59(3):527–605, Jul 1979. doi:10.1152/physrev.1979.59.3.527.

[266] Dionne KE, Colton CK, and Yarmush ML. Effect of hypoxia on insulin secretion by isolated rat and canine islets of Langerhans. Diabetes., 42(1):12–21, Jan 1993. doi:10.2337/diab.42.1.12.

[267] Sato Y, Endo H, Okuyama H, et al. Cellular hypoxia of pancreatic beta-cells due to high levels of oxygen consumption for insulin secretion in vitro. J Biol Chem., 286(14):12524–32, Apr 2011. doi:10.1074/jbc.M110.194738.

[268] Lai Y, Brandhorst H, Hossain H, et al. Activation of NFkappaB dependent apoptotic pathway in pancreatic islet cells by hypoxia. Islets., 1(1):19–25, Jul-Aug 2009. doi:10.4161/isl.1.1.8530.

[269] Bensellam M, Maxwell EL, Chan JY, et al. Hypoxia reduces ER-to-Golgi protein trafficking and increases cell death by inhibiting the adaptive unfolded protein response in mouse beta cells. Diabetologia., 59(7):1492–502, Apr 2016. doi:10.1007/s00125-016-3947-y.

[270] Watanabe Y, Murdoch CE, Sano S, et al. Glutathione adducts induced by ischemia and deletion of glutaredoxin-1 stabilize HIF-1α and improve limb revascularization. Proc Natl Acad Sci U S A., 113(21):6011–6016, May 2016. doi:10.1073/pnas.1524198113.

[271] Surwit RS, Kuhn CM, Cochrane C, et al. Diet-induced type II diabetes in C57BL/6J mice. Diabetes., 37(9):1163–7, Sep 1988. doi:10.2337/diab.37.9.1163.

[272] Siersbæk MS, Ditzel N, Hejbøl EK, et al. C57BL/6J substrain differences in response to high-fat diet intervention. Sci Rep., 10(1):14052, Aug 2020. doi:10.1038/s41598-020-70765-w.

[273] Carlessi R, Keane KN, Mamotte C, et al. Nutrient regulation of β-cell function: what do islet cell/animal studies tell us? Eur J Clin Nutr., 71(7):890–895, Jul 2017. doi:10.1038/ejcn.2017.49.

[274] Dos Santos KC, Olofsson C, Cunha JPMCM, et al. The impact of macronutrient composition on metabolic regulation: An Islet-Centric view. Acta Physiol (Oxf)., 236(4):e13884, Dec 2022. doi:10.1111/apha.13884.

[275] Winzell MS and Ahrén B. The high-fat diet-fed mouse: a model for studying mechanisms and treatment of impaired glucose tolerance and type 2 diabetes. Diabetes., 53 Suppl 3:S215–9, Dec 2004. doi:10.2337/diabetes.53.suppl_3.s215.

[276] Sumiyoshi M, Sakanaka M, and Kimura Y. Chronic intake of high-fat and high-sucrose diets differentially affects glucose intolerance in mice. J Nutr., 136(3):582–7, Mar 2006. doi:10.1093/jn/136.3.582.

[277] Ortlepp JR, Kluge R, Giesen K, et al. A metabolic syndrome of hypertension, hyperinsulinaemia and hypercholesterolaemia in the New Zealand obese mouse. Eur J Clin Invest., 30(3):195–202, Mar 2000. doi:10.1046/j.1365-2362.2000.00611.x.

[278] Kluth O, Mirhashemi F, Scherneck S, et al. Dissociation of lipotoxicity and glucotoxicity in a mouse model of obesity associated diabetes: role of forkhead box O1 (FOXO1) in glucose-induced beta cell failure. Diabetologia., 54(3):605–16, Mar 2011. doi:10.1007/s00125-010-1973-8.

[279] Cheng CW, Villani V, Buono R, et al. Fasting-Mimicking Diet Promotes Ngn3-Driven beta-Cell Regeneration to Reverse Diabetes. Cell., 168(5):775–788.e12, 02 2017. ISSN 1097-4172. doi:10.1016/j.cell.2017.01.040.

[280] Wei S, Li C, Luo X, et al. Intermittent protein restriction protects islet β cells and improves glucose homeostasis in diabetic mice. Sci Bull (Beijing)., 67(7):733–747, Apr 2022. doi:10.1016/j.scib.2021.12.024.

[281] Shinjo T, Nakatsu Y, Iwashita M, et al. High-fat diet feeding significantly attenuates anagliptin-induced regeneration of islets of Langerhans in streptozotocin-induced diabetic mice. Diabetol Metab Syndr., 7:50, 2015. doi:10.1186/s13098-015-0047-y.

[282] Magkos F, Fraterrigo G, Yoshino J, et al. Effects of Moderate and Subsequent Progressive Weight Loss on Metabolic Function and Adipose Tissue Biology in Humans with Obesity. Cell Metab., 23(4):591–601, Apr 2016. doi:10.1016/j.cmet.2016.02.005.

[283] Lim EL, Hollingsworth KG, Aribisala BS, et al. Reversal of type 2 diabetes: normalisation of beta cell function in association with decreased pancreas and liver triacylglycerol. Diabetologia., 54(10):2506–14, Oct 2011. doi:10.1007/s00125-011-2204-7.

[284] Lv C, Sun Y, Zhang ZY, et al. β-cell dynamics in type 2 diabetes and in dietary and exercise interventions. J Mol Cell Biol., 14(7):mjac046, Nov 2022. doi:10.1093/jmcb/mjac046.

[285] Ahn JH, Kim MH, Kwon HJ, et al. Protective Effects of Oleic Acid Against Palmitic Acid-Induced Apoptosis in Pancreatic AR42J Cells and Its Mechanisms. Korean J Physiol Pharmacol., 17(1):43–50, Feb 2013. doi:10.4196/kjpp.2013.17.1.43.

[286] Schenkel LC and Bakovic M. Palmitic acid and oleic acid differentially regulate choline transporter-like 1 levels and glycerolipid metabolism in skeletal muscle cells. Lipids., 49(8):731–44, Aug 2014. doi:10.1007/s11745-014-3925-4.

[287] Liu X, Zeng X, Chen X, et al. Oleic acid protects insulin-secreting INS-1E cells against palmitic acid-induced lipotoxicity along with an amelioration of ER stress. Endocrine., 64(3):512–524, Jun 2019. doi:10.1007/s12020-019-01867-3.

[288] Pareja A, Tinahones FJ, Soriguer FJ, et al. Unsaturated fatty acids alter the insulin secretion response of the islets of Langerhans in vitro. Diabetes Res Clin Pract., 38(3):143–9, Dec 1997. doi:10.1016/s0168-8227(97)00103-4.

[289] Sato K, Arai H, Mizuno A, et al. Dietary palatinose and oleic acid ameliorate disorders of glucose and lipid metabolism in Zucker fatty rats. J Nutr., 137(8):1908–15, Aug 2007. doi:10.1093/jn/137.8.1908.

[290] Park JB and Levine M. The human glutaredoxin gene: determination of its organization, transcription start point, and promoter analysis. Gene., 197(1-2):189–93, Sep 1997. doi:10.1016/s0378-1119(97)00262-x.

[291] Cai H, Li M, Jian W, et al. A novel lncRNA BADLNCR1 inhibits bovine adipogenesis by repressing GLRX5 expression. J Cell Mol Med., 24(13):7175–7186, Jul 2020. doi:10.1111/jcmm.15181.

[292] Schneider MR, Zettler S, Rathkolb B, et al. TXNIP overexpression in mice enhances streptozotocin-induced diabetes severity. Mol Cell Endocrinol., 565:111885, Apr 2023. doi:10.1016/j.mce.2023.111885.

[293] Shalev A. Minireview: Thioredoxin-interacting protein: regulation and function in the pancreatic β-cell. Mol Endocrinol., 28(8):1211–20, Aug 2014. doi:10.1210/me.2014-1095.

[294] Wondafrash DZ, Nire'a AT, Tafere GG, et al. Thioredoxin-Interacting Protein as a Novel Potential Therapeutic Target in Diabetes Mellitus and Its Underlying Complications. Diabetes Metab Syndr Obes., 13:43–51, 2020. doi:10.2147/DMSO.S232221.

[295] Chou FC and Sytwu HK. Overexpression of thioredoxin in islets transduced by a lentiviral vector prolongs graft survival in autoimmune diabetic NOD mice. J Biomed Sci., 16(1):71, Aug 2009. doi:10.1186/1423-0127-16-71.

[296] Cohen-Kutner M, Khomsky L, Trus M, et al. Thioredoxin-mimetic peptides (TXM) reverse auranofin induced apoptosis and restore insulin secretion in insulinoma cells. Biochem Pharmacol., 85(7):977–90, Apr 2013. doi:10.1016/j.bcp.2013.01.003.

[297] Kikutani H and Makino S. The murine autoimmune diabetes model: NOD and related strains. Adv Immunol., 51:285–322, 1992. doi:10.1016/s0065-2776(08)60490-3.

[298] Tagaya Y, Maeda Y, Mitsui A, et al. ATL-derived factor (ADF), an IL-2 receptor/Tac inducer homologous to thioredoxin; possible involvement of dithiol-reduction in the IL-2 receptor induction. EMBO J., 8(3):757–64, Mar 1989. doi:10.1002/j.1460-2075.1994.tb06502.x.

[299] Ericson ML, Hörling J, Wendel-Hansen V, et al. Secretion of thioredoxin after in vitro activation of human B cells. Lymphokine Cytokine Res., 11(5):201–7, Oct 1992.

[300] Schenk H, Vogt M, Dröge W, et al. Thioredoxin as a potent costimulus of cytokine expression. J Immunol., 156(2):765–71, Jan 1996. doi:10.4049/jimmunol.156.2.765.

[301] Stancill JS and Corbett JA. Hydrogen peroxide detoxification through the peroxiredoxin/thioredoxin antioxidant system: A look at the pancreatic β-cell oxidant defense. Vitam Horm., 121:45–66, 2023. doi:10.1016/bs.vh.2022.11.001.

[302] Huh KH, Cho Y, Kim BS, et al. The role of thioredoxin 1 in the mycophenolic acid-induced apoptosis of insulin-producing cells. Cell Death Dis., 4(7):e721, Jul 2013. doi:10.1038/cddis.2013.247.

[303] Liu C, Cao B, Zhang Q, et al. Inhibition of thioredoxin 2 by intracellular methylglyoxal accumulation leads to mitochondrial dysfunction and apoptosis in INS-1 cells. Endocrine., 68(1):103–115, Apr 2020. doi:10.1007/s12020-020-02191-x.

[304] Nonn L, Williams RR, Erickson RP, et al. The absence of mitochondrial thioredoxin 2 causes massive apoptosis, exencephaly, and early embryonic lethality in homozygous mice. Mol Cell Biol., 23(3):916–22, Feb 2003. doi:10.1128/mcb.23.3.916-922.2003.

[305] Stancill JS, Hansen PA, Mathison AJ, et al. Deletion of Thioredoxin Reductase Disrupts Redox Homeostasis and Impairs β-Cell Function. Function (Oxf)., 3(4):zqac034, 2022. doi:10.1093/function/zqac034.

[306] Brüning D, Hatlapatka K, Lier-Glaubitz V, et al. Pharmacological inhibition of thioredoxin reductase increases insulin secretion and diminishes beta cell viability. Naunyn Schmiedebergs Arch Pharmacol., 394(6):1133–1142, Jun 2021. doi:10.1007/s00210-020-02046-2.

[307] Liu X, Liu Z, Li D, et al. Mitochondria play a key role in oxidative stress-induced pancreatic islet dysfunction after severe burns. J Trauma Acute Care Surg., 92(6):1012–1019, Jun 2022. doi:10.1097/TA.0000000000003490.

[308] Stancill JS, Broniowska KA, Oleson BJ, et al. Pancreatic β-cells detoxify H(2)O(2) through the peroxiredoxin/thioredoxin antioxidant system. J Biol Chem., 294(13):4843–4853, Mar 2019. doi:10.1074/jbc.RA118.006219.

[309] Zhou R, Tardivel A, Thorens B, et al. Thioredoxin-interacting protein links oxidative stress to inflammasome activation. Nat Immunol., 11(2):136–40, Feb 2010. doi:10.1038/ni.1831.

8. Erklärung

Hiermit erkläre ich, dass ich die vorliegende Arbeit bzw. die mir zuzuordnenden Teile im Rahmen einer kumulativen Habilitationsschrift, selbstständig und ohne zulässige Hilfe oder Benutzung anderer als der angegebenen Hilfsmittel angefertigt habe. Alle Textstellen, die wörtlich oder sinngemäß aus veröffentlichten oder nichtveröffentlichten Schriften entnommen sind, und alle Angaben, die auf mündlichen Auskünften beruhen, sind als solche kenntlich gemacht. Ich versichere, dass ich für die nach §2 (3) der Habilitationsordnung angeführten bereits veröffentlichten Originalarbeiten als Erst- oder Seniorautor fungiere, da ich den größten Teil der Daten selbst erhoben habe, für das Design der Arbeiten verantwortlich bin und die Manuskripte maßgeblich gestaltet habe. Für alle von mir erwähnten Untersuchungen habe ich die in der „Satzung der Justus-Liebig-Universität zur Sicherung guter wissenschaftlicher Praxis“ niedergelegten Grundsätze befolgt. Ich versichere, dass alle an der Finanzierung der Arbeiten beteiligten Geldgeber in den jeweiligen Publikationen genannt worden sind. Ich versichere außerdem, dass die vorgelegte Arbeit weder im Inland noch im Ausland in gleicher oder ähnlicher Weise einer anderen Prüfungsbehörde vorgelegt wurde oder Gegenstand eines anderen Prüfungsverfahrens war. Mit der Überprüfung meiner Arbeit durch eine Plagiatserkennungssoftware bzw. ein internetbasiertes Softwareprogramm erkläre ich mich einverstanden.

Dr. med. Sebastian Friedrich Petry

9. Danksagungen

Die Erstellung dieser Arbeit ging im privaten, beruflichen und wissenschaftlichen Umfeld einher mit dem Kontakt zu zahlreichen Menschen, die mich auf meinem Weg auf vielfältige Weise unterstützt, motiviert und inspiriert haben. Vielen herzlichen Dank!

Insbesondere bin ich Herrn **Prof. Dr. med. Thomas Linn** für seine fortwährende Förderung und Unterstützung dankbar. Von Anbeginn meiner Tätigkeit für meine Dissertation bis hin zur Fertigstellung dieser Arbeit stand er mir stets mit Rat und Tat zur Seite. Prof. Linn räumte mir bei der Gestaltung und der Ausrichtung meiner Forschung große Freiräume ein. Ihm habe ich es maßgeblich zu verdanken, dass diese Habilitation entstehen konnte.

Ich bedanke mich ganz herzlich bei Frau **Doris Erb**, Frau **Gundula Hertl** und Frau **Birte Hußmann** für die stets angenehme und produktive Zusammenarbeit und unermüdliche Hilfe bei all den durchgeführten Experimenten.
Auch danke ich Herrn **Axel Römer, M. Sc.**, welcher mit seinem Fleiß, Ehrgeiz und seiner Gewissenhaftigkeit maßgeblich zu diversen Publikationen beigetragen und mich mit vielen kritischen Diskussionen inspiriert hat.

Herrn **Prof. Dr. med. Andreas Schäffler** danke ich für meine Ausbildung zum Internisten und Endokrinologen. Ich weiß das mir durchgehend entgegengebrachte Vertrauen und die kontinuierliche Förderung und Unterstützung meiner klinischen, außerklinischen und wissenschaftlichen Aktivitäten überaus zu schätzen.
Großer Dank gebührt auch den Herren **Prof. Dr. med. Thomas Karrasch** und **Dr. med. Michael Eckhard**, welchen ich grundlegende medizinische Fähigkeiten verdanke, und welche mich ebenso kontinuierlich gefördert und ausgebildet haben.
Ich lerne nach wie vor von Ihnen allen und stoße immer auf ein offenes Ohr.

Selbstverständlich bin ich meinen Eltern, **Dr. med. Ulrike** und **Friedrich Wilhelm Petry**, und meinem Bruder, **Johannes Petry, B. Sc.**, für den immerfort währenden Beistand und ihre Förderung und Hilfe in allen Lebenslagen dankbar.

Ich danke meinem engsten Freundeskreis, den Herren **Dr. rer. nat. Marcel Diwisch**, **Dr. rer. nat. Wayne Lippert**, **Dr. med. Sebastian Reimann** und **Christian Drucker, M. sc.** für die vielen heiteren Stunden und die lange Freundschaft.

Ich danke Dir, **Luisa Schreiber, M. Sc.**, für Deine Geduld und Dein Verständnis gegenüber meiner vielen medizinischen Aktivitäten. Ich danke Dir für die gemeinsame Zeit und Deine Liebe.

10. Publikationsverzeichnis

Mazrouei S, **Petry SF**, Sharifpanah F, Javanmard SH, Kelishadi R, Schulze PC, Franz M, Jung C. Pathophysiological correlation of arginase-1 in development of type 2 diabetes from obesity in adolescents. Biochim Biophys Acta Gen Subj. 2023 Feb;1867(2):130263. doi: 10.1016/j.bbagen.2022.130263.

Petry SF, Römer A, Rawat D, Brunner L, Lerch N, Zhou M, Grewal R, Sharifpanah F, Sauer H, Eckert GP, Linn T. Loss and Recovery of Glutaredoxin 5 Is Inducible by Diet in a Murine Model of Diabesity and Mediated by Free Fatty Acids In Vitro. Antioxidants (Basel). 2022 Apr 15;11(4):788. doi: 10.3390/antiox11040788.

Petry SF*, Kandula ND*, Günther S, Helker C, Schagdarsurengin U, Linn T. Valproic Acid Initiates Transdifferentiation of the Human Ductal Adenocarcinoma Cell-line Panc-1 Into α-Like Cells. Exp Clin Endocrinol Diabetes. 2022 Apr 21. doi: 10.1055/a-1750-9190. *Gleichberechtige Erstautorenschaft.

Römer A, Rawat D, Linn T, **Petry SF**. Preparation of fatty acid solutions exerts significant impact on experimental outcomes in cell culture models of lipotoxicity. Biol Methods Protoc. 2021 Dec 3;7(1):bpab023. doi: 10.1093/biomethods/bpab023.

Reutzel M, Grewal R, Esselun C, **Petry SF**, Linn T, Brandt A, Bergheim I, Eckert GP. Effects of different standard and special diets on cognition and brain mitochondrial function in mice. Nutr Neurosci. 2022 Sep;25(9):1823-1835. doi: 10.1080/1028415X.2021.1906392.

Römer A, Linn T, **Petry SF**. Lipotoxic Impairment of Mitochondrial Function in β-Cells: A Review. Antioxidants (Basel). 2021 Feb 15;10(2):293. doi: 10.3390/antiox10020293.

Khatri R, **Petry SF**, Linn T. Intrapancreatic MSC transplantation facilitates pancreatic islet regeneration. Stem Cell Res Ther. 2021 Feb 12;12(1):121. doi: 10.1186/s13287-021-02173-4.

Khatri R, Mazurek S, **Petry SF, Linn T.** Mesenchymal stem cells promote pancreatic β-cell regeneration through downregulation of FoxO1 pathway. Stem Cell Res Ther. 2020 Nov 25;11(1):497. doi: 10.1186/s13287-020-02007-9.

Jiang Q, Maresch CC, **Petry SF**, Paradowska-Dogan A, Bhushan S, Chang Y, Wrenzycki C, Schuppe HC, Houska P, Hartmann MF, Wudy SA, Shi L, Linn T. Elevated CCL2 causes Leydig cell malfunction in metabolic syndrome. JCI Insight. 2020 Nov 5;5(21):e134882. doi: 10.1172/jci.insight.134882.

Hanschmann EM*, **Petry SF***, Eitner S, Maresch CC, Lingwal N, Lillig CH, Linn T. Paracrine regulation and improvement of β-cell function by thioredoxin. Redox Biol. 2020 Jul;34:101570. doi: 10.1016/j.redox.2020.101570. *Gleichberechtige Erstautorenschaft.

Schröder C, Khatri R, **Petry SF**, Linn T. Class I and II Histone Deacetylase Inhibitor LBH589 Promotes Endocrine Differentiation in Bone Marrow Derived Human Mesenchymal Stem Cells and Suppresses Uncontrolled Proliferation. Exp Clin Endocrinol Diabetes. 2021 May;129(5):357-364. doi: 10.1055/a-1103-1900.

Doering L, Khatri R, **Petry SF**, Sauer H, Howaldt HP, Linn T.Regulation of somatostatin expression by vitamin D3 and valproic acid in human adipose-derived mesenchymal stem cells. Stem Cell Res Ther. 2019 Aug 6;10(1):240. doi: 10.1186/s13287-019-1330-x.

Petry SF, Sun LM, Knapp A, Reinl S, Linn T. Distinct Shift in Beta-Cell Glutaredoxin 5 Expression Is Mediated by Hypoxia and Lipotoxicity Both In Vivo and In Vitro. Front Endocrinol (Lausanne). 2018 Mar 12;9:84. doi: 10.3389/fendo.2018.00084.

Petry SF, Sharifpanah F, Sauer H, Linn T. Differential expression of islet glutaredoxin 1 and 5 with high reactive oxygen species production in a mouse model of diabesity. PLoS One. 2017 May 24;12(5):e0176267. doi: 10.1371/journal.pone.0176267.

Maresch CC, **Petry SF**, Theis S, Bosy-Westphal A, Linn T. Low Glycemic Index Prototype Isomaltulose-Update of Clinical Trials. Nutrients. 2017 Apr 13;9(4):381. doi: 10.3390/nu9040381.

11. Anhang mit den Originalarbeiten

Folgende Arbeiten liegen dieser Schrift zugrunde (in der Reihenfolge der Bearbeitung):

Römer A, Linn T, **Petry SF**. Lipotoxic Impairment of Mitochondrial Function in β-Cells: A Review. Antioxidants (Basel). 2021 Feb 15;10(2):293. doi: 10.3390/antiox10020293.

Römer A, Rawat D, Linn T, **Petry SF**. Preparation of fatty acid solutions exerts significant impact on experimental outcomes in cell culture models of lipotoxicity. Biol Methods Protoc. 2021 Dec 3;7(1):bpab023. doi: 10.1093/biomethods/bpab023.

Petry SF, Sharifpanah F, Sauer H, Linn T. Differential expression of islet glutaredoxin 1 and 5 with high reactive oxygen species production in a mouse model of diabesity. PLoS One. 2017 May 24;12(5):e0176267. doi: 10.1371/journal.pone.0176267.

Petry SF, Sun LM, Knapp A, Reinl S, Linn T. Distinct Shift in Beta-Cell Glutaredoxin 5 Expression Is Mediated by Hypoxia and Lipotoxicity Both In Vivo and In Vitro. Front Endocrinol (Lausanne). 2018 Mar 12;9:84. doi: 10.3389/fendo.2018.00084.

Petry SF, Römer A, Rawat D, Brunner L, Lerch N, Zhou M, Grewal R, Sharifpanah F, Sauer H, Eckert GP, Linn T. Loss and Recovery of Glutaredoxin 5 Is Inducible by Diet in a Murine Model of Diabesity and Mediated by Free Fatty Acids In Vitro. Antioxidants (Basel). 2022 Apr 15;11(4):788. doi: 10.3390/antiox11040788.

Hanschmann EM*, **Petry SF***, Eitner S, Maresch CC, Lingwal N, Lillig CH, Linn T. Paracrine regulation and improvement of β-cell function by thioredoxin. Redox Biol. 2020 Jul;34:101570. doi: 10.1016/j.redox.2020.101570. *Gleichberechtige Erstautorenschaft.

antioxidants

MDPI

Review

Lipotoxic Impairment of Mitochondrial Function in β-Cells: A Review

Axel Römer, Thomas Linn and Sebastian F. Petry *

Clinical Research Unit, Center of Internal Medicine, Justus Liebig University, 35392 Giessen, Germany; Axel.Roemer@ernaehrung.uni-giessen.de (A.R.); Thomas.Linn@innere.med.uni-giessen.de (T.L.)
* Correspondence: sebastian.petry@innere.med.uni-giessen.de; Tel.: +49-641-985-42841; Fax: +49-641-985-42849

Abstract: Lipotoxicity is a major contributor to type 2 diabetes mainly promoting mitochondrial dysfunction. Lipotoxic stress is mediated by elevated levels of free fatty acids through various mechanisms and pathways. Impaired peroxisome proliferator-activated receptor (PPAR) signaling, enhanced oxidative stress levels, and uncoupling of the respiratory chain result in ATP deficiency, while β-cell viability can be severely impaired by lipotoxic modulation of PI3K/Akt and mitogen-activated protein kinase (MAPK)/extracellular-signal-regulated kinase (ERK) pathways. However, fatty acids are physiologically required for an unimpaired β-cell function. Thus, preparation, concentration, and treatment duration determine whether the outcome is beneficial or detrimental when fatty acids are employed in experimental setups. Further, ageing is a crucial contributor to β-cell decay. Cellular senescence is connected to loss of function in β-cells and can further be promoted by lipotoxicity. The potential benefit of nutrients has been broadly investigated, and particularly polyphenols were shown to be protective against both lipotoxicity and cellular senescence, maintaining the physiology of β-cells. Positive effects on blood glucose regulation, mitigation of oxidative stress by radical scavenging properties or regulation of antioxidative enzymes, and modulation of apoptotic factors were reported. This review summarizes the significance of lipotoxicity and cellular senescence for mitochondrial dysfunction in the pancreatic β-cell and outlines potential beneficial effects of plant-based nutrients by the example of polyphenols.

Keywords: lipotoxicity; free fatty acids; oxidative stress; mitochondrial dysfunction; beta cell; diabetes mellitus; polyphenol; ageing

Citation: Römer, A.; Linn, T.; Petry, S.F. Lipotoxic Impairment of Mitochondrial Function in β-Cells: A Review. *Antioxidants* **2021**, *10*, 293. https://doi.org/10.3390/antiox10020293

Academic Editors: Volker Böhm and Gunter Peter Eckert

Received: 28 November 2020
Accepted: 11 February 2021
Published: 15 February 2021

1. Introduction

The onset and progression of diabetes mellitus (DM) is crucially determined by the deterioration of the glucose-stimulated insulin secretion (GSIS) of pancreatic β-cells. In 2019, there were more than 460 million patients with DM worldwide with a steadily rising prevalence (9.3%) over the last few decades [1]. The impaired action of insulin in these patients leads to elevated plasma glucose levels. Chronic hyperglycemia can damage various molecules and tissues by glycation [2]. To prevent these complications, the supply with an adequate amount of insulin is necessary. As insulin secretion demands a lot of biochemical energy [3] and mitochondria contribute to 98% of cellular adenosine triphosphate (ATP) [4], their proper function becomes a major aspect in developing β-cell dysfunction and decay.

The progression of type 2 diabetes mellitus (T2DM) is accompanied by elevated free fatty acids (FFAs) [5–7] as well as the deterioration of the lipid metabolism. FFA are known to impair the function of β-cells and promote their failure by various mechanisms [8], among others, by toxic metabolites of lipid degradation, the activation or dysregulation of signaling pathways, oxidative stress, and an altered energy production. By mediating this so-called lipotoxicity, FFA can impair the mitochondrial metabolism and other compartments of the β-cell and disturb its capacity of both insulin synthesis and release. FFAs increase insulin resistance by several signaling pathways, including altered translocation

of glucose transporter (GLUT). FFAs are therefore one of the major promotors of developing T2DM [9]. Nevertheless, FFAs are physiologically required for energy demands, as components of membranes or signaling molecules, and there is no defined qualitative or quantitative cut-off at which toxic effects commence. In general, lipotoxicity is defined as the impairment of cellular functions like mitochondrial respiration, protein translation and function, and induction of cell death mediated by the accumulation of FFAs. However, the underlying mechanisms are more complex and involve an imbalance between uptake, storage, and utilization of FFAs.

Beside elevation of FFA blood and tissue levels, and associated disorders of lipid metabolism, cellular senescence [10] is the second major contributor to the increasing prevalence of T2DM [11]. The rate of apoptotic events is increased while proliferation is disfavored with age, leading to an incremented decay of the endocrine pancreas. Increased levels of reactive oxygen species (ROS) and DNA damage diminish the regenerative capacity and function of β-cells correlating with a general impairment of insulin production and secretion machinery as well as an increased rate of apoptosis. There is also a connection between enhanced cellular stress leading to an age-dependent impairment of the lipid metabolism marked by increased plasma triglyceride (TG) levels and reduced postprandial TG clearance rates [12]. Likewise, there is a correlation between increased plasma FFA and age [13]. Concomitant with a decreased antioxidative capacity of β-cells [14], which is yet challenged by both FFA and age [15], this would promote lipotoxic effects ultimately leading to an acceleration of senescence and dysfunction of β-cells.

There are available data which point towards beneficial effects of plant-based nutrients [16]. Their beneficial effects are mainly, but not completely, thought to be mediated by their phytochemicals, consisting of heterogeneous substances with a variety of different bioactive molecules [17]. Beside e.g., carotenoids, glucosinolates, lectins, terpenes, alkaloids, and polysaccharides [18,19], the vast group of polyphenols has been investigated extensively for positive effects to improve insulin resistance and blood glucose levels [20]. Polyphenols can contain molecules like tannins, flavonoids, anthocyanins, proanthocyanidins, or derivatives of different organic acids [21–23], which are able to enhance action of insulin [24], glucose transport [25], or decrease intestinal carbohydrate hydrolysis [26–28]. These compounds can modulate antioxidative enzymes or cellular stress responses by gene expression [29–31] or regulation of cytokines and signaling pathways to improve β-cell function. By scavenging radicals and inducing the upregulation of antioxidative enzymes, phytochemicals can mitigate oxidative stress [32]. They directly control single steps in the lipid metabolism like uptake and storage of FFA to abate their toxic intermediates [33]. Moreover, phytochemicals can directly reverse the lipotoxic effects of FFAs by counteracting their adverse regulatory effects, e.g., by downregulating the respective signal pathways of insulin secretion or apoptosis [34]. There is a growing body of evidence that polyphenols could be able to reverse the negative effects of lipotoxicity and preserve, restore, and promote the physiological functions of β-cells.

The aim of this review is to (I) summarize the knowledge of basic research on lipotoxicity directed against β-cells, in particular their mitochondria, with special regard to methodology, (II) elucidate the connection with cellular senescence, and (III) outline potential beneficial effects of dietary measures employing polyphenols as an example.

2. Literature Search

The literature search based for this review was executed on 7th of September and 31st of December 2020 on PubMed. The search term (lipotox * OR "free fatty acid *") AND (mitochondria * OR polyphenol * OR flavonoid * OR ageing) AND "beta cell *" yielded a total of 149 primary articles. The publication dates ranged from February 1977 to September 2020. After screening literature, 22 articles were excluded. Exclusion criteria were no suitable topic (11 exclusions), not written in English (five exclusions), reviews with no primary data (five exclusions) and no available full-texts (one exclusion), leaving 127 articles. Three

reviews with primary data have been included. A flow chart of the literature search is given in Figure 1. A list of all screened articles is provided in Supplementary Material.

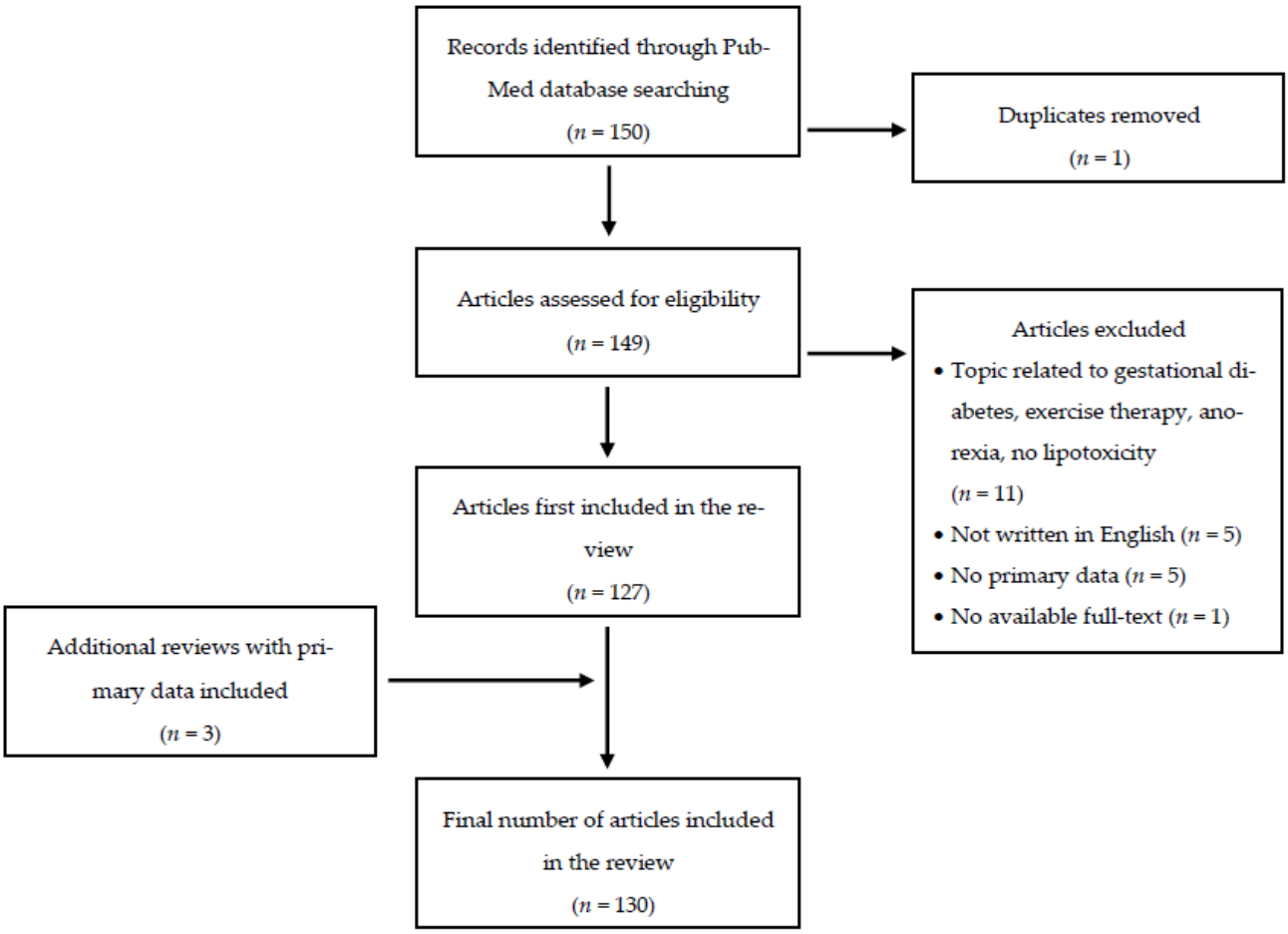

Figure 1. Flow diagram of the literature search on PubMed, www.ncbi.nlm.nih.gov/pubmed.

3. Factors Influencing Lipotoxic Outcomes in Tissue Culture

Since lipotoxicity cannot merely be defined by exceeding a specified concentration of FFA, the respective experimental setup must be considered closely when assessing experimental outcomes.

The employed amount of FFA is one of the key factors for activating lipotoxic pathways. However, only few authors state the rationale for the chosen concentrations. A point of reference could be the serum FFA level of healthy and diabetic subjects and animals.

Spectroscopic analysis of blood samples revealed that the total FFA concentration in diabetic human serum is ranging from 3.5 to 15 mM, also giving concentrations of specific FFA like oleic acid (OA) with 0.74–3.9 mM and palmitic acid (PA) with 1.0–3.8 mM [35–38]. These data also reveal an increase of OA and PA concentrations in diabetic compared to healthy individuals of approximately 10% [36]. Serum concentrations of rodents are lower with a total FFA serum concentration of 0.8–1.5 mM [39,40]. Authors claim that a FFA concentration range of 0.5–2.0 mM is suitable to mimic lipotoxicity in T2DM [41,42]. There is no detailed information about specific FFA concentrations for pancreatic tissue, which would indicate suitable concentrations for experimental models. Given the distinct magnitude of β-cell dysfunction on parameters like ATP production or insulin secretion, the increase of 10% in FFA concentration appears to be insignificant. These facts could indicate that considering the total FFA concentration is not a satisfactory parameter to determine a lipotoxic environment. A small increase of FFA concentrations could be sufficient to have greater impact on deteriorations of β-cell metabolism. All these facts

are raising the issue which concentrations should be employed for inducing lipotoxicity in an experimental setup. The screening of the available literature revealed significant differences. Most commonly 500 µM were used with a total range of 10–2000 µM. From the total of performed treatments with FFA (n = 104), there are available data for the following concentration ranges: 10–99 µM (n = 12), 100–499 µM (n = 53), 500 µM (n = 49), 501–2000 µM (n = 18) (Table 1). Single (n = 82) as well as multiple concentrations (n = 22) have been employed.

Table 1. Frequency of FFA concentrations used in screened literature focused on lipotoxicity (n = 132). Free fatty acids (FFA).

Concentration of FFA	Frequency in Screened Articles
10–99 µM	12
100–499 µM	53
500 µM	49
501–2000 µM	18

Insulin secretion and ATP levels were frequently examined. Treatment with 400 or 500 µM FFA led to a 6–90% decrease in ATP [4,43–45]. An incremented concentration of 2000 µM did not mediate higher toxicity [46]. A 15–70% diminished insulin secretion was induced by a short-or medium-term treatment (up to 72 h) with 400 or 500 µM FFA [47,48]. Exposure to 100 µM for several weeks led to a 20% decrease [49]. Glucose stimulation treatment was conducted with comparable concentrations of around 25 mM. The available data did neither reveal a dose dependent effect of FFA on insulin secretion, nor on ATP levels. Since the described protocols differed a lot in detail, e.g., regarding solvents, bovine serum albumin (BSA) amount, and incubation times, results were only comparable to a limited extent. For other readouts, the number of studies was too small to examine dose dependency.

In most tissue culture reports single rather than multiple FFA were examined. Hence, another key modulator for in vitro tissue culture is the selected type of FFA. It is noteworthy that only a small number of FFA have been used repeatedly for studying molecular pathways of cells. The most common design was the usage of single PA (n = 52), followed by the combination of PA + OA (n = 20), the combination of PA + OA + any additional FFA (n = 8), the combination of PA + any additional FFA (n = 6), treatment with single OA (n = 6), or with any single FFA (n = 4). Concentration range of combined FFA culture was 100–2000 µM (PA + OA), 200–1000 µM (PA + OA + any FFA) and 10–500 µM (PA + any FFA). The group of FFA used occasionally includes myristic, stearic, palmitoleic, linoleic, linolenic, methylpalmitic, docosahexaenoic, and arachidonic acid (Table 2). The combination of different types of FFA could be a suitable model for mimicking a physiological FFA composition [50].

Table 2. Frequency of FFA and FFA combinations used in screened literature (n = 96). Free fatty acids (FFA). Palmitic acid (PA). Oleic acid (OA). Any FFA is referring to myristic, stearic, palmitoleic, linoleic, linolenic, methylpalmitic, docosahexaenoic, and arachidonic acid.

FFA	Frequency in Screened Articles
PA	52
PA and OA	20
PA and OA and any FFA	8
PA and any FFA	6
OA	6
Any FFA	4

Furthermore, the preparation of FFA solutions can have a major impact on the outcome depending on the applied assays. For dissolving FFA, the reviewed articles used ethanol (n = 25), NaOH or NaCl (n = 12), dimethyl sulfoxide (n = 4), and methanol (n = 3), while most articles did not specify how the FFA solutions have been prepared (n = 54) (Table 3). The use of solvents should be tested on key parameters like viability and also insulin concentration because they can affect the outcome by varying cytotoxic properties [51,52]. In addition, the total BSA concentration as well as the molar FFA:BSA ratio can have a drastic impact on the mediated lipotoxicity as well as specifically on the MTT viability assay [53,54], and were only described in detail in half of the studies (n = 53). The utilized BSA content in the respective cell culture media varied markedly, ranging between 0.05–5% for comparable FFA concentrations [55,56]. The molar FFA:BSA ratio determines the amount of unbound FFA in the treatment media, representing a more decisive parameter when compared to the total FFA concentration according to some authors [57]. Commonly used molar FFA:BSA ratios within the literature were at maximum 5:1. It was suggested to not exceed this ratio [57], whereas due to hyperlipidemia, higher ratios could be suitable for modeling the pathophysiological state in T2DM [58].

Table 3. Frequency of used solvents in screened literature (n = 98).

Solvent	Frequency in Screened Articles
Ethanol	25
NaOH or NaCl	12
Dimethyl sulfoxide	4
Methanol	3
No further information	54

The vast amount of the reviewed data (n = 199) were obtained from rodent cell culture (rodent n = 96, human n = 12, monkey n = 1) and animal models (Table 4). If comparing the results obtained from cell lines and primary β-cells, there are no remarkable differences if same FFA concentrations are applied [59,60]. There is no indication that there is an adaption of applied FFA concentrations depending on whether rodent cell lines and isolated human islets are used. This leads to the question if FFA concentrations used in rodents are suitable for studying human-based systems.

Table 4. Frequency of cell culture models used in screened literature (n = 109). Insulinoma (INS-1). Mouse insulinoma 6 (MIN6). Human embryonic kidney 293 (HEK 293). Rat insulinoma (Rinm5f). Hamster islet transformed-tioguanine resistant clone 15 (HIT-T15). Hepatoblastoma (HepG2). Chinese hamster ovary (CHO). NOD/Lt (NIT1). β-tumour cell (βTC6). CV-1 in origin simain-1 (COS1).

Cell Line	Frequency in Screened Articles
INS-1 (rodent)	57
MIN6 (rodent)	23
HEK 293 (human)	7
Rinm5f (rodent)	5
HIT-T15 (rodent)	5
HepG2 (human)	3
CHO (rodent)	2
EndoC-βH1 (human)	2
NIT1 (rodent)	2
βTC6 (rodent)	1
BRIN-BD11 (rodent)	1
COS1 (monkey)	1

4. Factors Influencing Lipotoxic Outcomes in Animal Models

In animal experiments a high fat diet ranging from 20–60% fat content (n = 12) was reported. There was no direct treatment of animals with isolated FFA (n = 18).

Animal models (n = 73) included 23 studies using wild types (C57BL/6 n = 15, C57BL/6J n = 8) and 11 using specific mutations of metabolism (C57BL/6 mutants n = 8, C57BL/6J mutants n = 3), Wistar rats (n = 11), Sprague Dawley rats (n = 9), db/db (n = 4), ob/ob, CD1 mice, Zucker diabetic fatty rats (each n = 3) and ICR, NMRI, KK-Ay, Atg7f/f, HcB19 and nu/nu mice (each n = 1) (Table 5). In 17 articles, isolated islets from humans were investigated. The mentioned parameters like chosen model, type, and concentration of FFA as well as preparation of FFA stock solutions must be carefully considered while comparing the different results.

Table 5. Frequency of animal models used in screened literature (n = 73). Institute for Cancer Research (ICR). Naval Medical Research Institute (NMRI). Diabetic KK and lethal yellow (Ay) mice (KK-Ay). Ubiquitin-like modifier-activating enzyme (ATG7). TXNIP deficiency (HcB19).

Animal Model	Frequency in Screened Articles
wild type C57BL/6 and C57BL/6J mouse	15 and 8
mutant C57BL/6 and C57BL/6J mouse	8 and 3
Wistar rat	11
Sprague Dawley rat	9
db/db mouse	4
ob/ob mouse	3
CD1 mouse	3
Zucker diabetic fatty rat	3
ICR mouse	1
NMRI mouse	1
KK-Ay mouse	1
Atg7f/f mouse	1
HcB19 mouse	1
nu/nu mouse	1

5. Lipotoxic Action of FFA on Mitochondria in β-Cells

5.1. Detrimental Effects of Elevated FFA in Type 1 and Type 2 Diabetes Mellitus

FFA are well known to mediate toxic effects and impair the function of β-cells enhancing blood glucose levels and increasing the cellular abundance of glucose molecules. Since T2DM patients are exposed to elevated FFA blood levels, they are considered at special risk to suffer from lipotoxic effects including damaged β-cells.

Both reduced insulin levels and action promote lipolysis, but the specific cause why FFA are elevated remain mostly unclear [61]. The abundance of energy generated by the so-called "obesogenic" environment, hallmarked by low physical activity and high caloric, Western-style diet rich in short-chain carbohydrates and animal fats [11], is considered an important link between elevated FFA in T2DM, obesity, and related deteriorations in lipid metabolism. Importantly, a pathological insulin resistance is promoted by lipotoxic effects [43], representing a major mechanism for obesity as a risk factor for T2DM. In type 1 DM, there is no predominant correlation between lipotoxicity and destruction of β-cells [62].

FFA are able to mediate lipotoxicity at different stages of their metabolism covering the range from uptake [63] to degradation [64]. Therefore, lipotoxicity is of a multifactorial etiology and not restricted to a single specific pathway. The following sections will elucidate the underlying pathophysiological mechanisms.

5.2. Cellular Uptake of FFA by CD36 and Impairment of Calcium Concentration

FFA uptake into the cell is mediated by fatty acid transporter, also known as cluster of differentiation (CD) 36 [65]. It is known that β-cells abundantly express CD36 [66], probably to ensure a constant FFA supply for energy allocation. CD36 does have substrate specificity, preferring long chain over medium chain FFA [67]. By the binding of long chain FFA to CD36, a pro-inflammatory response is promoted [68] inducing elevated levels of oxidative stress and cellular damage. A relief from oxidative stress can be detected by deletion of CD36 [69]. Another mechanism of FFA uptake is by binding to the free fatty acid receptor 1, also known as the G protein-coupled receptor (GPR) 40 [70]. GPR40 activates phospholipase C (PLC) [71] which is degrading phosphatidylinositol-4,5-bisphosphate into the signaling molecules inositol trisphosphate (IP3) and diacylglycerol to increase the cytosolic calcium (Ca) concentration [72]. Furthermore, Ca storages of the mitochondria are released by PLC, and the endoplasmic reticulum (ER) can release its Ca storages through the activation of GPR40 [71]. The increase of the cytosolic Ca concentration induces exocytosis of insulin vesicles [73]. The replenishment of Ca storages is facilitated by the activation of the sarcoplasmic/endoplasmic reticulum calcium ATPase (SERCA). SERCA activity is stress-sensitive and can be impaired by abundant FFA. As a result, depleted Ca storages render GSIS impossible [74], and Ca-sensitive enzymes of the tricarboxylic acid (TCA) cycle or the transport of NADH as well as the electron transport chain in mitochondria are dysregulated [73].

5.3. Mitochondrial Uptake and Processing of FFA

Cytosolic FFA must be activated to acyl-CoA by coenzyme A for further reactions. Acyl-CoA can be transported into the mitochondria by carnitine palmitoyltransferase (CPT) 1, also known as carnitine acyltransferase I [75]. CPT1, the key enzyme of lipid metabolism [76], will exchange the CoA residue with carnitine and initiate the transport across the outer mitochondrial membrane. The transport across the inner mitochondrial membrane is facilitated by carnitine-acylcarnitine translocase and finally, CPT2 will perform the cleavage into carnitine and acyl-CoA in the mitochondrial matrix. Acyl-CoA will be degraded through several enzymatically catalyzed steps of β-oxidation leading to the formation of acetyl-CoA and the reduction equivalents NADH and $FADH_2$ [77]. Glycolysis will generate acetyl-CoA and the respective reduction equivalents. Acetyl-CoA from FFA or glucose will be used in the TCA cycle to generate more reduction equivalents.

An important biochemical feature of lipotoxicity is the impaired activity of glycolytic and TCA cycle-related enzymes with the associated ability for anaplerotic reactions. The impaired enzymes, among others the citrate synthase [78], cause a shortage of intermediates required for the TCA cycle like oxaloacetate, citrate, and α-ketoglutarate [79], which might also be caused by a reduced activity of pyruvate carboxylase [80–82], and is also directly proportional to GSIS [83]. The gene expression of those enzymes is impaired [84], and the

exchange of pyruvate with TCA cycle intermediates like citrate or malate is abolished and blunts GSIS [85].

5.4. FFA-Induced Deterioration of Anaplerosis

FFA decrease glutamine levels [86], an amino acid which supports pyruvate transport [87]. Elevated FFA are thought to influence glutamine by increasing the transformation into glutamate [88] and impairing the activity of glutamine synthetase [89]. Decreased glutamine levels further impair the function of β-cells by inhibiting cellular respiration and glucagon-like peptide 1 (GLP-1)-promoted GSIS [86,90] incrementing ROS and the unfolded protein response (UPR).

Interestingly, Lee et al. reported that pyruvate carboxylase inhibition, both by phenylacetic acid (PAA) as well as by high glucose/PA treatment, mitigates AMP-activated protein kinase (AMPK), promoting apoptosis in insulinoma (INS-1) cells. By contrast, AMPK activation was protective against lipotoxic cytotoxicity. PAA and PA treatment promoted CCAAT/enhancer binding protein homologous protein (CHOP) [79] and phosphorylated c-Jun N-terminal kinases (JNK) [91]. The activation of CHOP mediates ATP depletion, consequently reducing GSIS [92]. The reduced flux of metabolites like oxaloacetate, citrate, and α-ketoglutarate worsens the harmful effects of lipotoxicity, whereas the reconstitution of anaplerosis alleviates the consequences of lipotoxicity, as reactions providing intermediates for TCA cycle are enhanced [79]. The authors suggest that the cause for lipotoxicity is closely related to fuel supply by TCA cycle.

In diabetic mouse models it was observed that T2DM correlates with a decreased activity of the pyruvate dehydrogenase complex [93]. This enzyme complex is necessary for glucose utilization and energy production in the TCA cycle. Glucose will be degraded to pyruvate, and through pyruvate dehydrogenase shortened to acetyl-CoA, implicating pyruvate and its related metabolic pathways exert a crucial role for the mitochondrial function [79].

5.5. Impairment of Iron-Sulfur Cluster Biosynthesis and Ferroptosis Is Induced by FFA

The impaired formation of iron-sulfur (Fe/S) clusters [94,95] was reported to be affected by elevated FFA. These clusters are generated in mitochondria by the iron-sulfur cluster assembly machinery (ISC) [96]. The ISC contains more than 18 proteins responsible for the formation, transfer, or insertion of Fe/S clusters into apoproteins [97]. Fe/S clusters contribute to three-dimensional molecular structure, transfer electrons, or are enzymatic co-substrates. Some of the Fe/S enzymes are involved in energy metabolism like complex I [98], II [99], and III [100] of the respiratory chain. Other Fe/S enzymes serve as sensors for oxygen [101], are involved in gene expression [102] or lipid metabolism [103]. Aconitase, an Fe/S cluster containing enzyme, is especially interesting in this context [104]. It has different functions in the cell depending on its localization. While the mitochondrial aconitase is part of the TCA cycle, the cytosolic aconitase has a regulatory function in Fe-homeostasis and is accordingly termed iron regulatory protein 1 (IRP1) [105]. While losing its Fe/S cluster in an Fe-deficient state, IRP1 binds the iron regulatory element (IRE) of mRNA. IREs are part of the cellular iron-regulatory machinery like ferritin, transferrin receptor 1, divalent metal transporter 1, or ferroportin. By binding IRP1 to IRE, the Fe-uptake into the mitochondria is increased, thus providing more Fe for the Fe/S cluster formation. This regulation by IRP1 is highly conserved and found in yeast, plants, animals, and humans [106]. As previously shown, FFA-induced deficiency of glutaredoxin 5 (Glrx5), a protein of the ISC transferring Fe/S clusters, disrupted the Fe/S cluster insertion into apoproteins [94,95]. FFA-mediated cellular stress or impaired protein maturation could be detrimental for the sensitive clusters and enzymes. Consequently, enzymes of the TCA cycle and complexes of the respiratory chain act less efficiently leading to reduced production of ATP. Furthermore, the Fe-regulation by the cytosolic aconitase is impaired inducing uncontrolled Fe-uptake into the mitochondria. Mitochondrial Fe-overload in combination with elevated ROS promotes the generation of lipid peroxides leading to an Fe-dependent form of non-apoptotic

cell death [107] called ferroptosis [60]. Glutathione peroxidase (GPx) 4 is an enzyme which has protective properties by lowering lipid peroxides in a glutathione (GSH) dependent reaction [108] thereby counteracting ferroptosis. Furthermore, FFA also deplete GSH, therefore debilitating the detoxification of lipid peroxides by GPx4 [109]. By increasing oxidative stress, FFA can induce the transformation of GSH into glutathione disulfide [110]. A lipotoxic-induced deficiency of Glrx5 might therefore impair mitochondrial metabolism by lowering activity of TCA cycle enzymes and complexes I-III as well as the induction of β-cell decay by ferroptosis and could be correlated to lower GSIS. Glrx5 mutations have been described in seven human case reports [106,111–114], of which three describe a link to DM, ferroptosis, and impaired enzyme activities [106,112,114].

5.6. FFA Utilization in Energy Metabolism Contributes to Oxidative Stress

In cells with adequate oxygen supply complexes I-IV use reduction equivalents generated by acetyl-CoA to build up a proton gradient in the respiratory chain to generate ATP at complex V (ATP synthase). The electron transfer caused by complex I, complex II, and complex III will generate ROS in a reaction with oxygen [115], complex I contributing to the largest extent [116]. The excessive use of FFA or glucose for energy production will lead to an increased amount of ROS, eventually damaging the cells by reactions with molecules like DNA or enzymes or producing lipid peroxide, triggering ferroptosis.

Another way of generating ROS out of FFA is the β-oxidation in peroxisomes. Again, it is difficult to define at which specific concentrations ROS become harmful for cell physiology. It is important to note that the imbalance between ROS production and detoxification is the detrimental key factor for oxidative stress. As β-cells have reduced amounts of antioxidative enzymes, it seems likely that the threshold of an overwhelmed antioxidative defense is lower compared to other types of cells.

There are some data indicating that FFAs mediate an increasing level of toxicity depending on their carbon chain length. Especially long chain fatty acids are suspected to be preferably metabolized in peroxisomes due to specific FFA importers in mitochondria and peroxisomes while less toxic short chain and middle chain FFAs are degraded in the mitochondria [115]. Thus, a diet rich in middle chain fatty acids is not detrimental to β-cells and even promotes GSIS [117], presumably mediated through GPR40.

In human plasma, the five most abundant FFAs, namely OA, PA, stearic, linoleic, and palmitoleic acid, do have a minimum carbon chain length of 16 carbon units and belong to the group of long chain fatty acids. These represent more than 90% of the total amount of FFA in human plasma [118]. The reactions of β-oxidation in peroxisomes are mostly similar to the reactions in the mitochondria, except for the initial step that is facilitated by different enzymes. In peroxisomes the acyl-CoA oxidase will reduce FAD to $FADH_2$ and form a double binding in the carbon chain of fatty acids. The acyl-CoA dehydrogenase will perform the same reaction in mitochondria [119]. While the electron transfer to $FADH_2$ in mitochondria by acyl-CoA dehydrogenase can be further used for ATP production, in peroxisomes the electrons will interact with oxygen to form hydrogen peroxide (H_2O_2). Loading with FFA leads to an increased formation of H_2O_2 in peroxisomes as compared to mitochondria [120]. H_2O_2 is membrane permeable [121] and can induce negative effects also outside of these organelles and impair insulin secretion. These observations support the hypothesis that ROS production by peroxisomal β-oxidation as well as by mitochondrial respiratory chain complexes are the major reasons for lipotoxicity. Due to a lack of the expression of catalase, GPx1, and superoxide dismutase (SOD), β-cells seem to have only weak protection against oxidative stress [14,122]. Other authors are raising issues that β-cells are also equipped with other antioxidant systems like proteins of the thioredoxin family making them more resistant to stress conditions as generally assumed [123].

5.7. Uncoupling and GLP-1 Agonists Relieve Cellular Stress

As an adaptive response to increased oxidative stress, β-cells are able to induce the expression of uncoupling protein (UCP) 2. UCP2 is a proton channel localized at the

inner mitochondria membrane dissipating proton gradients [124]. There are four existing isoforms, while only UCP2 is occurring in β-cells [125]. Uncoupling of mitochondria in brown adipose tissue by UCP1 is known as a useful process for generating heat [126]. However, uncoupling in β-cells by UCP2 is not proven as part of thermogenesis [127]. The uncoupling in β-cells is probably a rather adaptive response to increased oxidative stress. The elevation of ROS, especially superoxide as produced by complexes I and III, is required for the upregulation of UCP2 [128,129]. Increased H_2O_2 concentrations further activate calcium-independent phospholipase A2 γ (iPLA$_2$γ) and fuel UCP2 uncoupling [56]. iPLA$_2$γ alleviates oxidative stress, but it is also a phospholipid remodeling and repair factor of the inner mitochondrial membrane targeting oxidized cardiolipin. Cardiolipin is important for mitochondrial function by regulating gene expression and influencing electron transfer at the respiratory chain complexes [130]. Exendin-4, a GLP-1 agonist used in DM therapy, can increase insulin secretion and reduce β-cell apoptosis by mechanisms including acetylation of iPLA$_2$ γ [131,132] as well as upregulation of pancreatic and duodenal homeobox 1 (Pdx1) also known as insulin promotor factor 1 [133]. The regulation of Pdx1 is additionally mediated by a FFA induced increase of Small heterodimer partner interacting leucine zipper protein, which again increments apoptosis [134]. FFA are ligands for the peroxisome proliferator-activated receptor (PPAR), a receptor responsible for modulation of various pathways in lipid metabolism. There are three subtypes of PPAR, namely PPAR α, PPARβ/δ, and PPARγ [135]. All of these subtypes can be activated by FFA and will increase the transcription of UCP2 [4,76,136–139]. Polymorphisms in the promotor area can also lead to a deterioration of lipid metabolism leading to obesity [140].

5.8. ATP Production Is Diminished by Uncoupling and Reduction of ATP Synthase Activity

The promotor region of UCP2 contains a sterol regulatory element (SRE). Binding by sterol regulatory element binding protein (SREBP)-1c can increase UCP2 expression [141,142]. This process is promoted by FFA. Furthermore, hormone sensitive lipase, an enzyme degrading TG into FFA, activates UCP2 linking elevated FFA levels to UCP2 activation [137].

It was shown that the uncoupling of the proton gradient is dependent on the structure of FFA, and saturated FFA promote uncoupling and exert cytotoxic effects [143]. The uncoupling of the respiratory chain by UCP2 will reduce the amount of ROS, though also lowering the ATP production at complex V. FFA can also influence the ATP synthase regardless of uncoupling factors. The ATP synthase consists of two complexes, F1 and F0. While F0 will decrease the proton gradient, F1 is the catalytic complex forming ATP [144]. The F1 complex is build up by several subunits. Among these, the β-subunit has a crucial role in ATP production because of its ATP binding site. It is reported that FFA can reduce the expression of that specific subunit leading to a decreased ATP production [145]. FFA can also induce acetylation of Sirtuin, which modulates the activity of complex V [146].

5.9. Membrane Potential Is Modulated by the Abundance of Glucose and FFA, and Impairs Insulin Secretion

The mitochondrial membrane potential (MMP) is dependent on a sufficiently high proton gradient within the mitochondria. FFA are well known to decrease the MMP by an UCP2-induced lowered proton gradient [49]. The reduced MMP is not only linked to reduced ATP amounts and mitochondrial dysfunction, but also to the early stage of apoptosis and therefore β-cell decay [147]. A decreased MMP and a lowered cellular ATP/ADP ratio are counteracting insulin production and secretion of insulin vesicles, connecting mitochondrial function to insulin release. The uncoupling of respiratory chain complexes is a mechanism to relieve cells of oxidative stress, whereas extensive uncoupling subsides the ATP production. As the aerobic ATP production and reduced hyperpolarization of MMP is a crucial factor for inducing insulin secretion [148,149], extensive uncoupling is not favorable for β-cells. If studied in vitro, the lipotoxic effect by uncoupling of the respiratory chain is mostly seen in states of elevated glucose concentrations [59,78]. In a glucose-stimulated state, β-cells are more depending on ATP rendering them more vulnera-

ble against inefficiencies of the respiratory chain activity. Further suggestions indicate, that the lipotoxic uncoupling requires a high membrane potential reached at elevated glucose levels [150]. Interestingly, the impact of different glucose concentrations is suggested to be highly dependent on the employed model. While INS-1 cells show a glucose-dependent increase in apoptosis, no such effect was detectable in mouse insulinoma 6 (MIN6) cells or cultured human islets [151]. In the screened literature, few articles were able to observe such a glucose dependency in other cell lines than INS-1 [59,116,152–156].

5.10. PPAR Activity Is Incremented By FFA

Glucose can decrease the action of PPARα leading to limited fatty acid metabolization [138]. This so-called glucose fatty-acid cycle (Randle cycle) ensures a sufficient energy supply to the cells as lipid storages are not used for energy production if enough glucose is available and remain unaffected for phases of starvation. In general, a downregulated rate of fat metabolism with decreased FFA clearance enhances lipotoxic effects by accumulation of lipid intermediates [157] such as acyl-CoA and malonyl-CoA. The accumulation of especially long chain acyl-CoA in the cytosol induces functional impairment and apoptosis by mediating signaling effects and Ca release. Acyl-CoA interacts with PPARα [138] promoting apoptosis [72], uncoupling of respiratory complexes [133], and storage as TG [158], ultimately impairing GSIS [157]. Based on the acyl-CoA content of hamster islet transformed-tioguanine resistant clone 15 (HIT-T15) cells and the average distribution of cytosolic and mitochondrial mass in mouse pancreas [159], it is estimated that the cytosolic acyl-CoA concentration in rodent β-cells is 90 µM, while tissue concentrations are unknown [160]. Malonyl-CoA inhibits CPT1 preventing the mitochondrial uptake of acyl-CoA [156]. Yet, there are contrary conclusions regarding the influence of CPT1 in the context of lipotoxicity. While two publications indicate that mitochondrial FFA oxidation is required for lipotoxic effects and can be counteracted by the inhibition of CPT1 [93,138], another study suggests that the inhibition of CPT1 has no effect on lipotoxicity [57] indicating that FFA mediate lipotoxicity independently from mitochondrial metabolism.

5.11. The Process of Autophagy Is Disturbed by FFA

PPARγ regulates the gene expression responsible for autophagy [139] and apoptosis. While low grade autophagy activity is a requirement for remodeling of damaged cellular components [161], enhanced autophagy leads to disintegration of the β-cell [162]. In case of mitochondria, this process is called mitophagy. In the first step, damaged cellular components form autophagosomes [43], which are degraded by lysosomes. The activity of lysosomes is depending on ATP needed for acidification [43]. Thereby, FFA can reduce the lysosomal activity [163,164]. This will lead to an accumulation of autophagosomes [161]. Additionally, FFAs can disturb the process of autophagy by lowering the expression of the mechanistic target of rapamycin (mTOR) [43] and overexpression of optic atrophy protein 1 [163] or dynamin-related protein 1 [165]. An increase in mTOR by FFAs is also related to insulin resistance [43].

5.12. Acyl-CoA Abates Insulin Synthesis in B-Cells

Acyl-CoA is able to degrade the proton gradient of the respiratory chain through the formation of mitochondrial permeability transition pore [166] disturbing GSIS [71]. An increase in long chain acyl-CoA can inhibit the closure of ATP-dependent potassium (K)-channels [167,168]. Factors involved in this effect are the acyl group, the CoA component, and protein kinase C [169]. FFA can open K-channels by direct interaction [170] or as a consequence of GPR40 mediated Ca influx, which is both decreasing the ability of glucose to stimulate insulin secretion. In addition, the mRNA level of insulin is reduced by acyl-CoA [156] and palmitoylation [57,171], as well as the interaction with hepatic nuclear factor 4a, which could be related to uncoupling by UCP2 [45]. Some authors claim that the activation of FFA into acyl-CoA is one of the most essential aspects mediating harmful

effects as the inhibition of acyl-CoA synthase could suppress lipotoxicity-mediated cell death [172,173].

5.13. Ceramides Increase Oxidative Stress through Inducible Nitric Oxide Synthase

Palmitoyl-CoA, the activated form of PA, is substrate for the *de novo* formation of ceramides and upregulates sphingosine kinase 2 (SK2), a key enzyme of ceramide synthesis. Ceramides have impact on various pathways including proliferation, differentiation, growth arrest, and apoptosis [174,175]. They can impair insulin sensitivity by protein kinase C [138] and phosphorylation of insulin receptor substrate 1 (IRS-1) [176] as well as reduce insulin expression by Pdx1 [78]. IRS-1, which is likewise regulated by SREBP-1c [153], is integrated in proliferation signals by PI3K and Akt, while Akt also regulates glucose uptake by GLUT4. Furthermore, ceramides disrupt the acetylation of proteins of the mitochondrial metabolism [177], inhibit complex III, and decrease MMP [42]. They increase cellular oxidative stress through the activity of inducible nitric oxide synthase (iNOS) producing nitrogen oxide [57,79,139,178,179] and NADPH oxidase 2 (NOX2) producing superoxide [55,178,180–182]. The activation of both iNOS and NOX2 induces apoptosis by damaging mitochondrial DNA [155], which is more susceptible to harm due to the absence of introns [179]. Damaged DNA can be recognized by stimulator of interferon genes (STING), increasing inflammation and apoptosis. The STING pathway is enhanced under lipotoxic conditions and activates interferon regulatory factor 3 [47]. It has been shown that the presence of ceramides is crucial for the induction of apoptosis. While the regulation of mitogen-activated protein kinase (MAPK) pathway including JNK and extracellular-signal-regulated kinase (ERK) as well as Pi3K/Akt pathway are undoubtedly essential for cell survival, there are contrasting data regarding their exact role for the β-cell. According to literature, effects differ crucially between cell types and highly depend on the chosen treatment conditions [132,183], e.g., PA inhibited ERK and induced apoptosis in INS-1 cells [184], but exposure of glucose and interleukin (IL)-1β triggered apoptosis concomitant with elevated ERK levels in human β-cells [44,185].

Additionally, SK2 was reported to increase apoptosis through Bcl-2, while SK2 inhibition prevented lipotoxic cell death [186]. The regulation of apoptosis by ceramides is seen as one of the most important factors for β-cell decay mediated by lipotoxicity [187]. While unsaturated FFA are not able to increase ceramides [188], other data indicate facilitated ceramide production through an increased ω6:ω3 ratio of fatty acids [189].

5.14. Augmented Apoptosis in B-Cells by Long-Chain and Saturated FFAs

The initiation and execution of the mitochondrial apoptosis pathway is complex and highly regulated. Briefly, the membrane of damaged cells starts to permeabilize, which is enhanced by Bax or p53-upregulated modulator of apoptosis and suppressed by Bcl-2 [190]. The permeabilization is promoted by several stress markers related to the ER, like CHOP, or the activating transcription factor [191]. The release of pro-apoptotic factors eventually triggers downstream caspases like caspase 3. In consequence, chromatin will condensate, DNA will be fragmented, and apoptosis is executed. Particularly long chain and saturated FFA as opposed to intermediate chain length and unsaturated FFAs induce ER stress [64] and counteract protective factors such as Sirtuin3 [44,91]. The fragmentation of DNA is further promoted by oxidative stress sensitive transient receptor potential melastatin-2 channels, inducible by lipotoxicity [55].

6. Positive Effects of FFA on β-Cell Function

The number of articles reporting beneficial effects of FFA to β-cells and insulin secretion is remarkably low. Most intriguingly, they share the same underlying pathways as detrimental effects. Although this seems to pose a contradiction at first, a more detailed look into the respective methodologies can give possible explanations.

FFA concentrations employed in studies delivering evidence for a beneficial impact were notably lower [71,170,171,192]. While publications reporting detrimental effects of

FFA usually applied concentrations around 500 μM, favorable effects were reported with concentrations far below 100 μM. Furthermore, shorter treatment times were associated with positive results indicating a difference between the acute and chronic exposure to FFA. Acute effects were observed after a few hours of treatment while chronic effects were noticeable after at least 24 h. Exposure of INS-1 cells to 100 μM for several weeks severely blunted their insulin secretion (−80%) [49], whereas it was promoted by 1 h incubation with 150 μM PA [56]. The short time treatment with low FFA concentration led to the activation of PPARγ coactivator 1α/β [193] and a depletion of Ca storages by GPR40, mediating insulin release [170]. The so-called "fatty acid stimulated insulin secretion" (FASIS) is induced by acute FFA uptake and oxidation through the activation of cellular energy production [72,158,194]. Resulting physiological low concentrations of ROS are also promoting insulin secretion, which is referred to as "redox stimulated insulin secretion" (RSIS) [56]. This effect is explained by PTEN-induced kinase 1 (PINK1)-mediated autophagy activation, which is improving net insulin release pattern by disposal of damaged cells [162]. In contrast, chronic elevation of FFA exerts a detrimental impact on insulin secretion through permanent depletion of Ca-storages, and an abundance of ROS.

Another decisive aspect in lipotoxicity is the homeostasis between FFA and fat storage mobilization. The available data indicate that stored neutral TG do not act lipotoxic in contrast to FFA [195]. Therefore, it is crucial to differentiate between an energy surplus leading to an excess of FFA on one hand and a storage as neutral TG on the other hand. While adipocytes have a nearly unlimited TG storing capacity, fat storing in β-cells is limited [195,196]. There are some articles implying that unsaturated FFA promote TG storage, thereby counteracting the toxic effect of saturated FFA [195,197]. Other authors assume that the protective effect is independent from fat storage [198], but rather reliant on a positive effect of unsaturated FFA to proapoptotic factors [46], while also inducing mitochondrial apoptosis [199]. Further data suggest an anti-lipotoxic effect of unsaturated FFA [200]. However, the underlying mechanisms have not yet been elucidated. Unsaturated FFA reveal their anti-lipotoxic effect mainly in co-treatment with saturated FFA. As sole treatment with unsaturated FFA is also toxic, enhanced lipid storing by unsaturated FFA should be further investigated as protective mechanism. It has been shown that the amount of unbound FFA is a better parameter for lipotoxicity instead of total concentration of FFA [57]. A summary of beneficial effects to β-cell physiology can be found in Table 6.

Table 6. Summary of metabolic effects of FFA treatment and respective pathways. Palmitic acid (PA). Insulinoma (INS-1). Glucose-stimulated insulin secretion (GSIS). Adenosine triphosphate (ATP). Calcium (Ca). Free fatty acids (FFA). Hamster islet transformed-tioguanine resistant clone 15 (HIT-T15). Phospholipase C (PLC). Endoplasmic reticulum (ER). Peroxisome proliferator-activated receptor (PPAR). Institute for Cancer Research (ICR). Chinese hamster ovary (CHO). Human embryonic kidney 293 (HEK 293). Hepatoblastoma (HepG2). Mouse insulinoma 6 (MIN6). Uncoupling protein (UCP). G protein-coupled receptor (GPR). PTEN-induced kinase 1 (PINK1). Oleic acid (OA). Triglyceride (TG).

Article	Treatment	Model	Results and Respective Pathways
Green et al., 2009 [192]	50 μM PA, 1 h	INS-1 cells, human islets	- liver X receptor improved GSIS - β-oxidation provided ATP for GSIS - lipid signaling supported Ca influx
Komatsu et al., 1999 [171]	10 μM PA, 1 h	Wistar Rat islets	- FFA supported GSIS within first 10 min of secretion
Remizov et al., 2003 [170]	100 μM PA, 30-60 min	HIT-T15 cells, primary mice β-cells	- FFA caused Ca mobilization from internal storages
Zhao et al., 2013 [71]	20 μM linoleic acid, 2-10 min	Sprague Dawley rat islets	- FFA stimulated Ca increase. Effect depended on Acyl-CoA synthase, PLC, and ER/mitochondrial Ca storages
Oropeza et al., 2015 [193]	100 μM PA, 1 h	C57BL/6J mice islets	- FFA increased PPARγ coactivator 1α expression, regulating key enzymes in lipolysis and the glycerolipid/free fatty acid cycle
Chen et al., 2020 [72]	10 μM linolenic acid, 1 h	INS-1 cells, KO mice islets, Wistar Rat islets	- FFA receptor 1 agonist supported insulin secretion by increased mitochondrial function and β-oxidation
Li et al., 2020 [194]	10 μM linolenic acid, 1 h	ob/ob mice, ICR mice, C57BL/6 mice, CHO cells, HEK293 cells, HepG2 cells, MIN6 cells	- FFA receptor 1 agonist supported insulin secretion and glycemic control
Li et al., 2020 [158]	No FFA	C57BL/6 mice, ob/ob mice, db/db mice	- FFA receptor 1/PPAR agonist supported β-cell function and fatty acid metabolism
Ježek et al., 2015 [56]	150 μM PA, 1 h	INS-1 cells	- FFA activated UCP2. Oxidative stress by physiological FFA uptake was prevented. - PA increased insulin secretion by GPR40
Guo et al., 2019 [162]	100–500 μM PA, 24–48 h	RIN-m5f cells	- sonodynamic therapy increased insulin secretion of damaged cells by activated PINK1 autophagy
Cho et al., 2012 [195]	100–500 μM PA, 24 h and 10–62 μM arachidonic acid and 20–120 μM unsaturated FFA (OA, arachidonic acid, palmitoleic acid)	HIT-T15 cells	- unsaturated fatty acids protected against PA damages, probably by TG accumulation
Tuo et al., 2011 [199]	50–500 μM linoleic acid, 48 h	INS-1 cells	- negative effects occurred from 250 μM upwards for viability, effect depended on high glucose concentrations
Ježek et al., 2018 [200]	100 μM PA, 10-60 min	C57BL6J mice islets	- monoacylglycerol bound to GPR119 and enhanced insulin secretion
Cnop et al., 2001 [57]	125–500 μM PA and OA, 2 d and 8 d	Wistar Rat islets	- OA treatment accumulated more TG than PA, ameliorating the detrimental effects of FFA

7. Influence of Ageing on β-Cell Function

Since there are multiple mechanisms by which lipotoxicity can impair β-cell function, this section will review which of the underlying pathways are especially related to accelerated ageing and senescence of β-cells and the pancreas. Cellular senescence is defined by a cell cycle arrest triggered by damaged DNA, exerting an anti-tumorigenic purpose [201]. It can be induced due to telomere shortening at the end of a cell's life span, or, dependent on the physiological conditions, as part of the cellular stress response. Lipotoxicity is linked to cellular senescence by the p38 MAPK pathway which is age-dependently correlating

with decreased cell proliferation and insulin release in β-cells. Lipotoxicity can contribute to the activation of p38 MAPK by elevated ROS and ceramides. p38 MAPK promotes senescence through different pathways, which are dependent on and independent of telomerase length [202]. As autophagy can be regulated by MAPK, it is tempting to speculate that lipotoxicity might thereby impair the degradation of damaged organelles and cellular regeneration. Age-dependently, ROS and levels of radicals tend to accumulate and lead to enhanced damaging of mitochondrial proteins and DNA, leading to cellular dysfunction. Beside cellular damaging and signal pathways, glucose and insulin homeostasis is impaired by decline in mitochondrial ATP synthesis capacity and reduced expression and translocation of GLUT2 [117]. In addition, depending on age, the insulin dependent uptake by GLUT4 is decreased by Ras-related C3 botulinum toxin substrate 1 (Rac1), a protein which is correlating with ceramide-mediated senescence [203]. In presence of ceramides, the activation of Rac1 could also influence oxidative stress by induction of NOX2 [178]. With increasing age, the activity of insulin like growth factor (IGF) binding protein 3 as well as the total amount of IGF decline. A reduced binding of IGF leads to the deterioration of glucose tolerance, lipid metabolism, and increased stress by absent UCP regulation [204]. FFA can further have negative effects on the activity of the subunits of farnesyl transferase (FTase) and geranylgeranyl transferase (GGTase). FTase and GGTase are enzyme complexes required for the prenylation of proteins determining localization and transport of proteins. The degradation of subunits of FTase and GGTase by FFA activation of caspase is chronically activating Rac1 leading to increased cellular stress. The impairment of protein prenylation has negative consequences on GSIS and is connected to ageing syndromes [180]. A further increase of senescence has been seen in involving caveolin-1, a membrane protein inducing apoptosis by Src family kinases-mediated phosphorylation of tyrosine-14, which is promoted by FFA [42]. While they are known ways, how lipotoxicity is correlating with acceleration of β-cell senescence, the data in this literature search are limited to few articles (n = 15).

8. Potential Protective Effects of Plant-Based Nutrients

A healthy lifestyle involving sufficient exercise and a balanced diet is a pivotal part of the treatment of T2DM. Plant-based nutrients as mainly recommended in the so-called Mediterranean diet contain numerous phytochemicals mediating wholesome effects. In particular, the major group of polyphenols was reported to wield protective properties, e.g., ameliorating glucotoxicity [205,206], oxidative stress [207], and ER stress [208] as well as inhibiting α-amylase [209,210] and preventing protein glycation [211]. Yet, their effects on the mitochondria of β-cells have been barely investigated (in cell lines: n = 5, in animal experiments: n = 5). Most interestingly, the beneficial effects of polyphenols are targeting pathways affected by lipotoxicity. They counteract the dysregulation of the MAPK and Pi3K pathway [22,23,212–214], and mitigate apoptosis by altering Bax/Bcl ratio and up-regulation of Pdx1, protein kinase A, and cAMP response element-binding protein signaling [215]. They stabilize the mitochondrial membrane preventing the release of proapoptotic factors and enhancing Ca signaling [23]. Moreover, polyphenols support insulin release through interaction with Pdx1 [212] in a forkhead box protein O1 (FoxO1)-dependent manner [214] and inhibit dipeptidylpeptidase-4 (DPP4) to increase GLP-1 levels–a pathway successfully used in clinical practice by DPP4 inhibitors and GLP-1 receptor agonists [33,216,217]. In addition, the dysregulation of GLUT2 and GLUT4 can be reversed by polyphenols improving elevated blood glucose levels and increasing insulin sensitivity [22]. Furthermore, relief from oxidative stress due to their radical scavenging capacity [33], and amelioration of ROS production by iNOS was reported. Polyphenols promote the activity and regeneration of antioxidative enzymes like SOD, catalase, GSH reductase, and GPx [21,33,212,218]. Particularly, GPx4 reduces lipid peroxides in the context of ferroptosis. As lipotoxicity-induced ferroptosis is also closely related to restrictions of Fe/S enzymes, plant-based nutrients rich in polyphenols were shown to sustain the activity of those enzymes, e.g., cytochrome C oxidase or succinate dehydrogenase, which

showed lowered activity in an animal study with high fat diet [212] counteracting mitochondrial dysfunction. Possible beneficial effects of polyphenols could be also mediated by improved fat metabolism through upregulation of SREBP-1c including signals from Akt or the estrogen receptor α [22,23] and lipid storing, improving lipid parameters [21,218]. Polyphenols further exert anti-inflammatory effects through decreased cytokine levels and ER stress [212,219].

According to these data, plant-based nutrients rich in polyphenols might be promising agents to counteract lipotoxic damage to β-cell mitochondria in diabetes and account for the beneficial effects of the Mediterranean diet. Yet, their clinical and therapeutical benefit has not been studied in clinical trials, and some authors even claim that toxic effects might arise from dosages required to achieve therapeutic levels in humans [33]. A summary of the described effects is given in Table 7.

Table 7. Summary of metabolic effects mediated by plant-based polyphenols and respective pathways. Oleic acid (OA). Mouse insulinoma 6 (MIN6). Glutathione peroxidase (GPx). Free fatty acids (FFA). Glucagon-like peptide 1 (GLP-1). Dipeptidylpeptidase-4 (DPP4). Reactive oxygen species (ROS). Superoxide dismutase (SOD). Triglyceride (TG). Palmitic acid (PA). Insulinoma (INS-1). Pancreatic and duodenal homebox 1 (Pdx1). Extracellular-signal-regulated kinase (ERK). Glucose-stimulated insulin secretion (GSIS). Endoplasmic reticulum (ER). Insulin receptor substrate 1 (IRS-1). Glucose transporter (GLUT). Rat insulinoma (Rinm5f). AMP-activated protein kinase (AMPK). Mechanistic target of rapamycin (mTOR). High fat diet (HFD). Interleukin (IL). Tumor necrosis factor α (TNFα). Forkhead box protein O1 (FoxO1).

Article	Treatment	Model	Extract, Substance	Results and Respective Pathways
Zakłos-Szyda et al., 2020 [33]	100 μM OA, 24 h	MIN6 cells	*Viburnum opulus* L., fresh juice and phenolic rich fraction with chlorogenic acid, flavanols, procyanidins	- reduced oxidative stress by radical scavenging and activation of antioxidative enzymes (GPx) - increased FFA uptake and lipid droplets accumulation - increased GLP-1 secretion by inhibited DPP4 activity - higher extract dosages increased necrosis/apoptosis by caspase activation and elevated ROS
Renganathan et al., 2020 [21]	No induction	Wistar rats	Dhanwantaram kashayam, polyherbal formulation containing *Sida spinosa* L., *Hordeum vulgare* L., *Aegle marmelos* (L.) Corrêa, *Bauhinia forficata* Link.	- less oxidative stress by activation of antioxidative enzymes (catalase, SOD, GPx, glutathion reductase) - improved lipid parameters (total cholesterol, FFA, phospholipids, TG) - extract abated antioxidative enzymes in control rats

Table 7. *Cont.*

Article	Treatment	Model	Extract, Substance	Results and Respective Pathways
Liu et al., 2019 [34]	200 µM PA, 24–96 h	INS-1 cells, C57BL/6J mice islets	Dracorhodin perchlorate	- increased Pdx1 expression by ERK1/2 - decreased apoptosis by Bax/Bcl-2 ratio - lowered blood glucose by improved GSIS, increased islet size/number - diminished ER stress
Sun et al., 2019 [23]	100 µM PA, 48 h	INS-1 cells	Silibinin	- improved viability, GSIS, lipid metabolism by estrogen receptor - increased mitochondrial mass and improved mitochondrial membrane potential
Gharib and Montasser Kouhsari, 2019 [22]	No induction	Wistar rats	*Punica granatum* L., fruit extract with punicalagin, anthocyanins, ellagic acid, gallic acid, caffeic acid, catechins, quercetin, rutin	- lowered fasting glucose by modulations of IRS-1, Akt, GLUT2/4 mRNA - enhanced lipid parameters (FFA, TG)
Gharib et al., 2018 [213]	No induction	Wistar rats	*Punica granatum* L., fruit extract with punicalagin, anthocyanins, ellagic acid, gallic acid, caffeic acid, catechins, quercetin, rutin	- improved lipid parameters (FFA, TG) - increased insulin sensitivity by decreased p53, p65, miR-145 and elevated IRS-1 - reduced ROS
Huang et al., 2017 [216]	100 µM PA, 24 h	RINm5F cells	*Abelmoschus esculentus* (L.) Moench, extract with quercetin glucosides, pentacyclic triterpene ester, carbohydrates, polysaccharides	- increased GLP-1 effect by decreased DPP4 activity - reduced apoptosis by AMPK, mTOR, PI3K signaling
Liu et al., 2017 [212]	HFD, 6 weeks	Sprague dawley rats islets	*Morus nigra* L., leaf extract with polysaccharides	- improved lipid parameters (FFA, TG, low-density lipoprotein) - decreased IL-6, TNFα - lowered fasting glucose - promoted mitochondrial enzymes (succinate dehydrogenase, cytochrome C oxidase) - morphological improvement of β-cells
Hao et al., 2015 [214]	500 µM PA, 24 h	MIN6 cells	Curcumin	- reduced apoptosis by caspase and Bax/Bcl-2 ratio - improved GSIS by mitochondrial membrane potential, Akt, FoxO1 - reduced oxidative stress by antioxidative enzymes (MnSOD, catalase, GPx, glutathione reductase)

9. Conclusions

Mitochondrial function is a key parameter crucially determining energy supply and cell survival. By those factors, it plays a central role in β-cell decay and development of T2DM. FFAs are well known to impair the glucose metabolism by mediating negative effects on mitochondria generally known as lipotoxicity. As lipotoxicity is multifactorial, most of the reviewed studies described lipotoxic effects mediated by increased oxidative stress, uncoupling of energy production by UCP2, deterioration of lipid homeostasis by PPAR and SREBP-1c signaling, extra-mitochondrial signaling through accumulation of acyl-CoA, and eventually enhanced apoptosis. While lipotoxicity can accelerate senescence of β-cells, there is evidence for a sustained mitochondrial metabolism and reversed effects of lipotoxicity by polyphenols as apparent in plant-based nutrients. However, the data are extremely limited and covering a wide range of different plants and ingredients, preventing a distinct verdict on their significance for T2DM and lipotoxicity. When studying the effects of FFAs, parameters like structure, concentration, treatment duration, and preparation should be considered carefully since they have massive impact on the outcome of the experimental setup. Especially the employed concentration substantially determines if FFAs will have an adverse or beneficial effect on β-cells. Judging cautiously from literature it can be generally assumed that in vitro FFAs mediate physiological effects in the lower micromolar range (Table 6), whereas concentrations in the upper micromolar range and higher exert lipotoxic effects. In contrast, concentrations are considerably higher in vivo with human serum containing levels in the lower millimolar range and murine serum with approximately 10% of this amount.

The different results of FFAs and polyphenol treatment as well as the multifactorial presentation of lipotoxicity leaves several questions unanswered. Therefore, further studies with clearly defined experimental setups would benefit this promising field of research and further elucidate the execution of lipotoxicity and respective protective mechanisms for the pancreatic β-cell.

Supplementary Materials: The following are available online at https://www.mdpi.com/2076-3921/10/2/293/s1; Supplement S1: Articles included after literature search on PubMed (n = 130).

Author Contributions: A.R.: conceptualization, methodology, original draft preparation, and visualization. T.L.: conceptualization, critical review, and editing. S.F.P.: conceptualization, critical review, editing, and supervision. All authors have read and agreed to the published version of the manuscript.

Funding: This research received no external funding.

Conflicts of Interest: The authors declare no conflict of interest.

Abbreviations

AMPK, AMP-activated protein kinase; ATG7, Ubiquitin-like modifier-activating enzyme; ATP, adenosine triphosphate; BSA, bovine serum albumin; βTC6, β-tumour cell; Ca, calcium; CD, cluster of differentiation; CHO, Chinese hamster ovary; CHOP, CCAAT/enhancer binding protein homologous protein; COS1, CV-1 in origin simain-1; CPT, carnitine palmitoyltransferase; DM, diabetes mellitus; DPP4, dipeptidylpeptidase-4; ER, endoplasmic reticulum; ERK, extracellular-signal-regulated kinase; FASIS, fatty acid stimulated insulin secretion; Fe/S, iron-sulfur; FFA, free fatty acids; FoxO1, forkhead box protein O1; FTase, farnesyl transferase; GGTase, geranylgeranyl transferase; GLP-1, glucagon-like peptide 1; Glrx5, glutaredoxin 5; GLUT, glucose transporters; GPR, G protein-coupled receptor; GPx, glutathione peroxidase; GSH, glutathione; GSIS, glucose-stimulated insulin secretion; H_2O_2, hydrogen peroxide; HcB19, TXNIP deficiency; HEK 293, Human embryonic kidney 293; HepG2, Hepatoblastoma; HFD, high fat diet; HIT-T15, Hamster islet transformed-tioguanine resistant clone 15; ICR, Institute for Cancer Research; IGF, insulin like growth factor; IL, interleukin; iNOS, inducible nitric oxide synthase; INS-1, insulinoma; IP3, inositol trisphosphate; iPLA$_2\gamma$, calcium-independent phospholipase A2 γ; IRE, iron regulatory element; IRP1, iron regulatory protein 1; IRS-1, insulin receptor substrate 1; ISC, iron-sulfur cluster assembly machinery; JNK, phosphorylated

c-Jun N-terminal kinases; K, potassium; KK-Ay, Diabetic KK and lethal yellow (Ay) mice; MAPK, mitogen-activated protein kinase; MIN6, Mouse insulinoma 6; MMP, mitochondrial membrane potential; mTOR, mechanistic target of rapamycin; NIT1, NOD/Lt; NMRI, Naval Medical Research Institute; NOX2, NADPH oxidase 2; OA, oleic acid; PA, palmitic acid; PAA, phenylacetic acid; Pdx1, pancreatic and duodenal homebox 1; PINK1, PTEN-induced kinase 1; PLC, phospholipase C; PPAR, peroxisome proliferator-activated receptor; Rac1, Ras-related C3 botulinum toxin substrate 1; Rinm5f, Rat insulinoma; ROS, reactive oxygen species; RSIS, redox stimulated insulin secretion; SERCA, sarcoplasmic/endoplasmic reticulum calcium ATPase; SK2, sphingosine kinase 2; SOD, superoxide dismutase; SRE, sterol regulatory element; SREBP, sterol regulatory element binding protein; STING, stimulator of interferon genes; T2DM, type 2 diabetes mellitus; TCA, tricarboxylic acid; TG, triglyceride; TNFα, tumor necrosis factor α; UCP, uncoupling protein; UPR, unfolded protein response.

References

1. Saeedi, P.; Petersohn, I.; Salpea, P.; Malanda, B.; Karuranga, S.; Unwin, N.; Colagiuri, S.; Guariguata, L.; Motala, A.A.; Ogurtsova, K.; et al. Global and regional diabetes prevalence estimates for 2019 and projections for 2030 and 2045: Results from the International Diabetes Federation Diabetes Atlas, 9th edition. *Diabetes Res. Clin. Pract.* **2019**, *157*, 107843. [CrossRef] [PubMed]
2. Kawahito, S.; Kitahata, H.; Oshita, S. Problems associated with glucose toxicity: Role of hyperglycemia-induced oxidative stress. *World J. Gastroenterol.* **2009**, *15*, 4137. [CrossRef]
3. Sato, Y.; Endo, H.; Okuyama, H.; Takeda, T.; Iwahashi, H.; Imagawa, A.; Yamagata, K.; Shimomura, I.; Inoue, M. Cellular hypoxia of pancreatic β-cells due to high levels of oxygen consumption for insulin secretion in vitro. *J. Biol. Chem.* **2011**, *286*, 12524–12532. [CrossRef]
4. Jiang, L.; Wan, J.; Ke, L.Q.; Lü, Q.G.; Tong, N.W. Activation of PPARδ promotes mitochondrial energy metabolism and decreases basal insulin secretion in palmitate-treated β-cells. *Mol. Cell. Biochem.* **2010**, *343*, 249–256. [CrossRef] [PubMed]
5. Reaven, G.M.; Hollenbeck, C.; Jeng, C.Y.; Wu, M.S.; Chen, Y.D.I. Measurement of plasma glucose, free fatty acid, lactate, and insulin for 24 h in patients with NIDDM. *Diabetes* **1988**, *37*, 1020–1024. [CrossRef] [PubMed]
6. Bikopoulos, G.; da Silva Pimenta, A.; Lee, S.C.; Lakey, J.R.; Der, S.D.; Chan, C.B.; Ceddia, R.B.; Wheeler, M.B.; Rozakis-Adcock, M. Ex vivo transcriptional profiling of human pancreatic islets following chronic exposure to monounsaturated fatty acids. *J. Endocrinol.* **2008**, *196*, 455–464. [CrossRef] [PubMed]
7. Salgin, B.; Ong, K.K.; Thankamony, A.; Emmett, P.; Wareham, N.J.; Dunger, D.B. Higher fasting plasma free fatty acid levels are associated with lower insulin secretion in children and adults and a higher incidence of type 2 diabetes. *J. Clin. Endocrinol. Metab.* **2012**, *97*, 3302–3309. [CrossRef] [PubMed]
8. Ye, R.; Onodera, T.; Scherer, P.E. Lipotoxicity and B cell maintenance in obesity and type 2 diabetes. *J. Endocr. Soc.* **2019**, *3*, 617–631. [CrossRef]
9. Boden, G. Effects of Free Fatty Acids (FFA) on Glucose Metabolism: Significance for Insulin Resistance and Type 2 Diabetes. *Exp. Clin. Endocrinol. Diabetes* **2003**, *111*, 121–124. [CrossRef]
10. Kushner, J.A. The role of aging upon β cell turnover. *J. Clin. Investig.* **2013**, *123*, 990–995. [CrossRef]
11. Kalyani, R.R.; Golden, S.H.; Cefalu, W.T. Diabetes and aging: Unique considerations and goals of care. *Diabetes Care* **2017**, *40*, 440–443. [CrossRef]
12. Spitler, K.M.; Davies, B.S.J. Aging and Plasma Triglyceride Metabolism. *J. Lipid Res.* **2020**, *61*, 1161–1167. [CrossRef] [PubMed]
13. Houtkooper, R.H.; Argmann, C.; Houten, S.M.; Cant'o, C.; Jeninga, E.H.; Andreux, P.A.; Thomas, C.; Doenlen, R.; Schoonjans, K.; Auwerx, J. The metabolic footprint of aging in mice. *Sci. Rep.* **2011**, *1*, 1–11. [CrossRef]
14. Lei, X.G.; Vatamaniuk, M.Z. Two Tales of Antioxidant Enzymes on β Cells and Diabetes. *Antioxid. Redox Signal.* **2011**, *14*, 489–503. [CrossRef]
15. Okoduwa, S.I.R.; Umar, I.A.; Ibrahim, S.; Bello, F.; Habila, N. Age-dependent alteration of antioxidant defense system in hypertensive and type-2 diabetes patients. *J. Diabetes Metab. Disord.* **2015**, *14*. [CrossRef]
16. Rupasinghe, H.P.V.; Balasuriya, N.; Wang, Y. Prevention of Type 2 Diabetes by Polyphenols of Fruits. In *Nutritional Antioxidant Therapies: Treatments and Perspectives*; Springer International Publishing: Cham, Germany, 2017; pp. 447–466. ISBN 9783319676258.
17. Guaadaoui, A.; Benaicha, S.; Elmajdoub, N.; Bellaoui, M.; Hamal, A. What is a bioactive compound? A combined definition for a preliminary consensus. *Int. J. Food Sci. Nutr.* **2014**, *3*, 174–179. [CrossRef]
18. Campos-Vega, R.; Oomah, B.D. Chemistry and classification of phytochemicals. In *Handbook of Plant Food Phytochemicals*; John Wiley & Sons Ltd.: Oxford, UK, 2013; pp. 5–48. ISBN 9781444338102.
19. Ganesan, K.; Xu, B. Anti-diabetic effects and mechanisms of dietary polysaccharides. *Molecules* **2019**, *24*, 2556. [CrossRef] [PubMed]
20. Cao, H.; Ou, J.; Chen, L.; Zhang, Y.; Szkudelski, T.; Delmas, D.; Daglia, M.; Xiao, J. Dietary polyphenols and type 2 diabetes: Human Study and Clinical Trial. *Crit. Rev. Food Sci. Nutr.* **2019**, *59*, 3371–3379. [CrossRef] [PubMed]

21. Renganathan, S.; Srivastava, A.; Pillai, R.G. Dhanwantaram kashayam, an Ayurvedic polyherbal formulation, reduces oxidative radicals and reverts lipids profile towards normal in diabetic rats. *Biochem. Biophys. Rep.* **2020**, *22*. [CrossRef]
22. Gharib, E.; Kouhsari, S.M. Study of the antidiabetic activity of Punica granatum L. Fruits aqueous extract on the alloxan-diabetic wistar rats. *Iran. J. Pharm. Res.* **2019**, *18*, 358–368. [CrossRef]
23. Sun, Y.; Yang, J.; Liu, W.; Yao, G.; Xu, F.; Hayashi, T.; Onodera, S.; Ikejima, T. Attenuating effect of silibinin on palmitic acid-induced apoptosis and mitochondrial dysfunction in pancreatic β-cells is mediated by estrogen receptor alpha. *Mol. Cell. Biochem.* **2019**, *460*, 81–92. [CrossRef]
24. Liu, I.-M.; Tzeng, T.-F.; Liou, S.-S.; Lan, T.-W. Myricetin, a naturally occurring flavonol, ameliorates insulin resistance induced by a high-fructose diet in rats. *Life Sci.* **2007**, *81*, 1479–1488. [CrossRef] [PubMed]
25. Samadder, A.; Chakraborty, D.; De, A.; Bhattacharyya, S.S.; Bhadra, K.; Khuda-Bukhsh, A.R. Possible signaling cascades involved in attenuation of alloxan-induced oxidative stress and hyperglycemia in mice by ethanolic extract of Syzygium jambolanum: Drug-DNA interaction with calf thymus DNA as target. *Eur. J. Pharm. Sci.* **2011**, *44*, 207–217. [CrossRef] [PubMed]
26. Johnson, M.H.; Lucius, A.; Meyer, T.; Gonzalez De Mejia, E. Cultivar evaluation and effect of fermentation on antioxidant capacity and in vitro inhibition of α-amylase and α-glucosidase by highbush blueberry (vaccinium corombosum). *J. Agric. Food Chem.* **2011**, *59*, 8923–8930. [CrossRef] [PubMed]
27. Grussu, D.; Stewart, D.; McDougall, G.J. Berry polyphenols inhibit α-amylase in vitro: Identifying active components in rowanberry and raspberry. *J. Agric. Food Chem.* **2011**, *59*, 2324–2331. [CrossRef]
28. Liu, T.; Song, L.; Wang, H.; Huang, D. A high-throughput assay for quantification of starch hydrolase inhibition based on turbidity measurement. *J. Agric. Food Chem.* **2011**, *59*, 9756–9762. [CrossRef] [PubMed]
29. Krajka-Kuźniak, V.; Paluszczak, J.; Szaefer, H.; Baer-Dubowska, W. The activation of the Nrf2/ARE pathway in HepG2 hepatoma cells by phytochemicals and subsequent modulation of phase II and antioxidant enzyme expression. *J. Physiol. Biochem.* **2015**, *71*, 227–238. [CrossRef]
30. Muraoka, K.; Shimizu, K.; Sun, X.; Tani, T.; Izumi, R.; Miwa, K.; Yamamoto, K. Flavonoids exert diverse inhibitory effects on the activation of NF-κB. *Transplant. Proc.* **2002**, *34*, 1335–1340. [CrossRef]
31. Moon, S.K.; Cho, G.O.; Jung, S.Y.; Gal, S.W.; Kwon, T.K.; Lee, Y.C.; Madamanchi, N.R.; Kim, C.H. Quercetin exerts multiple inhibitory effects on vascular smooth muscle cells: Role of ERK1/2, cell-cycle regulation, and matrix metalloproteinase-9. *Biochem. Biophys. Res. Commun.* **2003**, *301*, 1069–1078. [CrossRef]
32. Forni, C.; Facchiano, F.; Bartoli, M.; Pieretti, S.; Facchiano, A.; D'Arcangelo, D.; Norelli, S.; Valle, G.; Nisini, R.; Beninati, S.; et al. Beneficial Role of Phytochemicals on Oxidative Stress and Age-Related Diseases. *Biomed Res. Int.* **2019**, *2019*, 1–16. [CrossRef] [PubMed]
33. Zakłos-Szyda, M.; Kowalska-Baron, A.; Pietrzyk, N.; Drzazga, A.; Podsędek, A. Evaluation of viburnum opulus l. Fruit phenolics cytoprotective potential on insulinoma min6 cells relevant for diabetes mellitus and obesity. *Antioxidants* **2020**, *9*, 433. [CrossRef]
34. Liu, L.; Liang, C.; Mei, P.; Zhu, H.; Hou, M.; Yu, C.; Song, Z.; Bao, Y.; Huang, Y.; Yi, J.; et al. Dracorhodin perchlorate protects pancreatic β-cells against glucotoxicity-or lipotoxicity-induced dysfunction and apoptosis in vitro and in vivo. *FEBS J.* **2019**, *286*, 3718–3736. [CrossRef] [PubMed]
35. Kish-Trier, E.; Schwarz, E.L.; Pasquali, M.; Yuzyuk, T. Quantitation of total fatty acids in plasma and serum by GC-NCI-MS. *Clin. Mass Spectrom.* **2016**, *2*, 11–17. [CrossRef]
36. Sergeant, S.; Ruczinski, I.; Ivester, P.; Lee, T.C.; Morgan, T.M.; Nicklas, B.J.; Mathias, R.A.; Chilton, F.H. Impact of methods used to express levels of circulating fatty acids on the degree and direction of associations with blood lipids in humans. *Br. J. Nutr.* **2016**, *115*, 251–261. [CrossRef] [PubMed]
37. de Oliveira, C.; Khatua, B.; Noel, P.; Kostenko, S.; Bag, A.; Balakrishnan, B.; Patel, K.S.; Guerra, A.A.; Martinez, M.N.; Trivedi, S.; et al. Pancreatic triglyceride lipase mediates lipotoxic systemic inflammation. *J. Clin. Investig.* **2020**, *130*, 1931–1947. [CrossRef] [PubMed]
38. Navina, S.; Acharya, C.; DeLany, J.P.; Orlichenko, L.S.; Baty, C.J.; Shiva, S.S.; Durgampudi, C.; Karlsson, J.M.; Lee, K.; Bae, K.T.; et al. Lipotoxicity causes multisystem organ failure and exacerbates acute pancreatitis in obesity. *Sci. Transl. Med.* **2011**, *3*, 107ra110. [CrossRef]
39. Paye, F.; Presset, O.; Chariot, J.; Molas, G.; Rozé, C. Role of nonesterified fatty acids in necrotizing pancreatitis: An in vivo experimental study in rats. *Pancreas* **2001**, *23*, 341–348. [CrossRef]
40. Christeff, N.; Homo-Delarche, F.; Thobie, N.; Durant, S.; Dardenne, M.; Nunez, E.A. Free fatty acid profiles in the non-obese diabetic (NOD) mouse: Basal serum levels and effects of endocrine manipulation. *Prostaglandins Leukot. Essent. Fat. Acids* **1994**, *51*, 125–131. [CrossRef]
41. Shimabukuro, M.; Higa, M.; Zhou, Y.T.; Wang, M.Y.; Newgard, C.B.; Unger, R.H. Lipoapoptosis in beta-cells of obese prediabetic fa/fa rats. Role of serine palmitoyltransferase overexpression. *J. Biol. Chem.* **1998**, *273*, 32487–32490. [CrossRef] [PubMed]
42. Wehinger, S.; Ortiz, R.; Díaz, M.I.; Aguirre, A.; Valenzuela, M.; Llanos, P.; Mc Master, C.; Leyton, L.; Quest, A.F.G. Phosphorylation of caveolin-1 on tyrosine-14 induced by ROS enhances palmitate-induced death of beta-pancreatic cells. *Biochim. Biophys. Acta Mol. Basis Dis.* **2015**, *1852*, 693–708. [CrossRef]
43. Mir, S.U.R.; George, N.M.; Zahoor, L.; Harms, R.; Guinn, Z.; Sarvetnick, N.E. Inhibition of autophagic turnover in β-cells by fatty acids and glucose leads to apoptotic cell death. *J. Biol. Chem.* **2015**, *290*, 6071–6085. [CrossRef] [PubMed]

44. Kim, M.; Lee, J.S.; Oh, J.E.; Nan, J.; Lee, H.; Jung, H.S.; Chung, S.S.; Park, K.S. SIRT3 overexpression attenuates palmitate-induced pancreatic β-cell dysfunction. *PLoS ONE* **2015**, *10*, e0124744. [CrossRef] [PubMed]
45. Lameloise, N.; Muzzin, P.; Prentki, M.; Assimacopoulos-Jeannet, F. Uncoupling protein 2: A possible link between fatty acid excess and impaired glucose-induced insulin secretion? *Diabetes* **2001**, *50*, 803–809. [CrossRef] [PubMed]
46. Rachek, L.I.; Thornley, N.P.; Grishko, V.I.; LeDoux, S.P.; Wilson, G.L. Protection of INS-1 cells from free fatty acid-induced apoptosis by targeting hOGG1 to mitochondria. *Diabetes* **2006**, *55*, 1022–1028. [CrossRef] [PubMed]
47. Hu, H.Q.; Qiao, J.T.; Liu, F.Q.; Wang, J.B.; Sha, S.; He, Q.; Cui, C.; Song, J.; Zang, N.; Wang, L.S.; et al. The STING-IRF3 pathway is involved in lipotoxic injury of pancreatic β cells in type 2 diabetes. *Mol. Cell. Endocrinol.* **2020**, 110890. [CrossRef] [PubMed]
48. Cripps, M.J.; Bagnati, M.; Jones, T.A.; Ogunkolade, B.W.; Sayers, S.R.; Caton, P.W.; Hanna, K.; Billacura, M.P.; Fair, K.; Nelson, C.; et al. Identification of a subset of trace amine-associated receptors and ligands as potential modulators of insulin secretion. *Biochem. Pharmacol.* **2020**, *171*, 113685. [CrossRef]
49. Zhang, Q.; Cui, Q.; Hou, Y.; Wang, H.; Xu, Y.; Pi, J. The impairment of glucose-stimulated insulin secretion in pancreatic β-cells caused by prolonged glucotoxicity and lipotoxicity is associated with elevated adaptive antioxidant response. *Food Chem. Toxicol.* **2017**, *100*, 161–167. [CrossRef]
50. Qureshi, F.M.; Dejene, E.A.; Corbin, K.L.; Nunemaker, C.S. Stress-induced dissociations between intracellular calcium signaling and insulin secretion in pancreatic islets. *Cell Calcium* **2015**, *57*, 366–375. [CrossRef]
51. Alsabeeh, N.; Chausse, B.; Kakimoto, P.A.; Kowaltowski, A.J.; Shirihai, O. Cell culture models of fatty acid overload: Problems and solutions. *Biochim. Biophys. Acta Mol. Cell Biol. Lipids* **2018**, *1863*, 143–151. [CrossRef]
52. Timm, M.; Saaby, L.; Moesby, L.; Hansen, E.W. Considerations regarding use of solvents in in vitro cell based assays. *Cytotechnology* **2013**, *65*, 887–894. [CrossRef] [PubMed]
53. Roche, M.; Rondeau, P.; Singh, N.R.; Tarnus, E.; Bourdon, E. The antioxidant properties of serum albumin. *FEBS Lett.* **2008**, *582*, 1783–1787. [CrossRef] [PubMed]
54. Huang, K.T.; Chen, Y.H.; Walker, A.M. Inaccuracies in MTS assays: Major distorting effects of medium, serum albumin, and fatty acids. *Biotechniques* **2004**, *37*, 406–412. [CrossRef]
55. Li, F.; Munsey, T.S.; Sivaprasadarao, A. TRPM2-mediated rise in mitochondrial Zn 2+ promotes palmitate-induced mitochondrial fission and pancreatic β-cell death in rodents. *Cell Death Differ.* **2017**, *24*, 1999–2012. [CrossRef] [PubMed]
56. Ježek, J.; Dlasková, A.; Zelenka, J.; Jabůrek, M.; Ježek, P. H2O2-activated mitochondrial phospholipase iPLA2γ prevents lipotoxic oxidative stress in synergy with UCP2, amplifies signaling via G-protein-coupled receptor GPR40, and regulates insulin secretion in pancreatic β-cells. *Antioxidants Redox Signal.* **2015**, *23*, 958–972. [CrossRef] [PubMed]
57. Cnop, M.; Hannaert, J.C.; Hoorens, A.; Eizirik, D.L.; Pipeleers, D.G. Inverse Relationship between Cytotoxicity of Free Fatty Acids in Pancreatic Islet Cells and Cellular Triglyceride Accumulation. *Diabetes* **2001**, *50*, 1771–1777. [CrossRef] [PubMed]
58. Oliveira, A.F.; Cunha, D.A.; Ladriere, L.; Igoillo-Esteve, M.; Bugliani, M.; Marchetti, P.; Cnop, M. In vitro use of free fatty acids bound to albumin: A comparison of protocols. *Biotechniques* **2015**, *58*, 228–233. [CrossRef] [PubMed]
59. Saitoh, Y.; Hongwei, W.; Ueno, H.; Mizuta, M.; Nakazato, M. Candesartan attenuates fatty acid-induced oxidative stress and NAD(P)H oxidase activity in pancreatic β-cells. *Diabetes Res. Clin. Pract.* **2010**, *90*, 54–59. [CrossRef]
60. Hansen, J.B.; Dos Santos, L.R.B.; Liu, Y.; Prentice, K.J.; Teudt, F.; Tonnesen, M.; Jonas, J.C.; Wheeler, M.B.; Mandrup-Poulsen, T. Glucolipotoxic conditions induce β-cell iron import, cytosolic ROS formation and apoptosis. *J. Mol. Endocrinol.* **2018**, *61*, 69–77. [CrossRef]
61. Sobczak, A.I.S.; A. Blindauer, C.; J. Stewart, A. Changes in Plasma Free Fatty Acids Associated with Type-2 Diabetes. *Nutrients* **2019**, *11*, 2022. [CrossRef]
62. Cnop, M.; Welsh, N.; Jonas, J.C.; Jörns, A.; Lenzen, S.; Eizirik, D.L. Mechanisms of pancreatic β-cell death in type 1 and type 2 diabetes: Many differences, few similarities. *Diabetes* **2005**, *54* (Suppl. 2), 97–107. [CrossRef]
63. Wu, P.; Yang, L.; Shen, X. The relationship between GPR40 and lipotoxicity of the pancreatic β-cells as well as the effect of pioglitazone. *Biochem. Biophys. Res. Commun.* **2010**, *403*, 36–39. [CrossRef]
64. Plötz, T.; von Hanstein, A.S.; Krümmel, B.; Laporte, A.; Mehmeti, I.; Lenzen, S. Structure-toxicity relationships of saturated and unsaturated free fatty acids for elucidating the lipotoxic effects in human EndoC-βH1 beta-cells. *Biochim. Biophys. Acta Mol. Basis Dis.* **2019**, *1865*, 165525. [CrossRef] [PubMed]
65. Clarke, D.C.; Miskovic, D.; Han, X.-X.; Calles-Escandon, J.; Glatz, J.F.C.; Luiken, J.J.F.P.; Heikkila, J.J.; Bonen, A. Overexpression of membrane-associated fatty acid binding protein (FABPpm) in vivo increases fatty acid sarcolemmal transport and metabolism. *Physiol. Genomics* **2004**, *17*, 31–37. [CrossRef] [PubMed]
66. Ly, L.D.; Xu, S.; Choi, S.K.; Ha, C.M.; Thoudam, T.; Cha, S.K.; Wiederkehr, A.; Wollheim, C.B.; Lee, I.K.; Park, K.S. Oxidative stress and calcium dysregulation by palmitate in type 2 diabetes. *Exp. Mol. Med.* **2017**, *49*, e291-12. [CrossRef]
67. Pepino, M.Y.; Kuda, O.; Samovski, D.; Abumrad, N.A. Structure-function of CD36 and importance of fatty acid signal transduction in fat metabolism. *Annu. Rev. Nutr.* **2014**, *34*, 281–303. [CrossRef] [PubMed]
68. Okamura, D.M.; Pennathur, S.; Pasichnyk, K.; López-Guisa, J.M.; Collins, S.; Febbraio, M.; Heinecke, J.; Eddy, A.A. CD36 regulates oxidative stress and inflammation in hypercholesterolemic CKD. *J. Am. Soc. Nephrol.* **2009**, *20*, 495–505. [CrossRef]
69. Kim, Y.W.; Moon, J.S.; Seo, Y.J.; Park, S.Y.; Kim, J.Y.; Yoon, J.S.; Lee, I.K.; Lee, H.W.; Won, K.C. Inhibition of fatty acid translocase cluster determinant 36 (CD36), stimulated by hyperglycemia, prevents glucotoxicity in INS-1 cells. *Biochem. Biophys. Res. Commun.* **2012**, *420*, 462–466. [CrossRef]

70. Kristinsson, H.; Sargsyan, E.; Manell, H.; Smith, D.M.; Göpel, S.O.; Bergsten, P. Basal hypersecretion of glucagon and insulin from palmitate-exposed human islets depends on FFAR1 but not decreased somatostatin secretion. *Sci. Rep.* **2017**, *7*, 4657. [CrossRef] [PubMed]
71. Zhao, Y.; Wang, L.; Qiu, J.; Zha, D.; Sun, Q.; Chen, C. Linoleic Acid Stimulates [Ca2+]i Increase in Rat Pancreatic Beta-Cells through Both Membrane Receptor- and Intracellular Metabolite-Mediated Pathways. *PLoS ONE* **2013**, *8*, e60255. [CrossRef]
72. Chen, Y.; Ren, Q.; Zhou, Z.; Deng, L.; Hu, L.; Zhang, L.; Li, Z. HWL-088, a new potent free fatty acid receptor 1 (FFAR1) agonist, improves glucolipid metabolism and acts additively with metformin in ob/ob diabetic mice. *Br. J. Pharmacol.* **2020**, *177*, 2286–2302. [CrossRef]
73. Ly, L.D.; Da Ly, D.; Nguyen, N.T.; Kim, J.H.; Yoo, H.; Chung, J.; Lee, M.S.; Cha, S.K.; Park, K.S. Mitochondrial Ca2+ Uptake Relieves Palmitate-Induced Cytosolic Ca2+ Overload in MIN6 Cells. *Mol. Cells* **2020**, *43*, 66–75. [CrossRef]
74. Biden, T.J.; Boslem, E.; Chu, K.Y.; Sue, N. Lipotoxic endoplasmic reticulum stress, β cell failure, and type 2 diabetes mellitus. *Trends Endocrinol. Metab.* **2014**, *25*, 389–398. [CrossRef]
75. Schreurs, M.; Kuipers, F.; van der Leij, F.R. Regulatory enzymes of mitochondrial β-oxidation as targets for treatment of the metabolic syndrome. *Obes. Rev.* **2010**, *11*, 380–388. [CrossRef] [PubMed]
76. Wan, J.; Jiang, L.; Lü, Q.; Ke, L.; Li, X.; Tong, N. Activation of PPARδ up-regulates fatty acid oxidation and energy uncoupling genes of mitochondria and reduces palmitate-induced apoptosis in pancreatic β-cells. *Biochem. Biophys. Res. Commun.* **2010**, *391*, 1567–1572. [CrossRef] [PubMed]
77. Talley, J.T.; Mohiuddin, S.S. *Biochemistry, Fatty Acid Oxidation*; StatPearls Publishing: Treasure Island, FL, USA, 2020.
78. Maris, M.; Robert, S.; Waelkens, E.; Derua, R.; Hernangomez, M.H.; D'Hertog, W.; Cnop, M.; Mathieu, C.; Overbergh, L. Role of the saturated nonesterified fatty acid palmitate in beta cell dysfunction. *J. Proteome Res.* **2013**, *12*, 347–362. [CrossRef]
79. Lee, J.H.; Jung, I.R.; Choi, S.E.; Lee, S.M.; Lee, S.J.; Han, S.J.; Kim, H.J.; Kim, D.J.; Lee, K.W.; Kang, Y. Toxicity generated through inhibition of pyruvate carboxylase and carnitine palmitoyl transferase-1 is similar to high glucose/palmitate-induced glucolipotoxicity in INS-1 beta cells. *Mol. Cell. Endocrinol.* **2014**, *383*, 48–59. [CrossRef] [PubMed]
80. Abdul-Ghani, M.A.; Muller, F.L.; Liu, Y.; Chavez, A.O.; Balas, B.; Zuo, P.; Chang, Z.; Tripathy, D.; Jani, R.; Molina-Carrion, M.; et al. Deleterious action of FA metabolites on ATP synthesis: Possible link between lipotoxicity, mitochondrial dysfunction, and insulin resistance. *Am. J. Physiol. Endocrinol. Metab.* **2008**, *295*, 678–685. [CrossRef]
81. Lu, H.; Koshkin, V.; Allister, E.M.; Gyulkhandanyan, A.V.; Wheeler, M.B. Molecular and metabolic evidence for mitochondrial defects associated with β-cell dysfunction in a mouse model of type 2 diabetes. *Diabetes* **2010**, *59*, 448–459. [CrossRef] [PubMed]
82. MacDonald, M.J.; Longacre, M.J.; Langberg, E.C.; Tibell, A.; Kendrick, M.A.; Fukao, T.; Ostenson, C.G. Decreased levels of metabolic enzymes in pancreatic islets of patients with type 2 diabetes. *Diabetologia* **2009**, *52*, 1087–1091. [CrossRef] [PubMed]
83. Nagaraju, R.; Rajini, P.S. Adaptive response of rat pancreatic β-cells to insulin resistance induced by monocrotophos: Biochemical evidence. *Pestic. Biochem. Physiol.* **2016**, *134*, 39–48. [CrossRef]
84. Cunha, D.A.; Igoillo-Esteve, M.; Gurzov, E.N.; Germano, C.M.; Naamane, N.; Marhfour, I.; Fukaya, M.; Vanderwinden, J.M.; Gysemans, C.; Mathieu, C.; et al. Death protein 5 and p53-upregulated modulator of apoptosis mediate the endoplasmic reticulum stress-mitochondrial dialog triggering lipotoxic rodent and human β-cell apoptosis. *Diabetes* **2012**, *61*, 2763–2775. [CrossRef] [PubMed]
85. Boucher, A.; Lu, D.; Burgess, S.C.; Telemaque-Potts, S.; Jensen, M.V.; Mulder, H.; Wang, M.Y.; Unger, R.H.; Sherry, A.D.; Newgard, C.B. Biochemical mechanism of lipid-induced impairment of glucose-stimulated insulin secretion and reversal with a malate analogue. *J. Biol. Chem.* **2004**, *279*, 27263–27271. [CrossRef]
86. Carlessi, R.; Rowlands, J.; Ellison, G.; Helena de Oliveira Alves, H.; Newsholme, P.; Mamotte, C. Glutamine deprivation induces metabolic adaptations associated with beta cell dysfunction and exacerbate lipotoxicity. *Mol. Cell. Endocrinol.* **2019**, *491*, 110433. [CrossRef] [PubMed]
87. Yang, C.; Ko, B.; Hensley, C.T.; Jiang, L.; Wasti, A.T.; Kim, J.; Sudderth, J.; Calvaruso, M.A.; Lumata, L.; Mitsche, M.; et al. Glutamine oxidation maintains the TCA cycle and cell survival during impaired mitochondrial pyruvate transport. *Mol. Cell* **2014**, *56*, 414–424. [CrossRef]
88. Roberts, L.D.; Koulman, A.; Griffin, J.L. Towards metabolic biomarkers of insulin resistance and type 2 diabetes: Progress from the metabolome. *Lancet Diabetes Endocrinol.* **2014**, *2*, 65–75. [CrossRef]
89. Stančáková, A.; Civelek, M.; Saleem, N.K.; Soininen, P.; Kangas, A.J.; Cederberg, H.; Paananen, J.; Pihlajamäki, J.; Bonnycastle, L.L.; Morken, M.A.; et al. Hyperglycemia and a common variant of GCKR are associated with the levels of eight amino acids in 9369 finnish men. *Diabetes* **2012**, *61*, 1895–1902. [CrossRef]
90. Van Loon, L.J.C.; Kruijshoop, M.; Menheere, P.P.C.A.; Wagenmakers, A.J.M.; Saris, W.H.M.; Keizer, H.A. Amino acid ingestion strongly enhances insulin secretion in patients with long-term type 2 diabetes. *Diabetes Care* **2003**, *26*, 625–630. [CrossRef]
91. Zhou, Y.; Chung, A.C.K.; Fan, R.; Lee, H.M.; Xu, G.; Tomlinson, B.; Chan, J.C.N.; Kong, A.P.S. Sirt3 Deficiency Increased the Vulnerability of Pancreatic Beta Cells to Oxidative Stress-Induced Dysfunction. *Antioxidants Redox Signal.* **2017**, *27*, 962–976. [CrossRef]
92. Tran, K.; Li, Y.; Duan, H.; Arora, D.; Lim, H.Y.; Wang, W. Identification of small molecules that protect pancreatic β cells against endoplasmic reticulum stress-induced cell death. *ACS Chem. Biol.* **2014**, *9*, 2796–2806. [CrossRef]
93. Zhou, Y.P.; Berggren, P.O.; Grill, V. A fatty acid-induced decrease in pyruvate dehydrogenase activity is an important determinant of β-cell dysfunction in the obese diabetic db/db mouse. *Diabetes* **1996**, *45*, 580–586. [CrossRef]

94. Rodríguez-Manzaneque, M.T.; Tamarit, J.; Bellí, G.; Ros, J.; Herrero, E. Grx5 is a mitochondrial glutaredoxin required for the activity of iron/sulfur enzymes. *Mol. Biol. Cell* **2002**, *13*, 1109–1121. [CrossRef] [PubMed]
95. Petry, S.F.; Sun, L.M.; Knapp, A.; Reinl, S.; Linn, T. Distinct shift in beta-cell glutaredoxin 5 expression is mediated by hypoxia and lipotoxicity both in vivo and in vitro. *Front. Endocrinol.* **2018**, *9*, 1–11. [CrossRef]
96. Stehling, O.; Wilbrecht, C.; Lill, R. Mitochondrial iron–sulfur protein biogenesis and human disease. *Biochimie* **2014**, *100*, 61–77. [CrossRef] [PubMed]
97. Braymer, J.J.; Lill, R. Iron–sulfur cluster biogenesis and trafficking in mitochondria. *J. Biol. Chem.* **2017**, *292*, 12754–12763. [CrossRef]
98. Flemming, D.; Schlitt, A.; Spehr, V.; Bischof, T.; Friedrich, T. Iron-Sulfur Cluster N2 of the Escherichia coli NADH:Ubiquinone Oxidoreductase (Complex I) Is Located on Subunit NuoB. *J. Biol. Chem.* **2003**, *278*, 47602–47609. [CrossRef] [PubMed]
99. Albracht, S.P.J. The prosthetic groups in succinate dehydrogenase Number and stoichiometry. *BBA Enzymol.* **1980**, *612*, 11–28. [CrossRef]
100. Ding, H.; Robertson, D.E.; Daldal, F.; Dutton, P.L. Cytochrome bc1 complex [2Fe-2S] cluster and its interaction with ubiquinone and ubihydroquinone at the Qo site: A double-occupancy Qo site model. *Biochemistry* **1992**, *31*, 3144–3158. [CrossRef] [PubMed]
101. Khoroshilova, N.; Popescu, C.; Münck, E.; Beinert, H.; Kiley, P.J. Iron-sulfur cluster disassembly in the FNR protein of Escherichia coli by O2: [4Fe-4S] to [2Fe-2S] conversion with loss of biological activity. *Proc. Natl. Acad. Sci. USA* **1997**, *94*, 6087–6092. [CrossRef]
102. Fuss, J.O.; Tsai, C.L.; Ishida, J.P.; Tainer, J.A. Emerging critical roles of Fe-S clusters in DNA replication and repair. *Biochim. Biophys. Acta Mol. Cell Res.* **2015**, *1853*, 1253–1271. [CrossRef]
103. Rosenbohm, A.; Süssmuth, S.D.; Kassubek, J.; Müller, H.-P.; Pontes, C.; Abicht, A.; Bulst, S.; Ludolph, A.C.; Pinkhardt, E. Novel *ETFDH* mutation and imaging findings in an adult with glutaric aciduria type II. *Muscle Nerve* **2014**, *49*, 446–450. [CrossRef]
104. Robbins, A.H.; Stout, C.D. Structure of activated aconitase: Formation of the [4Fe-4S] cluster in the crystal. *Proc. Natl. Acad. Sci. USA* **1989**, *86*, 3639–3643. [CrossRef]
105. Rouault, T.A. The role of iron regulatory proteins in mammalian iron homeostasis and disease. *Nat. Chem. Biol.* **2006**, *2*, 406–414. [CrossRef] [PubMed]
106. Camaschella, C.; Campanella, A.; De Falco, L.; Boschetto, L.; Merlini, R.; Silvestri, L.; Levi, S.; Iolascon, A. The human counterpart of zebrafish shiraz shows sideroblastic-like microcytic anemia and iron overload. *Blood* **2007**, *110*, 1353–1358. [CrossRef]
107. Dixon, S.J.; Lemberg, K.M.; Lamprecht, M.R.; Skouta, R.; Zaitsev, E.M.; Gleason, C.E.; Patel, D.N.; Bauer, A.J.; Cantley, A.M.; Yang, W.S.; et al. Ferroptosis: An iron-dependent form of nonapoptotic cell death. *Cell* **2012**, *149*, 1060–1072. [CrossRef]
108. Koulajian, K.; Ivovic, A.; Ye, K.; Desai, T.; Shah, A.; George Fantus, I.; Ran, Q.; Giacca, A. Overexpression of glutathione peroxidase 4 prevents β-cell dysfunction induced by prolonged elevation of lipids in vivo. *Am. J. Physiol. Endocrinol. Metab.* **2013**, *305*, E254-62. [CrossRef]
109. Santangelo, C.; Matarrese, P.; Masella, R.; Di Carlo, M.C.; Di Lillo, A.; Scazzocchio, B.; Vecci, E.; Malorni, W.; Perfetti, R.; Anastasi, E. Hepatocyte growth factor protects rat RINm5F cell line against free fatty acid-induced apoptosis by counteracting oxidative stress. *J. Mol. Endocrinol.* **2007**, *38*, 147–158. [CrossRef] [PubMed]
110. Xu, P.; Qiao, K.; Stephanopoulos, G. Engineering oxidative stress defense pathways to build a robust lipid production platform in Yarrowia lipolytica. *Biotechnol. Bioeng.* **2017**, *114*, 1521–1530. [CrossRef] [PubMed]
111. Baker, P.R.; Friederich, M.W.; Swanson, M.A.; Shaikh, T.; Bhattacharya, K.; Scharer, G.H.; Aicher, J.; Creadon-Swindell, G.; Geiger, E.; Maclean, K.N.; et al. Variant non ketotic hyperglycinemia is caused by mutations in LIAS, BOLA3 and the novel gene GLRX5. *Brain* **2014**, *137*, 366–379. [CrossRef] [PubMed]
112. Liu, G.; Guo, S.; Anderson, G.J.; Camaschella, C.; Han, B.; Nie, G. Heterozygous missense mutations in the GLRX5 gene cause sideroblastic anemia in a Chinese patient. *Blood* **2014**, *124*, 2750–2751. [CrossRef]
113. Chiu, C.F.; Lin, J.L.; Lin, J.J.; Tseng, M.H.; Lo, F.S.; Chiang, M.C. Nonketotic Hyperglycinemia of Infants in Taiwan. *Pediatr. Neonatol.* **2016**, *57*, 420–426. [CrossRef]
114. Daher, R.; Mansouri, A.; Martelli, A.; Bayart, S.; Manceau, H.; Callebaut, I.; Moulouel, B.; Gouya, L.; Puy, H.; Kannengiesser, C.; et al. GLRX5 mutations impair heme biosynthetic enzymes ALA synthase 2 and ferrochelatase in Human congenital sideroblastic anemia. *Mol. Genet. Metab.* **2019**, *128*, 342–351. [CrossRef]
115. Elsner, M.; Gehrmann, W.; Lenzen, S. Peroxisome-generated hydrogen peroxide as important mediator of lipotoxicity in insulin-producing cells. *Diabetes* **2011**, *60*, 200–208. [CrossRef]
116. Koshkin, V.; Wang, X.; Scherer, P.E.; Chan, C.B.; Wheeler, M.B. Mitochondrial functional state in clonal pancreatic β-cells exposed to free fatty acids. *J. Biol. Chem.* **2003**, *278*, 19709–19715. [CrossRef]
117. Pujol, J.B.; Christinat, N.; Ratinaud, Y.; Savoia, C.; Mitchell, S.E.; Dioum, E.H.M. Coordination of GPR40 and ketogenesis signaling by medium chain fatty acids regulates beta cell function. *Nutrients* **2018**, *10*, 473. [CrossRef] [PubMed]
118. Quehenberger, O.; Armando, A.M.; Brown, A.H.; Milne, S.B.; Myers, D.S.; Merrill, A.H.; Bandyopadhyay, S.; Jones, K.N.; Kelly, S.; Shaner, R.L.; et al. Lipidomics reveals a remarkable diversity of lipids in human plasma1. *J. Lipid Res.* **2010**, *51*, 3299–3305. [CrossRef] [PubMed]
119. Osumi, T.; Hashimoto, T. Acyl-CoA oxidase of rat liver: A new enzyme for fatty acid oxidation. *Biochem. Biophys. Res. Commun.* **1978**, *83*, 479–485. [CrossRef]

120. Gehrmann, W.; Elsner, M.; Lenzen, S. Role of metabolically generated reactive oxygen species for lipotoxicity in pancreatic β-cells. *Diabetes. Obes. Metab.* **2010**, *12*, 149–158. [CrossRef]
121. Laporte, A.; Lortz, S.; Schaal, C.; Lenzen, S.; Elsner, M. Hydrogen peroxide permeability of cellular membranes in insulin-producing cells. *Biochim. Biophys. Acta Biomembr.* **2020**, *1862*, 183096. [CrossRef]
122. Lenzen, S.; Drinkgern, J.; Tiedge, M. Low antioxidant enzyme gene expression in pancreatic islets compared with various other mouse tissues. *Free Radic. Biol. Med.* **1996**, *20*, 463–466. [CrossRef]
123. Stancill, J.S.; Broniowska, K.A.; Oleson, B.J.; Naatz, A.; Corbett, J.A. Pancreatic β-cells detoxify H2O2 through the peroxiredoxin/thioredoxin antioxidant system. *J. Biol. Chem.* **2019**, *294*, 4843–4853. [CrossRef]
124. Klingenberg, M.; Winkler, E. The reconstituted isolated uncoupling protein is a membrane potential driven H+ translocator. *EMBO J.* **1985**, *4*, 3087–3092. [CrossRef] [PubMed]
125. Chan, C.B.; MacDonald, P.E.; Saleh, M.C.; Johns, D.C.; Marbàn, E.; Wheeler, M.B. Overexpression of uncoupling protein 2 inhibits glucose-stimulated insulin secretion from rat islets. *Diabetes* **1999**, *48*, 1482–1486. [CrossRef] [PubMed]
126. Fedorenko, A.; Lishko, P.V.; Kirichok, Y. Mechanism of fatty-acid-dependent UCP1 uncoupling in brown fat mitochondria. *Cell* **2012**, *151*, 400–413. [CrossRef] [PubMed]
127. Solmonson, A.; Mills, E.M. Uncoupling Proteins and the Molecular Mechanisms of Thyroid Thermogenesis. *Endocrinology* **2016**, *157*, 455–462. [CrossRef] [PubMed]
128. Echtay, K.S.; Roussel, D.; St-Pierre, J.; Jekabsons, M.B.; Cadenas, S.; Stuart, J.A.; Harper, J.A.; Roebuck, S.J.; Morrison, A.; Pickering, S.; et al. Superoxide activates mitochondrial uncoupling proteins. *Nature* **2002**, *415*, 96–99. [CrossRef]
129. Hu, M.; Lin, H.; Yang, L.; Cheng, Y.; Zhang, H. Interleukin-22 restored mitochondrial damage and impaired glucose-stimulated insulin secretion through down-regulation of uncoupling protein-2 in INS-1 cells. *J. Biochem.* **2017**, *161*, 433–439. [CrossRef]
130. Birk, A.V.; Chao, W.M.; Bracken, C.; Warren, J.D.; Szeto, H.H. Targeting mitochondrial cardiolipin and the cytochrome c /cardiolipin complex to promote electron transport and optimize mitochondrial ATP synthesis. *Br. J. Pharmacol.* **2014**, *171*, 2017–2028. [CrossRef]
131. Li, Z.; Zhou, Z.; Huang, G.; Hu, F.; Xiang, Y.; He, L. Exendin-4 Protects Mitochondria from Reactive Oxygen Species Induced Apoptosis in Pancreatic Beta Cells. *PLoS ONE* **2013**, *8*, e76172. [CrossRef] [PubMed]
132. Gu, J.; Wei, Q.; Zheng, H.; Meng, X.; Zhang, J.; Wang, D. Exendin-4 Promotes Survival of Mouse Pancreatic β -Cell Line in Lipotoxic Conditions, through the Extracellular Signal-Related Kinase 1/2 Pathway. *J. Diabetes Res.* **2016**, *2016*, 1–8. [CrossRef] [PubMed]
133. Ciregia, F.; Giusti, L.; Ronci, M.; Bugliani, M.; Piga, I.; Pieroni, L.; Rossi, C.; Marchetti, P.; Urbani, A.; Lucacchini, A. Glucagon-like peptide 1 protects INS-1E mitochondria against palmitate-mediated beta-cell dysfunction: A proteomic study. *Mol. Biosyst.* **2015**, *11*, 1696–1707. [CrossRef] [PubMed]
134. Lee, K.M.; Seo, Y.J.; Kim, M.K.; Seo, H.A.; Jeong, J.Y.; Choi, H.S.; Lee, I.K.; Park, K. gyu Mediation of glucolipotoxicity in INS-1 rat insulinoma cells by small heterodimer partner interacting leucine zipper protein (SMILE). *Biochem. Biophys. Res. Commun.* **2012**, *419*, 768–773. [CrossRef]
135. Tyagi, S.; Gupta, P.; Saini, A.; Kaushal, C.; Sharma, S. The peroxisome proliferator-activated receptor: A family of nuclear receptors role in various diseases. *J. Adv. Pharm. Technol. Res.* **2011**, *2*, 236–240. [CrossRef]
136. Poitout, V. β-Cell Lipotoxicity: Burning Fat into Heat? *Endocrinology* **2004**, *145*, 3563–3565. [CrossRef] [PubMed]
137. Winzell, M.S.; Svensson, H.; Enerbäck, S.; Ravnskjaer, K.; Mandrup, S.; Esser, V.; Arner, P.; Alves-Guerra, M.C.; Miroux, B.; Sundler, F.; et al. Pancreatic β-cell lipotoxicity induced by overexpression of hormone-sensitive lipase. *Diabetes* **2003**, *52*, 2057–2065. [CrossRef]
138. Tordjman, K.; Standley, K.N.; Bernal-Mizrachi, C.; Leone, T.C.; Coleman, T.; Kelly, D.P.; Semenkovich, C.F. PPARα suppresses insulin secretion and induces UCP2 in insulinoma cells. *J. Lipid Res.* **2002**, *43*, 936–943. [CrossRef]
139. Higa, M.; Zhou, Y.T.; Ravazzola, M.; Baetens, D.; Orci, L.; Unger, R.H. Troglitazone prevents mitochondrial alterations, β cell destruction, and diabetes in obese prediabetic rats. *Proc. Natl. Acad. Sci. USA* **1999**, *96*, 11513–11518. [CrossRef] [PubMed]
140. Joseph, J.W.; Koshkin, V.; Saleh, M.C.; Sivitz, W.I.; Zhang, C.Y.; Lowell, B.B.; Chan, C.B.; Wheeler, M.B. Free fatty acid-induced β-cell defects are dependent on uncoupling protein 2 expression. *J. Biol. Chem.* **2004**, *279*, 51049–51056. [CrossRef]
141. Yamashita, T.; Eto, K.; Okazaki, Y.; Yamashita, S.; Yamauchi, T.; Sekine, N.; Nagai, R.; Noda, M.; Kadowaki, T. Role of uncoupling protein-2 up-regulation and triglyceride accumulation in impaired glucose-stimulated insulin secretion in a β-cell lipotoxicity model overexpressing sterol regulatory element-binding protein-1c. *Endocrinology* **2004**, *145*, 3566–3577. [CrossRef] [PubMed]
142. Medvedev, A.V.; Robidoux, J.; Bai, X.; Cao, W.; Floering, L.M.; Daniel, K.W.; Collins, S. Regulation of the uncoupling protein-2 gene in INS-1 β-cells by oleic acid. *J. Biol. Chem.* **2002**, *277*, 42639–42644. [CrossRef] [PubMed]
143. Oberhauser, L.; Granziera, S.; Colom, A.; Goujon, A.; Lavallard, V.; Matile, S.; Roux, A.; Brun, T.; Maechler, P. Palmitate and oleate modify membrane fluidity and kinase activities of INS-1E β-cells alongside altered metabolism-secretion coupling. *Biochim. Biophys. Acta Mol. Cell Res.* **2020**, *1867*, 118619. [CrossRef]
144. Papa, S.; Guerrieri, F.; Zanotti, F.; Fiermonte, M.; Capozza, G.; Jirillo, E. The γ subunit of F1 and the PVP protein of Fo (FoI) are components of the gate of the mitochondrial FoF1 H+-ATP synthase. *FEBS Lett.* **1990**, *272*, 117–120. [CrossRef]
145. Köhnke, R.; Mei, J.; Park, M.J.; York, D.A.; Erlanson-Albertsson, C. Fatty acids and glucose in high concentration down-regulates ATP synthase β-subunit protein expression in INS-1 cells. *Nutr. Neurosci.* **2007**, *10*, 273–278. [CrossRef]

146. Ciregia, F.; Bugliani, M.; Ronci, M.; Giusti, L.; Boldrini, C.; Mazzoni, M.R.; Mossuto, S.; Grano, F.; Cnop, M.; Marselli, L.; et al. Palmitate-induced lipotoxicity alters acetylation of multiple proteins in clonal β cells and human pancreatic islets. *Sci. Rep.* **2017**, *7*, 13445. [CrossRef] [PubMed]
147. Amo, T.; Sato, S.; Saiki, S.; Wolf, A.M.; Toyomizu, M.; Gautier, C.A.; Shen, J.; Ohta, S.; Hattori, N. Mitochondrial membrane potential decrease caused by loss of PINK1 is not due to proton leak, but to respiratory chain defects. *Neurobiol. Dis.* **2011**, *41*, 111–118. [CrossRef] [PubMed]
148. Grubelnik, V.; Markovič, R.; Lipovšek, S.; Leitinger, G.; Gosak, M.; Dolenšek, J.; Valladolid-Acebes, I.; Berggren, P.O.; Stožer, A.; Perc, M.; et al. Modelling of dysregulated glucagon secretion in type 2 diabetes by considering mitochondrial alterations in pancreatic α-cells. *R. Soc. Open Sci.* **2020**, *7*, 191171. [CrossRef] [PubMed]
149. Grubelnik, V.; Zmazek, J.; Markovič, R.; Gosak, M.; Marhl, M. Modelling of energy-driven switch for glucagon and insulin secretion. *J. Theor. Biol.* **2020**, *493*, 110213. [CrossRef] [PubMed]
150. Köhnke, D.; Ludwig, B.; Kadenbach, B. A threshold membrane potential accounts for controversial effects of fatty acids on mitochondrial oxidative phosphorylation. *FEBS Lett.* **1993**, *336*, 90–94. [CrossRef]
151. Sargsyan, E.; Bergsten, P. Lipotoxicity is glucose-dependent in INS-1E cells but not in human islets and MIN6 cells. *Lipids Health Dis.* **2011**, *10*, 115. [CrossRef] [PubMed]
152. Nakata, M.; Shintani, N.; Hashimoto, H.; Baba, A.; Yada, T. Intra-islet PACAP protects pancreatic β-cells against glucotoxicity and lipotoxicity. *J. Mol. Neurosci.* **2010**, *42*, 404–410. [CrossRef]
153. Kato, T.; Shimano, H.; Yamamoto, T.; Ishikawa, M.; Kumadaki, S.; Matsuzaka, T.; Nakagawa, Y.; Yahagi, N.; Nakakuki, M.; Hasty, A.H.; et al. Palmitate impairs and eicosapentaenoate restores insulin secretion through regulation of SREBP-1c in pancreatic islets. *Diabetes* **2008**, *57*, 2382–2392. [CrossRef] [PubMed]
154. Hirota, N.; Otabe, S.; Nakayama, H.; Yuan, X.; Yamada, K. Sequential activation of caspases and synergistic β-cell cytotoxicity by palmitate and anti-Fas antibodies. *Life Sci.* **2006**, *79*, 1312–1316. [CrossRef]
155. Maedler, K.; Oberholzer, J.; Bucher, P.; Spinas, G.A.; Donath, M.Y. Monounsaturated fatty acids prevent the deleterious effects of palmitate and high glucose on human pancreatic β-cell turnover and function. *Diabetes* **2003**, *52*, 726–733. [CrossRef] [PubMed]
156. Briaud, I.; Harmon, J.S.; Kelpe, C.L.; Segu, V.B.G.; Poitout, V. Lipotoxicity of the pancreatic β-cell is associated with glucose-dependent esterification of fatty acids into neutral lipids. *Diabetes* **2001**, *50*, 315–321. [CrossRef]
157. Frigerio, F.; Chaffard, G.; Berwaer, M.; Maechler, P. The antiepileptic drug topiramate preserves metabolism-secretion coupling in insulin secreting cells chronically exposed to the fatty acid oleate. *Biochem. Pharmacol.* **2006**, *72*, 965–973. [CrossRef] [PubMed]
158. Li, Z.; Zhou, Z.; Hu, L.; Deng, L.; Ren, Q.; Zhang, L. ZLY032, the first-in-class dual FFA1/PPARδ agonist, improves glucolipid metabolism and alleviates hepatic fibrosis. *Pharmacol. Res.* **2020**, *159*, 105035. [CrossRef] [PubMed]
159. Dean, P.M. Ultrastructural morphometry of the pancreatic β-cell. *Diabetologia* **1973**, *9*, 115–119. [CrossRef]
160. Deeney, J.T.; Tornheim, K.; Korchak, H.M.; Prentki, M.; Corkey, B.E. Acyl-CoA esters modulate intracellular Ca2+ handling by permeabilized clonal pancreatic beta-cells. *J. Biol. Chem.* **1992**, *267*, 19840–19845. [CrossRef]
161. Fujitani, Y.; Ebato, C.; Uchida, T.; Kawamori, R.; Watada, H. β-cell autophagy: A novel mechanism regulating β-cell function and mass- Lessons from β-cell-specific Atg7-deficient mice. *Islets* **2009**, *1*, 151–153. [CrossRef] [PubMed]
162. Guo, T.; Liu, T.; Sun, Y.; Liu, X.; Xiong, R.; Li, H.; Li, Z.; Zhang, Z.; Tian, Z.; Tian, Y. Sonodynamic therapy inhibits palmitate-induced beta cell dysfunction via PINK1/Parkin-dependent mitophagy. *Cell Death Dis.* **2019**, *10*, 457. [CrossRef] [PubMed]
163. Petcherski, A.; Trudeau, K.M.; Wolf, D.M.; Segawa, M.; Lee, J.; Taddeo, E.P.; Deeney, J.T.; Liesa, M. Elamipretide Promotes Mitophagosome Formation and Prevents Its Reduction Induced by Nutrient Excess in INS1 β-cells. *J. Mol. Biol.* **2018**, *430*, 4823–4833. [CrossRef] [PubMed]
164. Assali, E.A.; Shlomo, D.; Zeng, J.; Taddeo, E.P.; Trudeau, K.M.; Erion, K.A.; Colby, A.H.; Grinstaff, M.W.; Liesa, M.; Las, G.; et al. Nanoparticle-mediated lysosomal reacidification restores mitochondrial turnover and function in β cells under lipotoxicity. *FASEB J.* **2019**, *33*, 4154–4165. [CrossRef]
165. Peng, L.; Men, X.; Zhang, W.; Wang, H.; Xu, S.; Fang, Q.; Liu, H.; Yang, W.; Lou, J. Involvement of Dynamin-Related Protein 1 in Free Fatty Acid-Induced INS-1-Derived Cell Apoptosis. *PLoS ONE* **2012**, *7*, e49258. [CrossRef] [PubMed]
166. Taddeo, E.P.; Alsabeeh, N.; Baghdasarian, S.; Wikstrom, J.D.; Ritou, E.; Sereda, S.; Erion, K.; Li, J.; Stiles, L.; Abdulla, M.; et al. Mitochondrial proton leak regulated by Cyclophilin D elevates insulin secretion in islets at nonstimulatory glucose levels. *Diabetes* **2020**, *69*, 131–145. [CrossRef] [PubMed]
167. Larsson, O.; Deeney, J.T.; Bränström, R.; Berggren, P.O.; Corkey, B.E. Activation of the ATP-sensitive K+ channel by long chain acyl-CoA: A role in modulation of pancreatic β-cell glucose sensitivity. *J. Biol. Chem.* **1996**, *271*, 10623–10626. [CrossRef] [PubMed]
168. Bränström, R.; Aspinwall, C.A.; Välimäki, S.; Östensson, C.G.; Tibell, A.; Eckhard, M.; Brandhorst, H.; Corkey, B.E.; Berggren, P.O.; Larsson, O. Long-Chain CoA esters activate human pancreatic beta-cell KATP channels: Potential role in Type 2 diabetes. *Diabetologia* **2004**, *47*, 277–283. [CrossRef]
169. Antollini, S.S.; Barrantes, F.J. Fatty Acid Regulation of Voltage- and Ligand-Gated Ion Channel Function. *Front. Physiol.* **2016**, *7*, 573. [CrossRef]
170. Remizov, O.; Jakubov, R.; Düfer, M.; Drews, P.K.; Drews, G.; Waring, M.; Brabant, G.; Wienbergen, A.; Rustenbeck, I.; Schöfl, C. Palmitate-induced Ca2+-signaling in pancreatic beta-cells. *Mol. Cell. Endocrinol.* **2003**, *212*, 1–9. [CrossRef] [PubMed]

171. Komatsu, M.; Yajima, H.; Yamada, S.; Kaneko, T.; Sato, Y.; Yamauchi, K.; Hashizume, K.; Aizawa, T. Augmentation of Ca2+-stimulated insulin release by glucose and long- chain fatty acids in rat pancreatic islets: Free fatty acids mimic ATP- sensitive K+ channel-independent insulinotropic action of glucose. *Diabetes* **1999**, *48*, 1543–1549. [CrossRef]
172. El-Assaad, W.; Buteau, J.; Peyot, M.L.; Nolan, C.; Roduit, R.; Hardy, S.; Joly, E.; Dbaibo, G.; Rosenberg, L.; Prentki, M. Saturated fatty acids synergize with elevated glucose to cause pancreatic β-cell death. *Endocrinology* **2003**, *144*, 4154–4163. [CrossRef]
173. Maestre, I.; Jordán, J.; Calvo, S.; Reig, J.A.; Ceña, V.; Soria, B.; Prentki, M.; Roche, E. Mitochondrial dysfunction is involved in apoptosis induced by serum withdrawal and fatty acids in the β-cell line INS-1. *Endocrinology* **2003**, *144*, 335–345. [CrossRef] [PubMed]
174. MATHIAS, S.; PEÑA, L.A.; KOLESNICK, R.N. Signal transduction of stress via ceramide. *Biochem. J.* **1998**, *335*, 465–480. [CrossRef]
175. Maedler, K.; Spinas, G.A.; Dyntar, D.; Moritz, W.; Kaiser, N.; Donath, M.Y. Distinct effects of saturated and monounsaturated fatty acids on β-cell turnover and function. *Diabetes* **2001**, *50*, 69–76. [CrossRef] [PubMed]
176. Sokolowska, E.; Blachnio-Zabielska, A. The Role of Ceramides in Insulin Resistance. *Front. Endocrinol.* **2019**, *10*, 577. [CrossRef]
177. Itami, N.; Shirasuna, K.; Kuwayama, T.; Iwata, H. Palmitic acid induces ceramide accumulation, mitochondrial protein hyper-acetylation, and mitochondrial dysfunction in porcine oocytes. *Biol. Reprod.* **2018**, *98*, 644–653. [CrossRef] [PubMed]
178. Syed, I.; Szulc, Z.M.; Ogretmen, B.; Kowluru, A. L-threo-C 6 -pyridinium-ceramide bromide, a novel cationic ceramide, induces NADPH oxidase activation, mitochondrial dysfunction and loss in cell viability in INS 832/13 β-cells. *Cell. Physiol. Biochem.* **2012**, *30*, 1051–1058. [CrossRef] [PubMed]
179. Grishko, V.; Rachek, L.; Musiyenko, S.; LeDoux, S.P.; Wilson, G.L. Involvement of mtDNA damage in free fatty acid-induced apoptosis. *Free Radic. Biol. Med.* **2005**, *38*, 755–762. [CrossRef] [PubMed]
180. Veluthakal, R.; Arora, D.K.; Goalstone, M.L.; Kowluru, R.A.; Kowluru, A. Metabolic Stress Induces Caspase-3 Mediated Degradation and Inactivation of Farnesyl and Geranylgeranyl Transferase Activities in Pancreatic β-Cells. *Cell. Physiol. Biochem.* **2016**, *39*, 2110–2120. [CrossRef] [PubMed]
181. Yuan, H.; Zhang, X.; Huang, X.; Lu, Y.; Tang, W.; Man, Y.; Wang, S.; Xi, J.; Li, J. NADPH oxidase 2-derived reactive oxygen species mediate FFAs-Induced dysfunction and apoptosis of b- Cells via JNK, p38 MAPK and p53 pathways. *PLoS ONE* **2010**, *5*, e15726. [CrossRef] [PubMed]
182. Barlow, J.; Affourtit, C. Novel insights into pancreatic β-cell glucolipotoxicity from real-time functional analysis of mitochondrial energy metabolism in INS-1E insulinoma cells. *Biochem. J.* **2013**, *456*, 417–426. [CrossRef]
183. Saksida, T.; Stosic-Grujicic, S.; Timotijevic, G.; Sandler, S.; Stojanovic, I. Macrophage migration inhibitory factor deficiency protects pancreatic islets from palmitic acid-induced apoptosis. *Immunol. Cell Biol.* **2012**, *90*, 688–698. [CrossRef] [PubMed]
184. Zhu, Y.; Ren, C.; Zhang, M.; Zhong, Y. Perilipin 5 Reduces Oxidative Damage Associated With Lipotoxicity by Activating the PI3K/ERK-Mediated Nrf2-ARE Signaling Pathway in INS-1 Pancreatic β-Cells. *Front. Endocrinol.* **2020**, *11*, 166. [CrossRef] [PubMed]
185. Maedler, K.; Størling, J.; Sturis, J.; Zuellig, R.A.; Spinas, G.A.; Arkhammar, P.O.G.; Mandrup-Poulsen, T.; Donath, M.Y. Glucose- and interleukin-1β-induced β-cell apoptosis requires Ca2+ influx and extracellular signal-regulated kinase (ERK) 1/2 activation and is prevented by a sulfonylurea receptor 1/inwardly rectifying K+ channel 6.2 (SUR/Kir6.2) selective potassium channel opener in human islet. *Diabetes* **2004**, *53*, 1706–1713. [CrossRef] [PubMed]
186. Song, Z.; Wang, W.; Li, N.; Yan, S.; Rong, K.; Lan, T.; Xia, P. Sphingosine kinase 2 promotes lipotoxicity in pancreatic β-cells and the progression of diabetes. *FASEB J.* **2019**, *33*, 3636–3646. [CrossRef]
187. Tomita, T. Apoptosis in pancreatic β-islet cells in Type 2 diabetes. *Bosn. J. basic Med. Sci.* **2016**, *16*, 162–179. [CrossRef]
188. Koshkin, V.; Dai, F.F.; Robson-Doucette, C.A.; Chan, C.B.; Wheeler, M.B. Limited mitochondrial permeabilization is an early manifestation of palmitate-induced lipotoxicity in pancreatic β-cells. *J. Biol. Chem.* **2008**, *283*, 7936–7948. [CrossRef] [PubMed]
189. Velasquez, C.; Vasquez, J.S.; Balcazar, N. In vitro effect of fatty acids identified in the plasma of obese adolescents on the function of pancreatic β-cells. *Diabetes Metab. J.* **2017**, *41*, 303–315. [CrossRef] [PubMed]
190. Prause, M.; Christensen, D.P.; Billestrup, N.; Mandrup-Poulsen, T. JNK1 protects against glucolipotoxicity-mediated beta-cell apoptosis. *PLoS ONE* **2014**, *9*, e87067. [CrossRef]
191. Song, H.; Wohltmann, M.; Tan, M.; Ladenson, J.H.; Turk, J. Group VIA phospholipase A2 mitigates palmitate-induced β-cell mitochondrial injury and apoptosis. *J. Biol. Chem.* **2014**, *289*, 14194–14210. [CrossRef] [PubMed]
192. Green, C.D.; Jump, D.B.; Olson, L.K. Elevated insulin secretion from liver X receptor-activated pancreatic β-cells involves increased de novo lipid synthesis and triacylglyceride turnover. *Endocrinology* **2009**, *150*, 2637–2645. [CrossRef] [PubMed]
193. Oropeza, D.; Jouvet, N.; Bouyakdan, K.; Perron, G.; Ringuette, L.J.; Philipson, L.H.; Kiss, R.S.; Poitout, V.; Alquier, T.; Estall, J.L. PGC-1 coactivators in β-cells regulate lipid metabolism and are essential for insulin secretion coupled to fatty acids. *Mol. Metab.* **2015**, *4*, 811–822. [CrossRef]
194. Li, Z.; Liu, C.; Zhou, Z.; Hu, L.; Deng, L.; Ren, Q.; Qian, H. A novel FFA1 agonist, CPU025, improves glucose-lipid metabolism and alleviates fatty liver in obese-diabetic (ob/ob) mice. *Pharmacol. Res.* **2020**, *153*, 104679. [CrossRef] [PubMed]
195. Cho, Y.S.; Kim, C.H.; Kim, K.Y.; Cheon, H.G. Protective effects of arachidonic acid against palmitic acid-mediated lipotoxicity in HIT-T15 cells. *Mol. Cell. Biochem.* **2012**, *364*, 19–28. [CrossRef]
196. Schaffer, J.E. Lipotoxicity: When tissues overeat. *Curr. Opin. Lipidol.* **2003**, *14*, 281–287. [CrossRef] [PubMed]

197. Nakajima, S.; Gotoh, M.; Fukasawa, K.; Murakami-Murofushi, K.; Kunugi, H. Oleic acid is a potent inducer for lipid droplet accumulation through its esterification to glycerol by diacylglycerol acyltransferase in primary cortical astrocytes. *Brain Res.* **2019**, *1725*, 146484. [CrossRef]
198. Plötz, T.; Hartmann, M.; Lenzen, S.; Elsner, M. The role of lipid droplet formation in the protection of unsaturated fatty acids against palmitic acid induced lipotoxicity to rat insulin-producing cells. *Nutr. Metab.* **2016**, *13*, 16. [CrossRef]
199. Tuo, Y.; Wang, D.; Li, S.; Chen, C. Long-term exposure of INS-1 rat insulinoma cells to linoleic acid and glucose in vitro affects cell viability and function through mitochondrial-mediated pathways. *Endocrine* **2011**, *39*, 128–138. [CrossRef] [PubMed]
200. Ježek, P.; Jabůrek, M.; Holendová, B.; Plecitá-Hlavatá, L. Fatty Acid-Stimulated Insulin Secretion vs. Lipotoxicity. *Molecules* **2018**, *23*, 1483. [CrossRef] [PubMed]
201. Lee, S.; Lee, J.-S. Cellular senescence: A promising strategy for cancer therapy. *BMB Rep.* **2019**, *52*, 35–41. [CrossRef]
202. Sone, H.; Kagawa, Y. Pancreatic beta cell senescence contributes to the pathogenesis of type 2 diabetes in high-fat diet-induced diabetic mice. *Diabetologia* **2005**, *48*, 58–67. [CrossRef] [PubMed]
203. Deshpande, S.S.; Qi, B.; Park, Y.C.; Irani, K. Constitutive activation of rac1 results in mitochondrial oxidative stress and induces premature endothelial cell senescence. *Arterioscler. Thromb. Vasc. Biol.* **2003**, *23*, e1–e6. [CrossRef] [PubMed]
204. Hoa Nguyen, K.; Yao, X.H.; Erickson, A.G.; Mishra, S.; Grégoire Nyomba, B.L. Glucose intolerance in aging male igfbp-3 transgenic mice: Differential effects of human igfbp-3 and its mutant igfbp-3 devoid of igf binding ability. *Endocrinology* **2015**, *156*, 462–474. [CrossRef]
205. Civelek, M.; Flory, S.; Meloh, H.; Fitzenberger, E.; Wenzel, U. The polyphenol quercetin protects from glucotoxicity depending on the aggresome in Caenorhabditis elegans. *Eur. J. Nutr.* **2020**, *59*, 485–491. [CrossRef] [PubMed]
206. Moens, C.; Bensellam, M.; Himpe, E.; Muller, C.J.F.; Jonas, J.; Bouwens, L. Aspalathin Protects Insulin-Producing β Cells against Glucotoxicity and Oxidative Stress-Induced Cell Death. *Mol. Nutr. Food Res.* **2020**, *64*, e1901009. [CrossRef]
207. Ben Salem, M.; Ben Abdallah Kolsi, R.; Dhouibi, R.; Ksouda, K.; Charfi, S.; Yaich, M.; Hammami, S.; Sahnoun, Z.; Zeghal, K.M.; Jamoussi, K.; et al. Protective effects of Cynara scolymus leaves extract on metabolic disorders and oxidative stress in alloxan-diabetic rats. *BMC Complement. Altern. Med.* **2017**, *17*, 328. [CrossRef]
208. Galli, A.; Marciani, P.; Marku, A.; Ghislanzoni, S.; Bertuzzi, F.; Rossi, R.; Di Giancamillo, A.; Castagna, M.; Perego, C. Verbascoside Protects Pancreatic β-Cells against ER-Stress. *Biomedicines* **2020**, *8*, 582. [CrossRef]
209. Zakłos-Szyda, M.; Majewska, I.; Redzynia, M.; Koziołkiewicz, M. Antidiabetic Effect of Polyphenolic Extracts from Selected Edible Plants as α-Amylase, α -Glucosidase and PTP1B Inhibitors, and β Pancreatic Cells Cytoprotective Agents—A Comparative Study. *Curr. Top. Med. Chem.* **2015**, *15*, 2431–2444. [CrossRef] [PubMed]
210. Mollica, A.; Stefanucci, A.; Zengin, G.; Locatelli, M.; Macedonio, G.; Orlando, G.; Ferrante, C.; Menghini, L.; Recinella, L.; Leone, S.; et al. Polyphenolic composition, enzyme inhibitory effects ex-vivo and in-vivo studies on two Brassicaceae of north-central Italy. *Biomed. Pharmacother.* **2018**, *107*, 129–138. [CrossRef]
211. Ben Khedher, M.R.; Hafsa, J.; Haddad, M.; Hammami, M. Inhibition of Protein Glycation by Combined Antioxidant and Antiglycation Constituents from a Phenolic Fraction of Sage (*Salvia officinalis* L.). *Plant Foods Hum. Nutr.* **2020**, *75*, 505–511. [CrossRef] [PubMed]
212. Liu, C.G.; Ma, Y.P.; Zhang, X.J. Effects of mulberry leaf polysaccharide on oxidative stress in pancreatic β-cells of type 2 diabetic rats. *Eur. Rev. Med. Pharmacol. Sci.* **2017**, *21*, 2482–2488.
213. Gharib, E.; Kouhsari, S.M.; Izad, M. Punica granatum L. Fruit aqueous extract suppresses reactive oxygen species-mediated p53/p65/miR-145 expressions followed by Elevated Levels of irs-1 in alloxan-diabetic rats. *Cell J.* **2018**, *19*, 520–527. [CrossRef]
214. Hao, F.; Kang, J.; Cao, Y.; Fan, S.; Yang, H.; An, Y.; Pan, Y.; Tie, L.; Li, X. Curcumin attenuates palmitate-induced apoptosis in MIN6 pancreatic β-cells through PI3K/Akt/FoxO1 and mitochondrial survival pathways. *Apoptosis* **2015**, *20*, 1420–1432. [CrossRef]
215. Zhang, Y.; Zhen, W.; Maechler, P.; Liu, D. Small molecule kaempferol modulates PDX-1 protein expression and subsequently promotes pancreatic β-cell survival and function via CREB. *J. Nutr. Biochem.* **2013**, *24*, 638–646. [CrossRef] [PubMed]
216. Huang, C.N.; Wang, C.J.; Lee, Y.J.; Peng, C.H. Active subfractions of Abelmoschus esculentus substantially prevent free fatty acid-induced ß cell apoptosis via inhibiting dipeptidyl peptidase-4. *PLoS ONE* **2017**, *12*, e0180285. [CrossRef]
217. McCarty, M.F. A chlorogenic acid-induced increase in GLP-1 production may mediate the impact of heavy coffee consumption on diabetes risk. *Med. Hypotheses* **2005**, *64*, 848–853. [CrossRef] [PubMed]
218. Paolisso, G.; Giugliano, D.; D'Amore, A.; Varricchio, M.; Galzerano, D.; D'Onofrio, F.; Balbi, V. Daily vitamin E supplements improve metabolic control but not insulin secretion in elderly type II diabetic patients. *Diabetes Care* **1993**, *16*, 1433–1437. [CrossRef] [PubMed]
219. Kwak, H.J.; Yang, D.; Hwang, Y.; Jun, H.S.; Cheon, H.G. Baicalein protects rat insulinoma INS-1 cells from palmitate-induced lipotoxicity by inducing HO-1. *PLoS ONE* **2017**, *12*, e0176432. [CrossRef]

BIOLOGY Methods & Protocols

Biology Methods and Protocols, 2021, 1–9

https://doi.org/10.1093/biomethods/bpab023
Advance Access Publication Date: 3 December 2021
Methods Article

METHODS ARTICLE

Preparation of fatty acid solutions exerts significant impact on experimental outcomes in cell culture models of lipotoxicity

Axel Römer , Divya Rawat, Thomas Linn and Sebastian F. Petry *

Clinical Research Unit, Center of Internal Medicine, Justus Liebig University Giessen, 35392 Giessen, Germany

*Correspondence address. Clinical Research Unit, Center of Internal Medicine, Justus Liebig University Giessen, Klinikstraße 33, 35392 Giessen, Germany. Tel: +49 641 985 57010; Fax: +49 641 985 57029; E-mail: sebastian.petry@innere.med.uni-giessen.de

Abstract

Free fatty acids are essentially involved in the pathogenesis of chronic diseases such as diabetes mellitus, non-alcoholic fatty liver disease, and cardiovascular disease. They promote mitochondrial dysfunction, oxidative stress, respiratory chain uncoupling, and endoplasmic reticulum stress and modulate stress-sensitive pathways. These detrimental biological effects summarized as lipotoxicity mainly depend on fatty acid carbon chain length, degree of unsaturation, concentration, and treatment time. Preparation of fatty acid solutions involves dissolving and complexing. Solvent toxicity and concentration, amount of bovine serum albumin (BSA), and ratio of albumin to fatty acids can vary significantly between equal concentrations, mediating considerable harmful effects and/or interference with certain assays such as 3-(4,5-dimethylthiazol-2-yl)-2,5-diphenyltetrazolium bromide (MTT). Herein, we studied the impact of commonly used solvents ethanol and dimethyl sulfoxide and varying concentrations of BSA directly and in solution with oleic acid on MTT to formazan conversion, adenosine triphosphate level, and insulin content and secretion of murine β-cell line MIN6 employing different treatment duration. Our data show that experimental outcomes and assay readouts can be significantly affected by mere preparation of fatty acid solutions and should thus be carefully considered and described in detail to ensure comparability and distinct evaluation of data.

Keywords: free fatty acid; oleic acid; lipotoxicity; beta cell; BCRJ Cat# 0293; RRID: CVCL_0431; diabetes mellitus; sample preparation

Introduction

Lipotoxicity

Visceral obesity is one of the major causes of insulin resistance and development of type 2 diabetes mellitus (T2DM) [1, 2]. Abundance of energy fuels insulin resistance and leads to dyslipidemia marked by pathological increase of free fatty acids (FFA). Detrimental effects mediated by FFA were first described in 1994 and termed as “lipotoxicity” [3]. Interactions between FFA and cells are complex and comprise multiple pathways eventually interfering with lipid metabolism. Dysregulation of uptake, utilization, and/or storage of triglycerides and FFA [4, 5] leads to accumulation of bioactive molecules such as acyl-CoA and ceramides [6, 7] triggering pathways including mitogen-activated protein kinase (MAPK), extracellular-signal-regulated kinase (ERK), sterol regulatory element binding protein-1c (SREBP-1c), and uncoupling protein 2 (UCP2) or promoting release of intracellular Ca storages [8–11]. Apart from diabetes

Received: 5 October 2021; **Revised:** 25 November 2021; **Editorial Decision:** 29 November 2021; **Accepted:** 30 November 2021

research, lipotoxicity plays a role in the pathogenesis of non-alcoholic fatty liver disease [12], cardiovascular disease [13], and apoptosis promoted by cytochrome C release [14]. Therefore, establishment of standardized protocols for *in vitro* models with defined FFA as lipid stressors is required for the investigation of underlying mechanisms.

Preparation of FFA solutions applicable for immortalized or primary cell lines comprises dissolving and complexing FFA. According to our review of over 100 articles about lipotoxic effects on mitochondria in pancreatic β-cells, protocols frequently do not contain essential information on how FFA solutions were prepared [15]. Since equally concentrated FFA solutions can be composed distinctly differently and thus have significant impact on experimental outcomes, we aim to have a closer look at the respective experimental parameters.

Type of FFA and solubility

Each FFA is characterized by physicochemical properties including solubility by carbon chain length and number of double bonds. Frequently used FFA in diabetes research are long-chain fatty acids namely palmitic (PA) and oleic acid (OA) representing the most abundant saturated and unsaturated FFA in T2DM, respectively [16]. For solubilizing FFA and preparing a high molecular stock solution, most frequently employed protocols include ethanol (26%), saponification (12%), dimethyl sulfoxide (DMSO) (4%), and methanol (3%), while 55% of articles do not specify the substance used [15]. However, solubility of FFA and respective composition of solutions differ significantly among solvents. Solubility of PA in DMSO is 80 mM compared with 350 mM for OA (Cayman Chemical, Ann Arbor, MI, USA). In contrast, there seems to be no relevant difference in ethanol solubility for preparing stock solutions. A concentration as high as 1800 mM for PA/OA was achieved with ethanol [17]. While toxicity of DMSO in different models is lower than ethanol at same concentrations [18], the amount of ethanol in the final FFA concentration can be lowered to a greater extent because of higher dilution factors. Therefore, ethanol allows studying higher FFA concentrations with low levels of solvent. Methanol is rarely used as solvent, but seems to be less toxic in human and rat cell lines, while solubility is comparable to ethanol [19]. In contrast, saponification doesn't yield harmful solvent effects as sodium salts of FFA are created by usage of NaOH or NaCl. To saponify FFA, higher temperatures have to be used.

Bovine serum albumin

Fraction V fatty acid-free bovine serum albumin (BSA) is used to complex FFA in aqueous conditions like cell culture media. FFA are physiologically complexed to albumin [20]. The biopolymer BSA has different functions depending on respective experimental settings. In cellular systems, cholesterol [21] and opioid binding characteristics are described [22]. Thiol groups of BSA can act as antioxidant [23] and inhibition of angiotensin-converting enzyme was described in a cell model of hypertension for human serum albumin [24]. It is used as a blocking agent for methods based on antibody interactions and as protein standard. Its complexation ability can be used for complexing metals or FFA. As BSA carries FFA it is involved in energy metabolism and composition of biomembranes. BSA will increase FFA bioavailability in organisms [25]. For complexing FFA, BSA can be added into cell culture media and after gently mixing FFA stock solution is added. FFA can be protected from oxidation by overlaying with nitrogen and will complex to BSA by shaking for several hours at 37°C. After sterile filtration, FFA media can be stored at −20°C. The amount of BSA will determine the final molar FFA:BSA ratio. The higher the FFA:BSA ratio the greater is the amount of FFA unbound to BSA. FFA-mediated detrimental effects on cellular functions are crucially determined by the amount of unbound FFA [26]. It is suggested that a 5:1 ratio is suitable to mimic pathological conditions and should not be exceeded [27]. When a stable FFA:BSA ratio is maintained, the amount of BSA will increment with increasing concentrations of FFA interfering with substrates employed in experimental settings like 3-(4,5-dimethylthiazol-2-yl)-2,5-diphenyltetrazolium bromide (MTT) [27, 28]. Conversion of MTT to formazan assesses the reduction potential of a cell, that is the biofunctionality of dehydrogenase enzymes depending on reducing compounds to drive cellular energetics [29]. The assay can distinguish living from dead cells, as active mitochondria are required to perform this reaction. A high conversion rate of MTT is taken as parameter for metabolically active cells with high capacity of reduction equivalents. By examining various control conditions, we have observed that this reaction can be induced by BSA.

Aim of research

We studied the impact of ethanol and DMSO, BSA, treatment duration, and differentially prepared OA solutions on MTT to formazan conversion, adenosine triphosphate (ATP) level, and insulin content and secretion of murine β-cell line MIN6.

Material and methods

Cell culture

Mouse insulinoma (MIN6) cells (BCRJ Cat# 0293, RRID: CVCL_0431) were obtained from Prof. Lenzen of Hannover Medical School, Hannover, Germany [30]. Cells of passages 50–60 were cultured in an incubator at 37°C with 5% CO_2 in Dulbecco's modified Eagle's medium (DMEM) enriched with 25 mM glucose and 1 mM pyruvate (Gibco, Thermo Fisher Scientific, Waltham, MA, USA) and supplemented with 16% v/v heat inactivated fetal bovine serum (Biowest, Riverside, MO, USA), 80 U/mL penicillin/streptomycin (Gibco, Thermo Fisher Scientific), and 50 μM 2-mercaptoethanol (Gibco, Thermo Fisher Scientific). Change of culture media was performed every 2–3 days. After reaching a confluency of 70–80%, PBS (Lonza, Basel, Switzerland) washed cells were collected by trypsinization with 0.05% Trypsin-EDTA (Gibco, Thermo Fisher Scientific). After centrifugation at 1200 rpm for 4 min, supernatant was removed and MIN6 cells were resuspended in fresh DMEM. Cell count was determined using a Neubauer counting chamber (Brand, Wertheim, Germany) after staining with Trypan blue (Sigma-Aldrich, St. Louis, MO, USA).

Preparation of treatment solutions

BSA, DMSO, ethanol

Ethanol (purity >99.8%, Sigma, Munich, Germany), DMSO (purity >99.5%, Sigma), or fraction V fatty acid free BSA (SERVA Electrophoresis, Heidelberg, Germany) was added to cell culture DMEM. Prior to treatment, solutions containing ethanol or DMSO were mixed properly for several seconds. BSA was dissolved overnight on a shaker at 37°C, followed by sterile filtration (0.22 μm).

FFA solution

OA (purity >99%, Enzo Life Sciences, New York, USA) was dissolved in ethanol (purity >99.8%, Sigma) to prepare stock solutions of 150, 225, 450, and 900 mM. Stock solutions were diluted

1:300 with DMEM complexed with fraction V fatty acid-free BSA (SERVA Electrophoresis, Heidelberg, Germany) to prepare FFA concentrations of 0.5, 0.75, 1.5, and 3 mM. The molar FFA:BSA ratio was 5:1 and ethanol concentration was 0.23–0.32% w/w. The prepared FFA media were overlayed with nitrogen (Linde, Dublin, Ireland) and placed on a shaker overnight at 37°C. After sterile filtration (0.22 μm), stock solutions were stored at −20°C. Control media contained matching amounts of ethanol and BSA. For comparison of solvent effects, a 150 mM OA stock solution and control medium were prepared with DMSO (purity >99.5%, Sigma). Stock solution was diluted to generate 1.5 mM OA media. A suggested standard protocol for preparation of FFA solutions is given in the Supplementary Data.

MTT assay

MTT assay was chosen for evaluation of cell functionality. After $1 * 10^4$ MIN6 cells in 200 μL DMEM had attached to a 96-well plate (Greiner Bio-One, Kremsmünster, Austria) for 24 h, DMEM was replaced by fresh DMEM, control, or treatment medium, respectively, for 24 or 120 h (5 days). In case of 120 h treatment medium was changed after 0 (attachment time), 48, and 96 h. Ten milligrams of MTT (purity >98%, Abcam, Cambridge, UK) was dissolved in 5 mL PBS (c = 2 mg/mL). After sterile filtration (0.22 μm), 50 μL of media was replaced by MTT solution, protected from light. Samples were incubated at 37°C for 4 h. Afterward the entire medium was replaced by 200 μL DMSO. Formazan crystals dissolved for 15 min on a plate shaker and absorption values were measured at 570 and 620 nm (background) by a Multimode Microplate Reader (Berthold Technologies, Bad Wildbad, Germany). Absorption value of DMEM without MIN6 cells was subtracted as a blank value.

ELISA

$4 * 10^5$ MIN6 cells in 3 mL DMEM were seeded into a six-well plate (Greiner Bio-One, Kremsmünster, Austria). After attaching to the plate for 24 h, cells were exposed to 1.5 mM OA for 24 h. One milliliter of culture medium was collected and centrifuged at 2000 rpm for 5 min at 4°C. Supernatant was collected for further analysis. PBS-washed cells were lysed with 300 μL of NP-40 buffer (10% aqueous solution, Merck Millipore, Burlington, MA, USA) supplemented with 3% v/v protease inhibitor cocktail 100× (Halt, Thermo Fisher Scientific, Waltham, MA, USA) for 20 min at 4°C. After centrifugation at 12,000 rpm for 15 min at 4°C, supernatant of cell lysate was collected. Insulin content of cell lysate and culture medium was measured by direct sandwich ELISA (DRG Diagnostics, Marburg, Germany). An aliquot of lysate samples was analyzed for total protein by Bradford protein assay (Bio-Rad Laboratories, Hercules, CA, USA) to normalize insulin results to total protein [31]. In total, 0.1–1 mg/mL BSA was used as standard.

ATP bioluminescence

$5 * 10^4$ MIN6 cells were seeded into a 96 luminescence-well plate (Corning Inc., Corning, NY, USA) and attached for 24 h. After attaching solvent treatment was performed for 24 h. ATP level was determined by adding a NaOH lysis buffer and a solution containing luciferase, luciferin, and co-substrates. The assay was performed according to manufacturer's instructions (PerkinElmer, Waltham, MA, USA). Luminescence was measured using a Multimode Microplate Reader (CLARIOstar, BMG LABTECH, Ortenberg, Germany).

Statistical analysis

Statistical analysis was performed by GraphPad Prism 7 (GraphPad Software, San Diego, CA, USA) using one- or two-way ANOVA with Tukey's multiple comparisons test. Data are represented as mean ± SD. A P-value <0.05 was considered significant and marked with *. $P < 0.01$, <0.001, and <0.0001 were marked with **, ***, and ****, respectively.

Results

BSA increases MIN6 cell-dependent MTT conversion to formazan

After 24 h cultivation of MIN6 cells with 0.5–12.5% w/w BSA, the conversion of MTT to formazan was increased by BSA (Fig. 1A). This effect was observable up to a maximum concentration of 6% BSA increasing conversion by ∼60%. After exceeding a concentration of 12.5% a negative effect set in. Cultivation with 12.5% BSA led to an overall increased conversion of ∼25% compared with DMEM-treated cells. Treatment with 5% w/w ethanol was chosen as toxic treatment decreasing reducing activity measured by MTT conversion by ∼60%. In contrast, prolonged cultivation for 5 days led to a non-significant increase with 1% and 3% BSA, whereas 6–10% BSA inhibited MTT to formazan conversion by up to 50% (Fig. 1B). Absorption levels with 6%, 8%, and 10% BSA were below controls after 5 days culture.

BSA increases MIN6 cell-dependent and independent MTT conversion to formazan

The impact of BSA concentrations ranging from 1% to 10% w/w on MTT assay with (Fig. 2A) or without (Fig. 2B) MIN6 cells was studied. Conversion of MTT to formazan in medium containing BSA without cells was dose-dependently rising. Relative enhancement was significant for higher concentrations of BSA while the absolute increase in absorption was minimal.

To take into account the MIN6-independent effect of BSA absorption readings of solutions without cells was subtracted from corresponding cell samples. This normalization resulted in a 25% decrease in absorption for 10% BSA when compared with lower concentrations (Fig. 3) in contrast to a 17% decrease without normalization (Fig. 2A).

Increased treatment duration intensifies lipotoxic effects and MTT to formazan conversion

To study the effects of treatment duration, MIN6 cells were exposed to 0.5–3 mM OA with corresponding control solutions for 24 h (Fig. 4A) and 5 days (Fig. 4B), respectively. For both setups, a dose-dependent toxic effect was observed. It was more pronounced after 5 days of treatment. Prolonged culture doubled absorption readouts in comparison with 24 h cultivation.

DMSO and ethanol significantly affect MTT to formazan conversion in a dose-dependent manner

DMSO treatment of MIN6 cells for 24 h showed a negative effect on MTT to formazan conversion for 4% w/w, whereas 0.5–2% w/w increased optical density slightly (Fig. 5). 1–4% w/w ethanol mediated a more pronounced reduction of MTT conversion, while 0.5% and 1% did not show a significant difference in optical density after 24 h.

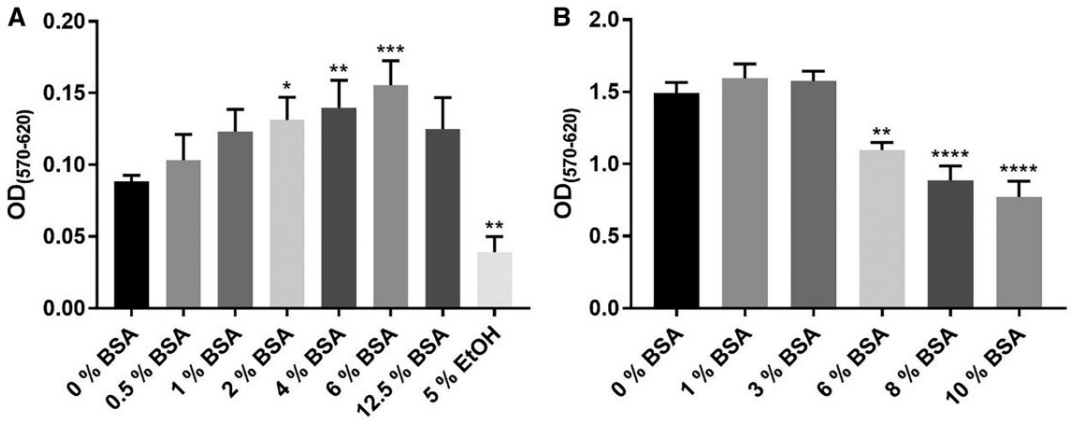

Figure 1: Optical density obtained from MTT assay after (**A**) 24 h treatment of MIN6 cells with different BSA concentrations and ethanol as toxic treatment ($n = 4$) and (**B**) 120 h (5 days) treatment of MIN6 cells with different BSA concentrations ($n = 3$). *$P < 0.05$, **$P < 0.01$, ***$P < 0.001$, ****$P < 0.0001$ compared with 0% BSA.

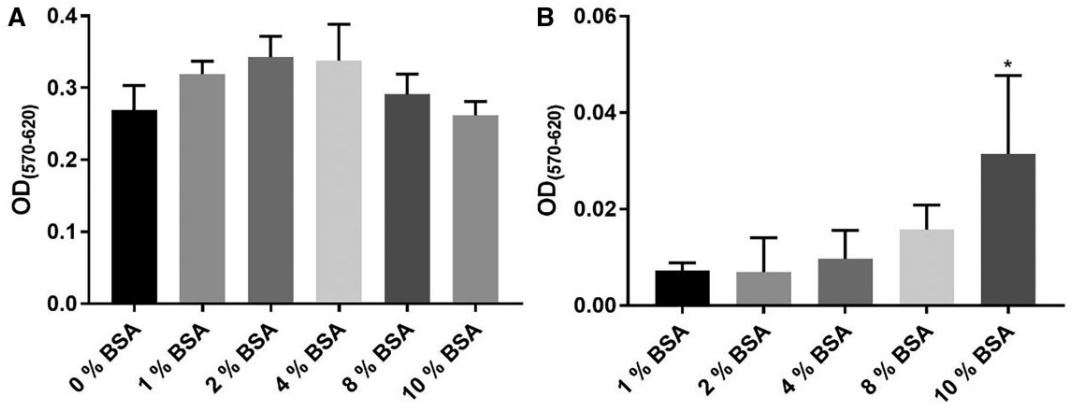

Figure 2: Optical density obtained from MTT assay (**A**) after treatment of MIN6 cells with different BSA concentrations for 24 h ($n = 3$) and (**B**) for different BSA concentrations without MIN6 cells ($n = 3$). *$P < 0.05$ compared with (B) 1% BSA.

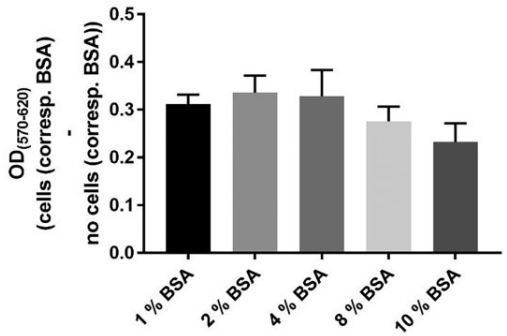

Figure 3: Normalized optical density after 24 h treatment with BSA ($n = 3$). Readings of solutions without cells were subtracted from corresponding cell samples.

24 h ethanol treatment decreases ATP content of MIN6 cells

Treatment with ethanol for 24 h decreased intracellular ATP level (Fig. 6). The effect was more pronounced by higher ethanol concentration and significant for 0.45% w/w and 0.9% w/w. Treatment with 0.225% led to a non-significant decrease of 30% while 0.9% decreased ATP by 50%.

Ethanol-prepared FFA exhibit greater impairment of insulin than DMSO-prepared FFA

For comparison of solvent effect on insulin synthesis, 1.5 mM OA was dissolved in ethanol (final concentration = 0.45% w/w) or DMSO (final concentration = 0.96% w/w). 1.5 mM OA dissolved in ethanol mediated a ~90% decrease of insulin concentration in cell lysate (Fig. 7A) and in culture media (Fig. 7B), indicating abated insulin secretion. Preparation with DMSO diminished lysate insulin by ~40% and secreted insulin in medium by ~85%. The presence of DMSO did not impair insulin production to such extent as the presence of ethanol did despite its higher concentration.

Discussion

It is acknowledged that the effects of FFA treatment are essentially dependent on carbon chain length, degree of unsaturation, and concentration of the respective fatty acid as well as treatment duration [15]. However, preparation of FFA can vary significantly, and little is known about a possible impact on assay readouts and experimental outcomes.

Bovine serum albumin

BSA initially enhanced conversion of MTT to formazan in a concentration-dependent manner in MIN6 culture before a

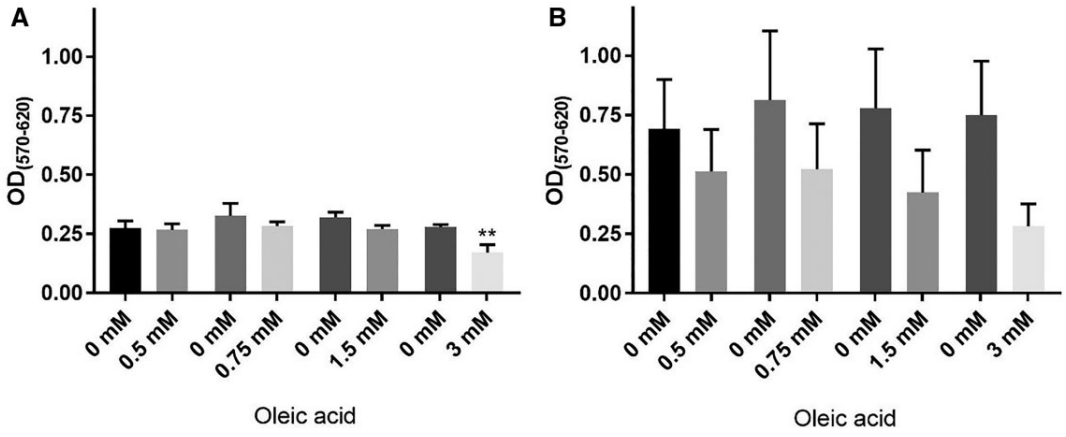

Figure 4: Optical density obtained from MTT assay of MIN6 cells after (**A**) 24 h and (**B**) 120 h (5 days) treatment duration with different concentrations of OA or corresponding controls ($n = 3$). $^{**}P < 0.01$ compared with respective control treatment without fatty acid.

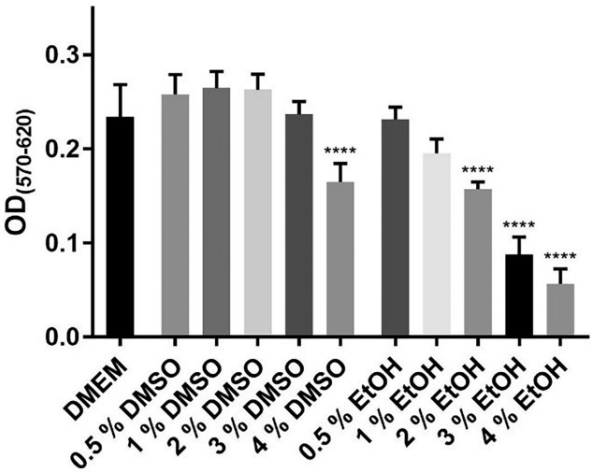

Figure 5: Optical density obtained from MTT assay of MIN6 cells treated for 24 h with solvents DMSO and ethanol ($n = 5$). $^{****}P < 0.0001$ compared with cell culture with DMEM.

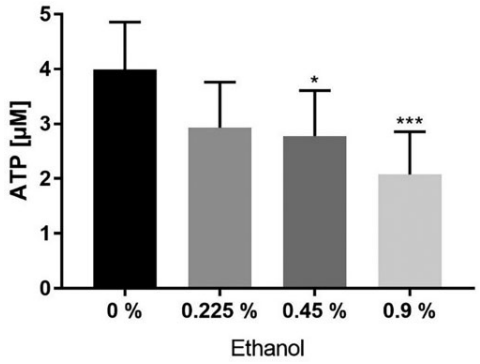

Figure 6: ATP level of MIN6 cells after 24 h treatment with ethanol ($n = 8$). $^{*}P < 0.05$, $^{***}P < 0.001$ compared with 0% ethanol.

decrease was observed at higher concentrations. In a setup without MIN6 cells, conversion increased steadily. The impact of BSA on experimental outcomes has not been studied extensively. It is unclear whether it is caused by an interference with conversion of MTT to formazan or altered cytobiological function. Possible mechanisms underlying a cell-dependent effect are growth factors; carrier function for small molecules; binding of toxic substances; or the supplementation of cell culture media with essential compounds like lipids, amino acids, and metal ions [32, 33]. As Huang *et al.* [34] have demonstrated BSA significantly reduces hydroxyl groups taking effect on antibody reactions. Secretion of IL-1β and TNF-α was promoted by BSA in microglial cells [35]. In brain tissue, BSA increased oxidation in mitochondria particularly by activation of succinate dehydrogenase [36]. Ponte *et al.* [37] demonstrated that BSA can modulate muscle cell response to calcium release of the sarcoplasmic reticulum. Remarkably, high concentrations of BSA led to lower conversion of MTT in MIN6 samples. General proteotoxic effects [38] might explain this decrease. By assumption those high concentrations of 6% or more with impairing effects are not used in regular cell culture work. For cell-independent effects, a direct effect of BSA on MTT was strikingly evident. Although absolute absorption levels were only affected marginally, normalization with corresponding cell-independent BSA controls can be a helpful tool to clarify the cellular effects, especially in models with small differences between samples. A major concern is that cellular viability as determined by MTT assay is overestimated if BSA in control media is not adjusted. Maximum effect in our experiments was +50% in MTT to formazan conversion. It should also be considered that absolute absorption levels are time-dependent. After 5 days of culture, optical density approximately doubled when compared with 24 h (Fig. 4). So far it is not known if prolonged treatment with BSA containing media has a greater effect on cell-independent MTT reaction. Judging from our data, a cell-dependent and -independent effect might be possible. By rough estimation, 1% of BSA in DMEM increased MIN6 viability by 10%. By assuming a 5:1 ratio, most used models investigating 0.5 mM FFA apply 0.1 mM BSA representing 0.66% BSA. Exposition against low molecular FFA concentration should physiologically only lead to a slightly reduced viability [39–41]. Therefore, BSA exerts a relevant impact on MTT outcome when compared with its lipotoxic effect and might conceal FFA-mediated effects. In dosages mediating a significant level of lipotoxicity, this impact becomes negligible. The significance of these effects is highly depending on the experimental setup. If multiple concentrations are tested, greater differences between employed amounts of BSA occur. According to our previous work, this is the case for approximately 21% of articles on lipotoxicity in diabetic models [15]. To be able to assess the impact of BSA, an exact

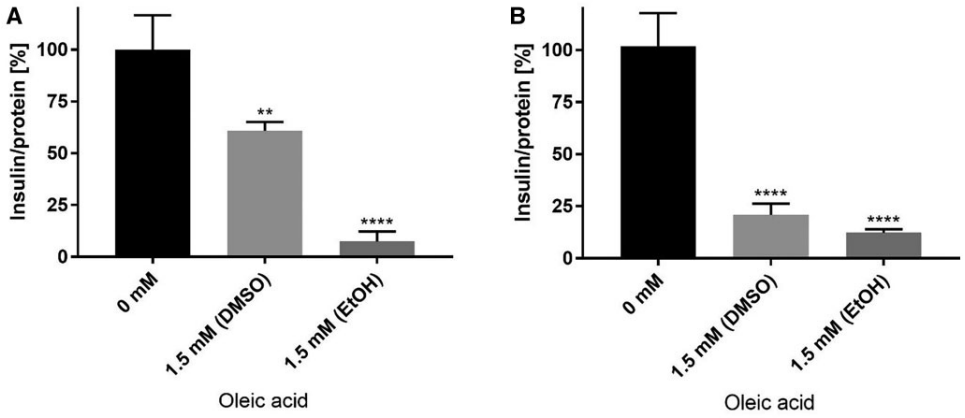

Figure 7: Insulin amount of (**A**) MIN6 cell lysate and (**B**) culture medium after 24 h treatment with 1.5 mM OA prepared with DMSO or ethanol ($n = 4$). $^{**}P < 0.01$, $^{****}P < 0.0001$ compared with 0 mM.

methodological description is necessary. A concentration range of 0.5–2 mM FFA would result in a BSA range of 0.1–0.4 mM representing 0.66–2.77% BSA. This could lead to a change of viability of 20%. Therefore, it is necessary to prepare individual control solutions for all treatment conditions in MTT assays. In diabetes research, outcomes also depend on FFA concentration as concentrations below 0.1 mM exert positive effects on insulin secretion as opposed to concentrations of 0.5 mM and above. Underlying mechanisms involve promoted insulin secretion by depletion of Ca storages induced by interaction of peroxisome proliferator-activated receptor γ (PPARγ) and G protein-coupled receptor 40 (GPR40), an effect which is especially seen after acute treatment [42–44]. Physiological levels of FFA can be further used for energy production increasing insulin secretion by elevated ATP levels [45]. By chronic exposure, energy production is impaired by SREBP-1c-induced uncoupling of respiratory chain complexes by UCP2. Beside possible interactions of BSA, both FFA concentration and treatment duration can change experimental outcomes. Also, molar ratio is a decisive parameter in lipotoxic research. The chosen ratio of FFA:BSA can generally determine lipotoxic effects throughout different assays. It was shown that mere changes can induce apoptotic effects [26] which are prevented by lower molecular ratios [27]. These changes in toxicity can also be apparent due to different preparations of BSA. The amount of albumin can be affected by using commercially available FFA-free albumin or charcoal-absorbed BSA which can be used for removing bovine FFA, potentially altering the outcome of certain assays. There are vast differences in ratios employed throughout literature ranging from 74:1 [46] to 1:3 [47] or 1:5 [44]. To achieve the same FFA concentration of 0.5 mM, different protocols give markedly divergent concentrations of BSA like 0.045% [46], 10% [47], or 16.6% [44]. As 54% of reviewed articles neither state the amount of BSA nor the FFA:BSA ratio, it is doubtful that the general impact of BSA is commonly taken into account. It would be helpful to state that BSA and solvents were used as controls and their effects on cell viability were evaluated [48]. The matter is further complicated by the enrichment of cell culture medium by BSA-containing serum.

Solvents

Direct toxic effects of solvents for FFA preparation have to be considered carefully. Possible solvents have differential toxic impact on cellular systems as shown by MTT and insulin ELISA. DMSO seems to be less toxic for equimolar concentrations compared with ethanol. Due to restrictions in solubility especially the use of highly concentrated PA requires high concentrations of DMSO. Systematic evaluations of common solvents in organisms serve as reference [18]. Embryotoxic effects commence at ethanol concentrations above 1%. Equal concentrations led to negative effects in performed MTT assays (Fig. 5). It can't be excluded that metabolic restrictions also occur at lower concentrations.

The majority of articles does not provide the used solvent and/or different concentrations are not discriminated in terms of solvent concentration. When multiple concentrations of FFA are used, a detailed description of respective preparations favoring the preparation of individual stock solutions would be desirable. A single stock solution applied for a range of concentrations leads to decreased levels of solvents at higher dilution and vice versa. Lipotoxic and solvent-induced effects might thus be difficult to be distinguished. Similarly, solvent controls should be prepared for each concentration. This becomes especially relevant for articles studying higher FFA concentrations due to solubility characteristics. As 0.5 mM is the most frequently chosen concentration applied, few articles are exceeding the concentration. Nine out of 132 articles reviewed for FFA-mediated effects on mitochondrial function [15] employed a concentration between 1 and 2 mM. Three working groups gave sufficient information to calculate final ethanol solution which was lower than 0.31%. Two articles used saponification. There was not sufficient or no data at all on preparation of FFA solutions in the remaining articles. Without these information, respective solvent-mediated effects cannot be considered. As an example, a 1 mM OA solution prepared from a 300 mM stock solution will contain a final ethanol concentration of 0.3%, while using a 100 mM stock solution will result in 0.97% ethanol, potentially exerting significant toxic impact on sensitive cell lines or assays as demonstrated by our data (Fig. 5–7).

Limitations

Our aim was to generate a systematic approach to study relevant parameters in FFA preparation employing a widely used β-cell model. Data presented herein have been collected from 2019 to 2021 and were consistent with previously mostly unpublished data gathered by multiple researchers from our group during the last 5 years. However, there are limitations to this study. Only single effectors were tested, leaving the question if

and how respective concentrations take impact on experimental outcomes once combined in the final treatment solution. We mainly focused on MTT assay as predictor of cellular function. Future studies should thus evaluate the impact of FFA solution preparation on a broader range of assays. Our data further revealed that the quantitative impact on experimental outcomes depends on the respective assay. Treatment with 1% ethanol only changed MTT results slightly whereas cellular ATP content was diminished by 50% and exposure to 1.5 mM OA led to a 20% decrease in MTT reaction but a 90% decrease in insulin ELISA readout. The impact of the effectors employed in this study on mere assay results must thus be carefully delineated from their biological effects and considered for interpretation of experimental outcomes, especially regarding potential implications for *in vivo* studies. Comparison of albumin levels and experimental parameters to mimic physiological conditions is difficult. Level of human serum albumin ranges from 550 to 700 μM in healthy individuals [49] with very limited data on the effects of BSA. Respective studies involve various experimental models and concentrations applying 0.7–30 μM [35–37] while BSA concentration and/or FFA:albumin molar ratio in diabetic research are often not stated [15, 27]. Applied BSA concentration in the current study comprised 100–600 μM correlating with (sub-)physiological levels. However, medical conditions such as diabetes mellitus [50] or liver disease [51] can significantly affect serum albumin levels. Drawing conclusions from our data on the significance for *in vivo* assays does thus not seem feasible.

Conclusion

Our data demonstrate that preparation of FFA solutions can exert significant impact on experimental outcomes when studying lipotoxic effects. Effects of utilized solvents, amount of BSA, molar relation of FFA to BSA, treatment time, and choice of controls can exponentiate or counteract each other to a great extent. Popular assays used for estimating cell viability like MTT to formazan conversion are susceptible to BSA. Solvents in general have detrimental effects on cells. It is difficult to predict and analyze the outcomes of these effects, especially since information on preparation of FFA solutions is frequently omitted or incomplete in literature. We recommend that researchers give respective information to allow for comparability and appropriate interpretation of data. A suggested protocol is given in the Supplementary Data.

Supplementary data

Supplementary data are available at *Biology Methods and Protocols* online.

Data availability

All data are included within this manuscript and its Supplementary Files.

Funding

Supported by a Research Grant of the University Medical Center Giessen and Marburg (UKGM).

Author contributions

A.R.: conceptualization, methodology, acquisition, analysis, interpretation of data, original draft preparation, and visualization. D.R.: critical review and editing. T.L.: conceptualization, critical review, and editing. S.F.P.: conceptualization, critical review, editing, and supervision. All authors have read and agreed to the published version of the manuscript.

Conflict of interest statement

The authors declare no conflicts of interest.

References

1. Al-Goblan AS, Al-Alfi MA, Khan MZ. Mechanism linking diabetes mellitus and obesity. *Diabetes Metab Syndr Obes* 2014; **7**:587–91. doi:10.2147/DMSO.S67400.
2. Sinclair A, Saeedi P, Kaundal A *et al.* Diabetes and global ageing among 65–99-year-old adults: Findings from the International Diabetes Federation Diabetes Atlas. *Diabetes Res Clin Pract* 2020;**162**:108078.doi:10.1016/J.DIABRES.2020.108078.
3. Lee Y, Hirose H, Ohneda M *et al.* Beta-cell lipotoxicity in the pathogenesis of non-insulin-dependent diabetes mellitus of obese rats: impairment in adipocyte-beta-cell relationships. *Proc Natl Acad Sci USA* 1994;**91**:10878–82. doi:10.1073/PNAS.91.23.10878.
4. Li Z, Zhou Z, Hu L *et al.* ZLY032, the first-in-class dual FFA1/PPARδ agonist, improves glucolipid metabolism and alleviates hepatic fibrosis. *Pharmacol Res* 2020;**159**:105035.doi:10.1016/j.phrs.2020.105035.
5. Zakłos-Szyda M, Kowalska-Baron A, Pietrzyk N *et al.* Evaluation of *Viburnum opulus* l. Fruit phenolics cytoprotective potential on insulinoma min6 cells relevant for diabetes mellitus and obesity. *Antioxidants* 2020;**9**:433.doi:10.3390/antiox9050433.
6. Velasquez C, Vasquez JS, Balcazar N. In vitro effect of fatty acids identified in the plasma of obese adolescents on the function of pancreatic β-cells. *Diabetes Metab J* 2017;**41**:303–15. doi:10.4093/dmj.2017.41.4.303.
7. Tang Y, Plötz T, Gräler MH et al. Sphingosine-1 phosphate lyase regulates sensitivity of pancreatic beta-cells to lipotoxicity. *Int J Mol Sci* 2021;**22**:10893.doi:10.3390/IJMS221910893.
8. Kim M, Lee JS, Oh JE *et al.* SIRT3 overexpression attenuates palmitate-induced pancreatic β-cell dysfunction. *PLoS ONE* 2015;**10**:e0124744.doi:10.1371/journal.pone.0124744.
9. Ly LD, Ly DD, Nguyen NT *et al.* Mitochondrial Ca^{2+} uptake relieves palmitate-induced cytosolic Ca^{2+} overload in MIN6 cells. *Mol Cells* 2020;**43**:66–75. doi:10.14348/molcells.2019.0223.
10. Ishikawa M, Iwasaki Y, Yatoh S *et al.* Cholesterol accumulation and diabetes in pancreatic beta-cell-specific SREBP-2 transgenic mice: A new model for lipotoxicity. *J Lipid Res* 2008; **49**:2524–34. doi:10.1194/JLR.M800238-JLR200.
11. Hu M, Lin H, Yang L *et al.* Interleukin-22 restored mitochondrial damage and impaired glucose-stimulated insulin secretion through down-regulation of uncoupling protein-2 in INS-1 cells. *J Biochem* 2017;**161**:433–9. doi:10.1093/jb/mvw084.
12. Mazi TA, Borkowski K, Newman JW *et al.* Ethnicity-specific alterations of plasma and hepatic lipidomic profiles are related to high NAFLD rate and severity in Hispanic Americans, a pilot study. *Free Radic Biol Med* 2021;**172**:490–502. doi:10.1016/J.FREERADBIOMED.2021.06.024.

13. Chumakova G, Gritsenko O, Gruzdeva O *et al.* Analysis of probable lipotoxic damage and myocardial fibrosis in epicardial obesity. *Aging (Albany NY)* 2021;**13**:14806–15. doi:10.18632/aging.203148.
14. Barrios-Maya M, Ruiz-Ramírez A, Quezada H *et al.* Palmitoyl-CoA effect on cytochrome c release, a key process of apoptosis, from liver mitochondria of rat with sucrose diet-induced obesity. *Food Chem Toxicol* 2021;**154**:112351.doi:10.1016/J.FCT.2021.112351.
15. Römer A, Linn T, Petry SF. Lipotoxic impairment of mitochondrial function in β-cells: A review. *Antioxidants (Basel, Switzerland)* 2021;**10**:293.doi:10.3390/antiox10020293.
16. Quehenberger O, Armando AM, Brown AH *et al.* Lipidomics reveals a remarkable diversity of lipids in human plasma1. *J Lipid Res* 2010;**51**:3299–305. doi:10.1194/jlr.M009449.
17. Wehinger S, Ortiz R, Díaz MI *et al.* Phosphorylation of caveolin-1 on tyrosine-14 induced by ROS enhances palmitate-induced death of beta-pancreatic cells. *Biochim Biophys Acta* 2015;**1852**:693–708. doi:10.1016/j.bbadis.2014.12.021.
18. Hallare A, Nagel K, Köhler H et al. Comparative embryotoxicity and proteotoxicity of three carrier solvents to zebrafish (*Danio rerio*) embryos. *Ecotoxicol Environ Saf* 2006;**63**:378–88. doi:10.1016/J.ECOENV.2005.07.006.
19. Jover R, Ponsoda X, Castell JV et al. Evaluation of the cytotoxicity of ten chemicals on human cultured hepatocytes: Predictability of human toxicity and comparison with rodent cell culture systems. *Toxicol Vitr* 1992;**6**:47–52. doi:10.1016/0887-2333(92)90084-5.
20. van der Vusse GJ. Albumin as fatty acid transporter. *Drug Metab Pharmacokinet* 2009;**24**:300–7. doi:10.2133/DMPK.24.300.
21. Sankaranarayanan S, de la Llera-Moya M, Drazul-Schrader D *et al.* Serum albumin acts as a shuttle to enhance cholesterol efflux from cells. *J Lipid Res* 2013;**54**:671–6. doi:10.1194/JLR.M031336.
22. Zhou R, Perez-Aguilar JM, Meng Q *et al.* Opioid binding sites in human serum albumin. *Anesth Analg* 2012;**114**:122–8. doi:10.1213/ANE.0B013E318232E922.
23. Faure P, Troncy L, Lecomte M *et al.* Albumin antioxidant capacity is modified by methylglyoxal. *Diabetes Metab* 2005;**31**:169–77. doi:10.1016/S1262-3636(07)70183-0.
24. Fagyas M, Úri K, Siket IM *et al.* New perspectives in the renin–angiotensin–aldosterone system (RAAS) II: Albumin suppresses angiotensin converting enzyme (ACE) activity in human. *PLoS ONE* 2014;**9**:e87844.doi:10.1371/JOURNAL.PONE.0087844.
25. Saifer A, Goldman L. The free fatty acids bound to human serum albumin. *J Lipid Res* 1961;**2**:268–70. doi:10.1016/S0022-2275(20)39014-3.
26. Cnop M, Hannaert JC, Hoorens A *et al.* Inverse relationship between cytotoxicity of free fatty acids in pancreatic islet cells and cellular triglyceride accumulation. *Diabetes* 2001;**50**:1771–7. doi:10.2337/diabetes.50.8.1771.
27. Oliveira AF, Cunha DA, Ladriere L *et al.* In vitro use of free fatty acids bound to albumin: A comparison of protocols. *Biotechniques* 2015;**58**:228–33. doi:10.2144/000114285.
28. Funk D, Schrenk H-H, Frei E. Serum albumin leads to false-positive results in the XTT and the MTT assay. *Biotechniques* 2007;**43**:178–86. doi:10.2144/000112528.
29. Mosmann T. Rapid colorimetric assay for cellular growth and survival: Application to proliferation and cytotoxicity assays. *J Immunol Methods* 1983;**65**:55–63. doi:10.1016/0022-1759(83)90303-4.
30. Baltrusch S, Lenzen S. Novel insights into the regulation of the bound and diffusible glucokinase in MIN6 β-cells. *Diabetes* 2007;**56**:1305–15. doi:10.2337/db06-0894.
31. Bradford MM. A rapid and sensitive method for the quantitation of microgram quantities of protein utilizing the principle of protein-dye binding. *Anal Biochem* 1976;**72**:248–54. doi:10.1016/0003-2697(76)90527-3.
32. Lane BP, Miller SL. Preparation of large numbers of uniform tracheal organ cultures for long term studies. *In Vitro* 1976;**12**:147–54. doi:10.1007/BF02796363.
33. Keenan J, Doherty G, Clynes M. Separation of growth-stimulating activity of BSA fraction V from the bulk of albumin using heparin sepharose chromatography. *Cytotechnology* 1995;**19**:63–72. doi:10.1007/BF00749756.
34. Huang Z, Gengenbach T, Tian J *et al.* Effect of bovine serum albumin treatment on the aging and activity of antibodies in paper diagnostics. *Front Chem* 2018;**6**:161.doi:10.3389/fchem.2018.00161.
35. Zhao T, Xia Y, Li L *et al.* Bovine serum albumin promotes IL-1beta and TNF-alpha secretion by N9 microglial cells. *Neurol Sci* 2009;**30**:379–83. doi:10.1007/S10072-009-0123-X.
36. Panov A, Vavilin V, Lyakhovich V *et al.* Effect of bovine serum albumin on mitochondrial respiration in the brain and liver of mice and rats. *Bull Exp Biol Med* 2010;**149**:187–90. doi:10.1007/S10517-010-0904-5.
37. Ponte C, Oliveira C, Suarez-Kurtz G. Bovine serum albumin potentiates caffeine- or ATP-induced tension in human skinned skeletal muscle fibers. *Braz J Med Biol Res* 1997;**30**:675–8. doi:10.1590/S0100-879X1997000500017.
38. Boyer F, Diotel N, Girard D *et al.* Enhanced oxidative stress in adipose tissue from diabetic mice, possible contribution of glycated albumin. *Biochem Biophys Res Commun* 2016;**473**:154–60. doi:10.1016/J.BBRC.2016.03.068.
39. Wang W, Zhang D, Zhao H *et al.* Ghrelin inhibits cell apoptosis induced by lipotoxicity in pancreatic β-cell line. *Regul Pept* 2010;**161**:43–50. doi:10.1016/j.regpep.2009.12.017.
40. Gu J, Wei Q, Zheng H *et al.* Exendin-4 promotes survival of mouse pancreatic β-cell line in lipotoxic conditions, through the extracellular signal-related kinase 1/2 pathway. *J Diabetes Res* 2016;**2016**:5294025–8. doi:10.1155/2016/5294025.
41. Oberhauser L, Granziera S, Colom A *et al.* Palmitate and oleate modify membrane fluidity and kinase activities of INS-1E β-cells alongside altered metabolism-secretion coupling. *Biochim Biophys Acta Mol Cell Res* 2020;**1867**:118619.doi:10.1016/j.bbamcr.2019.118619.
42. Remizov O, Jakubov R, Düfer M *et al.* Palmitate-induced Ca^{2+}-signaling in pancreatic beta-cells. *Mol Cell Endocrinol* 2003;**212**:1–9. doi:10.1016/j.mce.2003.09.026.
43. Oropeza D, Jouvet N, Bouyakdan K *et al.* PGC-1 coactivators in β-cells regulate lipid metabolism and are essential for insulin secretion coupled to fatty acids. *Mol Metab* 2015;**4**:811–22. doi:10.1016/j.molmet.2015.08.001.
44. Ježek J, Dlasková A, Zelenka J *et al.* H_2O_2-activated mitochondrial phospholipase iPLA2γ prevents lipotoxic oxidative stress in synergy with UCP2, amplifies signaling via G-protein-coupled receptor GPR40, and regulates insulin secretion in pancreatic β-cells. *Antioxid Redox Signal* 2015;**23**:958–72. doi:10.1089/ars.2014.6195.
45. Green CD, Jump DB, Olson LK. Elevated insulin secretion from liver X receptor-activated pancreatic β-cells involves increased de novo lipid synthesis and triacylglyceride turnover. *Endocrinology* 2009;**150**:2637–45. doi:10.1210/en.2008-1039.
46. Hu HQ, Qiao JT, Liu FQ *et al.* The STING-IRF3 pathway is involved in lipotoxic injury of pancreatic β cells in type 2

diabetes. *Mol Cell Endocrinol* 2020;**518**:110890.doi:10.1016/j.mce.2020.110890.
47. Li F, Munsey TS, Sivaprasadarao A. TRPM2-mediated rise in mitochondrial Zn 2+ promotes palmitate-induced mitochondrial fission and pancreatic β-cell death in rodents. *Cell Death Differ* 2017;**24**:1999–2012. doi:10.1038/cdd.2017.118.
48. Laporte A, Lortz S, Schaal C *et al.* Hydrogen peroxide permeability of cellular membranes in insulin-producing cells. *Biochim Biophys Acta Biomembr* 2020;**1862**:183096.doi:10.1016/j.bbamem.2019.183096.
49. Levitt DG, Levitt MD. Human serum albumin homeostasis: A new look at the roles of synthesis, catabolism, renal and gastrointestinal excretion, and the clinical value of serum albumin measurements. *Int J Gen Med* 2016;**9**:229–55. doi:10.2147/IJGM.S102819.
50. Jun JE, Lee S-E, Lee Y-B *et al.* Increase in serum albumin concentration is associated with prediabetes development and progression to overt diabetes independently of metabolic syndrome. *PLoS ONE* 2017;**12**:e0176209.doi:10.1371/JOURNAL.PONE.0176209.
51. Spinella R, Sawhney R, Jalan R. Albumin in chronic liver disease: Structure, functions and therapeutic implications. *Hepatol Int* 2016;**10**:124–32. doi:10.1007/S12072-015-9665-6.

Preparation of fatty acid solutions exerts significant impact on experimental outcomes in cell culture models of lipotoxicity

Axel Römer, Divya Rawat, Thomas Linn, and Sebastian F. Petry

Preparation of fatty acid solutions

The following protocol describes the preparation of a 150 mM oleic acid (OA) stock solution dissolved in ethanol. OA will be complexed to bovine serum albumin (BSA) in Dulbecco's modified eagle's medium (DMEM) at a concentration of 2 mM. Aliquots can be diluted by factor 4 prior to utilization to receive the final fatty acid concentration of 0.5 mM. Molar FFA:BSA ratio is 5:1.

This protocol is also suitable to prepare stocks of 225 mM, 450 mM, and 900 mM for BSA-complexed aliquots of 3 mM, 6 mM, and 12 mM to achieve final concentrations of 0.75 mM, 1.5 mM, and 3 mM.

Dissolving fatty acids in ethanol

1. Calculate the desired amount of fatty acid and ethanol (absolute).
    - Preparation of 150 mM OA in ethanol requires 42.37 mg OA in 1000 µl of solution (MW_{OA} = 282.47 g/mol). By density of OA (ρ = 0.895 g/ml), this corresponds to 47.34 µl OA and 952.66 µl of ethanol are required.

      Note: Final fatty acid solution of 0.5 mM is achieved by 1:300 dilution. Therefore, final ethanol concentration will be 0.316 % w/w. This can be calculated by density of ethanol (ρ = 0.7893 g/ml). Mind the difference between % w/w, % w/v, and % v/v.

      Note: OA is liquid at room temperature and too viscid for precise pipetting. A scale is recommended to weigh 42.37 mg OA.
2. Remove fatty acid from fridge/freezer and prepare a beaker with small volume and a scale suitable for milligram.

3. Weigh the required amount of OA. Pipette the required volume of ethanol to the beaker.

   Note: Carefully consider the volatility of ethanol.

   Note: To avoid long-time storage it is recommended to prepare an aliquot adapted to the planned experiments.

4. Mix the solution with a pipette and transfer it into a tube suitable for freezing.

   Note: Stock solution can be used directly or stored at -20° C for several months. They should be protected by overlaying with nitrogen. Plastic tubes are not suitable for storing organic solvents.

<u>Complexing dissolved fatty acids with BSA</u>

5. Calculate the required amount of fatty acid free BSA. Molar ratio of FFA:BSA will be 5:1.

   0 mM control media will comprise equal amounts of both BSA and ethanol.

   - Preparation of 0.4 mM BSA requires 531.7 mg BSA in 20 ml of solution (MW_{BSA} = 66463 g/mol).

     Note: It is not recommended to complex fatty acids in high concentrations (> 30 mM) or to prepare big volumes at once (> 30 ml) due to viscosity of FFA and weak solubility of BSA in aqueous media.

     Note: Preparation of aliquots with 12 mM fatty acid and 2.4 mM BSA for a total volume of 20 ml is suitable with respect to the BSA and fatty acid characteristics.

6. Weigh 531.7 mg BSA in two 50 ml tubes each (fatty acid tube and control tube).
7. Add 19.73 ml of pre-warmed cell culture medium to the fatty acid tube and 19.67 ml to the control tube. Gently shake tubes for several minutes.
8. After most of BSA is dissolved add 266.67 µl of 150 mM OA stock solution to the fatty acid tube and 319.82 µl of ethanol to the control tube. Mix it with a pipette.
9. Cover tubes with nitrogen to protect from oxidation.
10. Place tubes on a platform rocker and let it shake overnight in an incubator at 37° C and 5 % CO_2.

11. Fatty acid and control medium will be sterile filtered (0.22 µm) into 15 ml tubes. Quality of media is enhanced if they are filled into tubes with less remaining oxygen.
12. Tubes can be stored at -20° C for several months. On the day of treatment fatty acid medium and control medium will be thawed in a water bath (37° C) and diluted with cell culture medium by factor 4 prior to application.

Table 1: Preparation of higher oleic acid stock concentrations in absolute ethanol. Required amount of oleic acid and volume of ethanol.

Stock concentration	Oleic acid	Ethanol
900 mM	254.22 mg	715.95 µl
450 mM	127.11 mg	857.98 µl
225 mM	63.56 mg	928.99 µl

Table 2: Preparation of BSA-complexed oleic acid or respective control group. Required amount of BSA and volume of cell culture medium, oleic acid stock (for fatty acid tube) or ethanol (for control tube).

Aliquot oleic acid concentration	Step 6	Fatty acid tube		Control tube	
		Step 7	Step 8	Step 7	Step 8
	BSA	Medium	Oleic acid (stock concentration)	Medium	Ethanol
12 mM	3190.22 mg	19.73 ml	266.67 µl (900 mM stock)	19.77 ml	233.02 µl
6 mM	1595.11 mg	19.73 ml	266.67 µl (450 mM stock)	19.72 ml	284.45 µl
3 mM	797.56 mg	19.73 ml	266.67 µl (225 mM stock)	19.69 ml	310.89 µl

PLOS ONE

RESEARCH ARTICLE

Differential expression of islet glutaredoxin 1 and 5 with high reactive oxygen species production in a mouse model of diabesity

Sebastian Friedrich Petry[1]*, Fatemeh Sharifpanah[2], Heinrich Sauer[2], Thomas Linn[1]

1 Clinical Research Unit, Center of Internal Medicine, Justus Liebig University, Giessen, Germany, **2** Department of Physiology, Faculty of Medicine, Justus Liebig University, Giessen, Germany

* sebastian.petry@innere.med.uni-giessen.de

Citation: Petry SF, Sharifpanah F, Sauer H, Linn T (2017) Differential expression of islet glutaredoxin 1 and 5 with high reactive oxygen species production in a mouse model of diabesity. PLoS ONE 12(5): e0176267. https://doi.org/10.1371/journal.pone.0176267

Editor: Massimo Pietropaolo, Baylor College of Medicine, UNITED STATES

Received: January 31, 2017

Accepted: April 7, 2017

Published: May 24, 2017

Data Availability Statement: All relevant data are within the paper and its Supporting Information files.

Funding: General funding from University of Giessen and Center of Internal Medicine granted to Clinical Research Unit were used for realization of this study. The funders had no role in study design, data collection and analysis, decision to publish, or preparation of the manuscript.

Competing interests: The authors have declared that no competing interests exist.

Abstract

The onset and progression of diabetes mellitus type 2 is highly contingent on the amount of functional beta-cell mass. An underlying cause of beta-cell decay in diabetes is oxidative stress, which markedly affects the insulin producing pancreatic cells due to their poor antioxidant defence capacity. Consequently, disturbances of cellular redox signaling have been implicated to play a major role in beta-cell loss in diabetes mellitus type 2. There is evidence suggesting that the glutaredoxin (Grx) system exerts a protective role for pancreatic islets, but the exact mechanisms have not yet been elucidated. In this study, a mouse model for diabetes mellitus type 2 was used to gain further insight into the significance of Grx for the islets of Langerhans in the diabetic metabolism. We have observed distinct differences in the expression levels of Grx in pancreatic islets between obese, diabetic db mice and lean, non-diabetic controls. This finding is the first report about a decrease of Grx expression levels in pancreatic islets of diabetic mice which was accompanied by declining insulin secretion, increase of reactive oxygen species (ROS) production level, and cell cycle alterations. These data demonstrate the essential role of the Grx system for the beta-cell during metabolic stress which may provide a new target for diabetes mellitus type 2 treatment.

Introduction

Diabetes mellitus type 2 is hallmarked by a progressive loss of functional beta-cell mass. As from the early prediabetic stages of the disease onwards, the Islets of Langerhans suffer the detrimental effects of hyperglycaemia, free fatty acids, and inflammation [1]. As stress levels exceed the beta-cell's coping capacity, insulin secretion fades [2, 3]. Furthermore, oxidative stress and impaired redox signaling play a pivotal role in beta-cell decay [4]. The redox regulation of cellular processes ensures cell viability and function [5]. A major actor in redox signaling and maintenance of redox balance is the glutaredoxin (Grx) system. It consists of NAPDH, glutathione, glutathione reductase and the oxidoreductase glutaredoxin. Its influence on cellular processes is based on reversible post-translational de-glutathionylation of their target's cysteine residues. In mammals, there are four glutaredoxins, characterized as mono- or dithiol

Grx depending on the number of redox-active cysteine-residuals in their active center. The dithiol Grx1 was originally found to reduce ribonucleotides and thus to ensure DNA synthesis in E. coli [6, 7]. It is mainly located in the cytoplasm, but was also reported in the intermembrane space of mitochondria and the nucleus [8, 9]. It is a major actor in the thiol-disulfide exchange and thereby involved in keeping cellular structures reduced and functional [10]. Grx1 has influence on cell differentiation [11] and regulates transcription factors, including NF-kappaB [12, 13]. NF-kappaB exerts an anti-apoptotic function in most cell types, whereas its role in the beta-cell is dependent on its activators. A protective effect against apoptosis induced by TNF-alpha is suggested [14]. Furthermore, researchers demonstrated that Grx1 promotes insulin secretion in MIN6 cells and isolated rat islets [15] while Grx1 knockout resulted in impaired insulin secretion [16]. The second dithiol, Grx2, forms iron-sulfur clusters which act as a redox sensor [17, 18]. As a regulatory mechanism of the redox state in the mitochondria [19] it has protective effects from apoptosis [20]. The monothiol Grx3 can form iron-sulfur clusters [21] as well and is necessary for haem synthesis [22]. It has protective and immunomodulatory effects, too [23, 24]. Grx5 was studied in yeast mutants lacking the enzyme. These featured increased susceptibility to oxidative and osmotic stress. Elevated ROS production, accumulation of iron and inactivation of enzymes requiring Fe-S clusters were noted [25, 26]. These affected enzymes are not only required for glucose processing and thereby insulin secretion, but iron accumulation is also known to induce secondary complications in diabetes [27]. Due to their diverse functions and their substrate specifity, alterations in glutaredoxin activity and expression can have massive impact on cellular pathways. Therefore, a key role in diabetes has been implicated [28]. The metabolically highly active beta-cell suffers from low antioxidant capacity. Several enzymes, including superoxide dismutase, catalase and glutathione peroxidase were shown to be expressed less in mouse islets in comparison to other tissues [29]. Oxidative stress disrupts the physiology of insulin secretion at several stages. GLUT2 (Glucose transporter 2) expression is reduced in rodent models for diabesity [30, 31] and mitochondrial dysfunction [32–34] was reported. Furthermore, oxidative modifications of ATP-sensitive potassium channels as well as hyperpolarization of the cell membrane conducted by ROS can both take influence on insulin secretion [35, 36]. Surprisingly, there are few data regarding glutaredoxins in the islets of diabetic mice. We hypothesized that they play a role in the challenged beta-cell during the onset and progression of diabetes mellitus type 2. Therefore, we screened islets of diabetic db/db mice in comparison to lean db/+ littermates. Homozygote db mice are marked by total leptin resistance due to a receptor mutation [37] and thus develop obesity and diabetes ("diabesity") [38]. We found lower expression of all four glutaredoxins in diabetic mice in comparison to lean controls. The effect was most pronounced for Grx1 and 5, which lead us to further investigate both redoxins. For the first time we detected distinguished differences in Grx expression in the islets of Langerhans in a mouse model for diabetes mellitus type 2 which could be correlated to insulin expression, cell cycle, and ROS production.

Materials and methods

Ethics statement

Animal research was approved by and conducted in accordance with institutional animal welfare officer, Chair of Animal Welfare of the Justus Liebig University Giessen, and Regional Administrative Council Giessen, Veterinary Department, under the code GI20/11-Nr.A18/2010. 3Rs were applied for reducing the number of required mice and reduce potential suffering, enrichment was applied to the IVC. Scoring was done daily. Mice were anaesthetized with ketamin / xylazin i.p. and bled to death by incision of the abdominal aorta before removing the

pancreas and other organs. The ARRIVE Guidelines Checklist (Animal Research: Reporting In Vivo Experiments) is available in the Supporting information section (S1 File).

Animal model

40 male BKS(D)-Leprdb/JOrlRj (db/db) mice and 40 BKS(D)-Leprdb/JOrlRj Témoin (db/+) control mice aged 5 weeks were bought from Charles River (Sulzfeld, Germany) and given one week to adapt to the animal facility. Number of required mice was calculated regarding manifestation rate of diabetes according to literature with type I error of 0.05 and type II error of 0.2. Animals were housed according to institutional guidelines (room temperature 22 ± 0.5˚C, 12 hours light / dark cycle, 60% humidity) with tap water and standard diet pellet food (Altromin, Lage, Germany) ad libitum in individually ventilated cages in groups of five mice. Mice were observed from 6 to 18 weeks of age. Blood glucose (Glucometer OneTouch Ultra 2, LifeScan, Neckargemünd, Germany) and body weight were measured weekly. Blood for glucose measurement was collected by puncturing the tip of the tail on conscious animals after overnight fasting. Pancreatectomy for IHC and islet isolation for qRT-PCR were done at 6, 12 and 18 weeks of age. In order to harvest pancreata mice were sedated by narcotic agent (1 ml Ketamine 10%, 0.8 ml Xylazine 2%, 8.2 ml NaCl 0.9%; 0.1 ml / 10 g body weight). Next, the abdominal wall was excised to expose the aorta which was cut to drain the blood before the organ was removed.

Islet isolation

Islets were isolated as described before by our department [39]. Briefly, the extracted pancreas was perfused with 4 mg / ml collagenase B (Roche, Mannheim, Germany) dissolved in 1% Hank's solution (Biochrom, Berlin, Germany) supplemented with 35 ml Hepes buffer (Biochrom, Berlin, Germany), 10 ml Ciprofloxacin, 10 ml Penicillin-Streptomycin, and 1 ml Gentamycin through the ductus pancreaticus. The perfused pancreas was mechanically chopped with scissors before 10 minutes of incubation in collagenase solution at 37˚C in a shaking water bath. After every 3 minutes of collagenase digestion the sample was vortexed for 10 seconds. The digested tissue was shaken by hand for two more minutes and the digestion process was eventually stopped by placing the tube containing the tissue on ice and adding cold Hank's solution. Following 3 minutes of centrifugation at 1500 rpm, the supernatant was discarded and the pellet was dissolved in 15% P/FCS dissolved in Medium 199 (Gibco, Karlsruhe, Germany) and fetal bovine serum (biowest, Nuaillé, France) at room temperature. The islets were hand-picked under stereomicroscope and incubated overnight at 37˚C to overcome the isolation stress.

Immunohistochemistry

IHC was used for detection of insulin (Dako, Hamburg, Germany), Grx1 (Santa Cruz Biotechnology, USA) and 5 (kindy provided by Prof. Lillig / Dr. Hanschmann as described in [40]), Ki-67 (Dako, Hamburg, Germany) as a marker for proliferation and activated caspase-3 (Cell Signaling, Frankfurt, Germany) as a marker for apoptosis. Pancreata were fixed with Zamboni (paraformaldehyde in picric acid and PBS as described in [41]) for four hours, then washed and stored in PBS supplemented with 18% sucrose solution overnight. Organs were embedded in cryoblock embedding medium (Biosystems, Nunningen, Switzerland) and frozen at -80˚C. Sectioning was done using Leica Crysostat CM1850 (Leica, Wetzlar, Germany). Slides were washed with PBS and blocked with 1% donkey serum dissolved in PBS containing 0.3% Triton X-100 (0.3% PBST) for 20 minutes. For Ki-67 staining, antigen retrieval was performed with NaOH 0.09 M for three minutes followed by another wash cycle. Sections were incubated with

primary antibodies diluted in 1% donkey serum dissolved in 0.3% PBST overnight at 4˚C. Secondary antibodies in 5% mouse serum were applied for one hour at room temperature. Nuclei were stained with Hoechst (Calbiochem, Darmstadt, Germany) in 0.1% TRIS buffer pH 7.6 and samples were preserved with ProLong Gold (Invitrogen, Karlsruhe, Germany). Pancreata were entirely sectioned. Sections were assessed for their quality, i.e. structurally damaged ones were not used. Two consecutive sections were regarded as one (results were divided by two for analysis). An interval of 140 μm was maintained between these pairs of slides which were included in the analysis in order to avoid multiple inclusion of islets. When islet area exceeded 140 μm in 12 weeks old db/db mice, double inclusion was carefully avoided by manual comparison of slides. 12 slides per pancreas, including 24 to 384 islets per organ, were observed. Total islet count included in the study was 2221 with 123 islets per mouse on average. Islet count was consistent with the number of islets isolated during islet isolation. Slides were prepared simultaneously in batches during immunohistology for appropriate comparability. For qualitative assessment of redoxin staining patterns in islets, immunostained slides were screened for islets. Images were taken, background staining was removed, and images were converted to gray scale for more effective and accurate comparison. Representative images were then selected manually.

Measurement of islet area and protein expression level

Size of islet area as well as protein expression level of Grx1, Grx5 and insulin were measured by using custom scripts for ImageJ (Wayne Rasband, National Institutes of Health, USA). Images were taken with Leica Application Suite v 3.8.0 using digital microscope camera DFC 420 C (Leica, Wetzlar, Germany) as described before [42]. Software was calibrated to match the images' scale and mean islet area was obtained. For analysis of protein expression level of insulin, Grx1 and 5, gray scaled pictures taken from a batch of simultaneously prepared stainings were normalized by removing background using slides without primary antibodies and calculating mean fluorescent intensity in islets. This resulted in mean grey values ranging from 0 (0%) to 255 (100%). In order to quantify redoxin staining area, the area stained by the antibody against the respective redoxin was set into relation with the area stained by insulin.

RNA isolation, cDNA synthesis and qRT-PCR

Extraction of RNA from harvested islets was done using RNeasy Plus Micro Kit (Qiagen, Düsseldorf, Germany). Total RNA concentration was determined by OD260 nm method using NanoDrop 1000 spectrophotometer (Thermo Scientific, Schwerte, Germany). cDNA was synthesised with SuperScript III Reverse Transcriptase kit (Invitrogen, Darmstadt, Germany). qRT-PR was carried out on Real-Time PCR System StepOnePlus (Applied Biosystems). Each PCR consisted of 10 min denaturation at 95˚C, followed by 40 cycles of denaturation (95˚C, 10 s) and annealing / extension (60˚C, 1 min). Primer concentration for qRT-PCR was 20 pM. Primer (Invitrogen, Darmstadt, Germany) sequences were as follows:

beta-actin (housekeeping):
fwd GTG GGA ATG GGT CAG AAG G, rev GAG GCA TAC AGG GAC AGC A;
INS1:
fwd TAT AAA GCT GGT GGG CAT CC, rev GGG ACC ACA AAG ATG CTG TT;
Grx1:
fwd GAG CAG TTG GAC GCG CTG G, rev CTC GCC ATT GAG GTA CAC TTG C;
Grx5:
fwd GAA GAA GGA CAA GGT GGT GGT CTT C, rev GCA TCT GCA GAA GAA TGT CAC AGC

Relative mRNA expression values were obtained by normalizing CT values of the target genes in comparison with CT values of the housekeeping gene using the delta-CT method.

Measurement of ROS production

Intracellular reactive oxygen species (ROS) production level in isolated islets were detected using 2',7'-dichlorofluorescein diacetate (DCFH-DA) indicator dye (Sigma, Munich, Germany). DCFH-DA is a non-fluorescent, cell-permeable compound which is cleaved by intracellular esterases to 2',7'-dichlorofluorescein (DCFH) and thereby trapped within cells. DCFH is membrane impermeable and a variety of intracellular ROS rapidly oxidize it to the highly fluorescent DCF (2',7'-dichloro-fluorescein) [43, 44]. Isolated islet cells of 24 weeks old animals were categorized in three different groups as untreated control, high glucose treated (20 mM for 2 hours) and TNF-alpha treated (1μM for 15 minutes). The above mentioned samples were incubated in serum-free medium containing 10μM DCFH-DA indicator dye dissolved in dimethylsulfoxide (DMSO) (Sigma, Munich, Germany). After 30 min incubation at 37˚C in the dark, samples were rinsed with pre-warmed serum-free medium and immediately analyzed with confocal laser scanning microscope. Intracellular DCF fluorescence (corrected for background fluorescence) was evaluated in 3600 μm^2 regions of interest using an overlay mask unless otherwise indicated. For fluorescence excitation, the 488 nm band of the argon ion laser of a confocal laser scanning microscope (Leica SP2 AOBS, Bensheim, Germany) was used. Emission was recorded using a longpass LP515 nm filter set. All islet cells per condition were photographed and fluorescence intensities were quantified with Leica Simulator software.

Statistical analysis

Statistical analysis was performed using Graph Pad Prism 5 (GraphPad Software, San Diego, USA) using Mann Whitney test and two-way Anova as appropriate. Data are given as mean values ± SEM, with n denoting the number of experiments unless otherwise indicated. A p-value < 0.05 was considered significant.

Results

A phenotype of diabesity in rodents

The leptin-resistant db mouse was employed for investigation of glutaredoxins in diabetes. It is known that homozygous db mice exhibit a distinct aspect of diabesity. Consecutively, a strong obese and diabetic phenotype was developed during the 12 weeks study period. Homozygous animals constantly showed a significantly higher body weight as well as fasting blood glucose during the observation period from 6 to 18 weeks of age ($p < 0.0001$). At the end of the observation period, homozygotes with 57 g on average were twice as heavy as heterozygotes with 26 g (Fig 1a). Their fasting blood glucose exceeded 200 mg/dl from 13 weeks of age onwards while heterozygotes showed no significant increase from 12 to 18 weeks of age (Fig 1b).

Pathohistomorphic changes with distinct morphology and high cell turnover

After having ensured a strong phenotype in the selected strain of db mice as well as the suitability of heterozygous animals as controls, the histology of their pancreatic islets was examined. Assessment of islet count during islet isolation revealed more islets in db/db animals at all time points ($p < 0.001$ at 6 weeks of age, $p < 0.05$ on average, data not shown). In both groups, lowest pancreatic islet count was observed at the age of 12 weeks. Morphological

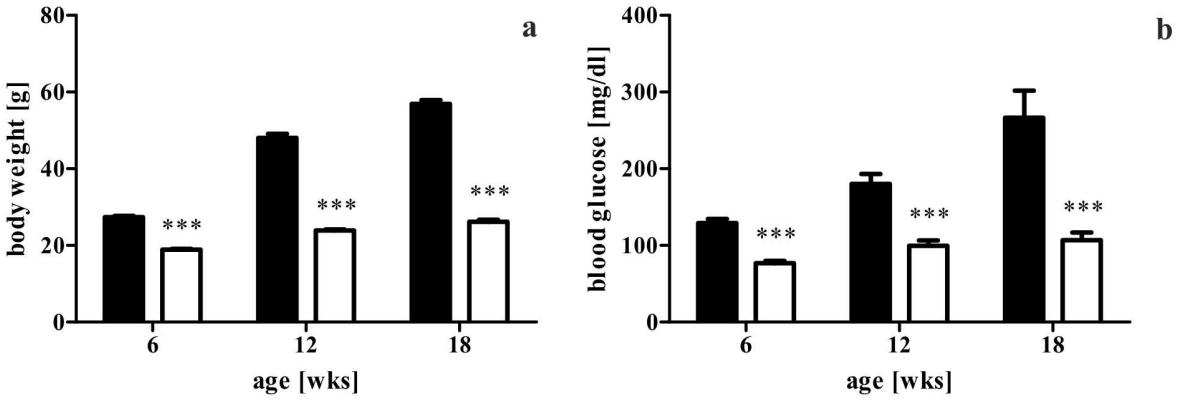

Fig 1. Body weight and fasting blood glucose level of db/db and db/+ mice. (a) Body weight of db/db and db/+ mice. (b) Fasting blood glucose levels of db/db and db/+ mice. Data depicted from 6, 12, and 18 weeks of age, corresponding to pancreatectomy. Values are mean ± SEM (n = 11-40 mice), black bars represent db/db mice, white bars represent db/+ mice, *** denotes $p < 0.0001$.

https://doi.org/10.1371/journal.pone.0176267.g001

studies by immunohistology exposed larger islets occuring together with fragmented small ones in homozygotes (Fig 2). At the age of 6 weeks islets of homozygotes were already enlarged but shaped normally (Fig 2a). Larger islets in 12 weeks old db/db mice resulted in vast islet formations (Fig 2f). As homozygotes grew older, small abnormally shaped islets increased in number (Fig 2k). Changes in islets of heterozygotes were more moderate (Fig 2b, 2g and 2l).

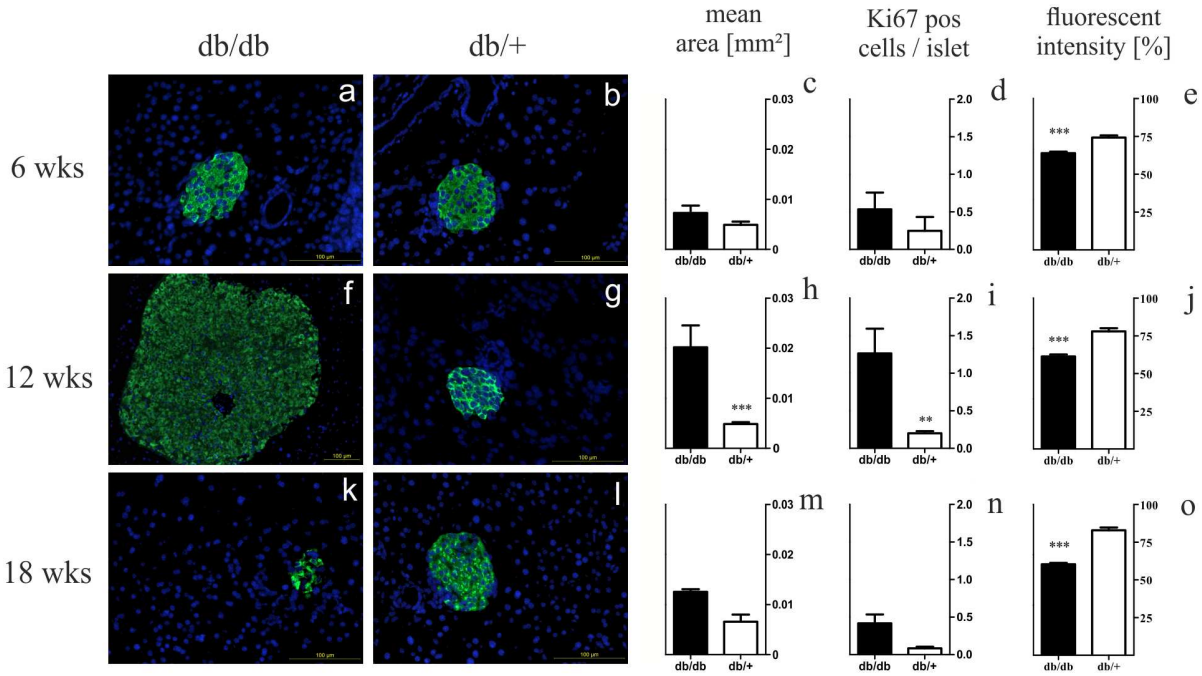

Fig 2. Morphology and quantification of area, proliferation rate, and fluorescent intensity of db/db and db/+ islets. (a, b, f, g, k, l) Representative images taken of immunostained islets at 6, 12 and 18 weeks are shown in comparison (green: insulin, blue: nuclei; bars indicate 100 μm^2). (c, h, m) Quantification of mean islet area as measured with ImageJ corresponding to insulin staining area. (d, i, n) Proliferation of islet cells analyzed by Ki-67 positive cells per islet. (e, j, o) Semiquantitative analysis of insulin staining. Black bars represent db/db mice, white bars represent db/+ mice, n = 3 mice, *** denotes $p < 0.001$, ** denotes $p < 0.005$.

https://doi.org/10.1371/journal.pone.0176267.g002

These findings were quantified by measuring islet area in immunostained slides. We found larger mean islet area in db/db animals at all time points with a maximum at 12 weeks ($p < 0.001$ at 12 weeks and $p < 0.005$ on average) (Fig 2c, 2h and 2m). On average, db/db mice had 2.5-fold larger islets. Respectively, islet proliferation was measured by counting of cells positive for Ki-67 staining. We found higher proliferation of db/db islets ($p < 0.005$ at 12 weeks and on average) (Fig 2d, 2i and 2n). Again, a peak was found at 12 weeks in homozygotes, while proliferation decreased in ageing animals of both groups. On average, homozygotes featured a four-fold higher proliferation rate. Slides were also stained against activated caspase-3 and analysed qualitatively. Apoptosis was higher in 6 and 12 weeks old homozygotes in comparison to heterozygotes (data not shown).

Receding insulin content in the islets of Langerhans

Both the phenotype of diabesity as well as the marked histological alterations in db/db mice were accompanied by a depletion of insulin content in islets, as our respective analysis revealed. This loss correlated to the extent of body weight and blood glucose levels of db/db animals. Quantification of insulin staining of immunohistology confirmed the impression of lower insulin content in db/db islets when compared to db/+ specimen ($p < 0.0001$) (Fig 2e, 2j and 2o). Regarding the genetic level, homozygotes showed a 70-fold drop in *INS1* expression from 6 to 18 weeks of age ($p < 0.0001$) (Fig 3a). In comparison to heterozygotes, *INS1* expression was twice as low at 6 and 12 weeks of age ($p < 0.05$) and 45-fold lower at 18 weeks ($p < 0.0001$). Heterozygote expression was declining less markedly.

Marked differences in islet redoxin expression

Our aim was to correlate the witnessed differences between obese, diabetic and lean, non-diabetic mice with changes in glutaredoxin expression. For screening, we assessed the pattern as well as fluorescent intensity of immunohistologically stained islets from 12 weeks old mice of both groups. This timepoint appeared most promising for the observed marked differences in shape, insulin content and proliferation detected in our previous analysis. We discovered visible differences with more dense and extense staining in db/+ animals for all four glutaredoxins, which were most pronounced for Grx1 and 5 (Fig 4).

Reduced glutaredoxin 1 and 5 levels in islets during diabesity

Based on the screening of glutaredoxins in islets, we carried out further analysis for Grx 1 and 5. Staining in db/db islets was more scarce and extended over a smaller area when compared to control islets. Furthermore, Grx5 staining patterns were more intense and more extensive than Grx1 patterns. Findings were confirmed by semiquantitative analysis of Grx fluorescent intensity as well as quantification of Grx to insulin staining ratio (Fig 5). Control islets featured higher Grx fluorescent intensity and Grx to insulin ratio for both redoxins and all time points. Grx5 was the redoxin with higher expression. To confirm the findings on the genome level, gene expression of *Grx1* and *5* was analysed by qRT-PCR in isolated islets. Corresponding to higher fluorescent intensity and area, heterozygotes showed higher gene expression ($p < 0.0001$ at 6 and 12 weeks) for *Grx1* at all time points (Fig 3b). In homozygote islets, a nadir was found at 12 weeks, while expression im heterozygote islets was stable. Analysis of *Grx5* expression revealed a significant decrease ($p < 0.0001$) in both db/db and db/+ animals with controls exhibiting higher expression at all time points ($p < 0.0001$ at 6 and 12 weeks) (Fig 3c). qRT-PCR revealed a markedly higher expression of *Grx5* when compared to *Grx1*.

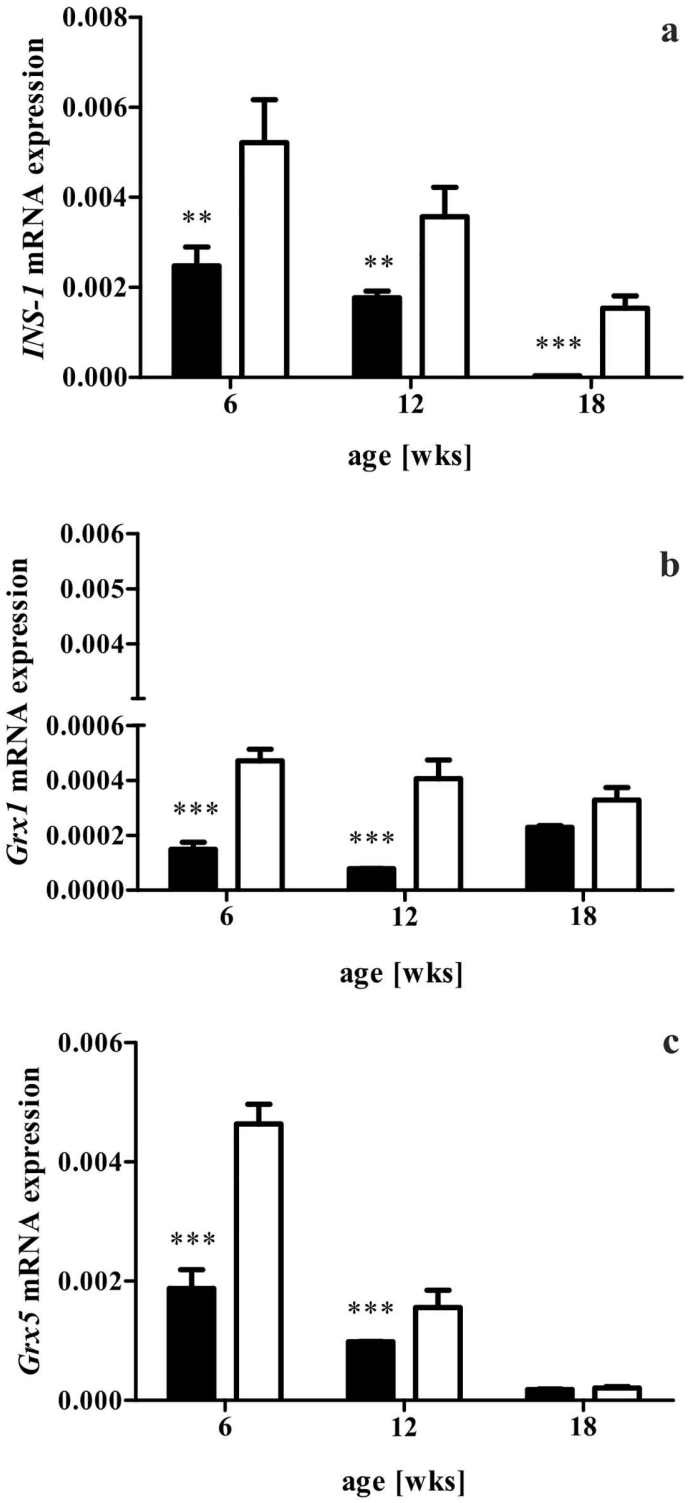

Fig 3. Gene expression of *INS1*, *Grx1*, and *Grx5* in db/db and db/+ islets. Gene expression was evaluated by qRT-PCR. (a) *INS1* expression declined in both groups of mice in relation to their age, but controls exhibited significantly higher expression levels at all time points. (b) *Grx1* expression was higher in db/+ mice at all time points. A slight decrease in controls was observed, while db/db animals featured a gap at 12 weeks of age. (c) *Grx5* expression decreased in both groups with age with higher levels in db/+ islets.

Values are mean ± SEM (n = 4—6 mice) and normalized with beta-actin, black bars represent db/db mice, white bars represent db/+ mice, *** denotes $p < 0.0001$, ** denotes $p < 0.005$.

https://doi.org/10.1371/journal.pone.0176267.g003

Enhanced ROS production in Grx-deficient islets

In order to further evaluate the significance of Grx-deficiency in mouse islets in diabetes, we analyzed ROS production level in isolated pancreatic islets using DCF staining. It was evaluated in untreated islets as well as islets pretreated with high glucose and TNF-alpha in order to stimulate hyperglycaemic and inflammatory stress as apparent during diabetes mellitus type 2. Isolated pancreatic islets from homozygous mice indicated higher ROS production level without any stimulation as well as upon treatment with either glucose or TNF-alpha compared to heterozygotes ($p < 0.0001$). Both groups showed an elevation in ROS content upon treatment with either glucose or TNF-alpha, but with a markedly higher level in db/db islets (Fig 6).

Discussion

The course of diabetes mellitus type 2 is highly dependent on the preservation of a healthy beta-cell mass and insulin secretion capacity, which both are notably impaired by oxidative stress and disturbed redox signaling [45]. It was previously shown that the Grx system has positive impact on insulin secretion [16, 46, 47]. Furthermore, tissue-specific expression of Grx was reported [48]. Plasmatic Grx activity differs between healthy subjects and patients suffering from diabetes mellitus type 2 [49]. Evidence for a protective role of the Grx system in the diabetic metabolism has arisen [50–54], but its exact significance for the beta-cell is still unknown. Thus, the aim of this study was to evaluate the relevance of the glutathione-dependent oxidoreductase system as a potential protection machinery in an in vitro model for diabetes mellitus type 2. A high level of oxidative phosphorylation is mandatory for the metabolically active beta-cell, especially when challenged by metabolic stress. As a result, mitochondrial ROS are considered a requirement for unimpaired insulin secretion [55, 56]. However, it is accepted that an abundance of ROS induces oxidative stress, exerts detrimental effects on cellular structures and proteins, and disturbs redox signaling. Accordingly, permanent excess of ROS is seen as noxious to insulin secretion [57]. Elevated ROS production in islets of

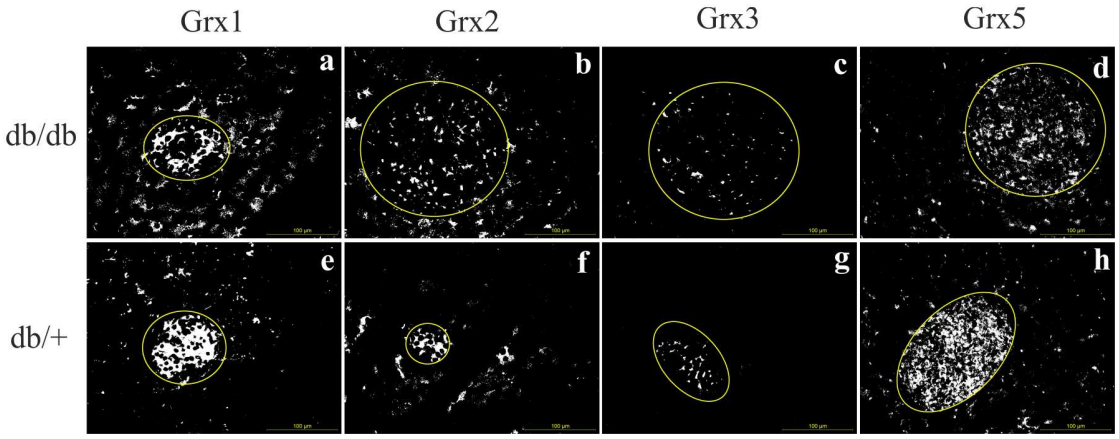

Fig 4. Qualitative comparison of the Grx system in db/db and db/+ islets. Representative monochrome pictures of Grx staining pattern captured of islets of 12 weeks old db/db and db/+ mice. (a, e) Grx1, (b, f) Grx2, (c, g) Grx3, (d, h) Grx5. Staining patterns suggested higher expression in db/+ mice. The difference was most pronounced for Grx1 and 5. 200x, yellow circles indicate islets, bars indicate 100 μm^2.

https://doi.org/10.1371/journal.pone.0176267.g004

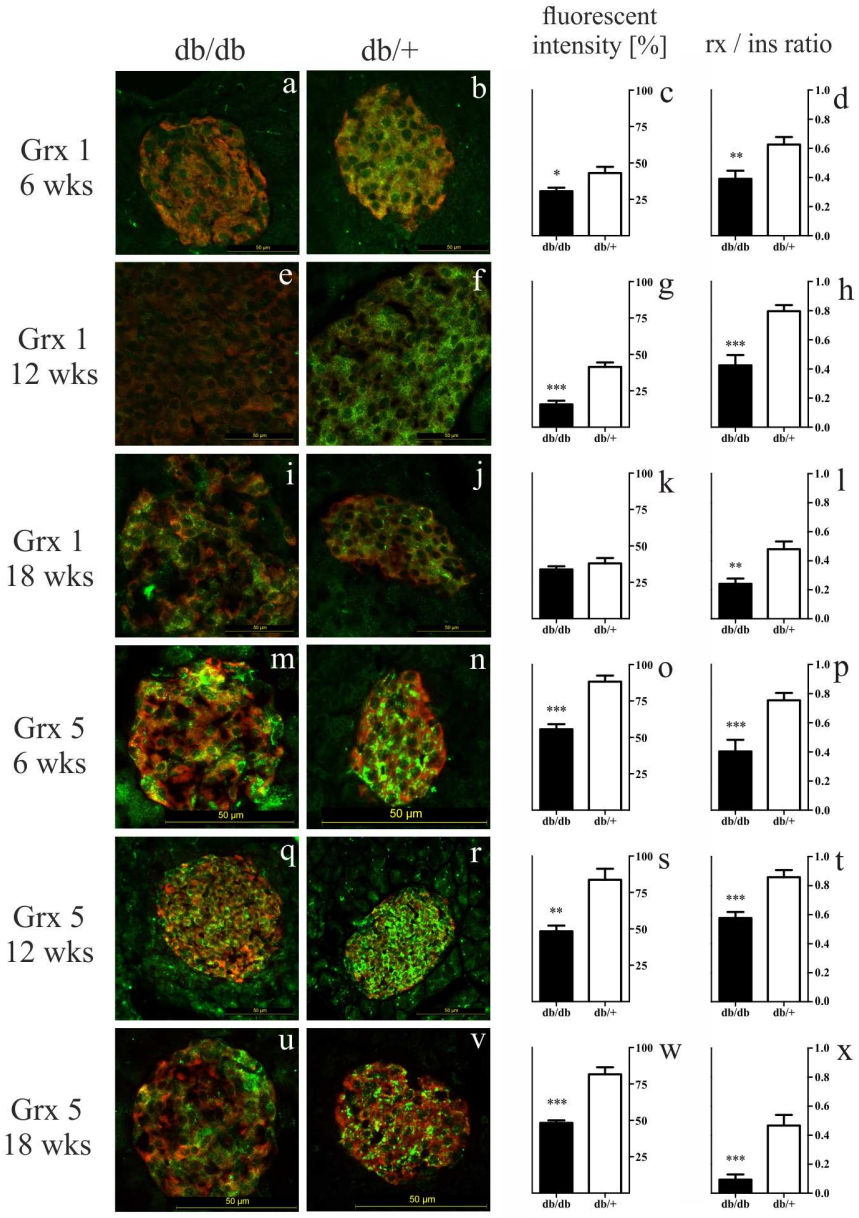

Fig 5. Representative images of Grx1 and 5 staining, quantification of Grx to insulin ratio, and fluorescent intensity of db/db and db/+ islets. (a, b, e, f, i, j, m, n, q, r, u, v) Representative images taken of immunostained islets at 6, 12 and 18 weeks are shown in comparison (green: Grx1 / 5, red: insulin, bars indicate 50 μm^2). (c, g, k, o, s, w) Semiquantitative analysis of Grx1 / 5 staining. (d, h, l, p, t, x) Quantification of Grx 1 / 5 to insulin staining ratio. Black bars represent db/db mice, white bars represent db/+ mice, n = 3 mice, *** denotes $p < 0.0001$, ** denotes $p < 0.005$, * denotes $p < 0.05$.

https://doi.org/10.1371/journal.pone.0176267.g005

diabetic rodents were confirmed by others [58], and overexpression of radical-scavenging enzymes resulted in protection of ROS-mediated induction of diabetes [59]. The beta-cell is especially prone to oxidative damage for its low expression of enzymes such as catalase and glutathione peroxidase, which are mainly involved in detoxification of H_2O_2 [29]. The glutaredoxin system has been proven to be expressed in mice islets [48] and may represent an

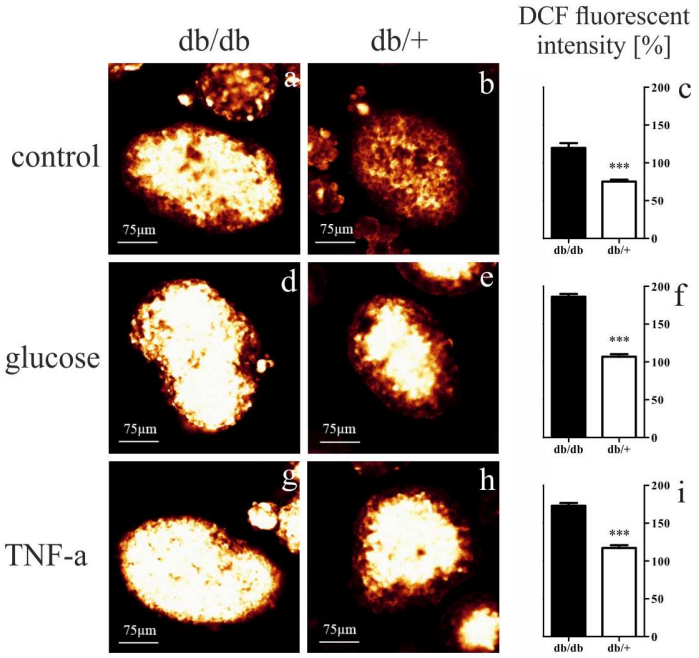

Fig 6. Representative images of ROS measurements and quantification in islets of db/db and db/+ mice. (a, b, d, e, g, h) Representative images show DCF stained pancreatic islets without any treatment as well as upon treatment with either glucose or TNF-alpha (bars represent 75 μm). (c, f, i) Quantification of DCT fluorescence intensity revealed significantly higher ROS production in db/db islets with a more pronounced rise after exposure to high glucose and TNF-alpha treatment in comparison to db/+ islets. Values are mean ± SEM (n = 54—139 islets), black bars represent db/db islets, white bars represent db/+ islets, *** denotes $p < 0.0001$.

https://doi.org/10.1371/journal.pone.0176267.g006

important alternative pathway in detoxification of ROS for the beta-cell. The four mammalian glutaredoxins are located in the major cellular compartments [8, 21, 26, 60] and are thereby involved in a broad range of functions. Thus, it is acknowledged that they feature varying expression patterns and activity when the beta-cell is challenged by metabolic stress. In the present study, we identified significant differences in Grx expression between diabese mice and lean controls for all four oxidoreductases, which were most pronounced for the mainly cytoplasmic Grx1 as well as the mitochondrial Grx5. Our data indicate that Grx1 expression correlated negatively with average size of pancreatic islets as well as proliferation rate, and positively with islet count in homozygotes. Grx1 protein and mRNA expression were elevated at 6 and 18 weeks when beta-cell turnover was at its minimum. At these time points homozygous mice featured high islet count and small islets with low proliferation rate. By contrast, we found reduced mRNA and protein expression of Grx1 at 12 weeks when islet count was low, but islets were large and showed elevated proliferation. Furthermore, a correlation was found between higher and stable expression in heterozygotes and less apoptosis of islet cells, elevated insulin expression and stable blood glucose levels when compared to homozygotes. These observations support the anti-apoptotic [61, 62] and pro-proliferative role [11] of Grx1. Grx1 is a major catalyst of post-translational modification of proteins via de-glutathionylation [61, 63], reversing detrimental glutathionylation by ROS. Among its targets are NF-kappaB, a key regulator of apoptosis [64], and PKC-alpha [65]. Previous studies suggest a positive impact of PKC-alpha on insulin secretion via maintenance of calcium channels [66, 67]. Further, Grx1 restores aldose reductase [68], an enzyme which is required for glucose processing if

hexokinase is saturated due to glucose overload. A recent study linked Grx to adenosine monophosphate-activated protein kinase (AMPK) activation and thereby stabilization of insulin secretion [54]. Consequently, Grx1 might support generation of new islets as well as growth of pre-existing islets, and further sustain islet metabolic activity in attempt to maintain glucose homeostasis and preserve insulin secretion capacity. In this study, Grx5 featured a significant reduction in both groups of mice, which was markedly more pronounced in db/db animals and correlated with fading insulin expression and rising blood glucose levels. The Grx5 enzyme is an important actor in composition of iron-sulfur clusters in the mitochondria [26]. Therefore, it is essential for a broad range of enzymes relying on these clusters, among which numerous have relevance for the respiratory chain [26]. Thus, the connection between Grx5 and oxidative phosphorylation might explain the co-occurrence of reduced insulin as well as Grx5 expression in this study. It has been reported that Grx5-deficiency increases the susceptibility to oxidative stress [25]. Furthermore, a lack of Grx5 enzyme was also correlated to cellular iron overload [69]. Iron is known to catalyze ROS production and thereby mediate apoptosis [70]. The link between metabolic stress and iron metabolism was shown in an in vivo model for diabetes mellitus type 2 with defective iron channels which featured stronger beta-cell viability [71]. Also, iron chelator treatment and dietary iron restriction had beneficial effects on glucose homeostasis in rodents [72]. Therefore, Grx5 might play a key role in maintaining mitochondrial functionality and prevent detrimental impact of iron accumulation. At the present time, the exact significance of reduced Grx1 and 5 levels in diabese db/db mice remains to be studied. Functional experiments will elucidate whether reduced redoxin levels are cause or result of impaired insulin secretion in islets of diabese animals. Regulators and effectors of islet redoxins have to be identified and modulation of redoxin expression should

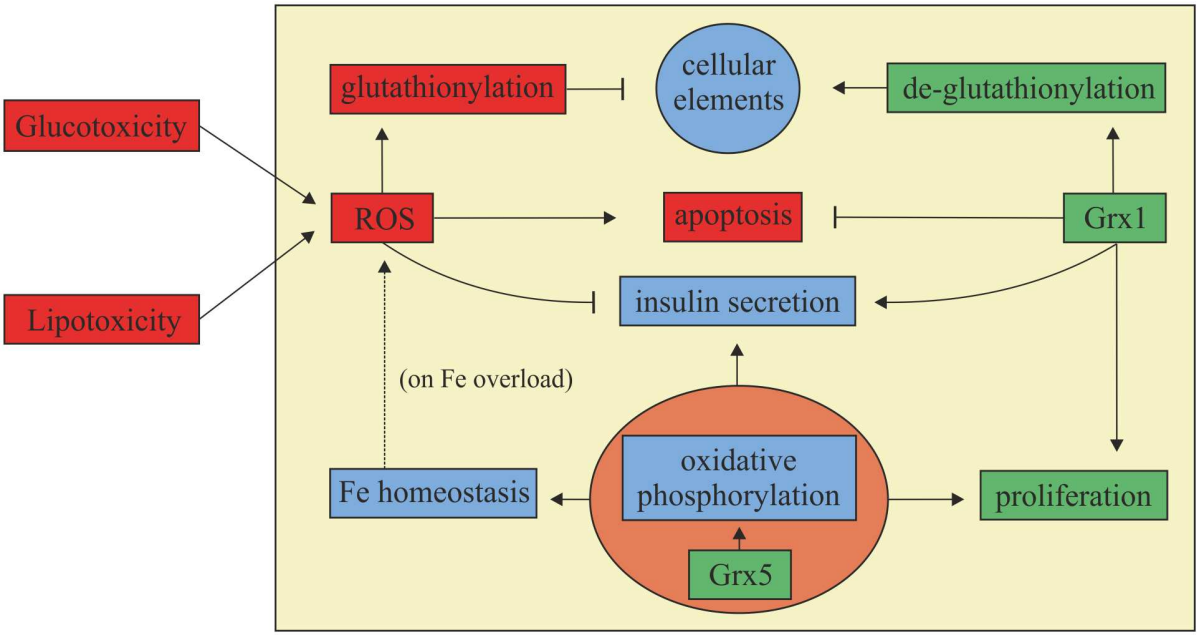

Fig 7. Summary. Both gluco- and lipotoxicity are extracellular promoters of ROS generation. ROS are harmful to cellular elements as they catalyze their glutathionylation. When the cell's antioxidant capacity is depleted, cell death occurs. Regarding the beta-cell, ROS impair insulin secretion. Grx1 and 5 wield protective properties. Grx1 is a major actor in de-glutathionylation, thereby reversing the harmful effects of ROS on its targets, exerting anti-apoptotic and pro-proliferative effects, and preserving insulin secretion. Grx5 has impact on the respiratory chain and cellular iron homeostasis by transferring iron-sulfur clusters to respective apoproteins. Hence, it supports cell viability and function, allows proliferation and counteracts iron accumulation which would promote ROS formation.

https://doi.org/10.1371/journal.pone.0176267.g007

be investigated regarding its influence on islet viability and metabolic activity. Further, immunohistological analysis in this study was limited by a low number of mice (n = 3). However, an appropriate amount of islets per animal was used for analysis and results were consistent among animals. Moreover, genome analysis via mRNA expression was carried out in 4 to 6 mice per timepoint and results were consistent with protein analysis.

Conclusion

In conclusion, our findings demonstrate a correlation between glutaredoxins and dysfunction of the islets of Langerhans in a mouse model for diabesity, which has not been described before. We propose that deficiency of Grx1 and 5 is connected to impaired insulin secretion and beta-cell decay in diabetes mellitus type 2. A summary of the obeserved correlations in reference to literature is given in Fig 7.

Supporting information

S1 File. The ARRIVE guidelines checklist. The ARRIVE Guidelines Checklist (Animal Research: Reporting In Vivo Experiments) was followed and is available.
(PDF)

Acknowledgments

Prof. Dr. Linn is the guarantor of this work and, as such, had full access to all of the data in the study and takes responsibility for the integrity of the data and the accuracy of the data analysis. The authors thank Gundula Hertl, Birte Hussmann, and Doris Erb for expert advice and technical assistance, as well as Prof. Dr. Sauer, Department of Physiology, Faculty of Medicine, Justus Liebig University, Giessen, Germany, for enabling us to measure ROS production in mouse islets in his facility. The authors thank Prof. Dr. Lillig, Department of Medical Biochemistry and Molecular Biology, Ernst-Moritz Arndt-University Greifswald, Germany, and Dr. Hanschmann, Department of Neurology, Heinrich Heine University Düsseldorf, Germany, for providing the antibody against Grx5.

Author Contributions

Conceptualization: TL.

Data curation: SFP.

Formal analysis: SFP FS.

Funding acquisition: TL.

Investigation: SFP FS.

Methodology: SFP FS HS TL.

Project administration: SFP TL.

Resources: HS TL.

Software: SFP.

Supervision: TL.

Validation: TL.

Visualization: SFP.

Writing – original draft: SFP.

Writing – review & editing: SFP FS TL.

References

1. Robertson RP, Harmon J, Tran PO, Tanaka Y, Takahashi H. Glucose toxicity in beta-cells: type 2 diabetes, good radicals gone bad, and the glutathione connection. Diabetes. 2003; 52(3):581–7. https://doi.org/10.2337/diabetes.52.3.581 PMID: 12606496
2. American Diabetes Association. Report of the Expert Committee on the Diagnosis and Classification of Diabetes Mellitus. Diabetes Care. 2003; 26:Suppl 1:S5–20. PMID: 12502614
3. DeFronzo RA. Pathogenesis of type 2 diabetes mellitus. Med Clin North Am. 2004; 88(4):787–835. https://doi.org/10.1016/j.mcna.2004.04.013 PMID: 15308380
4. Robertson RP, Harmon J, Tran PO, Poitout V. Beta-cell glucose toxicity, lipotoxicity, and chronic oxidative stress in type 2 diabetes. Diabetes. 2004; 53:Suppl 1:S119–24. https://doi.org/10.2337/diabetes.53.2007.S119 PMID: 14749276
5. Ullrich V, Kissner R. Redox signaling: bioinorganic chemistry at its best. J Inorg Biochem. 2006; 100 (12):2079–86. https://doi.org/10.1016/j.jinorgbio.2006.09.019 PMID: 17095095
6. Holmgren A. Hydrogen donor system for Escherichia coli ribonucleoside-diphosphate reductase dependent upon glutathione. Proc Natl Acad Sci U S A. 1976; 73(7):2275–9. https://doi.org/10.1073/pnas.73.7.2275 PMID: 7783
7. Holmgren A. Glutathione-dependent synthesis of deoxyribonucleotides. Purification and characterization of glutaredoxin from Escherichia coli. J Biol Chem. 1979; 254(9):3664–71. PMID: 372193
8. Lundberg M, Fernandes AP, Kumar S, Holmgren A. Cellular and plasma levels of human glutaredoxin 1 and 2 detected by sensitive ELISA systems. Biochem Biophys Res Commun. 2004; 319(3):801–9. https://doi.org/10.1016/j.bbrc.2004.04.199 PMID: 15184054
9. Pai HV, Starke DW, Lesnefsky EJ, Hoppel CL, Mieyal JJ. What is the functional significance of the unique location of glutaredoxin 1 (GRx1) in the intermembrane space of mitochondria? Antioxid Redox Signal. 2007; 9(11):2027–33. https://doi.org/10.1089/ars.2007.1642 PMID: 17845131
10. Holmgren A. Thioredoxin and glutaredoxin systems. J Biol Chem. 1989; 264(24):13963–6. PMID: 2668278
11. Takashima Y, Hirota K, Nakamura H, Nakamura T, Akiyama K, Cheng FS, et al. Differential expression of glutaredoxin and thioredoxin during monocytic differentiation. Immunol Lett. 1999; 68(2-3):397–401. https://doi.org/10.1016/S0165-2478(99)00087-5 PMID: 10424449
12. Hirota K, Matsui M, Murata M, Takashima Y, Cheng FS, Itoh T, et al. Nucleoredoxin, glutaredoxin, and thioredoxin differentially regulate NF-kappaB, AP-1, and CREB activation in HEK293 cells. Biochem Biophys Res Commun. 2000; 274(1):177–82. https://doi.org/10.1006/bbrc.2000.3106 PMID: 10903915
13. Daily D, Vlamis-Gardikas A, Offen D, Mittelman L, Melamed E, Holmgren A, et al. Glutaredoxin protects cerebellar granule neurons from dopamine-induced apoptosis by activating NF-kappa B via Ref-1. J Biol Chem. 2001; 276(2):1335–44. https://doi.org/10.1074/jbc.M008121200 PMID: 11035035
14. Kim S, Millet I, Kim HS, Kim JY, Han MS, Lee MK, et al. NF-kappa B prevents beta cell death and autoimmune diabetes in NOD mice. Proc Natl Acad Sci U S A. 2007; 104(6):1913–8. https://doi.org/10.1073/pnas.0610690104 PMID: 17267600
15. Ivarsson R, Quintens R, Dejonghe S, Tsukamoto K, in't Veld P, Renström E, et al. Redox control of exocytosis: regulatory role of NADPH, thioredoxin, and glutaredoxin. Diabetes. 2005; 54(7):2132–42. https://doi.org/10.2337/diabetes.54.7.2132 PMID: 15983215
16. Reinbothe TM, Ivarsson R, Li DQ, Niazi O, Jing X, Zhang E, et al. Glutaredoxin-1 mediates NADPH-dependent stimulation of calcium-dependent insulin secretion. J Mol Endocrinol. 2009; 23(6):893–900. https://doi.org/10.1210/me.2008-0306
17. Berndt C, Hudemann C, Hanschmann EM, Axelsson R, Holmgren A, Lillig CH. How does iron-sulfur cluster coordination regulate the activity of human glutaredoxin 2? Antioxid Redox Signal. 2007; 9 (1):151–7. PMID: 17115894
18. Lillig CH, Berndt C, Vergnolle O, Lönn ME, Hudemann C, Bill E, et al. Characterization of human glutaredoxin 2 as iron-sulfur protein: A possible role as redox sensor. Proc Natl Acad Sci U S A. 2005; 102 (23):8168–73. https://doi.org/10.1073/pnas.0500735102 PMID: 15917333
19. Beer SM, Taylor ER, Brown SE, Dahm CC, Costa NJ, Runswick MJ, et al. Glutaredoxin 2 catalyzes the reversible oxidation and glutathionylation of mitochondrial membrane thiol proteins: implications for mitochondrial redox regulation and antioxidant DEFENSE. J Biol Chem. 2004; 279(46):47939–51. https://doi.org/10.1074/jbc.M408011200 PMID: 15347644

20. Enoksson M, Fernandes AP, Prast S, Lillig CH, Holmgren A, Orrenius S. Overexpression of glutaredoxin 2 attenuates apoptosis by preventing cytochrome c release. Biochem Biophys Res Commun. 2005; 327(3):774–9. https://doi.org/10.1016/j.bbrc.2004.12.067 PMID: 15649413

21. Haunhorst P, Berndt C, Eitner S, Godoy JR, Lillig CH. Characterization of the human monothiol glutaredoxin 3 (PICOT) as iron-sulfur protein. Biochem Biophys Res Commun. 2010; 394(2):372–6. https://doi.org/10.1016/j.bbrc.2010.03.016 PMID: 20226171

22. Haunhorst P, Hanschmann E, Bräutigam L, Stehling O, Hoffmann B, Mühlenhoff U, et al. Crucial function of vertebrate glutaredoxin 3 (PICOT) in iron homeostasis and hemoglobin maturation. Mol Biol Cell. 2013; 24(12):1895–903. https://doi.org/10.1091/mbc.E12-09-0648 PMID: 23615448

23. Witte S, Villalba M, Bi K, Liu Y, Isakov N, Altman A. Inhibition of the c-Jun N-terminal kinase/AP-1 and NF-kappaB pathways by PICOT, a novel protein kinase C-interacting protein with a thioredoxin homology domain. J Biol Chem. 2000; 275(3):1902–9. https://doi.org/10.1074/jbc.275.3.1902 PMID: 10636891

24. Kato N, Motohashi S, Okada T, Ozawa T, Mashima K. PICOT, protein kinase C theta-interacting protein, is a novel regulator of FcepsilonRI-mediated mast cell activation. Cell Immunol. 2008; 251(1):62–7. https://doi.org/10.1016/j.cellimm.2008.04.005 PMID: 18479680

25. Rodríguez-Manzaneque MT, Ros J, Cabiscol E, Sorribas A, Herrero E. Grx5 glutaredoxin plays a central role in protection against protein oxidative damage in Saccharomyces cerevisiae. Mol Cell Biol. 1999; 19(12):8180–90. https://doi.org/10.1128/MCB.19.12.8180 PMID: 10567543

26. Rodríguez-Manzaneque MT, Tamarit J, Bellí G, Ros J, Herrero E. Grx5 is a mitochondrial glutaredoxin required for the activity of iron/sulfur enzymes. Mol Biol Cell. 2002; 13(4):1109–21. https://doi.org/10.1091/mbc.01-10-0517 PMID: 11950925

27. Ikeda Y, Enomoto H, Tajima S, Izawa-Ishizawa Y, Kihira Y, Ishizawa K, et al. Dietary iron restriction inhibits progression of diabetic nephropathy in db/db mice. Am J Physiol Renal Physiol. 2013; 304(7): F1028–36. https://doi.org/10.1152/ajprenal.00473.2012

28. Hanschmann EM, Godoy JR, Berndt C, Hudemann C, Lillig CH. Thioredoxins, glutaredoxins, and peroxiredoxins–molecular mechanisms and health significance: from cofactors to antioxidants to redox signaling. Antioxid Redox Signal. 2013; 19(13):1539–605. https://doi.org/10.1089/ars.2012.4599 PMID: 23397885

29. Lenzen S, Drinkgern J, Tiedge M. Low antioxidant enzyme gene expression in pancreatic islets compared with various other mouse tissues. Free Radic Biol Med. 1996; 20(3):463–6. https://doi.org/10.1016/0891-5849(96)02051-5 PMID: 8720919

30. Thorens B, Wu YJ, Leahy JL, Weir GC. The loss of GLUT2 expression by glucose-unresponsive beta cells of db/db mice is reversible and is induced by the diabetic environment. J Clin Invest. 1992; 90 (1):77–85. https://doi.org/10.1172/JCI115858 PMID: 1634622

31. Kluth O, Mirhashemi F, Scherneck S, Kaiser D, Kluge R, Neschen S, et al. Dissociation of lipotoxicity and glucotoxicity in a mouse model of obesity associated diabetes: role of forkhead box O1 (FOXO1) in glucose-induced beta cell failure. Diabetologia. 2011; 54(3):605–16. https://doi.org/10.1007/s00125-010-1973-8 PMID: 21107520

32. Anello M, Lupi R, Spampinato D, Piro S, Masini M, Boggi U, et al. Functional and morphological alterations of mitochondria in pancreatic beta cells from type 2 diabetic patients. Diabetologia. 2005; 48 (2):282–9. https://doi.org/10.1007/s00125-004-1627-9 PMID: 15654602

33. Tretter L, Adam-Vizi V. Inhibition of Krebs Cycle Enzymes by Hydrogen Peroxide: A Key Role of a-Ketoglutarate Dehydrogenase in Limiting NADH Production under Oxidative Stress. J Neurosci. 2000; 20 (24):8972–9. PMID: 11124972

34. Hasan NM, Longacre MJ, Stoker SW, Boonsaen T, Jitrapakdee S, Kendrick MA, et al. Impaired anaplerosis and insulin secretion in insulinoma cells caused by small interfering RNA-mediated suppression of pyruvate carboxylase. J Biol Chem. 2008; 283(42):28048–59. https://doi.org/10.1074/jbc.M804170200 PMID: 18697738

35. Islam MS, Berggren PO, Larsson O. Sulfhydryl oxidation induces rapid and reversible closure of the ATP-regulated K+ channel in the pancreatic beta-cell. FEBS Lett. 1993; 319(1-2):128–32. https://doi.org/10.1016/0014-5793(93)80051-U PMID: 8454044

36. Krippeit-Drews P, Lang F, Häussinger D, Drews G. H2O2 induced hyperpolarization of pancreatic B-cells. Pflugers Arch. 1994; 426(6):552–4. https://doi.org/10.1007/BF00378534 PMID: 8052526

37. Chen H, Charlat O, Tartaglia LA, Woolf EA, Weng X, Ellis SJ, et al. Evidence that the diabetes gene encodes the leptin receptor: identification of a mutation in the leptin receptor gene in db/db mice. Cell. 1996; 84(3):491–5. https://doi.org/10.1016/S0092-8674(00)81294-5 PMID: 8608603

38. Hummel KP, Dickie MM, Coleman DL. Diabetes, a new mutation in the mouse. Science. 1966; 153 (3740):1127–8. https://doi.org/10.1126/science.153.3740.1127 PMID: 5918576

39. Lai Y, Schneider D, Kidszun A, Hauck-Schmalenberger I, Breier G, Brandhorst D, et al. Vascular endothelial growth factor increases functional beta-cell mass by improvement of angiogenesis of isolated human and murine pancreatic islets. Transplantation. 2005; 79(11):1530–6. PMID: 15940042

40. Hanschmann EM. Thioredoxin family proteins in physiology and disease.; 2011. Dissertation.

41. Stefanini M, De Martino C, Zamboni L. Fixation of ejaculated spermatozoa for electron microscopy. Nature. 1967; 216(173–174).

42. Kilimnik G, Kim A, Jo J, Miller K, Hara M. Quantification of pancreatic islet distribution in situ in mice. Am J Physiol Endocrinol Metab. 2009; 297(6):E1331–E8. https://doi.org/10.1152/ajpendo.00479.2009 PMID: 19808908

43. Sauer H, Engel S, Milosevic N, Sharifpanah F, Wartenberg M. Activation of AMP-kinase by AICAR induces apoptosis of DU-145 prostate cancer cells through generation of reactive oxygen species and activation of c-Jun N-terminal kinase. Int J Oncol. 2012; 2(2):501–8.

44. Bolt HN, Hengstler JG, Stewart J. Analyses of reactive oxygen species. EXCLI J. 2009; 8:241–5.

45. Evans JL, Goldfine ID, Maddux BA, Grodsky GM. Oxidative stress and stress-activated signaling pathways: a unifying hypothesis of type 2 diabetes. Endocr Rev. 2002; 23(5):599–622. https://doi.org/10.1210/er.2001-0039 PMID: 12372842

46. Liu X, Han S, Yang Y, Kang J, Wu J. Glucose-induced glutathione reduction in mitochondria is involved in the first phase of pancreatic beta-cell insulin secretion. Biochem Biophys Res Commun. 2015; 464 (3):730–6. https://doi.org/10.1016/j.bbrc.2015.07.016 PMID: 26164230

47. Takahashi HK, Santos LR, Roma LP, Duprez J, Broca C, Wojtusciszyn A, et al. Acute nutrient regulation of the mitochondrial glutathione redox state in pancreatic beta-cells. Biochem J. 2014; 460(3):411–23. https://doi.org/10.1042/BJ20131361 PMID: 24678915

48. Godoy JR, Funke M, Ackermann W, Haunhorst P, Oesteritz S, Capani F, et al. Redox atlas of the mouse. Immunohistochemical detection of glutaredoxin-, peroxiredoxin-, and thioredoxin-family proteins in various tissues of the laboratory mouse. Biochim Biophys Acta. 2011; 1810(1):2–92. https://doi.org/10.1016/j.bbagen.2010.05.006 PMID: 20682242

49. Du Y, Zhang H, Montano S, Hegestam J, Ekberg NR, Holmgren A, et al. Plasma glutaredoxin activity in healthy subjects and patients with abnormal glucose levels or overt type 2 diabetes. Acta Diabetol. 2013; 9(2):225–32.

50. Shelton MD, Kern TS, Mieyal JJ. Glutaredoxin regulates nuclear factor kappa-B and intercellular adhesion molecule in Müller cells: model of diabetic retinopathy. J Biol Chem. 2007; 282(17):12467–74. https://doi.org/10.1074/jbc.M610863200 PMID: 17324929

51. Lekli I, Mukherjee S, Ray D, Gurusamy N, Kim YH, Tosaki A, et al. Functional recovery of diabetic mouse hearts by glutaredoxin-1 gene therapy: role of Akt-FoxO-signaling network. Gene Ther. 2010; 17(4):478–85. https://doi.org/10.1038/gt.2010.9 PMID: 20182516

52. Di Simplicio P, de Giorgio LA, Cardaioli E, Lecis R, Miceli M, Rossi R, et al. Glutathione, glutathione utilizing enzymes and thioltransferase in platelets of insulin-dependent diabetic patients: relation with platelet aggregation and with microangiopatic complications. Eur J Clin Invest. 1995; 25(9):665–9. https://doi.org/10.1111/j.1365-2362.1995.tb01983.x PMID: 7498240

53. Seghieri G, di Simplicio P, de Giorgio LA, Anichini R, Alberti L, Franconi F. Relationship between metabolic glycaemic control and platelet content of glutathione and its related enzymes, in insulin-dependent diabetes mellitus. Clin Chim Acta. 2000; 299(1-2):109–17. https://doi.org/10.1016/S0009-8981(00)00283-7 PMID: 10900297

54. Dong K, M W, Liu X, Huang Y, Zhang D, Wang Y, et al. Glutaredoxins concomitant with optimal ROS activate AMPK through S-glutathionylation to improve glucose metabolism in type 2 diabetes. Free Radic Biol Med. 2016; 101:334–47. https://doi.org/10.1016/j.freeradbiomed.2016.10.007 PMID: 27743883

55. Leloup C, Tourrel-Cuzin C, Magnan C, Karaca M, Castel J, Carneiro L, et al. Mitochondrial reactive oxygen species are obligatory signals for glucose-induced insulin secretion. Diabetes. 2009; 58(3):673–81. https://doi.org/10.2337/db07-1056 PMID: 19073765

56. Munhoz AC, Riva P, Simões D, Curi R, Carpinelli AR. Control of Insulin Secretion by Production of Reactive Oxygen Species: Study Performed in Pancreatic Islets from Fed and 48-Hour Fasted Wistar Rats. PLoS One. 2016; 11(6):e0158166. https://doi.org/10.1371/journal.pone.0158166 PMID: 27362938

57. Li N, Li B, Brun T, Deffert-Delbouille C, Mahiout Z, Daali Y, et al. NADPH oxidase NOX2 defines a new antagonistic role for reactive oxygen species and cAMP/PKA in the regulation of insulin secretion. Diabetes. 2012; 61(11):2842–50. https://doi.org/10.2337/db12-0009 PMID: 22933115

58. Bindokas VP, Kuznetsov A, Sreenan S, Polonsky KS, Roe MW, Philipson LH. Visualizing superoxide production in normal and diabetic rat islets of Langerhans. J Biol Chem. 2003; 278(11):9796–801. https://doi.org/10.1074/jbc.M206913200 PMID: 12514170

59. Kubisch HM, Wang J, Bray TM, Phillips JP. Targeted overexpression of Cu/Zn superoxide dismutase protects pancreatic beta-cells against oxidative stress. Diabetes. 1997; 46(10):1563–6. https://doi.org/10.2337/diabetes.46.10.1563 PMID: 9313750

60. Lundberg M, Johansson C, Chandra J, Enoksson M, Jacobsson G, Ljung J, et al. Cloning and expression of a novel human glutaredoxin (Grx2) with mitochondrial and nuclear isoforms. J Biol Chem. 2001; 276(28):26269–75. https://doi.org/10.1074/jbc.M011605200 PMID: 11297543

61. Chrestensen CA, Starke DW, Mieyal JJ. Acute cadmium exposure inactivates thioltransferase (Glutaredoxin), inhibits intracellular reduction of protein-glutathionyl-mixed disulfides, and initiates apoptosis. J Biol Chem. 2000; 275(34):26556–65. https://doi.org/10.1074/jbc.M004097200 PMID: 10854441

62. Murata H, Ihara Y, Nakamura H, Yodoi J, Sumikawa K, Kondo T. Glutaredoxin exerts an antiapoptotic effect by regulating the redox state of Akt. J Biol Chem. 2003; 278(50):50226–33. https://doi.org/10.1074/jbc.M310171200 PMID: 14522978

63. Gravina SA, Mieyal JJ. Thioltransferase is a specific glutathionyl mixed disulfide oxidoreductase. Biochemistry. 1993; 32(13):3368–76. https://doi.org/10.1021/bi00064a021 PMID: 8461300

64. Reynaert NL, van der Vliet A, Guala AS, McGovern T, Hristova M, Pantano C, et al. Dynamic redox control of NF-kappaB through glutaredoxin-regulated S-glutathionylation of inhibitory kappaB kinase beta. Proc Natl Acad Sci U S A. 2006; 103(35):13086–91. https://doi.org/10.1073/pnas.0603290103 PMID: 16916935

65. Ward NE, Stewart JR, Ioannides CG, O'Brian CA. Oxidant-induced S-glutathiolation inactivates protein kinase C-alpha (PKC-alpha): a potential mechanism of PKC isozyme regulation. Biochemistry. 2000; 39(33):10319–29. https://doi.org/10.1021/bi000781g PMID: 10956021

66. Warwar N, Efendic S, Ostenson CG, Haber EP, Cerasi E, Nesher R. Dynamics of glucose-induced localization of PKC isoenzymes in pancreatic beta-cells: diabetes-related changes in the GK rat. Diabetes. 2006; 55(3):590–9. https://doi.org/10.2337/diabetes.55.03.06.db05-0001 PMID: 16505220

67. Arkhammar P, Juntti-Berggren L, Larsson O, Welsh M, Nånberg E, Sjöholm A, et al. Protein kinase C modulates the insulin secretory process by maintaining a proper function of the beta-cell voltage-activated Ca2+ channels. J Biol Chem. 1994; 269(4):2743–9. PMID: 8300606

68. Wetzelberger K, Baba SP, Thirunavukkarasu M, Ho YS, Maulik N, Barski OA, et al. Postischemic deactivation of cardiac aldose reductase: role of glutathione S-transferase P and glutaredoxin in regeneration of reduced thiols from sulfenic acids. J Biol Chem. 2010; 285(34):26135–48. https://doi.org/10.1074/jbc.M110.146423 PMID: 20538586

69. Camaschella C, Campanella A, De Falco L, Boschetto L, Merlini R, Silvestri L, et al. The human counterpart of zebrafish shiraz shows sideroblastic-like microcytic anemia and iron overload. Blood. 2007; 110(4):1353–8. https://doi.org/10.1182/blood-2007-02-072520 PMID: 17485548

70. Dixon SJ, Stockwell BR. The role of iron and reactive oxygen species in cell death. Nat Chem Biol. 2014; 10(1):9–17. https://doi.org/10.1038/nchembio.1416 PMID: 24346035

71. Hansen JB, Tonnesen MF, Madsen AN, Hagedorn PH, Friberg J, Grunnet LG, et al. Divalent metal transporter 1 regulates iron-mediated ROS and pancreatic β cell fate in response to cytokines. Cell Metab. 2012; 16(4):449–61. https://doi.org/10.1016/j.cmet.2012.09.001 PMID: 23000401

72. Cooksey RC, Jones D, Gabrielsen S, Huang J, Simcox JA, Luo B, et al. Dietary iron restriction or iron chelation protects from diabetes and loss of beta-cell function in the obese (ob/ob lep-/-) mouse. Am J Physiol Endocrinol Metab. 2010; 298(6):E1236–43. https://doi.org/10.1152/ajpendo.00022.2010 PMID: 20354157

frontiers in Endocrinology

ORIGINAL RESEARCH
published: 12 March 2018
doi: 10.3389/fendo.2018.00084

Distinct Shift in Beta-Cell Glutaredoxin 5 Expression Is Mediated by Hypoxia and Lipotoxicity Both *In Vivo* and *In Vitro*

Sebastian Friedrich Petry, Lia Mingzhe Sun, Anna Knapp, Sabrina Reinl and Thomas Linn*

Clinical Research Unit, Center of Internal Medicine, Justus Liebig University, Giessen, Germany

Histomorphological and functional alterations in pancreatic islet composition directly correlate with hyperglycemia severity. Progressive deterioration of metabolic control in subjects suffering from type 2 diabetes is predominantly caused by impaired beta-cell functionality. The glutaredoxin system is supposed to wield protective properties for beta-cells. Therefore, we sought to identify a correlation between the structural changes observed in diabetic pancreatic islets with altered glutaredoxin 5 expression, in order to determine an underlying mechanism of beta-cell impairment. Islets of db/db mice presenting with uncontrolled diabetes were assessed in terms of morphological structure and insulin, glucagon, and glutaredoxin 5 expression. MIN6 cell function and glutaredoxin 5 expression were analyzed after exposure to oleic acid and hypoxia. Islets of diabese mice were marked by typical remodeling and distinct reduction of, and shifts, in localization of glutaredoxin 5-positive cells. These islets featured decreased glutaredoxin 5 as well as insulin and glucagon content. In beta-cell culture, glutaredoxin 5 protein and mRNA expression were decreased by hypoxia and oleic acid but not by leptin treatment. Our study demonstrates that glutaredoxin 5 expression patterns are distinctively altered in islets of rodents presenting with uncontrolled diabesity. *In vitro*, reduction of islet-cell glutaredoxin 5 expression was mediated by hypoxia and oleic acid. Thus, glutaredoxin 5-deficiency in islets during diabetes may be caused by lipotoxicity and hypoxia.

Keywords: diabetes mellitus type 2, glutaredoxin, islet remodeling, rodent diabesity, db mouse, MIN6, lipotoxicity, hypoxia

OPEN ACCESS

Edited by:
Åke Sjöholm,
Gävle Hospital, Sweden

Reviewed by:
Toshiro Arai,
Nippon Veterinary and Life Science University, Japan
Yukihiro Fujita,
Asahikawa Medical University, Japan
Matteo A. Russo,
IRCCS San Raffaele Pisana, Italy

****Correspondence:***
Sebastian Friedrich Petry
sebastian.petry@innere.med.uni-giessen.de

Specialty section:
This article was submitted to Diabetes, a section of the journal Frontiers in Endocrinology

Received: *12 December 2017*
Accepted: *22 February 2018*
Published: *12 March 2018*

Citation:
Petry SF, Sun LM, Knapp A, Reinl S and Linn T (2018) Distinct Shift in Beta-Cell Glutaredoxin 5 Expression Is Mediated by Hypoxia and Lipotoxicity Both In Vivo and In Vitro. Front. Endocrinol. 9:84. doi: 10.3389/fendo.2018.00084

1. INTRODUCTION

Type 2 diabetes mellitus is hallmarked by deprivation of the microarchitecture of pancreatic islets and progressive loss of beta-cells due to gluco- and lipotoxicity as well as a chronic state of inflammation (1). In particular, lipotoxicity, as mediated by free fatty acids, is a pivotal pathogenetic factor in type 2 diabetes as it induces pronounced insulin resistance (2) concomitant with significant impairment of insulin secretion (3). Free fatty acids mediate beta-cell death by induction of ER stress (4) and ROS production (5). During high metabolic activity, beta-cells further suffer from a hypoxia-like condition (6), which exhibits substantial damage to its secretory apparatus (7). However, the islets of Langerhans broadly express members of the glutaredoxin (Grx) system (8). These proteins are mainly involved in redox regulation of cellular processes and biogenesis of iron–sulfur proteins. Glutaredoxins (Grxs) are assumed to wield protective properties. Mammals express four Grxs

classified as mono- or dithiol Grx dependent on the number of cysteine residues in their active center.

Dithiol oxidoreductases Grx1 and 2 are major actors in thiol-disulfide exchange (9–11). They exercise control over their targets by reversible posttranslational de-glutathionylation of cysteine residues in dependence of glutathione reductase and glutathione. Monothiol Grx3 and 5 have no known catalytic activity. They are essential for biogenesis of proteins containing iron–sulfur clusters (12, 13). Mitochondrial Grx5 is directly involved in the composition of iron–sulfur clusters and thereby essential for mitochondrial, as well as cytosolic iron–sulfur proteins, which are essential for cell function (14). Grx5-deficiency results in elevated susceptibility to oxidative and osmotic stress together with cellular iron overload in yeast (14, 15). In zebra fish lacking Grx5, these pathologies occur together with anemia (16). The relevance of Grx5 for unimpaired heme biosynthesis and iron homeostasis is also apparent in human erythroblasts. An example of the effects of Grx5-deficiency was demonstrated in a patient suffering from defective homozygous GLRX5 mRNA-splicing. This patient presented a distinct phenotype including diabetes mellitus mediated by pancreatic iron overload, indicating the crucial role of Grx5 for unimpaired glucose metabolism (17).

Rodents feature a defined composition of the islets of Langerhans. Predominantly, islets consist of insulin-producing beta- and glucagon-producing alpha-cells. The vast majority of beta-cell mass is located in islet center, while alpha-cells are located in islet periphery, together with delta-, gamma- and epsilon cells (18, 19). In humans, cells are distributed randomly throughout islets (20). It is well accepted that disruption of physiological islet cell compositions occurs in diabetes and has remarkable functional impact (21, 22). Apart from apoptosis, beta-cell loss involves dedifferentiation (23–25) and autophagocytosis, where by the islets undergo remodeling (26, 27). However, the exact mechanisms underlying islet remodeling are not entirely understood and apart from documented expression of Grxs in the islets of Langerhans there is little knowledge about their significance for islet physiology. Despite alpha-cell dysfunction in diabetes mellitus being well known in human subjects and rodents (28, 29), there are no publications addressing Grx expression in glucagon-producing cells. However, data indicate that in contrast to beta-cells, alpha-cells are well-provided with antioxidant enzymes (30).

The aim of this study was to determine whether; (I) islets of db/db mice presenting with uncontrolled diabetes differ qualitatively and quantitatively from lean, leptin-susceptible wild types in terms of Grx5 expression, (II) changes in islet Grx5 protein pattern correlate with structural alterations and shifts in the cellular composition of the islets of Langerhans, (III) leptin action can be delineated from changes in glutaredoxin expression *in vitro*, and (IV) hypoxia and lipotoxicity have an effect on beta-cell Grx5 expression.

We report reduced Grx5 content in islets, loss of insulin content, and loss of glucagon content in pancreases of db/db mice presenting with uncontrolled diabesity in comparison to lean, non-diabetic C57BL/6 littermates. Islet Grx5 patterns were associated with a reduction of structural complexity of islets. We also describe novel data for a connection between Grx5 and beta-cell insulin secretion capacity *in vitro*. Changes in beta-cell Grx5 content were shown to be independent from leptin-resistance but were dependent on hypoxia and oleic acid in a dose-dependent manner. This is the first report of distinct histomorphological alterations of islet Grx5 expression patterns during uncontrolled rodent diabesity in context with altered islet composition and a possibly lipotoxicity-mediated loss of beta-cell Grx5 expression.

2. MATERIALS AND METHODS

2.1. Animal Model

15 male BKS(D)-Leprdb/JOrlRj (db/db) mice and 12 male C57BL/6NRj (C57) mice were acquired at the age of 10 weeks from Janvier Labs and were given 2 weeks to adapt to local animal facility. Number of required mice was calculated regarding manifestation rate of diabetes according to our previous study with type I error of 0.05 and type II error of 0.2. Housing conditions involved room temperature of 22 ± 0.5°C, 12 h light/dark cycle, 60% humidity, and tap water and standard diet pellet food (Altromin, Lage, Germany) *ad libitum* in individually ventilated cages in groups of five mice in accordance with institutional guidelines. Mice were sedated by isoflurane (5%). Thereafter, pancreas retrieval for histological studies was carried out at 12 or 13 weeks of age for db/db animals and 12 or 14 weeks of age for controls as diabetic animals were symptomatic and could thus not be kept for a prolonged period. Respective time points were pooled for both groups.

2.2. Histochemistry and Immunohistochemistry

Light microscopy was used for detection of insulin (Dako, Hamburg, Germany) and primary assessment of islet morphology. Organs were fixated with 3.5–3.7% formaldehyde, rinsed with 70% ethanol, and stored overnight. Embedding was carried out with paraffin after treatment in ascending alcohol series. Prior to staining, paraffin was removed using terpene (Roti-Histol, Roth, Karlsruhe, Germany) and descending alcohol series. Slides were washed with Tris and blocked with 1% goat serum for 20 min. Primary antibodies diluted in 1% goat serum dissolved in TBS containing 0.3% Triton X-100 (0.3% PBST) were applied overnight at 4°C. Secondary antibodies in 5% mouse serum were applied thereafter for 1 h at room temperature. Fuchsine red staining was used in order to visualize insulin. Staining progress was observed with light microscope and stopped after 1 min in Tris. Staining procedure was finished by counterstaining with hemalum–eosin 10% for 1 min (hemalum) and 5 min (eosin) before preservation and conservation with VectaMount (Vector Laboratories, Burlingame, CA, USA).

2.3. Immunofluorescence

Immunofluorescent staining was used for detection of insulin (Dako, Hamburg, Germany), Glucagon (Novus Biologicals, USA), and Grx5 (kindly provided and validated by Prof. Lillig/Dr. Hanschmann as described in Ref. (31)). Organs were stored overnight in PBS supplemented with 18% sucrose solution,

embedded in cryoblock embedding medium (Biosystems, Nunningen, Switzerland) and frozen at −80°C. Organs were sectioned using Leica Crysostat CM1850 (Leica, Wetzlar, Germany) in order to acquire slides of 7 µm thickness. Frozen tissue was fixated with Zamboni (paraformaldehyde in picric acid and PBS as described in Ref. (32)) for 15 min. Slides were washed with Tris-buffer and blocked with 1% donkey serum dissolved in 0.3% TBST for 20 min. Incubation with primary antibodies diluted in 1% donkey serum dissolved in 0.3% PBST took place overnight at 4°C. Secondary antibodies in 5% mouse serum were applied for 1 h at room temperature. Nuclei were stained with Hoechst (Calbiochem, Darmstadt, Germany) in 0.1% TRIS buffer pH 7.6 and samples were preserved with ProLong Gold (Invitrogen, Karlsruhe, Germany).

Extracted pancreases were sectioned entirely. Manual optical assessment for quality was employed, i.e., slides with damaged structure were rejected. Multiple inclusion of the same islets was avoided by maintaining an interval of 140 µm between slides used for analysis and by manual comparison of islets. Appropriate comparability of immunohistological staining was achieved by preparation in batches. Slides were screened entirely, all islets were included. Successful staining of target antigen and avoidance of extensive background staining was verified by comparison against samples prepared without the respective primary antibody.

2.4. Measurement of Islet Area and Quantification of Fluorescent Signals

Images were taken with Leica Application Suite v 3.8.0 using digital microscope camera DFC 420 C (Leica, Wetzlar, Germany). Analysis of islet area and quantification of fluorescent signal of insulin, glucagon, and Grx5 was employed using custom scripts for ImageJ (Wayne Rasband, National Institutes of Health, USA) as described before (33). Briefly, ImageJ was calibrated to match image scale. Single islets were optically selected. Exact islet area was identified using combined overlay images (staining of nuclei, insulin, and glucagon). Islet region was carefully tagged manually by use of freehand selection according to outline of insulin and glucagon staining and typical clusters of stained nuclei. Area of selection was measured, and ROI of identified islets were saved for following analysis.

Absolute area of insulin, glucagon, and Grx5 staining per islet was acquired by applying a threshold value to previously saved ROI. Threshold value was manually adapted to limit selection to staining of the respective antibody. Area of selection was measured and ROI were saved for analysis of fluorescent intensity. Relative area of the respective target antigen per islet was normalized to respective islet area to achieve better comparability between islets of different area. As third parameter of staining area quantification, absolute Grx5 area was set in relation to absolute insulin area for every islet to correlate islet Grx with insulin content.

Quantification of fluorescent intensity of insulin, glucagon, and Grx5 as quantification of respective protein content was obtained by measuring mean fluorescent intensity in the previously identified ROI for areas stained by respective antibodies. Therefore, images were normalized by removing background using slides without primary antibodies and converted to gray scale. Fluorescent intensity was measured in emitted fluorescence and given in mean gray values ranging from 0 (0%) to 255 (100%) and normalized against islet extent to achieve better comparability between islets of different area.

Number of Grx5-positive cells per islet was quantified by manually counting all nuclei per islet and identifying those presenting Grx5 staining. Results were given in percentage of cells displaying Grx5 fluorescence.

For each analysis mean of three individual runs was calculated to limit influence of manual selection of ROI and adaption of threshold values.

2.5. Cell Culture and Protein Analysis

Mouse insulinoma cells 6th subclone (MIN6 cells) cell line was obtained from Dr. Sigurd Lenzen (Institute of Clinical Biochemistry, Hannover Medical School, Hannover, Germany) (34) (originally from Dr. Miyazaki, Institute for Medical Genetics, Kumamoto University Medical School, Japan (35)) and cells were routinely maintained in Dulbecco's modified Eagle medium (DMEM, Life Technologies, Darmstadt, Germany) containing 25 mM glucose, supplemented with 10% fetal calf serum (biowest, Nuaillé, France), 2 mM L-glutamine, 25 mM Hepes (Biochrom, Berlin, Germany), 285 µM 2-mercaptoethanol (Life Technologies, Darmstadt, Germany), and 1% penicillin/streptomycin (Life Technologies, Darmstadt, Germany). Subculture and maintenance were performed as reported repeatedly in publications from our group (36, 37). MIN6 cells presented in this study were at passages 50-60. We compared earlier passage cells ($P < 30$) and they did not differ in normal glucose stimulated insulin secretion (GSIS) from $P > 30$ (data not shown). All assays used MIN6 cells grown to 70-80% confluence unless otherwise stated.

Cells were cultured at 37°C and 5% CO_2 and split by trypsinization. Washing was done with PBS before adding 0.5% Trypsin-EDTA (Gibco, Darmstadt, Germany) solution. Detachment was carried out by dilution with DMEM and centrifugation for 4 min at 1,200 RPM before seeding into new flasks.

For leptin cultivation, prior to analysis recombinant mouse leptin (R&D, Wiesbaden, Germany) was applied for 2 and 48 h, respectively. Leptin was pre-diluted to 0.1% in 20 mM Tris–HCl, pH 8.0. Concentrations of 0, 0.075, 0.45, and 2 ng/ml were applied. For fatty acid treatment, oleic acid was applied for 24 h under normoxic and hypoxic (2% O_2) atmosphere, respectively. Concentrations of 0, 0.5, and 0.75 mM were applied, respectively. Lysates and supernatant was collected for ELISA/PCR analysis.

Protein expression for insulin and Grx5 was measured in MIN6 cell lysates and supernatant. Prior to lysis, 1 ml supernatant was extracted before cells were washed in ice-cold PBS. Cells were incubated on ice for 20 min in NP-40 lysis buffer (United States Biological, Swampscott, USA). Supernatant was gathered by centrifugation for 20 min at 1,200 RPM. Insulin (DRG Instruments GmbH, Marburg, Germany) and Grx5 (CUSABIO Biotech, Wuhan, China) content was analyzed using ELISA technique. As Grx5 concentration exceeded largest measured standard (1,609.05 pg/ml) at 48 h leptin treatment, data were extrapolated. As absorbance in ELISA reached a plateau, it has to be noted that

Grx5 protein level at 2 ng/ml leptin treatment was omitted for analysis.

Cell viability was assessed by Vybrant MTT Cell Proliferation Assay Kit following manufacturer's instructions (Molecular Probes, Inc., Waltham, MA, USA).

2.6. RNA Isolation, cDNA Synthesis, and qRT-PCR

MIN6 cell RNA was extracted using RNeasy Plus Micro Kit (Qiagen, Düsseldorf, Germany). Total RNA concentration was determined by OD260 nm method using NanoDrop 1000 spectrophotometer (Thermo Scientific, Schwerte, Germany). SuperScript III Reverse Transcriptase kit (Invitrogen, Darmstadt, Germany) was employed to synthesize cDNA. qRT-PR was carried out on real-time PCR System StepOnePlus (Applied Biosystems). PCR included 615 s of activation/denaturation at 95°C and 40 cycles of annealing and elongation (95°C, 30 s each). Primer (Invitrogen, Darmstadt, Germany) concentration for qRT-PCR was 20 pM. Sequences were as follows:

beta-actin (housekeeping in leptin culture):
fwd CGT GAA AAG ATG ACC CAG ATC A, rev CAC AGC CTG GAT GGC TAC GT;
rpl32 (housekeeping in oleic acid culture):
fwd GGA GAA GGT TCA AGG GCC AG, rev GCG TTG GGA TTG GTG ACT CT;
Grx5:
fwd GAA GAA GGA CAA GGT GGT GGT CTT C, rev GCA TCT GCA GAA GAA TGT CAC AGC

Relative mRNA expression values were obtained by normalizing CT values of the target genes in comparison with CT values of the housekeeping gene using the delta-CT method.

2.7. Statistical Analysis

Statistical analysis was performed using Graph Pad Prism 5 (GraphPad Software, San Diego, CA, USA) using Mann–Whitney test and two-way ANOVA as appropriate. Data are given as mean values ± SEM, with n denoting the number of experiments unless otherwise indicated. A p-value < 0.05 was considered significant.

3. RESULTS

3.1. Uncontrolled Diabesity on the Genetic Background of the db Mutation

Obese homozygous leptin-resistant db/db mice were utilized for comparison with lean wild-type C57BL/6 animals as the db strain is typically presenting a strong phenotype of diabesity. Homozygotes featured uncontrolled diabetes mellitus with polyuria and weight loss exhibiting significantly ($p < 0.0001$) higher blood glucose levels than their lean, non-diabetic littermates. Mean blood glucose value was 471 mg/dl and thus 2.6-fold higher than in controls whose average blood glucose level was 179 mg/dl (**Figure 1A**). Furthermore, a distinct phenotype of rodent obesity was still apparent despite beginning weight loss in db animals. Average body weight was 52 g in db/db animals in comparison to 29 g in controls ($p < 0.0001$, **Figure 1B**).

3.2. Loss of Islet Structure and Elevated Islet Area in Rodent Diabesity

To relate the phenotype of uncontrolled diabetes to histomorphological alterations, islet structure was assessed histologically. Light microscopy was used as it allowed for easier discrimination between endocrine and exocrine tissue. Analysis revealed marked differences between islets of diabetic db/db mice and non-diabetic C57BL/6 controls. Pancreases of db animals contained two types of islets: small deformed ones with lost demarcation to exocrine tissue (**Figure 2A**) as well as a vast number of remarkably extensive islets (**Figure 2B**). In contrast, C57 islets were clearly defined from exocrine tissue and presented a notably lower variability of islet size (**Figure 2C**). The optical impression of elevated islet extent was confirmed by quantification of islet area using stained slides. Despite high variability, islets of db/db mice were significantly larger ($p < 0.05$) than C57 islets (**Figure 2D**), on average by 1.5-fold.

3.3. Shift in Islet Cell Composition As a Sign of Uncontrolled Diabetes

In line with the diabetic phenotype images acquired for morphological studies also revealed faint insulin appearance in db/db when compared to the intense staining of C57BL/6 islets (**Figures 3A–F**). To further evaluate cell-specific pathologies, immunofluorescence staining of insulin and glucagon was conducted. This allowed for individual assessment of islet beta- and alpha-cell areas per islet and estimation of islet insulin and glucagon content from the same section.

Analysis of immunostained slides indicated a shift in islet cell composition in db/db animals. Islets featured staining of alpha-cells in both the periphery and center with an overall increase in alpha-cell area as defined by positive staining of glucagon (**Figures 3A–C**). By contrast, C57 islets presented typical murine distribution patterns of peripheral alpha-cells (**Figures 3D–F**). Quantification of insulin and glucagon area per islet exposed a non-significant trend for higher absolute insulin area in

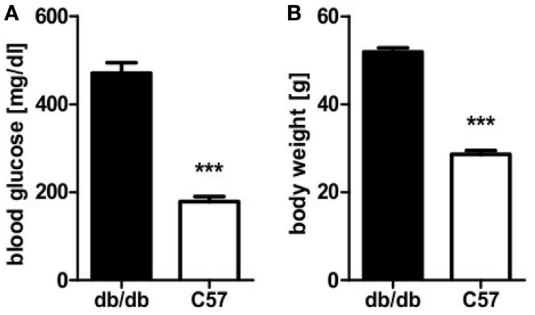

FIGURE 1 | Blood glucose level and body weight of db/db and C57BL/6 mice. **(A)** Blood glucose level of db/db and C57BL/6 mice. **(B)** Body weight of db/db and C57BL/6 mice. Values are mean ± SEM (n = 12–15 mice), black bars represent db/db mice, white bars represent C57BL/6 mice, *** denotes $p < 0.0001$.

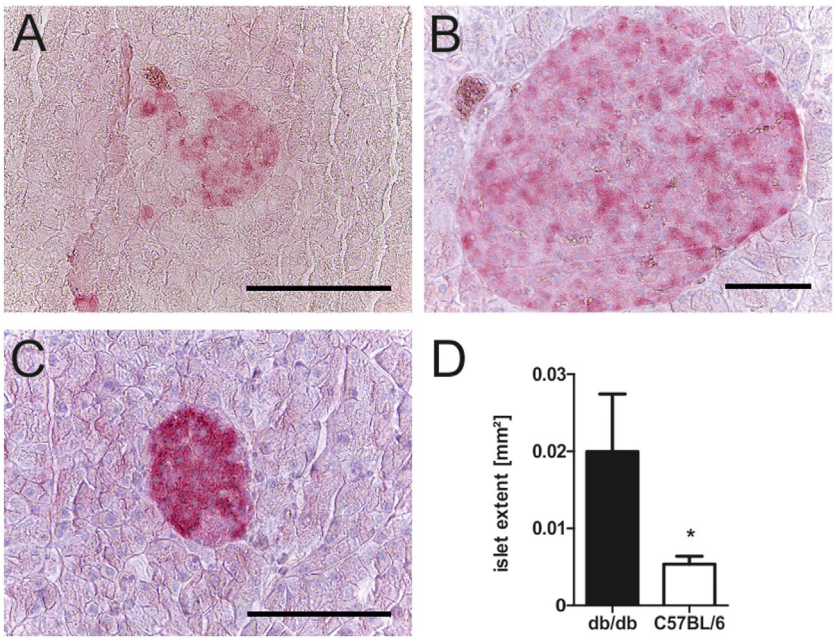

FIGURE 2 | Morphology and quantification of db/db and C57BL/6 islet extent. **(A–C)** Representative images taken of db/db and C57BL/6 islets using light microscopy in comparison: **(A)** typical small db islet with lost demarcation to exocrine issue, **(B)** example of extensive db islets, and **(C)** generic C57 islet (fuchsine red: insulin, bars indicate 50 µm). **(D)** Quantification of mean islet area as measured with ImageJ corresponding to islet extent. Black bars represent db/db mice, white bars represent C57BL/6 mice, n = 6 mice, * denotes $p < 0.05$.

non-diabetic wild-type mice (data not shown). However, relative insulin area normalized to islet extent demonstrated a significantly ($p < 0.005$) decreased value in db/db islets (**Figure 3G**). In contrast, absolute glucagon area in diabetic animals was significantly ($p < 0.05$) elevated (**Figure 3H**), while normalized glucagon area showed no significant difference between both strains of mice (data not shown). This shift in alpha- to beta-cell mass ratio in islets of diabetic mice was significant despite high variability in db/db islets ($p < 0.005$, **Figure 3I**).

Apart from this alteration of islet alpha- and beta-cell area, loss of staining intensity for insulin as well as glucagon was apparent. Quantitative analysis of fluorescent intensity was employed to assess islet insulin and glucagon content, confirming the optical impression of fainter staining in db/db islets with significantly lower fluorescent intensity for both proteins ($p < 0.005$ for insulin, $p < 0.05$ for glucagon, **Figures 3J,K**).

3.4. Distinct Grx5 Expression Patterns in Diabesity

In order to correlate the observed phenotypical and morphological differences between leptin-resistant, diabetic db/db animals and leptin-susceptible, non-diabetic controls with changes in expression of Grx5, we assessed islet Grx5 staining patterns in both strains of mice.

Both strains of mice featured global staining of islets cells with emphasis on nuclei as identified by comparing Grx5 and nucleus staining (**Figures 4A–H**). However, in db/db islets detection of Grx5-positive cells with nuclear staining was not as striking as in C57BL/6 islets. They exhibited a rather global and indistinct distribution of Grx5 with decreased intensity, and significantly ($p < 0.005$) lower Grx5-positive cell count. Quantification resulted in, on average, 25% Grx5-positive cells with nuclear staining in db/db islets and 49% in C57 islets (**Figure 4L**). In correspondence to generally enlarged islet size, diabetic mice were marked by significantly ($p < 0.05$) elevated Grx5 area (data not shown). When Grx5-positive cell area was normalized to islet extent this relation was reversed and a significant ($p < 0.05$) relative loss of Grx5 immunostaining was observed (**Figure 4I**). The differences in Grx5 expression between diabese and non-diabetic, lean controls could be further defined by quantification of Grx5 fluorescent intensity. Fluorescent intensity was significantly reduced in db/db islets, despite an increase in the area of positively stained cells, correlating with reduced islet Grx5 content (**Figure 4J**). The Grx5 to insulin content ratio was significantly ($p < 0.0001$) reduced in db/db islets (**Figure 4K**).

3.5. No Effect of Leptin on Grx5 Expression in Mouse Beta-Cells

Since the homozygous db mouse is an extreme example of total leptin resistance, our aim was to study whether leptin exposure to mouse beta-cells has influence on Grx expression. MIN6 cells were incubated with several concentrations of recombinant leptin for 2 and 48 h. As a control, MIN6 insulin content (**Figure 5A**) was measured in cell lysates and insulin secretion measured (**Figure 5B**) in supernatant. While insulin secretion declined significantly after 48 h of culture, no effect of leptin on insulin

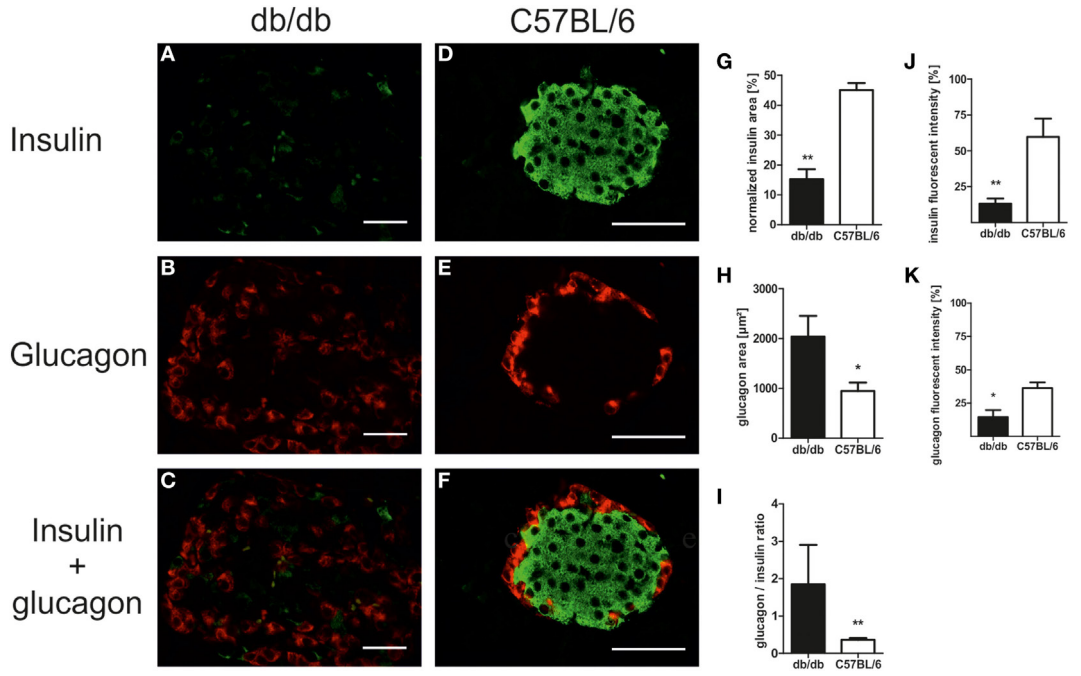

FIGURE 3 | Islet composition and insulin/glucagon content of db/db and C57BL/6 islets. **(A–F)** Representative images taken of immunostained db/db and C57BL/6 islets stained for insulin and glucagon (green: insulin, red: glucagon, bars indicate 50 µm). **(G,H)** Quantification of relative islet insulin and absolute glucagon area. **(I)** Quantification of islet glucagon/insulin area ratio. **(J,K)** Quantification of insulin and glucagon fluorescent intensity. Black bars represent db/db mice, white bars represent C57BL/6 mice, n = 6 mice, ** denotes $p < 0.005$, * denotes $p < 0.05$.

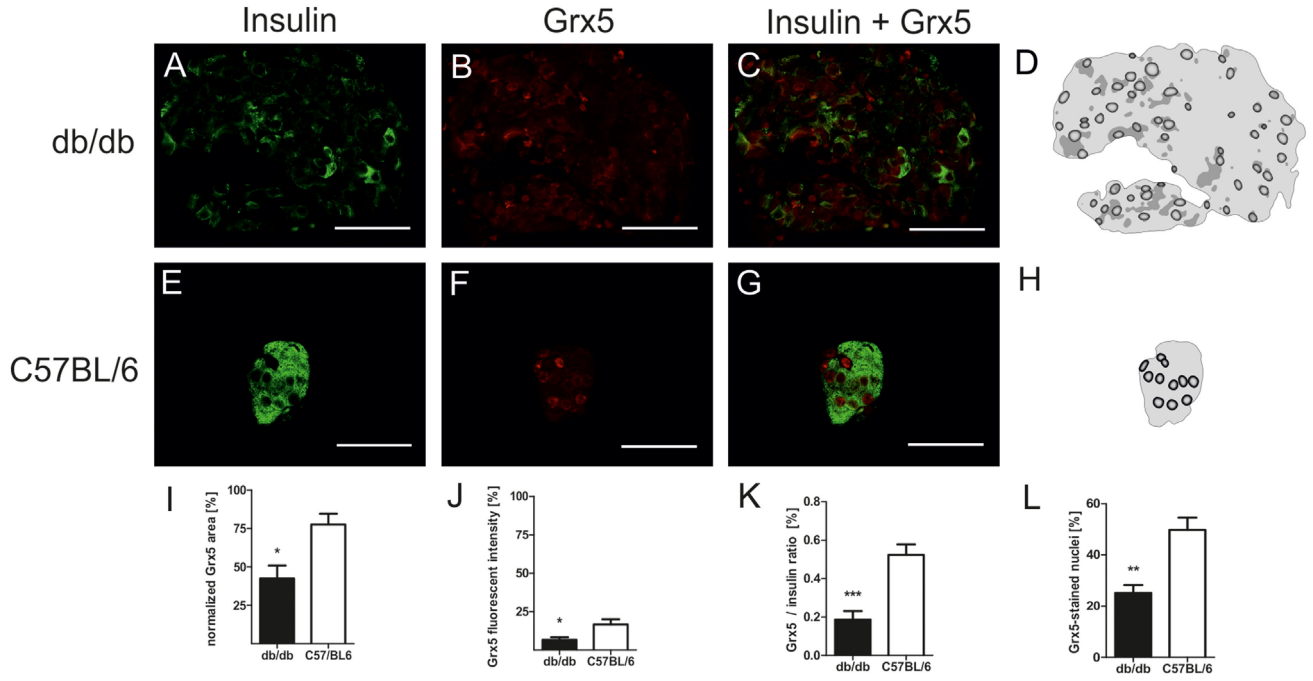

FIGURE 4 | Grx5 expression patterns in db/db and C57BL/6 mice and quantification of Grx5 area, fluorescent intensity, Grx5 to insulin ratio and nuclei staining. **(A–C,E–G)** Representative images taken of immunostained db/db and C57BL/6 islets stained for insulin and Grx5 (green: insulin, red: Grx5, bars indicate 50 µm). **(D,H)** Schematics of Grx5 staining in db/db and C57BL/6 islets (black: high intensity staining to white: no signal detected). **(I)** Quantification of islet Grx5 area normalized to islet extent. **(J)** Quantification of Grx5 fluorescent intensity. **(K)** Quantification of Grx5 to insulin ratio. **(L)** Quantification of nuclei stained for Grx5. Black bars represent db/db mice, white bars represent C57BL/6 mice, n = 6 mice, *** denotes $p < 0.0001$, ** denotes $p < 0.005$, * denotes $p < 0.05$.

secretion was detected. Grx5 protein and mRNA expression were studied in MIN6 cells exposed to leptin. Grx5 protein expression featured a time-dependent non-significant increase toward 48 h which was independent of leptin concentration (**Figure 5C**). *Grx5* mRNA expression decreased with time and was also not influenced by leptin (**Figure 5D**). Grx5 was not detected in cell supernatant (data not shown).

3.6. Beta-Cell Grx5 Expression Is Regulated by Hypoxia and Oleic Acid

Islet isolation of diabetic db/db mice presenting with uncontrolled diabesity for protein and mRNA analysis was not successful, due to the low yield of intact islets from db/db pancreases. Possible mechanisms behind deficiency of islet Grx5 content were, therefore, evaluated *in vitro*. MIN6 cells were exposed to oleic acid and hypoxia (2% O_2) for 24 h. MIN6 secretion as measured by insulin content in cell supernatant was significantly attenuated under hypoxic treatment ($p < 0.001$). Exposure to oleic acid resulted in a non-significant trend of reduced insulin secretion (**Figure 6A**). Hypoxia significantly ($p < 0.01$) reduced *INS2* mRNA expression, whereas treatment with oleic acid resulted in decreased expression; however, this was not significant (**Figure 6B**). Functional impairment of MIN6 cells upon hypoxic and oleic acid treatment was then correlated with Grx5 protein content and mRNA expression. In concordance with reduced insulin secretion and mRNA expression, MIN6 cells presented significantly reduced Grx5 protein content upon hypoxic ($p < 0.01$) and oleic acid ($p < 0.05$) incubation (**Figure 6C**). Both treatments attenuated *Grx5* mRNA expression; however, effects were not significant (data not shown). To exclude beta-cell decay as a mediator for secretory impairment and reduction of Grx5, an MTT assay was conducted. MIN6 cells maintained strong viability upon exposure to oleic acid for 24 h under normoxia (**Figure 6D**).

4. DISCUSSION

The glutaredoxin system has been repeatedly reported to exert protective effects on pancreatic beta-cells. In this study, we aimed to further elucidate these findings and evaluate a possible connection to histomorphological deviations of the islets of Langerhans occurring during uncontrolled diabesity as well as possible underlying mechanisms. Diabetic mice suffering from leptin-resistance on the db/db background were employed as a rodent model for diabetes mellitus type 2 and C57BL/6 wild-type animals without impairment of leptin signaling served as controls. As the utilized strain of db/db mice originates from a mixture of the C57BL/KsJ substrain and C57BL/6 wild-type mice (38, 39), they share a genetic background and thus provide a reasonable mouse model for our experimental setting.

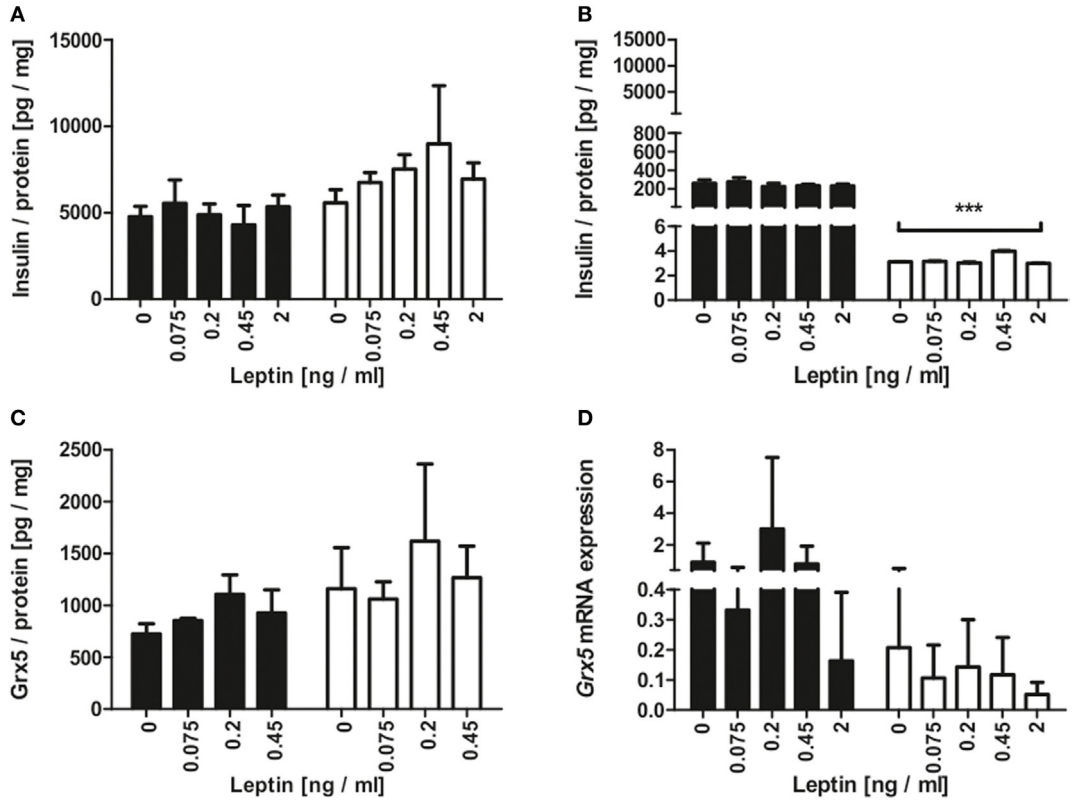

FIGURE 5 | Insulin and Grx5 protein expression and *Grx5* mRNA expression in MIN6 cells upon exposure to recombinant leptin for 2 and 48 h. **(A)** MIN6 lysate insulin content. **(B)** MIN6 supernatant insulin content. **(C)** MIN6 lysate Grx5 content. **(D)** MIN6 *Grx5* mRNA expression. Black bars represent 2 h, white bars represent 48 h. n = 9 runs, *** denotes $p < 0.001$.

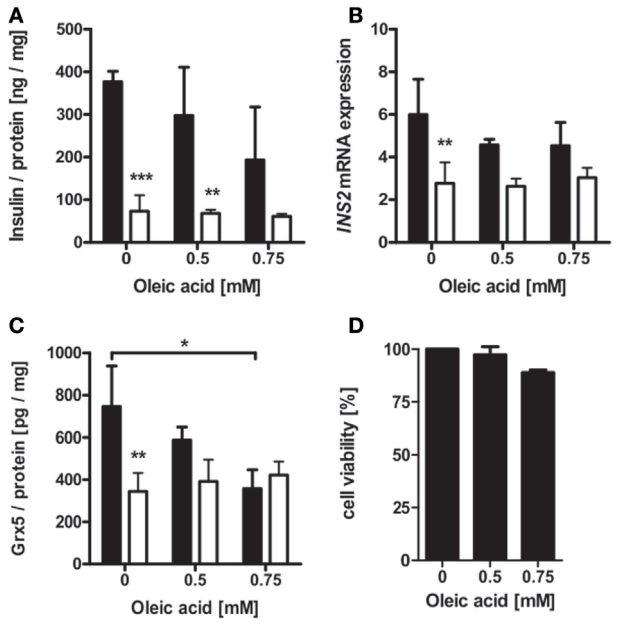

FIGURE 6 | Insulin and Grx5 protein and mRNA expression in MIN6 cells upon exposure to hypoxia (2% O_2) and oleic acid for 24 h. **(A)** MIN6 supernatant insulin content. **(B)** MIN6 *INS2* mRNA expression. **(C)** MIN6 lysate Grx5 content. **(D)** MIN6 MTT assay after 24 h of normoxic oleic acid treatment. Black bars represent normoxic atmosphere, white bars hypoxic atmosphere. n = minimum of 3 runs. *** denotes $p < 0.001$, ** denotes $p < 0.01$, * denotes $p < 0.05$.

A shift in islet cell composition associated with experimental diabetes is well documented (21, 22, 40, 41), but the underlying mechanisms are not fully understood. However, there is evidence that altered beta-cell functionality is profoundly involved in these histomorphological changes of the insulin-producing pancreatic micro organs. For instance, beta-cells were shown to express markers typically associated with endocrine progenitor cells in diabetes. Marked beta-cell plasticity was observed during progression of hyperglycemia as researchers reported beta-cell dedifferentiation into alpha-cells (23–25). Accordingly, beta-cells of hyperglycemic rodents including db/db mice feature loss of transcription factor Forkhead box protein O1 (FoxO1), an important regulator of beta-cell mass and stress response, which is accompanied by dedifferentiation into alpha-cells (23). Furthermore, levels of oxidative stress rise in pancreatic islets during diabetes (42). Oxidative stress is an acknowledged trigger of islet dysfunction (43) and maintenance of beta-cell differentiation is challenged by oxidative conditions (44). Islets of db/db mice typically present altered antioxidant enzyme expression, apart from Grxs (45), and modulation of oxidative stress markers (46) as well as increased ROS (33). Hypoxia has been described to occur in the beta-cells during high metabolic activity due to immensely high levels of oxidative phosphorylation (6, 7). As a result, a HIF-mediated hypoxic stress response is triggered (6) and apoptosis (6), upregulation of NF-κB, and oxidative stress (36) occur. Beta-cells are exceptionally vulnerable to hypoxia. In consequence, db/db islets present a marked increase in HIF and HIF target gene transcription (47) as well as NF-κB-mediated apoptosis (37). Free fatty acids have been reported to interfere significantly with beta-cell turnover (48) and induce functional and structural aberration of islets (49). These data indicate that the observed shift in islet cell composition is directly linked to impaired islet functionality mediated by gluco-/lipotoxicity and hypoxia. As a result, islets of db/db mice present pronounced structural deviations marked by a considerable amount of degranulated, i.e., endocrine inactive, beta-cells (50). Interestingly, Grxs are involved in regulation of oxidative stress, HIF (51) as well as NF-κB (52, 53). Beneficial effects of the Grx system on insulin secretion (54–56), as well as its impact on key enzymes of glucose metabolism (57–59), have been described. However, their role in pancreatic beta-cell function remains vague.

In the present histomorphological study, we identified distinct staining patterns of Grx5 with notable differences in expression between diabese mice and lean controls. Main features of Grx5 staining involved rarefication and loss of staining area as well as fluorescent intensity and Grx5 to insulin ratio in islets of diabetic mice. Strikingly, Grx5 presented a distinct staining of nuclei, which was mostly lost in diabetic islets. While Grx5 is an acknowledged mitochondrial glutaredoxin in yeast (14), it has been detected in rodent nuclei (8). However, the significance of this finding has yet to be elucidated. Grx5 is so far not known to exhibit catalytical activity, but Grx5-deficiency increases the susceptibility to oxidative stress (15) and correlates with cellular iron overload (17). These findings might account for Grx5 loss upon extensive metabolic stress; however, the observed loss of nucleic localization requires further study.

The homozygous db mice used in this study are hallmarked by complete leptin resistance (60) and thus exhibit a severe phenotype of diabesity (61). Adipokines and adipose-derived hormones are acknowledged mediators of inflammation, glucose and lipid metabolism, and energy balance (62). Leptin is an extensively studied hormone deriving from white adipose tissue (63). It is a key regulator of energy homeostasis (64) and exerts regulatory control on glucose metabolism and on the beta-cell itself in the so-called adipo-insular feedback loop. Leptin inhibits insulin secretion (65) and gene expression (66). In contrast, insulin increases leptin secretion (67) and gene expression (68). Expression of leptin correlates with fat mass leading to elevated levels in obese subjects (69, 70) as well as rodents (71). Homozygous db mice present complete leptin resistance. Therefore, influence of leptin excess on db/db islet Grx expression is highly unlikely. Our experimental setting was unable to deduce effects of leptin on insulin secretion or on Grx5 expression. In rodents, leptin plasma levels ranging from below 0.5 (72) up to 4,000 ng/ml (73) have been described. We deliberately chose leptin concentrations in a low physiological range to assess physiological influence on Grx5. Significant alterations of MIN6 insulin content and secretion occurred over time, as expected. While this poses a contradiction toward the adipo-insular axis, there are several differing reports in the current body of literature. Highly contingent on experimental settings and leptin dosage, studies reported no stimulation (74), stimulatory (75), and dose-dependent U-shaped responses in beta-cell lines, perfused pancreases, and isolated islets (76–78).

Interestingly, beta-cell Grx5 protein level correlated with insulin content. A non-significant decrease in *Grx5* mRNA occurred over time, which we interpreted as a sign of sufficient Grx5 protein levels in beta-cells under physiological conditions in contrast to fading expression in islets of diabese animals. To elucidate a possible mechanism behind reduced Grx5 levels, MIN6 cells were exposed to hypoxia and oleic acid. Oleic acid as a monounsaturated fatty acid is typically elevated in the diabetic metabolism of db/db mice (79) and is a mediator of lipotoxicity. Concentrations characteristically occurring in diabetes (2, 80, 81) were used in beta-cell culture. Both stressors induced significantly attenuated Grx5 protein levels in MIN6 cells in correlation with reduced insulin secretion *in vitro*. Thus, Grx5 might be depleted in diabese rodents as part of the beta-cell's extensive stress response to lipotoxicity and hypoxia. Especially as a mitochondrial protein, beta-cell and islet Grx5 content might further be reduced due to structural and functional deviations of mitochondria typically occurring in type 2 diabetes (82). Elevated mitochondrial ROS caused by lipotoxicity and hypoxia might be the link between mitochondrial damage and decreased levels of Grx5. Increased susceptibility to oxidative damage and impaired iron-homeostasis with iron-mediated ROS catalyzation as caused by Grx5-deficiency (15, 17) would even fuel this process.

Given our present data and little available literature, we can only speculate as to a connection between pronounced adjustment in Grx expression and islet remodeling under metabolic stress. Further studies are required, particularly functional *in vivo* experiments to gain deeper insights into the specific role of Grx5 for the islets of Langerhans. Glutaredoxin-regulated pathways involved in beta-cell physiology as well as targets and effectors of Grx need to be identified. No causal link between islet Grx expression and islet remodeling has been previously reported, but we have shown that it represents a promising target for future research. However, we were able to demonstrate clear qualitative and quantitative deviations in histomorphological glutaredoxin patterns in uncontrolled rodent diabesity when compared to lean wild-type controls and we were able to delineate the phenomenon from leptin resistance *in vitro*. Oleic acid and hypoxia were identified as possible mediators of beta-cell and islet Grx5-deficiency. The influence of further typical stressors present during diabesity on beta-cell Grx5 expression should be evaluated using a broader range of dosage. Results could hereafter be validated using a different rodent model. In addition, the direct link between hypoxic/lipotoxic stress and reduced islet Grx5 must be evaluated *in vivo*. The potential influence of HIF-dependent cell remodeling and gene transcription as source of altered endocrine beta-cell function should be ruled out.

In conclusion, we provide evidence for a connection between Grx5 expression and islet dysfunction during diabesity *in vivo* as well as a direct link between Grx5 and beta-cell insulin secretion which is independent from leptin resistance. *In vitro* culture of beta-cells under the influence of hypoxia and oleic acid reveals a potential mechanism of action. Our data support the role of Grx5 as a protective factor for the pancreatic beta-cell.

ETHICS STATEMENT

This study was carried out in accordance with the recommendations of institutional animal welfare officer, Chair of Animal Welfare of the Justus Liebig University Giessen, and Regional Administrative Council Giessen, Veterinary Department, under the code GI20/11-Nr.A18/2010. Both committees approved the protocol. All experiments were performed in accordance with German Animal Welfare Law. 3Rs were applied for reducing the number of required mice and reduce potential suffering, enrichment was applied to the IVC. Scoring for adverse events was done daily. Mice were anesthetized with isoflurane using a desiccator and sacrificed by cervical dislocation before removing the pancreas and other organs.

AUTHOR CONTRIBUTIONS

Conceptualization: SFP and TL. Data curation, formal analysis, investigation: SFP, LMS, AK, and SR. Writing—original draft preparation: SP. Writing—review and editing: SFP, LMS, AK, SR, and TL. Guarantor of the research: TL.

ACKNOWLEDGMENTS

TL is the guarantor of this work and, as such, had full access to all of the data in the study and takes responsibility for the integrity of the data and the accuracy of the data analysis. The authors thank Gundula Hertl, Birte Hussmann, and Doris Erb for expert advice and technical assistance. The authors thank Prof. Dr. Lillig, Department of Medical Biochemistry and Molecular Biology, Ernst-Moritz Arndt-University Greifswald, Germany, and Dr. Hanschmann, Department of Neurology, Heinrich Heine University Düsseldorf, Germany, for providing the antibody against Grx5. The authors thank Dr. Fiona Cousins for proofreading the manuscript.

FUNDING

This work was supported by Third Party Resources to TL from Clinical Research Unit and Justus Liebig University.

REFERENCES

1. Robertson RP, Harmon J, Tran PO, Tanaka Y, Takahashi H. Glucose toxicity in beta-cells: type 2 diabetes, good radicals gone bad, and the glutathione connection. *Diabetes* (2003) 52(3):581–7. doi:10.2337/diabetes.52.3.581
2. Thiébaud D, DeFronzo RA, Jacot E, Golay A, Acheson K, Maeder E, et al. Effect of long chain triglyceride infusion on glucose metabolism in man. *Metabolism* (1982) 31(11):1128–36. doi:10.1016/0026-0495(82)90163-9
3. Solinas G, Naugler W, Galimi F, Lee M-S, Karin M. Saturated fatty acids inhibit induction of insulin gene transcription by JNK-mediated phosphorylation of insulin-receptor substrates. *Proc Natl Acad Sci U S A* (2006) 103(44):16454–9. doi:10.1073/pnas.0607626103
4. Cunha DA, Hekerman P, Ladrière L, Bazarra-Castro A, Ortis F, Wakeham MC, et al. Initiation and execution of lipotoxic ER stress in pancreatic beta-cells. *J Cell Sci* (2008) 121(Pt 14):2308–18. doi:10.1242/jcs.026062
5. Elsner M, Gehrmann W, Lenzen S. Peroxisome-generated hydrogen peroxide as important mediator of lipotoxicity in insulin-producing cells. *Diabetes* (2011) 60(1):200–8. doi:10.2337/db09-1401
6. Sato Y, Endo H, Okuyama H, Takeda T, Iwahashi H, Imagawa A, et al. Cellular hypoxia of pancreatic beta-cells due to high levels of oxygen consumption for

insulin secretion in vitro. *J Biol Chem* (2011) 286(14):12524–32. doi:10.1074/jbc.M110.194738
7. Dionne KE, Colton CK, Yarmush ML. Effect of hypoxia on insulin secretion by isolated rat and canine islets of Langerhans. *Diabetes* (1993) 42(1):12–21. doi:10.2337/diabetes.42.1.12
8. Godoy JR, Funke M, Ackermann W, Haunhorst P, Oesteritz S, Capani F, et al. Redox atlas of the mouse. Immunohistochemical detection of glutaredoxin-, peroxiredoxin-, and thioredoxin-family proteins in various tissues of the laboratory mouse. *Biochim Biophys Acta* (2011) 1810(1):2–92. doi:10.1016/j.bbagen.2010.05.006
9. Holmgren A. Thioredoxin and glutaredoxin systems. *J Biol Chem* (1989) 264(24):13963–6.
10. Chrestensen CA, Starke DW, Mieyal JJ. Acute cadmium exposure inactivates thioltransferase (Glutaredoxin), inhibits intracellular reduction of protein-glutathionyl-mixed disulfides, and initiates apoptosis. *J Biol Chem* (2000) 275(34):26556–65. doi:10.1074/jbc.M004097200
11. Gravina SA, Mieyal JJ. Thioltransferase is a specific glutathionyl mixed disulfide oxidoreductase. *Biochemistry* (1993) 32(13):3368–76. doi:10.1021/bi00064a021
12. Lill R, Dutkiewicz R, Freibert SA, Heidenreich T, Mascarenhas J, Netz DJ, et al. The role of mitochondria and the CIA machinery in the maturation of cytosolic and nuclear iron-sulfur proteins. *Eur J Cell Biol* (2015) 94(7–9):280–91. doi:10.1016/j.ejcb.2015.05.002
13. Stehling O, Wilbrecht C, Lill R. Mitochondrial iron-sulfur protein biogenesis and human disease. *Biochimie* (2014) 100:61–77. doi:10.1016/j.biochi.2014.01.010
14. Rodríguez-Manzaneque MT, Tamarit J, Bellí G, Ros J, Herrero E. Grx5 is a mitochondrial glutaredoxin required for the activity of iron/sulfur enzymes. *Mol Biol Cell* (2002) 13(4):1109–21. doi:10.1091/mbc.01-10-0517
15. Rodríguez-Manzaneque MT, Ros J, Cabiscol E, Sorribas A, Herrero E. Grx5 glutaredoxin plays a central role in protection against protein oxidative damage in *Saccharomyces cerevisiae*. *Mol Cell Biol* (1999) 19(12):8180–90. doi:10.1128/MCB.19.12.8180
16. Wingert RA, Galloway JL, Barut B, Foott H, Fraenkel P, Axe JL, et al. Deficiency of glutaredoxin 5 reveals Fe-S clusters are required for vertebrate haem synthesis. *Nature* (2005) 436(7053):1035–9. doi:10.1038/nature03887
17. Camaschella C, Campanella A, De Falco L, Boschetto L, Merlini R, Silvestri L, et al. The human counterpart of zebrafish shiraz shows sideroblastic-like microcytic anemia and iron overload. *Blood* (2007) 110(4):1353–8. doi:10.1182/blood-2007-02-072520
18. Baetens D, Malaisse-Lagae F, Perrelet A, Orci L. Endocrine pancreas: three-dimensional reconstruction shows two types of islets of Langerhans. *Science* (1979) 206(4424):1323–5. doi:10.1126/science.390711
19. Elayat AA, el Naggar MM, Tahir M. An immunocytochemical and morphometric study of the rat pancreatic islets. *J Anat* (1995) 186:629–37.
20. Steiner DJ, Kim A, Miller K, Hara M. Pancreatic islet plasticity: interspecies comparison of islet architecture and composition. *Islets* (2010) 2(3):135–45. doi:10.4161/isl.2.3.11815
21. McEvoy RC, Hegre OD. Morphometric quantitation of the pancreatic insulin-, glucagon-, and somatostatin-positive cell populations in normal and alloxan-diabetic rats. *Diabetes* (1977) 26(12):1140–6. doi:10.2337/diabetes.26.12.1140
22. Pipeleers D, in't Veld PI, Maes E, Van De Winkel M. Glucose-induced insulin release depends on functional cooperation between islet cells. *Proc Natl Acad Sci U S A* (1982) 79(23):7322–5. doi:10.1073/pnas.79.23.7322
23. Talchai C, Xuan S, Lin HV, Sussel L, Accili D. Pancreatic beta cell dedifferentiation as a mechanism of diabetic beta cell failure. *Cell* (2012) 150(6):1223–34. doi:10.1016/j.cell.2012.07.029
24. White MG, Marshall HL, Rigby R, Huang GC, Amer A, Booth T, et al. Expression of mesenchymal and alpha-cell phenotypic markers in islet beta-cells in recently diagnosed diabetes. *Diabetes Care* (2013) 36(11):3818–20. doi:10.2337/dc13-0705
25. Gao T, McKenna B, Li C, Reichert M, Nguyen J, Singh T, et al. Pdx1 maintains beta cell identity and function by repressing an alpha cell program. *Cell Metab* (2014) 19(2):259–71. doi:10.1016/j.cmet.2013.12.002
26. Ebato C, Uchida T, Arakawa M, Komatsu M, Ueno T, Komiya K, et al. Autophagy is important in islet homeostasis and compensatory increase of beta cell mass in response to high-fat diet. *Cell Metab* (2008) 8(4):325–32. doi:10.1016/j.cmet.2008.08.009
27. Riahi Y, Wikstrom JD, Bachar-Wikstrom E, Polin N, Zucker H, Lee MS, et al. Autophagy is a major regulator of beta cell insulin homeostasis. *Diabetologia* (2016) 59(7):1480–91. doi:10.1007/s00125-016-3868-9
28. Unger RH, Aguilar-Parada E, Müller WA, Eisentraut AM. Studies of pancreatic alpha cell function in normal and diabetic subjects. *J Clin Invest* (1970) 49(4):837–48. doi:10.1172/JCI106297
29. Dusaulcy R, Handgraaf S, Heddad-Masson M, Visentin F, Vesin C, Reimann F, et al. alpha-cell dysfunctions and molecular alterations in male insulinopenic diabetic mice are not completely corrected by insulin. *Endocrinology* (2016) 157(2):536–47. doi:10.1210/en.2015-1725
30. Bloch K, Shichman E, Vorobeychik M, Bloch D, Vardi P. Catalase expression in pancreatic alpha cells of diabetic and non-diabetic mice. *Histochem Cell Biol* (2007) 127(2):227–32. doi:10.1007/s00418-006-0248-4
31. Hanschmann EM. *Thioredoxin Family Proteins in Physiology and Disease [Dissertation]* Marburg, Germany: Philipps-Universität Marburg (2011). doi:10.17192/z2011.0712
32. Stefanini M, De Martino C, Zamboni L. Fixation of ejaculated spermatozoa for electron microscopy. *Nature* (1967) 216:173–4. doi:10.1038/216173a0
33. Petry SF, Sharifpanah F, Sauer H, Linn T. Differential expression of islet glutaredoxin 1 and 5 with high reactive oxygen species production in a mouse model of diabesity. *PLoS One* (2017) 12(5):e0176267. doi:10.1371/journal.pone.0176267
34. Baltrusch S, Lenzen S. Novel insights into the regulation of the bound and diffusible glucokinase in MIN6 beta-cells. *Diabetes* (2007) 56(5):1305–15. doi:10.2337/db06-0894
35. Miyazaki J, Araki K, Yamato E, Ikegami H, Asano T, Shibasaki Y, et al. Establishment of a pancreatic beta cell line that retains glucose-inducible insulin secretion: special reference to expression of glucose transporter isoforms. *Endocrinology* (1990) 127(1):126–32. doi:10.1210/endo-127-1-126
36. Lai Y, Brandhorst H, Hossain H, Bierhaus A, Chen C, Bretzel RG, et al. Activation of NFkappaB dependent apoptotic pathway in pancreatic islet cells by hypoxia. *Islets* (2009) 1(1):19–25. doi:10.4161/isl.1.1.8530
37. Chen C, Moreno R, Samikannu B, Bretzel RG, Schmitz ML, Linn T. Improved intraportal islet transplantation outcome by systemic IKK-beta inhibition: NF-kappaB activity in pancreatic islets depends on oxygen availability. *Am J Transplant* (2011) 11(2):215–24. doi:10.1111/j.1600-6143.2010.03390.x
38. Hummel KP, Coleman DL, Lane PW. The influence of genetic background on expression of mutations at the diabetes locus in the mouse. I. C57BL-KsJ and C57BL-6J strains. *Biochem Genet* (1972) 7(1):1–13. doi:10.1007/BF00487005
39. Coleman DL. Obese and diabetes: two mutant genes causing diabetes-obesity syndromes in mice. *Diabetologia* (1978) 14(3):141–8. doi:10.1007/BF00429772
40. Cerf ME, Chapman CS, Louw J. High-fat programming of hyperglycemia, hyperinsulinemia, insulin resistance, hyperleptinemia, and altered islet architecture in 3-month-old Wistar rats. *ISRN Endocrinol* (2012):627270. doi:10.5402/2012/627270
41. Brereton MF, Iberl M, Shimomura K, Zhang Q, Adriaenssens AE, Proks P, et al. Reversible changes in pancreatic islet structure and function produced by elevated blood glucose. *Nat Commun* (2014) 22(5):4639. doi:10.1038/ncomms5639
42. Lenzen S. Chemistry and biology of reactive species with special reference to the antioxidative defence status in pancreatic beta-cells. *Biochim Biophys Acta* (2017) 1861(8):1929–42. doi:10.1016/j.bbagen.2017.05.013
43. Robertson RP. Chronic oxidative stress as a central mechanism for glucose toxicity in pancreatic islet beta cells in diabetes. *J Biol Chem* (2004) 279(41):42351–4. doi:10.1074/jbc.R400019200
44. Kondo T, El Khattabi I, Nishimura W, Laybutt DR, Geraldes P, Shah S, et al. p38 MAPK is a major regulator of MafA protein stability under oxidative stress. *Mol Endocrinol* (2009) 23(8):1281–90. doi:10.1210/me.2008-0482
45. Chan JY, Luzuriaga J, Bensellam M, Biden TJ, Laybutt DR. Failure of the adaptive unfolded protein response in islets of obese mice is linked with abnormalities in β-cell gene expression and progression to diabetes. *Diabetes* (2013) 62(5):1557–68. doi:10.2337/db12-0701
46. Lee Y-E, Kim J-W, Lee E-M, Ahn Y-B, Song K-H, Yoon K-H, et al. Chronic resveratrol treatment protects pancreatic islets against oxidative stress in db/db mice. *PLoS One* (2012) 7(11):e50412. doi:10.1371/journal.pone.0050412
47. Bensellam M, Maxwell EL, Chan JY, Luzuriaga J, West PK, Jonas JC, et al. Hypoxia reduces ER-to-Golgi protein trafficking and increases cell death

by inhibiting the adaptive unfolded protein response in mouse beta cells. *Diabetologia* (2016) 59(7):1492–502. doi:10.1007/s00125-016-3947-y
48. Maedler K, Spinas GA, Dyntar D, Moritz W, Kaiser N, Donath MY. Distinct effects of saturated and monounsaturated fatty acids on beta-cell turnover and function. *Diabetes* (2001) 50(1):69–76. doi:10.2337/diabetes.50.1.69
49. Milburn J Jr, Hirose H, Lee YH, Nagasawa Y, Ogawa A, Ohneda M, et al. Pancreatic beta-cells in obesity. Evidence for induction of functional, morphologic, and metabolic abnormalities by increased long chain fatty acids. *J Biol Chem* (1995) 270(3):1295–9. doi:10.1074/jbc.270.3.1295
50. Leiter EH, Gapp DA, Eppig JJ, Coleman DL. Ultrastructural and morphometric studies of delta cells in pancreatic islets from C57BL/Ks diabetes mice. *Diabetologia* (1979) 17(5):297–309. doi:10.1007/BF01235886
51. Watanabe Y, Murdoch CE, Sano S, Ido Y, Bachschmid MM, Cohen RA, et al. Glutathione adducts induced by ischemia and deletion of glutaredoxin-1 stabilize hif-1α and improve limb revascularization. *Proc Natl Acad Sci U S A* (2016) 113(21):6011–6. doi:10.1073/pnas.1524198113
52. Hirota K, Matsui M, Murata M, Takashima Y, Cheng FS, Itoh T, et al. Nucleoredoxin, glutaredoxin, and thioredoxin differentially regulate NF-kappaB, AP-1, and CREB activation in HEK293 cells. *Biochem Biophys Res Commun* (2000) 274(1):177–82. doi:10.1006/bbrc.2000.3106
53. Daily D, Vlamis-Gardikas A, Offen D, Mittelman L, Melamed E, Holmgren A, et al. Glutaredoxin protects cerebellar granule neurons from dopamine-induced apoptosis by activating NF-kappa B via Ref-1. *J Biol Chem* (2001) 276(2):1335–44. doi:10.1074/jbc.M101400200
54. Reinbothe TM, Ivarsson R, Li DQ, Niazi O, Jing X, Zhang E, et al. Glutaredoxin-1 mediates NADPH-dependent stimulation of calcium-dependent insulin secretion. *J Mol Endocrinol* (2009) 23(6):893–900. doi:10.1210/me.2008-0306
55. Liu X, Han S, Yang Y, Kang J, Wu J. Glucose-induced glutathione reduction in mitochondria is involved in the first phase of pancreatic beta-cell insulin secretion. *Biochem Biophys Res Commun* (2015) 464(3):730–6. doi:10.1016/j.bbrc.2015.07.016
56. Takahashi HK, Santos LR, Roma LP, Duprez J, Broca C, Wojtusciszyn A, et al. Acute nutrient regulation of the mitochondrial glutathione redox state in pancreatic beta-cells. *Biochem J* (2014) 460(3):411–23. doi:10.1042/BJ20131361
57. Dong K, Wu M, Liu X, Huang Y, Zhang D, Wang Y, et al. Glutaredoxins concomitant with optimal ROS activate AMPK through S-glutathionylation to improve glucose metabolism in type 2 diabetes. *Free Radic Biol Med* (2016) 101:334–47. doi:10.1016/j.freeradbiomed.2016.10.007
58. Ward NE, Stewart JR, Ioannides CG, O'Brian CA. Oxidant-induced S-glutathiolation inactivates protein kinase C-alpha (PKC-alpha): a potential mechanism of PKC isozyme regulation. *Biochemistry* (2000) 39(33):10319–29. doi:10.1021/bi000781g
59. Wetzelberger K, Baba SP, Thirunavukkarasu M, Ho YS, Maulik N, Barski OA, et al. Postischemic deactivation of cardiac aldose reductase: role of glutathione S-transferase P and glutaredoxin in regeneration of reduced thiols from sulfenic acids. *J Biol Chem* (2010) 285(34):26135–48. doi:10.1074/jbc.M110.146423
60. Chen H, Charlat O, Tartaglia LA, Woolf EA, Weng X, Ellis SJ, et al. Evidence that the diabetes gene encodes the leptin receptor: identification of a mutation in the leptin receptor gene in db/db mice. *Cell* (1996) 84(3):491–5. doi:10.1016/S0092-8674(00)81294-5
61. Hummel KP, Dickie MM, Coleman DL. Diabetes, a new mutation in the mouse. *Science* (1966) 153(3740):1127–8. doi:10.1126/science.153.3740.1127
62. Flier JS, Cook KS, Usher P, Spiegelman BM. Severely impaired adipsin expression in genetic and acquired obesity. *Science* (1987) 237(4813):405–8. doi:10.1126/science.3299706
63. Zhang Y, Proenca R, Maffei M, Barone M, Leopold L, Friedman JM. Positional cloning of the mouse obese gene and its human homologue. *Nature* (1994) 372(6505):425–32. doi:10.1038/372425a0
64. Friedman JM, Halaas JL. Leptin and the regulation of body weight in mammals. *Nature* (1998) 395(6704):763–70. doi:10.1038/27376
65. Kulkarni RN, Wang ZL, Wang RM, Hurley JD, Smith DM, Ghatei MA, et al. Leptin rapidly suppresses insulin release from insulinoma cells, rat and human islets and, in vivo, in mice. *J Clin Invest* (1997) 100(11):2729–36. doi:10.1172/JCI119818
66. Seufert J, Kieffer TJ, Habener JF. Leptin inhibits insulin gene transcription and reverses hyperinsulinemia in leptin-deficient ob/ob mice. *Proc Natl Acad Sci U S A* (1999) 96(2):674–9. doi:10.1073/pnas.96.2.674
67. Laferrère B, Caixas A, Fried SK, Bashore C, Kim J, Pi-Sunyer FX. A pulse of insulin and dexamethasone stimulates serum leptin in fasting human subjects. *Eur J Endocrinol* (2002) 146(6):839–45. doi:10.1530/eje.0.1460839
68. Moreno-Aliaga MJ, Stanhope KL, Havel PJ. Transcriptional regulation of the leptin promoter by insulin-stimulated glucose metabolism in 3t3-l1 adipocytes. *Biochem Biophys Res Commun* (2001) 283(3):544–8. doi:10.1006/bbrc.2001.4822
69. Fain JN, Madan AK, Hiler ML, Cheema P, Bahouth SW. Comparison of the release of adipokines by adipose tissue, adipose tissue matrix, and adipocytes from visceral and subcutaneous abdominal adipose tissues of obese humans. *Endocrinology* (2004) 145(5):2273–82. doi:10.1210/en.2003-1336
70. Haleem DJ, Sheikh S, Fawad A, Haleem MA. Fasting leptin and glucose in normal weight, over weight and obese men and women diabetes patients with and without clinical depression. *Metab Brain Dis* (2017) 32(3):757–64. doi:10.1007/s11011-017-9964-9
71. Maffei M, Fei H, Lee GH, Dani C, Leroy P, Zhang Y, et al. Increased expression in adipocytes of ob RNA in mice with lesions of the hypothalamus and with mutations at the db locus. *Proc Natl Acad Sci U S A* (1995) 92(15):6957–60. doi:10.1073/pnas.92.15.6957
72. Hamad EM, Sato M, Uzu K, Yoshida T, Higashi S, Kawakami H, et al. Milk fermented by *Lactobacillus gasseri* sbt2055 influences adipocyte size via inhibition of dietary fat absorption in zucker rats. *Br J Nutr* (2009) 101(5):716–24. doi:10.1017/S0007114508043808
73. Singer G, Stokes KY, Terao S, Granger DN. Sepsis-induced intestinal microvascular and inflammatory responses in obese mice. *Shock* (2009) 31(3):275–9. doi:10.1097/SHK.0b013e3181834ab3
74. Leclercq-Meyer V, Malaisse WJ. Failure of human and mouse leptin to affect insulin, glucagon and somatostatin secretion by the perfused rat pancreas at physiological glucose concentration. *Mol Cell Endocrinol* (1998) 141(1–2):111–8. doi:10.1016/S0303-7207(98)00087-2
75. Tanizawa Y, Okuya S, Ishihara H, Asano T, Yada T, Oka Y. Direct stimulation of basal insulin secretion by physiological concentrations of leptin in pancreatic beta cells. *Endocrinology* (1997) 138(10):4513–6. doi:10.1210/endo.138.10.5576
76. Zhao AZ, Bornfeldt KE, Beavo JA. Leptin inhibits insulin secretion by activation of phosphodiesterase 3B. *J Clin Invest* (1998) 102(5):869–73. doi:10.1172/JCI3920
77. Brown JE, Dunmore SJ. Leptin decreases apoptosis and alters BCL-2: Bax ratio in clonal rodent pancreatic beta-cells. *Diabetes Metab Res Rev* (2007) 23(6):497–502. doi:10.1002/dmrr.726
78. Kieffer TJ, Heller RS, Leech CA, Holz GG, Habener JF. Leptin suppression of insulin secretion by the activation of ATP-sensitive K+ channels in pancreatic beta-cells. *Diabetes* (1997) 46(6):1087–93. doi:10.2337/diab.46.6.1087
79. Deepa SS, Walsh ME, Hamilton RT, Pulliam D, Shi Y, Hill S, et al. Rapamycin modulates markers of mitochondrial biogenesis and fatty acid oxidation in the adipose tissue of db/db mice. *J Biochem Pharmacol Res* (2013) 1(2):114–23.
80. Gordon E. Non-esterified fatty acids in blood of obese and lean subjects. *Am J Clin Nutr* (1960) 8(5):740–7. doi:10.1093/ajcn/8.5.740
81. Reaven GM, Hollenbeck C, Jeng CY, Wu MS, Chen YD. Measurement of plasma glucose, free fatty acid, lactate, and insulin for 24 h in patients with NIDDM. *Diabetes* (1988) 37(8):1020–4. doi:10.2337/diab.37.8.1020
82. Anello M, Lupi R, Spampinato D, Piro S, Masini M, Boggi U, et al. Functional and morphological alterations of mitochondria in pancreatic beta cells from type 2 diabetic patients. *Diabetologia* (2005) 48(2):282–9. doi:10.1007/s00125-004-1627-9

Conflict of Interest Statement: The authors declare that the research was conducted in the absence of any commercial or financial relationships that could be construed as a potential conflict of interest.

antioxidants

MDPI

Article

Loss and Recovery of Glutaredoxin 5 Is Inducible by Diet in a Murine Model of Diabesity and Mediated by Free Fatty Acids In Vitro

Sebastian Friedrich Petry [1,*,†], Axel Römer [1,†], Divya Rawat [1], Lara Brunner [1], Nina Lerch [1], Mengmeng Zhou [1], Rekha Grewal [2], Fatemeh Sharifpanah [3,4], Heinrich Sauer [5], Gunter Peter Eckert [2] and Thomas Linn [1]

1 Clinical Research Unit, Medical Clinic and Polyclinic III, Center of Internal Medicine, Justus Liebig University, 35392 Giessen, Germany; axel.roemer@ernaehrung.uni-giessen.de (A.R.); divyarawat21@gmail.com (D.R.); lara.s.brunner@med.uni-giessen.de (L.B.); nina.f.lerch@stud.mh-hannover.de (N.L.); mengmeng.zhou@med.uni-giessen.de (M.Z.); thomas.linn@innere.med.uni-giessen.de (T.L.)
2 Laboratory for Nutrition in Prevention & Therapy, Department of Nutritional Sciences, Justus Liebig University, 35392 Giessen, Germany; rekha.grewal@ernaehrung.uni-giessen.de (R.G.); gunter.eckert@ernaehrung.uni-giessen.de (G.P.E.)
3 Faculty of Medicine, Philipps University, 35037 Marburg, Germany; fatemeh.sharifpanah@gmail.com
4 Cyntegrity Germany GmbH, 60438 Frankfurt, Germany
5 Department of Physiology, Faculty of Medicine, Justus Liebig University, 35392 Giessen, Germany; heinrich.sauer@physiologie.med.uni-giessen.de
* Correspondence: sebastian.petry@innere.med.uni-giessen.de; Tel.: +49-641-985-57010
† These authors contributed equally to this work.

check for updates

Citation: Petry, S.F.; Römer, A.; Rawat, D.; Brunner, L.; Lerch, N.; Zhou, M.; Grewal, R.; Sharifpanah, F.; Sauer, H.; Eckert, G.P.; et al. Loss and Recovery of Glutaredoxin 5 Is Inducible by Diet in a Murine Model of Diabesity and Mediated by Free Fatty Acids In Vitro. *Antioxidants* **2022**, *11*, 788. https://doi.org/10.3390/antiox11040788

Academic Editors: Mirko Zaffagnini, Jeremy Couturier and Raffaella Mastrocola

Received: 13 February 2022
Accepted: 14 April 2022
Published: 15 April 2022

Publisher's Note: MDPI stays neutral with regard to jurisdictional claims in published maps and institutional affiliations.

Abstract: Free fatty acids (FFA), hyperglycemia, and inflammatory cytokines are major mediators of β-cell toxicity in type 2 diabetes mellitus, impairing mitochondrial metabolism. Glutaredoxin 5 (Glrx5) is a mitochondrial protein involved in the assembly of iron–sulfur clusters required for complexes of the respiratory chain. We have provided evidence that islet cells are deprived of Glrx5, correlating with impaired insulin secretion during diabetes in genetically obese mice. In this study, we induced diabesity in C57BL/6J mice in vivo by feeding the mice a high-fat diet (HFD) and modelled the diabetic metabolism in MIN6 cells through exposure to FFA, glucose, or inflammatory cytokines in vitro. qRT-PCR, ELISA, immunohisto-/cytochemistry, bioluminescence, and respirometry were employed to study Glrx5, insulin secretion, and mitochondrial biomarkers. The HFD induced a depletion of islet Glrx5 concomitant with an obese phenotype, elevated FFA in serum and reactive oxygen species in islets, and impaired glucose tolerance. Exposure of MIN6 cells to FFA led to a loss of Glrx5 in vitro. The FFA-induced depletion of Glrx5 coincided with significantly altered mitochondrial biomarkers. In summary, we provide evidence that Glrx5 is regulated by FFA in type 2 diabetes mellitus and is linked to mitochondrial dysfunction and blunted insulin secretion.

Keywords: glutaredoxin; β-cell; high fat diet; diabetes; obesity; mitochondria

1. Introduction

Visceral obesity is one of the major risk factors for developing glucose intolerance and type 2 diabetes mellitus. A sedentary lifestyle combined with Western dietary habits promotes diabetes in genetically predisposed individuals. A misbalance of calorie intake and muscular activity leads to sustained nutritional overflow in tissues with predominantly insulin-dependent glucose uptake. An insulin-resistant metabolism is hallmarked by hyperglycemia, elevated free fatty acids (FFA), and a chronic state of inflammation mediated through cytokines such as interleukin-1β (IL-1β), interferon-γ (IFN-γ), and tumor necrosis factor-α (TNF-α) [1]. This adverse metabolic condition challenges the pancreatic β-cells which are imperative for maintaining glucose homeostasis. They feature a marked metabolic activity and therefore rely on a vast amount of energy supplied by their mitochondria, especially when a supraphysiologically high level of insulin secretion is required

to overcome insulin resistance [2] and ameliorate hyperglycemia. This immense substrate turnover in the respiratory chain promotes the formation of superoxide and hydrogen peroxide at complexes I–III [3], eventually leading to the functional and structural decay of mitochondria [4]. Ultimately, the secretory apparatus of the β-cells is impaired. The excess of FFA further fuels these processes by promoting the formation of reactive oxygen species (ROS) through peroxisomal β-oxidation [5], the phosphorylation of insulin receptor substrates [6], the induction of the p53-dependent mitochondrial apoptotic pathway [7], and interference with the cell cycle [7]. Activated FFA form acyl-CoA, which accumulates due to mitochondrial dysfunction, activating PPARγ and the sterol regulatory element-binding protein (SREBP)-1c-dependent pathways with detrimental effects on insulin release, cell proliferation and survival, and leads to an increased uncoupling of mitochondria [8].

Glutaredoxin 5 (Glrx5) is a mitochondrial enzyme of the thioredoxin family. It is an acknowledged actor in the iron–sulfur (Fe/S) cluster assembly and consecutively for the biogenesis of enzymes containing these clusters [9,10]. Glrx5, with a Cys-Gly-Phe-Ser active site, binds Fe/S clusters and transfers them to specific target apoproteins where they are required for structural conformation, electron transfer, or as co-substrates (for an overview, see [11]). Fe/S clusters form reactive centers in complexes I–III of the respiratory chain and prosthetic groups in cytosolic aconitase (Aco1) and mitochondrial ferrochelatase. In several cell models including human cells, it has been demonstrated that Glrx5 deficiency leads to an increased susceptibility to oxidative and osmotic stress and cellular iron overload [12–15]. A human subject suffering from Glrx5 deficiency was reported to present anemia, type 2 diabetes mellitus/type 3c diabetes mellitus (i.e., by damage to the exocrine pancreas), hepatosplenomegaly, and cirrhosis of the liver due to cellular iron overload [16]. The application of iron chelators markedly ameliorated these conditions in line with data derived from a murine model of cellular iron overload [17]. Free cellular iron induces oxidative damage to membrane lipids and the formation of lipid peroxides, resulting in oxidative, non-apoptotic cell decay known as ferroptosis [18].

Little is known about the role of Glrx5 in pancreatic β-cells and its regulation. Therefore, we employed a dietary-induced model of murine diabesity to study the expression of Glrx5 in pancreatic islets under a high-fat diet (HFD) versus standard chow. The animals featured a considerable loss of islet Glrx5 concomitant with elevated serum FFA, obesity, and impaired glucose tolerance after HFD feeding. In vitro, murine β-cells were exposed to fatty acids, high glucose, or inflammatory cytokines. The nutritional regimen employed in vivo was modelled by pre-incubation with free fatty acids followed by exposure to high glucose. Only culture conditions involving FFA led to a decline in Glrx5 and impaired mitochondrial metabolism.

In summary, this study delivers in vivo and in vitro evidence for a distinct regulation of islet Glrx5 by FFA and links the loss of Glrx5 with failing insulin secretion due to impaired mitochondrial metabolism.

2. Materials and Methods

2.1. Research Animals

A total of 88 male C57BL/6J mice were acquired from Charles River (Sulzfeld, Germany) at the age of 5 weeks and were given two weeks to adapt to the local animal facility. They were housed at 22 ± 2 °C, with a 14:10 h light/dark cycle, a relative humidity of 55 ± 10%, and provided with tap water ad libitum in individually ventilated cages in groups of five mice. All animal research was carried out in accordance with recommendations from our institutional animal welfare officer, the Chair of Animal Welfare of the Justus Liebig University, Giessen, and the Regional Administrative Council of Giessen, the Veterinary Department, under codes GI 20/11 No. G 3/2017 and No. G 48/2018. Both committees approved the protocol. All experiments were performed in accordance with the German Animal Welfare Law.

During adaption to our animal facility, both groups of mice were fed a control diet (CD, 3514 kcal/kg, 10% of energy from fat, 66% from carbohydrates, and 24% from protein; diet C 1090-10, Altromin, Lage, Germany) ad libitum. The control group did not undergo a

change of diet throughout the study period of 22 weeks. The experimental group received a high-fat diet (HFD, 5389 kcal/kg, 70% of energy from fat, 14% from carbohydrates, and 16% from protein; diet C 1090-70, Altromin, Lage, Germany) for 13 weeks (from 7 to 20 weeks of age). Afterwards, the experimental group was switched back to the CD until 23 weeks of age (3 weeks in total) before it was fed the HFD again for 4 more weeks (age 23 to 27 weeks). A summary of the experimental setup is given in Figure 1.

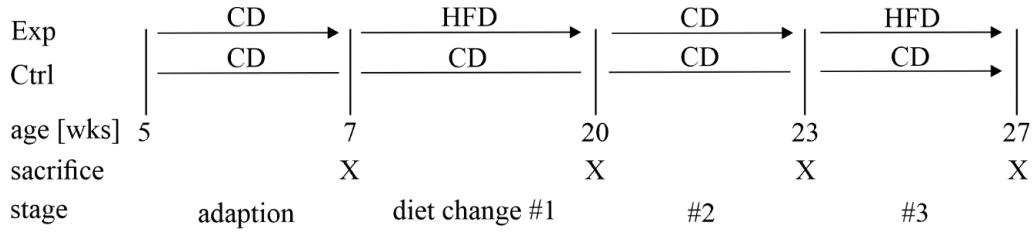

Figure 1. Experimental setup of the animal experiment. Male C57BL/6J mice were divided into the experimental (Exp) and control (Ctrl) groups at the age of 7 weeks after 2 weeks of adaption to our animal housing. Control animals were fed a control diet (CD, ca. 3514 kcal/kg, 10% of energy from fat, 66% from carbohydrates, and 24% from protein) throughout the study period. The experimental group was fed a high-fat diet (HFD, ca. 5389 kcal/kg, 70% of energy from fat, 14% from carbohydrates, and 16% from protein) from 7 to 20 weeks of age, followed by rescue feeding with the CD for 3 weeks, and another cycle of the HFD for 4 weeks. Euthanasia was carried out in both groups at 7, 20, 23, and 27 weeks of age.

Blood glucose levels were monitored with a glucometer (OneTouch Ultra 2, LifeScan, Düsseldorf, Germany) using blood samples collected by puncturing the tip of the tail after overnight fasting. Animals of both groups were euthanized at 7, 20, 23, and 27 weeks of age. Intraperitoneal glucose tolerance tests (IPGTT) were conducted at these time points. The fasting blood glucose level was measured before glucose (1 mg per g body weight) was injected intraperitoneally and 30, 60, 90, and 120 min thereafter.

2.2. Pancreatic Islet Isolation

Mice were anesthetized with 1 mg and 0.2 mg of ketamine (Medistar, Ascheberg, Germany) and xylazine (Ceva, Düsseldorf, Germany), respectively, which were dissolved in 0.9% NaCl per 10 g of body weight and administered via intraperitoneal injection. To harvest the pancreas in ischemia, the abdominal wall was excised, the aorta was cut, and the blood was drained and collected for further analysis before the removal and processing of the pancreas for either immunohistology or islet isolation.

For immunohistochemistry, organs were fixed with 4% phosphate-buffered paraformaldehyde in picric acid (pH 7.3) following the protocol established by Stefanini et al. [19] for four hours, then washed and stored in PBS supplemented with 18% sucrose solution overnight. Organs were embedded in a cryoblock embedding medium (Biosystems, Nunningen, Switzerland) and frozen at −80 °C.

Islet isolation was carried out as described previously by our department [20]. Briefly, the pancreas was perfused with 4 mg/mL collagenase B (Roche, Mannheim, Germany) dissolved in 1% Hank's solution (Biochrom, Berlin, Germany) and supplemented with 35 mL HEPES buffer (Biochrom), 10 mL ciprofloxacin, 10 mL penicillin–streptomycin, and 1 mL gentamycin through the ductus pancreaticus. To facilitate the process of digestion, the perfused organ was mechanically chopped with a pair of scissors before incubation in a collagenase solution at 37 °C in a shaking water bath for 10 min. Every 3 min, tissue was vortexed for 10 s. Digested tissue was then shaken by hand for another 2 min, and the process was eventually stopped by adding cold Hank's solution. Following 3 min of centrifugation at 375 g, the supernatant was discarded, and the pellet was dissolved in 15% Parker/fetal calf serum dissolved in Medium 199 (Gibco, Darmstadt, Germany) and fetal bovine serum (Biowest, Nuaillé, France) at room temperature. Islets were hand-picked under a stereomicroscope and incubated overnight at 37 °C to overcome isolation stress.

2.3. Immunohistochemistry

Immunohistological staining was employed for the detection of insulin and Glrx5. Frozen organs were thawed and sectioned entirely. Slides with a thickness of 7 µm were created using a Leica Cryostat CM1850 (Leica, Wetzlar, Germany). A manual optical assessment for quality was employed and slides with a damaged structure were rejected. An interval of 140 µm between slides was maintained to avoid the multiple inclusion of islets. Slides were washed with PBS and blocked with 1% donkey serum dissolved in PBS containing 0.3% Triton X-100 (0.3% PBST) for 20 min. Sections were incubated with respective primary antibodies (insulin: 1:100, Bio-Rad, Feldkirchen, Germany; Glrx5: 1:100, Bioss, Woburn, MA, USA) diluted in 1% donkey serum dissolved in 0.3% PBST overnight at 4 °C in a wet chamber. Secondary antibodies (1:400, FITC and Rhodamine Red, Jackson, Newmarket, UK) in 5% mouse serum were applied for one hour at room temperature in the dark before nuclei were stained with Hoechst 33,342 (Calbiochem, Darmstadt, Germany) in 0.1% TRIS buffer with a pH of 7.6, and samples were preserved with ProLong Gold (Invitrogen, Darmstadt, Germany). Slides without primary antibodies were used as negative controls.

Images of stained samples were taken with Leica Application Suite V 3.8.0 using a DFC420 C digital microscope camera (Leica, Wetzlar, Germany). The ImageJ software (Wayne Rasband, National Institutes of Health, Bethesda, MD, USA) was used for this analysis. The islet area and the respective staining area of the insulin or Glrx5 were measured by the optical identification of islets and manual selection by use of the freehand selection tool after calibrating ImageJ to match the scale. The absolute staining area of the insulin or Glrx5 staining inside the respective islets was then acquired by applying a threshold value and manual adaption to exclude regions without staining. The staining of Glrx5 was quantified by dividing its staining area by the area of insulin staining for each islet.

2.4. ROS Production Analysis

Intracellular ROS production in islets was detected employing the 2′,7′-dichlorofluorescein diacetate (DCFH-DA, Sigma-Aldrich, Taufkirchen, Germany) staining method as previously described [21–23]. Briefly, isolated primary islets were incubated in the dark in a serum-free medium containing a 10-µM DCFH-DA indicator dye dissolved in dimethylsulfoxide (DMSO, Sigma-Aldrich) for 30 min at 37 °C. Samples were rinsed with a pre-warmed serum-free medium and immediately analyzed. DCF fluorescence was evaluated in 3600 μm^2 regions of interest by a confocal laser scanning microscope (Leica SP2 AOBS, Bensheim, Germany) and the 488 nm band of its argon ion laser. Emission was measured using a long-pass LP515 nm filter set. The fluorescence was quantified with the Leica Simulator software using an overlay mask and correction for background fluorescence.

2.5. mRNA Expression Analysis

RNA was extracted from isolated islets using the RNeasy Plus Micro Kit (Qiagen, Düsseldorf, Germany). A NanoDrop 1000 spectrophotometer (Thermo Scientific, Schwerte, Germany) was employed to determine the total RNA concentration (OD 260/280 nm). cDNA was synthesized with the SuperScript III Reverse Transcriptase kit (Invitrogen). Quantitative real-time PCR (qRT-PCR) was carried out on the StepOnePlus Real-Time PCR System (Applied Biosystems, Waltham, MA, USA) conducting activation for 10 min at 95 °C, 40 cycles of denaturation (95 °C for 10 s), and carrying out annealing/extension at 60 °C for 1 min. The primer concentration was 10 µM. The sequences of the employed primers (Invitrogen) were as follows:

Beta-actin (reference):
fwd GTG GGA ATG GGT CAG AAG G,
rev GAG GCA TAC AGG GAC AGC A;
Ins1:
fwd TAT AAA GCT GGT GGG CAT CC,
rev GGG ACC ACA AAG ATG CTG TT;
Glrx5:

fwd GAA GAA GGA CAA GGT GGT GGT CTT C,
rev GCA TCT GCA GAA GAA TGT CAC AGC

Relative mRNA expression values were obtained by normalizing the respective Ct values of target genes with the reference gene using the delta Ct method. Delta delta Ct values were calculated for the controls vs. the HFD group for each time point and the fold change in mRNA expression was calculated.

2.6. Glucose Stimulation of Pancreatic Islets

Islets were isolated from the HFD and control mice as described above, and were hand-picked, transferred to a petri dish with TCM-199 (Biochrom) with a low glucose medium (30 mg/dL), and incubated for 30 min at 37 °C. They were then further incubated with 30 mg/dL or 300 mg/dL glucose in TCM-99 at 37 °C in a shaking water bath for 90 min. A total of five islets of equivalent size were used per condition. After incubation, the supernatant was collected and islets were sonicated in an immunoreactive insulin (IRI) buffer (7.12 g $Na_2HPO_4 \times H_2O$, 6 g NaCl, 3 g BSA, in 1000 mL distilled water) for lysis. Samples were stored at −20 °C before analysis.

2.7. Cell Culture

The employed murine β-cell line, mouse insulinoma 6 (MIN6), was maintained in Dulbecco's Modified Eagle Medium (DMEM, Gibco) enriched with 25 mM glucose, 1 mM pyruvate, 15.8% heat-inactivated fetal calf serum (Biowest, Nuaillé, France), 50 µM 2-mercaptoethanol (Life Technologies, Carlsbad, CA, USA), and 80 U/mL penicillin/streptomycin (Life Technologies), as previously described by our group [24,25]. We used cells at passages 50–60 grown up to a confluence of 70–80%. The culture conditions were 37 °C and 5% CO_2. The culture media were replaced every 2–3 days. Splitting was carried out by trypsinization with 0.05% trypsin–EDTA (Gibco) after washing with PBS. Beforehand, seeding cells were detached by applying DMEM and centrifugation at 250 *g* for 4 min.

Oleic (Enzo Life Sciences, Lörrach, Germany) and palmitic acid (Sigma-Aldrich) were dissolved in absolute ethanol (Sigma-Aldrich, with a purity higher than 99.8%) to prepare stock solutions of 300 mM and were added to DMEM (Gibco) with fatty acid-free BSA fraction V (Sigma-Aldrich) to reach final fatty acid concentrations of 0.75, 1.5, and 3 mM. The molar FFA:BSA ratio was 4:1. After being overlayed with nitrogen (Linde, Pullach, Germany) overnight at 37 °C on a shaker and sterile filtration, the stock solutions were stored at −20 °C. The ethanol concentrations for 0.75, 1.5, and 3 mM of final fatty acid solution were 0.23, 0.45, and 0.9%, respectively. The control medium was prepared to match the respective alcohol and BSA concentrations. For treatment with cytokines, 10 ng/mL TNF-α, 5 ng/mL IL-1β, and 100 ng/mL IFN-γ (all from R&D Systems) were dissolved in a standard cell culture medium. For the glucose treatment, the culture medium was replaced by a fresh medium without glucose for 2 h, after which it was renewed and enriched with the respective concentrations of glucose. MIN6 cells were pre-incubated with palmitic acid (0 or 400 µM for 48 h) prior to starving them in a Krebs–Ringer–HEPES (KRH) buffer (129 mM NaCl, 5 mM $NaHCO_3$, 4.8 mM KCL, 2.5 mM $CaCl_2$, 1.2 mM $MgSO_4$ and 0.1% (*w*/*v*) BSA, 10 mM HEPES, pH 7.4) for 1 h followed by exposing the cells to glucose (0, 3, or 16 mM) for 1 h.

2.8. Cell Metabolic Activity

The cell metabolic activity was assessed by a 3-(4,5-dimethylthiazol-2-yl)-2,5-diphenyltetrazolium bromide (MTT, Abcam, Cambridge, UK, purity > 98%) assay. We employed 10^4 MIN6 cells in 200 µL DMEM attached to a 96-well plate. The medium was replaced with a fatty acid medium for 24 h. After treatment, 50 µL of the medium was replaced by 2 mg/mL MTT freshly dissolved in PBS to achieve a final concentration of 0.5 mg/mL, and then sterile filtered (0.22 µm) and incubated at 37 °C in 5% CO_2. After 4 h, the medium was replaced by 200 µL DMSO. After formazan crystals were dissolved for 15 min on a plate shaker, the absorbance was measured at 570 nm and 620 nm (background) using a multimode microplate reader (Berthold Technologies, Bad Wildbad, Germany).

2.9. Immunocytochemistry

For immunocytochemistry, adherent cells were trypsinized using 0.05% trypsin-EDTA. Cells were collected and centrifuged at 250 *g* for 4 min before seeding them on petri dishes where treatment was conducted for 24 h. The medium was removed, and the cells were washed with PBS and trypsinized in an incubator at 37 °C for 2–3 min. Detached cells were centrifuged in PBS at 250 *g* for 4 min. The cell pellets were diluted with PBS, and 10–20 µL containing 2000–5000 cells were dropped on slides. The cells were dried for 20–40 min and stored at −20 °C before staining was conducted, following the protocol described for immunohistology. The protein levels of insulin and Glrx5 were quantified with ImageJ using the mean fluorescent intensity normalized by the cell area. This resulted in the integrated density (IntDen), as previously described [26]. Briefly, all eligible single cells were selected manually. The IntDen, area, and mean fluorescent intensity of the background were measured. The IntDen was normalized by subtracting the product of the cell area and mean background fluorescent intensity.

2.10. Determination of Cellular ATP Levels

Twenty-four hours prior to incubation, 5×10^4 cells/well were seeded into 96-well luminescence plates (Corning Inc., Corning, NY, USA). The cells were incubated with oleic acid (0.75, 1.5, or 3 mM) or ethanol as the solvent control for 24 h. ATP levels were determined using a luciferase-based bioluminescence assay. Cells were lysed by a NaOH lysis buffer, followed by adding a solution containing luciferase, luciferin, and co-substrates (PerkinElmer, Waltham, MA, USA). The luminescence was measured using a multimode microplate reader (CLARIOstar, BMG LABTECH, Ortenberg, Germany).

2.11. Mitochondrial Respiration

Respiratory states were measured at 37 °C using the Oxygraph-2k (OROBOROS Instruments, Innsbruck, Austria) based on a silver chloride (Clarke) electrode and DatLab software version 7.0.0.2 (OROBOROS Instruments). For the analysis of the respiratory system, a complex multiple substrate–uncoupler–inhibitor titration (SUIT) protocol (elaborated by Prof. Dr. Erich Gnaiger, University of Innsbruck [27]) was applied including different substrates, uncouplers, and inhibitors. After 24 h of treatment with 0.75 mM oleic acid or respective ethanol solvent controls, cells were harvested in mitochondrial respiration medium MIR05 (0.5 mM EGTA, 3 mM $MgCl_2$, 60 mM K-lactobionate, 20 mM taurine, 10 mM KH_2PO_4, 20 mM HEPES, 110 mM sucrose, 1 mg/mL BSA, pH 7.1) developed by OROBOROS [28]. The cells were centrifuged and resuspended in MIR05 to obtain a solution containing 5×10^5 cells/mL. After adding 2 mL of cell suspension into each chamber of the oxygraph, the respiration stabilized (endogenous respiration). The cell membranes were permeabilized with digitonin (5 µL/10^6 cells), leaving the mitochondrial outer and inner membranes intact. The capacity of the oxidative phosphorylation (OXPHOS) of complexes I and II was determined by adding complex I substrates glutamate (10 mM) and malate (2 mM), and complex V substrate ADP (2 mM) followed by the complex II substrate succinate (10 mM). Adding the complex V inhibitor oligomycin (2 µg/mL) led to a leak in the respiration. Uncoupled electron transfer system (ETS) capacity was achieved by the titration of protonophore FCCP. After adding the complex I inhibitor rotenone (0.5 µM), uncoupled complex II respiration was achieved. The inhibition of complex III by applying antimycin A (2.5 µM) determined the residual oxygen consumption (caused by enzymes which do not belong to the electron transfer system), which was subtracted from all respiratory states. By adding N,N,N′,N′-tetramethyl-p-phenylenediamine (0.5 mM) and ascorbate (2 mM), complex IV was measured. The autoxidation rate was determined using sodium azide (≥100 mM). Complex IV respiration was additionally corrected for autoxidation [29]. The results of mitochondrial respiration were normalized with the activity of citrate synthase measured by the conversion of DTNP into TNP at 412 nm by a GENESYS 10S photometer (Thermo Fisher Scientific, Waltham, MA, USA).

2.12. ELISA Analysis

ELISA was employed for the quantitative analysis of protein content in cell and islet lysates and medium and FFA levels in murine blood. Commercial kits were used according to the respective manufacturers' instructions: insulin (DRG Diagnostics, Marburg, Germany), Glrx5 (CUSABIO Technology, Houston, TX, USA), and FFA (Abcam, Cambridge, UK). Prior to the cell lysis of 4×10^5 MIN6 cells per condition, 1 mL of culture medium was extracted, centrifuged at 330 g for 5 min at 4 °C, and supernatant was preserved for analysis. Cells were washed twice in ice-cold PBS and incubated on ice for 20 min in 10% NP-40 alternative lysis buffer (Merck Millipore, Burlington, MA, USA) with 3% v/v proteinase inhibitor 100× (Halt, Thermo Fisher Scientific, Waltham, MA, USA). Cell debris was removed by centrifugation at 12,000 g at 4 °C for 15 min, leaving the supernatant for further use. Pancreatic islets were prepared as described above. The amount of insulin and Glrx5 protein was normalized to the total lysate protein as determined by the Bradford protein assay (Bio-Rad Laboratories, Hercules, CA, USA).

2.13. Statistical Analysis

The statistical analysis was performed using GraphPad Prism 7 (GraphPad Software, San Diego, CA, USA) using an unpaired *t*-test or one- or two-way ANOVA with Dunnett or Sidak multiple comparison tests when appropriate. The Pearson correlation coefficient was calculated for correlation analyses. Data are given as mean values ± SEM, unless otherwise stated. A p-value of <0.05 was considered significant.

3. Results

3.1. A Mouse Model of Dietary-Induced Diabesity

To study the effect of the dietary-induced abundance of FFA on the expression of Glrx5 in the islets of Langerhans in C57BL/6J-mice, the mice were switched from a high-fat diet to standard chow and back during the study period (as described in Materials and Methods and Figure 1). The control mice gained weight physiologically as they aged, whereas the animals from the experimental group gained weight quickly when fed the HFD. During the switch to the CD from 20 to 23 weeks of age, a rapid weight loss was observed before another increase in body weight after the second phase of the HFD. After both stages with the HFD at 20 and 27 weeks, the mice exhibited a significantly higher body weight compared to the control group (27.85 ± 1.59 vs. 37.3 ± 5.89 g, *** $p < 0.001$ at 20 weeks; 28.8 ± 3.19 vs. 43 ± 3 g, *** $p < 0.001$ at 27 weeks, Figure 2A). Along with this, the amount of FFA in the blood of the experimental animals increased from 20 weeks of age onwards, especially after both stages of HFD feeding at 20 and 27 weeks of age (1.24 ± 0.32 vs. 2.32 ± 0.06 mM, * $p < 0.05$ at 20 weeks; 1.43 ± 1.07 vs. 2.77 ± 0.23 mM, ** $p < 0.005$ at 27 weeks, Figure 2C). The fasting blood glucose levels were only significantly elevated at the end of the study at 27 weeks of age (78.56 ± 20.53 vs. 102.6 ± 22.76 mg/dL, ** $p < 0.005$, Figure 2B). The dynamic glucose metabolism, as measured by IPGTT, showed obvious signs of impairment after HFD feeding. Although no difference between respective blood glucose values was detected when both groups of mice were compared at the beginning of the study at seven weeks of age (AUC 18,732 ± 1518 vs. 21,107 ± 1880 mg/dL x min, n.s., Figure 2E), HFD-fed mice showed significantly higher glucose levels at 20 weeks of age (AUC 22,667 ± 1610 vs. 29,403 ± 1512 mg/dL x min, * $p < 0.05$, Figure 2F) as a sign of an impaired first phase of glucose-stimulated insulin secretion (GSIS). When switched to the CD, this difference could no longer be detected (AUC 24,703 ± 1604 vs. 26,180 ± 1761 mg/dL x min, n.s., Figure 2G). After four more weeks of HFD feeding, the respective mice exhibited significantly worse glycemic control (AUC 25,377 ± 1732 vs. 32,393 ± 2211 mg/dL x min, * $p < 0.05$, Figure 2H). Neither pancreas weight (Figure 2D) nor islet count (data not shown) differed significantly between both groups, although a trend in higher organ weight and increased islet count was detected towards the end of the study.

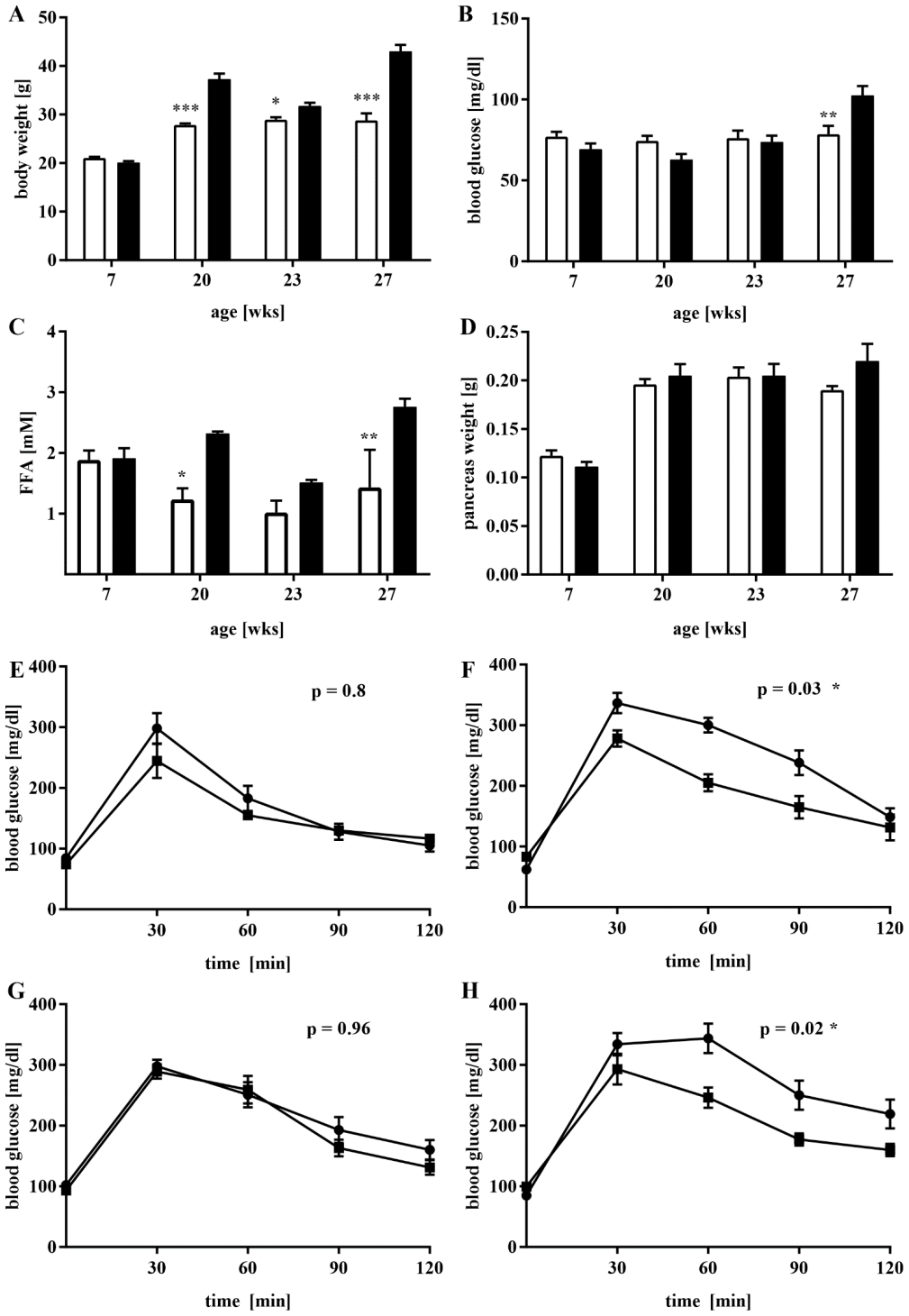

Figure 2. Fasting and dynamic blood glucose levels, body weight, free fatty acid levels, and pancreas weight of the research animals. IPGTT and euthanasia was conducted before dietary changes and at the end of the experimental procedure at 7, 20, 23, and 27 weeks of age. Fasting blood glucose levels and body weight were monitored every two weeks until 20 weeks of age, and then weekly. (**A**) Body weight and (**B**) fasting blood glucose values at 7, 20, 23, and 27 weeks of age; n = 5–33 mice/timepoint/group. (**C**) Blood FFA levels as determined by ELISA; n = three mice/timepoint/group. (**D**) Pancreas weight; n = six mice/timepoint/group. (**E**–**H**) IPGTT results at (**E**) 7, (**F**) 20, (**G**) 23, and (**H**) 27 weeks of age; n = five mice/timepoint/group. For each graph, the white bars represent the controls, and the black bars represent the experimental group. *** denotes $p < 0.001$, ** $p < 0.005$, and * $p < 0.05$ ((**A**–**D**): two-way ANOVA, (**E**–**H**): unpaired t-test).

3.2. The Islet Glrx5 Content Is Diet-Dependent

Having ensured a diabese phenotype, we aimed to study the effects of dietary changes on islet Glrx5 content. Immunohistology was employed on harvested pancreases and mRNA expression was assessed in isolated islets. The optical assessment of the islets of Langerhans was conducted. No obvious difference in islet morphology and size could be detected when age-matched HFD and control animals were compared (Figure 3A–C controls vs. D–F HFD at 7 weeks, J–L controls vs. M–O HFD at 20 weeks, S–U controls vs. V–X HFD at 23 weeks, AB–AD controls vs. AE–AG HFD at 27 weeks). The quantification of the mean islet area by immunohistology confirmed this observation, revealing no significant difference between both groups of mice (data not shown). The Glrx5 staining pattern indicated a loss of Glrx5 staining in terms of density and intensity in islets of HFD mice throughout the study period. The quantification showed a significantly reduced Glrx5-to-insulin ratio in HFD animals from 20 weeks of age onwards when compared with controls. Interestingly, after switching the diet from the HFD to CD from 20 to 23 weeks of age, HFD mice's islets presented a recovery of Glrx5 content followed by a pronounced decrease towards the end of the study after 4 more weeks of HFD feeding (Glrx5-to-insulin ratio: 0.107 ± 0.103 vs. 0.102 ± 0.076, n.s. at 7 weeks; 0.135 ± 0.212 vs. 0.02 ± 0.019, **** $p < 0.0001$ at 20 weeks; 0.147 ± 0.104 vs. 0.056 ± 0.081, ** $p < 0.005$ at 23 weeks; 0.048 ± 0.058 vs. 0.008 ± 0.007, **** $p < 0.0001$ at 27 weeks, Figure 3G,P,Y,AH). *Glrx5* mRNA expression was found to follow a similar pattern. The HFD group exhibited a significantly lower expression after both stages of HFD feeding at 20 and 27 weeks of age. The switch to CD resulted in a recovery of expression as measured at 23 weeks of age (fold change control vs. HFD group 0.69-fold, n.s., at 7 weeks, 2.91-fold, * $p < 0.05$, at 20 weeks, 1.32-fold, n.s., at 23 weeks, and 3.29-fold, * $p < 0.05$, at 27 weeks, Figure 3H,Q,Z,AI). *Ins1* mRNA expression correlated with this pattern and the diabese phenotype (fold change control vs. HFD group 1.64-fold, n.s., at 7 weeks, 2.95-fold, * $p < 0.05$, at 20 weeks, 0.49-fold, n.s., at 23 weeks, and 1.43-fold, * $p < 0.05$, at 27 weeks, Figure 3I,R,AA,AJ).

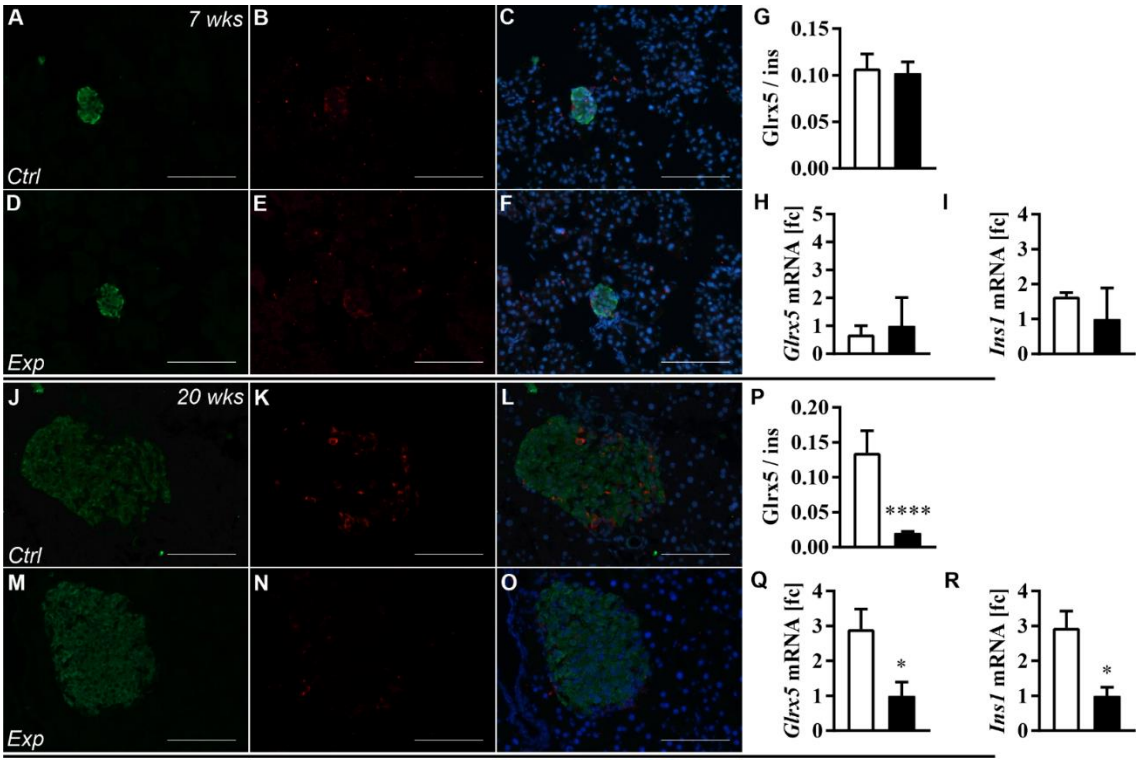

Figure 3. *Cont.*

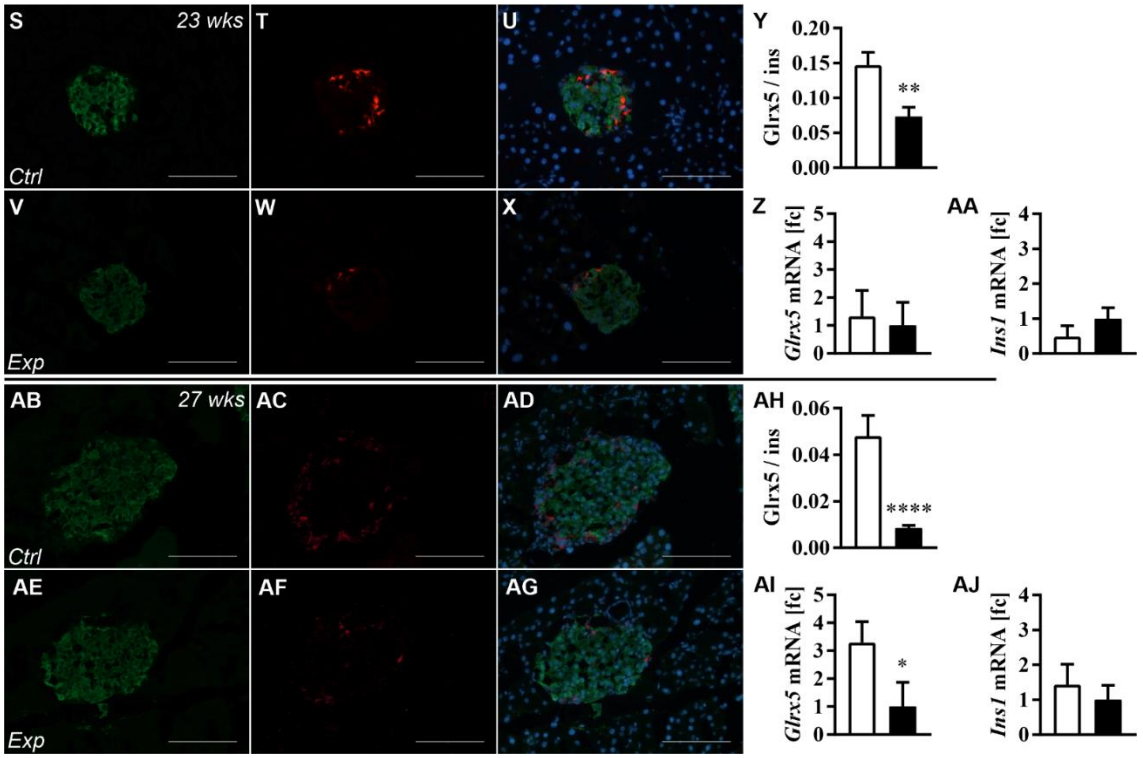

Figure 3. Immunohistological and Ins1 and Glrx5 mRNA expression analysis. The immunohistological staining patterns of insulin and Glrx5 were analyzed at 7, 20, 23, and 27 weeks of age. Glrx5 staining was quantified by calculating the ratio of the Glrx5/insulin staining area. The mRNA expression of *Ins1* and *Glrx5* was studied using qRT-PCR. (**A**–**F**, **J**–**O**, **S**–**X**, **AB**–**AG**) Representative images taken from the immunohistological analysis of insulin and Glrx5 presenting size-matched representative islets of both groups of mice ((**A**–**C**) controls, 7 weeks; (**D**–**F**) HFD, 7 weeks; (**J**–**L**) controls, 20 weeks; (**M**–**O**) HFD, 20 weeks; (**S**–**U**) controls, 23 weeks; (**V**–**X**) HFD, 23 weeks; (**AB**–**AD**) controls, 27 weeks; (**AE**–**AG**) HFD, 27 weeks). Green = insulin, red = Glrx5, blue = nuclei. Scale bars represent 100 µm. Images were taken at 200× magnification. n = 33–67 islets of three to four mice/timepoint/group. (**G**,**P**,**Y**,**AH**) The quantification of Glrx5 staining. (**H**,**Q**,**Z**,**AI**) The islet mRNA expression of Glrx5 and (**I**,**R**,**AA**,**AJ**) of Ins1 given as fold change controls vs. HFD for each time point. n = six mice/timepoint/group. For each graph, the white bars represent the controls, and the black bars represent the experimental group. **** denotes $p < 0.0001$, ** $p < 0.005$, and * $p < 0.05$ (two-way ANOVA).

3.3. Elevated ROS Production and Impaired GSIS in HFD-Fed Mice

ROS production was significantly increased in the islets of the HFD group at 20 and 23 weeks of age (99.8 ± 24.5 vs. 148.5 ± 29.5%, **** $p < 0.0001$ at 20 weeks; 88 ± 15 vs. 131.7 ± 24.2%, **** $p < 0.0001$ at 23 weeks, Figure 4A). We decided to conduct a glucose stimulation and protein analysis instead of ROS measurements at 27 weeks of age. The amount of insulin in the islets of HFD mice showed a non-significant increase when stimulated with glucose, whereas control islets featured a significant drop in cellular insulin (0.07 ± 0.02 vs. 0.2 ± 0.01 µg/mg, ** $p < 0.005$, Figure 4B). The level of insulin in the culture medium increased after stimulating the control islets, whereas stimulating the experimental group's islets even showed a decrease (0.07 ± 0.004 vs. 0.05 ± 0.05 µg/mg, * $p < 0.05$, Figure 4C). Results indicate elevated basal insulin secretion and confirm defective GSIS, as detected in IPGTT.

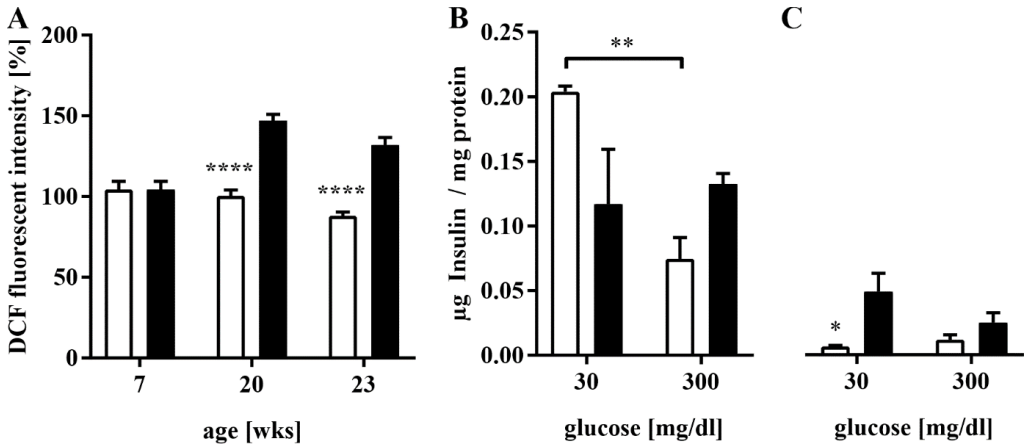

Figure 4. Pancreatic islet ROS production and glucose stimulation. ROS were quantified in pancreatic islets from animals of both groups at 7, 20, and 23 weeks of age by DCFH-DA staining and analysis with a confocal microscope. The glucose stimulation and consecutive measurements of insulin in islet lysates and the medium were conducted in both groups at 27 weeks of age. (**A**) The ROS production of primary islets at 7, 20, and 23 weeks of age. n = 63–65 islets of three mice/timepoint/group. (**B**,**C**) The amount of insulin in the (**B**) lysates and (**C**) culture medium of the islets before and after stimulation with 300 mg/dL glucose. n = five islets of three mice/timepoint/group, four runs. For each graph, the white bars represent the controls, and the black bars represent the experimental group. **** denotes $p < 0.0001$, ** $p < 0.005$, and * $p < 0.05$ (two-way ANOVA).

3.4. FFA Mediate the Loss of Glrx5 in MIN6 Cells

To model the observed fluctuation of blood FFA levels in vitro, we pre-incubated MIN6 cells with 400 µM palmitate for 48 h followed by 1 h of starvation and consecutive exposure to glucose (3 and 16 mM) for 24 h. Although the Glrx5 protein level was not significantly affected by exposure to glucose alone, pre-treated cell glucose dependently featured a significantly mitigated level of Glrx5 (82.8 ± 9.5 vs. 46.3 ± 11.8 pg/mg, * $p < 0.05$ at 3 mM glucose, Figure 5A). The amount of insulin in the medium was significantly lower in pre-treated cells, indicating a correlation between insulin secretion and Glrx5 (0.56 ± 0.14 vs. 0.14 ± 0.03 µg/mg, ** $p < 0.005$ at 16 mM glucose, Figure 5B). The exposure to oleic acid alone led to similar results. In a dose-dependent manner, the amount of Glrx5 (91.32 ± 13.11 vs. 43.03 ± 10.91 vs. 20.82 ± 7.56 vs. 8.76 ± 0.85 pg/mg, **** $p < 0.0001$, Figure 5C) as well as the amount of insulin in the medium (0.38 ± 0.2 vs. 0.08 ± 0.01 vs. 0.03 ± 0.01 vs. 0.02 ± 0.002 µg/mg, ** $p < 0.005$ at 0.75 mM, *** $p < 0.001$ at 1.5 and 3 mM, Figure 5D) decreased. Similar results were observed for palmitic acid (data not shown). To separate the effects of FFA and hyperglycemia on Glrx5 in β-cells, incubation with glucose in varying concentrations for 24 h was conducted after 2 h of starvation. No significant impact on Glrx5 was detected (41.17 ± 13.93 vs. 58.63 ± 14.24 vs. 48.44 ± 2.43 vs. 58.05 ± 19.05 vs. 40.11 ± 3.85 pg/mg, n.s., Figure 5E), whereas insulin in the culture medium increased (0.074 ± 0.002 vs. 0.089 ± 0.001 vs. 0.094 ± 0.004 vs. 0.091 ± 0.003 vs. 0.093 ± 0.005 µg/mg, * $p < 0.05$ at 5 mM glucose, *** $p < 0.001$ at 10 mM glucose, ** $p < 0.005$ at 20 and 30 mM glucose, Figure 5F). Since inflammation is an important factor in the diabetic metabolism, we also studied the effect of inflammatory cytokines. Cells were exposed to a cytokine mix consisting of 10 ng/mL TNF-α, 5 ng/mL IL-1β, and 100 ng/mL IFN-γ [30] for 24 and 48 h, respectively. As displayed in Figure 5G, no significant change in Glrx5 was observed upon treatment (385.1 ± 190.6 vs. 352 ± 154.9 pg/mg after 24 h, 275.1 ± 57.64 vs. 268.4 ± 84.34 pg/mg after 48 h, n.s.). The insulin in the culture medium declined non-significantly (0.16 ± 0.07 vs. 0.08 ± 0.02 µg/mg at 24 h; 0.14 ± 0.1 vs. 0.11 ± 0.05 µg/mg at 48 h, n.s., Figure 5H).

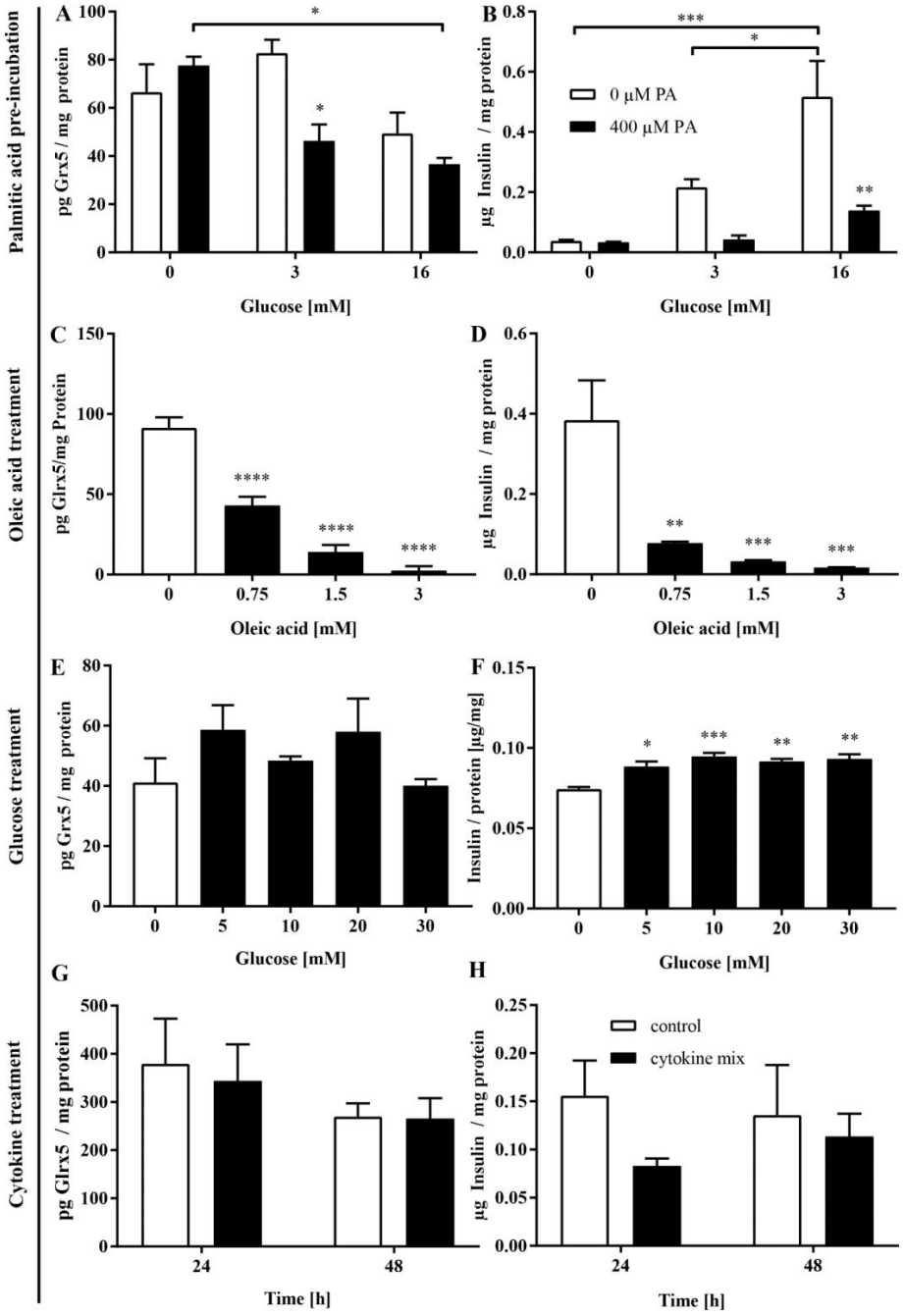

Figure 5. MIN6 Glrx5 level and insulin secretion. (**A**,**B**) Diabetic conditions were modelled in MIN6 cells employing a 48 h period of pre-incubation with 400 µM palmitic acid (PA) followed by 1 h of starvation and exposure to increasing concentrations of glucose for 24 h. (**C**,**D**) Furthermore, we employed a treatment with 0.75, 1.5, or 3 mM oleic acid for 24 h, (**E**,**F**) and a 2 h period of starvation followed by exposure to 5, 10, 20, or 30 mM glucose for 24 h, or (**G**,**H**) a cytokine mix (10 ng/mL TNF-α, 5 ng/mL IL-1β, and 100 ng/mL IFN-γ) for 24 or 48 h, respectively. The protein level of Glrx5 in lysate and insulin in the culture medium of β-cells exposed to (**A**,**B**) glucose for 24 h after and without pre-incubation with 400 µM palmitate and 1h of starvation; (**C**,**D**) oleic acid for 24 h; (**E**,**F**) glucose for 24 h after 2 h of starvation; and (**G**,**H**) a mix of 10 ng/mL TNF-α, 5 ng/mL IL-1β, and 100 ng/mL IFN-γ for 24 or 48 h. Insulin and Glrx5 were measured by ELISA and normalized by total protein. The white bars represent the controls, and the black bars represent the (pre)-treated cells. n = 3–5. **** denotes $p < 0.0001$, *** $p < 0.001$, ** $p < 0.005$, and * $p < 0.05$ (one-/two-way ANOVA).

The correlation between MIN6 insulin and Glrx5 content on a single-cell level was studied by employing immunocytochemistry. The quantification of insulin staining correlated well with Glrx5 staining both without treatment (Figure 6A, r = 0.78, **** $p < 0.0001$) and after 24 h of exposure to 1.5 mM oleic acid (Figure 6B, r = 0.83, **** $p < 0.0001$).

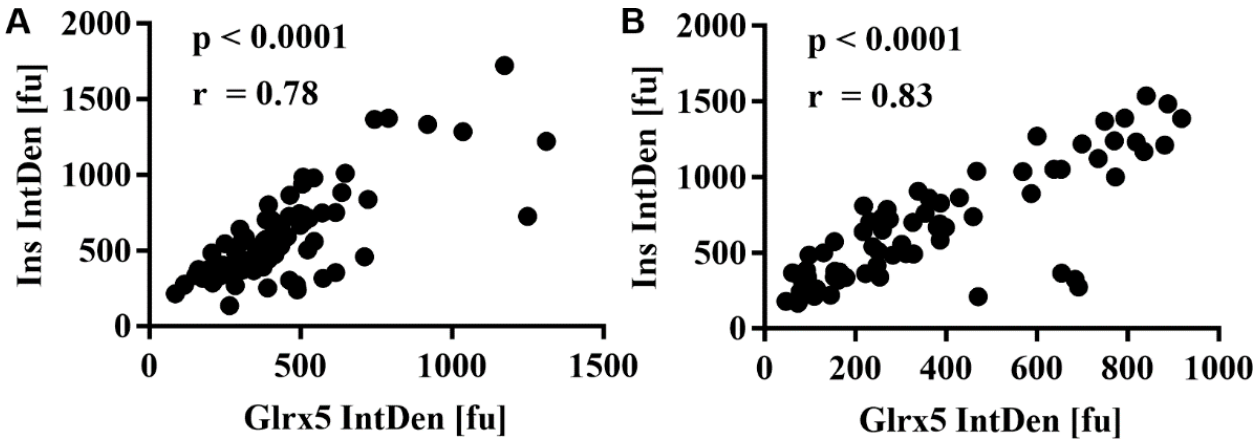

Figure 6. Cytological analysis of MIN6 insulin and Glrx5 content. MIN6 cells exposed to 1.5 mM oleic acid for 24 h were stained for insulin and Glrx5 and compared with the controls. Staining was quantified by measuring the integrated density using ImageJ software. The values for insulin and Glrx5 were correlated. (**A**) The correlation of insulin with Glrx5 in the control cells and (**B**) after treatment with 1.5 mM oleic acid for 24 h. $n = 4$ (9–35 cells/run, Pearson).

3.5. The Loss of Glrx5 Is Correlated with Mitigated ATP and Impaired O_2 Flux in the Respiratory Chain

The impact of diminished levels of Glrx5 on the respiratory chain was analyzed by the available amount of ATP in MIN6 cells. A dose-dependent exposure to oleic acid as well as pre-incubation with 400 µM palmitate led to a significant decrease in ATP (3.99 ± 0.87 vs. 2.12 ± 0.63 vs. 1.6 ± 0.45 vs. 0.89 ± 0.25 µM, **** $p < 0.0001$, Figure 7A and 3.6 ± 0.43 vs. 2.69 ± 0.46 µM at 3 mM glucose, ** $p < 0.005$, Figure 7B). To gain insight into the reason behind this energy deficiency, we examined the O_2 flux through the respiratory chain. Endogenous respiration was significantly increased in treated cells, indicating an increased substrate turnover which was less efficient due to increased uncoupling already in the basal state (650.5 ± 41.86 vs. 727 ± 109 pmol/(s*U), * $p < 0.05$, Figure 7C). The maximum possible O_2 flux was measured upon saturation with respective substrates and revealed a significantly decreased maximum capacity of oxidative phosphorylation in treated cells (2935 ± 537.2 vs. 2340 ± 399.4 pmol/(s*U), *** $p < 0.001$, Figure 7D). Maximum electron transfer capacity, analyzed after adding an uncoupler, was also significantly lower after exposure to oleic acid (3672 ± 784 vs. 3173 ± 603.1 pmol/(s*U), *** $p < 0.001$, Figure 7E). Ultimately, the O_2 flux through both complex I and II was significantly diminished (1332 ± 230 vs. 984.5 ± 156.7 pmol/(s*U), *** $p < 0.001$, Figure 7F, 2537 ± 394.7 vs. 2057 ± 370 pmol/(s*U), *** $p < 0.001$, Figure 7G), whereas complex IV was not affected (2516 ± 416.8 vs. 2437 ± 375 pmol/(s*U), n.s., Figure 7H).

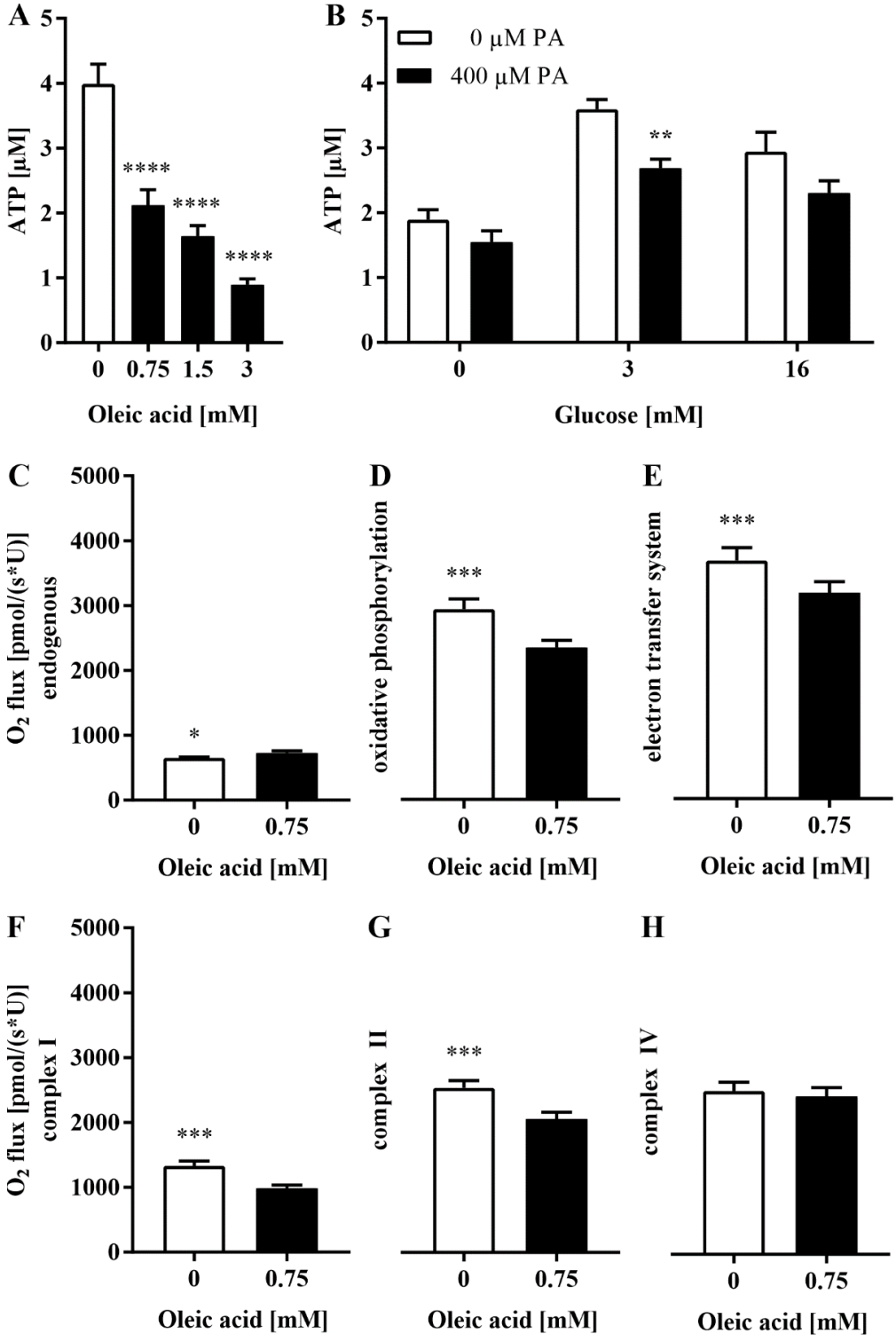

Figure 7. ATP production and the O_2 flux in the respiratory chain after FFA treatment. Cellular ATP levels were analyzed employing a luciferase-based bioluminescence assay. Respiratory states were measured with an Oxygraph and an O_2 probe. (**A**) ATP after exposure to oleic acid for 24 h or (**B**) after pre-incubation with 400 µM palmitate, 1 h of starvation, and exposure to glucose. (**C**–**H**) The O_2 flux in the respiratory chain after exposure to 0.75 mM oleic acid for 24 h. The white bars represent the controls, and the black bars represent the (pre-)treated cells. $n = 12$. **** denotes $p < 0.0001$, *** $p < 0.001$, ** $p < 0.005$ and * $p < 0.05$ (one-way ANOVA/unpaired *t*-test).

4. Discussion

It is acknowledged that chronic hyperglycemia and elevated FFA exert deleterious effects on the pancreatic β-cell, and continuous advances in research have identified numerous underlying pathways and mechanisms [31,32]. In particular, mitochondria, which are essential for insulin secretion due to their crucial role in fuel metabolism, are affected significantly, presenting a severely altered expression of carrier proteins [33], morphology [34], and increased volume [35]. Little is known about the role of mitochondrial glutaredoxins. We have previously reported a loss of Glrx5 in islets of monogenetically diabese db/db-mice [21,25]. However, this model is hardly comparable with type 2 diabetes mellitus, as it occurs in human subjects, since this complex metabolic disorder is of a polygenetic and multifactorial origin. In this study, we could demonstrate that the loss of Glrx5 is also apparent in an HFD-induced murine model of diabesity. Moreover, standard chow led to the reconstitution of islet Glrx5 and ameliorated glucose tolerance (Figures 2 and 3). Serum FFA levels correlated with the diabese phenotype and the amount of islet Glrx5. This leads to the conclusion that FFA mediate the loss of Glrx5 in vivo. This hypothesis was confirmed in vitro, where the exposure of MIN6 cells to FFA led to a loss of Glrx5 concomitant with a decrease in insulin secretion, while treatment with glucose or inflammatory cytokines had no such effect (Figures 5 and 6).

It is generally recognized that FFA can exert both positive and negative effects on the β-cell's viability and insulin secretion, and are dependent on their carbon chain length and concentration. Furthermore, exposure time and the presence of hyperglycemia or inflammatory cytokines modulate their effects. An acute increase in FFA is linked to increased β-cell mass and insulin secretion mediated through the FFA receptor GPR40/FFAR [36,37] and PPAR [38]. The chronic elevation of FFA fuels insulin resistance and exerts detrimental effects on insulin secretion [39], gene expression [40], and β-cell survival [41] as well, mostly due to increased oxidative and endoplasmic reticulum stress, GLUT translocation, and inflammation [7,42]. However, the impact of FFA on basal insulin release and GSIS is differential. GSIS is inhibited but basal insulin is even increased [39,43,44] due to the decreased activity of citrate synthase which ultimately results in increased hexokinase activity, enhancing β-cell glucose usage [45]. Hyperglycemia enhances the detrimental effects of FFA since the respiratory chain uncoupling by UCP2 requires high membrane potential as reached at high glucose concentrations [46]. Excessive uncoupling favors mitochondrial dysfunction. Elevated glucose turnover inhibits AMPK [47] and increases the concentration of malonyl-CoA. An abundance of malonyl-CoA diminishes the oxidation of FFA by inhibiting the mitochondrial fatty acid transporter CPT1 [48]. The subsequent accumulation of FFA activates caspases [49], promoting apoptosis. Consistently, our findings show both enhanced ROS production and elevated basal insulin secretion with the failure of GSIS in pancreatic islets (Figure 4) after the HFD-induced abundance of FFA. In human subjects with normal glucose tolerance, elevated fasting FFA levels were associated with decreased insulin secretion and the risk of developing impaired glucose tolerance [50].

Our data indicate a significant loss of ATP and a decrease in oxidative phosphorylation and O_2 flux through the respiratory chain (Figure 7) as correlates for mitochondrial dysfunction. Similar observations were made in islets of C57BL/6J after 12 weeks of high-fat diet feeding. Islets featured diminished glucose oxidation upon stimulation with glucose and increased palmitate oxidation in the basal state, indicating a switch in substrates during this insulin-resistant state [35]. Comparable findings were achieved in human islets [34]. The availability of ATP is a prerequisite for insulin secretion, but GSIS requires mitochondrial respiration [51,52]. The main source of ATP production depends on glucose responsiveness in MIN6 cells. Less responsive MIN6 cells allocate ATP mainly through nonoxidative pathways [53], whereas insulin secretion is dependent on oxidative phosphorylation [54,55]. This was demonstrated for MIN6 cells which become less sensible to glucose and have diminished ATP content as well as low lipid oxidation at high passages [56]. In vivo studies even identified heterogenic islet populations marked by varying glucose sensitivity and mitochondrial respiration in mice and humans [57].

Most interestingly, the O_2 flux was significantly impaired in both complex I and II, which both rely on Fe/S clusters, but not in complex IV, which does not contain any Fe/S clusters (Figure 7). Glrx5 is known to be essential for the activity of Fe/S enzymes [58,59]. Camaschella et al. described diminished cytosolic and mitochondrial aconitase activity and expression in a Glrx5-deficient human subject [16] which was also found in murine osteoblasts [12]. Corbett et al. had previously related the loss of mitochondrial aconitase activity with cytokine-induced NO production and abolished insulin secretion in rat β-cell and human islets [60–62]. Diminished Fe/S cluster biosynthesis was shown to mitigate the function of Cdkal1, an Fe/S cluster enzyme crucial for proinsulin processing in iron-regulatory protein 2-deficient mice and rat insulinoma cells [63]. These data indicate that the impact of iron metabolism on insulin production and secretion is more complex and not limited to the abundance of free iron, which is well known to act in a diabetogenic manner. Rather, this suggests that the impaired Fe/S clusters might function as a possible link between mitigated mitochondrial function and the deprivation of Glrx5.

There are limitations to our study. Although our data indicate a 90% reduction in Glrx5 after exposure to oleic acid in MIN6 cells, the absolute amount of cellular Glrx5 was very low and we did not study iron metabolism in our models; thus, the question of whether Glrx5 is a cause of mitochondrial dysfunction and impaired insulin secretion remains open. General toxic effects of diabetic stressors on the mitochondria might account for our observations. Thus, further studies, especially employing models with Glrx5 knockout and overexpression and investigations focusing on human material, need to be conducted to further characterize the significance of Glrx5 for the pancreatic β-cell.

5. Conclusions

We deliver further evidence for the role of Glrx5 in β-cell deficiency in type 2 diabetes mellitus. Our data indicate that Glrx5 is downregulated by FFA and that recovery can be achieved by diet. We propose mitochondrial dysfunction as a possible underlying mechanism linking the loss of Glrx5 to mitigated insulin secretion.

Author Contributions: Conceptualization, S.F.P. and T.L.; methodology, S.F.P., A.R., D.R., R.G., F.S., H.S., G.P.E. and T.L.; software, S.F.P., A.R., D.R., R.G., F.S., H.S., G.P.E. and T.L.; validation, S.F.P., A.R. and T.L.; formal analysis, S.F.P., A.R., D.R., L.B. and N.L.; investigation, S.F.P., A.R., D.R., L.B., N.L., F.S. and H.S.; resources, H.S., G.P.E. and T.L.; data curation, S.F.P. and A.R.; writing—original draft preparation, S.F.P.; writing—review and editing, S.F.P., A.R., D.R., L.B., N.L., M.Z., R.G., F.S., H.S., G.P.E. and T.L.; visualization, S.F.P.; supervision, G.P.E. and T.L.; project administration, S.F.P. and T.L.; funding acquisition, S.F.P. and T.L. All authors have read and agreed to the published version of the manuscript.

Funding: This research was funded by a research grant of the University Medical Center Giessen and Marburg (UKGM), grant number 18/2019 GI.

Institutional Review Board Statement: Animal research was carried out in accordance with recommendations of our institutional animal welfare officer, the Chair of Animal Welfare of the Justus Liebig University, Giessen, and the Regional Administrative Council of Giessen, the Veterinary Department, under codes GI 20/11 No. G 3/2017 and No. G 48/2018. Both committees approved the protocol. All experiments were performed in accordance with the German Animal Welfare Law.

Informed Consent Statement: Not applicable.

Data Availability Statement: All data are included within this manuscript.

Acknowledgments: The authors thank Gundula Hertl, Birte Hussmann, and Doris Erb for their expert advice and technical assistance.

Conflicts of Interest: The authors declare no conflict of interest. The funders had no role in the design of the study; in the collection, analyses, or interpretation of data; in the writing of the manuscript, or in the decision to publish the results.

References

1. Barlow, J.; Solomon, T.P.J.; Affourtit, C. Pro-inflammatory cytokines attenuate glucose-stimulated insulin secretion from INS-1E insulinoma cells by restricting mitochondrial pyruvate oxidation capacity—Novel mechanistic insight from real-time analysis of oxidative phosphorylation. *PLoS ONE* **2018**, *13*, e0199505. [CrossRef] [PubMed]
2. Thiébaud, D.; DeFronzo, R.A.; Jacot, E.; Golay, A.; Acheson, K.; Maeder, E.; Jéquier, E.; Felber, J.P. Effect of long chain triglyceride infusion on glucose metabolism in man. *Metabolism* **1982**, *31*, 1128–1136. [CrossRef]
3. Nishikawa, T.; Edelstein, D.; Du, X.L.; Yamagishi, S.; Matsumura, T.; Kaneda, Y.; Yorek, M.A.; Beebe, D.; Oates, P.J.; Hammes, H.P.; et al. Normalizing mitochondrial superoxide production blocks three pathways of hyperglycaemic damage. *Nature* **2000**, *404*, 787–790. [CrossRef] [PubMed]
4. Ma, Z.; Wirström, T.; Borg, L.A.H.; Larsson-Nyrén, G.; Hals, I.; Bondo-Hansen, J.; Grill, V.; Björklund, A. Diabetes reduces beta-cell mitochondria and induces distinct morphological abnormalities, which are reproducible by high glucose in vitro with attendant dysfunction. *Islets* **2012**, *4*, 233–242. [CrossRef] [PubMed]
5. Elsner, M.; Gehrmann, W.; Lenzen, S. Peroxisome-generated hydrogen peroxide as important mediator of lipotoxicity in insulin-producing cells. *Diabetes* **2011**, *60*, 200–208. [CrossRef]
6. Solinas, G.; Naugler, W.; Galimi, F.; Lee, M.S.; Karin, M. Saturated fatty acids inhibit induction of insulin gene transcription by JNK-mediated phosphorylation of insulin-receptor substrates. *Proc. Natl. Acad. Sci. USA* **2006**, *103*, 16454–16459. [CrossRef]
7. Maedler, K.; Spinas, G.A.; Dyntar, D.; Moritz, W.; Kaiser, N.; Donath, M.Y. Distinct effects of saturated and monounsaturated fatty acids on beta-cell turnover and function. *Diabetes* **2001**, *50*, 69–76. [CrossRef]
8. Lee, K.M.; Seo, Y.J.; Kim, M.K.; Seo, H.A.; Jeong, J.Y.; Choi, H.S.; Lee, I.K.; Park, K.G. Mediation of glucolipotoxicity in INS-1 rat insulinoma cells by small heterodimer partner interacting leucine zipper protein (SMILE). *Biochem. Biophys. Res. Commun.* **2012**, *419*, 768–773. [CrossRef]
9. Lill, R.; Dutkiewicz, R.; Freibert, S.A.; Heidenreich, T.; Mascarenhas, J.; Netz, D.J.; Paul, V.D.; Pierik, A.J.; Richter, N.; Stümpfig, M.; et al. The role of mitochondria and the CIA machinery in the maturation of cytosolic and nuclear iron-sulfur proteins. *Eur. J. Cell Biol.* **2015**, *94*, 280–291. [CrossRef]
10. Stehling, O.; Wilbrecht, C.; Lill, R. Mitochondrial iron-sulfur protein biogenesis and human disease. *Biochimie* **2014**, *100*, 61–77. [CrossRef]
11. Braymer, J.J.; Lill, R. Iron-sulfur cluster biogenesis and trafficking in mitochondria. *J. Biol. Chem.* **2017**, *292*, 12754–12763. [CrossRef] [PubMed]
12. Linares, G.R.; Xing, W.; Govoni, K.E.; Chen, S.T.; Mohan, S. Glutaredoxin 5 regulates osteoblast apoptosis by protecting against oxidative stress. *Bone* **2009**, *44*, 795–804. [CrossRef] [PubMed]
13. Rodríguez-Manzaneque, M.T.; Ros, J.; Cabiscol, E.; Sorribas, A.; Herrero, E. Grx5 glutaredoxin plays a central role in protection against protein oxidative damage in Saccharomyces cerevisiae. *Mol. Cell Biol.* **1999**, *19*, 8180–8190. [CrossRef] [PubMed]
14. Wingert, R.A.; Galloway, J.L.; Barut, B.; Foott, H.; Fraenkel, P.; Axe, J.L.; Weber, G.J.; Dooley, K.; Davidson, A.J.; Schmid, B.; et al. Deficiency of glutaredoxin 5 reveals Fe-S clusters are required for vertebrate haem synthesis. *Nature* **2005**, *436*, 1035–1039. [CrossRef] [PubMed]
15. Ye, H.; Jeong, S.Y.; Ghosh, M.C.; Kovtunovych, G.; Silvestri, L.; Ortillo, D.; Uchida, N.; Tisdale, J.; Camaschella, C.; Rouault, T.A. Glutaredoxin 5 deficiency causes sideroblastic anemia by specifically impairing heme biosynthesis and depleting cytosolic iron in human erythroblasts. *J. Clin. Investig.* **2010**, *120*, 1749–1761. [CrossRef] [PubMed]
16. Camaschella, C.; Campanella, A.; De Falco, L.; Boschetto, L.; Merlini, R.; Silvestri, L.; Levi, S.; Iolascon, A. The human counterpart of zebrafish shiraz shows sideroblastic-like microcytic anemia and iron overload. *Blood* **2007**, *110*, 1353–1358. [CrossRef] [PubMed]
17. Cooksey, R.C.; Jones, D.; Gabrielsen, S.; Huang, J.; Simcox, J.A.; Luo, B.; Soesanto, Y.; Rienhoff, H.; Abel, E.D.; McClain, D.A. Dietary iron restriction or iron chelation protects from diabetes and loss of beta-cell function in the obese (ob/ob lep-/-) mouse. *Am. J. Physiol. Endocrinol. Metab.* **2010**, *298*, E1236–E1243. [CrossRef]
18. Stockwell, B.R.; Friedmann Angeli, J.P.; Bayir, H.; Bush, A.I.; Conrad, M.; Dixon, S.J.; Fulda, S.; Gascón, S.; Hatzios, S.K.; Kagan, V.E.; et al. Ferroptosis: A Regulated Cell Death Nexus Linking Metabolism, Redox Biology, and Disease. *Cell* **2017**, *171*, 273–285. [CrossRef]
19. Stefanini, M.; De Martino, C.; Zamboni, L. Fixation of ejaculated spermatozoa for electron microscopy. *Nature* **1967**, *216*, 173–174. [CrossRef]
20. Lai, Y.; Schneider, D.; Kidszun, A.; Hauck-Schmalenberger, I.; Breier, G.; Brandhorst, D.; Brandhorst, H.; Iken, M.; Brendel, M.D.; Bretzel, R.G.; et al. Vascular endothelial growth factor increases functional beta-cell mass by improvement of angiogenesis of isolated human and murine pancreatic islets. *Transplantation* **2005**, *79*, 1530–1536. [CrossRef]
21. Petry, S.F.; Sharifpanah, F.; Sauer, H.; Linn, T. Differential expression of islet glutaredoxin 1 and 5 with high reactive oxygen species production in a mouse model of diabesity. *PLoS ONE* **2017**, *12*, e0176267. [CrossRef] [PubMed]
22. Taha, A.; Sharifpanah, F.; Wartenberg, M.; Sauer, H. Omega-3 and Omega-6 polyunsaturated fatty acids stimulate vascular differentiation of mouse embryonic stem cells. *J. Cell Physiol.* **2020**, *235*, 7094–7106. [CrossRef] [PubMed]
23. Bolt, H.N.; Hengstler, J.G.; Stewart, J. Analyses of reactive oxygen species. *EXCLI J.* **2009**, *8*, 241–245.
24. Lai, Y.; Brandhorst, H.; Hossain, H.; Bierhaus, A.; Chen, C.; Bretzel, R.G.; Linn, T. Activation of NFkappaB dependent apoptotic pathway in pancreatic islet cells by hypoxia. *Islets* **2009**, *1*, 19–25. [CrossRef]

25. Petry, S.F.; Sun, L.M.; Knapp, A.; Reinl, S.; Linn, T. Distinct Shift in Beta-Cell Glutaredoxin 5 Expression Is Mediated by Hypoxia and Lipotoxicity Both In Vivo and In Vitro. *Front. Endocrinol.* **2018**, *9*, 84. [CrossRef]
26. Burgess, A.; Vigneron, S.; Brioudes, E.; Labbé, J.C.; Lorca, T.; Castro, A. Loss of human Greatwall results in G2 arrest and multiple mitotic defects due to deregulation of the cyclin B-Cdc2/PP2A balance. *Proc. Natl. Acad. Sci. USA* **2010**, *107*, 12564–12569. [CrossRef]
27. Gnaiger, E. Mitochondrial pathways and respiratory control: An introduction to OXPHOS analysis, 5th ed. *Bioenerg. Commun.* **2020**, *2020*, 2.
28. Stadlmann, S.; Renner, K.; Pollheimer, J.; Moser, P.L.; Zeimet, A.G.; Offner, F.A.; Gnaiger, E. Preserved coupling of oxidative phosphorylation but decreased mitochondrial respiratory capacity in IL-1beta-treated human peritoneal mesothelial cells. *Cell Biochem. Biophys.* **2006**, *44*, 179–186. [CrossRef]
29. Pohland, M.; Hagl, S.; Pellowska, M.; Wurglics, M.; Schubert-Zsilavecz, M.; Eckert, G.P. MH84: A Novel g-Secretase Modulator/PPARg Agonist–Improves Mitochondrial Dysfunction in a Cellular Model of Alzheimer's Disease. *Neurochem. Res.* **2016**, *41*, 231–242. [CrossRef]
30. Hanschmann, E.M.; Petry, S.F.; Eitner, S.; Maresch, C.C.; Lingwal, N.; Lillig, C.H.; Linn, T. Paracrine regulation and improvement of β-cell function by thioredoxin. *Redox Biol.* **2020**, *34*, 101570. [CrossRef]
31. Robertson, R.P.; Harmon, J.; Tran, P.O.; Poitout, V. Beta-cell glucose toxicity, lipotoxicity, and chronic oxidative stress in type 2 diabetes. *Diabetes* **2004**, *53* (Suppl. 1), S119–S124. [CrossRef] [PubMed]
32. Poitout, V.; Robertson, R.P. Glucolipotoxicity: Fuel excess and beta-cell dysfunction. *Endocr. Rev.* **2008**, *29*, 351–366. [CrossRef] [PubMed]
33. Brun, T.; Scarcia, P.; Li, N.; Gaudet, P.; Duhamel, D.; Palmieri, F.; Maechler, P. Changes in mitochondrial carriers exhibit stress-specific signatures in INS-1Eb-cells exposed to glucose versus fatty acids. *PLoS ONE* **2013**, *8*, e82364. [CrossRef]
34. Anello, M.; Lupi, R.; Spampinato, D.; Piro, S.; Masini, M.; Boggi, U.; Del Prato, S.; Rabuazzo, A.M.; Purrello, F.; Marchetti, P. Functional and morphological alterations of mitochondria in pancreatic beta cells from type 2 diabetic patients. *Diabetologia* **2005**, *48*, 282–289. [CrossRef] [PubMed]
35. Fex, M.; Nitert, M.D.; Wierup, N.; Sundler, F.; Ling, C.; Mulder, H. Enhanced mitochondrial metabolism may account for the adaptation to insulin resistance in islets from C57BL/6J mice fed a high-fat diet. *Diabetologia* **2007**, *50*, 74–83. [CrossRef]
36. Ferdaoussi, M.; Bergeron, V.; Zarrouki, B.; Kolic, J.; Cantley, J.; Fielitz, J.; Olson, E.N.; Prentki, M.; Biden, T.; MacDonald, P.E.; et al. G protein-coupled receptor (GPR)40-dependent potentiation of insulin secretion in mouse islets is mediated by protein kinase D1. *Diabetologia* **2012**, *55*, 2682–2692. [CrossRef]
37. Itoh, Y.; Kawamata, Y.; Harada, M.; Kobayashi, M.; Fujii, R.; Fukusumi, S.; Ogi, K.; Hosoya, M.; Tanaka, Y.; Uejima, H.; et al. Free fatty acids regulate insulin secretion from pancreatic beta cells through GPR40. *Nature* **2003**, *422*, 173–176. [CrossRef]
38. Kim, H.S.; Hwang, Y.C.; Koo, S.H.; Park, K.S.; Lee, M.S.; Kim, K.W.; Lee, M.K. PPAR-g activation increases insulin secretion through the up-regulation of the free fatty acid receptor GPR40 in pancreatic b-cells. *PLoS ONE* **2013**, *8*, e50128. [CrossRef]
39. Sako, Y.; Grill, V.E. A 48-hour lipid infusion in the rat time-dependently inhibits glucose-induced insulin secretion and B cell oxidation through a process likely coupled to fatty acid oxidation. *Endocrinology* **1990**, *127*, 1580–1589. [CrossRef]
40. Ritz-Laser, B.; Meda, P.; Constant, I.; Klages, N.; Charollais, A.; Morales, A.; Magnan, C.; Ktorza, A.; Philippe, J. Glucose-induced preproinsulin gene expression is inhibited by the free fatty acid palmitate. *Endocrinology* **1999**, *140*, 4005–4014. [CrossRef]
41. Lupi, R.; Dotta, F.; Marselli, L.; Del Guerra, S.; Masini, M.; Santangelo, C.; Patané, G.; Boggi, U.; Piro, S.; Anello, M.; et al. Prolonged exposure to free fatty acids has cytostatic and pro-apoptotic effects on human pancreatic islets: Evidence that beta-cell death is caspase mediated, partially dependent on ceramide pathway, and Bcl-2 regulated. *Diabetes* **2002**, *51*, 1437–1442. [CrossRef] [PubMed]
42. Eguchi, K.; Manabe, I.; Oishi-Tanaka, Y.; Ohsugi, M.; Kono, N.; Ogata, F.; Yagi, N.; Ohto, U.; Kimoto, M.; Miyake, K.; et al. Saturated fatty acid and TLR signaling link b cell dysfunction and islet inflammation. *Cell Metab.* **2012**, *15*, 518–533. [CrossRef] [PubMed]
43. Mason, T.M.; Goh, T.; Tchipashvili, V.; Sandhu, H.; Gupta, N.; Lewis, G.F.; Giacca, A. Prolonged elevation of plasma free fatty acids desensitizes the insulin secretory response to glucose in vivo in rats. *Diabetes* **1999**, *48*, 524–530. [CrossRef] [PubMed]
44. Paolisso, G.; Gambardella, A.; Amato, L.; Tortoriello, R.; D'Amore, A.; Varricchio, M.; D'Onofrio, F. Opposite effects of short- and long-term fatty acid infusion on insulin secretion in healthy subjects. *Diabetologia* **1995**, *38*, 1295–1299. [CrossRef]
45. Liu, Y.Q.; Tornheim, K.; Leahy, J.L. Fatty acid-induced beta cell hypersensitivity to glucose. Increased phosphofructokinase activity and lowered glucose-6-phosphate content. *J. Clin. Investig.* **1998**, *101*, 1870–1875. [CrossRef]
46. Köhnke, D.; Ludwig, B.; Kadenbach, B. A threshold membrane potential accounts for controversial effects of fatty acids on mitochondrial oxidative phosphorylation. *FEBS Lett.* **1993**, *336*, 90–94. [CrossRef]
47. Salt, I.P.; Johnson, G.; Ashcroft, S.J.; Hardie, D.G. AMP-activated protein kinase is activated by low glucose in cell lines derived from pancreatic beta cells, and may regulate insulin release. *Biochem. J.* **1998**, *335 Pt 3*, 533–539. [CrossRef]
48. Briaud, I.; Harmon, J.S.; Kelpe, C.L.; Segu, V.B.; Poitout, V. Lipotoxicity of the pancreatic beta-cell is associated with glucose-dependent esterification of fatty acids into neutral lipids. *Diabetes* **2001**, *50*, 315–321. [CrossRef]
49. Hirota, N.; Otabe, S.; Nakayama, H.; Yuan, X.; Yamada, K. Sequential activation of caspases and synergistic beta-cell cytotoxicity by palmitate and anti-Fas antibodies. *Life Sci.* **2006**, *79*, 1312–1316. [CrossRef]

50. Salgin, B.; Ong, K.K.; Thankamony, A.; Emmett, P.; Wareham, N.J.; Dunger, D.B. Higher fasting plasma free fatty acid levels are associated with lower insulin secretion in children and adults and a higher incidence of type 2 diabetes. *J. Clin. Endocrinol. Metab.* **2012**, *97*, 3302–3309. [CrossRef]
51. Malmgren, S.; Nicholls, D.G.; Taneera, J.; Bacos, K.; Koeck, T.; Tamaddon, A.; Wibom, R.; Groop, L.; Ling, C.; Mulder, H.; et al. Tight coupling between glucose and mitochondrial metabolism in clonal beta-cells is required for robust insulin secretion. *J. Biol. Chem.* **2009**, *284*, 32395–32404. [CrossRef] [PubMed]
52. Noda, M.; Yamashita, S.; Takahashi, N.; Eto, K.; Shen, L.M.; Izumi, K.; Daniel, S.; Tsubamoto, Y.; Nemoto, T.; Iino, M.; et al. Switch to anaerobic glucose metabolism with NADH accumulation in the beta-cell model of mitochondrial diabetes. Characteristics of betaHC9 cells deficient in mitochondrial DNA transcription. *J. Biol.* **2002**, *277*, 41817–41826.
53. Minami, K.; Yano, H.; Miki, T.; Nagashima, K.; Wang, C.Z.; Tanaka, H.; Miyazaki, J.I.; Seino, S. Insulin secretion and differential gene expression in glucose-responsive and -unresponsive MIN6 sublines. *Am. J. Physiol. Endocrinol. Metab.* **2000**, *279*, E773–E781. [CrossRef] [PubMed]
54. Duchen, M.R.; Smith, P.A.; Ashcroft, F.M. Substrate-dependent changes in mitochondrial function, intracellular free calcium concentration and membrane channels in pancreatic beta-cells. *Biochem. J.* **1993**, *294 Pt 1*, 35–42. [CrossRef]
55. Daunt, M.; Dale, O.; Smith, P.A. Somatostatin inhibits oxidative respiration in pancreatic beta-cells. *Endocrinology* **2006**, *147*, 1527–1535. [CrossRef]
56. Cheng, K.; Delghingaro-Augusto, V.; Nolan, C.J.; Turner, N.; Hallahan, N.; Andrikopoulos, S.; Gunton, J.E. High passage MIN6 cells have impaired insulin secretion with impaired glucose and lipid oxidation. *PLoS ONE* **2012**, *7*, e40868. [CrossRef]
57. Taddeo, E.P.; Stiles, L.; Sereda, S.; Ritou, E.; Wolf, D.M.; Abdullah, M.; Swanson, Z.; Wilhelm, J.; Bellin, M.; McDonald, P.; et al. Individual islet respirometry reveals functional diversity within the islet population of mice and human donors. *Mol. Metab.* **2018**, *16*, 150–159. [CrossRef]
58. Rodríguez-Manzaneque, M.T.; Tamarit, J.; Bellí, G.; Ros, J.; Herrero, E. Grx5 is a mitochondrial glutaredoxin required for the activity of iron/sulfur enzymes. *Mol. Biol. Cell* **2002**, *13*, 1109–1121. [CrossRef]
59. Uzarska, M.A.; Dutkiewicz, R.; Freibert, S.A.; Lill, R.; Mühlenhoff, U. The mitochondrial Hsp70 chaperone Ssq1 facilitates Fe/S cluster transfer from Isu1 to Grx5 by complex formation. *Mol. Biol. Cell* **2013**, *24*, 1830–1841. [CrossRef]
60. Corbett, J.A.; Lancaster, J.R.J.; Sweetland, M.A.; McDaniel, M.L. Interleukin-1 beta-induced formation of EPR-detectable iron-nitrosyl complexes in islets of Langerhans. Role of nitric oxide in interleukin-1 beta-induced inhibition of insulin secretion. *J. Biol. Chem.* **1991**, *266*, 21351–21354. [CrossRef]
61. Corbett, J.A.; Sweetland, M.A.; Wang, J.L.; Lancaster, J.R.J.; McDaniel, M.L. Nitric oxide mediates cytokine-induced inhibition of insulin secretion by human islets of Langerhans. *Proc. Natl. Acad. Sci. USA* **1993**, *90*, 1731–1735. [CrossRef] [PubMed]
62. Scarim, A.L.; Heitmeier, M.R.; Corbett, J.A. Irreversible inhibition of metabolic function and islet destruction after a 36-h exposure to interleukin-1beta. *Endocrinology* **1997**, *138*, 5301–5307. [CrossRef] [PubMed]
63. Santos, M.C.F.D.; Anderson, C.P.; Neschen, S.; Zumbrennen-Bullough, K.B.; Romney, S.J.; Kahle-Stephan, M.; Rathkolb, B.; Gailus-Durner, V.; Fuchs, H.; Wolf, E.; et al. Irp2 regulates in-sulin production through iron-mediated Cdkal1-catalyzed tRNA modification. *Nat. Commun.* **2020**, *11*, 296. [CrossRef] [PubMed]

Redox Biology 34 (2020) 101570

Contents lists available at ScienceDirect

Redox Biology

journal homepage: www.elsevier.com/locate/redox

Research Paper

Paracrine regulation and improvement of β-cell function by thioredoxin

Eva-Maria Hanschmann[a,b,1], Sebastian Friedrich Petry[c,*,1], Susanne Eitner[a], Constanze Christin Maresch[c], Neelam Lingwal[c], Christopher Horst Lillig[a,1,***], Thomas Linn[c,1,**]

[a] Institute for Medical Biochemistry and Molecular Biology, University Medicine, University of Greifswald, Germany
[b] Department of Neurology, Medical Faculty, Heinrich-Heine-University, Düsseldorf, Germany
[c] Clinical Research Unit, Center of Internal Medicine, Justus-Liebig-University, Giessen, Germany

A B S T R A C T

The failure of insulin-producing β-cells is the underlying cause of hyperglycemia in diabetes mellitus. β-cell decay has been linked to hypoxia, chronic inflammation, and oxidative stress. Thioredoxin (Trx) proteins are major actors in redox signaling and essential for signal transduction and the cellular stress response. We have analyzed the cytosolic, mitochondrial, and extracellular Trx system proteins in hypoxic and cytokine-induced stress using β-cell culture, isolated pancreatic islets, and pancreatic islet transplantation modelling low oxygen supply.

Protein levels of cytosolic Trx1 and Trx reductase (TrxR) 1 significantly decreased, while mitochondrial Trx2 and TrxR2 increased upon hypoxia and reoxygenation. Interestingly, Trx1 was secreted by β-cells during hypoxia. Moreover, murine and human pancreatic islet grafts released Trx1 upon glucose stimulation. Survival of transplanted islets was substantially impaired by the TrxR inhibitor auranofin.

Since a release was prominent upon hypoxia, putative paracrine effects of Trx1 on β-cells were examined. In fact, exogenously added recombinant hTrx1 mitigated apoptosis and preserved glucose sensitivity in pancreatic islets subjected to hypoxia and inflammatory stimuli, dependent on its redox activity. Human subjects were studied, demonstrating a transient increase in extracellular Trx1 in serum after glucose challenge. This increase correlated with better pancreatic islet function. Moreover, hTrx1 inhibited the migration of primary murine macrophages.

In conclusion, our study offers evidence for paracrine functions of extracellular Trx1 that improve the survival and function of pancreatic β-cells.

1. Introduction

Inflammation and fluctuations in islet oxygen supply play a pivotal role in loss of insulin secreting β-cells of pancreatic islets during the onset and progression of diabetes mellitus [1–3]. Elevated levels of reactive oxygen species (ROS) and disturbed redox circuits, often referred to as oxidative stress, have been linked to this irreversible process [4]. Accordingly, it was shown that hyperglycemia creates a hypoxia-like condition in islets, which leads to activation of a hypoxic stress response [5]. β-cells are highly vulnerable to hypoxia resulting in functional impairment of insulin secretion and induction of apoptosis [5–7], accumulation of ROS [8], down-regulation of the unfolded protein response [7], up-regulation of NF-κB, and dys-regulation of cellular redox signaling [9,10].

Interestingly, NF-κB-induced apoptosis is redox-regulated by proteins of the thioredoxin (Trx) family (for an overview see Ref. [11]). The Trx system, composed of Trx, the seleno protein Trx reductase (TrxR), and NADPH regulates specific proteins via reversible disulfide-dithiol exchange reactions and de-nitrosylation of cysteine (Cys) residues. Moreover, recent data indicate that Trx is also involved in hydrogen sulfide (H2S) signaling [12].

Mammalian genomes encode two forms of thioredoxin proteins: the cytosolic (Trx1, TrxR1) and the mitochondrial (Trx2, TrxR2) ones. Trx1 was furthermore shown to translocate into the nucleus [13] and to be secreted [14]. The activity of Trx is regulated by its potential inhibitor Txnip (Thioredoxin-interacting protein) which binds to and inhibits reduced Trx. Due to distinct substrate specificity, Thioredoxin proteins have a broad range of functions in the regulation of DNA synthesis [15], gene expression [16], regulation of intracellular hydrogen peroxide levels [17], proliferation and apoptosis [18,19], changes in oxygen supply, and the modulation of the immune response [20]. Modification of activity, expression levels, or localization of thioredoxins was associated with dys-regulation of proteins in distinct cellular pathways and various diseases, including diabetes [11].

The expression and anti-apoptotic functions of Trx1 were shown to improve islet survival following pancreatic islet transplantation, a

* Corresponding author. Clinical Research Unit, Center of Internal Medicine, Klinikstrasse 33, 35392, Giessen, Germany.
** Corresponding author. Clinical Research Unit, Center of Internal Medicine, Klinikstrasse 33, 35392, Giessen, Germany.
*** Corresponding author. Institute for Medical Biochemistry and Molecular Biology, University Medicine Greifswald, Ferdinand-Sauerbruch-Strasse, DZ7, J03-35, 17475, Greifswald, Germany.
E-mail addresses: sebastian.petry@innere.med.uni-giessen.de (S.F. Petry), horst@lillig.de (C.H. Lillig), thomas.linn@innere.med.uni-giessen.de (T. Linn).
[1] These authors contributed equally to the manuscript.

https://doi.org/10.1016/j.redox.2020.101570
Received 11 April 2020; Accepted 7 May 2020
Available online 16 May 2020

therapeutic strategy to restore β-cell function [21], which inevitably involves hypoxia-reoxygenation injury as well as exposure of grafts to the host's inflammatory response. The general lack of oxygen and the generation of ROS, particularly during the reoxygenation period, may prevent long-term cell survival, cell regeneration, and restoration of insulin production and secretion. Moreover, the sensitive micro-milieu of pancreatic β-cells can further be disrupted by inflammatory processes, mediated by chemo- and cytokines, complement components, matrix metalloproteases, and infiltrating macrophages [22–24].

In the present study, evidence is provided that thioredoxin proteins of pancreatic β-cells are differentially regulated in cytosolic, mitochondrial, and extracellular compartments under hypoxic or inflammatory conditions. They are involved in the control of cellular processes facilitating cell survival, secretory function as well as extracellular signaling and cell communication of β-cells. Our data clearly confirm that distinct stimuli induce compartmentalized redox reactions and hold different effects on thioredoxin proteins. Moreover, this study shows that extracellular full-length hTrx1 possesses paracrine functions dependent on its redox activity, affecting β-cell survival and function.

2. Materials and methods

2.1. Materials and products

Mitochondrial and caspase activity kits of cells were purchased from Invitrogen (Karlsruhe, Germany) and Biozol (Eching, Germany), respectively. Insulin concentrations of isolated pancreatic islets or mouse β-cells were determined by specific sandwich ELISA assays from DRG Instruments (Marburg, Germany). hTrx1 activity was analyzed by Trx1-catalyzed reduction of insulin (Proteostat, Enzo, Lörrach, Germany). Primer sequences for qRT-PCR and antibodies are listed in Tables S1 and S2.

2.2. Protein expression, purification and activity

Recombinant human thioredoxin (hTrx1) was cloned into the pet20b plasmid and was expressed in E. coli and purified using HisTrap columns and the IMAC principle [25]. To produce endotoxin-free protein, expression was performed in ClearColi BL21(DE3) Electrocompetent Cells (Lucigen). In addition, hTrx1 with < 1.0 endotoxin units/μg protein was purchased from Biocat GmbH (Heidelberg, Germany). As control, hTrx1 was denatured at 90 °C for 30 min (dhTrx1). In addition, a redox-inactive Cys32Ser mutant of hTrx1 (C32S) was generated by rolling-circle PCR using specific oligonucleotides (Fig. S1).

2.3. Pancreatic islet isolation and culture

Porcine islets were harvested from retired breeders as previously described [26]. Briefly, islets from a single pancreas were retrieved after vascular flush with University of Wisconsin solution (Du Pont Critical Care, IL, USA). The quality of the islets was evaluated by trypan blue exclusion, dithizone staining and glucose-stimulated insulin secretion (GSIS) to verify cell viability, purity, and function. Pig islets were cultured at non-CO_2 air in CMRL 1066 (PAA, Pasching, Austria) supplemented with 25 mM HEPES, 20% heat-inactivated pig serum, 100 U/ml penicillin (Biochrom, Berlin, Germany), 100 μg/ml streptomycin, and 2 mg/ml glucose. Their insulin secretion was determined by calculating the ratio of stimulated and basal insulin concentrations measured at 22 and 2.8 mM glucose concentration in the medium, resulting in an insulin stimulation index (SI).

2.4. Cell culture and hypoxia

The murine β-cell line MIN6 was cultivated in high glucose DMEM medium (PAA, Pasching, Austria) supplemented with 20% heat-inactivated fetal calf serum, 100 U/ml penicillin and 100 μg/ml streptomycin, 1 mM sodium pyruvate, and 71 μM mercaptoethanol at 37 °C in a 90% humidified atmosphere containing 5% CO_2. Cells were grown under different oxygen concentrations (1%, 2% or 20%) using the New Brunswick Innova hypoxia chamber. Recombinant cytokines used in cell culture were 10 ng/ml TNF-α, 5 ng/ml IL-1β, 100 ng/ml IFN-γ purchased from R&D Systems (Marburg, Germany). Control cells were grown under standard cell culture conditions at 20% O_2. Cells were harvested, washed with PBS, incubated in NP40-containing lysis buffer (10 mM Tris/HCl, 0.1% NP40, 10 mM NaCl, 3 mM MgCl2, and protease and phosphatase inhibitors, pH 7.4) for 15 min at room temperature, and were flash frozen in liquid nitrogen. Cell extracts were centrifuged at 13,000 rpm for 15 min at 4 °C. Protein levels were determined using Bradford reagent (Biorad, CA, USA) or BCA (Pierce, MA, USA). The cells' constituent insulin secretion was determined by comparing the amount of insulin in their cell culture medium before and after the respective treatment.

2.5. Macrophage migration

Peritoneal macrophages were retrieved following thioglycollate challenge as described [24]. They were added to the insert of 12-well plates (Greiner bio-one, Kremsmünster, Austria) to give a volume of 250 μl with or without Trx1. Wells contained 600 μl of supernatant from pancreatic islet free floating tissue culture. Macrophages were allowed to migrate for 48 h at 37 °C in a 5% CO_2 humidified atmosphere and labelled adding 8 μM calcein AM. Cells migrating to the bottom surface of the filter were removed by using trypsin EDTA and detected using a fluorescence plate reader (Berthold Technologies-Mithras LB940, Germany).

2.6. Immunoblot

Samples (20 μg of total protein) were combined with sample loading buffer (0.3 M Tris-HCl, pH 7, 50% glycerol, 5% SDS, 0.1% bromphenol blue). Proteins were reduced by a 20 min incubation at RT with 100 mM DTT, followed by an additional incubation for 10 min at 94 °C. Proteins were separated on a reducing SDS-PAGE (Pierce, MA, USA) and transferred to a PVDF membrane, which was blocked with 5% milk powder and 1% BSA in Tris-buffered saline containing 0.05% Tween20. Proteins were detected using specific primary antibodies, a horseradish peroxidase-coupled secondary antibody and the electrogenerated chemiluminescence method. Images were obtained using the Chemostar system. ImageJ was employed for the densitometric quantification.

2.7. Enzyme linked immunosorbent assays (ELISA)

Detection of human or porcine Trx1 in plasma was performed customizing a sandwich procedure described by Lundberg [27]. Capture antibody (mouse monoclonal (mAb) MT17R6) was diluted in PBS (1.0 μg/ml) and absorbed to 96-well Maxisorp plates (Nunc) for 24 h at 4 °C. After washing steps with PBS/0.1% Tween20, a dilution buffer (ELISA diluent, Mabtech 3652-D2) was applied to prevent interference by heterophilic antibodies. Accordingly, assays were designed for quantification of Trx1, Trx2, TrxR1, TrxR2, and Txnip in MIN6 cell culture. Supernatants or lyzed cells taken from MIN6 cell culture were prepared as described for immunoblotting. Capture antibodies with reactivity to the respective mouse target proteins were coated to microtiter plates. These stationary phase antibodies bound sample or purified recombinant target proteins while non-bound proteins were removed by washing. Samples or standard proteins were added in appropriate dilution in triplicates and incubated at 4 °C overnight. After washing (PBS, 0.05% v/v Tween 20) three times, 100 μl of biotin-conjugated goat-anti-rabbit (Abcam, UK) detection antibody was added and incubated for 2 h at room temperature. 0.1 μg/ml streptavidin-horseradish peroxidase conjugate (SA-HRP, 50 ng/ml, Mabtech) was

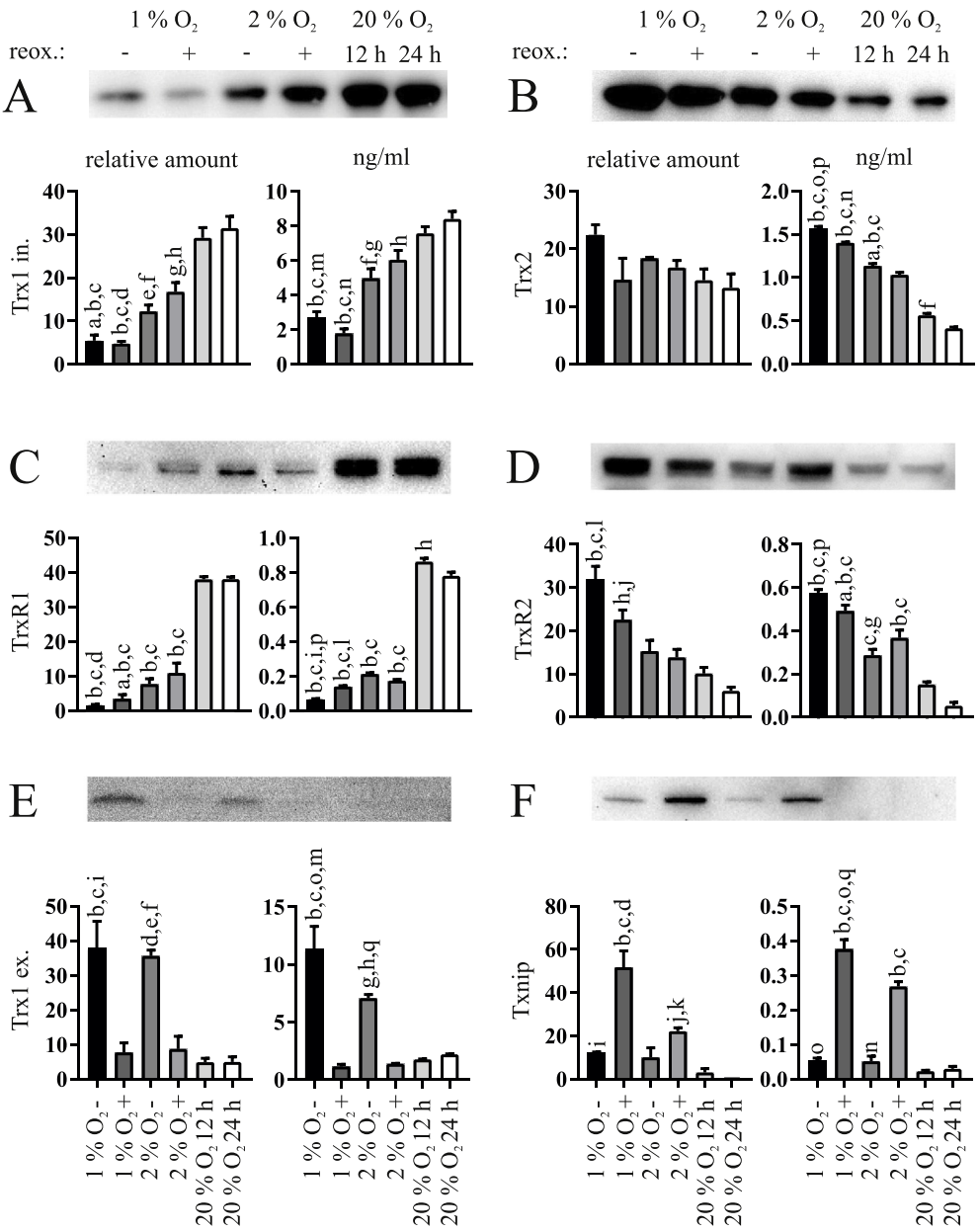

Fig. 1. Effects of hypoxia and reoxygenation on thioredoxin proteins in MIN6 cells. Each panel shows a representative western blot, the respective densitometric quantification data on the left, and the respective ELISA data on the right. (A) Intracellular Trx1, (B) Trx2, (C) TrxR1, (D) TrxR2, (E) extracellular Trx1, and (F) Txnip were analyzed in MIN6 cells cultured at 1% or 2% O_2 for 12 h with (+) or without (−) reoxygenation (reox.) for another 12 h. Normoxic cells cultured at 20% O_2 for 12 or 24 h were used as controls. Extracellular concentrations of Trx1 were determined in the supernatant of the cultivated cells. Actin or tubulin were not detected in these samples excluding the presence of cell lysis as potential source of extracellular Trx1. Images and densitometric quantifications are representative of n = 3–5 independent experiments. All ELISA data are normalized to 20 µg of protein lysate per well and given in ng/ml (n = 5). $^{a}p < 0.05$ vs. 2% O_2 +; $^{b}p < 0.0001$ vs. 20% O_2 12 h; , $^{c}p < 0.0001$ vs. 20% O_2 24 h; $^{d}p < 0.01$ vs. 2% O_2 +; $^{e}p < 0.001$ vs. 20% O_2 12 h; $^{f}p < 0.001$ vs. 20% O_2 24 h; $^{g}p < 0.01$ vs. 20% O_2 12 h; $^{h}p < 0.01$ vs. 20% O_2 24 h; $^{i}p < 0.001$ vs. 1% O_2 +; $^{j}p < 0.05$ vs. 20% O_2 12 h, $^{k}p < 0.05$ vs. 20% O_2 24 h; $^{l}p < 0.01$ vs. 2% O_2 -; $^{m}p < 0.05$ vs. 2% O_2 -; $^{n}p < 0.0001$ vs. 2% O_2 +; $^{o}p < 0.0001$ vs. 1% O_2 +; $^{p}p < 0.0001$ vs. 2% O_2 –; $^{q}p < 0.001$ vs. 2% O_2 +.

added to each well and incubated for 1 h. The assay was developed by addition of substrate 3,3′,5,5’ tetramethylbenzidine (TMB, Sigma) and stopped after 15 min using 1 M H2SO4. Absorbance at 450 nm was determined using the Multimode reader Mithras LB940 from Berthold, Bad Wildbad, Germany.

2.8. LDH activity

Extracellular LDH activity was analyzed in triplicates using the CytoTox 96-non- radioactive cytotoxicity assay (Promega) according to manufacturer's instructions. Plain medium was used as negative control. Absorbance was measured at 490 nm.

2.9. Immunohistochemistry

Consecutive frozen sections (7 µm) were prepared from liver transplanted with isolated pancreatic islets. Cryosections from mouse pancreas including islets were used as controls. Slides were incubated with polyclonal anti-insulin antibody (DAKO) from guinea pig for immunohistochemistry. Administration of primary antibodies against Trx1, TrxR1, Trx2, TrxR2, and Txnip from rabbit (Table S1) was customized to porcine tissue using the protocol of Godoy et al. [28]. Insulin co-staining was used to identify β-cells. Pancreata were used as control tissue. Sections were incubated with secondary antibodies, FITC-donkey anti-guinea pig and appropriate PE (phycoerythricin)-donkey anti-rabbit antibody (Jackson ImmunoResearch, Germany) for 1 h at 22 °C. Sections were washed, counterstained with DAPI and analyzed under the fluorescent microscope LB30T equipped with the digital camera DFC420C (Leica, Wetzlar, Germany). Images were taken at 400× magnification as islets were too small for analysis at 100× and 200x. Frames with pancreatic and transplanted islets were examined with ImageJ. Pixels were converted into mm^2 pre-programmed in a macro, and a threshold was set between 40 and 45 to adjust for unspecific background staining. The area stained by the antibody directed against the respective thioredoxin was expressed as the relation to the area stained with insulin. This resulted in a dimensionless quantity equivalent to the expression of the protein in β-cells.

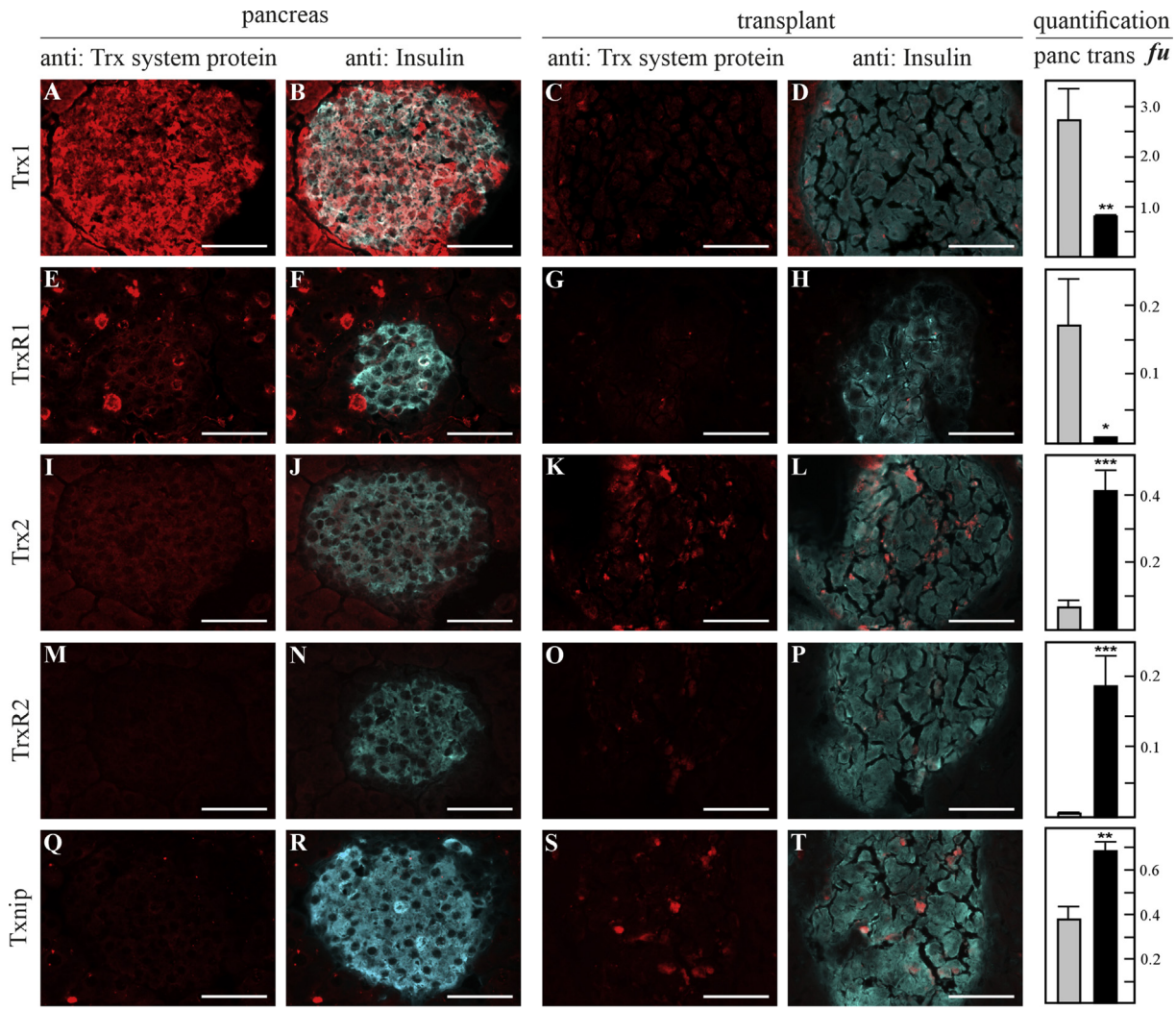

Fig. 2. Immunohistochemical analysis of thioredoxin proteins in native and transplanted pancreatic islets. Porcine islet grafts recovered 30 min after pig-to-mouse transplantation were stained with respective antibodies against the thioredoxin proteins and co-stained against insulin to identify islets. Thioredoxin proteins are represented by panels A, E, I, M, and Q in native pancreatic islets and C, G, K, O, and S in islets transplanted to the liver. Expression was compared between native pancreas and transplants for Trx1 (A–D), TrxR1 (E–H), Trx2 (I–L), TrxR2 (M–P), and Txnip (Q–T). White scale bars indicate 50 μm. Data presented as mean ± SEM. *p < 0.05, **p < 0.005, ***p < 0.0001 (*t*-test), n = 6–12 islet sections were evaluated for each condition.

2.10. Gene expression

Porcine pancreatic islets were lyzed and total RNA was extracted using the RNAeasy kit (Qiagen, Hilden, Germany). A sample of RNA (300 ng) was used as a template for the generation of cDNAs from Oligo (dT) 20 primers using the Superscript III first strand synthesis system (Invitrogen, Karlsruhe, Germany). Real-time PCR was performed with cDNA using specific primers (Table S2) and the Power SYBR Green PCR Master Mix reagents (Applied Biosystems, Darmstadt, Germany) using a StepOnePlus™ Real-Time PCR System. The expression of selected genes was assessed independently, and expression of ribosomal protein L13a (RPL13A) was used as a control for normalization. The effects of different treatments on individual gene expression were calculated as fold induction with the gene expression level in the control samples as fold one, with normoxic samples or hypoxic samples calculated separately and respectively to show the difference between these two environments.

2.11. Streptozotocin-induced diabetes and pancreatic islet transplantation

Animal research was approved by the Regional Administrative Council Giessen, Veterinary Department under the code GI20/11Nr.15/2006 and performed in accordance with the German Animal Welfare law and the ARRIVE guidelines. Diabetes was induced in NRMI nu/nu mice at the age of 12 weeks by a single injection of 180 mg/kg streptozotocin (Sigma, MS, USA) intraperitoneally. Blood glucose levels were monitored using the glucometer Elite (Bayer, Leverkusen, Germany). Mice with a non-fasting blood glucose concentration of more than 16.7 mM for three consecutive days were selected for transplantation (n = 16). Mice were divided into two groups and treated i.p. with 0.12 mg/kg/day thioredoxin reductase inhibitor auranofin (0.2 mg/ml in 0,9% saline, dissolved in 0.25 ml ethanol and 0.2 ml Cremophor EL) or vehicle (n = 8 per group) throughout the study period. Recipients were anaesthetized with avertine and maintained with isoflurane. 2000 pancreatic pig islet equivalents were transplanted into the liver via the portal vein with a 27-gauge needle as previously described [29]. Grafted livers and portal vein blood were recovered 30 min after transplantation of pancreatic islets. Healthy pancreata were used as controls. Grafted livers were embedded in TissueTek optimal cutting temperature compound (VWR International GmbH, Darmstadt, Germany) and snap-frozen in liquid nitrogen.

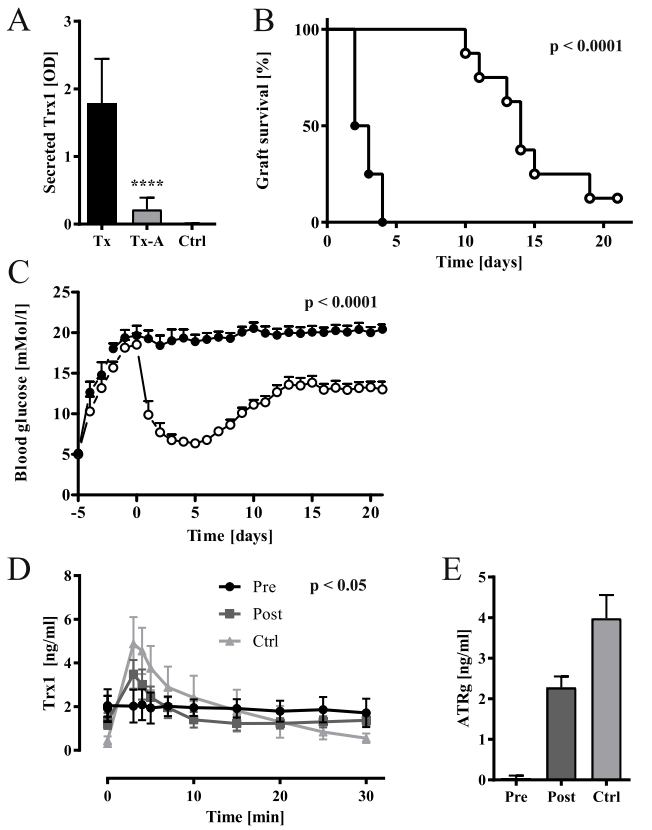

Fig. 3. Glucose-induced Trx secretion in pig and human islet grafts and the effect of TrxR inhibitor auranofin on Trx secretion and graft survival. (A) Trx1 protein release in transplanted mouse liver. Porcine Trx1 protein was specifically measured in portal vein blood retrieved 30 min after transplantation from transplanted mice (Tx), animals transplanted and treated with auranofin (Tx-A), and control mice (Ctrl) without transplanted pancreatic islets. Treatment with auranofin significantly inhibited Trx1 release from porcine islets. $p < 0.0001$ (one-way ANOVA), $n = 8$. (B, C) Auranofin treatment affected graft function in streptozotocin-induced diabetes. (B) Graft failure was characterized by recurrence of diabetes mellitus with elevated blood glucose > 11.1 mM. The overall percentage of dysfunctional grafts in auranofin-treated mice (filled circles) and controls (open circles) was significant during the observation period of 21 days. $p < 0.0001$ (Chi square), $n = 8$. (C) Daily blood glucose levels in each of the two experimental groups given as mean ± SEM. The overall mean concentrations over the 21 days were significantly different between groups. $p < 0.0001$ (two-way ANOVA), $n = 8$. (D, E) Glucose stimulated Trx1 in type 1 diabetic patients before (Pre), 12 months after (Post) pancreatic islet transplantation, and matched non-diabetic healthy probands (Ctrl). Prior to transplantation, patients completely lacked pancreatic islet cells as demonstrated by failing insulin release in Pre-Tx condition (not shown). The acute Thioredoxin (ATRg) response upon an intravenous glucose tolerance test (IVGTT) to 0.3 g/kg glucose was calculated by determining the mean value normalized by basal concentration from time points 3, 4, and 5 min after intravenous injection of glucose. Analysis of variance showed significant overall difference ($p = 0.0131$) of Pre-Tx, Post-Tx, and Ctrl groups for ATRg. Post-hoc analysis demonstrated significant differences of Trx1 responses to the glucose challenge. $p < 0.05$ (two-way ANOVA) $n = 8$.

2.12. Trx1 secretion in patients transplanted with pancreatic islets

Trial activities were acknowledged by the local Ethics Committee of the Faculty of Medicine, Justus Liebig University, Giessen, Germany under Reg.-No. 54/01. Intravenous glucose tolerance tests (IVGTT) were performed in patients before and after one year of pancreatic islet transplantation and in non-diabetic subjects as controls matched for age, sex and body weight.

Pancreatic islets were transplanted to type 1 diabetic patients with a history of hypoglycemia unawareness as part of the Edmonton trial at Giessen center [30]. Patients had a mean age of 41 ± 3 years, the mean time of diabetes since diagnosis was 28 ± 4 years, and the mean insulin requirement per day was 0.55 ± 0.06 U/kg. They received 14.743 ± 1278 (mean ± SD) total islet equivalents per kg body weight. Intravenous glucose tolerance test (IVGTT) was carried out as described [31,32]. Briefly, probands were advised to ingest > 150 g/day carbohydrates three days and remain fasting 10–16 h before the test. 0.3 g/kg glucose was injected in 1 min into a peripheral vein catheter, blood sampling times were −10, 0, 3, 4, 5, 7, 10, 15, 20, 25, and 30 min. Blood was collected into tubes containing EDTA. The samples were centrifuged immediately at 3000 rpm at 4 °C for 15 min and were stored in liquid nitrogen until analysis of thioredoxin concentration by ELISA. Acute thioredoxin (ATRg) response to glucose bolus injection was calculated as the mean concentration at 3, 4, and 5 normalized by basal level at 0 min.

2.13. Statistical analysis

Statistical analysis was performed using Graph Pad Prism 6 (GraphPad Software, San Diego, USA) using ANOVA with post hoc Tukey tests. Gene expressions without recombinant hTrx1 were normalized to the internal reference gene, genes that changed in the presence of hTrx1 to the expression level without hTrx1 ($2^{\Delta\Delta CT}$-method).

The graft rejection curve was generated according to Kaplan-Meier and analyzed by the Chi square test. A p-value < 0.05 was considered significant. Data were expressed as mean ± SD unless otherwise stated.

3. Results

3.1. Thioredoxin proteins in β-cells exposed to hypoxia in culture

MIN6 β-cells cultured for 12 h at 1% and 2% O_2 with and without subsequent reoxygenation for 12 h at 20% O_2 were analyzed for protein levels using Western Blot and ELISA (Fig. 1). Interestingly, the cytosolic and mitochondrial thioredoxin proteins showed opposite responses to the respective growth conditions. Protein amounts of cytosolic Trx1 (Fig. 1A) and TrxR1 (Fig. 1C) were significantly decreased upon hypoxia as compared to normoxia and were maintained during reoxygenation. By contrast, protein amounts of mitochondrial Trx2 (Fig. 1B) and TrxR2 (Fig. 1D) were enhanced during low oxygen and reoxygenation periods compared to the normoxic controls. Txnip (Fig. 1F) was detectable at hypoxia only and further accumulated in the reoxygenation period.

Because Trx1 is known to be secreted, we also analyzed the medium of cultivated cells for extracellular Trx1. Indeed, MIN6 cells secreted a significant quantity of Trx1 during hypoxia (Fig. 1E). We measured the extracellular protein levels of actin and tubulin to exclude a passive release of Trx1, for example due to cell death, and could detect neither of the two using Western Blot (data not shown). In addition, lactate dehydrogenase (LDH) activity was measured in the respective samples to analyze cell lysis/viability. It was significantly increased only at 1% O_2 without reoxygenation as well as after 24 h of normoxic culture when compared to 12 h of normoxic culture (Fig. S2).

3.2. Thioredoxin protein expression and secretion in transplanted pancreatic islets

Next, we analyzed if these dramatic changes could also be detected *in vivo* by employing a pig-to-mouse model of islet transplantation. Thioredoxin proteins were examined by immunohistochemistry in islet grafts recovered 30 min after transplantation. Indeed, compared to native islets (Fig. 2A, B and E, F), immunofluorescent signals representing Trx1 and TrxR1 were significantly reduced by 70% ($p < 0.005$) and 95% ($p < 0.05$) in islets transplanted to the liver (Fig. 2C, D and G, H), respectively. Immunofluorescence of Trx2

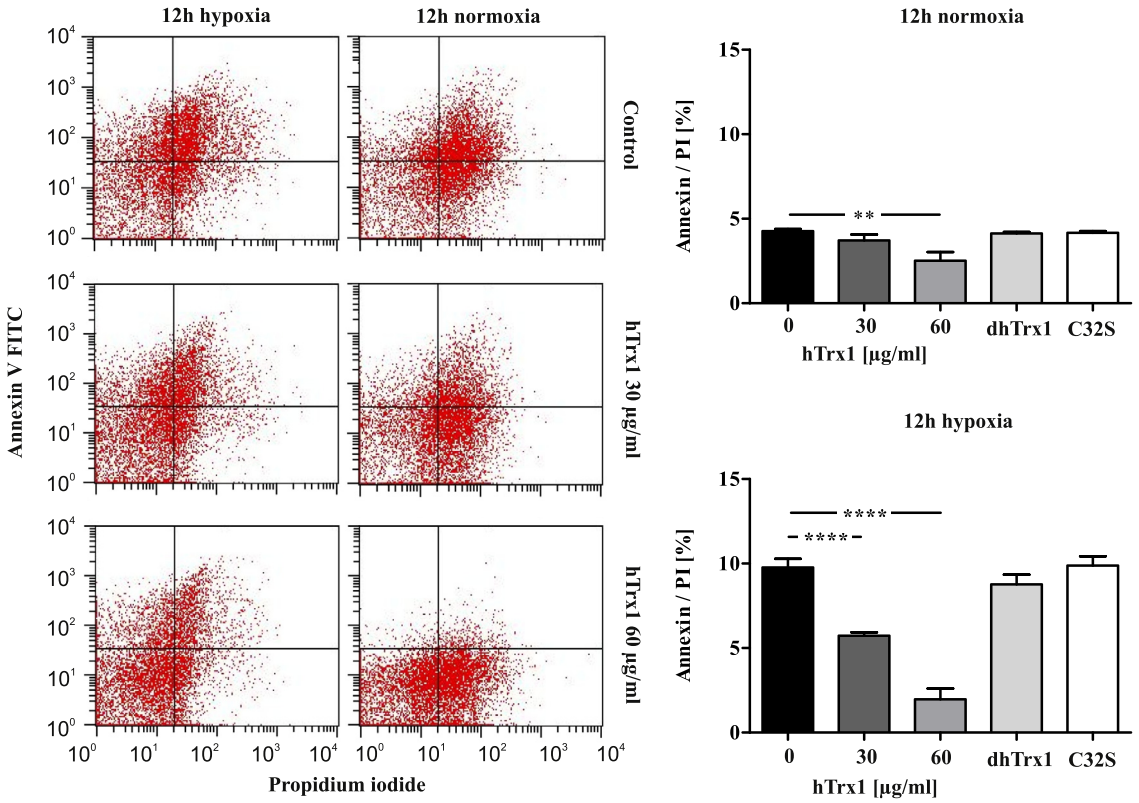

Fig. 4. Influence of hTrx1 on β-cell viability. Dissociated porcine pancreatic islet cells were analyzed for apoptosis and necrosis by fluorescence-activated cytometry (FACSCalibur and FACSuite Software, BD Biosciences, Heidelberg, Germany) probing them with annexin V and propidium iodide (PI). Cytometric analysis of islet cells treated with two concentrations of hTrx1 showed a significant ($p < 0.001$) reduction of Annexin V and PI (A/PI) double positive cells under 12 h normoxia (20% oxygen, 4.3 ± 0.3% to 2.5 ± 1.3%) with 60 µg/ml thioredoxin. Under 12 h hypoxia (2% oxygen), 30 µg/ml hTrx1 reduced A/PI cells also in significant way ($p < 0.0001$, one-way ANOVA) from 9.8 ± 1.3% to 5.7 ± 0.5% and 60 µg/ml hTrx1 to 2.0 ± 1.6%. As control for potential endotoxin contamination, we incubated hTrx1 for 30 min at 90 °C (dhTrx1). Thereby, we denatured and inactivated the protein. This process, however, does not affect endotoxins. Therefore, we tested the function of the redox-active domain of Trx1 using a redox-inactive Trx1 C32S mutant that lacks the N-terminal active site Cys. Both controls, 60 µg/ml denatured dhTrx1 and the redox-inactive C32S, did not affect the cells' viability. ****$p < 0.0001$, **$p < 0.001$ (one-way ANOVA), $n = 6$.

(Fig. 2I, J and K, L), TrxR2 (Figure 2M, N and O, P), and Txnip (Figure 2Q, R and S, T) was significantly elevated in grafts compared to pancreatic controls: 80% for Trx2 ($p < 0.0001$), 95% for TrxR2 ($p < 0.0001$), and 45% for Txnip ($p < 0.005$).

In correspondence with the secretion of Trx1 in MIN6 cells, Trx1 protein was found in portal vein blood 30 min after islet transplantation as opposed to non-transplanted mice (Ctrl, Fig. 3A). To gain deeper insight into the functional significance of the thioredoxin proteins, particularly the increase in mitochondrial Trx2 and TrxR2 protein levels for β-cell survival and function, a subgroup of mice transplanted with pancreatic islets was administered 0.12 mg/kg/day of the TrxR-inhibitor auranofin for 21 days. 50% of grafts failed within 2.5 days as opposed to 14 days in control mice receiving vehicle ($p < 0.0001$, Fig. 3B). Blood glucose levels normalized in control mice immediately after transplantation before slowly rising again later. Total mean blood glucose levels during the 21-day observation period were elevated for auranofin-as compared with vehicle-treated mice (18.7 ± 3.2 vs. 11.3 ± 3.5 mM, $p < 0.0001$, Fig. 3C). Secreted Trx1 was decreased by 85% in auranofin-as opposed to vehicle-treated mice (Tx vs. Tx-A, $p < 0.0001$, Fig. 3A).

Interestingly, when human probands were challenged with glucose bolus injection, an acute Trx1 (ATRg) response was triggered in the presence of functional pancreatic islets (Fig. 3D and E). In diabetic subjects eligible for pancreatic islet transplantation and completely lacking residual insulin (Pre) secretion of Trx1 was poor compared to both post transplantation (Post) and non-diabetic, non-transplanted individuals (Ctrl), respectively (ATRg Post 2.3 ± 0.5, Ctrl 4.0 ± .1.1 ng/ml, $p = 0.0131$). Hence, transplantation of pancreatic islets reconstituted a significant rise of Trx1 following the intravenous glucose challenge.

3.3. Addition of human recombinant Trx1 maintained cell viability and preserved insulin secretion in cultured β-cells

Transplantation of pancreatic islets has two major drawbacks, the low survival of transplanted cells due to hypoxia and an instant blood mediated immune response. Trx1 was shown to be involved in the regulation of apoptosis, specific transcription factors such as HIF-1α and NF-κB, and immunomodulation. Since we observed that the cytosolic Trx1 was significantly decreased *in vitro* and *in vivo* in favor of secretion, we aimed to analyze the impact of extracellular Trx1 on β-cell viability and function.

Therefore, porcine pancreatic islet cells were analyzed by staining with annexin V and propidium iodide (PI) (Fig. 4). Cytometric analysis showed a reduction of the percentage of A/PI double positive cells under normoxic conditions (20% oxygen) in the presence of 30 and 60 µg/ml hTrx1. 30 µg/ml hTrx1 reduced A/PI cells from 9.8 ± 1.3 to 5.7 ± 0.5% and 60 µg/ml hTrx1 to 2.0 ± 1.6% ($p < 0.0001$) in hypoxic (2% oxygen) culture. 60 µg/ml thermally inactivated, i.e. denatured, dhTrx1 and mutated redox-inactive hTrx1 C32S did not change the annexin/PI ratio under the analyzed culture conditions. Furthermore, MIN6 cells were subjected to 2% or to 20% oxygen in the absence or presence of a cytokine mix containing 100 ng/ml IFN-γ, 5 ng/ml IL-1β, and 10 ng/ml TNF-α. The local levels of these cytokines rise at the transplantation site due to tissue injury and remodeling [33]. Cell viability was analyzed using the MTT assay. The conversion of MTT

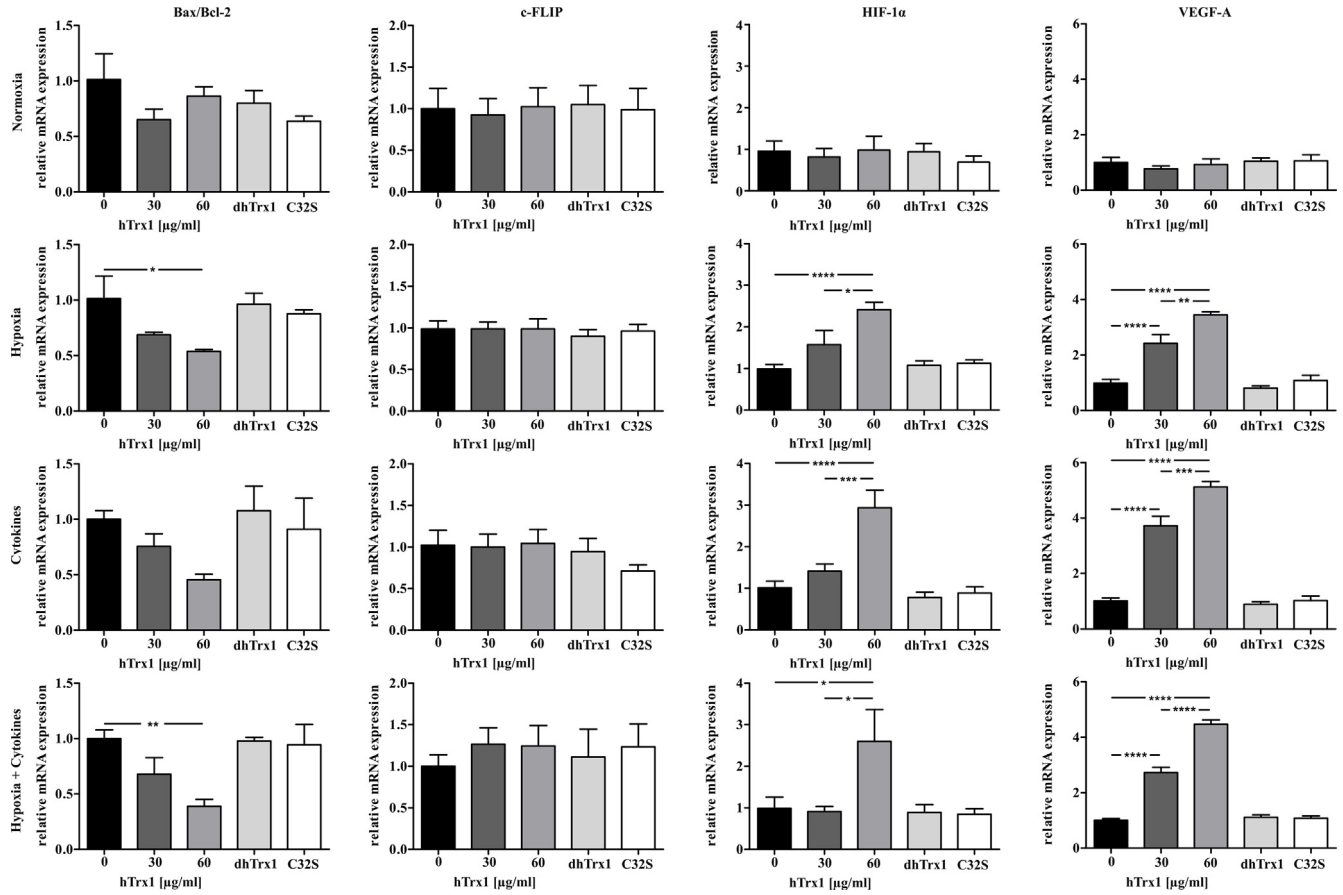

Fig. 5. Expression of genes in pancreatic islets at different oxygen levels and in the presence of cytokines. Target gene mRNA expression of Bax, Bcl2, c-FLIP, HIF1α and VEGF-A in porcine pancreatic islets cultured for 24 h under normoxia (20% oxygen) or hypoxia (2% oxygen) and in the presence of IFN-γ (100 ng/ml), IL-1β (5 ng/ml), and TNF-α (10 ng/ml) and 30 or 60 µg/ml hTrx1 or as control 60 µg/ml denatured hTrx1 (dhTrx1) or redox inactive hTrx1 C32S (C32S), respectively. The ratio of the mRNA expression of the proapoptotic gene Bax and antiapoptotic gene Bcl2 is given instead of the respective sole expression. Upon hypoxia, treatment with 60 µg/ml hTrx1 significantly reduced the relative mRNA expression ratio of Bax/Bcl-2 by 46%. Upon cytokine treatment during normoxia and hypoxia, as well as upon hypoxia without cytokine treatment, HIF-1α expression increased 2.9-fold, 2.6-fold and 2.4-fold, respectively. 60 µg/ml denatured dhTrx1 and the redox-inactive C32S served as controls and did not show any significant effects. Treatment time was 24 h ****$p < 0.0001$, ***$p < 0.001$, **$p < 0.005$, *$p < 0.05$ (one-way ANOVA), $n = 9$.

was amplified when 30 and 60 µg/ml hTrx1 was added, 25 and 56% upon hypoxia, 29 and 40% in the presence of cytokines, and even 93 and 174% at the combination of hypoxia and cytokines ($p = 0.0001$, Fig. S3). Concordantly, 30 and 60 µg/ml hTrx1 reduced caspase 3/7 activity measured with luminescence upon hypoxia by 21 and 39%, in the presence of the cytokines by 13 and 54%, and upon both hypoxia and cytokine treatment by 22 and 49%, respectively ($p < 0.0001$, Fig. S4). 60 µg/ml hTrx1 suppressed p65 phosphorylation at four and 8 h of hypoxia by 50 and 66% ($p = 0.0001$, Fig. S5). Again, dhTrx1 and Trx1 C32S did not induce any changes and showed comparable results as the untreated control.

To further examine the impact of hTrx1 on cell viability, levels of pro-apoptotic gene Bax/Bcl-2 and anti-apoptotic gene c-FLIP were measured in porcine islets (Fig. 5). hTrx1 decreased transcription of Bax/Bcl-2 during hypoxia and hypoxic culture enriched with cytokines. C-FLIP gene expression was not altered by hTrx1. The expression of the pro-survival gene VEGF-A displayed a significant increase with the presence of hTrx1. Moreover, hTrx1 amplified the expression of the HIF-1α gene. Thus, hTrx1 interfered with target genes, cytosolic, and membrane proteins involved in early and late stages of the apoptotic pathway in a specific pro-survival mode for pancreatic islets. None of the tested genes were altered following the treatment with dhTrx1 or Trx1 C32S. Taken together hTrx1 reduced apoptotic processes while increasing mitochondrial oxidative function. An overview of the observed effects of hTrx1 on β-cell viability is given in Table S3.

The significance of extracellular Trx1 for the constituent insulin secretion from MIN6 cells cultivated after 12 h at 2% oxygen was examined. Basal cell culture medium contained 2.5 ± 1 ng/mg insulin; when 30 or 60 µg/ml hTrx1 were added a concentration-dependent increase of secreted insulin 6.0 ± 1.8 and 10.3 ± 2.2 ng/mg ($p < 0.005$ compared with basal) was observed. The intracellular insulin content of cells without hTrx1 was 8.9 ± 0.9 ng/mg protein and 5.7 ± 0.2 or 4.4 ± 0.4 ng/mg with 30 or 60 µg/ml hTrx1, respectively (Fig. 6A). In isolated pancreatic islets, glucose stimulated insulin secretion given as stimulation index (SI) was measured. No significant increase of SI in the presence of hTrx1 was observed upon normoxia or hypoxia with 2% oxygen. However, with the combined hypoxia and inflammatory cytokine treatment, hTrx1 significantly ($p < 0.01$) increased the insulin release up to two-fold as compared to control (Fig. 6B).

3.4. hTrx1 mitigated macrophage migration

To assess a possible immunomodulatory effect under inflammatory conditions, the impact of hTrx1 on macrophage migration was studied. Spontaneous movements of macrophages were responsive to supernatant taken from pancreatic islet culture. Total migratory activity of macrophages stimulated by supernatant was suppressed 29 and 34% by 60 and 90 µg/ml hTrx1, respectively, as opposed to control wells without hTrx1 ($p < 0.0001$, Fig. 7). This inhibition was specific and

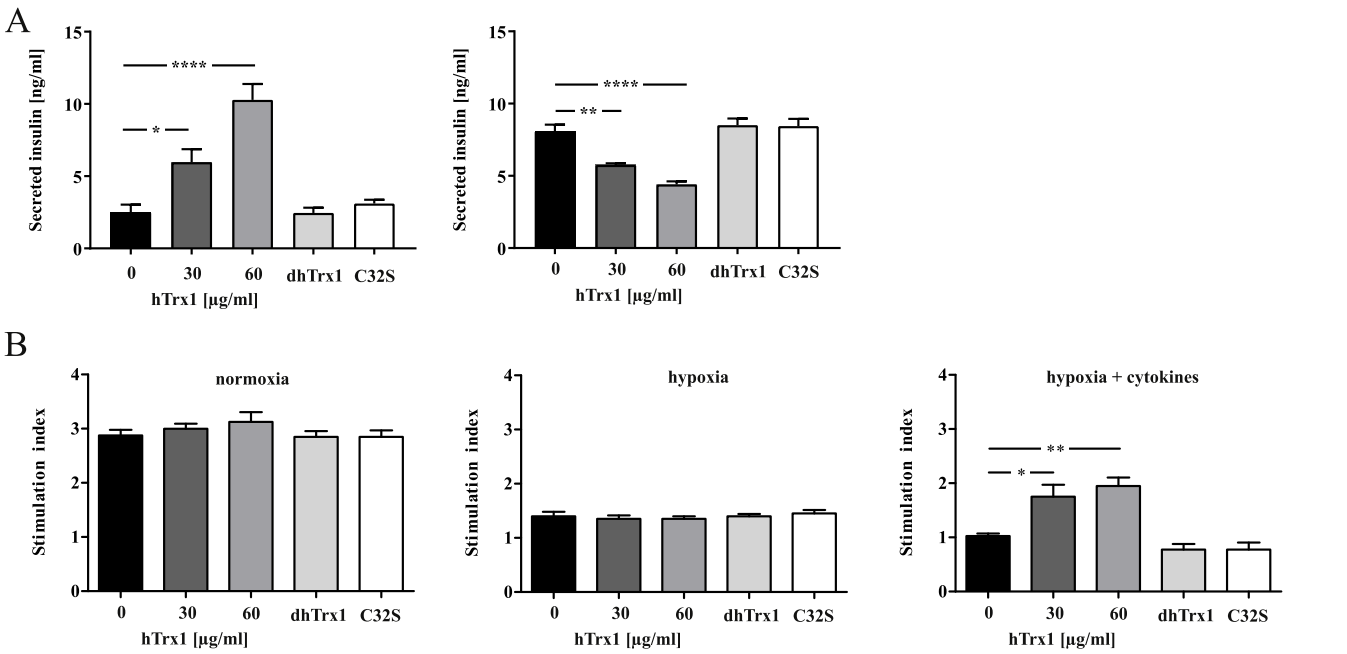

Fig. 6. Influence of hTrx1 on insulin secretion. The effect of reduced hTrx1 in tissue culture was studied at concentrations 0, 30, 60, and 90 µg/ml. As control for potential endotoxin contamination, we incubated the protein for 30 min at 90 °C (dhTrx1). Thereby, we denatured and inactivated the protein. This process, however, does not affect endotoxins. Therefore, we tested the function of the redox-active domain of Trx1 using a redox-inactive Trx1 C32S mutant that lacks the N-terminal active site Cys. (A) MIN6 cell lysates and supernatants with secreted insulin were collected following 12 h hypoxic (2% oxygen) cell culture in the absence or presence of 30 µg/ml or 60 µg/ml reduced hTrx1. Mouse insulin was analyzed using a specific ELISA. Intracellular insulin was normalized to the total protein amount. hTrx1 stimulated insulin secretion and likewise reduced intracellular insulin dose-dependently, whereas denatured or mutated hTrx1 had no effect. ****$p < 0.0001$, **$p < 0.01$, *$p < 0.05$ (one-way ANOVA), $n = 4$. (B) Porcine islets were cultured for 24 h under normoxic (20% oxygen) and hypoxic (2% oxygen) conditions in the absence or presence of cytokines IFN-γ (100 ng/ml), IL-1β (5 ng/ml), and TNF-α (10 ng/ml). The insulin stimulation index (SI) was calculated as the ratio of stimulated and basal insulin concentrations measured at 22 and 2.8 mM glucose concentrations in the medium. hTrx1 significantly restituted SI up to two-fold in combined hypoxic and inflammatory, but not in hypoxic condition alone. **$p < 0.01$, *$p < 0.05$ (one-way ANOVA), $n = 4$.

persisted when polymyxin B, an inhibitor for endotoxins, was added. Moreover, denatured dhTrx1 and mutated redox-inactive hTrx1 C32S only had 0.3 and 2.5% inhibitory effect on overall macrophage migration induced by pancreatic islets.

4. Discussion

As we and others have demonstrated previously, hypoxia and inflammation cause damage to pancreatic islets [1,7,9,24]. In particular, pancreatic islet transplantation is associated with acute injury as islets are deprived of their vascularization and encounter an instant blood-mediated inflammatory response. Overcoming conditions of hypoxia and reoxygenation is vital to maintain cell viability and insulin secretion capacity. Thioredoxin proteins as key enzymes of rapid, reversible, and specific redox reactions show varying expression patterns and activity in different compartments when β-cells are challenged by metabolic stress [34]. Moreover, their expression and activity are altered in models of ischemia/reperfusion [11].

Our findings clearly demonstrate a scenario of distinct changes in both the cytoplasmic and the mitochondrial systems along with the secretion of Trx1 in response to hypoxia and inflammation. Upon hypoxic stress, an up-regulation in mitochondrial Trx2/TrxR2 was accompanied by decreased protein levels of cytosolic Trx1/TrxR1. This opposite response to the same stimuli ex *vivo* and *in vivo* emphasizes the concept of compartmentalized redox signaling and specific functions of members of the Trx family of proteins. Interestingly, the potential endogenous inhibitor of Trx, Txnip, is upregulated by high glucose levels [8] and proinflammatory cytokines [35], while Txnip-deficient β-cells were characterized by augmented GSIS [36]. We found elevated Txnip levels ex *vivo* and *in vivo* as a response to hypoxia and inflammation. Increased Txnip protein levels were shown to correlate with an increase in caspase-3 cleavage and the induction of apoptosis [10]. Txnip was furthermore identified as an activator of the inflammasome in a ROS-dependent manner [22], and an opponent of Trx1 in having detrimental effects on the β-cell.

In phases of high metabolic activity islets suffer from a hypoxia-like condition [5] and thus depend highly on coping strategies in order to overcome deprivation of oxygen and to preserve secretory function [6]. A central actor linking hypoxia with thioredoxins is the Hypoxia-inducible factor-1α (HIF-1α). Overexpression of cytosolic Trx1 supports the stabilization and transactivation of HIF-1α upon hypoxia, whereas mitochondrial Trx2 opposes its activation [37]. Thus, decreased Trx1 and enhanced Trx2 intracellular concentrations observed in transplanted islets might jointly contribute to inhibition of HIF1α.

In contradiction to its generally accepted role as controlling element in conditions of nutritional and oxygen deprivation, the transcription factor HIF-1α was associated with a shift in glucose metabolism, switching from aerobic oxidative phosphorylation to anaerobic glycolysis and impaired glucose-stimulated insulin secretion [38]. It is tempting to speculate that HIF-1α might also be involved in the secretion of Trx1 and the up-regulation of Trx2 upon hypoxia. Interestingly, addition of hTrx1 protein increased the expression of hypoxia-induced HIF-1α when isolated pancreatic islets were compromised with hypoxia in the presence or absence of cytokines.

Extracellular Trx1 seemed to have a paracrine and autocrine influence that is vital for islet protection. As recently demonstrated, injection of recombinant Trx1 to mice transplanted with pancreatic islets significantly improved blood glucose control and islet viability, while overexpression of cellular Trx1 in grafted islet cells was not effective [39], supporting an essential role for extracellular Trx1.

Interestingly, Trx1 was originally described as T-cell leukemia-derived factor secreted by various cell types via an ER- and Golgi-independent pathway [11,13] and was later detected in blood of patients diagnosed with different diseases such as rheumatoid arthritis [40] or

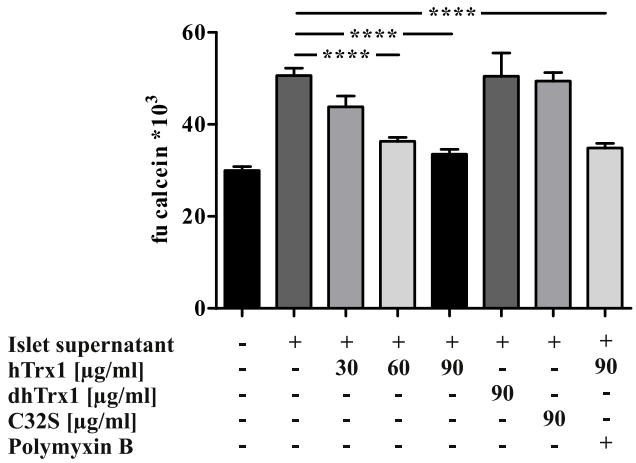

Fig. 7. Effects of hTrx1 on macrophage migration towards pancreatic islets. Cell migration assays were performed with primary murine macrophages cultured for 48 h in transwell plates using pancreatic islet culture medium as chemotactic stimulus in the presence or absence of reduced hTrx1 (final concentration 30, 60, 90 µg/ml), calcein-labelled migrated cells were counted. After 48 h of culture, islets were collected and washed three times with serum-free CMRL 1066 (PAA, Pasching, Austria). They were subsequently cultured for 48 h in serum-free CMRL 1066 supplemented with 2,5 mM L-Glutamine, 1 mM sodium pyruvate, 2 mg/ml glucose solution, 10 mM nicotinamide, Penicillin-Streptomycin and 200 mg Ciprofloxacin. The supernatant was collected for migration assay. As negative control, culture medium without islets was used. In addition, cells moving towards the islets' supernatant in the presence of 90 µg/ml denatured Trx1 (dhTrx1), redox-inactive hTrx1 C32S (C32S), or hTrx1 with 100 µM Polymyxin B were analyzed. The presence of 60 and 90 µg/ml hTrx1 significantly inhibited macrophage migration in contrast to dhTrx1 and C32S, which had no effect. Addition of Polymyxin B did not affect migration, ruling out LPS-mediated effects. ***p < 0.0001 (one-way ANOVA), n = 6.

diabetes mellitus [41]. A secretion of Trx1 was reported in macrophages stimulated with lipopolysaccharide (LPS) [42]. However, the exact secretory mechanisms remained indistinct and extracellular functions of thioredoxin proteins are not well understood. A few examples for redox regulation of membrane proteins by Trx1 have been described that show the induction of conformational changes and modulation of ligand binding and/or activity. Xu et al. suggested a direct interaction of Trx1 with transient receptor potential (TRP) channels [43]. Multiple subtypes of TRP channels, among others TRPM5 and TRPV4, exist on the β-cell and were shown to enhance insulin production upon activation [44,45]. Other examples comprise for instance tumor necrosis factor receptor superfamily member 8 (TNFRSF8) [46], HIV-1 gp120 [47], and transglutaminase 2 [48]. A receptor-agonist-like redox regulation of membrane channels and receptors might well account for the effects of extracellular Trx1 and their dose-dependency on insulin synthesis, protection of apoptosis, and macrophage migration, which we observed in our experiments. Furthermore, Kondo et al. showed that extracellular Trx1 can be transported into cells, indicating that it shuttles between the cytoplasm and the extracellular space [49]. Again, the exact mechanism is not fully understood. One suggested way of Trx1 uptake is internalization by lipid rafts [50]. Such specialized membrane domains contribute to exocytosis of insulin as part of the β-cell's surface proteome [51]. It is possible that re-internalization of secreted Trx1 is one mechanism in the restoration of intracellular Trx1 levels which we observed in β-cells during reoxygenation after exposure with 2%, but not 1% hypoxia (Fig. 1). In addition, we performed a macrophage migration assay to support the suggestion that extracellular, redox-active Trx1 is indeed functional in the inhibition of macrophage migration towards pancreatic islets. In line with our observation in peritoneal macrophages, extracellular Trx1 reduces the chemotaxis of human eosinophils [52], macrophage inflammatory protein 1 and 2-induced leukocyte chemotaxis [53], and LPS-induced neutrophil chemotaxis [54]. Further experiments are needed to confirm these characteristics of Trx1 as co-chemokine. Interestingly, Ro et al. reported that pancreatic islets subjected to hypoxia secreted chemoattractants for macrophages [55], and cytosolic Trx1 was shown to act as an inhibitor of this secretion process [56]. Exogenously administered Trx1 was shown to prolong cell survival during myocardial reperfusion injury [57] and expression of Trx1 in a redox-active form at the surface of endothelial cells inhibited complement deposition as well as neutrophil chemotaxis [58]. Migrant macrophages maintained local inflammation by secretion of IL-1β and other cytokines, which were shown to be counteracted by thioredoxin [39].

Besides the full-length Trx1, its secreted, truncated form Trx80 was described as an eosinophilic cytotoxicity enhancing factor and mitogenic cytokine [59,60]. Both proteins were shown to have different expression patterns [61], and whereas Trx1 is an oxidoreductase, the truncated Trx80 functions as a redox-inactive dimer [59,60]. Our experiments show that the paracrine functions of the full-length Trx1 on β-cell survival and function depend on a catalytically active enzyme, because the redox-inactive Cys32Ser mutant does not show significant changes compared to the control cells. Since pancreatic β-cells express the Toll-like receptor 4 (TLR4) and it is known that lipopolysaccharide affects cell viability and insulin release [62–65], we included denaturated protein and used polymyxin b as endotoxin-controls. Indeed, all our experiments rule out potential effects due to endotoxin contamination, attributing the observed experimental outcomes to redox-active full-length Trx.

In conclusion, we have shown that the cytosolic and mitochondrial Trx systems responded differentially to hypoxia- and cytokine-mediated stress *ex vivo* and *in vivo* using freshly transplanted β-cells. Cytosolic Trx1 was secreted. Chemical depletion of the activity of the mitochondrial Trx system by inhibition of TrxR2 in the absence of the cytosolic Trx1 and TrxR1 resulted in rapid islet decay, emphasizing important functions of these Trx proteins. Addition of extracellular Trx1 counteracted apoptosis and preserved insulin secretion. Notably, these paracrine effects are mediated by the redox-active, full-length Trx1. A graphical summary of the results was designed in Fig. S6.

Author contributions

Conceptualization: CHL, TL, EMH, Data Curation: EMH, SFP, SE, CCM, NL, CHL, TL, Formal Analysis: EMH, SFP, SE, CCM, NL, CHL, TL, Investigation: EMH, SFP, SE, NL, Writing, Review & Editing: EMH, SFP, SE, CCM, NL, CHL, TL, Guarantor of the research: TL.

Declaration of competing interest

None.

Acknowledgments

TL is the guarantor of this work and as such had full access to all of the data in the study and takes responsibility for the integrity of the data and the accuracy of the data analysis. Support from Klaus T. Preissner's lab, Biochemical Institute, Faculty of Medicine, Justus-Liebig University regarding design and establishment of the immunosorbent assays is highly acknowledged. The authors thank Gundula Hertl, Birte Hussmann, Doris Erb, and Divya Rawat for superb technical work.

This work was fully supported by grants of the Von Behring-Röntgen-Stiftung, Marburg, Germany to CHL and TL. It has been partially supported by current grants from Forschungscampus Mittelhessen and Federal Ministry of Education and Research (BMBF) to TL. The funders had no role in study design, data collection and analysis,

decision to publish, or preparation of the manuscript.

Appendix A. Supplementary data

Supplementary data to this article can be found online at https://doi.org/10.1016/j.redox.2020.101570.

References

[1] J.E. Gunton, et al., Loss of ARNT/HIF1beta mediates altered gene expression and pancreatic-islet dysfunction in human type 2 diabetes, Cell 122 (3) (2005) 337–349.
[2] P.A. Gerber, et al., Hypoxia lowers SLC30A8/ZnT8 expression and free cyto-solic Zn2+ in pancreatic beta cells, Diabetologia 57 (8) (2014) 1635–1644.
[3] M. Campbell-Thompson, et al., Insulitis and beta-cell mass in the natural history of type 1 diabetes, Diabetes 65 (3) (2016) 719–731.
[4] S. Lenzen, Chemistry and biology of reactive species with special reference to the antioxidative defence status in pancreatic β-cells, Biochim. Biophys. Acta 1861 (8) (2017) 1929–1942.
[5] Y. Sato, et al., Cellular hypoxia of pancreatic beta-cells due to high levels of oxygen consumption for insulin secretion in vitro, J. Biol. Chem. 286 (14) (2011) 12525–12532.
[6] K.E. Dionne, C.K. Colton, M.L. Yarmush, Effect of hypoxia on insulin secretion by isolated rat and canine islets of Langerhans, Diabetes 42 (1) (1993) 12–21.
[7] M. Bensellam, et al., Hypoxia reduces ER-to-Golgi protein trafficking and increases cell death by inhibiting the adaptive unfolded pro-tein response in mouse beta cells, Diabetologia 59 (7) (2016) 1492–1502.
[8] P.C. Schulze, J. Yoshioka, T. Takahashi, Z. He, G.L. King, R.T. Lee, Hyperglycemia promotes oxidative stress through inhibition of thioredoxin function by thior-edoxin-interacting protein, J. Biol. Chem. 279 (29) (2004) 30369–30374.
[9] Y. Lai, et al., Activation of NFkB depend-ent apoptotic pathway in pancreatic islet cells by hypoxia, Islets 1 (1) (2009) 19–25.
[10] J. Chen, G. Saxena, I.N. Mungrue, A.J. Lusis, A. Shalev, Thioredoxin-interacting protein: a critical link between glucose toxicity and beta-cell apoptosis, Diabetes 57 (4) (2008) 938–944.
[11] E.M. Hanschmann, J.R. Godoy, C. Berndt, C. Hudemann, C.H. Lillig, Thioredoxins, glutaredoxins, and peroxiredoxins–molecular mechanisms and health significance: from cofactors to antioxidants to redox signaling, Antioxidants Redox Signal. 19 (13) (2013) 1539–1605.
[12] Y. Mikami, N. Shibuya, Y. Kimura, N. Nagahara, Y. Ogasawara, H. Kimura, Thioredoxin and dihydrolipoic acid are required for 3-mercaptopyruvate sulfur-transferase to produce hydrogen sulfide, Biochem. J. 439 (3) (2011) 479–485.
[13] K. Hirota, et al., Distinct roles of thioredoxin in the cytoplasm and in the nucleus. A two-step mechanism of redox regulation of transcription factor NF-kappaB, J. Biol. Chem. 274 (39) (1999) 27891–27897.
[14] A. Rubartelli, A. Bajetto, G. Allavena, E. Wollman, R. Sitia, Secretion of thioredoxin by normal and neo-plastic cells through a leaderless secretory pathway, J. Biol. Chem. 267 (34) (1992) 24161–24164.
[15] T.C. Laurent, E.C. Moore, P. Reichard, Enzymatic synthesis of deoxyribonucleotides. IV. Isolation and characterization of thioredoxin, the hydrogen donor from Escherichia coli B, J. Biol. Chem. 239 (1964) 3436–3444.
[16] C. Abate, L. Patel, F.J. Rauscher 3rd, T. Curran, Redox regulation of fos and jun DNA-binding activity in vitro, Science 249 (4973) (1990) 1157–1161.
[17] M.I. Berggren, B. Husbeck, B. Samulitis, A.F. Baker, A. Gallegos, G. Powis, Thioredoxin peroxidase-1 (peroxiredoxin-1) is increased in thioredoxin-1 trans-fected cells and results in enhanced protection against apoptosis caused by hy-drogen peroxide but not by other agents including dexamethasone, etoposide, and doxorubicin, Arch. Biochem. Biophys. 392 (1) (2001) 103–109.
[18] M. Saitoh, et al., Mammalian thioredoxin is a direct inhibitor of apoptosis signal-regulating kinase (ASK) 1, EMBO J. 17 (9) (1998) 2596–2606.
[19] G. Powis, D.L. Kirkpatrick, M. Angulo, A. Baker, Thioredoxin redox control of cell growth and death and the effects of inhibitors, Chem. Biol. Interact. 111–112 (1998) 23–34.
[20] H. Steinbrenner, B. Speckmann, L.O. Klotz, Selenoproteins: antioxidant sele-noenzymes and beyond, Arch. Biochem. Biophys. 595 (2016) 113–119.
[21] F.C. Chou, H.K. Sytwu, Overexpression of thioredoxin in islets transduced by a lentiviral vector pro-longs graft survival in autoimmune diabetic NOD mice, J. Biomed. Sci. 16 (2009) 71.
[22] R. Zhou, A. Tardivel, B. Thorens, I. Choi, J. Tschopp, Thioredoxin-interacting protein links oxidative stress to inflammasome activation, Nat. Immunol. 11 (2) (2010) 136–140.
[23] K.U. Lee, et al., Preferential infiltration of macrophages during early stages of in-sulitis in diabetes-prone BB rats, Diabetes 37 (8) (1988) 1053–1058.
[24] N. Lingwal, M. Padmasekar, B. Samikannu, R.G. Bretzel, K.T. Preissner, T. Linn, Inhibition of gelatinase B (matrix metalloprotease-9) activity reduces cellular in-flammation and restores function of transplanted pancreatic islets, Diabetes 61 (8) (2012) 2045–2053.
[25] L. Banaei-Bouchareb, et al., Insulin cell mass is altered in Csf1op/Csf1op macro-phage-deficient mice, J. Leukoc. Biol. 76 (2) (2004) 359–367.
[26] H. Brandhorst, D. Brandhorst, B.J. Hering, R.G. Bretzel, Significant progress in porcine islet mass isola-tion utilizing liberase HI for enzymatic low-temperature pancreas digestion, Transplantation 68 (3) (1999) 355–361.
[27] M. Lundberg, et al., Methodological aspects of ELISA analysis of thioredoxin 1 in human plasma and cerebrospinal fluid, PloS One 9 (7) (2014) e103554.
[28] J.R. Godoy, et al., Redox atlas of the mouse. Immunohistochemical detection of glutaredoxin-, peroxiredoxin-, and thioredoxin-family proteins in various tissues of the laboratory mouse, Biochim. Biophys. Acta 1810 (1) (2011) 2–92.
[29] C. Chen, R. Kuehn, R.G. Bretzel, T. Linn, Anti-inflammatory thalidomide improves islet grafts survival and functions in a xenogenic environment, PloS One 4 (7) (2009) e6312.
[30] A.M. Shapiro, et al., International trial of the Edmonton protocol for islet trans-plantation, N. Engl. J. Med. 355 (13) (2006) 1318–1330.
[31] P.J. Bingley, et al., Standardization of the IVGTT to predict IDDM, Diabetes Care 15 (10) (1992) 1313–1316.
[32] S. Marcelli-Tourvieille, T. Hubert, F. Pattou, M.C. Vantyghem, Acute insulin re-sponse (AIR): review of protocols and clinical interest in islet transplantation, Diabetes Metab. 32 (4) (2005) 295–303.
[33] E.S. Xenos, et al., The role of nitric oxide in IL-1 beta-mediated dysfunction of ro-dent islets of Langerhans. Implications for the function of intrahepatic islet grafts, Transplantation 57 (8) (1994) 1208–1212.
[34] S. Lenzen, J. Drinkgern, M. Tiedge, Low antioxidant enzyme gene expression in pancreatic islets compared with various other mouse tissues, Free Radic. Biol. Med. 20 (3) (1996) 463–466.
[35] K. Hong, G. Xu, T.B. Grayson, A. Shalev, Cytokines regulate β-cell thioredoxin-in-teracting protein (TXNIP) via distinct mechanisms and pathways, J. Biol. Chem. 291 (16) (2016) 8428–8439.
[36] S. Rani, et al., Decreasing Txnip mRNA and protein levels in pancreatic MIN6 cells reduces reactive oxygen species and restores glucose regulated insulin secretion, Cell. Physiol. Biochem. 25 (6) (2010) 667–674.
[37] J. Zhou, A.E. Damdimopoulos, G. Spyrou, B. Brüne, Thioredoxin 1 and thioredoxin 2 have opposed regulatory functions on hypoxia-inducible factor-1alpha, J. Biol. Chem. 282 (10) (2007) 7482–7490.
[38] S. Puri, D.A. Cano, M. Hebrok, A role for von Hippel-Lindau protein in pancreatic beta-cell function, Diabetes 58 (2) (2009) 433–441.
[39] K. Asami, et al., Thioredoxin-1 attenuates early graft loss after intraportal islet transplantation in mice, PloS One 8 (8) (2013) e70259.
[40] T. Jikimoto, Y. Nishikubo, M. Koshiba, Thioredoxin as a biomarker for oxidative stress in patients with rheumatoid arthritis, Mol. Immunol. 38 (10) (2002) 765–772.
[41] Y. Kakisaka, et al., Elevation of serum thioredoxin levels in patients with type 2 diabetes, Horm. Metab. Res. 34 (3) (2002) 160–164.
[42] P. Checconi, et al., Redox proteomics of the inflammatory secretome identifies a common set of redoxins and other glutathionylated proteins released in in-flammation, influenza virus infection and oxidative stress, PloS One 10 (5) (2015) e0127086.
[43] S.Z. Xu, et al., TRPC channel activation by extracellular thioredoxin, Nature 451 (7174) (2008) 69–72.
[44] L.R. Brixel, et al., TRPM5 regulates glucose-stimulated insulin secretion, Pflügers Archiv 460 (1) (2010) 69–76.
[45] M. Skrzypski, et al., Activation of TRPV4 channel in pancreatic INS-1E beta cells enhances glucose-stimulated insulin secretion via calcium-dependent mechanisms, FEBS Lett. 587 (19) (2013) 3281–3287.
[46] U. Schwertassek, et al., Selective redox regulation of cytokine receptor signaling by extracellular thioredoxin-1, EMBO J. 26 (13) (2007) 3086–3097.
[47] I. Azimi, L.J. Matthias, R.J. Center, J.W. Wong, P.J. Hogg, Disulfide bond that constrains the HIV-1 gp120 V3 domain is cleaved by thioredoxin, J. Biol. Chem. 285 (51) (2010) 40072–40080.
[48] N.M. Plugis, B.A. Palanski, C.H. Weng, M. Albertelli, C. Khosla, Thioredoxin-1 se-lectively activates transglutaminase 2 in the extracellular matrix of the small in-testine: implications for celiac disease, J. Biol. Chem. 292 (5) (2017) 2000–2008.
[49] N. Kondo, et al., Redox sens-ing release of human thioredoxin from T lymphocytes with negative feedback loops, J. Immunol. 172 (1) (2004) 442–448.
[50] N. Kondo, et al., Lipid raft-mediated uptake of cysteine-modified thiore-doxin-1: apoptosis enhancement by inhibiting the endogenous thioredoxin-1, Antioxidants Redox Signal. 9 (9) (2007) 1439-1348.
[51] F. Xia, et al., Disruption of pancreatic beta-cell lipid rafts modifies Kv2.1 channel gating and insulin exocytosis, J. Biol. Chem. 279 (23) (2004) 24685–24691.
[52] N. Kobayashi, et al., Thioredoxin reduces C-C chemokine-induced chemotaxis of human eosinophils, Allergy 64 (8) (2009) 1130–1135.
[53] W. Liu, et al., Thioredoxin-1 ameliorates myosin-induced autoimmune myocarditis by suppressing chemokine expressions and leukocyte chemotaxis in mice, Circulation 110 (10) (2004) 1276–1283.
[54] H. Nakamura, et al., Circulating thioredoxin suppresses lipopolysaccharide-induced neutrophil chemotaxis, Proc. Natl. Acad. Sci. U. S. A. 98 (26) (2001) 15143–15148.
[55] H. Ro, E.W. Lee, J.H. Hong, Roles of islet Toll-like receptors in pig to mouse islet xenotransplantation, Cell Transplant. 22 (9) (2013) 1709–1722.
[56] S. Pagliei, et al., Thioredoxin specifically cross-desensitizes monocytes to MCP-1, Eur. Cytokine Netw. 13 (2) (2002) 261–267.
[57] L. Tao, et al., Cardioprotective effects of thioredoxin in myocardial ischemia and reperfusion: role of S-nitrosation, Proc. Natl. Acad. Sci. U. S. A. 101 (31) (2004) 11471–11476.
[58] B.C. King, J. Nowakowska, C.M. Karsten, J. Köhl, E. Renström, A.M. Blom, Truncated and full-length thioredoxin-1 have opposing activating and inhibitory properties for human complement with relevance to endothelial surfaces, J. Immunol. 188 (8) (2012) 4103–4112.
[59] K. Pekkari, R. Gurunath, E.S. Arner, A. Holmgren, Truncated thioredoxin is a mi-togenic cytokine for resting human peripheral blood mononuclear cells and is present in human plasma, J. Biol. Chem. 275 (48) (2000) 37474–37480.
[60] K. Pekkari, A. Holmgren, Truncated thioredoxin: physiological functions and me-chanism, Antioxidants Redox Signal. 6 (1) (2004) 53–61.
[61] B. Sahaf, et al., Thioredoxin expression and localization in human cell lines:

detection of full-length and truncated species, Exp. Cell Res. 236 (1) (1997) 181–192.
[62] H.M. Garay-Malpartida, R.F. Mourão, M. Mantovani, I.A. Santos, M.C. Sogayar, A.C. Goldberg, Toll-like receptor 4 (TLR4) expression in human and murine pancreatic beta-cells affects cell viability and insulin homeostasis, BMC Immunol. 12 (2011) 18.
[63] M. Vives-Pi, et al., Evidence of expression of endotoxin receptors CD14, toll-like receptors TLR4 and TLR2 and associated molecule MD-2 and of sensitivity to endotoxin (LPS) in islet beta cells, Clin. Exp. Immunol. 133 (2) (2003) 208–218.
[64] L. Witek-Janusek, J.P. Filkins, Insulin-like action of endotoxin: antagonism by steroidal and nonsteroidal anti-inflammatory agents, Circ. Shock 8 (5) (1981) 573–583.
[65] P. Acosta-Montaño, et al., Fatty acid and lipopolysaccharide effect on beta cells proteostasis and its impact on insulin secretion, Cells 8 (8) (2019) Pii: E884.

Supplementary Information for

Paracrine regulation and improvement of β-cell function by thioredoxin

Eva-Maria Hanschmann[1,2#], Sebastian Friedrich Petry[3*#], Susanne Eitner[1], Constanze Christin Maresch[3], Neelam Lingwal[3], Christopher Horst Lillig[1*§], and Thomas Linn[3*§]

[1]Institute for Medical Biochemistry and Molecular Biology, University Medicine, University of Greifswald

[2]Department of Neurology, Medical Faculty, Heinrich-Heine-University, Düsseldorf

[3]Clinical Research Unit, Center of Internal Medicine, Justus-Liebig-University, Giessen

[#§] These authors contributed equally to the manuscript

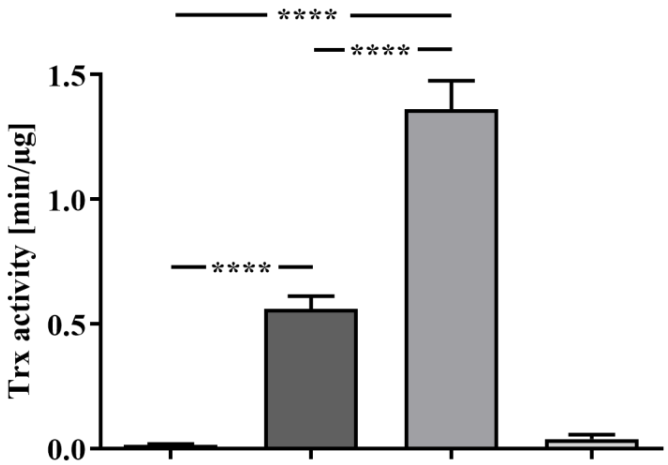

Fig. S1. Activity of recombinant hTrx1. Activity of 30 or 60 µg/ml hTrx1 was measured by fluorescence emitted during Trx1-catalyzed reduction of insulin. hTrx1 was absent in the negative control (0 hTrx1 µg/ml). Moreover, 30 min heated and denatured hTrx1 (dhTrx1) was analyzed. hTrx1 had a significantly higher activity in comparison to its absence. ****p<0.0001 (one-way ANOVA), n=5.

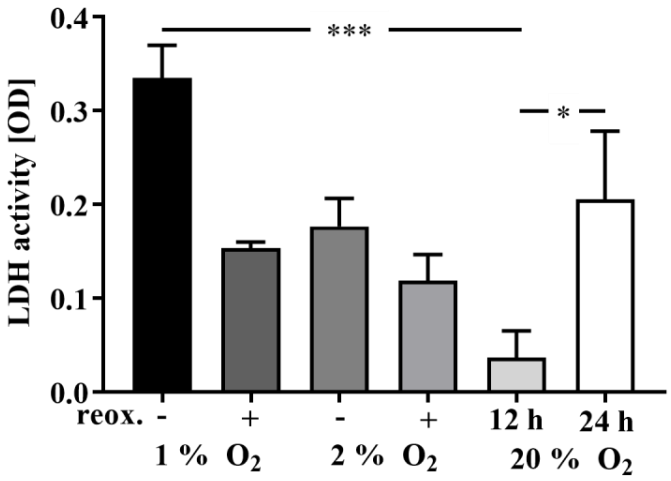

Fig. S2. Effects of hypoxia and reoxygenation on LDH activity in MIN6 cells. LDH activity of MIN6 cells cultured at 1 % or 2 % O_2 for 12 h with (+) or without (-) reoxygenation (reox.) for another 12 h. Normoxic cell culture was the control condition and performed at 20 % O_2 for 12 or 24 h as indicated. LDH activity was only significantly increased in cells cultured at 1 % O_2 without reoxygenation and at 20 % O_2 for 24 h in comparison with 20 % normoxic culture for 12 h. ***$p<0.001$, *$p<0.05$ (one-way ANOVA), n = 4.

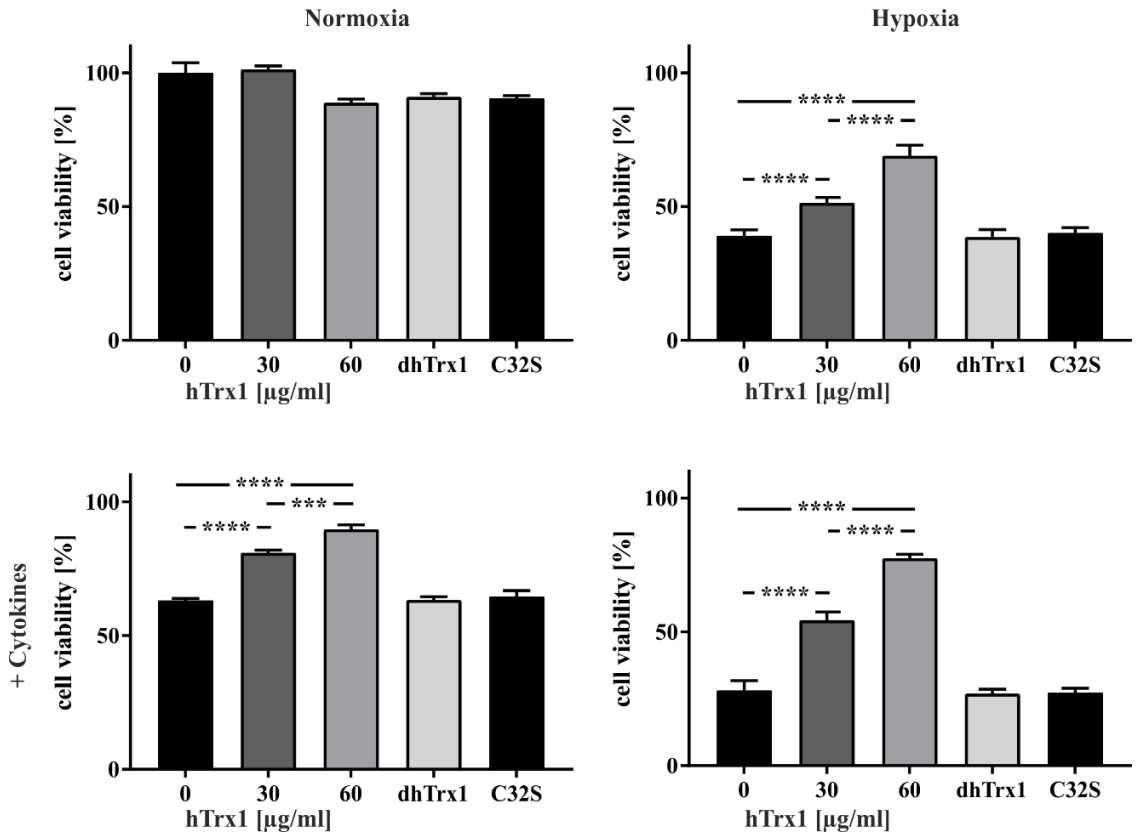

Fig. S3. Trx1 affects cell viability during hypoxia and inflammation. Mitochondrial activity of MIN6 cells was determined in a colorimetric assay using 3,4,5-dimethylthiazol-diphenyltetrazolium (MTT, Vybrant MTT kit, Molecular Probes, Invitrogen). The optical density (OD) data are given for MIN6 cells that were cultured in the presence of 0, 30 or 60 µg/ml hTrx1 and 60 µg/ml dhTrx1 or C32S, under normoxia and hypoxia (upper row) as well as under normoxia and hypoxia with additional cytokine treatment (10 ng/ml TNF-α, 5 ng/ml IL-1β, 100 ng/ml IFN-γ, lower row). The conversion of MTT was amplified when 30 and 60 µg/ml hTrx1 was added, 25 % and 56 % upon hypoxia, 29 % and 40 % in the presence of cytokines, and even 93 % and 174 % upon a combination of hypoxia and cytokines ****p<0.0001, ***p<0.005 (one-way ANOVA), n=5.

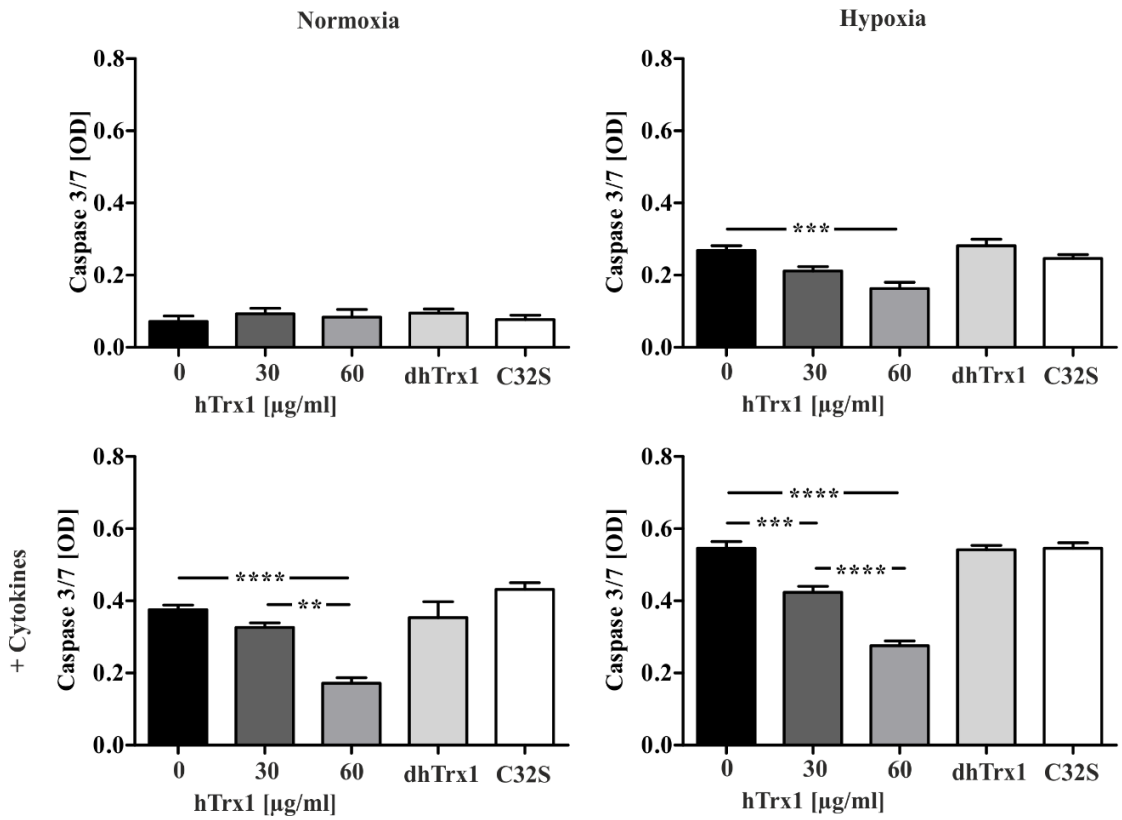

Fig. S4. Trx1 affects caspase activation during hypoxia and inflammation. Caspase 3/7 activity was measured following manufacturer's instructions and given as optical density. The OD data are given for MIN6 cells that were cultured in the presence of 0, 30 or 60 µg/ml hTrx1 and 60 µg/ml dhTrx1 or C32S, under normoxia and hypoxia (upper row) as well as under normoxia and hypoxia with additional cytokine treatment (10 ng/ml TNF-α, 5 ng/ml IL-1β, 100 ng/ml IFN-γ, lower row). hTrx1 treatment significantly reduced Caspase 3/7 expression during cytokine treatment with and without hypoxia by up to 80 %. ****p<0.0001, ***p<0.0005, **p<0.005 (one-way ANOVA), n=5.

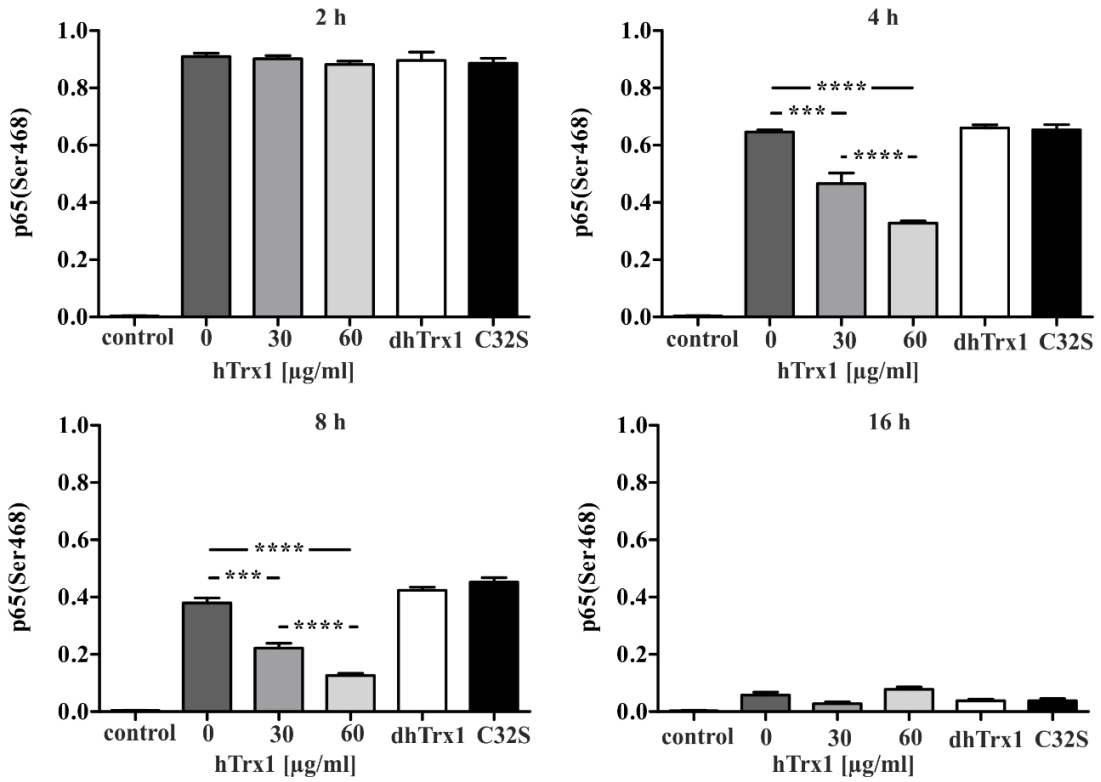

Fig. S5. Trx1 reduces NF-kB p65 (phospho-Ser468) activation during hypoxia and inflammation. Protein lysates were prepared from MIN6 cells. p65 activation was detected by a 10 min TNF-α pulse (10 ng/ml) of cells cultivated at normoxic or hypoxic conditions for 2, 4, 8, and 16 hours in the presence of 0, 30 or 60 µg/ml hTrx1 and 60 µg/ml dhTrx1 or C32S, respectively. 60 µg/ml hTrx1 suppressed p65 phosphorylation at four and eight hours of hypoxia by 50 % and 66 %. ****p<0.0001, ***p<0.001 (one-way ANOVA), n=5.

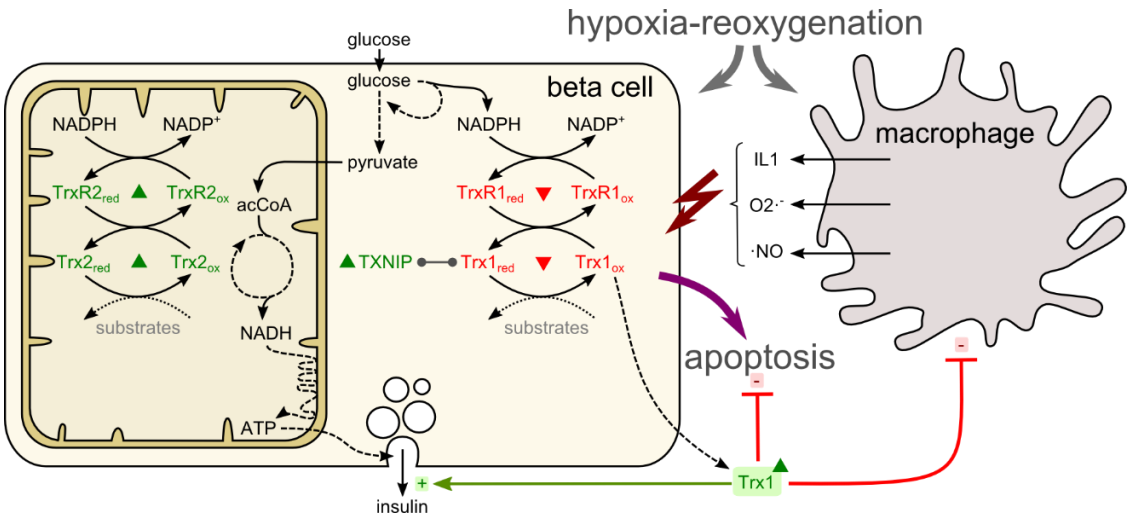

Fig. S6. Summary. Upon hypoxic and immune-mediated stress, there is a depletion of the cytosolic Trx1 system together with an up-regulation of the mitochondrial Trx2 system. Trx1 is released from the β-cell and counteracts cellular inflammation by e.g. inhibiting macrophage migration, increasing secretory capacities of the β-cell and reducing apoptosis and necrosis. Abrogation of both thioredoxin systems by auranofin leads to β-cell decay. Txnip is essential for glucose metabolism and β-cell function via binding of Trx1.

Table S1. List of antibodies and proteins.

Antigen	Manufacturer / product number	Method
Human antibodies		
Trx1	Mabtech (MT17R6)	Elisa
Murine antibodies		
Trx1	Elabscience (E-AB-16109)	Elisa
Trx2	Biorbyt (Orb4663)	Elisa
TrxR1	MyBioSource (MBS2017640)	Elisa
TrxR2	MyBioSource (MBS153657)	Elisa
Rabbit antibodies		
Goat Anti-Rabbit IgG	abcam (ab6720)	Elisa
Trx1	Boster (M01219-1)	IHC
TrxR1	Cell Signaling (#15140)	IHC
Trx2	myBioSource (MBS760526)	IHC
TrxR2	myBioSource (MBS852200)	IHC
Txnip	Cell Signaling (#14715)	IHC
Murine proteins		
Trx1	Abbexa (abx069263)	
TrxR1	Hoelzel (17667M)	
Trx2	Hoelzel (17653M)	
TrxR2	Hoelzel (17668M)	
Txnip	Cusabio (CSB-EP803849MO)	

Table S2. List of porcine and human primer sequences.

Primer	**fwd**	**rev**
Porcine		
Bcl-2	ATGTGTGTGGAGAGCGTCAA	CCTTCAGAGACAGCCAGGAG
c-FLIP	GAGCAAGCCCCTAGGAATCT	GTCTTGGTGTTGGGGCATAC
VEGF-A	CCTTGCCTTGCTGCTCTAC	GGTTTCTGGTCTCCTTCTGC
HIF1α	GCTTGCTCATCAGTTGCC	GCCTTCATTTCATCTTCAATATCC
Human		
hTrx1 C32S	CAGCCACGTGGTCTGGGCCTTG	CAAGGCCCAGACCACGTGGCTG

Table S3. Summary of β-cell viability data.

	hTrx1	Normoxia	+ Cytokines	Hypoxia	+ Cytokines
Annexin / PI[A] **[%]**	0	4.267 ± 0.3	7.9 ± 4.3	9.767 ± 1.3	13.27 ± 2.2
	30	3.717 ± 0.9	7.583 ± 2.3	5.733 ± 0.5****	7.950 ± 3.5**
	60	2.517 ± 1.3**	6.383 ± 1.4	1.967 ± 1.6****	6.950 ± 1.6***
MTT [OD] [B]	0	0.818 ± 0.07	0.516 ± 0.01	0.32 ± 0.02	0.23 ± 0.02
	30	0.828 ± 0.02	0.662 ± 0.01****	0.42 ± 0.02****	0.44 ± 0.03****
	60	0.726 ± 0.02	0.734 ± 0.03****	0.56 ± 0.05****	0.63 ± 0.02****
Casp. 3/7[C] **[absolute OD]**	0	0.072 ± 0.04	0.376 ± 0.03	0.268 ± 0.03	0.546 ± 0.04
	30	0.093 ± 0.04	0.326 ± 0.03	0.212 ± 0.03	0.424 ± 0.04***
	60	0.083 ± 0.05	0.172 ± 0.03****	0.163 ± 0.04***	0.276 ± 0.03****
Bax/Bcl-2[D] **[rel. mRNA expression]**	30	0.650 ± 0.3	0.756 ± 0.3	0.688 ± 0.1	0.678 ± 0.4
	60	0.863 ± 0.2	0.456 ± 0.2	0.538 ± 0.1*	0.389 ± 0.2**
c-Flip[E] **[rel. mRNA expression]**	30	0.925 ± 0.6	1.022 ± 0.5	0.988 ± 0.2	1.267 ± 0.6
	60	1.025 ± 0.6	1.044 ± 0.5	0.988 ± 0.3	1.244 ± 0.7
HIF-1α[F] **[rel. mRNA expression]**	30	0.838 ± 0.5	1.411 ± 0.5	1.575 ± 1.0	0.911 ± 0.4
	60	1.000 ± 0.9	2.933 ± 1.3****	2.413 ± 0.5****	2.600 ± 2.3*
VEGF-A[G] **[rel. mRNA expression]**	30	0.775 ± 0.3	3.722 ± 1.0****	2.425 ± 0.9****	2.722 ± 0.6****
	60	0.925 ± 0.6	5.122 ± 0.6****	3.450 ± 0.3****	4.467 ± 0.5****

MIN6 cells or islets were treated with hTrx1 (30 or 60 µg/ml) under conditions of normoxia (20 % oxygen) or hypoxia (2 % oxygen) in the presence or absence of cytokines (10 ng/ml TNF-α, 5 ng/ml IL-1β, and 100 ng/ml IFN-γ). As an overview the table includes data also shown graphically in ***Figures 4***, ***5***, ***S3***, and ***S4***.
[A]FACS analysis of porcine islets treated with annexin V and propidium iodide (PI) given as mean percentage of total cells with both annexin V and PI staining, see hypoxia and normoxia conditions depicted in ***Figure 4***. Cytokine treatment data were added to the table to show that the percentage of Annexin/PI double positive islet cells was significantly reduced by hTrx1 when hypoxia and cytokines were combined, but not in the condition of cytokines only. [B]MTT assay data of MIN6 cells given as optical density (OD, ***Figure S3***).
[C]Caspase 3/7 activity measured as absolute optical density (OD, Promega luminescent assay). OD is given in nm wavelength linearly correlated to caspase 3/7 activity (***Figure S4***). [D, E, F, G]mRNA fold expression in porcine islets relative to the expression level of the control without hTrx1 for pro-apoptotic genes Bax/Bcl-2, anti-apoptotic gene c-Flip, HIF-1α, and pro-survival gene VEGF-A (***Figure 5***). ****p<0.0001, ***p<0.001, **p<0.01, *p<0.05.